frontiers | Research Topics

Case reports in pulmonary medicine 2024

Edited by
Talat Kilic, Uday Kishore, Giuseppe Fiorentino and Karolina Henryka Czarnecka-Chrebelska

Published in
Frontiers in Medicine

ISSN 1664-8714
ISBN 978-2-8325-6825-5
DOI 10.3389/978-2-8325-6825-5

Generative AI statement
Any alternative text (Alt text) provided alongside figures in the articles in this ebook has been generated by Frontiers with the support of artificial intelligence and reasonable efforts have been made to ensure accuracy, including review by the authors wherever possible. If you identify any issues, please contact us.

About Frontiers

Frontiers is more than just an open access publisher of scholarly articles: it is a pioneering approach to the world of academia, radically improving the way scholarly research is managed. The grand vision of Frontiers is a world where all people have an equal opportunity to seek, share and generate knowledge. Frontiers provides immediate and permanent online open access to all its publications, but this alone is not enough to realize our grand goals.

Frontiers journal series

The Frontiers journal series is a multi-tier and interdisciplinary set of open-access, online journals, promising a paradigm shift from the current review, selection and dissemination processes in academic publishing. All Frontiers journals are driven by researchers for researchers; therefore, they constitute a service to the scholarly community. At the same time, the *Frontiers journal series* operates on a revolutionary invention, the tiered publishing system, initially addressing specific communities of scholars, and gradually climbing up to broader public understanding, thus serving the interests of the lay society, too.

Dedication to quality

Each Frontiers article is a landmark of the highest quality, thanks to genuinely collaborative interactions between authors and review editors, who include some of the world's best academicians. Research must be certified by peers before entering a stream of knowledge that may eventually reach the public - and shape society; therefore, Frontiers only applies the most rigorous and unbiased reviews. Frontiers revolutionizes research publishing by freely delivering the most outstanding research, evaluated with no bias from both the academic and social point of view. By applying the most advanced information technologies, Frontiers is catapulting scholarly publishing into a new generation.

What are Frontiers Research Topics?

Frontiers Research Topics are very popular trademarks of the *Frontiers journals series*: they are collections of at least ten articles, all centered on a particular subject. With their unique mix of varied contributions from Original Research to Review Articles, Frontiers Research Topics unify the most influential researchers, the latest key findings and historical advances in a hot research area.

Find out more on how to host your own Frontiers Research Topic or contribute to one as an author by contacting the Frontiers editorial office: frontiersin.org/about/contact

Case reports in pulmonary medicine 2024

Topic editors

Talat Kilic — İnönü University, Türkiye

Uday Kishore — United Arab Emirates University, United Arab Emirates

Giuseppe Fiorentino — Department of Respiratory Pathophysiology, Colli Hospital, Italy

Karolina Henryka Czarnecka-Chrebelska — Medical University of Lodz, Poland

Citation

Kilic, T., Kishore, U., Fiorentino, G., Czarnecka-Chrebelska, K. H., eds. (2025). *Case reports in pulmonary medicine 2024*. Lausanne: Frontiers Media SA.

doi: 10.3389/978-2-8325-6825-5

Table of contents

frontiers | Frontiers in Medicine

TYPE Editorial
PUBLISHED 26 August 2025
DOI 10.3389/fmed.2025.1680815

OPEN ACCESS

EDITED AND REVIEWED BY
Dawei Yang,
Fudan University, China

*CORRESPONDENCE
Karolina H. Czarnecka-Chrebelska
karolina_czarnecka@yahoo.co.uk;
karolina.czarnecka@umed.lodz.pl

RECEIVED 06 August 2025
ACCEPTED 11 August 2025
PUBLISHED 26 August 2025

CITATION
Czarnecka-Chrebelska KH and Kishore U (2025) Editorial: Case reports in pulmonary medicine 2024. *Front. Med.* 12:1680815. doi: 10.3389/fmed.2025.1680815

Editorial: Case reports in pulmonary medicine 2024

Karolina H. Czarnecka-Chrebelska[1]* and Uday Kishore[2]

[1]Department of Biomedicine and Genetics, Medical University of Lodz, Lodz, Poland, [2]Department of Veterinary Medicine (CAVM) and Zayed Centre for Health Sciences, United Arab Emirates University, Al Ain, United Arab Emirates

KEYWORDS

severe lung infections, pulmonary infection, Pneumonia—clinical features and management, next-generation sequencing—NGS, *Chlamydia psittaci* (*C. psittaci*), *Penicillium digitatum*, *Aeromonas dhakensis* AS3

Editorial on the Research Topic
Case reports in pulmonary medicine 2024

Recent clinical reports highlight a growing trend of unusual pulmonary infections affecting both immunocompetent and immunocompromised patients. Atypical pathogens such as *Chlamydia psittaci*, *Penicillium digitatum*, *Nocardia*, and *Aeromonas dhakensis* are increasingly recognized as causes of severe respiratory illnesses, often resulting in life-threatening complications. Identifying the infectious agent and reaching a final diagnosis are often delayed because initial symptoms and clinical signs are non-specific, resembling common respiratory infections. This similarity makes it difficult for healthcare providers to determine the exact cause of the illness promptly. Case studies show that traditional diagnostic tools often fall short, leading to delays and sometimes inappropriate treatments. The use of metagenomic next-generation sequencing (mNGS) has proven invaluable in detecting rare pathogens and guiding personalized therapies. However, the high cost of NGS and the need for rapid initiation of clinical antimicrobial treatment still contribute to delays in diagnosis (1).

Several reports highlight the often-overlooked burden of *Chlamydia psittaci* pneumonia. In two case studies, patients showed classic symptoms like fever, cough, dyspnea, and chest tightness—a non-specific clinical presentation that closely resembled common community-acquired pneumonia (Zhang et al.; Yan et al.). In one case, deep vein thrombosis complicated the course of the infection, and the patient did not respond to broad-spectrum antibiotics (Zhang et al.). In another case, despite thorough laboratory and radiological testing, the cause of pneumonia remained unknown (Yan et al.). In both cases, testing bronchoalveolar lavage fluid (BALF) samples with targeted next-generation sequencing (tNGS) enabled a quick and accurate diagnosis (Zhang et al.; Yan et al.). Similarly, mNGS played a key role in promptly confirming severe Legionnaires' disease, not identified with conventional testing (Fang et al.). The case describes two instances of *Legionellosis* with different outcomes. For the elderly immunocompromised patient, the delayed diagnosis led to the continued use of broad-spectrum antibiotics, allowing the infection to worsen unchecked. In contrast, the prompt use of mNGS in the case of the middle-aged patient enabled an accurate diagnosis and eventual recovery (Fang et al.).

Fungal and parasitic infections also merit attention in this regard. The first reported case in China of invasive *Penicillium digitatum* lung infection demonstrates how environmental fungi can cross into clinical pathology (Shi et al.). The patient's symptoms and imaging (chronic cough, consolidation on CT) resembled bacterial pneumonia, and

standard bacterial and fungal cultures failed to detect the pathogen. *P. digitatum* was identified only after mNGS on BALF and confirmatory targeted fungal culture, enabling tailored treatment that controlled the infection (Shi et al.).

Nocardia—and anthropozoonotic bacteria species have been increasingly reported as a cause of rapidly advancing pulmonary disease. Conventional diagnostic methods typically require long-lasting cultures (2–32 days) and can have low sensitivity, as fast-growing bacteria may overshadow/outnumber *Nocardia*, leading to missed detections despite strong clinical suspicion (2). Recent cases reveal that delayed *Nocardia* detection may cause life-threatening symptoms: a woman with gingival pain and pharyngeal discomfort, treated with oral metronidazole, quickly developed breathing difficulties. Her imaging resembled tuberculosis, but routine sputum and blood cultures were negative. Due to her deteriorating health, fiberoptic bronchoscopy was performed, revealing no tumor or severe inflammation. Yet, the lavage smear after a week of culture enabled the detection of *Nocardia*, allowing for targeted therapy and rapid disease control (Chen et al.). On the other hand, using NGS can provide results in about 48 h, with *Nocardia* species often ranking among the top two organisms detected (2). In the case of an immunosuppressed patient with Myasthenia gravis, 16S rRNA gene sequencing helped distinguish pulmonary nocardiosis from more common infections in an immunocompromised host, and ultimately, *Nocardia cyriacigeorgica* infection was confirmed (Zuo et al.).

In the case of a 19-year-old patient who presented with a simple sore throat but then deteriorated into septic shock with multiple serous effusions, repeated sputum cultures were negative. The mNGS analysis of blood and pericardial fluid led to the identification of the pathogen—anaerobe *Prevotella oris* (a member of the oral cavity microbiome, regarded as commensals in the oral cavity) that caused systemic pleural infection (Zhang et al.). Another case of pneumonia, which rapidly worsened to septic shock and severe pulmonary hypertension, was caused by the anaerobic pathogen *Aeromonas dhakensis*. Due to the severe acute respiratory distress syndrome, the mNGS of BALF and blood was performed promptly that subsequently led to the initiation of *A. dhakensis*-targeted treatment (Sha et al.). Rare human pathogen—zoonotic *Chlamydia abortus* can mimic community-acquired pneumonia, as seen in the 74-year-old female, who worsened rapidly. Standard bacterial, fungal, and viral tests were repeatedly negative, and a definitive diagnosis required mNGS on BALF, ultimately guiding effective targeted therapy (Yang and Shu). Similarly, a patient initially suffering from allergic and pulmonary infections, treated with allergic medications and broad-spectrum antibiotics for over a year, eventually developed symptoms that resembled tuberculosis both clinically and radiographically. After specialized culture and molecular testing, the diagnosis revealed the rare non-tuberculous mycobacteria—*Mycobacterium riyadhense* (Sawan et al.).

Pulmonary infection symptoms can sometimes result from severe parasitic invasion, as seen in a 75-year-old immunocompromised patient presenting with non-specific respiratory symptoms like cough and shortness of breath (Fang et al.). Initially, the diagnosis indicated a common bacterial or fungal pulmonary infection; however, symptoms persisted and worsened despite treatment. mNGS analysis of BALF samples detected *E. faecium, C. albicans*, *C. glabrata*, and unexpectedly, *Strongyloides stercoralis*—a soil-transmitted nematode common in tropical and subtropical regions (Fang et al.). Notably, uncomplicated strongyloidiasis is often asymptomatic, while severe cases can cause abdominal pain, diarrhea, vomiting, nausea, colitis, and gastrointestinal bleeding signs, though respiratory symptoms are rare (Fang et al.).

The commented cases highlight the importance of prompt pathogen identification, which enables targeted antibiotic therapy. This approach reduces the severity and duration of illness, prevents progression to multi-organ failure, and ultimately allows for complete recovery and hospital discharge. Some cases revealed novel associations, such as deep vein thrombosis secondary to psittacosis or fatal progression from oral infection. These findings stress the importance of considering rare etiologies in atypical pneumonias and support broader adoption of molecular diagnostics. In immunocompromised patients or those experiencing rapid clinical deterioration, early incorporation of genomic analysis—particularly metagenomic next-generation sequencing (mNGS)—is critical for timely and accurate pathogen identification when conventional diagnostics fail. This approach enables prompt, targeted treatment, which can significantly improve outcomes and, in many cases, be life-saving.

In the evolving field of respiratory medicine, recent case reports show an increasingly diverse range of pathogens responsible for severe lung infections. These cases—often involving rare or emerging microorganisms—highlight the diagnostic challenges of traditional methods and the clinical impact of delayed or incorrect treatment. On one hand, it is noted that the lungs are becoming increasingly susceptible to a broader range of emerging pathogens, including zoonotic bacteria and environmental fungi. On the other hand, more detailed analysis of clinical symptoms (with broader biomarker testing) and the use of advanced diagnostic tools could offer more precise and comprehensive ways to identify these threats early, leading to better clinical outcomes. Together, these cases emphasize the diagnostic and therapeutic importance of metagenomic next-generation sequencing (mNGS). By enabling rapid, unbiased pathogen detection, mNGS plays a transformative role in modern infectious disease management, particularly when traditional methods may overlook pathogens.

Author contributions

KHC-C: Conceptualization, Writing – original draft, Writing – review & editing, Formal analysis. UK: Writing – review & editing, Validation.

Acknowledgments

We thank all researchers who contributed to this Research Topic—Case reports in pulmonary medicine 2024 and the editorial team at *Frontiers in Medicine* for their support.

Conflict of interest

The authors declare that the research was conducted in the absence of any commercial or financial relationships that could be construed as a potential conflict of interest.

The author(s) declared that they were an editorial board member of Frontiers, at the time of submission. This had no impact on the peer review process and the final decision.

Generative AI statement

The author(s) declare that Gen AI was used in the creation of this manuscript. The Grammarly app was used to evaluate the quality of English. Grammarly features an AI assistant that utilizes generative AI to help rewrite paragraphs, eliminating errors and repetitions.

Any alternative text (alt text) provided alongside figures in this article has been generated by Frontiers with the support of artificial intelligence and reasonable efforts have been made to ensure accuracy, including review by the authors wherever possible. If you identify any issues, please contact us.

Publisher's note

References

1. Cao H, Chen Y, Ge L, Kwong JS, Lai H, Hu F, et al. An umbrella review of the diagnostic value of next-generation sequencing in infectious diseases. *Int J Clin Pharm*. (2024) 46:780–94. doi: 10.1007/s11096-024-01704-2

2. Weng SS, Zhang HY, Ai JW, Gao Y, Liu YY, Xu B, et al. Rapid detection of *Nocardia* by next-generation sequencing. *Front Cell Infect Microbiol*. (2020) 10:13. doi: 10.3389/fcimb.2020.00013

frontiers | Frontiers in Medicine

TYPE Case Report
PUBLISHED 11 June 2024
DOI 10.3389/fmed.2024.1381261

OPEN ACCESS

EDITED BY
Talat Kilic,
İnönü University, Türkiye

REVIEWED BY
Elizabeth A. Jacobsen,
Mayo Clinic Arizona, United States
Saltuk Buğra Kaya,
İnönü University, Türkiye

*CORRESPONDENCE
Yasuo Shimizu
✉ yasuo-s@dokkyomed.ac.jp

RECEIVED 03 February 2024
ACCEPTED 29 May 2024
PUBLISHED 11 June 2024

CITATION
Inaba M, Shimizu Y, Nakamura Y, Okutomi H, Takemasa A and Niho S (2024) Tezepelumab improved chronic eosinophilic pneumonia in severe asthma patients with liver cirrhosis. *Front. Med.* 11:1381261. doi: 10.3389/fmed.2024.1381261

Tezepelumab improved chronic eosinophilic pneumonia in severe asthma patients with liver cirrhosis

Mizuki Inaba[1], Yasuo Shimizu[1,2]*, Yusuke Nakamura[1], Hiroaki Okutomi[1], Akihiro Takemasa[1,2] and Seiji Niho[1]

[1]Department of Pulmonary Medicine and Clinical Immunology, Dokkyo Medical University, Mibu, Tochigi, Japan, [2]Respiratory Endoscopy Center, Dokkyo Medical University Hospital, Mibu, Japan

Systemic administration of corticosteroids is used in the treatment of chronic eosinophilic pneumonia (CEP). However, in patients with CEP as well as other comorbidities, the adverse effects of corticosteroids should be minimized as much as possible. A 71-year-old woman was presented with aggravating asthma with CEP and sinusitis, and she had uncompensated liver cirrhosis (LC) with a Child-Pugh score of 7. Initial treatment with a low dose of oral corticosteroids (OCSs) in combination with tezepelumab, an anti-thymic stromal lymphopoietin (TSLP) antibody, resulted in rapid improvement of asthma and CEP without deteriorating LC. Sinusitis also improved after ceasing OCS. This case suggested that tezepelumab may be useful as a treatment option for patients with CEP, especially those with liver dysfunction.

KEYWORDS

eosinophilic pneumonia, asthma, tezepelumab, thymic stromal lymphopoietin, liver fibrosis, sinusitis, eosinophilia, oral corticosteroids

1 Introduction

Asthma and chronic eosinophilic pneumonia (CEP) can be comorbid, and studies have shown that oral corticosteroids (OCSs) are successful in treating CEP (1). The metabolism of corticosteroids (CSs) in the liver is impaired in patients with severe liver cirrhosis (LC), and CS may further aggravate liver function and increase the risk of impaired consciousness by elevating the amount of circulating NH_3 (2). Therefore, providing treatment without worsening liver function is a challenge for patients with LC. Herein, a patient presented with shortness of breath and progressive hypoxemia, which was caused by poorly controlled asthma with CEP, complicated by sinusitis and LC. Initial treatment with a low dose of OCS in combination with tezepelumab, an anti-thymic stromal lymphopoietin (TSLP) antibody, resulted in rapid improvement of asthma and CEP without deteriorating LC. Furthermore, sinusitis also improved after ceasing OCS. This is the first case report of a successful CEP treatment with tezepelumab. Considering that there was a report of successful biologic therapy without OCS for CEP (3), when CEP patients have LC, the initial induction may be conducted with biologics alone, and OCS can be added after assessing the response to biologics.

2 Case presentation

A 71-year-old woman was presented in our hospital with a 2-month history of productive cough, shortness of breath, and hypoxia to SpO_2 of 92% in room air at a KT of 36.8°C. Auscultation revealed wheezing in both lungs. The respiratory symptoms were severe, presenting an asthma control test score of 6 points and a mean asthma control questionnaire score of 5.2 points. Laboratory examination revealed a normal leukocyte concentration of 5,800 cells/μL but an eosinophilia content of 1,200 cells/μL (20.7%) and reduced platelets (9.3 cells/μL), as well as 66% prothrombin activity and 3.3 g/dL of albumin. Liver enzymes were found in high concentrations, with 3.05 mg/dL of total bilirubin, 1.11 mg/dL of direct bilirubin, 1.94 mg/dL of indirect bilirubin, 158 U/L of alkaline phosphatase, and 43 μg/dL of NH_3. Eosinophils in sputum were prominent, exhibiting an average of 10–20 cells/field of view, measured by optical microscopy at 200× magnification on five fields. Chest X-rays showed infiltration shadows in the right upper and lower lung fields, chest computed tomography (CT) revealed predominant bilateral infiltration shadows in the upper lobes, which extended to both lower lobes, and sinus CT showed bilateral sinusitis (Figures 1A–D,I). Spirometry indicated a severe obstruction with a forced expiratory volume in 1 s (FEV_1) of 0.90 L/s and %FEV1 of 50.8%, and the fractional exhaled nitric oxide (FeNO) content was 91 ppb. The clinical diagnosis was CEP complicated by asthma, based on asthma-like symptoms, typical CEP shadows in the lungs, increased peripheral blood eosinophils, and prominent sputum eosinophils, as well as physical examination that revealed no collagen vascular disease (CVD) or rheumatoid arthritis. The patient had been sober for several years, but considering the uncompensated LC and a Child-Pugh score of 7, bronchoscopy was not performed because of the risk of coma following anesthesia (4). Treatment began with prednisolone (10 mg/day), inhaled fluticasone furoate/vilanterol (FF/VI, 200/25 μg/day), and tezepelumab (210 mg/month) (Figure 2). After 10 days, the asthma symptoms and chest XP markedly improved (Figure 1H), and after 1 month, the bilateral shadows disappeared (Figures 1E–G). Based on these improvements, the OCS dose was reduced to 3 mg/day. After 2 months of therapy, the asthma symptoms, pulmonary function, circulating eosinophils, and FeNO content markedly improved, but the NH_3 content increased from 43 μg/dL before therapy to 75 μg/dL at 2 months (Figures 3A–F). The blood tests performed on the day of the first visit provided no findings suggestive of CVD. Thus, OCS was terminated at 2 months and FF/VI and tezepelumab were continued. One month after the cessation of OCS, NH_3 was reduced to a baseline level of 43 μg/dL, and the other parameters and asthma symptoms remained under control, with no recurrence of CEP. At the same time, a marked improvement in sinusitis was observed (Figure 1J).

3 Discussion

In the treatment of CEP, the recommended initial OCS dose is 0.5 mg/kg, and because the patient weighed 49.4 kg, 25 mg/day would usually be used (1). However, this case was complicated by uncompensated LC. In LC, CS metabolism is impaired, and OCS administration does more harm than good, worsening the liver function and increasing the risk of coma, infection, diabetes, and gastrointestinal bleeding due to varices from the esophagus to the

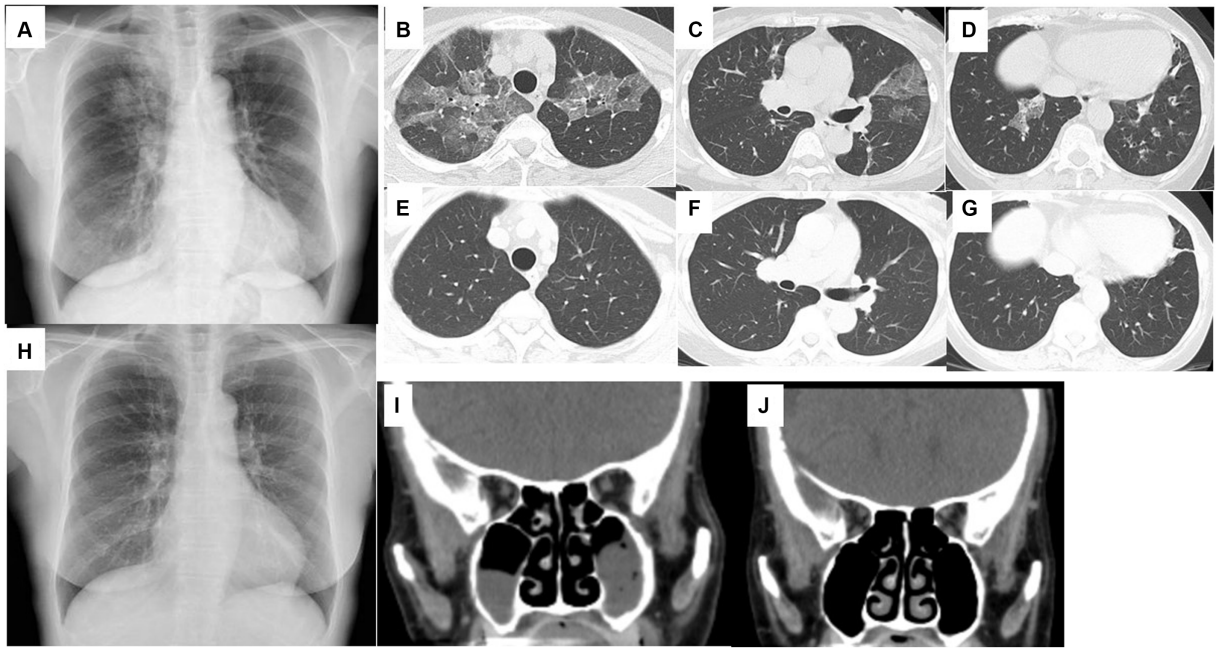

FIGURE 1
Chest X-ray **(A)** and chest CT **(B–D)** on the day of the first visit to the hospital. Bilateral ground-glass opacities in the upper lobes and bronchial wall thickening in the lower lobes. Chest X-ray on day 10 from starting therapy **(H)**. Bilateral ground-glass opacities disappeared. Chest CT performed 1 month after starting therapy **(E–G)**. Bilateral ground-glass opacities and bronchial wall thickening disappeared. Sinus CT on the day of the first visit to the hospital **(I)**. Bilateral sinusitis exists in the maxillary sinus. Sinus CT 3 months after starting therapy **(J)**. Bilateral sinusitis was improved.

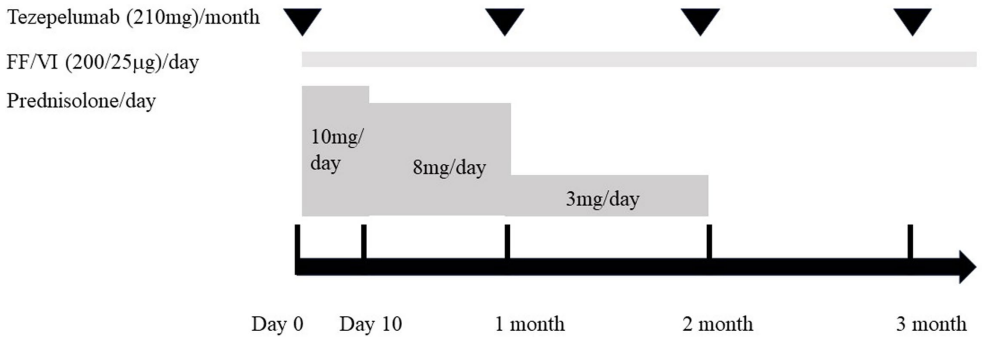

FIGURE 2
Clinical course of therapy for the present case. Initial therapy was started (day 0) with the combination of oral corticosteroid (prednisolone, 10 mg/day), inhaled fluticasone furoate/vilanterol (FF/VI, 200/25 μg/day), and tezepelumab (210 mg/month). Prednisolone was administered at 10 mg/day for 10 days. Then, the dose was reduced to 8 mg/day and continued for 1 month before being reduced to 3 mg/day during the next month. Two months after starting treatment, prednisolone was discontinued, while FF/VI and tezepelumab were continued.

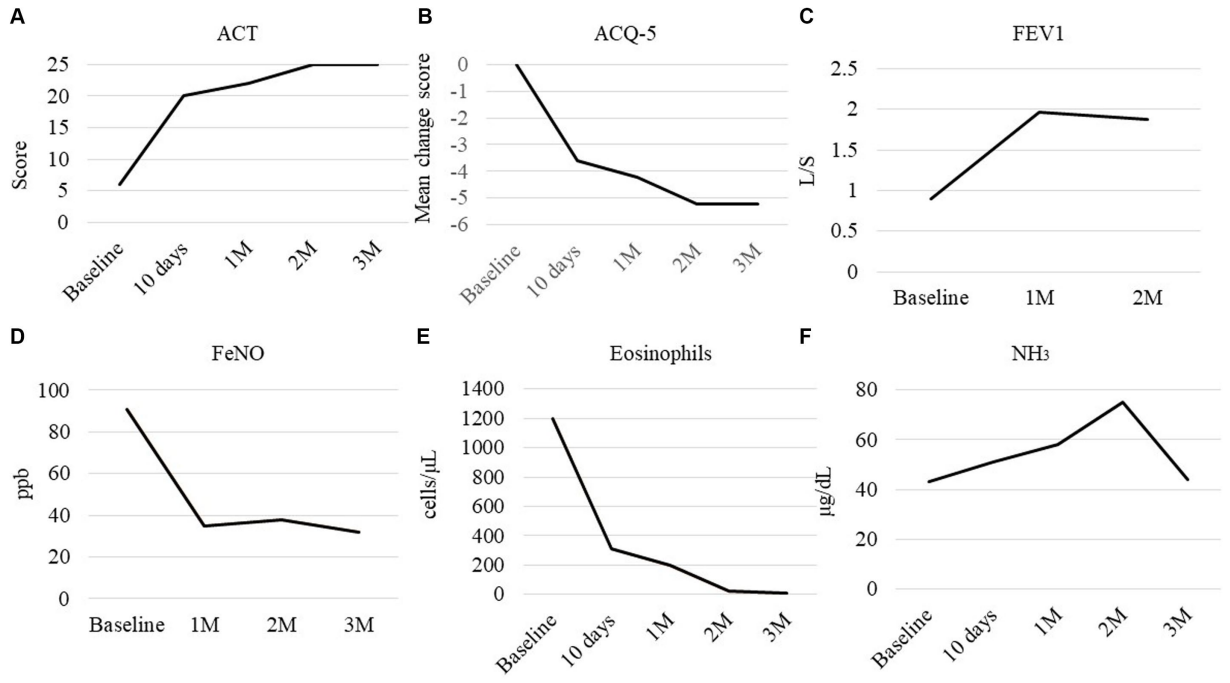

FIGURE 3
Clinical course of the parameters. **(A)** Asthma control test (ACT), **(B)** mean change from the baseline score of the asthma control questionnaire (ACQ-5), **(C)** forced expiratory volume in 1 s, **(D)** fractional exhaled nitric oxide (FeNO), **(E)** peripheral eosinophil count, and **(F)** NH_3 in peripheral blood. Baseline: measured on day 0, before starting therapy.

stomach. Therefore, the starting dose of OCS was reduced, and biologics were used in combination. Previous reports of long-term safety with tezepelumab were limited to non-asthmatic pulmonary eosinophilia or high OCS user patients in some of the trials (5). The treatment of the patients in the study showed no effects on liver function and no change in liver enzymes (6). As a result, it is suggested that tezepelumab has a low risk of liver injury; therefore, tezepelumab was used herein.

In the future practice of this patient, careful attention should be given to the development of eosinophilic granulomatosis with polyangiitis (EGPA). This patient had nasal polyps and elevated eosinophils, but the myeloperoxidase–anti-neutrophil cytoplasmic antibody (MPO-ANCA) was negative. However, since ANCA-negative EGPA patients also exist (7), careful attention to the development of EGPA is warranted. In the present patient, currently, 5 months have passed since OCS cessation, but no development of EGPA has occurred under tezepelumab therapy.

In conclusion, tezepelumab may be a treatment option for CEP and have a rapid sparing effect on OCS, safely leading to a reduced risk of OCS, even in LC patients. Moreover, TSLP activates group 2 innate lymphoid cells in the liver, promoting liver fibrosis (8, 9). Blocking the function of TSLP may help mitigate the worsening of LC.

Data availability statement

The original contributions presented in the study are included in the article/supplementary material, further inquiries can be directed to the corresponding author.

Ethics statement

Written informed consent was obtained from the individual(s) for the publication of any potentially identifiable images or data included in this article.

Author contributions

MI: Conceptualization, Data curation, Formal analysis, Investigation, Project administration, Visualization, Writing – original draft, Writing – review & editing. YS: Conceptualization, Data curation, Investigation, Project administration, Visualization, Writing – original draft, Writing – review & editing. YN: Writing – original draft, Writing – review & editing. HO: Writing – original draft, Writing – review & editing. AT: Writing – original draft, Writing – review & editing. SN: Writing – original draft, Writing – review & editing.

Funding

The author(s) declare that no financial support was received for the research, authorship, and/or publication of this article.

Conflict of interest

The authors declare that the research was conducted in the absence of any commercial or financial relationships that could be construed as a potential conflict of interest.

The author(s) declared that they were an editorial board member of Frontiers, at the time of submission. This had no impact on the peer review process and the final decision.

Publisher's note

References

1. Amratia DA, Viola H, Ioachimescu OC. Glucocorticoid therapy in respiratory illness: bench to bedside. *J Investig Med*. (2022) 70:1662–80. doi: 10.1136/jim-2021-002161

2. Madsbad S, Bjerregaard B, Henriksen JH, Juhl E, Kehlet H. Impaired conversion of prednisone to prednisolone in patients with liver cirrhosis. *Gut*. (1980) 21:52–6. doi: 10.1136/gut.21.1.52

3. Izhakian S, Pertzov B, Rosengarten D, Kramer MR. Successful treatment of acute relapse of chronic eosinophilic pneumonia with benralizumab and without corticosteroids: a case report. *World J Clin Cases*. (2022) 10:6105–9. doi: 10.12998/wjcc.v10.i18.6105

4. Tsai HC, Lin YC, Ko CL, Lou HY, Chen TL, Tam KW, et al. Propofol versus midazolam for upper gastrointestinal endoscopy in cirrhotic patients: a meta-analysis of randomized controlled trials. *PLoS One*. (2015) 10:e0117585. doi: 10.1371/journal.pone.0117585

5. Bethesda (MD): National Institute of Diabetes and Digestive and Kidney Diseases. *LiverTox: Clinical and research information on drug-induced liver injury* National Institute of Diabetes and Digestive and Kidney Diseases (NIDDK) (2012).

6. Menzies-Gow A, Wechsler ME, Brightling CE, Korn S, Corren J, Israel E, et al. DESTINATION study investigators. Long-term safety and efficacy of tezepelumab in people with severe, uncontrolled asthma (DESTINATION): a randomised, placebo-controlled extension study. *Lancet Respir Med*. (2023) 11:425–38. doi: 10.1016/S2213-2600(22)00492-1

7. Furuta S, Iwamoto T, Nakajima H. Update on eosinophilic granulomatosis with polyangiitis. *Allergol Int*. (2019) 68:430–6. doi: 10.1016/j.alit.2019.06.004

8. Vannella KM, Ramalingam TR, Borthwick LA, Barron L, Hart KM, Thompson RW, et al. Combinatorial targeting of TSLP, IL-25, and IL-33 in type 2 cytokine-driven inflammation and fibrosis. *Sci Transl Med*. (2016) 8:337ra65. doi: 10.1126/scitranslmed.aaf1938

9. Forkel M, Berglin L, Kekäläinen E, Carlsson A, Svedin E, Michaëlsson J, et al. Composition and functionality of the intrahepatic innate lymphoid cell-compartment in human nonfibrotic and fibrotic livers. *Eur J Immunol*. (2017) 47:1280–94. doi: 10.1002/eji.201646890

frontiers | Frontiers in Medicine

TYPE Case Report
PUBLISHED 17 July 2024
DOI 10.3389/fmed.2024.1424564

OPEN ACCESS

EDITED BY
Giuseppe Fiorentino,
Hospital of the Hills, Italy

REVIEWED BY
Serkan Surme,
Istanbul University-Cerrahpasa, Türkiye
Tohru Gonoi,
Chiba University, Japan

*CORRESPONDENCE
Jun Yang
✉ 705500524@qq.com
Guo-Ping Ai
✉ zbzqzyyagp@126.com

†These authors have contributed equally to this work and share first authorship

RECEIVED 28 April 2024
ACCEPTED 01 July 2024
PUBLISHED 17 July 2024

CITATION
Chen K, Wang Y, Dong J, Wu P-S, Yang J and Ai G-P (2024) Case report: From oral infection to life-threatening pneumonia: clinical considerations in Nocardia infection from a case.
Front. Med. 11:1424564.
doi: 10.3389/fmed.2024.1424564

Case report: From oral infection to life-threatening pneumonia: clinical considerations in Nocardia infection from a case

Kang Chen[1†], Ying Wang[2†], Jing Dong[3†], Ping-Shang Wu[1], Jun Yang[4*] and Guo-Ping Ai[5*]

[1]Department of Thoracic Cardiovascular Surgery, The Third Hospital of Wuhan, Wuhan, China, [2]Department of Otolaryngology, Qingdao Hospital, University of Health and Rehabilitation Sciences (Qingdao Municipal Hospital), Qingdao, China, [3]Department of Endocrinology, General Hospital of Central Theater Command of the People's Liberation Army, Wuhan, China, [4]Department of Stomatology, General Hospital of Central Theater Command of the People's Liberation Army, Wuhan, China, [5]Department of Radiology, General Hospital of Central Theater Command of the People's Liberation Army, Wuhan, China

Nocardia is an anthropozoonotic bacteria that occurs widely in the natural environment. However, because it is a gram-positive aerobic opportunistic pathogen, it rarely occurs in patients with no prior history of immune function disease. Since the symptoms are nonspecific the diagnosis of Nocardia pneumonia is challenging. Previous studies have not reported that this anthropozoonotic bacteria colonizing the human body could cause severe pneumonia by gingival pain and pharyngeal discomfort. This case report describes a previously healthy 60-year-old female farmer who presented to the doctor with gingival pain and pharyngeal discomfort. She was treated with a dental cleaning and oral metronidazole. The patient rapidly progressed to breathing difficulties. Lung shadow was found by computerized tomography examination. The radiologist diagnosed pulmonary tuberculosis as image-based. Through laboratory examination and culture of pathogenic microorganisms in the sputum and blood of the patient, no obvious positive findings were found. The disease progressed rapidly to tracheal intubation ventilator assisted breathing. Subsequently, the patient underwent alveolar lavatory examination under endotracheal intubation fiberbronchoscopy, and the culture of alveolar lavage fluid indicated Nocardia. According to this result, the patient's disease was quickly controlled after selecting the targeted drug compound sulfamethoxazole and intravenous meropenem for treatment. In view of the reason for the high misdiagnosis rate due to the low positive rate of Nocardia culture in most cases, the clinical thinking of diagnosis and treatment from oral infection symptoms to fatal pneumonia reported in this case has certain clinical popularization and enlighten significance, not only improved the diagnosis and treatment of rare diseases, but also be reduced medical disputes.

KEYWORDS

Nocardia, severe acute disease, intensive care, immunocompetent patient, pulmonary coinfection, case report

Introduction

The clinical manifestations and imaging examinations of pulmonary nocardiosis were nonspecific (1). In addition to the detection of pathogens by culture or next-generation sequencing (NGS) analysis of species, source, and drug sensitivity of pathogens, general laboratory tests also had no specificity and/or sensitivity indicators (2, 3). However, Nocardia pneumophila grew very slowly in *in vitro* medium and was easily covered by other fast-growing bacteria, which made it difficult to be detected (4, 5). Nocardia, as an opportunistic anthropozoonotic bacteria pathogen, is resistant to general antibiotics (6). As a result, infection of the lungs of even healthy people with this organism can lead to rapid progression and catastrophic consequences (7). We report a case of pulmonary nocardiosis with rapid progression from oral symptoms in order to promote the attention of clinicians to this disease.

Case report

A 60-year-old female farmer, previously healthy, with no immune-related diseases. The patient visited the hospital due to gingival pain and pharyngeal discomfort. The body temperature was 38.6°C, the gums were red and swollen (Figure 1A), the pharynx was congested, and the tonsils were bilateral II degree enlarged. A diagnosis of tonsillitis and gingivitis was made by the community doctor. She was treated with dental cleaning and oral metronidazole. However, the symptoms did not relieve. Three days later, the patient developed dyspnea. Physical examination revealed tachypnea (42 beats/min), moist rales in both lungs, low breath sounds in the right lower lung, a regular heart rate of 131 beats /min, and no obvious heart murmur. The abdomen was soft and non-tender. The patient underwent chest CT, which revealed multiple solid opacities in the right lung (Figures 1B–D). The radiologist believes that pulmonary tuberculosis should be the preferred consideration. The patient's hemocyte, blood biochemical, and blood tuberculosis laboratory tests are shown in Table 1. After multidisciplinary team (MDT) discussion based on the medical history, the diagnosis of this case should be considered pulmonary infection firstly, and the possibility of tuberculosis cannot be excluded. Therefore, the patient was treated with intravenous ceftriaxone sodium, an intravenous anti-inflammatory therapy. After 3 days of treatment, the patient's symptoms worsened tachypnea developed. A repeat CT scan of the chest was performed, which revealed a markedly enlarged area of patchy hyperdensity in the right lung and spread to the left lung (Figures 1E–G). In cases where respiration could not be maintained, the patient was placed a ventilator assisted respiration with endotracheal intubation. Blood and sputum cultures were obtained, and both were negative. After MDT discussion again, G test, GM test and cryptococcus detection should be improved, and fiberoptic bronchoscopy should be improved if conditions permit. Pulmonary fungal infection combined with bacterial infection should be considered in the diagnosis. Intravenous meropenem combined with voriconazole was given as anti-inflammatory treatment. Subsequent tests, G test, GM test, cryptococcal antigen were all negative. No abnormalities were found in the bronchi except for thick sputum. No tumor or severe inflammation was found in the trachea by fiberoptic bronchoscopy (Figures 2A–C). As an unexpected bonus, Nocardia was found the bronchoalveolar lavage fluid smear and a week of culture (Figures 2D–G). At this point, the patient was diagnosed multisite infection by Nocardia. Based on the drug susceptibility analysis of bacterial culture, compound sulfamethoxazole 1.5 g every 6 h was given nasal feeding combined with intravenous meropenem. Two days later, the patient's temperature got normalized, her spirits got improved gradually. The symptoms of gingival pain, pharyngeal discomfort and dyspnea with her did relieve also. Two weeks after treatment, the patient underwent a repeat CT scan of the chest, which revealed a reduction in the extent of bilateral lung shadow. The patient was scheduled to be discharged with oral trimethoprim-sulfamethoxazole for another 3 months. Subsequent follow-up chest CT showed that the lesions in both lungs were basically absorbed (Figures 3A–C). The symptoms of the oral and respiratory with her completely disappeared, and she was very satisfied with the treatment.

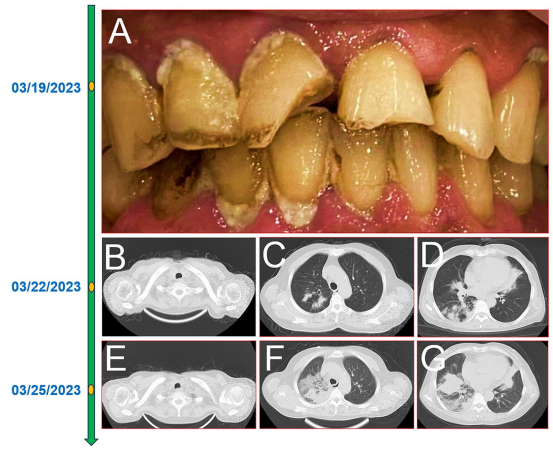

FIGURE 1
The timeline of the patient' disease progression. Gingivitis and oral hygiene of the patients **(A)**; 16-slice computerized tomography images of the chest at initial diagnosis of the patient, neck **(B)**, upper lobe **(C)**, lower lobe **(D)**; 16-slice computerized tomography images of the chest in the advanced stage of the patient, neck **(E)**, upper lobe **(F)**, lower lobe **(G)**.

Discussion

Nocardia is an aerobic prokaryotic actinomycete, widely exists in soil, air, decaying plants and other organic matter (8). It is an opportunistic pathogen of human, livestock and poultry. So far, a total of 791 nocardia isolates have been identified, of which 119 Nocardia species with effective names have been confirmed in literature, and 54 Nocardia species are related to human infection (9). It does not belong to the normal flora of human body, so it is not an endogenous infection. So, if this bacterium is detected in laboratory culture or NGS, it must be pathogenic. Unlike Candida, which can colonize the human body (10). Nocardia species often invade the human body from respiratory tract, oral mucosa lesions and skin lesions, and spread to lung, brain and other organs through respiratory tract and blood, which is easy to cause infection (11). Nocardial is aerobic, and the colonies were smooth and moist when cultured at 37° with general medium, grows into macroscopic colonies within 2–6 days, obtain satisfactory culture results requiring 4–6 weeks (12, 13). The colonies varied in color, including cheese, yellow, pink, coral red, and orange red (14, 15).

TABLE 1 Laboratory test results of the patient.

Laboratory tests	Normal range	Results
WBC (×109/L)	4 ~ 10	15.31
Neutrophile granulocyte percentage (%)	50 ~ 70	90.6
Eosinophils percentage (%)	0 ~ 5	0.5
Monocytes percentage (%)	3 ~ 8	2.1
C-reactive protein (mg/L)	<22	203
Erythrocyte sedimentation rate (mm/h)	0 ~ 10	22
Albumin (g/L)	0 ~ 40	31.3
Alanine aminotransferase (U/L)	7 ~ 40	31
Aspartate aminotransferase (U/L)	13 ~ 35	21
Direct bilirubin (μmol/L)	0 ~ 6.8	4.2
Creatinine (μmol/L)	41 ~ 81	46.2
Urea nitrogen (μmol/L)	3.6 ~ 9.5	5.11
Procalcitonin (ng/mL)	<0.05	90.36
Interleukin-6 (pg/mL)	0 ~ 40	>5,000
Mycoplasma pneumoniae antibody	Negative	Negative
Chlamydia pneumoniae antibody	Negative	Negative
T-SPOT-TB	Negative	Positive
Protein (Urinalysis routine)	Negative	0
Urobilinogen (Urinalysis routine)	Negative	0
Occult blood (Urinalysis routine)	Negative	0

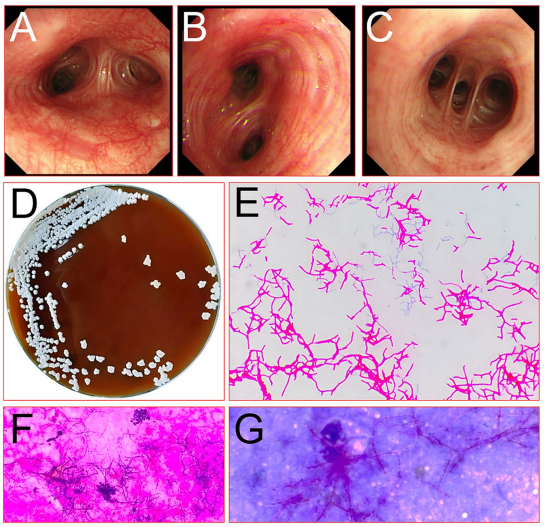

FIGURE 2
Picture of the bronchus of the right lung of the patient under a fiberoptic bronchoscope (**A**, main bronchus; **B**, lower lobe bronchus; **C**, basal segment bronchus) and microbe detected by fiberoptic bronchoscopic lavage fluid smear (**D**, culture original; **E**, micrograph of pathogenic bacteria; **F**, the standard acid-fast stain; **G**, the modified weakly acid-fast).

Besides, Nocardia belongs to the order actinomycetes, which was first isolated by Nocard in 1888 (16). It is similar to that of *Mycobacterium tuberculosis* (17). However, Nocardial mycelial ends did not show club-like expansion, different concentrations of decolorization solution were used for acid-fast staining, and the lower the concentration of decolorization solution used, the higher the positive rate of acid-fast staining (18). *Mycobacterium tuberculosis* has strong acid resistance and is not easy to decolorize. Therefore, the weakly acid-fast staining method can be used to distinguish Nocardia from Mycobacteria.

Nocardia pneumonia should be differentiated from actinomyces pneumonia and aspergillus pneumonia in chest imaging (19). Sulfur particles can be found in actinomyces pneumonia, and aspergillus pneumonia is the most common pulmonary fungal disease (20). The typical clinical manifestations of Nocardia pneumonia in the early stage were nodules or masses with halo sign around them, and crescent sign could be seen when cavitation was formed (20). However, their imaging identification is complicated and difficult in clinical practice (21).

These specific factors determine the complexity of the diagnosis of Nocardia, which is why the patient in this case was not diagnosed for days. It is difficult to culture Nocardia from sputum, for one thing, it is difficult to detect by smear staining, which is often misinterpreted by other bacteria and causes false positive results (15). On the other hand, it is because of the rapid growth of oral flora during sputum culture, which often leads to the suppression of nocardia. In addition, the commonly used media and culture conditions are not conducive to the cultivation of Nocardia, which will also lead to false negative results. In addition, the growth of Nocardia is slow, and the culture time is short in most laboratories, resulting in the missed detection of some nocardia. Nocardia is not the normal flora of the human body, so it is very important to detect the pathogen from tissue or body fluid secretions. Although the next generation sequencing (NGS) analysis testing of species, source, and drug sensitivity of pathogens has the advantages of fast speed and high sensitivity, the price is relatively expensive. In China, this testing has not been routinely carried out in hospital, can be shipped to commercial biological companies, so it is not very convenient. Bronchoalveolar lavage fluid obtained from

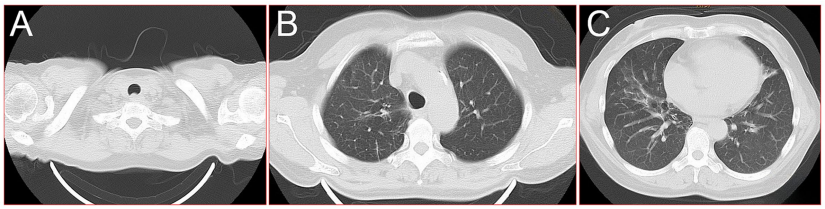

FIGURE 3
16-slice computerized tomography images of the chest during follow-up after the patient was cured. **(A)** Neck; **(B)** upper lobe; **(C)** lower lobe.

fiberoptic bronchoscopy can obtain pathogenic bacteria in the lower respiratory tract, and it is rarely contaminated by other bacteria, which is a valuable sampling material for pathogenic bacteria in clinical work (22, 23).

Previous studies showed that nocardial pneumonia accounted for 85% of all nocardiosis cases and the in-hospital mortality rate was 15.0% (6). Delays in diagnosis and treatment are the most common reasons. The diagnosis and treatment of this case was also tortuous. She started with gums inflammation by the unclean mouth, and it is understandable that metronidazole was given to the dentist. Then, the inflammation rapidly progressed to the lungs. After ruling out mycoplasma and chlamydia pneumonia, the patient was treated empiric with ceftriaxone. However, Nocardia is sensitive to sulfonamides, aminoglycosides, some cephalosporins, carbapenems and quinolones, and sulfonamides are the first choice for treatment (20, 24). The advantages of this drug are its good oral bioavailability and its good permeability into tissues and cerebrospinal fluid. The dosage should be adequate and the course of treatment should be long. Six weeks for immunocompetent patients with localized pulmonary nocardiosis and at least 6 months for immunocompromised patients (20). For patients with central nervous system spread, this should be extended to 12 months. For people with AIDS, 12 months or more (25).

Besides, low-dose maintenance therapy is recommended for immunosuppressed patients. At present, due to the high drug resistance rate of sulfonamides, the total drug resistance rate is more than 40%, and the combination therapy is advocated (20, 25). Carbapenems and linezolid are the two drugs with high sensitivity. Linezolid is the first to be sensitive to almost all nocardial species and is indicated for severe infections, disseminated nocardiosis, and sulfonamides allergy. It is suggested that the above drugs can be preferentially selected according to the condition of the patient in the treatment of refractory pulmonary nocardiosis. If the diagnosis is delayed, the mortality rate may reach 30–50% (6, 20, 26, 27). Therefore, early and rapid diagnosis and treatment are of great significance for the prognosis of patients.

Conclusion

This case illustrates the tortuous course of physician's diagnosis and treatment of a healthy peasant woman with typical infection progression from oral infection to life-threatening pneumonia. From this tortuous process, we can learn the harmfulness of nocardiosis and the difficulty of diagnosis. It can provide some clinical thoughts for explaining a class of infectious diseases with common clinical symptoms but catastrophic outcomes, reduce medical disputes, and improve the diagnosis and treatment of rare diseases.

Data availability statement

The original contributions presented in the study are included in the article/supplementary material, further inquiries can be directed to the corresponding authors.

Ethics statement

Written informed consent was obtained from the individual(s) for the publication of any potentially identifiable images or data included in this article.

Author contributions

KC: Data curation, Methodology, Project administration, Funding acquisition, Writing – review & editing. YW: Conceptualization, Formal analysis, Methodology, Resources, Software, Writing – original draft. JD: Data curation, Formal analysis, Investigation, Methodology, Software, Writing – original draft. P-SW: Conceptualization, Data curation, Formal analysis, Methodology, Writing – original draft. JY: Conceptualization, Data curation, Formal analysis, Funding acquisition, Investigation, Methodology, Project administration, Resources, Software, Supervision, Validation, Visualization, Writing – original draft, Writing – review & editing. G-PA: Conceptualization, Data curation, Formal analysis, Funding acquisition, Investigation, Methodology, Project administration, Resources, Software, Supervision, Validation, Visualization, Writing – review & editing.

Funding

The author(s) declare that no financial support was received for the research, authorship, and/or publication of this article.

Acknowledgments

The authors thank the patient who agreed to be included in this report for her cooperation and support in academic communication.

Conflict of interest

The authors declare that the research was conducted in the absence of any commercial or financial relationships that could be construed as a potential conflict of interest.

Publisher's note

References

1. Wang X, Liang Y, Cheng Q, Nong W, Hu L. Abdominal abscesses caused by *Nocardia farcinica* in an immunocompromised patient: a case report and literature review. *Infect Drug Resist.* (2023) 16:7447–54. doi: 10.2147/IDR.S441117

2. Tajima Y, Tashiro T, Furukawa T, Murata K, Takaki A, Sugahara K, et al. Pulmonary Nocardiosis with Endobronchial involvement caused by Nocardiaaraoensis. *Chest*. (2024) 165:e1–4. doi: 10.1016/j.chest.2023.07.067

3. Weng SS, Zhang HY, Ai JW, Gao Y, Liu YY, Xu B, et al. Rapid detection of Nocardia by next-generation sequencing. *Front Cell Infect Microbiol*. (2020) 10:13. doi: 10.3389/fcimb.2020.00013

4. Besteiro B, Coutinho D, Fragoso J, Figueiredo C, Nunes S, Azevedo C, et al. Nocardiosis: a single-center experience and literature review. *Braz J Infect Dis*. (2023) 27:102806. doi: 10.1016/j.bjid.2023.102806

5. Miyamoto M, Sasaki Y, Ohta K. Pulmonary nocardiosis caused by *Nocardia exalbida* mimicking lung cancer. *Respirol Case Rep*. (2019) 7:e00458. doi: 10.1002/rcr2.458

6. Yang M, Xu M, Wei W, Gao H, Zhang X, Zhao H, et al. Clinical findings of 40 patients with nocardiosis: a retrospective analysis in a tertiary hospital. *Exp Ther Med*. (2014) 8:25–30. doi: 10.3892/etm.2014.1715

7. Al Umairi RS, Pandak N, Al BM. The findings of pulmonary Nocardiosis on chest high resolution computed tomography: single Centre experience and review of literature. *Sultan Qaboos Univ Med J*. (2022) 22:357–61. doi: 10.18295/squmj.9.2021.131

8. Yuan D, Shen L, Qin BE, Xu X, Su Z, Liu J, et al. Central nervous system nocardiosis diagnosed by metagenomic next-generation sequencing: a case series and literature review. *Adv Clin Exp Med*. (2023) 32:1453–63. doi: 10.17219/acem/175818

9. Wang H, Zhu Y, Cui Q, Wu W, Li G, Chen D, et al. Epidemiology and antimicrobial resistance profiles of the Nocardia species in China, 2009 to 2021. *Microbiol Spectr*. (2022) 10:e0156021. doi: 10.1128/spectrum.01560-21

10. Miramón P, Pountain AW, Lorenz MC. Candida auris-macrophage cellular interactions and transcriptional response. *Infect Immun*. (2023) 91:e0027423. doi: 10.1128/iai.00274-23

11. Sun H, Goolam Mahomed M, Patel J. Brain metastasis or nocardiosis? A case report of central nervous system Nocardiosis with a review of the literature. *J Community Hosp Intern Med Perspect*. (2021) 11:258–62. doi: 10.1080/20009666.2021.1877399

12. Choquet E, Rodriguez-Nava V, Peltier F, Wankap-Mogo R, Bergeron E, Joseph C, et al. *Nocardia neocaledoniensis* as rare cause of spondylodiscitis. *Emerg Infect Dis*. (2023) 29:444–6. doi: 10.3201/eid2902.221389

13. Nouioui I, Pötter G, Jando M, Goodfellow M. *Nocardia noduli* sp. nov., a novel actinobacterium with biotechnological potential. *Arch Microbiol*. (2022) 204:260. doi: 10.1007/s00203-022-02878-x

14. Liang Y, Lin M, Qiu L, Chen M, Tan C, Tu C, et al. Clinical characteristics of hospitalized patients with Nocardia genus detection by metagenomic next generation sequencing in a tertiary hospital from southern China. *BMC Infect Dis*. (2023) 23:772. doi: 10.1186/s12879-023-08615-z

15. Toyokawa M, Taniguchi M, Uesaka K, Nishimura K. Complete genome sequence of multidrug-resistant strain *Nocardia wallacei* FMUON74, isolated from a sputum culture. *Microbiol Resour Announc*. (2020) 9:e01022–0. doi: 10.1128/MRA.01022-20

16. McNeil MM, Brown JM. The medically important aerobic actinomycetes: epidemiology and microbiology. *Clin Microbiol Rev*. (1994) 7:357–417. doi: 10.1128/CMR.7.3.357

17. Chen Y, Hu W. Co-infection with Mycobacterium tuberculosis and *Nocardia farcinica* in a COPD patient: a case report. *BMC Pulm Med*. (2023) 23:136. doi: 10.1186/s12890-023-02434-3

18. Muricy EC, Lemes RA, Bombarda S, Ferrazoli L, Chimara E. Differentiation between *Nocardia* spp. and *Mycobacterium* spp.: critical aspects for bacteriological diagnosis. *Rev Inst Med Trop São Paulo*. (2014) 56:397–401. doi: 10.1590/s0036-46652014000500005

19. Jouneau S, Ménard C, Lederlin M. Pulmonary alveolar proteinosis. *Respirology*. (2020) 25:816–26. doi: 10.1111/resp.13831

20. Lafont E, Conan PL, Rodriguez-Nava V, Lebeaux D. Invasive Nocardiosis: disease presentation, diagnosis and treatment - old questions, new answers? *Infect Drug Resist*. (2020) 13:4601–13. doi: 10.2147/IDR.S249761

21. Zhu J, Huang WC, Huang B, Zhu Y, Jiang XJ, Zou JN, et al. Clinical characteristics and prognosis of COVID-19 patients with initial presentation of lung lesions confined to a single pulmonary lobe. *Am J Transl Res*. (2020) 12:7501–9.

22. Wang L, Lu S, Guo Y, Liu J, Wu P, Yang S. Comparative study of diagnostic efficacy of sputum and bronchoalveolar lavage fluid specimens in community-acquired pneumonia children treated with fiberoptic bronchoscopy. *BMC Infect Dis*. (2023) 23:565. doi: 10.1186/s12879-023-08522-3

23. Li L, Li MJ, Sun L, Jiang YL, Zhu J. Neglected foreign body aspiration mimicking lung Cancer recurrence. *Risk Manag Healthc Policy*. (2022) 15:491–6. doi: 10.2147/RMHP.S361081

24. Benndorf R, Schwitalla JW, Martin K, de Beer ZW, Vollmers J, Kaster AK, et al. *Nocardia macrotermitis* sp. nov. and *Nocardia aurantia* sp. nov., isolated from the gut of the fungus-growing termite Macrotermes natalensis. *Int J Syst Evol Microbiol*. (2020) 70:5226–34. doi: 10.1099/ijsem.0.004398

25. Stefaniak J. HIV/AIDS presenting with stroke-like features caused by cerebral Nocardia abscesses: a case report. *BMC Neurol*. (2015) 15:183. doi: 10.1186/s12883-015-0437-7

26. Haussaire D, Fournier PE, Djiguiba K, Moal V, Legris T, Purgus R, et al. Nocardiosis in the south of France over a 10-years period, 2004-2014. *Int J Infect Dis*. (2017) 57:13–20. doi: 10.1016/j.ijid.2017.01.005

27. Zhong C, Huang P, Zhan Y, Yao Y, Ye J, Zhou H. Clinical features of pulmonary Nocardiosis in patients with different underlying diseases: a case series study. *Infect Drug Resist.* (2022) 15:1167–74. doi: 10.2147/IDR.S359596

frontiers | Frontiers in Medicine

TYPE Case Report
PUBLISHED 17 July 2024
DOI 10.3389/fmed.2024.1424586

OPEN ACCESS

EDITED BY
Uday Kishore,
United Arab Emirates University,
United Arab Emirates

REVIEWED BY
Somanon Bhattacharya,
Wuxi Advanced Therapeutics, Inc.,
United States
Jian Zhou,
Henan Provincial Cancer Hospital, China

*CORRESPONDENCE
Yumei Guo
✉ 325069675@qq.com
Lijie Zhang
✉ zhanglijie@hebmu.edu.cn

†These authors have contributed equally to this work and share first authorship

RECEIVED 28 April 2024
ACCEPTED 28 June 2024
PUBLISHED 17 July 2024

CITATION
Shi X, Ye J, Liu P, Gao W, Feng Z, Zheng C, Huang Y, Guo Y and Zhang L (2024) Case report: Rare pulmonary fungal infection caused by *Penicillium digitatum*: the first clinical report in China.
Front. Med. 11:1424586.
doi: 10.3389/fmed.2024.1424586

Case report: Rare pulmonary fungal infection caused by *Penicillium digitatum*: the first clinical report in China

Xiaojuan Shi[1†], Jiaqing Ye[2†], Peiling Liu[1], Weili Gao[3], Zhongjun Feng[2], Cuiying Zheng[2], Yinqi Huang[2], Yumei Guo[3*] and Lijie Zhang[2*]

[1]Department of Respiratory and Critical Care Medicine, Hebei Medical University Third Hospital, Shijiazhuang, China, [2]Department of Clinical Laboratory, Hebei Medical University Third Hospital, Shijiazhuang, China, [3]Hebei Key Laboratory of Intractable Pathogens, Shijiazhuang Center for Disease Control and Prevention, Shijiazhuang, China

Penicillium digitatum is a common plant pathogen that causes citrus rot, which is extremely rare in humans. We report a case of a 66-year-old man with a history of consuming large amounts of citrus fruits, smoking for 30 years, and a history of emphysema. He had experienced intermittent coughing with sputum for more than 10 years and was admitted to the hospital due to worsening of symptoms over the past month. Despite antibiotic treatment, his condition did not improve. Subsequently, bronchoalveolar lavage fluid (BALF) was detected by metagenomic next-generation sequencing (mNGS), which showed the presence of *P. digitatum*. The fungal culture of BALF also indicated the presence of the *Penicillium* genus. The diagnosis was lung infection caused by *P. digitatum*, and the patient was treated with itraconazole. The lung infection was controlled. This is the third reported case of invasive pulmonary fungal infection caused by *P. digitatum* worldwide at the genus level, and the first reported case in China. Although human infections caused by *P. digitatum* are rare, as an emerging opportunistic pathogen, the detection of this fungus in immunocompromised patients should still be clinically important.

KEYWORDS

***Penicillium digitatum*, fungal infection, mNGS, pulmonary infection, invasive pulmonary fungal infection**

Introduction

Penicillium species are among the most ubiquitous fungi in the environment (1) and rarely cause human infections. There have been only two reported cases of invasive pulmonary fungal infections caused by *Penicillium digitatum* at the genus level worldwide (2, 3). However, numerous reports suggest that *Penicillium spp.* can cause clinically significant diseases in immunocompromised individuals, such as urinary tract infections, corneal infections, cutaneous endocarditis, peritonitis, pneumonia, paravertebral infections, and brain infections (3–5). *Penicillium digitatum* belongs to the genus *Penicillium* and is one of the factors responsible for the decay of citrus fruits (6, 7). Although *P. digitatum* is a rare opportunistic pathogen causing human infections, we report a case of pulmonary fungal infection caused by *P. digitatum*, which is the first clinical case reported in China and the third reported worldwide.

Case presentation

A 66-year-old man from Hebei, China, was admitted to the hospital on 4 February 2023 (day 1) due to a worsened cough and phlegm for 1 month. Despite the self-administration of cefuroxime, the symptoms did not improve. The patient had a chronic cough and expectoration for over 10 years. Two months ago, he suffered from pelvic fractures and underwent surgery. Six weeks ago, he was infected with COVID-19, which mainly manifested as a fever for 3 days, accompanied by pharyngalgia, cough, and sputum, without dyspnea. The patient visited a community hospital, where he was advised to isolate himself at home and rest without receiving glucocorticoids or other related treatments. His symptoms were basically under control. The patient had been smoking and drinking for over 30 years but had quit both 2 months prior to the visit.

On admission, the physical examination revealed that the patient was emaciated (body mass index = 16.53), with a barrel chest and low respiratory sounds in both lungs, especially in the right lower lung. A computed tomography (CT) scan revealed inflammatory lesions and local consolidation in the right lower lobe, with a small amount of pleural effusion on the right side and bilateral lung emphysema (Figures 1A1, B1). The laboratory results were as follows: WBC was 5.87×10^9/L, but the lymphocyte count (LYM) was decreased to 0.7×10^9/L. Additionally, the patient had mild anemia. The erythrocyte sedimentation rate (ESR) was significantly increased at 118.00 mm/h, and the high-sensitivity C-reactive protein (hsCRP) was also significantly elevated at 136.85 mg/L. Furthermore, the patient had significantly decreased levels of plasma albumin (ALB) at 26.63 g/L, while the liver and kidney function and arterial blood gas analysis indicators were essentially normal.

The initial diagnosis suggested that the patient might have community-acquired pneumonia, thus benzylpenicillin and levofloxacin were administered intravenously. After 7 days of treatment, the patient's symptoms did not improve, and repeated chest CT scans revealed no improvement in the pulmonary infiltrates or pleural effusion. The initial treatment was evaluated as ineffective, and three sputum smears, namely, sputum bacterial, fungal cultures, and acid-fast staining, were all negative. Therefore, the patient received an empirical upgrade of antimicrobial therapy with cefoperazone-sulbactam sodium and levofloxacin. Then, the bronchoalveolar lavage fluid (BALF) was collected and sent for metagenomic next-generation sequencing (mNGS), bacterial and fungal cultures, and acid-fast staining. The mNGS (SimcereDx, Nanjing, China) results were reported on the 2nd day of sequencing (day 11), showing the presence of *Penicillium digitatum* (36 reads with a relative abundance value of 67.92%) (Figure 2). These sequences were submitted to the SRA database at NCBI with mNGS with the accession number PRJNA1102665 (https://dataview.ncbi.nlm.nih.gov/object/PRJNA1102665). The BALF smear and acid-fast staining were negative. On day 12, ESR and hsCRP did not significantly decrease, the patient's symptoms did not improve, and repeated chest CT showed no significant improvement (Figures 1A2, B2). Further inquiry of the patient revealed that he had regularly consumed "Shatangju" mandarin, a citrus fruit, in large quantities for the past 3 months. The patient was started on oral itraconazole capsules (200 mg each time, twice a day, taken immediately after meals) for antifungal therapy (day 12) without the above-mentioned antibiotics. Bronchoscopy (day 13) was performed again, and the BALF was collected for fungal and bacterial cultures. On day 16, *Penicillium* species were found in the fungal culture of the first BALF, and on day 19, the second BALF fungal culture also supported the growth of the same type of *Penicillium* species (Figure 3). The internal transcribed spacer (ITS) identification of the species was performed. The colony was identified as *P. digitatum*.

An experimental method for *in vitro* antifungal susceptibility testing

1. The surface of bacterial colonies is rinsed with sterile physiological saline to create a spore suspension with a concentration of 0.5–1 McFarland.
2. A sterile swab is dipped into the bacterial suspension and squeezed to dry. Then, the agar surface is gently and evenly streaked in three directions, ensuring that the moisture is absorbed by the agar in <15 min.
3. An Etest strip is placed on the agar surface (ensuring the agar surface is dry and uniformly smooth before applying) and then incubated at 35°C for 48–72 h until clear inhibition zones appear.

Result interpretation

The interpretation of results varies based on the different antimicrobial mechanisms of various drugs.

1. For amphotericin B, the MIC value is interpreted at the point where 100% of bacterial growth is inhibited.
2. For 5-fluorocytosine, the MIC value is interpreted at the point where 90% of bacterial growth is inhibited.
3. For azoles and echinocandins, the MIC value is interpreted at the point where 80% of bacterial growth is inhibited.

In vitro antifungal susceptibility testing by broth microdilution methods showed the following minimum inhibitory concentrations: amphotericin B at 2 μg/ml, voriconazole at 0.06 μg/ml, micafungin at ≤0.25 μg/ml, and itraconazole at 0.125 μg/ml. After antifungal therapy, the patient's ESR and hsCRP levels significantly decreased. The chest CT scan on day 18 showed improvement in pulmonary inflammation and pleural effusion compared to before (Figures 1A3, B3). The patient's infection was evaluated as being under control, and he was discharged to continue with outpatient treatment, with oral itraconazole (200 mg each time, twice a day).

After 15 days, considering the patient experienced mild gastrointestinal discomfort while the pulmonary condition was well controlled, the itraconazole dosage was reduced to 200 mg once daily for 1 month. A follow-up chest CT scan on 10 March 2023 showed further absorption of pulmonary lesions (Figures 1A4, B4). There has been no

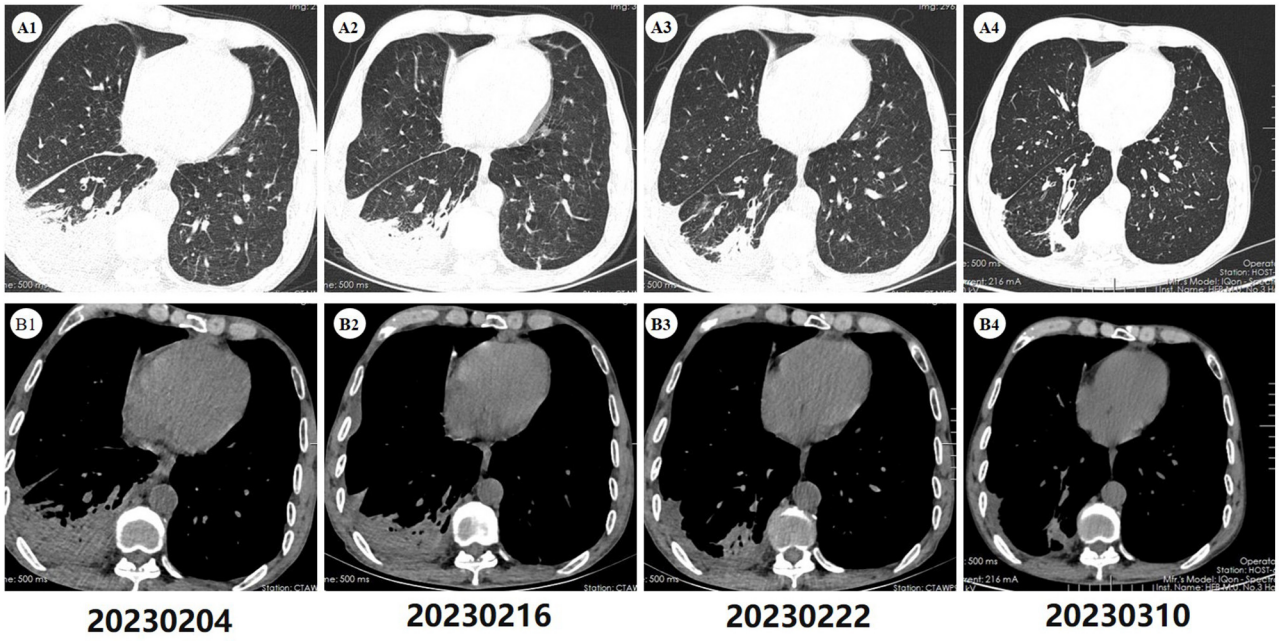

FIGURE 1
Computed tomography of the chest. **(A1, B1)** Upon admission, the scan (2023-02-04) revealed inflammatory lesions in the right lower lobe of the lung, along with localized consolidation. Furthermore, minimal pleural effusion was noted in the right pleural cavity and interlobar fissure. Bilateral pulmonary emphysema was also present. **(A2, B2)** A subsequent scan (2023-02-16), conducted after 12 days of antibiotic therapy, demonstrated persistent pulmonary lesions similar to those observed on the initial admission CT scan, with no apparent improvement. **(A3, B3)** A follow-up scan (2023-02-22), conducted after 6 days of antifungal therapy, exhibited improvement of pulmonary inflammation and pleural effusion compared to previous scans. **(A4, B4)** After 22 days of antifungal treatment, a follow-up scan (2023-03-10) demonstrated further absorption of the lung lesions, with only a small amount of residual fibrous streaky changes remaining.

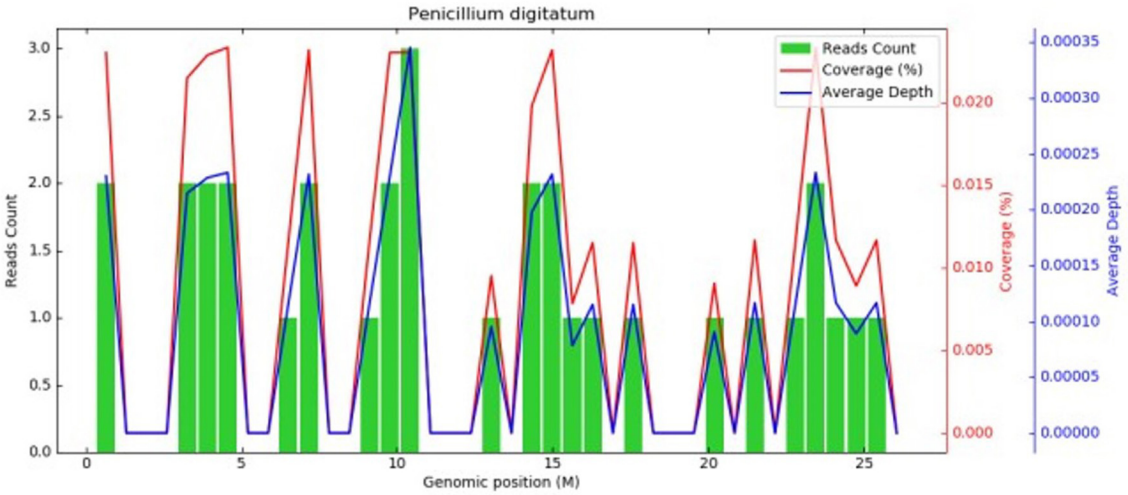

FIGURE 2
Metagenomic next-generation sequencing. Coverage graph of *P.digitatum* (36 reads, relative abundance value of 67.92%). The abscissa represents the genome position, the left ordinate is the number of reads of the pathogen aligned on the genome location (The number of map reads shown in green), and the right ordinate is the coverage and average sequencing depth at the corresponding position (coverage and depth, the red and blue lines in the figures).

recurrence during the 1 year follow-up period. Although no further CT scans were performed during this time, the patient remained in good health with no worsening of respiratory symptoms.

Discussion

Penicillium is a ubiquitous genus of mold, with many soil-borne saprophytic species, thriving in environments with moisture

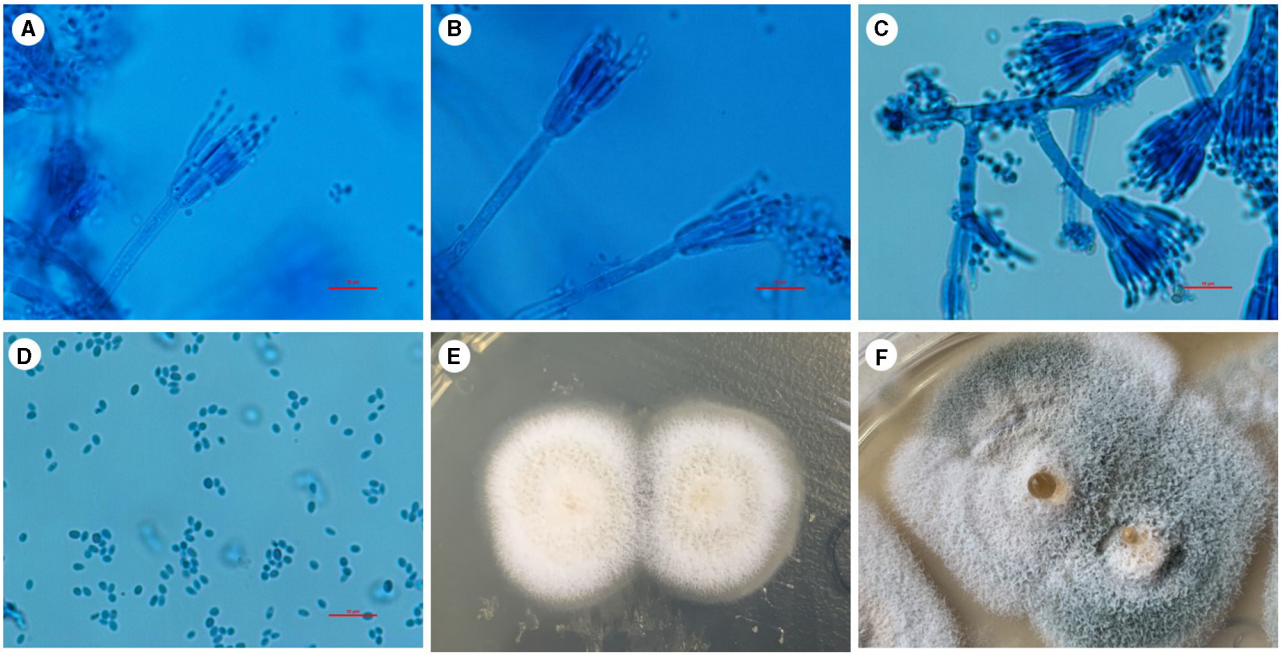

FIGURE 3
Penicillium digitatum was cultured for fungi in Sabouraud agar medium in a BALF sample at 28°C. **(A–C)** Positive colonies were cultured and stained with a lactophenol cotton blue staining solution. Under the microscope, the colonies showed a range of branching patterns, from simple to complex. The conidiophores had undergone multiple branchings and produced several rounds of symmetrical or asymmetrical small branches resembling brooms. **(D)** The spores of this *Penicillium* are typically elliptical under the microscope. **(E)** After 5 days of culture, the initial growth of *Penicillium* was observed, with white colonies exhibiting a velvety texture. **(F)** With the prolongation of growth time, the color of the colony gradually changes to light green or green, and liquid droplets appear in the center. Scale bars: 10 μm.

and decaying vegetation (8). In clinical samples, it is often isolated as a contaminant and overlooked, but it has become an opportunistic pathogen in immunocompromised patients. Except for *Talaromyces marneffei* (formerly known as *P. marneffei*), *Penicillium* infections are associated with allergic pneumonia and immunosuppressive diseases (9, 10) and, in severe cases, it can lead to systemic disseminated infections (11). *P. digitatum* is one of the most destructive pathogens of decaying citrus fruits, causing up to 90% of postharvest losses (12).

We searched for case reports and case series of pulmonary infections due to *Penicillium* species during 1995–2024 in PubMed using the keywords "(lung) AND (*Penicillium*)," except *Talaromyces marneffei*. Our search yielded 29 case reports that are summarized in Table 1. It summarizes data from 37 patients, of whom 15 (41%) were men and 13 (35%) were women. A total of 16 patients (43%) were over 50 years old, and 18 patients had their fungal species identified at the species level, with the following species being most common: *Penicillium citrinum* (4 patients, 11%), *P. digitatum* (2 patients, 5%), *Penicillium chrysogenum* (2 patients, 5%), *Penicillium brevicompactum* (2 patients, 5%), and *Penicillium purpurogenum* (2 patients, 5%). Regarding predisposing factors, 23 patients (62%) had occupational exposure, which mostly resulted in allergic pneumonia. Moreover, four patients (11%) had underlying pulmonary diseases, and seven patients (19%) were immunocompromised, including five (14%) with a history of cancer. In terms of treatment, 14 patients (38%) received steroid therapy, mainly for occupational exposure-related hypersensitivity pneumonitis. *Penicillium* infections were mostly treated with amphotericin B and itraconazole. Specifically, four patients (11%) were treated with amphotericin B, and nine patients (24%) received azole medications, with four out of these nine patients (4%) choosing itraconazole. Ultimately, 22 patients (59%) showed good recovery after treatment.

To the best of our knowledge, only two cases of pulmonary infection caused by *P. digitatum* have been reported (2, 3). Oshikata (2) reported the first case of pulmonary infection caused by *P. digitatum* in an elderly Japanese man who had emphysema and was undernourished. The second case was reported by Iturrieta-González et al. (3) in a late-term pregnant young woman who developed new nodular lesions in the lungs after being infected with SARS-CoV-2 and underwent termination of pregnancy, received treatment with corticosteroids, antibiotics, and mechanical ventilation. This infection was ultimately identified as *P. digitatum*.

The patient, in this case, had a clear history of consuming a large number of citrus fruits, including those with signs of mild rot, during the disease-onset period. There is also a possibility of inhaling spores of the *Penicillium* genus present in the air. Additionally, the patient was elderly and malnourished, had long-term smoking history and emphysema, had recently undergone major surgery, and was infected with COVID-19. The patient was in the recovery phase of COVID-19 infection, and his blood lymphocyte count remained below

TABLE 1 Case reports and case series of *Penicillium* species pulmonary infection during 1995–2024 in PubMed (M, male; F, female; RW, recover well).

References	Country/Age /gender	Pathogenic bacterium	Predisposing factors	Treatment	Outcome
Cámara et al. (13)	NA	*Penicillium brevicompactum*	Allogeneic bone marrow transplant recipient	NA	NA
D'Antoni et al. (14)	Italy/57/M	*Penicillium chrysogenum*	Lung cancer	Itraconazole	RW
Nakagawa-Yoshida et al. (15)	Canadian/79,66,76/3 M	*Penicillium brevicompactum, Penicillium olivicolor*	Occupational exposure	Steroid therapy/prednisone	Died
Mok et al. (16)	China/60/F	*Penicillium citrinum*	Acute leukemia	Amphotericin B, itraconazole	Died
Bates et al. (17)	England/38/M	*Penicillium species*	Occupational exposure	Prednisolone	RW
Qadir and Cunha et al. (18)	America/67/M	*Penicillium peritonitis*	Peritoneal dialysis	Fluconazole	RW
Cormier et al. (19)	Canada/54/M	*Penicillium species*	Occupational exposure	Prednisolone	RW
Perry et al. (20)	NA	*Penicillium species*	Occupational exposure	Steroids	RW
Breton et al. (21)	NA	*Penicillium purpurogenum*	Hematology disease	NA	NA
Rivero et al. (22)	Mar del Plata/56/F	*Penicillium species*	Occupational exposure	NA	NA
Novotny and Dixit et al. (23)	Hispanic-Filipino/<1/M	*Penicillium purpurogenum, Trichoderma species*	Occupational exposure	Methylprednisolone	RW
Ohnishi et al. (24)	Japan/37/F	*Penicillium corylophilum*	Occupational exposure	NA	NA
Lee et al. (25)	Korea/30/F	*Penicillium species*	Occupational exposure	Corticosteroid	RW
Yoshikawa et al. (26)	Japan/47/F	*Penicillium citrinum*	Occupational exposure	Methylprednisolone	RW
Laguna et al. (27)	Mexican/16/F	*Mycobacterium kansasii, Penicillium species*	Cystic fibrosis, abdominal pain	Amikacin, azithromycin, ethambutol, rifampin	NA
Guillot et al. (28)	France/27,49,38/3 NA	*Penicillium species*	Occupational exposure	Corticosteroid	RW
Amano et al. (29)	Japan/54/F	*Penicillium species*	Occupational exposure	NA	NA
Yasui et al. (30)	Japan/NA/3 NA	*Penicillium species*	Occupational exposure	NA	NA
Morell et al. (31)	Spain/avg. age 41/3 F	*Penicillium species*	Occupational exposure	NA	RW
Chien et al. (32)	Asian/57/F	*Penicillium species*	Franklin disease	Amphotericin B	RW
Geltner et al. (33)	Austria/56/M	*Penicillium chrysogenum*	Underwent left single lung transplant for α1-antitrypsin deficiency with severe lung emphysema	Posaconazole, caspofungin	Died
Chen et al. (34)	China/56/F	*Penicillium capsulatum*	Type 2 diabetes	Fluconazole, caspofungin	RW
Dillard and Ortega et al. (35)	American/44/M	*Cunninghamella species, Aspergillus fumigatus, Penicillium species*	History of pulmonary, tuberculosis	Itraconazole	RW
Oshikata et al. (2)	Japan/78/M	*Penicillium digitatum*	Bronchial asthma and pulmonary emphysema	Voriconazole, amphotericin B, fluconazole, itraconazole	RW
Shokouhi et al. (36)	Iran/44/M	*Penicillium notatum, Pneumocystis jiroveci*	Acute Myeloid Leukemia	Voriconazole, primaquine, clindamycin	RW
Zhao et al. (37)	China/67/M	*Penicillium citrinum*	Acute fibrinous and organizing pneumonitis, Type 2 diabetes	Methylprednisolone, amphotericin B, voriconazole	RW
Kutsuzaw et al. (38)	Japan/66/M	*Penicillium digitatum*	Occupational exposure, smoker	NA	RW
Beena et al. (39)	India/60/M	*Penicillium citrinum*	Multiple myeloma	NA	NA
Marruchella et al. (40)	Italy/42/F	*Penicillium species*	Occupational exposure	Corticosteroid therapy	RW

normal upon hospital admission. This indicates that the patient's cellular immune function has not yet fully recovered from the COVID-19 infection. These factors may have collectively contributed to the immunocompromise in the patient and facilitated the occurrence of lung infection due to *P. digitatum*.

Only individual case reports have documented successful treatment of *Penicillium* infections with itraconazole, amphotericin B, or fluconazole (4, 41). In the report by Oshikata et al. (2), the patient finally received a multidrug combination therapy of itraconazole, amphotericin B, and fluconazole, but the patient's condition did not improve. In the report by Iturrieta-González et al. (3), antifungal susceptibility testing showed *in vitro* activity of amphotericin B, voriconazole, and itraconazole, and the patient received itraconazole 400 mg/day, and the condition was effectively controlled after 10 days. The patient in our case also received itraconazole and showed a good therapeutic response. Currently, there are no relevant guidelines regarding the treatment of *Penicillium*. The preferred treatment involves administering Amphotericin B at a dosage of 0.5–1 mg/kg/day for 2 weeks, followed by maintenance therapy with Itraconazole at a dosage of 200 mg twice daily for 10 weeks (12–14). More research and reports are needed to explore the antifungal treatment regimens for Penicillium.

Conclusion

To the best of our knowledge, this is the first reported case of pulmonary infection caused by *P. digitatum* in China and the third case reported worldwide. The patient was an elderly man, undernourished, had emphysema, was in the recovery period of COVID-19 infection and surgery, and had a history of exposure to citrus fruit pathogens, which may have contributed to the occurrence of lung infection caused by *P. digitatum*. The patient's pulmonary fungal infection was effectively controlled with the use of itraconazole antifungal therapy. Although human infection with *P. digitatum* is considered rare, as an emerging opportunistic pathogen, clinical attention is still needed when it is isolated from immunocompromised patients.

Data availability statement

The datasets presented in this study can be found in online repositories. The names of the repository/repositories and accession number(s) can be found in the article/supplementary material.

Ethics statement

Written informed consent was obtained from the individual(s) for the publication of any potentially identifiable images or data included in this article. Written informed consent was obtained from the participant for the publication of this case report.

Author contributions

XS: Conceptualization, Writing – original draft. JY: Methodology, Writing – original draft. PL: Data curation, Writing – original draft. WG: Formal analysis, Writing – original draft. ZF: Supervision, Writing – review & editing. CZ: Writing – original draft. YH: Writing – original draft. YG: Formal analysis, Writing – original draft. LZ: Conceptualization, Supervision, Writing – review & editing.

Funding

The author(s) declare that no financial support was received for the research, authorship, and/or publication of this article.

Conflict of interest

The authors declare that the research was conducted in the absence of any commercial or financial relationships that could be construed as a potential conflict of interest.

Publisher's note

References

1. Visagie CM, Houbraken J, Frisvad JC, Hong SB, Klaassen CH, Perrone G, et al. Identification and nomenclature of the genus Penicillium. *Stud Mycol.* (2014) 78:343–71. doi: 10.1016/j.simyco.2014.09.001

2. Oshikata C, Tsurikisawa N, Saito A, Watanabe M, Kamata Y, Tanaka M, et al. Fatal pneumonia caused by Penicillium digitatum: a case report. *BMC Pulm Med.* (2013) 13:16. doi: 10.1186/1471-2466-13-16

3. Iturrieta-González I, Giacaman A, Godoy-Martínez P, Vega F, Sepúlveda M, Santos C, et al. Penicillium digitatum, First Clinical Report in Chile: Fungal Co-Infection in COVID-19 Patient. *J Fungi.* (2022) 8:961. doi: 10.3390/jof8090961

4. Avilés-Robles M, Gómez-Ponce C, Reséndiz-Sánchez J, Rodríguez-Tovar AV, Ceballos-Bocanegra A, Martínez-Rivera Á. Disseminated penicilliosis due to Penicillium chrysogenum in a pediatric patient with Henoch-Schönlein syndrome. *Int J Infect Dis.* (2016) 51:78–80. doi: 10.1016/j.ijid.2016.08.026

5. Garg A, Stuart A, Fajgenbaum M, Laidlaw DA, Stanford M. Chronic postoperative fungal endophthalmitis caused by Penicillium citrinum after cataract surgery. *J Cataract Refract Surg.* (2016) 42:1380–2. doi: 10.1016/j.jcrs.2016.07.025

6. Yang Q, Qian X, Dhanasekaran S, Boateng NAS, Yan X, Zhu H, et al. Study on the infection mechanism of penicillium digitatum on postharvest citrus (citrus reticulata blanco) based on transcriptomics. *Microorganisms.* (2019) 7:672. doi: 10.3390/microorganisms7120672

7. Ballester AR, González-Candelas L. EFE-mediated ethylene synthesis is the major pathway in the citrus postharvest pathogen penicillium digitatum during fruit infection. *J Fungi.* (2020) 6:172. doi: 10.3390/jof6030175

8. Bassett IJ, Crompton CW, Parmelee JA. *An atlas of airborne pollen grains and common fungus spores of Canada*. London: CABI (1978).

9. Deesomchok A, Tanprawate S. A 12-case series of Penicillium marneffei pneumonia. *J Med Assoc Thai.* (2006) 89:441–7.

10. Yoshikawa S, Tsushima K, Yasuo M, Fujimoto K, Kubo K, Kumagai T, et al. Hypersensitivity pneumonitis caused by *Penicillium citrinum*, not Enoki spores. *Am J Ind Med.* (2007) 50:1010–7. doi: 10.1002/ajim.20535

11. Ramírez I, Hidrón A, Cardona R. Successful treatment of pulmonary invasive fungal infection by Penicillium non-marneffei in lymphoblastic lymphoma: case report and literature review. *Clin Case Rep.* (2018) 6:1153–7. doi: 10.1002/ccr3.1527

12. Holmes GJ, Eckert JW. Sensitivity of Penicillium digitatum and P. *italicum* to postharvest citrus fungicides in California. *Phytopathology.* (1999) 89:716–21. doi: 10.1094/PHYTO.1999.89.9.716

13. de la Cámara R, Pinilla I, Muñoz E, Buendía B, Steegmann JL, Fernández-Rañada JM. Penicillium brevicompactum as the cause of a necrotic lung ball in an allogeneic bone marrow transplant recipient. *Bone Marrow Transplant.* (1996) 18:1189–93.

14. D'Antonio D, Violante B, Farina C, Sacco R, Angelucci D, Masciulli M, et al. Necrotizing pneumonia caused by Penicillium chrysogenum. *J Clin Microbiol.* (1997) 35:3335–7. doi: 10.1128/jcm.35.12.3335-3337.1997

15. Nakagawa-Yoshida K, Ando M, Etches RI, Dosman JA. Fatal cases of farmer's lung in a Canadian family. Probable new antigens, *Penicillium brevicompactum* and *P olivicolor*. *Chest.* (1997) 111:245–8. doi: 10.1378/chest.111.1.245

16. Mok T, Koehler AP Yu MY, Ellis DH, Johnson PJ, Wickham NW. Fatal Penicillium citrinum pneumonia with pericarditis in a patient with acute leukemia. *J Clin Microbiol.* (1997) 35:2654–6. doi: 10.1128/jcm.35.10.2654-2656.1997

17. Bates C, Read RC, Morice AH. A malicious mould. *Lancet (London, England).* (1997) 349:1598. doi: 10.1016/S0140-6736(97)03231-5

18. Qadir MT, Cunha BA. Penicillium peritonitis in a patient receiving continuous ambulatory peritoneal dialysis. *Heart Lung.* (1998) 27:67–8. doi: 10.1016/S0147-9563(98)90072-3

19. Cormier Y, Israël-Assayag E, Bédard G, Duchaine C. Hypersensitivity pneumonitis in peat moss processing plant workers. *Am J Respir Crit Care Med.* (1998) 158:412–7. doi: 10.1164/ajrccm.158.2.9712095

20. Perry LP, Iwata M, Tazelaar HD, Colby TV, Yousem SA. Pulmonary mycotoxicosis: a clinicopathologic study of three cases. *Modern Pathol.* (1998) 11:432–6.

21. Breton P, Germaud P, Morin O, Audouin AF, Milpied N, Harousseau JL. Rare pulmonary mycoses in patients with hematologic diseases. *Rev Pneumol Clin.* (1998) 54:253–7.

22. Rivero MG, Basile LM, Salvatore AJ, Fridlender H, Maxit M. Salami worker's lung. *Medicina.* (1999) 59:367–9.

23. Novotny WE, Dixit A. Pulmonary hemorrhage in an infant following 2 weeks of fungal exposure. *Arch Pediatr Adolesc Med.* (2000) 154:271–5. doi: 10.1001/archpedi.154.3.271

24. Ohnishi T, Yamada G, Tanaka H, Nakajima K, Tanaka S, Morita-Ichimura S, et al. A case of chronic hypersensitivity pneumonia with elevation of serum SP-D and KL-6. *Nihon Kokyuki Gakkai Zasshi.* (2002) 40:66–70.

25. Lee YM, Kim YK, Kim SO, Kim SJ, Park HS. A case of hypersensitivity pneumonitis caused by Penicillium species in a home environment. *J Korean Med Sci.* (2005) 20:1073–5. doi: 10.3346/jkms.2005.20.6.1073

26. Yoshikawa S, Tsushima K, Koizumi T, Kubo K, Kumagai T, Yamazaki Y. Hypersensitivity pneumonitis induced by spores of Penicillium citrinum in a worker cultivating Enoki mushroom. *Internal Med.* (2006) 45:537–41. doi: 10.2169/internalmedicine.45.1646

27. Laguna TA, Sagel SD, Sontag MK, Accurso FJ. The clinical course of a Mexican female with cystic fibrosis and the novel genotype S531P/S531P. *J Cystic Fibrosis.* (2008) 7:454–6. doi: 10.1016/j.jcf.2008.03.008

28. Guillot M, Bertoletti L, Deygas N, Raberin H, Faure O, Vergnon JM. Dry sausage mould hypersensitivity pneumonitis: three cases. *Rev Mal Respir.* (2008) 25:596–600. doi: 10.1016/S0761-8425(08)71617-6

29. Amano Y, Enomoto M, Bando M, Kawakami M, Sugiyama Y. Hypersensitity pneumonitis in a greenhouse rose grower. *Nihon Kokyuki Gakkai Zasshi.* (2009) 47:960–4.

30. Yasui H, Matsui T, Yokomura K, Nakano Y, Suda T, Chida K. Three cases of hypersensitivity pneumonitis in citrus farmers. *Nihon Kokyuki Gakkai Zasshi.* (2010) 48:172–7.

31. Morell F, Cruz MJ, Gómez FP, Rodriguez-Jerez F, Xaubet A, Muñoz X. Chacinero's lung - hypersensitivity pneumonitis due to dry sausage dust. *Scand J Work Environ Health.* (2011) 37:349–56. doi: 10.5271/sjweh.3151

32. Weng CH, Wang RC, Hsieh TY, Tsai CA, Lin TH. Penicillium pneumonia in a patient with newly diagnosed Franklin disease. *Am J Med Sci.* (2012) 344:69–71. doi: 10.1097/MAJ.0b013e31824a8927

33. Geltner C, Lass-Flörl C, Bonatti H, Müller L, Stelzmüller I. Invasive pulmonary mycosis due to Penicillium chrysogenum: a new invasive pathogen. *Transplantation.* (2013) 95:e21–3. doi: 10.1097/TP.0b013e31827ff214

34. Chen M, Houbraken J, Pan W, Zhang C, Peng H, Wu L, et al. Pulmonary fungus ball caused by Penicillium capsulatum in a patient with type 2 diabetes: a case report. *BMC Infect Dis.* (2013) 13:496. doi: 10.1186/1471-2334-13-496

35. Dillard TA, Ortega I. Multiple endobronchial mycetomas with varied appearances and mixed fungal flora. *J Bronchol Interv Pulmonol.* (2013) 20:147–9. doi: 10.1097/LBR.0b013e31828ab757

36. Shokouhi S, Tehrani S, Hemmatian M. Mixed pulmonary infection with *Penicillium notatum* and *Pneumocystis jiroveci* in a patient with acute myeloid leukemia. *Tanaffos.* (2016) 15:53–6.

37. Zhao J, Shi Y, Yuan D, Shi Q, Wang W, Su X, et al. case report of fungal infection associated acute fibrinous and organizing pneumonitis. *BMC Pulm Med.* (2020) 20:98. doi: 10.1186/s12890-020-1145-7

38. Kutsuzawa N, Takihara T, Shiraishi Y, Kajiwara H, Imanishi T, Fukutomi Y, et al. Occupational hypersensitivity pneumonitis in a Japanese citrus farmer. *Internal Med.* (2021) 60:3581–4. doi: 10.2169/internalmedicine.7588-21

39. Beena H, Gupta M, Kindo AJ. Pulmonary infection with Penicillium citrinum in a patient with multiple myeloma. *Indian J Med Microbiol.* (2021) 39:259–61. doi: 10.1016/j.ijmmb.2021.03.001

40. Marruchella A, Faverio P, Luppi F. Concurrent features of sarcoidosis and hypersensitivity pneumonitis in two patients exposed to fungal antigens. *BMC Pulm Med.* (2023) 23:427. doi: 10.1186/s12890-023-02642-x

41. Hoenigl M, Salmanton-García J, Walsh TJ, Nucci M, Neoh CF, Jenks JD, et al. Global guideline for the diagnosis and management of rare mould infections: an initiative of the European Confederation of Medical Mycology in cooperation with the International Society for Human and Animal Mycology and the American Society for Microbiology. *Lancet Infect Dis.* (2021) 21:e246–e57. doi: 10.1016/S1473-3099(20)30784-2

frontiers | Frontiers in Medicine

TYPE Case Report
PUBLISHED 17 July 2024
DOI 10.3389/fmed.2024.1404951

OPEN ACCESS

EDITED BY
Giuseppe Fiorentino,
Hospital of the Hills, Italy

REVIEWED BY
Indranil Chakrabarti,
All India Institute of Medical Sciences, Kalyani (AIIMS Kalyani), India
Yutaka Yoshii,
The Jikei University School of Medicine, Japan

*CORRESPONDENCE
Gani Oruqaj
✉ gani.oruqaj@innere.med.uni-giessen.de

†These authors have contributed equally to this work and share senior authorship

RECEIVED 21 March 2024
ACCEPTED 01 July 2024
PUBLISHED 17 July 2024

CITATION
Oruqaj G, Krombach G, Gattenloehner S, Herold S, Vadász I, Seeger W, Tello K and Hecker M (2024) Adenomatous hyperplasia induced by chronic cherry pit retention mimicking an endobronchial tumor-case series and systematic review of literature. *Front. Med.* 11:1404951. doi: 10.3389/fmed.2024.1404951

Adenomatous hyperplasia induced by chronic cherry pit retention mimicking an endobronchial tumor-case series and systematic review of literature

Gani Oruqaj[1]*, Gabriele Krombach[2], Stefan Gattenloehner[3], Susanne Herold[4], István Vadász[1], Werner Seeger[1], Khodr Tello[1†] and Matthias Hecker[1†]

[1]Department of Internal Medicine, Medical Clinic II, Universities of Giessen and Marburg Lung Center (UGMLC), Institute for Lung Health (ILH), Cardio-Pulmonary Institute (CPI), Member of the German Center for Lung Research (DZL), Giessen, Germany, [2]Department of Radiology, University Hospital Giessen, Giessen, Germany, [3]Department of Pathology, Justus-Liebig- University Giessen, Universities of Giessen and Marburg Lung Center (UGMLC), Giessen, Germany, [4]Department of Internal Medicine V, Universities of Giessen and Marburg Lung Center (UGMLC), Institute for Lung Health (ILH), Cardio-Pulmonary Institute (CPI), Member of the German Center for Lung Research (DZL), Giessen, Germany

Introduction: Endobronchial foreign body aspiration is not common in adults, but it is a life-threatening event. Recurrent pneumonias by chronic retention of foreign body often lead to initial medical presentation of the patient. However, lymphoplasmacellular bronchitis with adenomatous hyperplasia and squamous epithelium metaplasia with complete or partial blockage of lobar bronchus mimicking lung tumor is rare in literature, and this particular condition is often misdiagnosed.

Case presentation: we report our experience in the diagnostic and management of two elderly patients with recurrent pneumonia, admitted in hospital for further examination. In both patients, with no history of aspiration, the cherry pit was detected during bronchoscopy and recanalization with flexible cryoprobe, surrounded by purulent secretion, occluding completely the right upper lobe in the first case, and partially the left lower lobe associated with persistent actinomycosis in the second case, with signs of local inflammation, bronchial adenomatous hyperplasia mimicking lung tumor at initial bronchoscopic examination. Histology showed a lymphoplasmacellullar bronchitis with adenomatous hyperplasia and squamous epithelium metaplasia because of chronic retention of foreign body.

Conclusion: Bronchoscopy examination should be considered in cases where there is an unresolved chronic cough with recurrent pneumonia or persistent actinomycosis in patients with high risk. Cryoprobe is a safe and feasible approach for treatment of airway obstructions due to chronic foreign body retention. Furthermore, relevant findings are discussed here, along with a review of the pathologic alterations and treatment modalities seen in chronic retention of foreign body and airway injury.

KEYWORDS

adenomatous hyperplasia, squamous metaplasia, actinomycosis, cherry pit, mimicking lung

Introduction

Recurrent Pneumonia due to chronic retention of foreign body, which mimics a bronchial tumor is a rare observed condition in adults (1). Bronchoscopy is an uncommon indication for foreign body aspiration in adults, accounting for 1% of procedures (2). The diagnosis of the foreign body aspiration is often delayed or overlooked, leading to patients experiencing chronic cough, recurrent pulmonary infections and persisting dyspnea (3, 4). Cryotherapy with flexible cryoprobe is a safe technique for treatment of symptomatic endobronchial tumor stenosis, cryoextraction and quick removal of foreign bodies (5–8). Furthermore, actinomycosis associated with foreign body aspiration is a rare pulmonary infection, caused by inhalation of actinomyces contaminated aspiration (9).

Here, we report two unique cases of cherry pit aspiration, who unconsciously aspirated a cherry pit months or years prior to recurrent pulmonary infections. The patients were not aware of any aspiration. Bronchoscopy is the recommended initial management and diagnostic procedure for patients experiencing recurrent pulmonary infections, unresolved actinomycosis resistant to antibiotics regardless whether or not they have a history of aspiration.

Case 1 presentation

A 70-year old male patient with past medical history of hypertension, asthma, cardiovascular disease was admitted on December 14, 2023, because of persistent respiratory symptoms with intermittent coughing, dyspnea, fever in the last 2 days, and prior history of Pneumonia 2 weeks before admission which was treated with antibiotics. There was a slight improve after therapy, with persisting symptoms afterwards. Upon inquiry about aspiration, a suspicion of a foreign body in the bronchi was raised, in addition to suspicion of a tumor occlusion. History of choking due to foreign body aspiration and allergy were denied, but in last months has become more forgetful. Physical examination at admission showed a body temperature of 38°C, pulse rate of 89 beats per minute, blood pressure 113/78 mmHg, and respiratory rate of 29 breaths per minute, oxygen saturation on room air 92% with 2 L O_2. The patient had a clear consciousness. Physical examination appeared unremarkable, lungs with no wheezing, but diminished breath sounds on right upper side. The chest-X ray and a low dose CT scan demonstrated consolidation of the right upper lobe, with compression of the upper bronchus and poststenotic pneumonia and suspicious diagnosis of lung cancer (Figures 1A–D). A sputum analysis revealed a normal respiratory microbiota. Biochemical analysis revealed elevated C reactive protein of 159 mg/L (reference value <5 mg/L) and a white cell count of 10.3×10 9/l (reference value 3,9–10 giga/l). Renal function test normal, while liver function test slightly increased liver enzymes (GOT, GPT). C reactive protein (CRP) after therapy recovered and was again normal.

As next, the patient underwent fiberoptic bronchoscopic exploration with appropriate sedation using midazolam, propofol and hydromorphone, which lasted approximately 30 min. Flexible bronchoscopy showed a complete occlusion of the right upper lobar bronchus by adenomatous hyperplasia tissue and purulent secretion resembling macroscopically a lung tumor (Figures 2A–D). Purulent secretion distal to obstruction was cleared with suction, and hyperplasia tissue was carefully removed with cryoprobe, and finally cherry pit surrounded with epithelium hyperplasia and purulent secretion was successfully extracted with a cryoprobe (see Supplementary Video S1). Airways distal to obstruction were markedly bronchiectatic and altered (Figure 1). To our knowledge, this is the first case report regarding aspiration of cherry pit and subsequent pathologic-histologic alterations with adenomatous hyperplastic bronchitis, epithelium metaplasia mimicking a lung tumor.

Eight weeks after removal of the foreign body and adenomatous tissue, the patient underwent a follow-up CT scan that showed no longer consolidation of the right upper lobe, with minor bronchiectasia distally (Figures 1E–H).

The pathological examination of the tissue and foreign body revealed adenomatous hyperplasia and lympoplasmaceullar bronchitis with squamous epithelial metaplasia in the extracted tissue due to cherry pit aspiration, with no signs of dysplasia in the examined specimen (Figures 2E–H). The bronchial epithelial is reactively inflamed with chronic bronchitis and pseudopapillary epithelial hyperplasia and pronounced squamous epithelium metaplasia (Figure 2). The plant material (cherry pit) and secondary bacterial colonization by coccoid and filamentous bacteria could be well demonstrated (Figures 2A–H). Moreover, typical water-clear plant cells with very characteristic birefringence providing evidence of plant material, could be well observed with the use of polarized microscope (Figures 2G,H). Furthermore, in the final figure, the presence of a cherry pit foreign body within a specimen container, along with purulent secretions and bronchial hyperplasia tissue, was clearly visible (Figure 2D).

Case 2 presentation

A 74-year old patient with a history of COPD GOLD III, pulmonary hypertension presented with a productive cough yielding yellow sputum that had worsened over the past 8 weeks. The patient also reported generalized body weakness and a decreased appetite with the acute illness, but no fever or chills. The patient has intermittently symptoms in the past 2 years. Initially, there was performed a bronchoscopy fur further evaluation and diagnostics, which revealed a tumor like mass in the 8th segment of the left lower lobe. An endobronchial biopsy of the lesion showed an epithelium metaplasia, and revealed filamentous gram-positive organisms resembling actinomyces infection, which was treated with penicillin, and made good clinical improvement with radiological resolution.

At presentation 2 years later, he gave 8-week history of increasing breathlessness on exertion and cough productive of purulent sputum. He denied any haemoptysis, chest pain or weight loss but complained of episodic sweating three times per week. He was afebrile, with a pulse of 76 beats per minute and oxygen saturations of 91 percent on room air. White blood cell count was normal at 4.4 × 109/L. Chest radiograph revealed left lower zone consolidation with evidence of collapse (Figure 3A). Subsequent contrast enhanced computerized tomography (Figures 3A,B) demonstrated partial occlusion of left

Abbreviations: FBA, Foreign Body Aspiration; GOT, Glutamic-Oxaloacetic Transaminase; GPT, Glutamic Pyruvic Transaminase; CT, Computer Tomography; CRP, C-Reactive Protein.

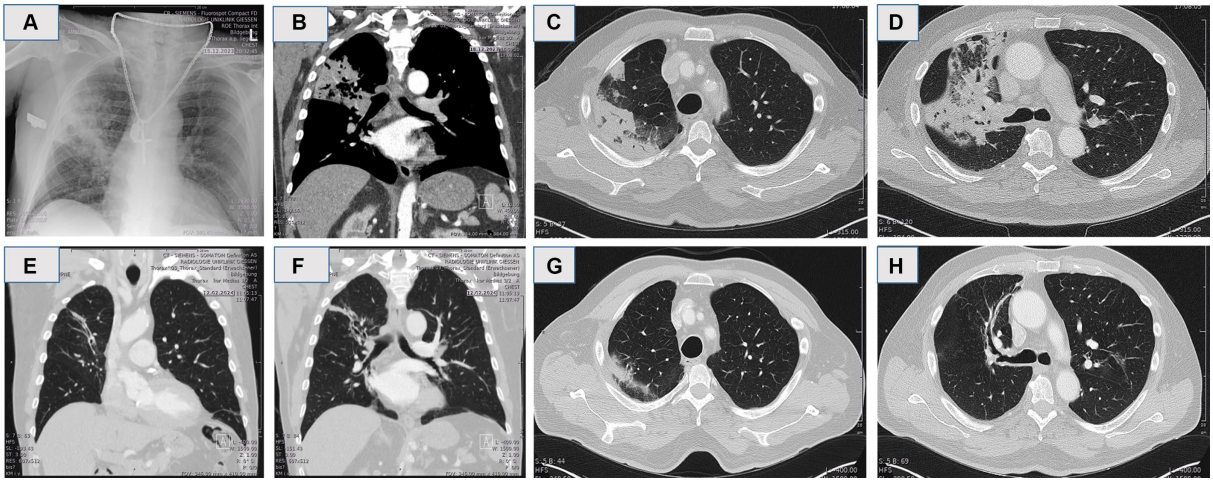

FIGURE 1
(A) Chest X-ray showing a consolidation in the right upper lobe indicating of pneumonia. **(B–D)** Computerized tomography (CT) in coronal and axial reconstruction demonstrated compression of the upper right bronchus and post-stenotic pneumonia of right upper lobe resembling lung cancer. **(E–H)** Computerized tomography in coronal and axial reconstruction 8 weeks post extraction of the cherry pit.

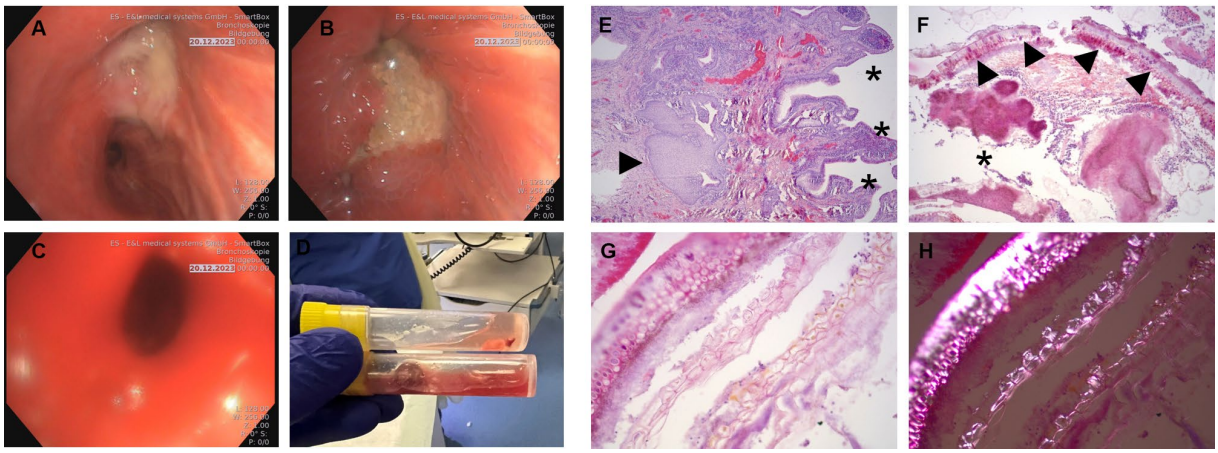

FIGURE 2
(A,B) Flexible bronchoscopy revealing total obstruction of the right upper lobar bronchus by amorphous bronchial adenomatous hyperplasia, purulent secretion and abundant granulation tissue. **(C)** The right upper lobar bronchus after retrieval of the foreign body and adenomatous hyperplasia by flexible cryoprobe. **(D)** Macroscopic appearance of the aspirated material cherry pit with hyperplasia tissue and purulent secretions in a specimen container, after removal with cryoprobe. **(E)** Pathological examination of bronchial epithelial hyperplasia with reactively inflamed bronchial mucosa with chronic bronchitis with pseudopapillary epithelial hyperplasia (stars) and pronounced squamous epithelium metaplasia (arrow) (**H&E**, 20x). **(F)** Immunostaining of plant material (arrows) and secondary bacterial colonization by coccoid and filamentous bacteria (star) (**H&E**, 50x). **(G,H)** Immunostaining of detailed typical water-clear plant cells **(G)**, polarized microscope image **(H)** with very characteristic birefringence as evidence of plant foreign material (**H&E**, 200x).

lower lobe with mucous secretion, bronchiectatic and altered, indicating for an actinomycosis infection.

Again, the flexible bronchoscopy examination was performed by using sedation with midazolam, propofol and hydromorphone, which lasted approximately 30 min. It revealed further the adenomatous hyperplasia and partial occlusion of the segment 8 in the left lower lobe. A grey tumor-like mass in bronchus 8th segment was noted. The mass was exerted with flexible cryoprobe (Figures 3E,F). Histology revealed chronically inflamed mucosa, cherry pit foreign material and filamentous gram-positive organisms resembling actinomyces, after years of latency.

In the follow-up CT scan after removal of the foreign body and adenomatous tissue, showed no longer consolidation of the left lower lobe, with remaining bronchiectasia distally (Figures 3C,D).

Discussion

Foreign body aspiration (FBA) is an uncommon event in the adult population. In these case series study, the patient in case 1 presented with symptoms of pneumonia, and his chest CT scan

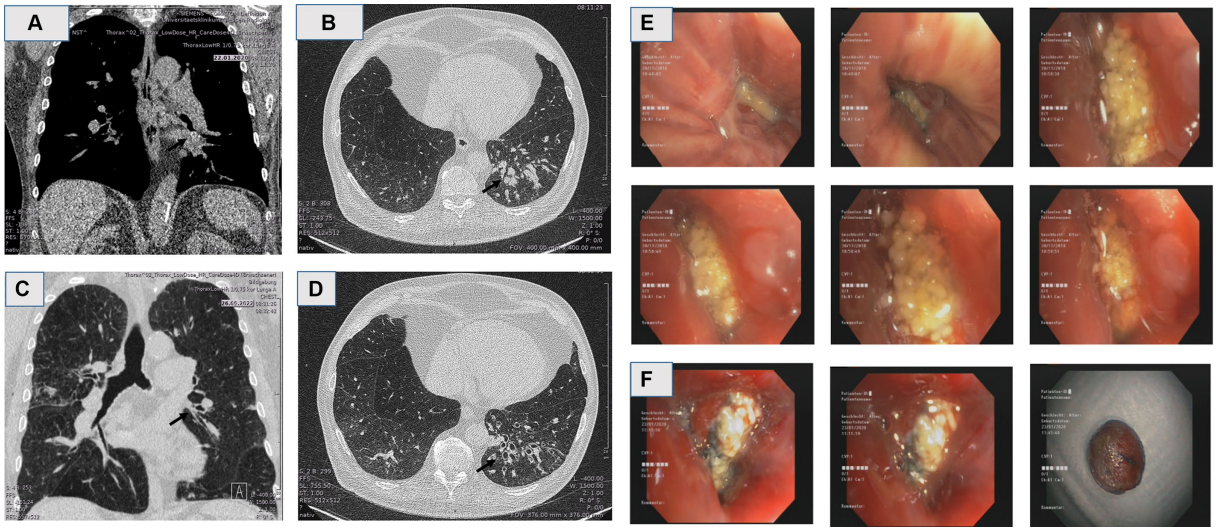

FIGURE 3
(A,B) Computerized tomography (CT) in coronal and axial reconstruction demonstrated compression of the lower left bronchus, followed by mucus obstruction of the bronchi, and post-stenotic bronchiectatic actinomycosis. **(C,D)** Computerized tomography in coronal and axial reconstruction in follow up, months post extraction of the cherry pit, revealing complete resolution with remaining bronchiectasia distally. **(E,F)** flexible bronchoscopy of the left lower lobe at initial presentation revealed an actinomycosis in biopsy **(E)**, and remaining obstruction in 2 years follow up, with the macroscopic appearance of the aspirated material, mimicking lung tumor **(F)**.

revealed a consolidation in the right upper lobe, and in case 2 presented with persistent actinomycosis infection resistant to antibiotics and dyspnea in exertion, in both cases resembling an endobronchial tumor. Since the recurrent pneumonia and persistent actinomycosis were the main reasons for admission to the hospital, we performed a bronchoscopy for further diagnostical purpose. However, in case 1 the patient can remember eating cherries 6–8 months before admission to hospital, but did not notice any aspiration of it, whereas in case 2 the patient did not notice any aspiration, after a long latency of the cherry pit. We suppose that the aspiration symptoms were mild due to their elderly and poor general condition. In case 1 during bronchoscopy showed a complete occlusion of the right upper lobar bronchus and hyperplasia tissue covered with purulent secretion resembling an endobronchial tumor. The obstruction including epithelium hyperplasia was carefully removed with a cryoprobe (Figure 2D; Supplementary Video S1). In case 2, in bronchoscopic examination revealed a partial occlusion of the left lower lobe with a tumor mass, hyperplasia tissue covered with purulent secretion mimicking also a lung tumor (Figures 3A–F), which was carefully removed with a cryoprobe (Figure 3F). Foreign body aspiration usually occurs in children, and the other peak at over 60 years of age accounting for 20% aspiration cases (10, 11). A foreign body aspiration can be tolerated in the elderly ages leading to recurrent pneumonia, and patients presenting with symptoms due to infection and other complications such as pneumothorax, or endobronchial tumor (12). Colleagues Li et al. prescribed a case report of watermelon seed aspiration in a cancer patient resembling a recurrence (3). Furthermore, actinomycosis is a purulent infection caused by filamentous bacilli, and pulmonary actinomycosis presented only 15% of actinomyces infection (13). Pulmonary actinomycosis is presented in various form, including pneumonia, a pseudo-tumor-like mass, draining fistulas, pulmonary abscess or tuberculosis (14, 15). Actinomycosis clinical cases due to nonorganic FBA have been reported in the literature such as secondary to pen end cap, or watermelon seed aspiration (16, 17).

However, there are no reports of cherry pit aspiration and adenomatous hyperplasia with lymphoplasmacellular bronchitis, squamous epithelium metaplasia, actinomycosis infection mimicking also macroscopically a lung cancer.

Foreign body aspirations are often characterized with histopathologic sequela of chronic inflammatory changes, including lymphocyte and plasma cell infiltration, fibrosis, and the formation of foreign body giant cells and granulomas (18). The changes resembling a tumor mass were seen in our clinical case, adenomatous hyperplasia adjacent to the aspirated cherry pit, which also revealed in addition squamous metaplasia. Secondary bacterial colonization by coccoid and filamentous bacteria were observed in H&E staining (Figure 2F). Interestingly in pathological specimen was observed clearly typical water-clear plant cells, with typical birefringence as evidence of foreign plant material (Figures 2E–H). Furthermore, a macroscopic view of a cherry pit foreign body could be finally observed in a specimen container (Figures 2D, 3F). Squamous epithelium metaplasia is normally seen as secondary to the toxic injury of the airways as precursor of squamous cell carcinoma (19). Squamous metaplasia has been documented to happen in smokers with chronic obstructive pulmonary disease, due to chronic toxic injury, expressing carcinoembryonic antigen (19). Additionally, epithelium squamous metaplasia possibly caused by aspiration of a pistachio shell, was detected during a CT-Screening for lung cancer, and supported in PET-CT scan for lung tumor (20). Similar cases of chronic inflammation and induction of squamous metaplasia due to retention of oral chaff debris in rat feed were observed in animal models (21). This phenomenon is also presented in our cases, in which adenomatous hyperplasia and epithelium squamous metaplasia were observed in addition to the chronic inflammation,

purulent secretion and aspirated cherry pit. Both chronic smoking and FBA have been shown to induce epithelium squamous metaplasia, it might be unclear if the cherry pit is only responsible factor, and smoking is additional factor contributed to the event. Juan et al. showed that DNA damage has the potential to drive the squamous metaplasia via mitotic checkpoints, opening novel molecular candidate targets for lung squamous cell carcinoma (22). Furthermore, atypical adenomatous hyperplasia is prescribed as risk factor for lung cancer (23).

Once the FBA is suspected with detailed clinical history and imaging findings, bronchoscopy is the next step in management of foreign body retrieval. Flexible bronchoscopy is a valuable procedure, with less discomfort, performing under light sedation, and enables access to the peripheral airways in medical centers where rigid bronchoscopy is not available (24). However, rigid bronchoscopy has been favored historically for foreign body removal in the pediatric population.

Cryotherapy with flexible cryoprobe is a safe technique for treatment of symptomatic endobronchial tumor stenosis, cryoextraction and quick removal of foreign bodies (5–8).

Cryobiopsy has emerged as a safe and effective method in diagnostics, with additional benefits over conventional biopsy when used in combination with radial endobronchial ultrasound (25, 26). Furthermore, cryoprobe plays a crucial role in the cryorecanalization of malignant airway obstruction, leading to improved patient survival (27). Additionally, use of cryoprobe has been proven safe and feasible for the retrieval of both organic and inorganic foreign body aspirations, providing a versatile tool for medical professionals (7).

The pneumonia in the follow-up CT in both cases were completely resolved (Figures 1E–H, 3C,D). Minor changes with persistent bronchiectasis in follow-up CT, are most likely in resolving process of pneumonia, or in chronic latency in case 2 associated with COPD.

In case 2 the tumor mass associated with pulmonary actinomycosis reported here was most likely due to the aspiration of the cherry pit, which had been present in the lung for a long duration, *ca.* 2 years. This indicates in addition, the importance of keeping actinomycosis of the lung in the differential diagnosis of pseudo-tumor of a lung lesion, a bronchoscopy after resolution of the local inflammation is imperative, and samples should be also for tissue diagnosis and regular culture. In elderly patients with aspiration risk, prevention of aspiration with upright positioning during meals, supervision from nurses, and routine oral care are crucial factors (28).

In conclusion, bronchoscopy examination should be considered as a diagnostic tool in cases of recurrent pneumonia or persistent actinomycosis that are resistant to antibiotics, to exclude any chronic foreign body retention as a potential underlying cause of the event. In addition, cryoprobe is safe, efficient and feasible method in retrieval of bronchial adenomatous hyperplasia resulting from chronic foreign body retention. This clinical novel rarity, with recurrent pneumonia or endobronchial actinomycosis associated with foreign body aspiration, which mimics a lung tumor with well-defined edges, requires special attention from medical staff in specific situations.

Data availability statement

The original contributions presented in the study are included in the article/Supplementary material, further inquiries can be directed to the corresponding author/s.

Ethics statement

The studies involving humans were approved by Justus Liebig University Medizinisches Lehrzentrum. The studies were conducted in accordance with the local legislation and institutional requirements. The participants provided their written informed consent to participate in this study. Written informed consent was obtained from the individual(s) for the publication of any potentially identifiable images or data included in this article.

Author contributions

GO: Conceptualization, Data curation, Formal analysis, Investigation, Writing – original draft, Writing – review & editing, Methodology, Software, Validation, Visualization. GK: Data curation, Formal analysis, Investigation, Writing – review & editing. SG: Formal analysis, Investigation, Resources, Writing – review & editing. SH: Data curation, Formal analysis, Investigation, Writing – review & editing. IV: Data curation, Formal analysis, Investigation, Writing – review & editing. WS: Conceptualization, Investigation, Supervision, Writing – review & editing. KT: Data curation, Formal analysis, Investigation, Supervision, Validation, Writing – review & editing, Writing – original draft, Conceptualization, Visualization. MH: Data curation, Formal analysis, Investigation, Supervision, Validation, Writing – review & editing, Writing – original draft, Conceptualization, Methodology, Visualization.

Funding

The author(s) declare that no financial support was received for the research, authorship, and/or publication of this article.

Conflict of interest

The authors declare that the research was conducted in the absence of any commercial or financial relationships that could be construed as a potential conflict of interest.

Publisher's note

Supplementary material

The Supplementary material for this article can be found online at: https://www.frontiersin.org/articles/10.3389/fmed.2024.1404951/full#supplementary-material

SUPPLEMENTARY VIDEO S1
Video of the flexible bronchoscopy: retrieval of the adenomatous hyperplasia and cherry pit foreign body.

References

1. Bajaj D, Sachdeva A, Deepak D. Foreign body aspiration. *J Thorac Dis*. (2021) 13:5159–75. doi: 10.21037/jtd.2020.03.94

2. Hewlett JC, Rickman OB, Lentz RJ, Prakash UB, Maldonado F. Foreign body aspiration in adult airways: therapeutic approach. *J Thorac Dis*. (2017) 9:3398–409. doi: 10.21037/jtd.2017.06.137

3. Li L, Li MJ, Sun L, Jiang YL, Zhu J. Neglected foreign body aspiration mimicking lung Cancer recurrence. *Risk Manag Healthc Policy*. (2022) 15:491–6. doi: 10.2147/RMHP.S361081

4. Madsen A, Madsen PH. Recurrent pneumonia due to endobronchial foreign body. *BMJ Case Rep*. (2014) 2014:bcr2013201959. doi: 10.1136/bcr-2013-201959

5. Hetzel M, Hetzel J, Schumann C, Marx N, Babiak A. Cryorecanalization: a new approach for the immediate management of acute airway obstruction. *J Thorac Cardiovasc Surg*. (2004) 127:1427–31. doi: 10.1016/j.jtcvs.2003.12.032

6. Schumann C, Hetzel M, Babiak AJ, Hetzel J, Merk T, Wibmer T, et al. Endobronchial tumor debulking with a flexible cryoprobe for immediate treatment of malignant stenosis. *J Thorac Cardiovasc Surg*. (2010) 139:997–1000. doi: 10.1016/j.jtcvs.2009.06.023

7. Fruchter O, Kramer MR. Retrieval of various aspirated foreign bodies by flexible cryoprobe: in vitro feasibility study. *Clin Respir J*. (2015) 9:176–9. doi: 10.1111/crj.12120

8. Sriratanaviriyakul N, Lam F, Morrissey BM, Stollenwerk N, Schivo M, Yoneda KY. Safety and clinical utility of flexible Bronchoscopic Cryoextraction in patients with non-neoplasm tracheobronchial obstruction: a retrospective chart review. *J Bronchol Interv Pulmonol*. (2015) 22:288–93. doi: 10.1097/LBR.0000000000000203

9. Chouabe S, Perdu D, Deslée G, Milosevic D, Marque E, Lebargy F. Endobronchial actinomycosis associated with foreign body: four cases and a review of the literature. *Chest*. (2002) 121:2069–72. doi: 10.1378/chest.121.6.2069

10. Tseng HJ, Hanna TN, Shuaib W, Aized M, Khosa F, Linnau KF. Imaging foreign bodies: ingested, aspirated, and inserted. *Ann Emerg Med*. (2015) 66:570–582.e5. doi: 10.1016/j.annemergmed.2015.07.499

11. Baharloo F, Veyckemans F, Francis C, Biettlot MP, Rodenstein DO. Tracheobronchial foreign bodies: presentation and management in children and adults. *Chest*. (1999) 115:1357–62. doi: 10.1378/chest.115.5.1357

12. Ha JH, Jeong BH. Airway foreign body mimicking an endobronchial tumor presenting with pneumothorax in an adult: A case report. *Medicina (Kaunas)*. (2021) 57:50. doi: 10.3390/medicina57010050

13. Kononen E, Wade WG. Actinomyces and related organisms in human infections. *Clin Microbiol Rev*. (2015) 28:419–42. doi: 10.1128/CMR.00100-14

14. Kim SR, Jung LY, Oh IJ, Kim YC, Shin KC, Lee MK, et al. Pulmonary actinomycosis during the first decade of 21st century: cases of 94 patients. *BMC Infect Dis*. (2013) 13:216. doi: 10.1186/1471-2334-13-216

15. Katsenos S, Galinos I, Styliara P, Galanopoulou N, Psathakis K. Primary bronchopulmonary Actinomycosis masquerading as lung Cancer: apropos of two cases and literature review. *Case Rep Infect Dis*. (2015) 2015:609637. doi: 10.1155/2015/609637

16. Singh S, Singh S, Jyotimallika J. Endobronchial actinomycosis associated with nonorganic foreign body aspiration after years of latency. *J Bronchol Interv Pulmonol*. (2015) 22:180–2. doi: 10.1097/LBR.0000000000000143

17. Kassab K, Karnib M, Bou-Khalil PK, Bizri AR. Pulmonary actinomycosis presenting as post-obstructive pneumonia. *Int J Infect Dis*. (2016) 48:29–31. doi: 10.1016/j.ijid.2016.04.009

18. Bozkurtlar E, Oksuzoglu K, Bostanci K, Aslan S, Kissa TN, Kocakaya D, et al. FDG PET/CT features of polysaccharide-based hemostatic agent: chronic inflammatory changes can mimic metastatic lesions. *Clin Nucl Med*. (2022) 47:e475–80. doi: 10.1097/RLU.0000000000004216

19. Rigden HM, Alias A, Havelock T, O'Donnell R, Djukanovic R, Davies DE, et al. Squamous metaplasia is increased in the bronchial epithelium of smokers with chronic obstructive pulmonary disease. *PLoS One*. (2016) 11:e0156009. doi: 10.1371/journal.pone.0156009

20. Purohit K, Grandfield S, Dhamija A, Abbasi A. Foreign body aspiration mimicking an endobronchial neoplasm: a case report and review of the literature. *Cureus*. (2023) 15:e36105. doi: 10.7759/cureus.36105

21. Madsen C. Squamous-cell carcinoma and oral, pharyngeal and nasal lesions caused by foreign bodies in feed. Cases from a long-term study in rats. *Lab Anim*. (1989) 23:241–7. doi: 10.1258/002367789780810572

22. Juan LS, Freije A, Sanz-Gómez N, Jiménez-Matías B, Pleguezuelos-Manzano C, Sanz JR, et al. DNA damage triggers squamous metaplasia in human lung and mammary cells via mitotic checkpoints. *Cell Death Discov*. (2023) 9:21. doi: 10.1038/s41420-023-01330-3

23. Wang GF, Lai MD, Yang RR, Chen PH, Su YY, Lv BJ, et al. Histological types and significance of bronchial epithelial dysplasia. *Mod Pathol*. (2006) 19:429–37. doi: 10.1038/modpathol.3800553

24. Ramos-Rossy J, Cantres O, Torres A, Casal J, Otero Y, Arzon-Nieves G, et al. Flexible Bronchoscopic removal of 3 foreign objects. *Fed Pract*. (2018) 35:24–6.

25. Thiboutot J, Illei PB, Maldonado F, Kapp CM, DeMaio A, Lee HJ, et al. Safety and feasibility of a sheath Cryoprobe for Bronchoscopic Transbronchial biopsy: the FROSTBITE trial. *Respiration*. (2022) 101:1131–8. doi: 10.1159/000526876

26. Nakai T, Watanabe T, Kaimi Y, Shiomi K, Ando K, Miyamoto A, et al. Diagnostic utility and safety of non-intubated Cryobiopsy technique using a novel ultrathin Cryoprobe in addition to conventional biopsy techniques for peripheral pulmonary lesions. *Respiration*. (2023) 102:503–14. doi: 10.1159/000531010

27. Ma Q, Shi B, Tian Y, Liu D. Fibrobronchoscopic cryosurgery for secondary malignant tumors of the trachea and main bronchi. *Thorac Cancer*. (2016) 7:459–66. doi: 10.1111/1759-7714.12337

28. Thomas LE, Lustiber L, Webb C, Stephens C, Lago AL, Berrios S. Aspiration prevention: a matter of life and breath. *Nursing*. (2019) 49:64–6. doi: 10.1097/01.NURSE.0000552698.50502.75

frontiers | Frontiers in Medicine

TYPE Case Report
PUBLISHED 22 July 2024
DOI 10.3389/fmed.2024.1426577

OPEN ACCESS

EDITED BY
Giuseppe Fiorentino,
Hospital of the Hills, Italy

REVIEWED BY
Hrishikesh Pandit,
National Heart, Lung, and Blood Institute (NIH), United States
Martina Maritati,
University of Ferrara, Italy

*CORRESPONDENCE
Qiong-Fang Yang
qfy195581@163.com

RECEIVED 01 May 2024
ACCEPTED 08 July 2024
PUBLISHED 22 July 2024

CITATION
Yang Q-F and Shu C-M (2024) Severe community-acquired pneumonia caused by *Chlamydia abortus* in China: a case report. *Front. Med.* 11:1426577. doi: 10.3389/fmed.2024.1426577

Severe community-acquired pneumonia caused by *Chlamydia abortus* in China: a case report

Qiong-Fang Yang * and Cai-Min Shu

Department of Respiratory Medicine, Affiliated Dongyang Hospital of Wenzhou Medical University, Dongyang, Zhejiang, China

Background: *Chlamydia abortus* causes abortions in ruminants; it can also cause miscarriages and stillbirths in pregnant women. However, it rarely causes pneumonia in humans. Here, we report a case of severe community-acquired pneumonia caused by *C. abortus*.

Case presentation: On admission to our hospital, a 74-year-old woman reported that she had had a fever, cough, phlegm in her throat, and shortness of breath for 10 days. In the local hospital, she was initially diagnosed with community-acquired pneumonia and treated with piperacillin–tazobactam for 4 days. However, her condition worsened, and she was therefore transferred to our hospital. On arrival at our emergency department, she was diagnosed with severe community-acquired pneumonia and treated with a high-flow nasal cannula and meropenem; she was then transferred to the Department of Respiratory Medicine. There, her condition continued to worsen despite continued treatment with the high-flow nasal cannula and omadacycline. After 24 h and emergency tracheal intubation, the patient was sent to the intensive care unit (ICU) for further treatment. The doctors in the ICU again adjusted the treatment, this time to meropenem along with mechanical ventilation; they also instituted methylprednisolone, ulinastatin, nadroparin calcium, and human immunoglobulin. In addition, bronchoalveolar lavage fluid was sent for metagenomic next-generation sequencing (mNGS). Subsequent mNGS suggested the presence of *C. abortus,* sequence number 5072; we therefore discontinued the meropenem and implemented a combination of doxycycline and moxifloxacin. After 8 days of treatment in the ICU, the patient's condition improved; she was then extubated and, 3 days later, transferred back to the respiratory medicine department. The respiratory physician continued to administer doxycycline and moxifloxacin for 4 days, after which the patient was discharged with medication. A month later, a repeat computed tomography (CT) scan of the chest suggested that the lesions in both lungs had been largely absorbed.

Conclusion: *C. abortus* can occasionally cause pneumonia in humans and, rarely, severe, life-threatening pneumonia. mNGS is uniquely suited for the early detection of this unusual infection. The combination of doxycycline and quinolones has been shown to be effective in severe pneumonia caused by *C. abortus*.

KEYWORDS

severe, community-acquired pneumonia, *Chlamydia abortus*, metagenomic next-generation sequencing, case report

Introduction

Chlamydia, as an obligate intracellular Gram-negative bacterium, is known to be responsible for several serious global healthcare challenges. Among these bacteria, *Chlamydia abortus* is an especially important zoonotic pathogen; it mainly causes infections in ruminants but, less frequently, may cause pneumonia in humans. Even more rarely, it can initiate an extremely severe pneumonia (1). Thus far, only six cases of pneumonia due to *C. abortus* have been reported worldwide; of these, five were not severe (2–6) and only one was severe (7). To further raise awareness of this rare disease, we here describe a case of severe pneumonia caused by *C. abortus*.

Case presentation

A 72-year-old woman was admitted to our emergency department on December 1, 2023, with complaints of fever as well as cough, phlegm in the throat, and shortness of breath, all of which had been present for 10 days. She had had a cerebral infarction a year earlier as well as an aneurysm of the left internal carotid artery but did not take medication regularly. Nevertheless, she said that she was able to take care of herself. Ten days earlier, she had developed a cold and a fever with a temperature of about 38.0°C along with a cough, phlegm in her throat, dyspnea, generalized muscle aches and pains, and intermittent diarrhea. Her symptoms were not relieved by cold medicine. Thus, after 5 days of illness, she went to her local hospital. There, after computed tomography (CT) of the chest, she was diagnosed with community-acquired pneumonia. The CT pointed to an infection in the upper lobe of the left lung (Figure 1: 1A–C), and she was given piperacillin–tazobactam (4.5 g q8h as an intravenous infusion) for 4 days. However, her condition did not improve. She was then admitted to the emergency department of our hospital.

On the patient's arrival at our emergency department, physical examination showed the following: temperature, 38.9°C; respirations, 26/min; pulse, 102/min; blood pressure, 130/75 mmHg; oxygen saturation, 72% (under mask oxygen of 4 L/min); clear consciousness; tachypnea; rhythmic dry and wet rales audible in both lungs; abdominal tenderness; and no swelling of the limbs. Laboratory tests showed the following: calcitonin, 9.0 ng/mL; C-reactive protein, 299 mg/L; leukocyte count, 11.12×10^9/L; neutrophil ratio, 96.4% (which was significantly higher than normal). Arterial blood gas analysis showed type I respiratory failure and an oxygenation index of 108 mmHg. Blood biochemistry suggested hyponatremia and hypochlorhydria. Blood creatinine, liver enzymes, and lactate dehydrogenase were significantly higher than normal. The levels of plasma pro-brain natriuretic peptide (pro-BNP) were 1150 pg/mL (Table 1). A repeat CT scan of the chest suggested infectious lesions in both lungs and a small pleural effusion on each side (Figure 1: 2A–C). Color Doppler ultrasound of the vasculature of both lower extremities revealed atherosclerosis and intermuscular venous thrombosis of both lower legs. Color Doppler ultrasound of the heart showed aortic arteriosclerosis. Tricuspid valve regurgitation was mild; the ejection fraction was 65%. The patient was diagnosed with severe community-acquired pneumonia and was ventilated by a high-flow nasal cannula (oxygen concentration, 80%; flow rate, 55 L/min) with the oxygen saturation maintained at about 95%; she was also medicated with meropenem (0.5 g q8h by intravenous infusion) and methylprednisolone (40 mg q12h by intravenous infusion). At one point during this procedure, her blood pressure dropped to 90/52 mmHg; however, it returned to the normal level after active fluid replacement.

The next day the patient was admitted to the respiratory ward, and ventilation by high-flow nasal cannula (oxygen concentration 75%, flow rate 50 L/min) was continued to maintain oxygen saturation at about 95%. The retest of her blood inflammation index was still significantly higher than normal (Table 1), and it was felt that the atypical pathogen infection had to be covered. The treatment was therefore adjusted to omadacycline (0.1 g qd by intravenous infusion with 0.2 g being given on the first day), methylprednisolone (40 mg q12h by intravenous infusion), ambroxol hydrochloride (30 mg bid by intravenous infusion) for phlegm, and nadroparin calcium (4100 U qd by hypodermic injection) for anticoagulant and symptom-supportive therapy.

To detect the etiology of her pneumonia, the patient underwent a series of microbiologic diagnostic tests for bacteria, fungi, and viruses, and including staining and culture, serologic testing, and others. However, all of the tests were negative (Table 2). Thus the patient's clinical symptoms continued to deteriorate, with oxygen saturation maintained between 89 and 95%. She experienced shortness of breath and—after being given an emergency tracheal intubation for mechanical ventilation 24 h after admission—was transferred to the ICU.

At the ICU, her treatment was adjusted to meropenem (1.0 g q8h by intravenous infusion) with continuing methylprednisolone, ambroxol hydrochloride, and nadroparin calcium plus the addition of thymopeptide (1.6 mg qd by hypodermic injection) and immunoglobulin (10 g qd by intravenous infusion) to improve the immunity. On the next day, bedside bronchoscopy showed that there was more white mucous sputum in both bronchi, and the lumen was clear after aspiration. The bronchoalveolar lavage fluid was then sent for mNGS examination. Two days later, the result suggested *C. abortus*, with 5072 sequence numbers and a relative abundance of 95.03%. A repeat bedside radiograph of the chest showed infection in both lungs, with greater infection in the right lung and partial absorption of infection in the left lung by comparison with the previous (December 1, 2023) CT localization film of the chest (Figure 1: 3B). Therefore the patient was given moxifloxacin (0.4 g qd by intravenous infusion) combined with doxycycline (0.1 g bid PO), and the meropenem was stopped. The patient's condition gradually stabilized under these treatments; methylprednisolone was reduced; and eventually—after 8 days of mechanical ventilation—the tracheal tube was removed to be replaced by a nasal cannula for the administration of oxygen. The bedside chest radiograph was then reviewed again; it pointed to infections in both lungs, similar to the previous one (December 6, 2023), with a small pleural effusion on the left side (Figure 1: 3C). After extubation, the patient appeared to have blood in her sputum. A review of the color Doppler ultrasound of her lower extremity vessels suggested that there was no increase in thrombus, so the

Abbreviations: ICU, intensive care unit; mNGS, metagenomic next-generation sequencing; CT, computed tomography; CRP, C-reactive protein; pro-BNP, pro-brain natriuretic peptide.

TABLE 1 Changes in laboratory indicators.

Test	Day 1	Day 3	Day 6	Day 9	Day 14	Day 18	Reference range
WBC	11.12	15.06	7.01	7.94	6.15	4.40	3.5–9.5 (10^9/L)
CRP	299.3	171.8	53.4	29.5	14.8	22.8	<8 (mg/L)
PCT	9.01	7.25	1.54	0.526	0.497	0.385	<0.1 (ng/ml)
IL-6	404.71	57.18	–	–	4.18	–	<5.4 (pg/ml)
D-dimer	4.52	5.55	–	2.66	2.65	12.79	<0.5 (ug/ml)
Cr	114	122	110	74	–	108	57–111 (umol/L)
Pro-BNP	1150	–	4102	1400	–	279.5	5–125 (pg/ml)
ALT	461	405	308	74	64	32	15–40 (U/L)
AST	72	217	195	36	40	13	9–50 (U/L)
Na	126.0	137.1	136.0	129.0	135.0	137.3	137–147 (mmol/L)
Cl	87.1	104.0	111.0	102.0	100.0	99.9	99–110 (mmol/L)
Alb	20.3	–	26.6	–	28.5	37.8	40–55 (g/L)
LDH	539	468	–	–	–	253	109–245 (U/L)

WBC, White blood cell count; CRP, C-reactive protein; PCT, Procalcitonin; interleukin-6, IL-6; Cr, creatinine; Pro-BNP, Pro-Brain Natriuretic Peptide; ALT, alanine aminotransferase; AST, aspartate aminotransferase; Na, serum sodium; Cl, serum chlorine; Alb, Albumin; LDH, lactate dehydrogenase.

nadroparin calcium was stopped. Three days after extubation, the patient was stable and transferred back to respiratory medicine.

In the respiratory medicine department, moxifloxacin and doxycycline were continued up to 14 days. During this period, CT pulmonary angiography did not indicate a thrombus. A repeat CT scan of the chest suggested partial resorption of the lesions whereas others had increased, as had the bilateral pleural effusions (Figure 1: 4A–C). After 14 days of antichlamydial treatment, the patient's blood inflammatory index had returned to normal; therefore, the antibiotics were stopped. Because the serum D-dimer level increased to 12.79 μg/mL, after communicating with the patient's family members, the patient was discharged with a prescription for rivaroxaban 10 mg qd PO. A month after discharge, the patient was reexamined by CT of the chest, indicating significant absorption of both lung lesions and pleural effusions (Figure 1: 5A–C). The full timeline of hospitalization and clinical treatment is shown in Figure 2.

Discussion

Chlamydia abortus used to be classified as a subspecies of *Chlamydia psittaci*, which caused mainly animal infections, with abortion and stillbirth being common among pregnant cows and sheep (8) and could also lead to miscarriage in pregnant women, sepsis in pregnancy, and pelvic inflammatory disease (3, 9, 10). However, thus far, only six cases of human pneumonia due to *C. abortus* have been found worldwide. *C. abortus* organisms can be excreted through urine, feces, lactated milk, amniotic fluid, placenta, aborted fetus, and other routes in diseased animals (11). Based on the findings of previously reported cases, most patients infected with *C. abortus* appear to have a history of direct or indirect contact with infected animals (2–7). This suggests that humans can become ill through direct contact with infected animals or secondary owing to contamination of the environment. The patient in this case was a farmer who fed small animals such as chickens, ducks, and pigs at home and had regular contact with these animals. Therefore we suspected that the patient might have developed pneumonia through direct contact with animals infected with *C. abortus*. No one else in the family was known to have had a similar infection.

C. abortus infection initially presents with flulike symptoms, causing fever, headache, and weakness in the limbs. Due to the lack of specificity of the clinical symptoms and clinicians' low level of knowledge of the disease, it is easy to miss or misdiagnose this disease. Chlamydial infection can also cause serious visceral complications; therefore, clinicians need to be alert to this possibility (12, 13). In this case, the patient presented with typical influenza-like symptoms (such as fever and generalized muscle pain) at the beginning of the disease, followed by respiratory symptoms (such as cough, phlegm, and dyspnea). These were accompanied by extrapulmonary manifestations such as diarrhea as well as laboratory tests suggesting hyponatremia and hypochlorhydria, impaired hepatic and renal function, and elevated lactate dehydrogenase. These are similar to the clinical features of *Legionella* pneumonitis (14) and *C. psittaci* pneumonia (15).

This patient's lung imaging showed rapid progression from a solid lesion in the upper lobe of the left lung to solid lesions in multiple lobes, with air bronchial signs at the site of the solid lesion accompanied by bilateral pleural effusions. These imaging features are nonspecific and are also seen in streptococcal and other atypical infections, making early diagnosis of the pathogen critical.

Pneumonia caused by *C. abortus* is very rare and cannot be detected by current detection methods, such as specimen culture, serologic detection, and the polymerase chain reaction. mNGS, as an unbiased method—with its high detection speed, high accuracy, wide coverage, and high throughput (16)—theoretically detects all pathogens in clinical samples and is particularly suitable for rare and complex infectious diseases with atypical etiology (17). In this case—after blood culture, sputum culture, and chlamydial nucleic

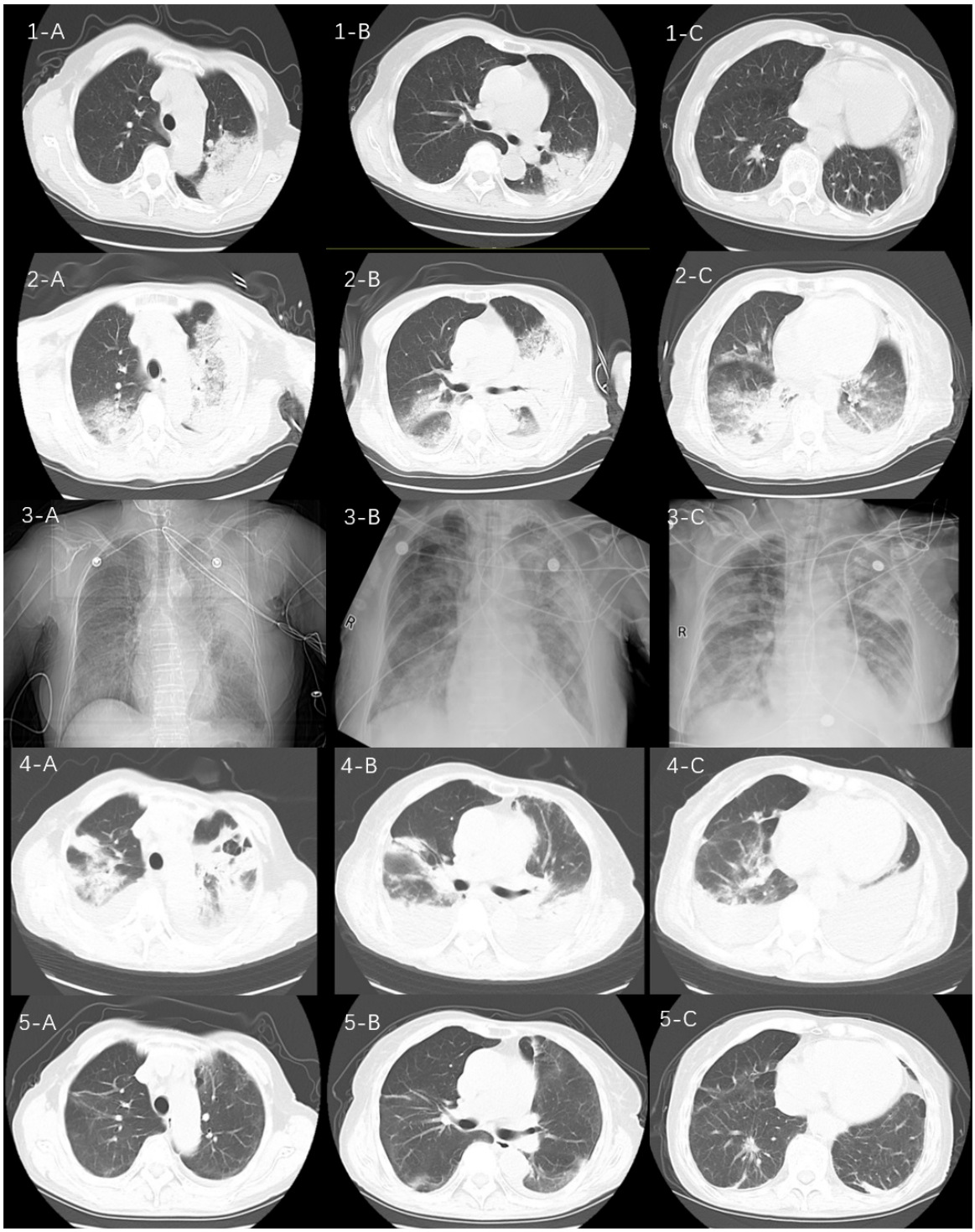

FIGURE 1
Sequential computed tomograms (CTs) of the patient's chest. CT at a local hospital (1A–C) appeared to show a solid shadow in the upper lobe of the left lung. CT on admission (2A–C) showed multiple exudative lesions in both lungs. The next images (3A–C) represent the patient's chest x-ray findings at the time of admission to our hospital, on the 5th and 10th days, respectively. CTs on the 15th day of admission (4A–C) suggested infection in both lungs with partially absorbed and partially enlarged lesions as well as an enlarging pleural effusion on the left side. CTs 1 month after discharge (5A–C) show substantial resorption of the lesions in both lungs.

acid testing were all found to be negative—we were able to diagnose *C. abortus* by mNGS.

C. abortus is unaffected by beta-lactam antibiotics because it lacks a cell wall. *Chlamydia* is usually sensitive to antibiotics that inhibit DNA and protein synthesis, including tetracyclines, macrolides, and quinolones. Therefore, tetracyclines are used as first-line therapeutic agents, whereas other approaches include macrolides and quinolones (18). The length of

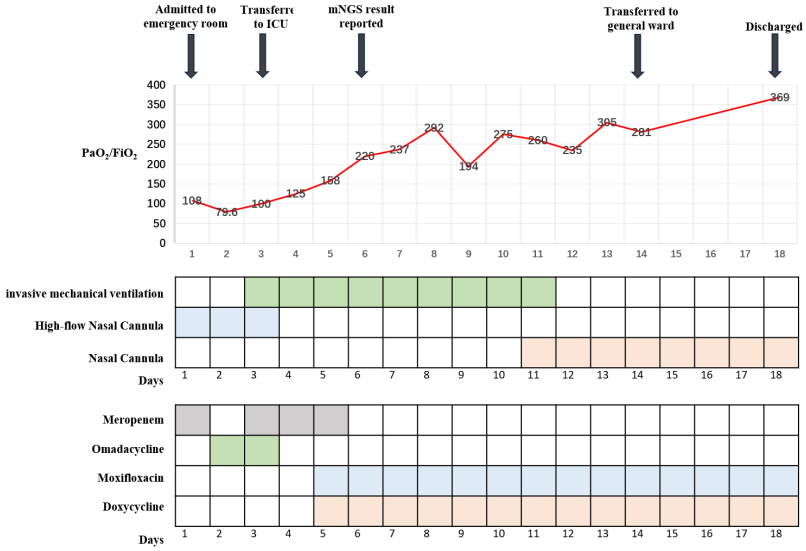

FIGURE 2
Hospitalization timeline and clinical treatments.

TABLE 2 Etiological examination results.

Test	Results	Reference range
Blood culture	Negative	Negative
Sputum bacterial culture	Negative	Negative
Cryptococcus antigen	Negative	Negative
T-SPOT	Non-reactive	Non-reactive
Fungus-D glucan determination	<40	<60 (Pg/ml)
Galactomannan determination	0.2	<0.25 (ug/L)
Sputum smear for acid-fast bacilli	Negative	Negative
Sputum tuberculosis culture	Negative	Negative
Influenza virus nucleic acid	Negative	Negative
COVID-19 nucleic acid	Negative	Negative
Adenovirus nucleic acid	Negative	Negative
Respiratory syncytial virus nucleic acid	Negative	Negative
Mycoplasma pneumoniae nucleic acid	Negative	Negative
Chlamydia nucleic acid	Negative	Negative
Legionella pneumophila nucleic acid	Negative	Negative
Streptococcus pneumoniae nucleic acid	Negative	Negative
Haemophilus influenzae nucleic acid	Negative	Negative
Bordetella pertussis nucleic acid	Negative	Negative

antibiotic administration is usually 10–14 days. In this case, immediately after confirmation of *C. abortus* infection, the antibiotics were adjusted to doxycycline combined with moxifloxacin, which had an immediate effect. Repeat CT of the chest 1 month later showed substantial resorption of both lung lesions.

In summary, ruminants can transmit *Chlamydia abortus* to humans. Its early diagnosis is low owing to nonspecific clinical signs and imaging features, making it hard to detect by conventional tests. Therefore, if early β-amide antibiotics are ineffective in patients with pneumonia who have a history of ruminant exposure, the possibility of infection with *Chlamydia abortus* must be considered. mNGS of the bronchoalveolar lavage fluid is an important method for diagnosing this disease.

Data availability statement

The original contributions presented in this study are included in this article/supplementary material, further inquiries can be directed to the corresponding author.

Ethics statement

Written informed consent was obtained from the individual(s) for the publication of any potentially identifiable images or data included in this article.

Author contributions

Q-FY: Writing – original draft, Writing – review and editing. C-MS: Writing – review and editing.

Funding

The author(s) declare that no financial support was received for the research, authorship, and/or publication of this article.

Acknowledgments

We would like to thank the nurses, and residents from the department of respiratory (Affiliated Dongyang Hospital of Wenzhou Medical University, Dongyang, China), who were involved in the management of the patient. We would also like to thank LetPub (www.letpub.com) for its linguistic assistance during the preparation of this manuscript.

Conflict of interest

The authors declare that the research was conducted in the absence of any commercial or financial relationships that could be construed as a potential conflict of interest.

Publisher's note

References

1. Xie G, Hu Q, Cao X, Wu W, Dai P, Guo W, et al. Clinical identification and microbiota analysis of *Chlamydia psittaci*- and *Chlamydia abortus*- pneumonia by metagenomic next-generation sequencing. *Front Cell Infect Microbiol.* (2023) 13:1157540. doi: 10.3389/fcimb.2023.1157540

2. Ortega N, Caro M, Gallego M, Murcia-Belmonte A, Álvarez D, Del Río L, et al. Isolation of *Chlamydia abortus* from a laboratory worker diagnosed with atypical pneumonia. *Irish Vet J.* (2015) 69:8. doi: 10.1186/s13620-016-0067-4

3. Pichon N, Guindre L, Laroucau K, Cantaloube M, Nallatamby A, Parreau S. *Chlamydia abortus* in pregnant woman with acute respiratory distress syndrome. *Emerg Infect Dis.* (2020) 26:628–9. doi: 10.3201/eid2603.191417

4. Zhu C, Lv M, Huang J, Zhang C, Xie L, Gao T, et al. Bloodstream infection and pneumonia caused by *Chlamydia abortus* infection in China: A case report. *BMC Infect Dis.* (2022) 22:181. doi: 10.1186/s12879-022-07158-z

5. Imkamp F, Albini S, Karbach M, Kimmich N, Spinelli C, Herren S, et al. Zoonotic *Chlamydiae* as rare causes of severe pneumonia. *Swiss Med Wkly.* (2022) 152:w30102. doi: 10.4414/smw.2022.w30102

6. Liu M, Wen Y, Ding H, Zeng H. Septic shock with *Chlamydia abortus* infection. *Lancet Infect Dis.* (2022) 22:912. doi: 10.1016/s1473-3099(21)00756-8

7. Huang J, Liu C, Zhou Z, Xia H, Zhu Z, Lu J, et al. Extracorporeal membrane oxygenation in severe acute respiratory distress syndrome caused by *Chlamydia abortus*: A case report. *Infect Drug Resist.* (2023) 16:3893–901. doi: 10.2147/idr.S411331

8. Caspe S, Ewing D, Livingstone M, Underwood C, Milne E, Sargison N, et al. The immune response in the uteri and placentae of *Chlamydia abortus*-infected ewes and its association with pregnancy outcomes. *Pathogens.* (2023) 12:846. doi: 10.3390/pathogens12060846

9. Pospischil A, Thoma R, Hilbe M, Grest P, Zimmermann D, Gebbers J. [Abortion in humans caused by *Chlamydophila abortus* (*Chlamydia psittaci* serovar 1)]. *Schweizer Arch Tierheilkunde.* (2002) 144:463–6. doi: 10.1024/0036-7281.144.9.463

10. Walder G, Meusburger H, Hotzel H, Oehme A, Neunteufel W, Dierich M, et al. *Chlamydophila abortus* pelvic inflammatory disease. *Emerg Infect Dis.* (2003) 9:1642–4. doi: 10.3201/eid0912.020566

11. Everett K, Bush R, Andersen A. Emended description of the order Chlamydiales, proposal of Parachlamydiaceae fam. nov. and Simkaniaceae fam. nov., each containing one monotypic genus, revised taxonomy of the family Chlamydiaceae, including a new genus and five new species, and standards for the identification of organisms. *Int J Syst Bacteriol.* (1999) 49:415–40. doi: 10.1099/00207713-49-2-415

12. Walder G, Hotzel H, Brezinka C, Gritsch W, Tauber R, Würzner R, et al. An unusual cause of sepsis during pregnancy: Recognizing infection with *Chlamydophila abortus*. *Obstetr Gynecol.* (2005) 106:1215–7. doi: 10.1097/01.AOG.0000161060.69470.9c

13. Rohde G, Straube E, Essig A, Reinhold P, Sachse K. Chlamydial zoonoses. *Deutsches Arzteblatt Int.* (2010) 107:174–80. doi: 10.3238/arztebl.2010.0174

14. Muggetti E, Fusi-Schmidhauser T, Schwarzenbach H, Pons M. [CME: *Legionella pneumonia*]. *Praxis.* (2020) 109:658–64. doi: 10.1024/1661-8157/a003467

15. Kong C, Zhu J, Lu J, Xu Z. Clinical characteristics of *Chlamydia psittaci* pneumonia. *Chin Med J.* (2021) 134:353–5. doi: 10.1097/cm9.0000000000001313

16. Liu H, Zhang Y, Yang J, Liu Y, Chen J. Application of mNGS in the etiological analysis of lower respiratory tract infections and the prediction of drug resistance. *Microbiol Spectr.* (2022) 10:e0250221. doi: 10.1128/spectrum.02502-21

17. Goldberg B, Sichtig H, Geyer C, Ledeboer N, Weinstock G. Making the leap from research laboratory to clinic: Challenges and opportunities for next-generation sequencing in infectious disease diagnostics. *mBio.* (2015) 6:e1888–1815. doi: 10.1128/mBio.01888-15

18. Kohlhoff S, Hammerschlag M. Treatment of Chlamydial infections: 2014 update. *Expert Opin Pharmacother.* (2015) 16:205–12. doi: 10.1517/14656566.2015.999041

frontiers | Frontiers in Medicine

TYPE Case Report
PUBLISHED 13 August 2024
DOI 10.3389/fmed.2024.1411338

OPEN ACCESS

EDITED BY
Karolina Henryka Czarnecka-Chrebelska,
Medical University of Lodz, Poland

REVIEWED BY
Cristiano Bortoluzzi,
Azienda Ulss 12 Veneziana, Italy
Tulika Chatterjee,
University of Illinois at Peoria, United States

*CORRESPONDENCE
Qingmin He
✉ 13095037353@163.com

†These authors have contributed equally to this work

RECEIVED 02 April 2024
ACCEPTED 30 July 2024
PUBLISHED 13 August 2024

CITATION
Deng Y, Lai J and He Q (2024) Pulmonary thromboembolism: a case report and misdiagnosis analysis of a 63-year-old female patient.
Front. Med. 11:1411338.
doi: 10.3389/fmed.2024.1411338

Pulmonary thromboembolism: a case report and misdiagnosis analysis of a 63-year-old female patient

Yingli Deng[1†], Jing Lai[1†] and Qingmin He[2*]

[1]Second Ward, Department of Respiratory and Critical Care Medicine, Ankang Central Hospital, Ankang, Shaanxi, China, [2]Department of Gastroenterology, Ankang Central Hospital, Ankang, Shaanxi, China

This paper presents a case of a 63-year-old female patient who was initially misdiagnosed with mycoplasma pneumonia due to symptoms such as chest pain, hemoptysis, and fever, but was later confirmed to have pulmonary thromboembolism (PTE) through further examination. This case highlights the similarities between PTE and pneumonia in terms of symptoms, as well as the complexity of PTE diagnosis. The article provides a detailed description of the patient's medical history, symptoms, examination process, and treatment outcomes. Furthermore, it discusses the possible reasons for the misdiagnosis, including insufficient awareness of PTE among physicians, lack of in-depth investigation into the causes of abnormally elevated D-dimer levels, the non-specific clinical manifestations of PTE, and the concerns of the patient's family regarding pulmonary artery CTA examination. Additionally, the article emphasizes the importance of clinicians in improving their ability to differentiate and diagnose PTE, rationally utilizing clinical examination methods, and ensuring timely diagnosis and treatment of PTE.

KEYWORDS

pulmonary thromboembolism, pneumonia, misdiagnosis, diagnosis, case report

1 Introduction

Pulmonary thromboembolism (PTE) is a disease triggered by thrombi originating from the venous system or right heart, which obstruct the pulmonary arteries or their branches, leading to impairments in pulmonary circulation and respiratory function (1, 2). As one of the common cardiopulmonary vascular diseases in China (3, 4), the primary clinical manifestations of PTE include dyspnea, chest pain, and cough. However, these symptoms closely resemble the respiratory symptoms of mycoplasma pneumonia, leading to frequent misdiagnosis and subsequent missed diagnosis, which can severely impact the prognosis of patients. This paper aims to illustrate a typical case of PTE that was misdiagnosed as pneumonia.

2 Case presentation

A 63-year-old female presented to our hospital with complaints of chest pain and hemoptysis for 18 days, accompanied by fever for 13 days. Her symptoms began while traveling

on a long-distance train, manifesting as right-sided chest pain and mild cough with scanty dark red bloody sputum, which gradually worsened. Despite receiving symptomatic treatment (including cough suppression, analgesia, and fever reduction) at the local health clinic, her condition did not improve. Thirteen days prior to admission, she developed fever and was diagnosed with mycoplasma pneumonia, where she was treated with piperacillin, moxifloxacin, and other medications. Although the fever resolved, her chest pain and hemoptysis persisted, and she developed shortness of breath. A chest CT scan revealed an increase in lung lesions.

Upon admission to our hospital, her initial physical examination revealed a blood pressure of 135/75 mmHg, a pulse oximetry reading of 92%, and decreased breath sounds in the right lower lung with few wet rales audible. The remaining lung fields had slightly coarse breath sounds. There was pitting edema in both lower extremities, with no other significant abnormalities noted. Her preliminary diagnoses were: (1) Community-acquired pneumonia (non-severe), (2) Pleural effusion, (3) Pulmonary hemorrhage, and (4) Hypoxemia. Differential diagnoses: (1) Acute lung abscess; (2) Bronchiectasis with infection. She was initially treated with anti-infective therapy (Intravenous infusion of moxifloxacin 0.4 g qd for 1 week), oxygen inhalation, and other symptomatic measures.

Subsequent investigations revealed sinus bradycardia and T-wave changes on ECG. Pulmonary artery CTA showed emboli in the main trunk of the right pulmonary artery and its branches in the upper, middle, and lower lobes of the right lung (Figures 1A–D). The scanned right lung appeared to have inflammatory changes, and partial pulmonary infarction could not be excluded. There were no significant abnormalities on bilateral lower extremity vascular ultrasonography. Echocardiography revealed mild tricuspid regurgitation and reduced left ventricular diastolic function. Blood gas analysis indicated an oxygen partial pressure of 67.00 mmHg at a 35% oxygen inhalation concentration, with a calculated oxygenation index <200 mmHg, suggesting type I respiratory failure. Coagulation studies revealed a fibrinogen concentration of 5.36 g/L and a D-dimer level of 10.80 mg/L. Blood tests showed a C-reactive protein level of 22.71 mg/L, a hypersensitive C-reactive protein level > 10.0 mg/L, and a procalcitonin level of 0.760 ng/mL. Both sputum TN-RNA and general bacterial cultures were negative. Chest ultrasonography detected a small amount of fluid in the right costophrenic angle.

Based on the aforementioned auxiliary examinations, the revised diagnoses are as follows: (1) Pulmonary embolism (submassive), (2) Type I respiratory failure, (3) Pulmonary infarction, (4) Pulmonary hemorrhage, (5) Community-acquired pneumonia (non-severe), (6) Mycoplasma infection, (7) Exudative pleural effusion, (8) Sinus bradycardia, and (9) Hyperfibrinogenemia. An anticoagulation regimen was initiated with subcutaneous injections of heparin calcium 5,000 IU twice daily for 5 days, concomitant with anti-infection therapy, oxygen inhalation, and symptomatic treatment. Following improvement in hemoptysis, oral rivaroxaban 15 mg twice daily was administered as sequential therapy, with no changes to the remainder of the treatment plan. After undergoing the aforementioned therapies, the patient exhibited significant alleviation of chest pain, hemoptysis, and shortness of breath, with no recurrence of fever.

Subsequent investigations were conducted to further evaluate the patient's condition. Sputum pathology revealed no malignant tumor cells. Dynamic electrocardiogram showed sinus bradycardia with occasional atrial and ventricular premature beats, while ST-T segments remained unremarkable. Pulmonary artery CTA demonstrated slight resorption of emboli in the main trunk of the right pulmonary artery and its branches in the upper, middle, and lower lobes of the right lung compared to previous images (Figures 1E–H). Additionally, the scanned lesions in the right lung showed slight resorption, suggestive of inflammation, although partial pulmonary infarction in the right lung could not be excluded. Repeat blood gas analysis was essentially normal, and D-dimer levels decreased significantly.

The discharge diagnoses encompassed the following: (1) Pulmonary embolism (submassive), (2) Type I respiratory failure, (3) Pulmonary infarction, (4) Pulmonary hemorrhage, (5) Community-acquired pneumonia (non-severe), (6) Mycoplasma infection, (7) Exudative pleural effusion, (8) Sinus bradycardia, (9) Hyperfibrinogenemia, (10) Atrial premature beats, and (11) Ventricular premature beats.

Following clinical improvement and stabilization after anticoagulation, anti-infection therapy, oxygen therapy, and other treatments, the patient requested discharge. Oral anticoagulation therapy with rivaroxaban was continued after discharge. One month later, during a follow-up visit, the patient reported no chest pain, dyspnea, or hemoptysis. Repeat pulmonary artery CTA showed a reduction in emboli in the main trunk of the right pulmonary artery and its branches in the upper, middle, and lower lobes of the right lung compared to previous images (Figures 1I–L). Moreover, the scanned lesions in the right lung had decreased in size. The detailed illustration of the entire treatment process is provided (Figure 2).

3 Discussion

PTE, the most common clinical type of pulmonary embolism, primarily results from the obstruction of pulmonary arteries and their branches by emboli formed due to the detachment of deep venous thrombi in the lower extremities. This blockage subsequently leads to a clinical syndrome caused by the interruption of tissue blood supply. In recent years, the incidence of PTE among the elderly population has been increasing year by year. According to relevant reports, the inpatient mortality rate of elderly PTE patients aged 65 and above is 3–10 times higher compared to younger patients, posing a severe threat to the health of the elderly.

The classic triad of symptoms in pulmonary infarction includes dyspnea, chest pain, and hemoptysis. However, these symptoms do not always occur simultaneously in patients with pulmonary infarction. Additionally, the nonspecific nature of their clinical manifestations often leads to delays in diagnosis. To facilitate more effective diagnosis of PTE, the following clinical examination methods may provide valuable assistance.

1. Pulmonary Embolism Rule-Out Criteria (PERC): The PERC score serves as a tool for assessing the risk of pulmonary embolism based on a series of clinical factors, encompassing patient age, oxygen saturation (SaO2), pulse rate, hemoptysis, recent trauma or surgery history, venous thromboembolism (VTE) history, unilateral leg swelling, and a history of oral steroid use (5). Specifically, a patient with an age under 50, absence of hemoptysis and unilateral leg swelling, pulse rate

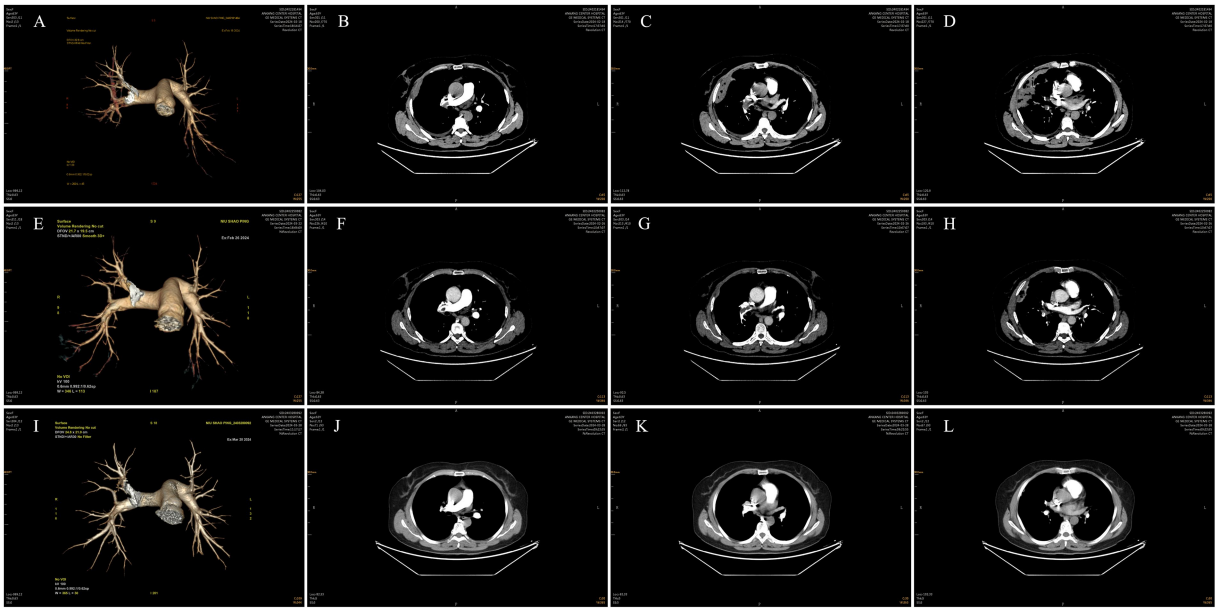

FIGURE 1
Pulmonary artery CTA. **(A–D)** Pulmonary artery CTA showed emboli in the main trunk of the right pulmonary artery and its branches in the upper, middle, and lower lobes of the right lung. **(E–H)** Pulmonary artery CTA demonstrated slight resorption of emboli in the main trunk of the right pulmonary artery and its branches in the upper, middle, and lower lobes of the right lung compared to previous images. **(I–L)** Pulmonary artery CTA showed a reduction in emboli in the main trunk of the right pulmonary artery and its branches in the upper, middle, and lower lobes of the right lung compared to previous images.

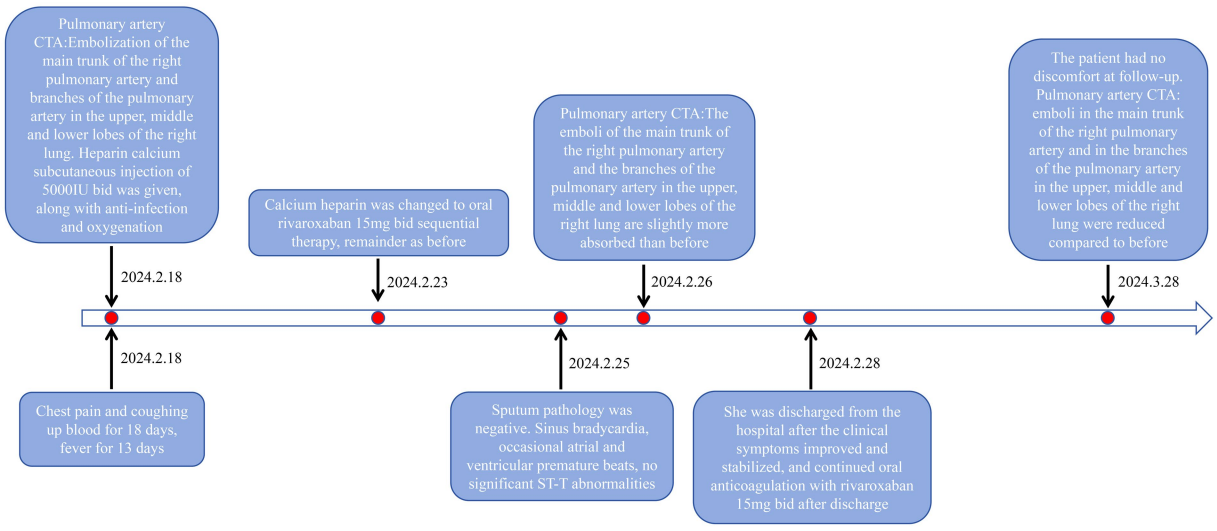

FIGURE 2
Treatment history of the case.

below 100 beats per minute, oxygen saturation above 94%, and no history of VTE, recent trauma or surgery, or oral steroid use, is considered to have a negative PERC score, indicating a relatively low risk of pulmonary embolism. Conversely, the presence of any one or more positive indicators among the aforementioned factors would result in a positive PERC score, suggesting a potentially higher risk of pulmonary embolism and thus necessitating further investigations and screenings for pulmonary embolism.

2. The relationship between D-dimer and PTE: D-dimer is an indicator that reflects the hypercoagulable state and fibrinolytic activity of the body. In the diagnosis of PTE, D-dimer demonstrates high sensitivity but relatively low specificity (6). Therefore, when utilizing D-dimer for PTE diagnosis, it is

necessary to comprehensively consider other clinical indicators to make a more accurate judgment.

3. The role of electrocardiogram (ECG) in PTE diagnosis: Following the occurrence of PTE, ECG changes exhibit diversity, and some PTE patients may even present with completely normal ECGs (7). The lack of specificity in ECG alterations poses significant challenges for clinical differential diagnosis, which may subsequently lead to delays in the diagnosis and treatment of PTE.
4. The association between lower extremity venous ultrasonography and PTE: Examination of the deep veins of the lower extremities in PTE patients has revealed that a considerable proportion of them have deep venous thrombosis (DVT). The prevalence of DVT is significantly higher in elderly patients compared to non-elderly individuals, and there is a close relationship between DVT and PTE. Therefore, performing lower extremity venous ultrasonography in elderly patients suspected of having PTE holds important clinical significance (8). However, it is worth noting that even if the lower extremity venous ultrasonography appears normal, the possibility of pulmonary embolism cannot be completely ruled out.
5. Application of Wells Score in PTE Assessment: According to large-scale data, a lower Wells score indicates a lower likelihood of pulmonary embolism as perceived by clinicians (9, 10). However, with the deepening of research on pulmonary embolism, it has been found that many patients assessed as low-risk by the Wells score are still diagnosed with acute pulmonary embolism after undergoing pulmonary artery CTA examination. Therefore, when elderly patients present with symptoms such as hypoxemia or have underlying diseases such as chronic obstructive pulmonary disease, even if their Wells score is low, we still need to be highly vigilant about the possibility of acute pulmonary embolism.
6. The Role of Pulmonary Artery CTA in PTE Diagnosis: Currently, pulmonary artery CTA has become an important method for diagnosing pulmonary embolism (11, 12). However, clinical observations have revealed an overuse of pulmonary artery CTA, primarily driven by the concerns of treating physicians about missing acute pulmonary embolism. This overuse not only increases the economic burden on patients but also exposes them to potential risks of malignancy due to excessive ionizing radiation and adverse effects such as nephropathy and allergic reactions caused by contrast agents. Therefore, pulmonary artery CTA should primarily be used for the confirmation or exclusion of suspected pulmonary embolism patients and should not be employed as a routine examination tool.

After a thorough analysis of the clinical data presented in this case study, we postulate that the misdiagnosis of the patient may have been attributed to several factors. Firstly, the patient's prominent clinical symptoms at the time of admission, including fever, chest pain, and hemoptysis, were highly similar to those of pneumonia and pleurisy, leading the treating physician to initially suspect a pulmonary infectious disease. Secondly, the patient exhibited several high-risk factors for PTE, such as prolonged sitting, bilateral lower extremity edema, bradycardia, and abnormally elevated D-dimer levels. However, due to the clinician's lack of experience, PTE-related examinations were not promptly initiated, and these symptoms were erroneously attributed to the patient's advanced age and hypercoagulable state. Thirdly, during the patient's stay at the primary hospital, neither echocardiography nor chest CT revealed any changes indicative of pulmonary embolism in the pulmonary arteries or right heart system, lacking typical evidence for a diagnosis of pulmonary embolism, which contributed to its easy misdiagnosis in clinical practice. Fourthly, the limited availability of equipment at the primary hospital precluded the possibility of performing comprehensive pulmonary artery CTA examinations, which is also one of the reasons for missed and misdiagnoses of pulmonary embolism in such settings. Fifthly, despite presenting with typical initial symptoms of pulmonary embolism, the patient's lack of attention to their own condition led to a delay in seeking medical attention until the onset of infectious complications, resulting in a diagnostic bias by the treating physician.

When encountering patients with high-risk factors for PTE but exhibiting non-typical PTE signs in clinical practice, if the patients subsequently develop pulmonary infection complications and fail to respond significantly to anti-infective therapy, we should reassess and consider conducting a screening for PTE. This approach aims to enhance the diagnostic rate of PTE, ensuring timely, accurate diagnosis and treatment for the patients. During the review of this case, we rigorously adhered to the epidemiological characteristics, predisposing factors, clinical manifestations, diagnostic criteria, and treatment protocols outlined in the guidelines (13). Through comprehensive evaluation, meticulous screening, and thorough related examinations, we ultimately confirmed the diagnosis of pulmonary embolism for the patient. This diagnosis was based on sufficient evidence, ensuring the accuracy and reliability of the diagnosis. In terms of treatment, we administered a reasonable therapeutic regimen tailored to the patient's specific condition and conducted follow-up evaluations. The current prognosis of the patient is acceptable, further validating the effectiveness of our diagnostic and therapeutic strategies.

The clinical symptoms of pneumonia are diverse and include fever, cough, chest tightness, and chest pain. In severe cases, difficulty breathing and hemoptysis may also occur. These symptoms share certain similarities with the clinical manifestations of pulmonary embolism, leading to potential confusion in diagnosis and subsequent missed diagnoses of pulmonary embolism, which can negatively impact patient prognosis. Given this, the accurate diagnosis of pulmonary embolism poses significant challenges, requiring clinicians to continuously enhance their differential diagnosis skills in daily practice to ensure timely identification and treatment of this disease.

Data availability statement

The original contributions presented in the study are included in the article/supplementary material, further inquiries can be directed to the corresponding author.

Ethics statement

The studies involving humans were approved by the Ethics Committee of Ankang Central Hospital. The studies were

conducted in accordance with the local legislation and institutional requirements. Written informed consent for participation was not required from the participants or the participants' legal guardians/next of kin in accordance with the national legislation and institutional requirements. Written informed consent was obtained from the individual(s) for the publication of any potentially identifiable images or data included in this article.

Author contributions

YD: Writing – original draft. JL: Writing – original draft. QH: Writing – original draft, Writing – review & editing.

Funding

The author(s) declare no financial support was received for the research, authorship, and/or publication of this article.

Acknowledgments

The authors would like to thank the editors and reviewers for their valuable comments and suggestions to improve the quality of the paper.

Conflict of interest

The authors declare that the research was conducted in the absence of any commercial or financial relationships that could be construed as a potential conflict of interest.

Publisher's note

References

1. Huisman MV, Barco S, Cannegieter SC, Le Gal G, Konstantinides SV, Reitsma PH, et al. Pulmonary embolism. *Nat Rev Dis Primers*. (2018) 4:18028. doi: 10.1038/nrdp.2018.28

2. Essien EO, Rali P, Mathai SC. Pulmonary embolism. *Med Clin North Am*. (2019) 103:549–64. doi: 10.1016/j.mcna.2018.12.013

3. Konstantinides SV, Meyer G, Becattini C, Bueno H, Geersing GJ, Harjola VP, et al. 2019 ESC guidelines for the diagnosis and management of acute pulmonary embolism developed in collaboration with the European Respiratory Society (ERS). *Eur Heart J*. (2020) 41:543–603. doi: 10.1093/eurheartj/ehz405

4. Raskob GE, Angchaisuksiri P, Blanco AN, Buller H, Gallus A, Hunt BJ, et al. Thrombosis: a major contributor to global disease burden. *Arterioscler Thromb Vasc Biol*. (2014) 34:2363–71. doi: 10.1161/ATVBAHA.114.304488

5. Freund Y, Cachanado M, Aubry A, Orsini C, Raynal PA, Féral-Pierssens AL, et al. Effect of the pulmonary embolism rule-out criteria on subsequent thromboembolic events among low-risk emergency department patients: the PROPER randomized clinical trial. *JAMA*. (2018) 319:559–66. doi: 10.1001/jama.2017.21904

6. Philbrick JT, Heim S. The d-dimer test for deep venous thrombosis: gold standards and bias in negative predictive value. *Clin Chem*. (2003) 49:570–4. doi: 10.1373/49.4.570

7. Tapson VF. Acute pulmonary embolism. *N Engl J Med*. (2008) 358:1037–52. doi: 10.1056/NEJMra072753

8. Johnson SA, Stevens SM, Woller SC, Lake E, Donadini M, Cheng J, et al. Risk of deep vein thrombosis following a single negative whole-leg compression ultrasound: a systematic review and meta-analysis. *JAMA*. (2010) 303:438–45. doi: 10.1001/jama.2010.43

9. Doherty S. Pulmonary embolism an update. *Aust Fam Physician*. (2017) 46:816–20.

10. Wells PS, Anderson DR, Rodger M, Stiell I, Dreyer JF, Barnes D, et al. Excluding pulmonary embolism at the bedside without diagnostic imaging: management of patients with suspected pulmonary embolism presenting to the emergency department by using a simple clinical model and d-dimer. *Ann Intern Med*. (2001) 135:98–107. doi: 10.7326/0003-4819-135-2-200107170-00010

11. Moores LK, Jackson WJ, Shorr AF, Jackson JL. Meta-analysis: outcomes in patients with suspected pulmonary embolism managed with computed tomographic pulmonary angiography. *Ann Intern Med*. (2004) 141:866–74. doi: 10.7326/0003-4819-141-11-200412070-00011

12. van Beek EJ, Brouwerst EM, Song B, Stein PD, Oudkerk M. Clinical validity of a normal pulmonary angiogram in patients with suspected pulmonary embolism--a critical review. *Clin Radiol*. (2001) 56:838–42. doi: 10.1053/crad.2001.0778

13. Khandait H, Harkut P, Khandait V, Bang V. Acute pulmonary embolism: diagnosis and management. *Indian Heart J*. (2023) 75:335–42. doi: 10.1016/j.ihj.2023.05.007

frontiers | Frontiers in Medicine

TYPE Case Report
PUBLISHED 21 August 2024
DOI 10.3389/fmed.2024.1399381

OPEN ACCESS

EDITED BY
Giuseppe Fiorentino,
Hospital of the Hills, Italy

REVIEWED BY
Sanjay Gautam,
International Vaccine Institute,
Republic of Korea
Madjid Morsli,
Center Hospitalier Universitaire de Nîmes,
France

*CORRESPONDENCE
Michael E. Otim
✉ dr.michael@dmcg.edu

RECEIVED 11 March 2024
ACCEPTED 01 July 2024
PUBLISHED 21 August 2024

CITATION
Sawan BA, Saleh LO, Al Shaltouni DZ, Sawan MA, Gawish S, Ahmed S, Gomez-Seco J and Otim ME (2024) Pulmonary infection by *Mycobacterium riyadhense*: first case report in United Arab Emirates.
Front. Med. 11:1399381.
doi: 10.3389/fmed.2024.1399381

Pulmonary infection by *Mycobacterium riyadhense*: first case report in United Arab Emirates

Batool A. Sawan[1], Leen O. Saleh[1], Dina Z. Al Shaltouni[1], Mohammad A. Sawan[2], Shefa Gawish[1], Samar Ahmed[1], Julio Gomez-Seco[3] and Michael E. Otim[1]*

[1]Department of Public Health, Dubai Medical College, Dubai, United Arab Emirates, [2]Department of Medicine, Near East University, Nicosia, Cyprus, [3]Fakeeh University Hospital, Dubai, United Arab Emirates

Mycobacterium riyadhense is an emerging slowly growing species that belongs to the group of nontuberculous mycobacteria (NTM) with approximately 20 cases reported worldwide. We highlight the first case of pulmonary infection by *Mycobacterium riyadhense* in United Arab Emirates (UAE). A 44-year-old female presented with chronic productive cough; a bronchial breathing pattern was appreciated on auscultation of her right upper lung. She was treated multiple times with allergic medications and antibiotics. Thorough investigations revealed *Mycobacterium riyadhense* and antitubercular drugs were started, eventually she was cured, however she had multiple relapses later. This case report holds a significant potential to make considerable contribution to the diagnosis of NTM, primarily because it presents the first documented case in UAE, as well as insights on how to address possible similar cases in the future.

KEYWORDS

non-tuberculous mycobacteria, *Mycobacterium riyadhense*, pulmonary cavity, chronic cough, antitubercular drugs

Introduction

Mycobacterium riyadhense (*M. riyadhense*), is a newly recognized slow-growing, non-photochromogenic NTM. *Mycobacterium riyadhense* was first isolated from a patient in Riyadh, Kingdom of Saudi Arabia (KSA) who presented with maxillary sinus infection in 2009 (1). To-date, about 20 cases have been reported in the literature.

Mycobacterium riyadhense seems to be capable of causing a spectrum of clinical presentations that are clinically indistinguishable from Tuberculosis (TB) (2). Despite pulmonary involvement being the most common form of non-tuberculous mycobacterial infections, a range of extra-pulmonary presentations have been reported. The clinical and radiologic findings of pulmonary infection caused by *M. riyadhense* are indifferent from those caused by *M. tuberculosis*, which is the most important human pathogen of the *Mycobacterium tuberculosis* complex (MTBC) (3).

Case presentation

A previously healthy 44-year-old female of German origin, living in UAE for more than 8 years, was referred to our care by an internist. She presented at Fakeeh University Hospital in Dubai, United Arab Emirates, in November 2021 with a chronic cough and purulent sputum lasting for 1 year. Earlier in mid-2020, she developed a persistent dry cough and sought medical attention from a general practitioner. Following an allergy test that revealed her sensitivity to pollen, she was prescribed Antihistamines, which were ineffective in alleviating her symptoms.

In May 2021, she was inaccurately treated in a local clinic for a bacterial infection with Ampicillin, which unfortunately triggered an allergic reaction. In September 2021, she returned to the local clinic with new onset yellowish sputum and was prescribed another course of antibiotics that the patient does not recall. In November 2021, she experienced a recurrence of the same symptoms, which drove her to Fakeeh University Hospital for medical advice. However, she did not exhibit any significant weight loss, night sweats, fever, or hemoptysis. Her past medical and family history is insignificant. She is a nonsmoker, a married housewife who lives at home with her family, none of whom are experiencing similar symptoms. Additionally, she stated having not had contact with TB patients and stated that there are no pets at home. It is also worth mentioning that she has never received the Bacille Calmette-Guerin (BCG) vaccine and travels annually to her homeland during the holidays.

Generally, she appeared alert, oriented, well-nourished, and not in distress. The physical examination showed no cervical lymphadenopathy. Auscultation of the chest revealed normal bilateral vesicular breathing, with a bronchial breathing pattern noted in the right upper lung. Sputum samples were collected for further investigations. In addition, a chest *x*-ray was done, revealing a pulmonary cavity as shown in Figure 1. The sputum culture, conducted over a 6-week period, reported growth of *Mycobacterium riyadhense* in December 2021 as seen in Table 1, with drug sensitivity tested and showed susceptibility to all first- and second-line anti-TB medications. Consequently, a 6-month course of anti-TB medications was initiated, consisting of 2 months of Isoniazid, Rifampin, Pyrazinamide, and Ethambutol, followed by 4 months of Isoniazid and Rifampin. Additionally, vitamin B6 supplements were given, along with a battery of serial investigations to detect any possible medication side effects. These side effects include: visual field assessment; uric acid levels; and liver function tests were monitored monthly and were all nearly normal. After completing the anti-TB regimen, symptoms subsided with radiological images showing improvement.

On July 27, 2022, the patient experienced a relapse characterized by fever and productive cough, NTM was confirmed again by PCR, but drug sensitivity was not retested at this point. Consequently, she was restarted on the same anti-TB medications, effectively alleviating the symptoms. An immunodeficiency workup was conducted in August 2022, and the findings are presented in Table 1. Additionally, a chest computed tomography (CT) scan was ordered to accurately evaluate the progression of her disease. The scan revealed a pulmonary cavity in the right lung (Figure 2A) and a "tree-in-bud" pattern, indicating the presence of mucus and pus causing the normally invisible peripheral airway to become visible (Figure 3A). 1 month later, a bronchoscopy with biopsy was performed to potentially identify other granulomatous diseases that resemble tuberculosis, given the patient's recent relapse. Biopsy results showed necrotizing granuloma in the submucosa of the right upper lung. For more details, refer to Table 1.

In early January 2023, just 1 month before completing her second anti-TB course (2 months of Isoniazid, Rifampin, Pyrazinamide, and Ethambutol, followed by 4 months of Isoniazid and Rifampin), she relapsed again for a week, presenting with night sweats, fever, productive cough, and pain in the upper right chest. Subsequently,

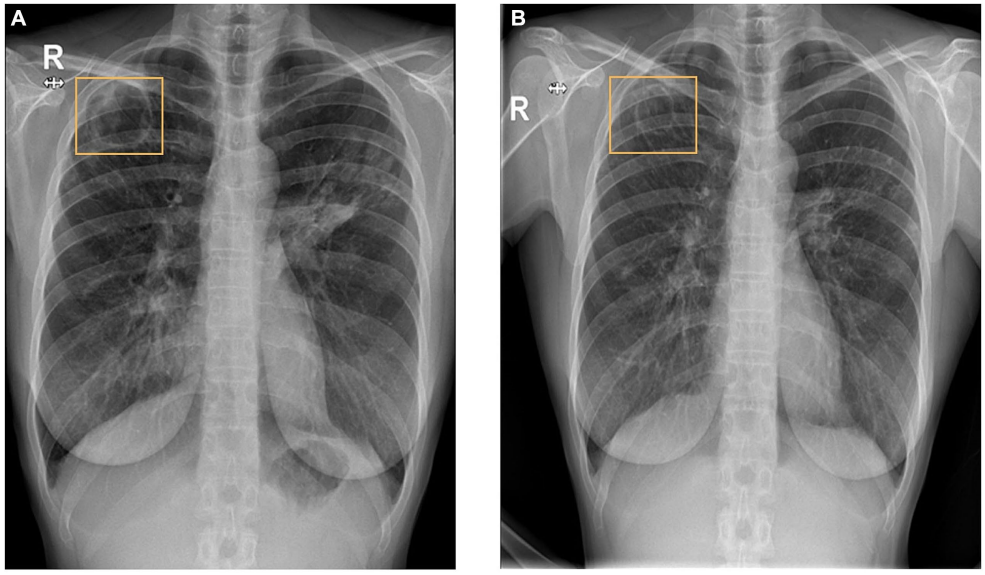

FIGURE 1
A well-defined cavity in the right upper lung measuring 4.5 cm and patchy consolidation in the left upper and middle lobes in November 2021 **(A)**. Over time, the cavity reduced in size to 3.5 cm then to 3.2 cm with regression of the infiltrates in the left upper lobe in December 2022 **(B)**.

TABLE 1 Timeline of disease course and serial investigations.

Date	Symptoms	Investigation/Intervention	Result
Nov./2021 (outpatient)	Chronic productive cough with yellowish sputum for 3 months.	- Sputum AFB stain	- After 2 days came Positive +3.
		- PCR	- After 1 week came positive NTM.
		- LJ culture for 6 weeks	- After 6 weeks came positive (*Mycobacterium Riyadhense*).
Feb./2022 (during first anti-TB course)	Asymptomatic	- AFB stain for sputum	- Negative
		- LJ medium for culture	- Negative
July/2022 (first relapse) (outpatient)	Fever and cough	- PCR	- After 1 week came positive NTM.
Aug./2022	Asymptomatic	- CTD panel	- All negative
		- IgA, IgM, IgG, and A1AT	- Normal
		- HIV IgM and IgG	- Negative
Sept./2022 (outpatient)		- Bronchoscopy with biopsies	- Trachea showed diffuse inflammation. - Right bronchial tree: inflammation with whitish phlegm and transbronchial biopsy taken from the posterior segment of RUL showed Necrotizing granuloma in submucosa. - Left bronchial tree: inflammation with whitish phlegm with stenosis of 60% in the anterior segment of LUL and the biopsy taken at the entry of it was benign. - Bronchoalveolar lavage done and when tested was acellular, Micro negative, AFB negative, and cytology negative.
Jan./2023 (second relapse) (outpatient)	Fever, cough, night sweats, and chest pain	- CRP	- CRP 11 mg/dL
		- ESR	- ESR 28 mm/h
		- Sputum AFB	- AFB Positive +4
Feb./2024 (inpatient)	Cough	- Right upper lobectomy (admitted for 5 days)	- Specimen showed caseating granulomas with no evidence of malignancy or vasculitis.
	1 week after surgery: Fever, productive cough, and night sweats.	- Thoracocentesis (admitted for 4 days)	- Pleural fluid analysis: 98% lymphocytes consistent with mycobacterial infection.

AFB, Acid fast Bacilli; PCR, Polymerase chain reaction; LJ, Lowenstein–Jensen; CTD, Connective tissue disease; HIV, Human immunodeficiency virus; RUL, Right upper lobe; LUL, Left upper lobe; CRP, C-reactive protein; and ESR, Erythrocyte sedimentation rate.

M. riyadhense was detected by sputum acid-fast bacilli (AFB) stain and culture, showing sensitivity to all four anti-TB medications (Table 1). Following a multidisciplinary team discussion to modify her medications, a decision was made to start Ethambutol and Pyrazinamide, along with Linezolid 600 mg and Moxifloxacin 400 mg. We also included biweekly electrocardiograms to monitor QTc for possible side effects. However, she did not opt for the new regimen, stating that she is feeling better. In addition, a consultation with a thoracic surgeon was planned to discuss the possibility of segmentectomy vs. right upper lobectomy. This consideration arises as the cavity likely functioned as a bacterial reservoir, contributing to her frequent relapses. Despite controversial radiologic findings with worsening pulmonary cavity seen in Figure 2B and regressing "tree-in-bud" pattern seen in Figure 3B, the patient appeared reluctant to undergo the latter procedure. After thorough discussion, the patient decided to wait and to get back to the hospital whenever she is ready to resume treatment.

In February 2024, the patient contacted the thoracic surgeon to proceed with right upper lung lobectomy, which was uneventful with good lung expansion and no pleural effusion. One week after discharge, she presented with fever, profuse night sweats, and productive cough, which was diagnosed as moderate right-sided pleural effusion for which she was admitted for 4 days. Ultrasound-guided thoracentesis (with pleural sampling) was performed, and the pleural fluid analysis showed lymphocytic exudate and a negative AFB stain, highly suggestive of mycobacterial pleural effusion. The previously suggested modified regimen was initiated, which includes Ethambutol 1,200 mg OD, Pyrazinamide 1,500 mg OD, Moxifloxacin 400 OD, and Linezolid 600 OD (+ Pyridoxine 10 mg OD). In March 2024, Moxifloxacin caused severe tendinitis,

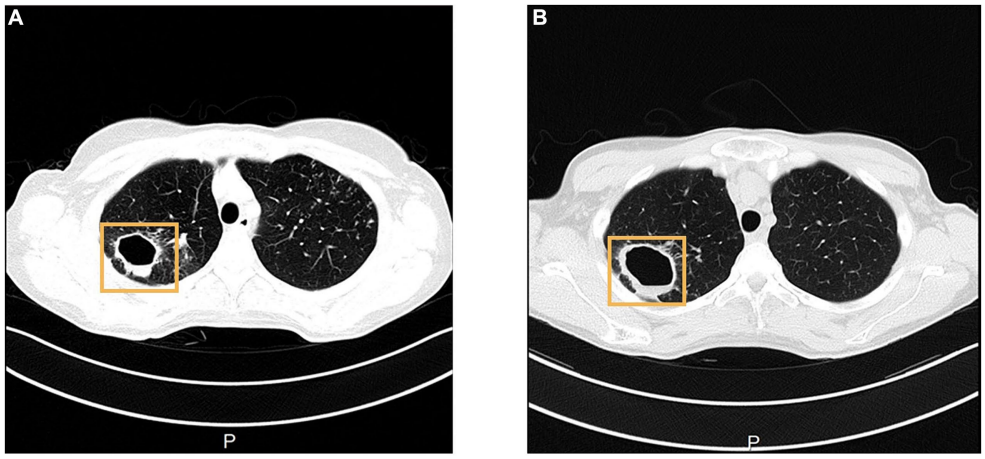

FIGURE 2
CT shows an increase in the size of right upper lung cavity, from 3.2 cm on 31st August 2022 **(A)**, to 4.5 cm on 16th January 2023 **(B)**. In the CT image, A stands for Anterior, and P stands for Posterior.

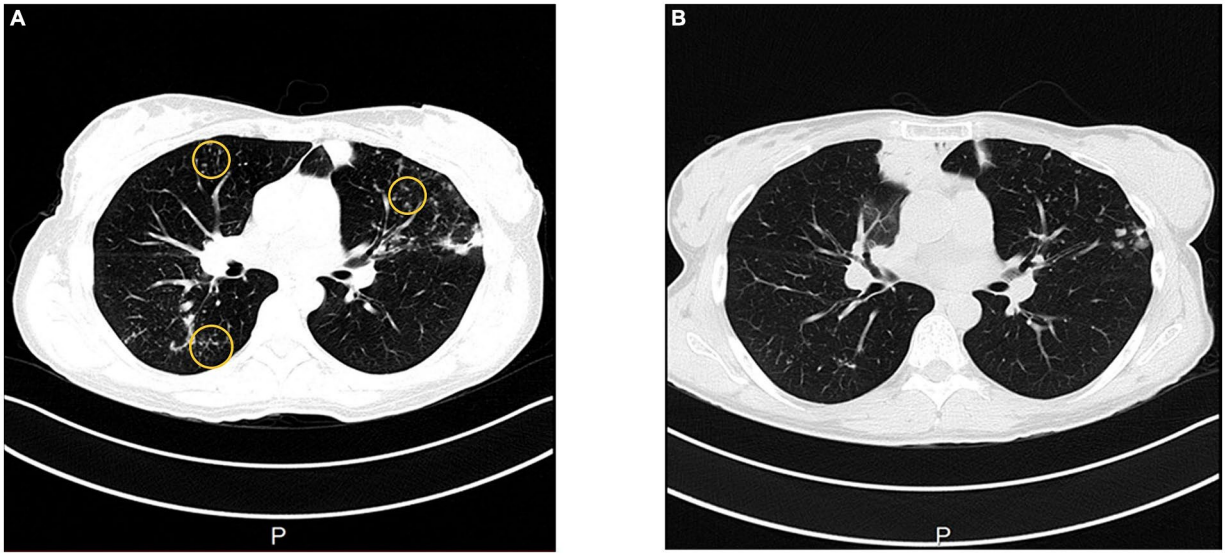

FIGURE 3
In August 2022, CT shows bronchiectasis with micronodular infiltrates with a "tree-in-bud" pattern in the right lower lobe and left lingula **(A)**, that have regressed over time in January 2023 **(B)**.

which was replaced by Rifampin with the rest of the regimen unchanged.

In April 2024, after the latest drug sensitivity results were received, the patient's treatment plan was modified to Isoniazid 300 mg OD, Rifampin 600 mg OD, Ethambutol 1,200 mg OD, Pyrazinamide 1,500 mg OD, and Clarithromycin 500 mg BID. After the final treatment plan, during the subsequent follow-up visit, the patient stated that her symptoms significantly improved apart from a minimal residual cough that is slowly improving. She expressed satisfaction with the results and the plan of care.

Discussion

Mycobacterium riyadhense is a nontuberculous species of bacteria belonging to the genus Mycobacterium, first identified in Riyadh, KSA, hence its name. The rising incidence of NTM infections constitutes a major epidemiological and public health threat worldwide (4). It seems that the infection is not limited to certain geographical locations since cases have been reported from France (5), Bahrain (5), and South Korea (6) in addition to Saudi Arabia.

Nontuberculous mycobacteria are generally rare, but they are a common cause of infection in immunocompromised hosts. *Mycobacterium riyadhense* has been lately described as an opportunistic infection that affects individuals with suppressed immune status as in HIV patients. Although HIV patients are prone to pulmonary infections by opportunistic pathogens in the late stage of AIDS, manifesting the disease with pulmonary infection caused by *Mycobacterium riyadhense* is extremely rare with only one case reported in the literature (7). Interestingly, two new cases have been reported in the literature with *Mycobacterium riyadhense* being the first presentation of an opportunistic infection that led to HIV diagnosis (7).

Mycobacterium riyadhense primarily affects the lungs but can also involve other organs. There is no evidence of human-to-human transmission yet reported (3). Not very different from other mycobacteria, symptoms of infection with *M. riyadhense* include persistent cough, fever, night sweats, asthenia, and weight loss. Diagnosis typically involves culturing the bacteria from clinical samples and performing molecular tests for accurate identification, as only culture can differentiate *M. riyadhense* from *M. tuberculosis*. Unfortunately, TB diagnosis is not always confirmed with cultures, and empirical treatment is sometimes started on a clinical basis. If this is added to reports that highlight the misidentification of NTM as *M. tuberculosis* (8), then a question arises as to whether at least some of the patients that are being treated as TB, might in fact have NTM infections. This is crucial because accurate diagnosis is essential for proper management and antibiotics choice. To date, no specific treatment regimen for *M. riyadhense* has been developed (1). Although resistance to Isoniazid is common, most patients responded well to standard anti-TB regimens and were cured (1).

In the other cases of *M. riyadhense*, incorrect diagnoses of TB were made, but in our case, misdiagnosis was prevented by PCR and culture, which excluded TB and warranted early treatment with serial laboratory and radiologic follow up. Regarding the culture medium used for the cultivation of *M. riyadhense*, a liquid medium (MGIT, "mycobacteria growth indicator tube," in the automated MGIT 960 system, BD) was used along with two different solid media (Lowenstein-Jensen and Stone brink medium). The isolate grew on all of them. Additionally, differentiation was performed by 16S sequencing. Limited knowledge about this pathogen raises questions about its infectivity and possible drug resistance that may challenge treatment used as in our case of *M. riyadhense*, which was initially (December 2021) susceptible to all anti-TB drugs but later developed resistance. In April 2023, using sputum culture, drug sensitivity showed resistance to Ciprofloxacin, Clarithromycin, Trimethoprim-sulfamethoxazole and intermediate resistance to Doxycycline. In April 2024, using the lung tissue sample obtained during lobectomy, drug sensitivity showed resistance to Trimethoprim-sulfamethoxazole and intermediate resistance Doxycycline, Ciprofloxacin and interestingly, showed susceptibility to Clarithromycin which explains why it was added in the final regimen.

Conclusion

Identification of this previously unknown pathogen raises concerns for human health and demonstrates the continuing threat caused by NTM. With the rising global prevalence of NTM, comes the need for accurate diagnosis and appropriate management of *Mycobacterium riyadhense* infections in the region. Therefore, clinicians should be skeptical and vigilant to the possible emergence of *M. riyadhense* as a more common pathogen.

Patient perspective

> Having experienced a complicated and rare case of Mycobacterium with three relapses over a span of more than 2 years, I found the treatment journey to be a mix of satisfaction and frustration. While the medications initially yielded a good response, the frequent relapses and the necessity of undergoing surgery left me feeling disheartened. Despite the challenges, I am immensely grateful to my doctor for their support and guidance throughout this difficult period. Currently, I am significantly improving and for that, I am truly thankful.

Data availability statement

The datasets presented in this article are not readily available because access to the data has to be through the Institutional Review Board or the corresponding author. Requests to access the datasets should be directed to MO, Dr.michael@dmcg.edu.

Ethics statement

The studies involving humans were approved by Institutional Research Board, Dubai Medical College, Dubai, UAE. The studies were conducted in accordance with the local legislation and institutional requirements. The participants provided their written informed consent to participate in this study. Written informed consent was obtained from the individual(s) for the publication of any potentially identifiable images or data included in this article.

Author contributions

BS: Formal Analysis, Writing – original draft, Writing – review & editing, Conceptualization, Methodology, Project administration, Resources, Validation, Investigation. LS: Conceptualization, Formal Analysis, Investigation, Methodology, Resources, Writing – original draft, Writing – review & editing, Validation, Funding acquisition, Supervision. DA: Conceptualization, Formal Analysis, Investigation, Methodology, Resources, Validation, Writing – original draft, Writing – review & editing, Data curation, Project administration. MS: Conceptualization, Data curation, Formal Analysis, Investigation, Methodology, Resources, Writing – original draft, Writing – review & editing. SG: Formal Analysis, Investigation, Methodology, Resources, Writing – original draft, Writing – review & editing, Project administration, Supervision. SA: Conceptualization, Formal Analysis, Investigation, Methodology, Resources, Writing – original draft, Writing – review & editing, Project administration, Supervision, Funding acquisition. JG-S: Formal Analysis, Investigation, Methodology, Project administration, Resources, Supervision, Writing – original draft, Writing – review & editing, Conceptualization, Data

curation, Validation. MO: Conceptualization, Formal Analysis, Methodology, Project administration, Resources, Supervision, Writing – original draft, Writing – review & editing, Validation.

Funding

The author(s) declare that no financial support was received for the research, authorship, and/or publication of this article.

Acknowledgments

The authors would like to thank the patient for accepting to participate in this study.

Conflict of interest

The authors declare that the research was conducted in the absence of any commercial or financial relationships that could be construed as a potential conflict of interest.

Publisher's note

References

1. Varghese B, Enani MA, Althawadi S, Johani S, Fernandez GM, Al-Ghafli H, et al. *Mycobacterium riyadhense* in Saudi Arabia. *Emerg Infect Dis*. (2017) 23:1732–4. doi: 10.3201/eid2310.161430

2. Saad M, Alshukairi A, Qutub M, Elkhizzi N, Hilluru H, Omrani A. *Mycobacterium riyadhense* infections. *Saudi Med J*. (2015) 36:620–5. doi: 10.15537/smj.2015.5.11226

3. Guan Q, Garbati M, Mfarrej S, AlMutairi T, Laval T, Singh A, et al. Insights into the ancestry evolution of the *Mycobacterium tuberculosis* complex from analysis of *Mycobacterium riyadhense*. *NAR Genom Bioinform*. (2021) 3:1–16. doi: 10.1093/nargab/lqab070

4. Jeon D. Infection source and epidemiology of nontuberculous mycobacterial lung disease. *Tuberc Respir Dis*. (2019) 82:94–101. doi: 10.4046/trd.2018.0026

5. Godreuil S, Marchandin H, Michon AL, Ponsada M, Chyderiotis G, Brisou P, et al. *Mycobacterium riyadhense* pulmonary infection, France and Bahrain. *Emerg Infect Dis*. (2012) 18:176–8. doi: 10.3201/eid1801.110751

6. Choi J, Lim J, Kim SR, Lee SH, Park JS, Seo KW, et al. Lung infection caused by *Mycobacterium riyadhense* confused with *Mycobacterium tuberculosis*: the first case in Korea. *Ann Lab Med*. (2012) 32:298–303. doi: 10.3343/alm.2012.32.4.298

7. Alenazi TH, Alanazi BS, Alsaedy A, Khair A, Solomon R, Al Johani SM. *Mycobacterium riyadhense* as the opportunistic infection that lead to HIV diagnosis: a report of 2 cases and literature review. *J Infect Public Health*. (2019) 12:285–8. doi: 10.1016/j.jiph.2018.05.006

8. Tortoli E, Pecorari M, Fabio G, MessinòM FA. Commercial DNA probes for mycobacteria incorrectly identify a number of less frequently encountered species. *J Clin Microbiol*. (2010) 48:307–10. doi: 10.1128/JCM.01536-09

frontiers | Frontiers in Medicine

TYPE Case Report
PUBLISHED 25 September 2024
DOI 10.3389/fmed.2024.1406515

OPEN ACCESS

EDITED BY
Giuseppe Fiorentino,
Colli Hospital, Italy

REVIEWED BY
Luis Mas,
Auna Oncosalud, Peru
Kui Zhang,
Sichuan University, China

*CORRESPONDENCE
Min Zhao
✉ 57103729@hebmu.edu.cn
Yu-Dong Wang
✉ wyd_999@hebmu.edu.cn

†These authors have contributed equally to this work and share first authorship

RECEIVED 25 March 2024
ACCEPTED 09 September 2024
PUBLISHED 25 September 2024

CITATION
Lyu H-X, Ma W-H, Zhang Y-Q, Jin H, Wang Y-D and Zhao M (2024) Case report: Emerging therapies for transformed small cell lung cancer: efficacy of serplulimab and a comprehensive case report.
Front. Med. 11:1406515.
doi: 10.3389/fmed.2024.1406515

Case report: Emerging therapies for transformed small cell lung cancer: efficacy of serplulimab and a comprehensive case report

Heng-Xu Lyu[1†], Wen-Hua Ma[1†], Yong-Qian Zhang[1], Hui Jin[2], Yu-Dong Wang[2*] and Min Zhao[1*]

[1]Department of Oncology, The First Hospital of Hebei Medical University, Shijiazhuang, China, [2]Department of Medical Oncology, The Fourth Hospital of Hebei Medical University, Shijiazhuang, China

This research reports a case of histological transformation from non-small cell lung cancer (NSCLC) to transformed small cell lung cancer (T-SCLC) in a patient undergoing EGFR-tyrosine kinase inhibitors (TKIs). The aggressive characteristics of the tumor diverged significantly from those commonly associated with lung adenocarcinomas, leading to further histological analysis. The subsequent histological examination confirmed the transformation to SCLC, consistent with established mechanisms of acquired resistance in NSCLC. Given the limited therapeutic options, the patient was administered a serplulimab-based immunochemotherapy regimen, achieving a progression-free survival (PFS) of 6 months post-transformation. The study underscores the potential of PD-1 inhibitors, particularly serplulimab, in the treatment landscape for T-SCLC and highlights the need for future comprehensive research.

KEYWORDS

transformed small cell lung cancer (T-SCLC), immune checkpoint inhibitors (ICIs), immunotherapy, non-small cell lung cancer (NSCLC), case report

Introduction

Lung cancer is traditionally classified into two main histological categories: small-cell lung cancer (SCLC) and non-small cell lung cancer (NSCLC), with SCLC comprising approximately 15% of cases (1, 2). Recognized for its aggressive nature and tendency for metastasis, SCLC presents a notably poor prognosis, reflected in a 5-year survival rate of <7% (2–4). In recent years, oncologists have observed a phenomenon known as lineage plasticity, particularly prevalent in the field of lung cancer (5). Specifically, NSCLC may transform into SCLC following treatments such as tyrosine kinase inhibitors (TKIs), chemotherapy, or immunotherapy, and approximately 15% of epidermal growth factor receptor (EGFR)-mutant lung adenocarcinomas (LUAD) undergo histological transformation to SCLC following acquired resistance to TKIs (6, 7).

Transformed small cell lung cancer (T-SCLC) shares a similarly poor prognosis with conventional SCLC, reflecting one of the most aggressive and lethal forms of lung cancer (8). Standardized treatment strategies are notably absent for T-SCLC, and patients are managed with platinum-etoposide (PE) chemotherapy predominantly (8, 9). Previous studies have reported a median overall survival (OS) of only 6 to 10 months and a median progression-free survival (PFS) of 3 or 4 months following a diagnosis of T-SCLC (8, 10, 11). The comparably short survival and therapeutic dilemmas highlight

the complexity of managing T-SCLC and emphasize the urgent need for more effective therapeutic strategies.

The IMpower 133 studies have demonstrated the efficacy of adding the programmed death-ligand 1 (PD-L1) inhibitor atezolizumab to the PE regimen (12, 13). Compared to chemotherapy alone, this combination has improved OS and PFS in patients with extensive-stage SCLC (ES-SCLC), establishing it as a first-line treatment option for ES-SCLC. Furthermore, the ASTRUM-005 also verified the survival benefit of programmed cell death protein 1 (PD-1) inhibitor serplulimab combined with etoposide and carboplatin in ES-SCLC (14). Recently, the National Medical Products Administration (NMPA) approved a marketing application for a new indication of anti-PD-1 monoclonal antibody drug toripalimab injection in combination with etoposide and platinum for the first-line treatment of ES-SCLC, which provides a new option for the treatment of ES-SCLC. These have prompted a revolutionary breakthrough in the immunochemotherapy of SCLC for over 30 years. In a retrospective study, the incorporation of atezolizumab and chemotherapy for T-SCLC patients has been found to indicate a trend toward extending PFS and OS (15). These findings provide a promising clinical insight, suggesting that immune therapies targeting the PD-L1/PD-1 axis, proven effective in SCLC, may also hold potential for treating T-SCLC.

This report details the case of a patient who transformed into SCLC from EGFR TKI-resistant LUAD. Initially diagnosed with EGFR-mutated LUAD, the patient was treated with the third-generation TKI, osimertinib, followed by anlotinib as a second-line therapy. After transformation to SCLC at month 14 after first-line treatment, the patient was administered a combination therapy of the PD-1 inhibitor serplulimab, along with etoposide and carboplatin, achieving a PFS of 6 months.

Case presentation

Initial management of lung adenocarcinoma

A 65-year-old female patient presented to the Fourth Hospital of Hebei Medical University in September 2021 with symptoms of cough, sputum production, and dyspnea. She reported no smoking or any notable medical history; general physical examination and routine laboratory tests showed no abnormalities. Chest CT imaging demonstrated a mass at the right hilum accompanied by obstructive pneumonitis, nodularities on the right pleural surface, a pleural effusion on the right leading to lung atelectasis, and prominent mediastinal lymph nodes (Figure 1A). Cytologic analysis from the thoracentesis identified an abundance of atypical cells. Immunocytochemical staining revealed positive markers for TTF1, CK7, CEA, and NapsinA, but negative for WT-1, CDX2, GATA3, and PD-L1 (22C3) (Figures 2A–D). Next-generation sequencing (NGS) identified an *EGFR* L858R mutation in exon 21 with a frequency of 68.0%, and a *PTEN* mutation abundance of 10.2%, with no mutations detected in *RB1* and *TP53* genes. Based on the radiographic findings combined with the cytologic evaluation from the pleural fluid, the patient was diagnosed with stage IV lung adenocarcinoma (T2N2M1) with an Eastern Cooperative Oncology Group (ECOG) performance status (PS) of 1.

Following the confirmed diagnosis and in line with clinical guidelines, the patient was initiated on osimertinib (80 mg daily, orally), complemented by concurrent intrapleural cisplatin hyperthermic perfusion therapy (120 mg, every 10 days for four cycles). The best objective response observed was partial response (PR) based on RECIST criteria, with a PFS of 9 months (Figure 1B). By August 2022, a PET/CT scan was conducted due to shoulder pain, which displayed further disease progression, signified by metastatic involvement in the right pleura, mediastinum, right hilar lymph nodes, right iliac bone, and the right second posterior rib. Upon observing disease progression, anlotinib was administered orally at a dosage of 12 mg daily for a cycle of 14 consecutive days, followed by a 7-day discontinuation as a second-line treatment (Figures 1C, D). However, an echocardiographic assessment in September 2022 revealed a decline in the left ventricular ejection fraction (LVEF) to 38%, indicating a potential cardiomyopathy linked to TKI therapy. As a result, anlotinib treatment was discontinued.

Histological transformation to SCLC and subsequent management

In November 2022, the patients came to the First Hospital of Hebei Medical University for further treatment. Following first-line osimertinib therapy, the patient demonstrated continuous and widespread disease progression. The tumor's biological behavior began to diverge from the typical characteristics of lung adenocarcinoma. Given literature reports suggesting that histological transformation could be one of the mechanisms underlying tumor drug resistance, a repeat tumor biopsy was performed in November 2022. Pathological analysis identified the presence of poorly differentiated carcinoma. The subsequent immunohistochemical findings were as follows: TTF-1(+), CK7(−), NapsinA(−), Syn(+), CgA(−), CD56(+), Ki-67(>90%+), CK5/6(−), P40(−), P63(−), PD-L1(−), and MOC31(+) (Figures 2E–K). NGS revealed an *EGFR* L858R mutation in exon 21 with a frequency of 29.93%, and a *PTEN* mutation abundance of 86.32%, with no mutations detected in *RB1* and *TP53* genes. Additionally, the LVEF measured in November 2022 was 41%. Based on these results, the patient was diagnosed with extensive-stage small cell lung cancer, with an ECOG PS of 3.

There's no consensus in the medical community on a definitive treatment strategy for patients with T-SCLC. Historically, treatment predominantly revolved around etoposide combined with platinum-based chemotherapy (cisplatin/carboplatin), but these regimens offered limited efficacy. Reports indicate that combining immunotherapy and platinum-based chemotherapy can extend the PFS for T-SCLC patients compared to chemotherapy alone (12, 13). Moreover, the ASTRUM-005 study demonstrated that the combination of serplulimab, etoposide, and carboplatin as first-line therapy significantly prolonged PFS and OS for patients with ES-SCLC. Based on this emerging evidence, our patient was prescribed a regimen of serplulimab (200 mg on day 1), etoposide (70 mg/m^2 from days 1–5), and carboplatin (AUC 5 on day 1),

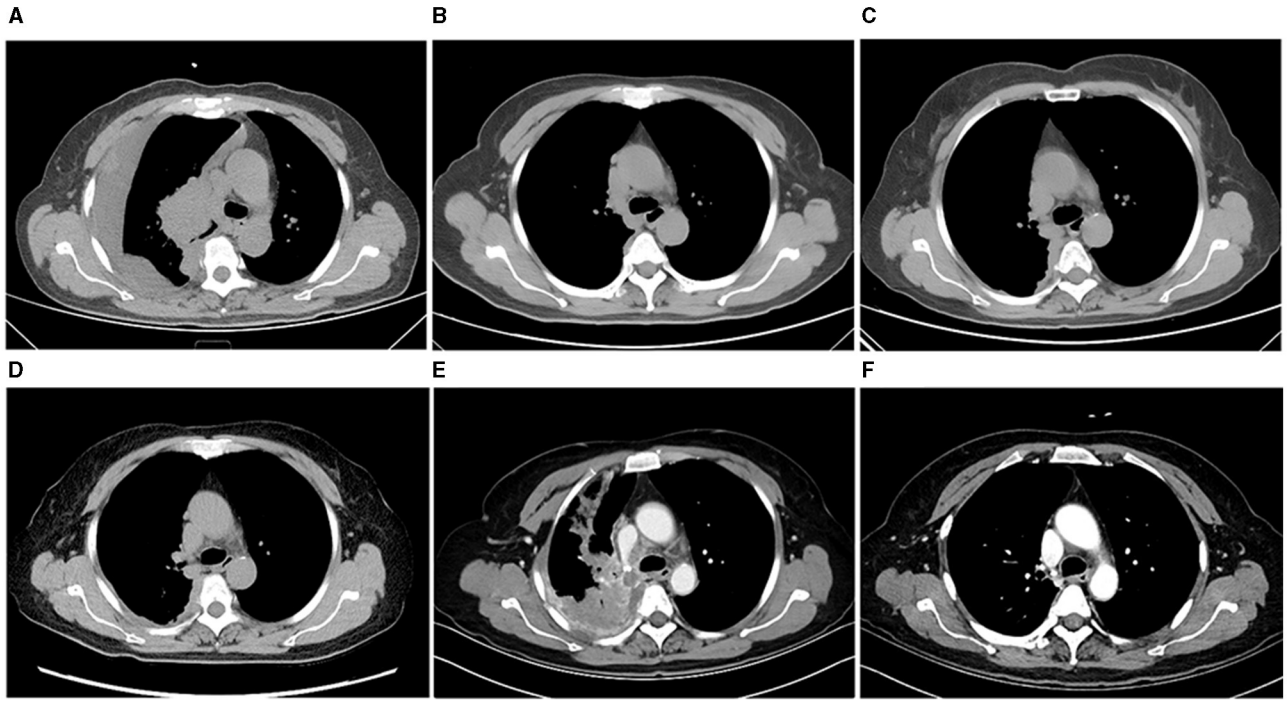

FIGURE 1
Evolution of thoracic tumor as revealed by chest CT imaging. **(A)** CT image at the time of initial diagnosis. **(B)** Partial response (PR) after first-line treatment. **(C)** Disease progression (PD) after first-line treatment. **(D)** Disease stable (SD) after second-line treatment. **(E)** PD after histological SCLC transformation. **(F)** PR after serplulimab-based treatment.

administered in 6-week cycles. The patient achieved a PR by the end of the second cycle in January 2023, and this response was maintained even after five cycles of the combination therapy, concluding in March 2023 (Figures 1E, F). The patient's general condition was alleviated rapidly following treatment. Alongside supportive care, there was a notable improvement in the LVEF, which normalized by the end of the second cycle. Additionally, the ECOG PS was evaluated as 1. However, the patient declined subsequent maintenance therapy with serplulimab.

In May 2023, the patient was readmitted presenting with symptoms of nausea and vomiting. Comprehensive diagnostic evaluations revealed that the pulmonary lesions remained stable. However, brain MRI and lumbar puncture conclusively identified metastasis to the central nervous system (CNS) (Figure 3). Unfortunately, localized radiation therapy yielded a suboptimal response. After a multidisciplinary team review, it was projected that her life expectancy is under 12 weeks, especially considering her deteriorated general health status reflected by an ECOG Performance Status of 4. Subsequently, the patient and her family chose to forego further treatment, opting for hospice care. The patient passed away later in the same month, marking an OS of 20 months since her lung cancer diagnosis.

Discussion

Acquired resistance following EGFR-TKI therapy is recognized as one of the mechanisms underlying the transformation from NSCLC to SCLC (6), and the transformation can only be conclusively diagnosed through histological methods. In the case we reported, the patient's PFS with the first-line osimertinib treatment was 9 months, significantly shorter than the previously reported 18.9 months (16). Moreover, the subsequent treatment with anlotinib yielded limited efficacy. After these two lines of systemic therapy, the patient's tumor exhibited a marked change in biological behavior, displaying increased aggressiveness, growth rate, and speed of metastasis, more akin to SCLC than the conventional lung adenocarcinomas typically associated with NSCLC. Coupled with literature evidence that histological transformation is one of the mechanisms of acquired resistance in treated NSCLC (especially in lung adenocarcinomas) (6, 17), these clues led us to suspect a potential histological transformation in this patient, prompting confirmation through a repeat biopsy. The patient's histological profile confirmed SCLC, originating from lung adenocarcinomas. Studies have generally demonstrated that histological transformation to SCLC occurs 16–19 months following treatment with EGFR-TKIs (5, 7, 8, 11). In contrast, the patient in our report experienced this transformation in the 14th month after osimertinib first-line treatment, slightly earlier than the literature.

Research into the complex molecular processes governing the transformation from NSCLC to SCLC has illuminated potential therapeutic pathways. Genomic sequencing revealed that the T-SCLC tumor tissue retains the *EGFR* mutation, although preclinical and clinical evidence indicates resistance to *EGFR* inhibition (18, 19). This feature is also observed in our case, where the

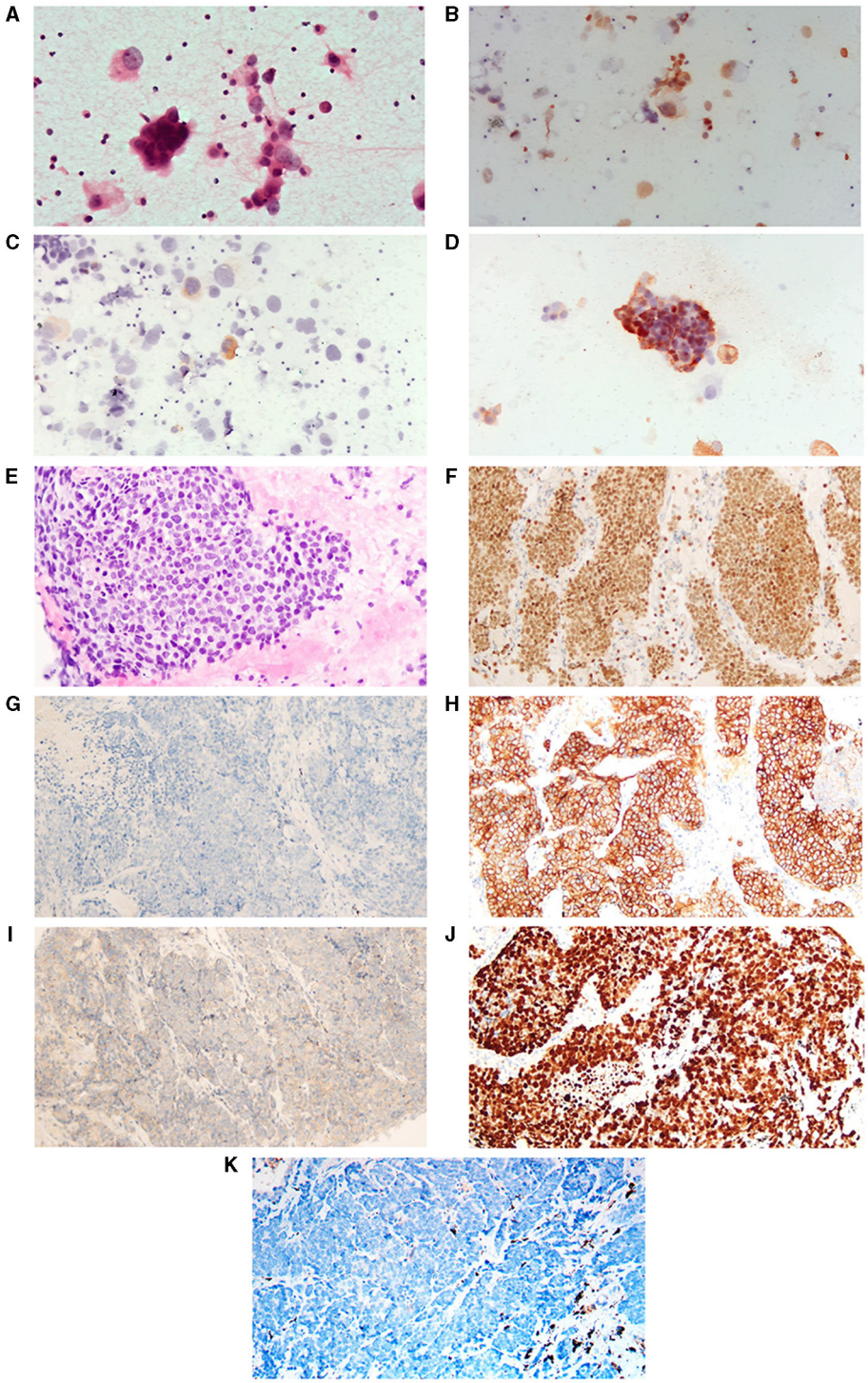

FIGURE 2
H&E and immunohistochemistry staining of tumor. **(A–D)** Represent cytologic photographs of lung adenocarcinoma (LAUD, before the histological transformation of the tumor). **(A)** Displays a hematoxylin and eosin (H&E) stained aspirate cytology sample. **(B–D)** Are positive immunohistochemical staining photographs for thyroid transcription factor-1 (TTF-1), Napsin A, and carcinoembryonic antigen (CEA), respectively. **(E–K)** Are pathological pictures following the SCLC transformation. **(E)** Shows H&E staining. **(F–K)** Are immunohistochemical images demonstrating positivity for TTF-1, negativity for Napsin A, and positivity for Synaptophysin (Syn), CD56, Ki-67, and negativity for programmed death-ligand 1 (PD-L1), respectively. All images are presented at 400x.

transformed tumor still harbors the *EGFR* mutation, albeit at a reduced abundance. Through histological analysis, we found that the transformed tumor tissue exhibits morphological and neuroendocrine characteristics identical to those of classical SCLC, which are consistent with previous research (7). The medical consensus generally attributes the histological transformation to

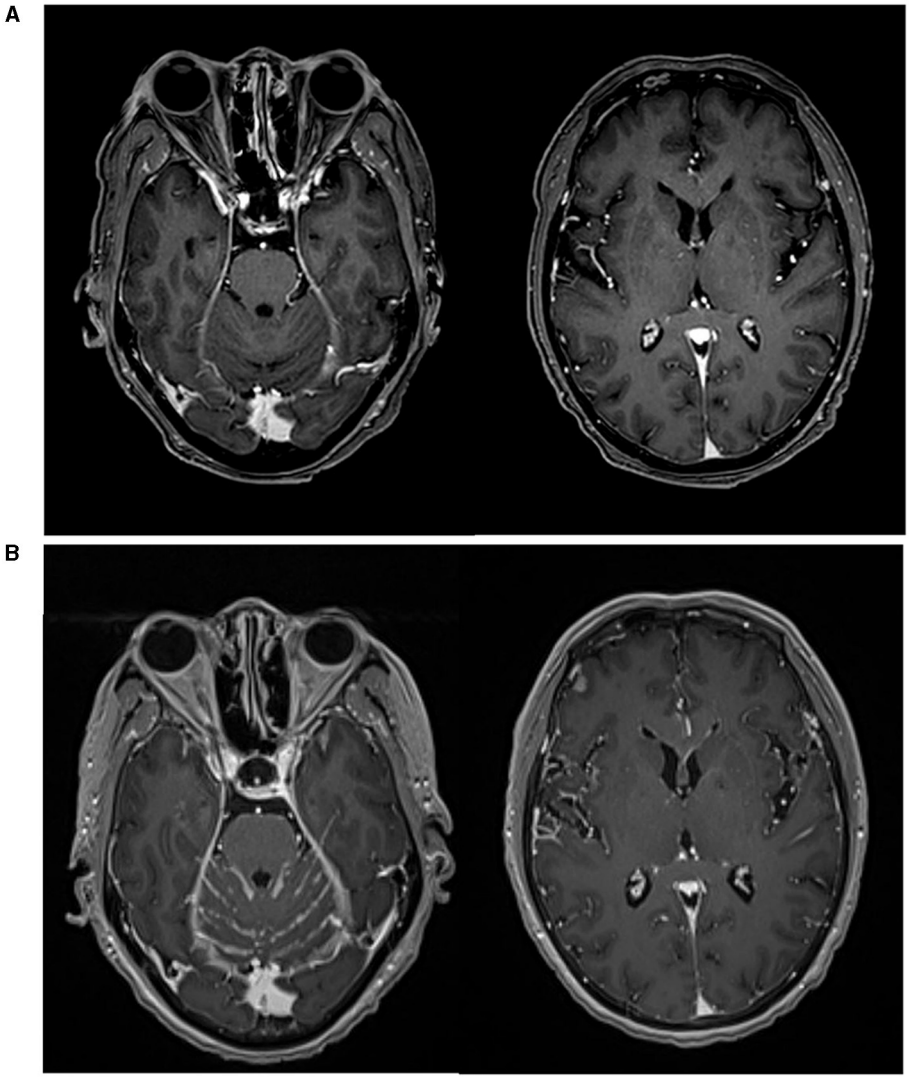

FIGURE 3
Brain MRI scans. **(A)** MRI image at the time of SCLC transformation. **(B)** MRI confirmed metastasis to the central nervous system (CNS).

the concomitant biallelic loss of *TP53* and *RB1* (7). Further studies have shown that T-SCLC patients are frequently characterized by molecular features mirroring those of classical SCLC, including the presence of an activating mutation in *PIK3CA*, loss of heterozygosity, loss of *RB1*, and an inactivating mutation in *TP53* (7, 20, 21). In our case, the patient did not exhibit mutations in *TP53* and *RB1*; however, a histological transformation still occurred. Indeed, while SCLC is characterized by cells that are functionally mutant for RB and p53 proteins, not all SCLC cases demonstrate inactivation of the *RB1* and *TP53* genes (22). It is important to consider that the undetected mutations in *RB1* and *TP53* in our patient could be attributed to the spatial heterogeneity of the tumor microenvironment (23), and hence, we cannot exclude the presence of alterations in *TP53* and *RB1*. In summary, the observed similarities in tumor histology and molecular characteristics between T-SCLC and classical SCLC indicate that therapeutic strategies for classical SCLC may also apply to patients with T-SCLC.

Notably, in this case, the patient experienced a substantial increase in the mutation abundance of PTEN (from 10.2% to 86.32%) following histological transformation. This observation suggests the potential involvement of the PI3K pathway in the patient's histological transition. Furthermore, the upregulation of the PI3K-AKT signaling pathway has been substantiated in this transition, as evidenced by EGFR-mutant patient-derived xenograft models where inhibition of the PI3K/AKT pathway arrested tumor growth and neuroendocrine transformation (24). Additional studies have illuminated the complexity of the transformation, revealing the downregulation of NOTCH signaling and overexpression of MYC and BCL2 (5, 24, 25). These studies also offer potential therapeutic strategies for patients with T-SCLC. Notably, the immune microenvironment between LUAD and T-SCLC exhibits distinct differences, particularly marked by downregulation of immune modulators and a conspicuous decline in CD8+ T cell presence in T-SCLC (26), highlighting the potential role of immunotherapy in managing this transformation.

A multicentre retrospective study reported by Fujimoto et al. showed that after 15 SCLC patients were treated with PD-1/PD-L1 inhibitor monotherapy, only 1 patient was adequate, with an mPFS of 1.3 months (27). ICIs alone have limited efficacy in transformed SCLC. Therefore, in our case, following the histological transformation of the patient, we initiated a serplulimab-based immunochemotherapy regimen, achieving a PFS of 6 months, which is superior to the previously reported PFS of <4 months (11).

Cardiotoxicity is a common adverse reaction to TKIs such as osimertinib. A study has indicated that cardiac adverse events (AEs) occur in approximately 5% of patients with EGFR-Mutated NSCLC treated with osimertinib (28). Although clinical research suggests that TKIs like osimertinib may increase the risk of cardiotoxicity, including heart failure, no evidence indicates that TKIs have direct treatment-related cardiotoxicity (29, 30). In this case, the patient experienced a severe reduction in LVEF and a significant decline in general condition following TKIs therapies. We consider that the patient's rapid tumor growth, following resistance to osimertinib and anlotinib, increased pulmonary burden, which in turn led to myocardial ischemia, thus triggering cardiotoxicity. Consequently, there was no notable improvement after discontinuation of the drug, which ultimately accelerated disease progression. The low LVEF state also posed challenges to the patient's safety medication. After a multidisciplinary consultation and considering the excellent safety profile of serplulimab in conjunction with the patient's preference, it was decided to administer serplulimab combined with EP chemotherapy for the treatment of T-SCLC, against the backdrop of supportive therapy to improve cardiac ejection function. The patient tolerated the serplulimab-based treatment well, rapidly improving the ECOG PS score and restoring cardiac function to normal levels.

For T-SCLC patients, recent research has begun to explore beyond traditional PE chemotherapy, seeking innovative solutions that reflect the complexity of the disease. In a retrospective study of 47 T-SCLC patients, incorporating atezolizumab into the existing chemotherapy treatment demonstrated a promising shift toward longer PFS (from 4.1 to 5.1 months) and substantially enhanced OS, increasing it from 7.9 to 20.2 months (15). Further corroborating these findings, a specific case of SCLC transformation from lung adenocarcinoma has shown a durable response to durvalumab (a PD-1 inhibitor) and PE regimen up to 19 months (31), reinforcing the potential efficiency of PD-1/PD-L1 inhibitors combined with chemotherapy for transformed SCLC. This initial evidence has been pivotal in motivating further investigations into immunochemotherapy as a viable alternative. Serplulimab, a novel PD-1 targeting monoclonal antibody developed by Shanghai Henlius Biotech, Inc., has emerged as a promising contender. Acting to reinvigorate the immune system's ability to recognize and attack tumor cells, serplulimab has shown encouraging results in trials such as ASTRUM-005 (NCT04063163) (14). The clinical success of serplulimab, achieving a PFS of 6 months in our case, extends beyond previous retrospective studies, laying the groundwork for a potential paradigm shift in treating T-SCLC.

Upon examining *ClinicalTrials*, we identified two prospective studies focused on T-SCLC. The first is an investigator-initiated, open-label, prospective phase II clinical trial, identified by NCT05957510, set to be conducted across various centers in China, aiming to enroll 36 patients with T-SCLC who have not received prior treatment after undergoing histological transformation, with the primary objective of evaluating the efficacy and safety of serplulimab in combination with chemotherapy in the treatment of EGFR-mutated NSCLC transformed into SCLC after treatment with safety and efficacy (32). The second, known by NCT04538378 in the United States, is designed to enroll 14 subjects with EGFR-mutated T-SCLC, having undergone transformation following EGFR-TKI and having been treated with platinum-based chemotherapy. While there are slight variations in the designs of these two studies, both aim to assess the antitumor activity and safety of immunochemotherapy regimens containing PD-1/PD-L1 inhibitors for T-SCLC patients.

In conclusion, this case report illustrates a promising response to serplulimab in a T-SCLC patient, providing a glimpse into the potential efficacy of incorporating PD-1 inhibitors with traditional chemotherapy. The complex landscape of T-SCLC, encompassing its early detection, underlying mechanisms, and clinical management, remains a fertile ground for exploration and discovery. Further comprehensive research, ranging from basic pre-clinical studies to retrospective and prospective clinical trials, is paramount to illuminating this unique subtype of lung cancer.

Data availability statement

The original contributions presented in the study are included in the article/supplementary material, further inquiries can be directed to the corresponding authors.

Ethics statement

According to internal institutional policies, ethics approval is not required for the present study. The studies were conducted in accordance with the local legislation and institutional requirements. The participants provided their written informed consent to participate in this study. Written informed consent was obtained from the individual(s) for the publication of any potentially identifiable images or data included in this article.

Author contributions

H-XL: Conceptualization, Data curation, Writing – original draft. W-HM: Conceptualization, Data curation, Writing – original draft. Y-QZ: Writing – review & editing. HJ: Investigation, Supervision, Writing – review & editing. Y-DW: Conceptualization, Data curation, Writing – review & editing. MZ: Conceptualization, Data curation, Writing – review & editing.

Funding

The author(s) declare that no financial support was received for the research, authorship, and/or publication of this article.

Conflict of interest

The authors declare that the research was conducted in the absence of any commercial or financial relationships that could be construed as a potential conflict of interest.

Publisher's note

References

1. Megyesfalvi Z, Gay CM, Popper H, Pirker R, Ostoros G, Heeke S, et al. Clinical insights into small cell lung cancer: tumor heterogeneity, diagnosis, therapy, and future directions. *CA Cancer J Clin.* (2023) 73:620–52. doi: 10.3322/caac.21785

2. Gazdar AF, Bunn PA, Minna JD. Small-cell lung cancer: what we know, what we need to know and the path forward. *Nat Rev Cancer.* (2017) 17:725–37. doi: 10.1038/nrc.2017.87

3. Wang Y, Zou S, Zhao Z, Liu P, Ke C, Xu S. New insights into small-cell lung cancer development and therapy. *Cell Biol Int.* (2020) 44:1564–76. doi: 10.1002/cbin.11359

4. Siegel RL, Miller KD, Fuchs HE, Jemal A. Cancer statistics, 2022. *CA Cancer J Clin.* (2022) 72:7–33. doi: 10.3322/caac.21708

5. Quintanal-Villalonga A, Chan JM, Yu HA, Pe'er D, Sawyers CL, Sen T, et al. Lineage plasticity in cancer: a shared pathway of therapeutic resistance. *Nat Rev Clin Oncol.* (2020) 17:360–71. doi: 10.1038/s41571-020-0340-z

6. Oser MG, Niederst MJ, Sequist LV, Engelman JA. Transformation from non-small-cell lung cancer to small-cell lung cancer: molecular drivers and cells of origin. *Lancet Oncol.* (2015) 16:e165–72. doi: 10.1016/S1470-2045(14)71180-5

7. Offin M, Chan JM, Tenet M, Rizvi HA, Shen R, Riely GJ, et al. Concurrent RB1 and TP53 alterations define a subset of EGFR-mutant lung cancers at risk for histologic transformation and inferior clinical outcomes. *J Thorac Oncol.* (2019) 14:1784–93. doi: 10.1016/j.jtho.2019.06.002

8. Ferrer L, Giaj Levra M, Brevet M, Antoine M, Mazieres J, Rossi G, et al. A brief report of transformation from NSCLC to SCLC: molecular and therapeutic characteristics. *J Thorac Oncol.* (2019) 14:130–4. doi: 10.1016/j.jtho.2018.08.2028

9. Wang S, Xie T, Hao X, Wang Y, Hu X, Wang L, et al. Comprehensive analysis of treatment modes and clinical outcomes of small cell lung cancer transformed from epidermal growth factor receptor mutant lung adenocarcinoma. *Thorac Cancer.* (2021) 12:2585–93. doi: 10.1111/1759-7714.14144

10. Roca E, Gurizzan C, Amoroso V, Vermi W, Ferrari V, Berruti A. Outcome of patients with lung adenocarcinoma with transformation to small-cell lung cancer following tyrosine kinase inhibitors treatment: a systematic review and pooled analysis. *Cancer Treat Rev.* (2017) 59:117–22. doi: 10.1016/j.ctrv.2017.07.007

11. Marcoux N, Gettinger SN, O'Kane G, Arbour KC, Neal JW, Husain H, et al. EGFR-mutant adenocarcinomas that transform to small-cell lung cancer and other neuroendocrine carcinomas: clinical outcomes. *J Clin Oncol.* (2019) 37:278–85. doi: 10.1200/JCO.18.01585

12. Mansfield AS, Kazarnowicz A, Karaseva N, Sanchez A, De Boer R, Andric Z, et al. Safety and patient-reported outcomes of atezolizumab, carboplatin, and etoposide in extensive-stage small-cell lung cancer (IMpower133): a randomized phase I/III trial. *Ann Oncol.* (2020) 31:310–7. doi: 10.1016/j.annonc.2019.10.021

13. Liu SV, Reck M, Mansfield AS, Mok T, Scherpereel A, Reinmuth N, et al. Updated Overall Survival and PD-L1 subgroup analysis of patients with extensive-stage small-cell lung cancer treated with atezolizumab, carboplatin, and etoposide (IMpower133). *J Clin Oncol.* (2021) 39:619–30. doi: 10.1200/JCO.20.01055

14. Cheng Y, Han L, Wu L, Chen J, Sun H, Wen G, et al. Effect of first-line serplulimab vs placebo added to chemotherapy on survival in patients with extensive-stage small cell lung cancer: the ASTRUM-005 randomized clinical trial. *JAMA.* (2022) 328:1223–32. doi: 10.1001/jama.2022.16464

15. Zhang CY, Sun H, Su JW, Chen YQ, Zhang SL, Zheng MY Li YF, et al. A potential treatment option for transformed small-cell lung cancer on PD-L1 inhibitor-based combination therapy improved survival. *Lung Cancer.* (2023) 175:68–78. doi: 10.1016/j.lungcan.2022.11.016

16. Soria JC, Ohe Y, Vansteenkiste J, Reungwetwattana T, Chewaskulyong B, Lee KH, et al. Osimertinib in untreated EGFR-mutated advanced non-small-cell lung cancer. *N Engl J Med.* (2018) 378:113–25. doi: 10.1056/NEJMoa1713137

17. Mambetsariev I, Arvanitis L, Fricke J, Pharaon R, Baroz AR, Afkhami M, et al. Small cell lung cancer transformation following treatment in EGFR-mutated non-small cell lung cancer. *J Clin Med.* (2022) 11:1429. doi: 10.3390/jcm11051429

18. Lin CA Yu SL, Chen HY, Chen HW, Lin SU, Chang CC Yu CJ, Yang PC, et al. EGFR-Mutant SCLC exhibits heterogeneous phenotypes and resistance to common antineoplastic drugs. *J Thorac Oncol.* (2019) 14:513–26. doi: 10.1016/j.jtho.2018.11.021

19. Liu Y. Small cell lung cancer transformation from EGFR-mutated lung adenocarcinoma: a case report and literatures review. *Cancer Biol Ther.* (2018) 19:445–9. doi: 10.1080/15384047.2018.1435222

20. van Meerbeeck JP, Fennell DA, De Ruysscher DK. Small-cell lung cancer. *Lancet.* (2011) 378:1741–55. doi: 10.1016/S0140-6736(11)60165-7

21. Rudin CM, Durinck S, Stawiski EW, Poirier JT, Modrusan Z, Shames DS, et al. Comprehensive genomic analysis identifies SOX2 as a frequently amplified gene in small-cell lung cancer. *Nat Genet.* (2012) 44:1111–6. doi: 10.1038/ng.2405

22. Sivakumar S, Moore JA, Montesion M, Sharaf R, Lin DI, Colon CI, et al. Integrative analysis of a large real-world cohort of small cell lung cancer identifies distinct genetic subtypes and insights into histologic transformation. *Cancer Discov.* (2023) 13:1572–91. doi: 10.1158/2159-8290.CD-22-0620

23. Yuan Y. Spatial heterogeneity in the tumor microenvironment. *Cold Spring Harb Perspect Med.* (2016) 6:a026583. doi: 10.1101/cshperspect.a026583

24. Quintanal-Villalonga A, Taniguchi H, Zhan YA, Hasan MM, Chavan SS, Meng F, et al. Multiomic analysis of lung tumors defines pathways activated in neuroendocrine transformation. *Cancer Discov.* (2021) 11:3028–47. doi: 10.1158/2159-8290.CD-20-1863

25. Nakagawa M, Takizawa N, Narita M, Ichisaka T, Yamanaka S. Promotion of direct reprogramming by transformation-deficient Myc. *Proc Natl Acad Sci U S A.* (2010) 107:14152–7. doi: 10.1073/pnas.1009374107

26. Huang J, Zhang SL, Zhou C, Huang W, Luo P, Chen HJ, et al. Genomic and transcriptomic analysis of neuroendocrine transformation in ALK-rearranged lung adenocarcinoma after treatments with sequential ALK inhibitors: a brief report. *JTO Clin Res Rep.* (2022) 3:100338. doi: 10.1016/j.jtocrr.2022.100338

27. Fujimoto D, Akamatsu H, Morimoto T, Wakuda K, Sato Y, Kawa Y, et al. Histologic transformation of epidermal growth factor receptor-mutated lung cancer. *Eur J Cancer.* (2022) 166:41–50. doi: 10.1016/j.ejca.2022.02.006

28. Kunimasa K, Kamada R, Oka T, Oboshi M, Kimura M, Inoue T, et al. Cardiac adverse events in EGFR-mutated non-small cell lung cancer treated with osimertinib. *JACC CardioOncol.* (2020) 2:1–10. doi: 10.1016/j.jaccao.2020.02.003

29. Anand K, Ensor J, Trachtenberg B, Bernicker EH. Osimertinib-induced cardiotoxicity: a retrospective review of the FDA adverse events reporting system (FAERS). *JACC CardioOncol.* (2019) 1:172–8. doi: 10.1016/j.jaccao.2019.10.006

30. Ewer MS, Tekumalla SH, Walding A, Atuah KN. Cardiac safety of osimertinib: a review of data. *J Clin Oncol.* (2021) 39:328–37. doi: 10.1200/JCO.20.01171

31. Li YC. Durable response to durvalumab-based immunochemotherapy in small-cell lung carcinoma transformation from EGFR-mutant non-small cell lung cancer: a case report. *Thorac Cancer.* (2022) 13:775–9. doi: 10.1111/1759-7714.14325

32. Huang J, Zhang XH, Cai Y, Yang D, Shi J, Xing P, et al. Rationale and design of a phase ii trial of combined serplulimab and chemotherapy in patients with histologically transformed small cell lung cancer: a prospective, single-arm and multicentre study. *Clin Oncol.* (2023) 36:39–45. doi: 10.1016/j.clon.2023.11.030

frontiers | Frontiers in Medicine

TYPE Case Report
PUBLISHED 27 September 2024
DOI 10.3389/fmed.2024.1444995

OPEN ACCESS

EDITED BY
Giuseppe Fiorentino,
Colli Hospital, Italy

REVIEWED BY
Cristiano Cesaro,
Hospital of the Hills, Italy
Armin Krvavac,
University of Missouri, United States

*CORRESPONDENCE
Shan Zhu
✉ zhuzhumao@126.com

†These authors have contributed equally to this work

RECEIVED 06 June 2024
ACCEPTED 09 September 2024
PUBLISHED 27 September 2024

CITATION
Li ZH, Kong L-X, Zhu S, Hu Y and Gao S (2024) Tracheobronchomegaly associated with tracheobronchopathia osteochondroplastica: a case report.
Front. Med. 11:1444995.
doi: 10.3389/fmed.2024.1444995

Tracheobronchomegaly associated with tracheobronchopathia osteochondroplastica: a case report

Zhen Hua Li†, Lu-Xia Kong†, Shan Zhu*, Yi Hu and Shan Gao

Department of Respiratory and Critical Care Medicine, The Central Hospital of Wuhan, Tongji Medical College, Huazhong University of Science and Technology, Wuhan, China

Tracheobronchomegaly (TBM) is a rare condition characterized by the dilatation of the trachea and bronchi due to severe atrophy of elastic fibers, accompanied by the thinning of the muscularis mucosae and the development of diverticula between cartilaginous rings. The etiology of this condition remains unclear. Tracheobronchopathia osteochondroplastica (TO) is another uncommon airway disease with an unknown etiology. The co-occurrence of these two diseases has not been reported. In this study, we report and discuss a case involving an elderly man with TBM and TO with a history of recurrent pneumonia over the past 6 years.

KEYWORDS

tracheobronchomegaly, Mounier-Kuhn syndrome, tracheobronchopathia osteochondroplastica, recurrent pneumonia, case report

Introduction

Tracheobronchomegaly (TBM), also known as Mounier-Kuhn syndrome (MKS), is different from other morphological abnormalities of the central airways (1). Tracheobronchopathia osteochondroplastica (TO) is another uncommon airway disease with an unknown etiology (2). This report presents an exceptional case of TBM in an adult, which can be attributed to TO. An 84-year-old man with a history of recurrent pneumonia in the same regions for the past 6 years underwent a chest computed tomography (CT) scan and fibroscopic examination, which revealed TO as the underlying cause of his condition. To the best of our knowledge, this is the firstdocumented case of adult TBM specifically associated with TO involving the trachea. The potential predictors of TBM and TO remain unclear. The diagnosis of this condition is challenging due to the presence of overlapping symptoms and a lack of awareness, often resulting in missed identification and unnecessary medical interventions.

Case description

The patient, an 84-year-old retired worker, presented with a 6-year history of chronic cough accompanied by mucopurulent expectoration. The onset of fever occurred the day before he was presented. He has a past medical history of recurrent pneumonia, requiring multiple hospitalizations. He is currently a non-smoker but had a 10-year history of smoking 20 cigarettes per day. In addition, the patient has a long-standing diagnosis of hyperlipidemia and is on atorvastatin calcium medication. His familial medical history only includes arterial

hypertension in his father. A computed tomography (CT) scan of the chest revealed tracheomegaly with a diameter of 62.6 mm and an increased caliber of the great bronchi (30.9 mm on the right and 37.9 mm on the left) (Figures 1A–E). The muscular layer of the tracheal wall was evidently thinner (Figures 1A–E), which is characterized by atrophy or the absence of elastic fibers or smooth muscle in the wall of the trachea and the main bronchi. A slice acquired during expiration demonstrated a partial collapse of the trachea and main bronchi (Figures 1A–E). The chest CT scan revealed an irregular calcified appearance of the tracheal wall and both main bronchi (Figure 1F). The video bronchoscopy revealed dynamic partial stenosis during expiration, indicating tracheomalacia (Figure 2). During the bronchoscopy, the increased tracheal diameter and the expiratory collapse due to tracheomalacia were observed, and the redundant tracheal wall might have even obstructed the view, which was consistent with the CT scan (Figure 3).

Discussion

Tracheobronchomegaly (TBM), first documented in 1932, is a rare and most likely congenital syndrome characterized by an enlarged trachea and main bronchi (3). To date, fewer than 400 cases have been documented in medical literature. TBM is distinguished by the dilation of the trachea and bronchi, setting it apart from other morphological abnormalities of the central airways. Its etiology remains unknown. However, it is considered to involve familial susceptibility and inheritance through autosomal recessive mechanisms, including Ehlers–Danlos syndrome, cystic fibrosis, Marfan's syndrome, and ankylosing spondylitis (4). The diagnosis of TBM is established through bronchoscopy and radiological imaging techniques. The use of CT has enabled better and easier visualization and determination of the airway size, facilitating the recognition of evidently abnormal cases. The tracheal diameter exceeding 3 cm or mainstem bronchi diameters greater than 2.4 cm strongly indicates the presence of the disease. For our patient, the transverse diameter of the trachea was 62.6 mm, the anteroposterior diameter was 31.2 mm, the diameter of the left main bronchus was 37.9 mm, and the diameter of the right main bronchus was 30.9 mm. A biopsy and necropsy examination of the tracheal wall revealed thinning of the muscularis mucosae, accompanied by the loss of elastic fibers (5). The effect of enlarged airways on spirometry derives from the weakness of the tracheobronchial walls and hypotonia in the myoelastic elements, resulting in dynamic airway compression (manifesting as an expiratory collapse during forced exhalation) and dynamic restriction. The clinical features are non-specific. Some patients remain asymptomatic with normal respiratory function, while others exhibit chronic cough and recurrent lower respiratory tract infections, which ultimately progress rapidly to severe respiratory failure and mortality (6). However, the etiology remains unclear and requires further follow-up. The condition known as tracheobronchopathia osteochondroplastica (TO) was initially documented by Rokitanski in 1855 (7). It is a rare, idiopathic, and benign disease that is often underdiagnosed. The reported incidence of TO is 0.11% (8). With the advancement of research and the widespread utilization of bronchoscopy, an increasing number of reports have been documented. Currently, there are over 600 recorded cases of TO (9). The condition is characterized by the presence of multiple submucosal nodules composed of cartilage and bone in the anterolateral walls of the tracheobronchial tree, with the exception of the posterior wall (10). The difficulty in clamping bronchoscopic nodules for a biopsy renders it unnecessary to perform biopsies in all cases (11). However, it is crucial to differentiate the histomorphology of TO from calcification resulting from other conditions such as tracheobronchial amyloidosis, atrophic polychondritis, and

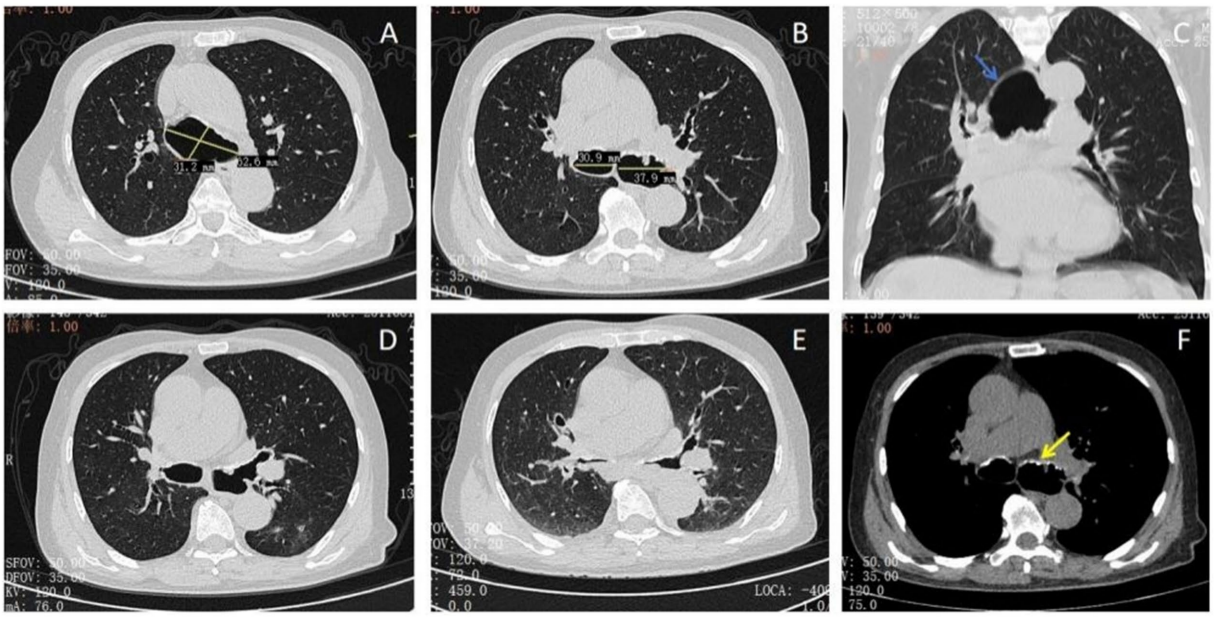

FIGURE 1
Thoracic computed tomography: **(A)** dilation of the trachea (62.6*31.2 mm). **(B)** Dilation of the main bronchi shown above. **(C)** The muscular layer of the tracheal wall was evidently thinner (blue arrow). **(D,E)** The constriction of the main bronchi was more than 50% during expiration. **(F)** CT images showed irregular submucosal nodular calcification (yellow arrow).

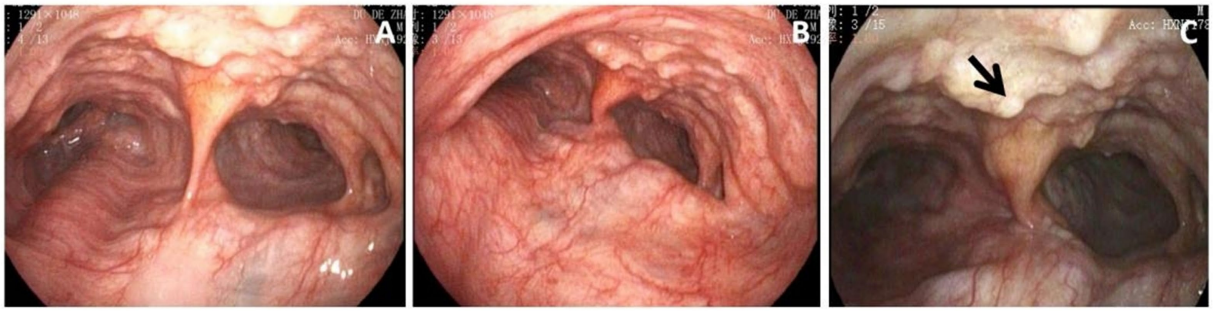

FIGURE 2
(A) Bronchoscopy showed massively dilated trachea. **(B)** The constriction of the main bronchi was approximately 50% during expiration. **(C)** Numerous cartilaginous and bony nodules protruding into the lumen from the submucosa of the tracheobronchial tree (black arrow). Histopathological examination of these lesions was performed to exclude neoplastic or chronic granulomatous etiologies. The results were suggestive of nodular cartilaginous tissue and mature bone tissue with calcification, as shown in Figure 3.

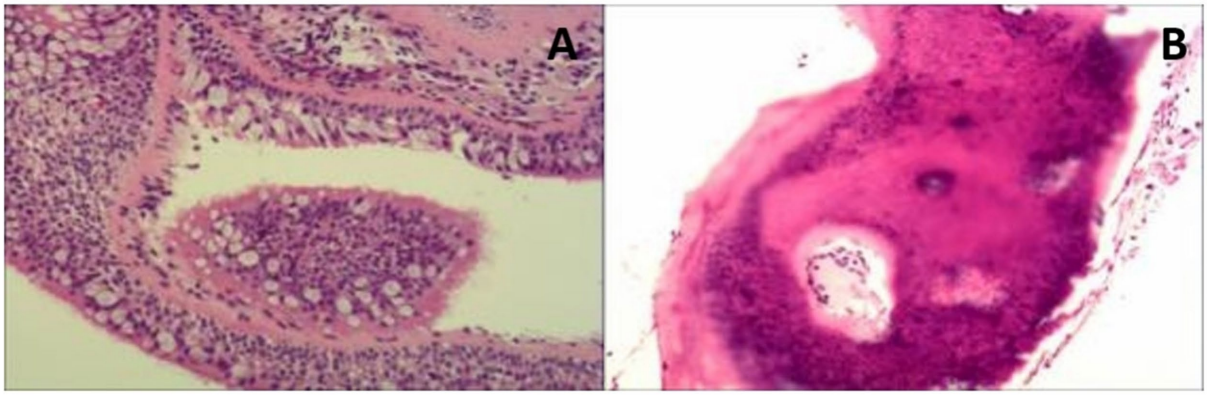

FIGURE 3
Histopathological images (biopsy taken during the bronchoscopy). **(A)** The bronchial mucous membrane tissue showed chronic inflammatory changes. **(B)** There was some calcified bone tissue in the local area. The patient was managed conservatively with close observation, demonstrating a gradual progression course over a 6-year follow-up period. Symptoms during each hospitalization period were alleviated through the administration of antibiotics.

granulomatous diseases, such as TB or sarcoidosis. The pathogenesis of TO remains elusive, with speculations suggesting that it may arise from submucosal elastic fibrosis, leading to the formation of elastic cartilage, which subsequently undergoes calcification and ossification. Alternatively, it is proposed that TO could result from the excessive proliferation of tracheal cartilage rings, giving rise to exophytic osteochondral warts that eventually ossify (12). The presence of TO has been found to be associated with certain malignancies, such as skin cancer and polyarteritis nodosa, as well as IgA deficiency. However, there is currently no established pathophysiological correlation between TO and these diseases (13, 14). The clinical manifestations are non-specific and resemble those of TBM, which include cough, recurrent respiratory infections, and hemoptysis (15). During progression to a severe stage, the nodules protrude into the lumen of the trachea and main bronchi, potentially causing airway obstruction. In our case report, we observed significant expansion of the main bronchi, which has not been previously documented. There is currently no clear pathological association between TBM and TO. The exploration of this issue requires further investigation. In our case report, we assumed that the ossified bronchial stenosis in the right lower lung potentially resulted in the weakening of the tracheal wall. The chronic high pressure generated by the stenosis during expiration most likely led to the gradual dilation of the trachea. More case reports are needed to confirm this hypothesis. The present case report highlights the importance of CT and fiberscopic examination for the diagnosis and shows that TBM can be associated with TO. Currently, for patients with tracheal stenosis caused by osteocartilaginous nodules, non-invasive continuous positive airway pressure ventilation, bi-level positive airway pressure ventilation, invasive stent placement, and surgical treatment are mainly used (16). However, while positive airway pressure ventilation can only temporarily relieve clinical symptoms, it cannot serve the purpose of treating the disease. Stent implantation is often associated with complications such as secretion retention, infection, and restenosis due to granulation. Surgical treatment causes significant damage to patients, involves high risks and complications, and has certain limitations. With increasing clinical awareness, it is essential to identify clinical risk factors and improve treatment outcomes. Laser tracheobronchoplasty is one of the less invasive new techniques. Laser tracheobronchoplasty treatment can reduce local nodule contracture and the formation of scar, thereby improving airway collapse. Currently, domestic and foreign studies have reported the effect of this treatment with good clinical feedback, and the clinical symptoms

of patients have been reported to significantly improve within 1 week after the surgery (17). Therefore, laser tracheobronchoplasty is a safe and effective technique for the treatment of osteocartilaginous nodules to achieve recanalization. However, future studies regarding the effectiveness of this technique are needed.

Data availability statement

The original contributions presented in the study are included in the article/supplementary material, further inquiries can be directed to the corresponding author.

Ethics statement

Written informed consent was obtained from the participant/patient(s) for the publication of this case report.

Author contributions

ZL: Conceptualization, Data curation, Formal analysis, Funding acquisition, Investigation, Methodology, Project administration, Resources, Software, Supervision, Validation, Visualization, Writing – original draft, Writing – review & editing. L-XK: Data curation, Formal analysis, Investigation, Resources, Writing – original draft. SZ: Conceptualization, Methodology, Resources, Supervision, Validation, Writing – original draft, Writing – review & editing. YH: Investigation, Supervision, Writing – review & editing. SG: Formal analysis, Methodology, Resources, Writing – review & editing.

Funding

The author(s) declare that no financial support was received for the research, authorship, and/or publication of this article.

Conflict of interest

The authors declare that the research was conducted in the absence of any commercial or financial relationships that could be construed as a potential conflict of interest.

Publisher's note

References

1. Lawrence DA, Branson B, Oliva I, Rubinowitz A. The wonderful world of the windpipe: a review of central airway anatomy and pathology. *Can Assoc Radiol J*. (2015) 66:30–43. doi: 10.1016/j.carj.2014.08.003

2. Liu Q, Hu Y, Lei M, Mei C, Yang C. Clinical characteristics of Tracheobronchopathia Osteochondroplastica: a retrospective study of 33 patients. *Int J Gen Med*. (2023) 16:3447–55. doi: 10.2147/IJGM.S418394

3. Mounier-Kuhn P. Dilatation de la trachee: constatations radiographiques et bronchoscopiques. *Lyon Med*. (1932) 150:106–9.

4. Babirye D, Walubembe J, Babirye JA, Baluku JB, Byakika-Kibwika P, Nabawanuka E. Tracheobronchomegaly (Mounier-Kuhn syndrome) in a 43-year-old male: a case report. *Int Med Case Rep J*. (2022) 15:631–7. doi: 10.2147/IMCRJ.S386083

5. Sailer S, Osona B, Peña-Zarza JA, Gil-Sanchez JA, Lacruz-Perez L, Mulet JF. Coincidence of Tracheobronchomegaly (Mounier-Kuhn syndrome) and juvenile idiopathic arthritis. *Klin Padiatr*. (2015) 227:290–2. doi: 10.1055/s-0035-1548837

6. Li ZH, Wang RJ, Gao S. Tracheobronchomegaly (Mounier-Kuhn syndrome): a case report. *QJM*. (2023) 116:792–3. doi: 10.1093/qjmed/hcad109

7. Hantous-Zannad S, Sebaï L, Zidi A, et al. Tracheobronchopathia osteochondroplastica presenting as a respiratory insufficiency: diagnosis by bronchoscopy and MRI. *Eur J Radiol*. (2003) 45:113–6. doi: 10.1016/S0720-048X(02)00028-1

8. García CA, Sangiovanni S, Zúñiga-Restrepo V, Morales EI, Sua LF, Fernández-Trujillo L. Tracheobronchopathia Osteochondroplastica-clinical, radiological, and endoscopic correlation: case series and literature review. *J Investig Med High Impact Case Rep*. (2020) 8:232470962092160. doi: 10.1177/2324709620921609

9. Guo R, Zhou M, Wei X, Niu L. Clinical characteristics of six cases of tracheobronchopathia osteochondroplastica. *Can Respir J*. (2020) 2020:1–6. doi: 10.1155/2020/8685126

10. Devaraja K, Sagar P, Chirom A. Tracheobronchopathia osteochondroplastica: awareness is the key for diagnosis and management. *BMJ Case Rep*. (2017) 2017:bcr2017220567. doi: 10.1136/bcr-2017-220567

11. Wang N, Long F, Jiang S. Tracheobronchopathia Osteochondroplastica: two cases reports and review of literature. *Medicine*. (2016) 95:e3396. doi: 10.1097/MD.0000000000003396

12. Juanola Pla J, Rejon Cabezas T, Ortega Castillo MP. Tracheobronchopathia osteochondroplastica. *Arch Bronconeumol*. (2020) 56:172. doi: 10.1016/j.arbres.2019.03.015

13. Laine M, Elfihri S, Kettani F, Bourkadi JE. Tracheobronchopathia osteochondroplastica associated with skin Cancer: a case report and review of the literature. *BMC Res Notes*. (2014) 7:637. doi: 10.1186/1756-0500-7-637

14. Dincer HE, Dunitz JM. Tracheobronchopathia osteochondroplastica and selective IgA deficiency. *J Bronchology Interv Pulmonol*. (2012) 19:54–6. doi: 10.1097/LBR.0b013e3182446949

15. Uchimura K, Yamasaki K, Yatera K, Nawata A, Ishimoto H, Mukae H. Multiple tracheobronchial polyposis caused by Tracheobronchopathia Osteochondroplastica. *Intern Med*. (2016) 55:3165–7. doi: 10.2169/internalmedicine.55.6774

16. Abia-Trujllo D, Majd A, Johnson MM, Mira-Avendano I, Patel NM, Makey IA, et al. Central airway collapse, an uderappreciated cause of respiratory morbidity. *Mayo Clin Proc*. (2020) 95:2747–54. doi: 10.1016/j.mayocp.2020.03.004

17. Castellanos P, MK M, Atallah I. Lasetracheobronchoplasty: a novel technique for the treatment ofsymptomatic tracheobronchomalacia|J. *Eur Arch Otorrinolaringol*. (2017) 274:1601–7. doi: 10.1007/s00405-016-4349-y

frontiers | Frontiers in Medicine

TYPE Correction
PUBLISHED 17 December 2024
DOI 10.3389/fmed.2024.1540232

OPEN ACCESS

APPROVED BY
Frontiers Editorial Office,
Frontiers Media SA, Switzerland

*CORRESPONDENCE
Shan Zhu
✉ zhuzhumao@126.com

†These authors have contributed equally to this work

RECEIVED 06 December 2024
ACCEPTED 06 December 2024
PUBLISHED 17 December 2024

CITATION
Li ZH, Kong L-X, Zhu S, Hu Y and Gao S (2024) Corrigendum: Tracheobronchomegaly associated with tracheobronchopathia osteochondroplastica: a case report. *Front. Med.* 11:1540232. doi: 10.3389/fmed.2024.1540232

Corrigendum: Tracheobronchomegaly associated with tracheobronchopathia osteochondroplastica: a case report

Zhen Hua Li†, Lu-Xia Kong†, Shan Zhu*, Yi Hu and Shan Gao

Department of Respiratory and Critical Care Medicine, The Central Hospital of Wuhan, Tongji Medical College, Huazhong University of Science and Technology, Wuhan, China

KEYWORDS

tracheobronchomegaly, Mounier-Kuhn syndrome, tracheobronchopathia osteochondroplastica, recurrent pneumonia, case report

A Corrigendum on
Tracheobronchomegaly associated with tracheobronchopathia osteochondroplastica: a case report

by Li, Z. H., Kong, L.-X., Zhu, S., Hu, Y., and Gao, S. (2024). *Front. Med.* 11:1444995. doi: 10.3389/fmed.2024.1444995

In the published article, there was an error in affiliation. Instead of "[1]The Centre Hospital of Wuhan, Wuhan, China, [2]Huazhong University of Science and Technology, Wuhan, China", it should be "Department of Respiratory and Critical Care Medicine, The Central Hospital of Wuhan, Tongji Medical College, Huazhong University of Science and Technology, Wuhan, China".

The authors apologize for this error and state that this does not change the scientific conclusions of the article in any way. The original article has been updated.

Publisher's note

All claims expressed in this article are solely those of the authors and do not necessarily represent those of their affiliated organizations, or those of the publisher, the editors and the reviewers. Any product that may be evaluated in this article, or claim that may be made by its manufacturer, is not guaranteed or endorsed by the publisher.

frontiers | Frontiers in Medicine

TYPE Case Report
PUBLISHED 02 October 2024
DOI 10.3389/fmed.2024.1423895

OPEN ACCESS

EDITED BY
Uday Kishore,
United Arab Emirates University,
United Arab Emirates

REVIEWED BY
Jorge García García,
Complejo Hospitalario Universitario de Albacete, Spain
Yanchang shang,
Chinese PLA General Hospital, China
Haijian Zhou,
National Institute for Communicable Disease Control and Prevention, China CDC, China

*CORRESPONDENCE
Zhenjun Zhao
✉ zzjhospital@sina.com
Lijie Zhang
✉ zhanglijie@hebmu.edu.cn

†These authors have contributed equally to this work and share first authorship

RECEIVED 26 April 2024
ACCEPTED 18 September 2024
PUBLISHED 02 October 2024

CITATION
Zuo H, Ye J, Li C, Li S, Gu J, Dong N, Zhao Y, Hao J, Song M, Guo Y, Gao W, Zhao Z and Zhang L (2024) Myasthenia gravis complicated with pulmonary infection by *Nocardia cyriacigeorgica*: a case report and literature review.
Front. Med. 11:1423895.
doi: 10.3389/fmed.2024.1423895

Myasthenia gravis complicated with pulmonary infection by *Nocardia cyriacigeorgica*: a case report and literature review

Huifen Zuo[1†], Jiaqing Ye[2†], Chenfei Li[3], Shijie Li[4], Jingxin Gu[1], Na Dong[1], Yihan Zhao[1], Jiahao Hao[2], Minghui Song[2], Yumei Guo[5], Weili Gao[5], Zhenjun Zhao[1*] and Lijie Zhang[2*]

[1]Department of Clinical Laboratory, Hebei Yiling Hospital, Shijiazhuang, China, [2]Department of Clinical Laboratory, Hebei Medical University Third Hospital, Shijiazhuang, China, [3]Department of Orthopedics, Hebei Medical University Third Hospital, Shijiazhuang, China, [4]Department of Myasthenia Gravis, Hebei Yiling Hospital, Shijiazhuang, China, [5]Hebei Key Laboratory of Intractable Pathogens, Shijiazhuang Center for Disease Control and Prevention, Shijiazhuang, China

Myasthenia gravis (MG) is an autoimmune disease. Patients with MG due to compromised autoimmune regulation, progressive muscle weakness, and prolonged use of immunosuppressants and glucocorticoid, often present with concomitant infections. However, cases of MG complicated by *Nocardia* infection are rare. In this case, we report MG complicated with pulmonary infection by *Nocardia cyriacigeorgica*. A 71-year-old male farmer who was admitted for management of MG. After 7 weeks of treatment of MG, the patient reported improvement. However, clinical presentation, inflammatory markers, and imaging findings supported a diagnosis of pulmonary infection. To further elucidate the etiology, *Nocardia* was identified in sputum smear microscopy and sputum culture, with 16S rRNA gene sequencing confirming *N. cyriacigeorgica*. The patient was prescribed trimethoprim-sulfamethoxazole. After 1 month of treatment, clinical symptoms of MG and pulmonary nocardiosis showed significant improvement. Additionally, we searched PubMed for case reports of *Nocardia cyriacigeorgica* pulmonary infection from 2010 to 2024 and conducted a statistical analysis of the case information. This report aims to highlights the increased risk of pulmonary Nocardia infection in MG patients after the use of steroids and immunosuppressants, thereby enhancing clinical awareness.

KEYWORDS

***Nocardia cyriacigeorgica*, myasthenia gravis, pulmonary infection, trimethoprim-sulfamethoxazole, immunosuppression**

Introduction

Myasthenia gravis (MG) is an autoimmune disease characterized by neuromuscular junction transmission impairment mediated by autoantibodies. *Nocardia* spp. are commonly found in soil, rotten plants and dust particles. Nocardiosis most commonly presents as primary skin infections, pulmonary infections, and disseminated infections (1). *Nocardia* infections are predominantly observed in immunocompromised individuals or those on long-term immunosuppressive therapy (2), also in patients with underlying lung disease (3). Patients with MG due to compromised autoimmune regulation, progressive muscle weakness, and

prolonged use of immunosuppressants and glucocorticoids, often present with concomitant infections. Muralidhar Reddy et al. reviewed 21 cases of MG patients with concurrent nocardiosis (4). Until now, only one case of pulmonary nocardiosis caused by *N. cyriacigeorgica* has been identified in a patient with MG at the species level (5).

Case presentation

A 71-year-old male farmer from Hebei, China, presented with left upper eyelid ptosis in July 2021. He sought medical attention at a local hospital where the edrophonium test yielded positive results. The symptoms fluctuated while receiving treatment with acetylcholinesterase inhibitors. Gradually, weakness in the limbs and difficulty swallowing emerged. In September 2021, further consultation was sought at Hebei Yiling Hospital. The clinical manifestations included bilateral ptosis of the upper eyelids; weakness and easy fatigue of the muscles in the face, neck and limbs; and shortness of breath, with symptoms worsening after activity. The absolute score for myasthenia gravis (MG) was 31 points. Repetitive nerve stimulation demonstrates a wave amplitude decrement >10% in the accessory nerve and bilateral facial nerves. Admitted on September 2nd for MG, with a medical history including right eye enucleation and coronary artery stent placement (regularly taking aspirin enteric-coated tablets, isosorbide dinitrate tablets, and metoprolol tartrate tablets).

Upon hospital admission, arterial blood gas analysis revealed a respiratory acidosis concomitant with metabolic alkalosis (pH 7.39, PO2 40.0 mmHg, PCO2 52.0 mmHg, HCO3 31.5 mmol/L). Some indicators in the blood routine were slightly elevated (WBC 7.53 × 10^9/L, NEUT% 75.8). Additionally, the patient exhibited elevated blood glucose levels (2-h postprandial blood glucose >11 mmol/L). In summary, the patient was treated diabetes with repaglinide tablets (1 mg, tid). For the treatment of MG, in September 2021, acetylcholinesterase inhibitor pyridostigmine bromide (60 mg, qid), glucocorticoid methylprednisolone tablets (20 mg, qd), and immunosuppressants tacrolimus and cyclophosphamide (tacrolimus capsules 2 mg qd AM, followed by 1 mg qd PM. IV infusion of 500 mL 0.9% NaCl with cyclophosphamide 0.4 g, biw). Concurrent traditional Chinese medicine can enhance the therapeutic effects. The efficacy of traditional Chinese medicine mainly lies in enhancing the body's yang energy through warming and tonifying methods, while simultaneously regulating the meridians to promote the circulation of qi and blood, supplementing nutrients or energy, and regulating the extraordinary meridians. The main components of the traditional Chinese medicine are Astragalus, Ginseng, Ophiopogon, Schisandra, Reishi Mushroom, Angelica, Deer Antler, Dodder Seed, Cistanche, Morinda, Platycodon, and Cimicifuga. After 7 weeks of treatment, the patient reported slight improvement in bilateral upper eyelid ptosis, reduced fatigue during swallowing, alleviated limb weakness, less neck fatigue, and improved shortness of breath than before.

On October 23, 2021, the patient presented with coughing, sputum production, nasal congestion, and rhinorrhea. Monitoring revealed blood glucose level of 18.2 mmol/L, and elevated inflammatory markers in blood routine (WBC 13.09 × 10^9/L, NEUT% 93.5, CRP 120.7 mg/L). Chest CT showed newly developed localized consolidation in the basal segment of the left lower lobe (Figures 1A,B). Clinical symptoms, inflammatory markers, and imaging support the diagnosis of pulmonary infection. Treatment with ceftriaxone sodium/tazobactam sodium for 5 days showed unsatisfactory results. To further clarify the etiology, filamentous rods with positive weak acid-fast staining were found in 3 days' consecutive sputum smears (Figure 2A), highly suggestive of *Nocardia*. White candida growth was observed in microbial culture after 48 h, with negative results in the G test, ruling out Candida infection. Dry, biting agar-like colonies grew on blood agar after 3 days. After 5 days, the colonies become wrinkled and stacked like leather, with velvety aerial mycelia on the surface (Figure 2B). Upon sequencing of the 16S rRNA gene, exhibited a 99.9% nucleotide homology with *N. cyriacigeorgica* (NR117334.1) in the NCBI database. These sequences were submitted to the SRA database at NCBI with the accession number PP178562.

Considering the possibility of infection related to immunosuppression, cyclophosphamide and methylprednisolone were discontinued while retaining traditional Chinese medicine, tacrolimus and pyridostigmine bromide. Additionally, the patient was prescribed trimethoprim–sulfamethoxazole (TMP-SMX; 2 tablets bid) for the treatment of *N. cyriacigeorgica* infection. After 7 weeks of treatment for MG, the patient reported slight improvement in bilateral upper eyelid ptosis, reduced fatigue during swallowing, alleviated limb weakness, reduced neck fatigue, and improved shortness of breath. After 1 month of standardized treatment for *N. cyriacigeorgica* infection, on December 1, 2021, the inflammatory indicators in the routine blood tests showed a significant decrease (WBC 7.25 × 109/L, 78.4% neutrophils, 16.4% lymphocytes, and CRP 16.9 mg/L). Chest CT showed a localized solid lesion in the basal segment of the lower lobe of the left lung, which was less extensive than before (Figures 1C,D). Bilateral drooping eyelids, shortness of breath, weakness in chewing, and weakness in both lower limbs improved. The absolute score for MG was 6 points, and the treatment outcome was judged as essentially cured. The clinical symptoms of MG and pulmonary *Nocardia* infection had improved, and it was agreed to discharge the patient. Until now, there has been no recurrence of the *Nocardia* infection in the lungs.

Discussion

MG is an autoimmune disorder characterized by impaired neuromuscular transmission mediated by autoantibodies. Patients are categorized into early-onset (≥18 and <50 years), late-onset (>50 years) and very late-onset MG (≥65 years) (6). Skeletal muscles throughout the body can be affected, manifesting as fluctuating weakness and fatigability, with symptoms showing a pattern of worsening in the morning and improving in the evening, they are exacerbated by activity and alleviated by rest. The genus *Nocardia* is a group of aerobic actinomycetes, Gram-positive bacteria, with some species exhibiting weak acid-fast staining. They are commonly found in soil, rotten plants and dust particles (2). The disease caused by *Nocardia* mainly manifests in three forms: pulmonary infection (the most common), disseminated infection, and primary cutaneous and soft tissue infections (7). Nocardiosis is prevalent among individuals with immunodeficiency or long-term use of immunosuppressive agents.

Research shows that patients with MG often experience concomitant infections due to the combined effects of compromised autoimmune regulation, progressive deterioration of myasthenia, and long-term use of immunosuppressants and hormones (8, 9).

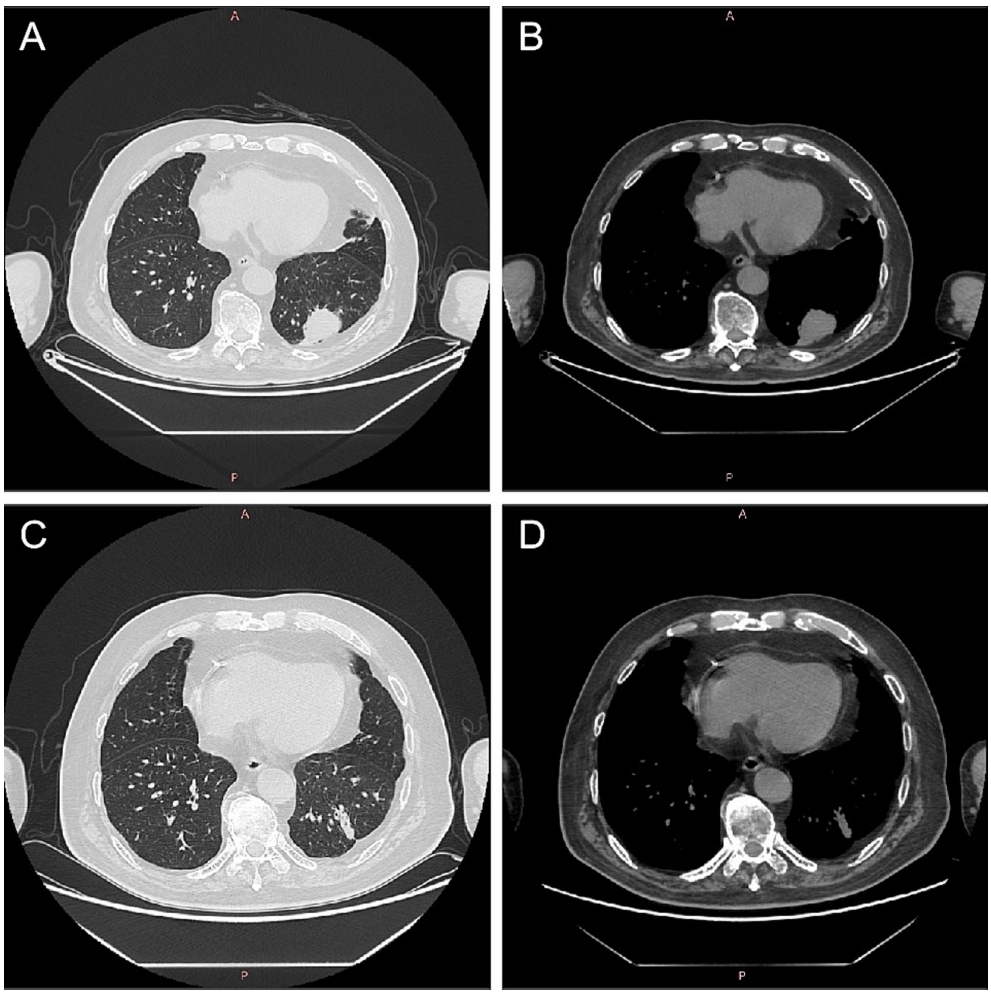

FIGURE 1
Computed tomography images of lungs before and after *Nocardia* treatment. After 2 months of treatment for myasthenia gravis, there was localized consolidation in the basal segment of the left lower lobe of the lung **(A,B)**. Following 1 month of treatment with trimethoprim–sulfamethoxazole for *Nocardia cyriacigeorgica*, chest CT showed a localized solid lesion in the basal segment of the lower lobe of the left lung, which was less extensive than before **(C,D)**. CT, computed tomography.

Muralidhar Reddy et al. conducted a statistical analysis on 21 cases of nocardiosis in MG patients, identifying risk factors for *Nocardia* infection, including elderly men, thymoma, immunosuppressive therapy, and pre-existing pulmonary diseases (4). *Nocardia farcinica* and *Nocardia asteroides* were more common pathogens (4). The investigation into the etiology of *N. cyriacigeorgica* infection in the patient reveals several key points. The patient in this case was an older man working in agriculture. It is possible that he inhaled *Nocardia* while working in the fields, initially resulting in colonization throughout the body. MG can induce respiratory muscle weakness, leading to symptoms such as respiratory distress, weak coughing, dyspnea, and dysphagia, which impede the clearance of pathogens. Systemic hormone therapy, especially when used in conjunction with other immunosuppressants, compromises the immune system. Misra et al. indicated that 88% of patients exhibit comorbidities, notably prevalent in the late-onset group, with cardiovascular diseases being common (10). Our patient had multiple comorbidities, including type 2 diabetes mellitus and a history of coronary artery stenting, which exacerbated the risk of infection.

Nocardiosis has three primary forms: primary cutaneous infection, pulmonary infection, and disseminated infection (1, 11). It can also present as central nervous system infections, eye infections, osteomyelitis, and septic arthritis (7). *Nocardia* infections are commonly seen in immunocompromised hosts undergoing immunosuppressive therapy, such as in cases of prolonged corticosteroid use, malignancies, organ transplants, and HIV. They can also occur in non-immunocompromised hosts, primarily those with structural lung diseases like cystic fibrosis and bronchiectasis (2). We have searched for case reports and case series of *N. cyriacigeorgica* pulmonary infection during 2010-2024 in PubMed using the key words "(pulmonary) AND (*Nocardia cyriacigeorgica*)." Our search yielded 35 case reports that are summarized in Table 1. The total number of patients was 36, with an equal distribution of 18 males and 18 females (50%). Among them, 27 patients (75%) were over the age of 50. *Nocardia* pulmonary infections are commonly seen in immunosuppressed patients and those with underlying pulmonary conditions. Our statistics revealed that 9 patients (25%) had underlying pulmonary diseases, and 21 patients (58%) were

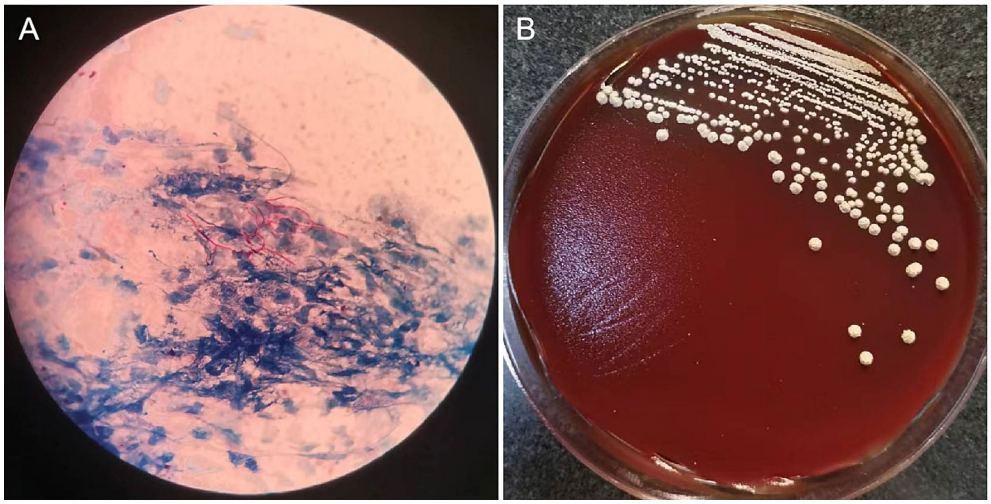

FIGURE 2
Microscopic pictures of *Nocardia* and colonies isolated from sputum sample.The sputum sample revealed filamentous rods with weak acid-fast staining **(A)**. On Colombia blood agar, grown at 37°C for 5 days, the colonies become wrinkled and stacked like leather, with velvety aerial mycelia on the surface **(B)**.

immunosuppressed. Among the immunosuppressed, 6 patients (17%) had a history of cancer, and 5 patients (14%) had autoimmune diseases. Moreover, we found that 5 patients (14%) had diabetes, and 5 patients (14%) were smokers. Regarding treatment, a significant number of patients, 28 (78%), were treated with TMP-SMX, and 28 patients (78%) showed a good recovery from their Nocardial lung infection symptoms.

On the basis of typical clinical manifestations such as fluctuating muscle weakness, diagnosis can be made by meeting any of the following three criteria: pharmacological examinations, electrophysiological characteristics, and serum anti-acetylcholinesterase receptor or other antibody detection. The clinical manifestations and pulmonary imaging of pulmonary nocardiosis lack specificity, posing challenges for early diagnosis. In the present case, the patient's sputum smear exhibited morphological features highly suggestive of *Nocardia* infection under the microscope. Combined with the slow growth characteristics of *Nocardia* species, it was cultured successfully through extending the incubation period. Therefore, for slow-growing bacteria like *Nocardia*, direct smear staining microscopy and prolonged incubation time are crucial.

Currently, the treatment of MG primarily revolves around cholinesterase inhibitors, glucocorticoids, immunosuppressants, intravenous immunoglobulin, plasmapheresis, and thymectomy (12). Many studies have indicated that some Chinese medical approaches demonstrate promising outcomes in managing MG. Integrating Chinese and western medical practices can reduce the recurrence rate of the disease, minimize adverse reactions and complications, as well as modulate the immune function (13–16). The relative severity of MG in patients is reflected by the absolute score of clinical evaluation, which assesses the degree of muscle weakness and fatigue without necessitating any instrumentation. Scoring ranges from 0 to 60 points, with higher scores indicating more severe symptoms. The approach utilized in this case involved integrating both traditional Chinese medicine and western medicine to treat severe MG. Upon admission, the absolute score was 31, which significantly decreased to 6 following treatment, indicating remarkable therapeutic efficacy. TMP–SMX is the preferred treatment for nocardiosis, with monotherapy often used for nonsevere cases. Empiric multidrug therapy (such as carbapenems, TMP–SMX, amikacin, linezolid, or parenteral cephalosporins) is recommended for severe pulmonary infections, disseminated infections, and central nervous system infections (17, 18). Sulfonamide–carbapenem combination therapy is used empirically for nocardiosis, but all *Nocardia* isolates should ideally be identified to the species level and subjected to susceptibility testing to guide optimal treatment. Patients with localized pulmonary infections should receive treatment for >6 months, while those with complicated or disseminated diseases should undergo antibacterial therapy for >9 months (18, 19). The present case utilized the TMP–SMX for anti-infective therapy. The significant decrease in inflammatory markers and improvement in clinical symptoms before and after treatment suggested a pronounced therapeutic effect. Based on the comprehensive assessment, the clinical symptoms of MG and pulmonary *Nocardia* infection improved, and reached the criteria for clinical cure. Therefore, the patient was approved for discharge. Until now, there has been no recurrence of the Nocardia infection in the lungs.

Conclusion

To our knowledge, cases of coexisting MG and *Nocardia* infection are relatively rare. This present case represents the second instance, which was aimed at further elucidating the relationship between MG and pulmonary *Nocardia* infection by adding another clinical example. It underscores the heightened risk of developing pulmonary Nocardiosis following the use of hormone and immunosuppressive agents in MG patients. Clinicians should be cognizant of this and consider the possibility of *Nocardia* infection when conventional empirical treatments fail, thereby facilitating timely communication with microbiology laboratories to appropriately extend culture duration and prevent misdiagnosis.

TABLE 1 Case reports and case series of *N. cyriacigeorgica* pulmonary infection during 2010-2024 in PubMed.

Reference	Country/Age/Gender	Predisposing factors	Treatment	Outcome	
Akcaglar, 2008	Turkey/37/M	Basedow–Graves disease, diabetes	TMP–SMX, amphotericin B, vancomycin, imipenem	Died	(20)
Cargill, 2010	United Kingdom/85/F	History of ischaemic heart disease, chronic obstructive pulmonary disease and polymyalgia rheumatica	Piperacillin/tazobactam, vancomycin, imipenem, doxycycline	Died	(21)
Chavez, 2011	United States of America/58/M	Obesity, hypertension, and diet-controlled type 2 diabetes mellitus	TMP–SMX	Recover well	(22)
Hadano, 2011	Japan/82/F	Colectomy for colon cancer history	TMP–SMX	Recover well	(23)
Madden, 2012	United States of America/9/M	Chronic granulomatous disease	TMP-SMX, linezolid, levofloxacin, voriconazole	Recover well	(24)
Lavalard, 2013	France/71/F	History included a diagnosed Waldenström's disease 20 years earlier, treated with cytotoxics, mitral and aortic insufficiency, excision of a frontal basal cell epithelioma, labial herpes, dry mouth and eyes without etiology and active smoking	TMP-SMX, rifampicin	Died	(25)
Severo, 2013	Brazil/77/F	Bronchiectasis, chronic obstructive pulmonary disease	NA	NA	(26)
Yagi, 2014	Japan/72/M; Japan/53/F	Rheumatoid arthritis, untreated *Mycobacterium avium* complex lung disease; 6-pack-year smoking history, a history of *Mycobacterium avium* complex lung disease	TMP–SMX; NA	Recover well; NA	(27)
Eshraghi, 2014	Iran/55/F	Kidney transplant	Trimoxazole, ceftriaxone	Recover well	(28)
Berring, 2014; Garcia,2015	Pakistan/6/M	Nephrotic syndrome	TMP-SMX, linezolid	Recover well	(29)
	United States of America/77/M	Myasthenia gravis, history of treated pulmonary tuberculosis	TMP-SMX, meropenem, linezolid	Recover well	(5)
Castellana, 2016	Italy/75/M	Chronic Obstructive Pulmonary Disease, smoking history	TMP–SMX	Recover well	(30)
Trastoy, 2017	Spain/81/F	Non-Hodgkin B-cell lymphoma and diabetes mellitus	TMP–SMX, meropenem, voriconazole (MI)	NA	(31)
Rivera, 2017	Puerto Rico/60/M	NA	TMP–SMX	Recover well	(32)
Vignesh, 2017	India/1M	Recurrent bloody stools, cervical and inguinal lymphadenitis, bilateral peri broncho vascular interstitial thickening with patchy consolidation in the left lower lobe, diffuse colon edema, polyclonal hypergammaglobulinemia	Mesalamine, anti-tubercular therapy (isoniazid, rifampicin, and ethambutol)	NA	(33)
Wu, 2018	China/55/F	Allergic bronchopulmonary aspergillosis	TMP–SMX and meropenem	Recover well	(34)
Kobayashi, 2018	Japan/52/F	Olfactory neuroblastoma	TMP-SMX	Recover well	(35)
Mahajan, 2019	United States of America/70/M	Low-dose prednisone, decreased appetite, proximal lower extremity weakness and leg spasms	TMP-SMX, meropenem, linezolid	Died	(36)
Karan, 2019	Serbia/70/M	Epileptic	Sulfamethoxazole and ceftriaxone	Recover well	(37)

(Continued)

TABLE 1 (Continued)

Reference	Country/Age/Gender	Predisposing factors	Treatment	Outcome	
AlMogbel, 2020	Saudi Arabias/65/F	End-stage renal disease, relied on hemodialysis, and suffered from ischemic heart disease, idiopathic thrombocytopenia and hypothyroidism	Vancomycin and ceftriaxone	Recover well	(38)
Yu, 2020	China/79/M	Membranous kidney disease	TMP-SMX, linezolid, methylprednisolone, and meropenem	Recover well	(39)
Saha, 2020	United States of America/72/M	Chronic obstructive pulmonary disease	TMP-SMX	Recover well	(40)
Lin, 2021	China/37/F	Chronic granulomatous disease	TMP–SMX	Recover well	(41)
Browne, 2021	Afghani/77/M	Diabetes, extensive history of chewing tobacco use	TMP–SMX, ceftriaxone and dexamethasone	Recover well	(42)
Colaneri, 2021	Italy/45/F	Human immunodeficiency virus infection infection	TMP/SMX, linezolid, and amikacin (MI)	Recover well	(43)
Tsuchiya, 2022	Japan/61/M	Diabetes, bronchiectasis	TMP–SMX	Recover well	(44)
Roy, 2022	United States of America/39M	Systemic lupus erythematosus	TMP–SMX, amikacin, voriconazole (MI)	Recover well	(45)
Kobashi, 2022	Japan/61/F	NA	TMP–SMX, meropenem, clarithromycin (MI)	Recover well	(46)
Bejcek, 2022	Hispanic/67/M	Non–small cell lung cancer	TMP–SMX	Recover well	(47)
Hong, 2023	China/55/F	CD4+ T cell deficiency	TMP–SMX	Recover well	(48)
Ye, 2023	China/63/F	Smoking history of over 40 years	TMP–SMX and voriconazole (MI)	Recover well	(49)
Gandham, 2023	India/41/M	Post-transplant	TMP–SMX	Recover well	(50)
Urbantat, 2023	Germany/14/F	Primary ciliary dyskinesia	TMP-SMX, meropenem	Recover well	(51)
Zhang, 2023	China/78/F	NA	Meropenem, linezolid, Sulfamethoxazole	Recover well	(52)
Bove, 2024	DOM/31/F	NA	TMP-SMX	Recover well	(53)

M, male; F, female; TMP–SMX, trimethoprim-sulfamethoxazole; MI. Mixed infections.

Data availability statement

The original contributions presented in the study are included in the article/supplementary material, further inquiries can be directed to the corresponding authors.

Ethics statement

Written informed consent was obtained from the individual(s) for the publication of any potentially identifiable images or data included in this article.

Author contributions

HZ: Conceptualization, Writing – original draft. JY: Conceptualization, Writing – original draft. CL: Methodology, Writing – original draft. SL: Formal analysis, Writing – original draft. JG: Formal analysis, Writing – original draft. ND: Formal analysis, Writing – original draft. YZ: Writing – original draft, Data curation. JH: Data curation, Writing – original draft. MS: Data curation, Writing – original draft. YG: Writing – review & editing. WG: Writing – review & editing. ZZ: Supervision, Writing – review & editing. LZ: Supervision, Writing – review & editing.

Funding

The author(s) declare that financial support was received for the research, authorship, and/or publication of this article. This work was fund by research project of Hebei Provincial Administration of Traditional Chinese Medicine (No. 2024143).

Conflict of interest

The authors declare that the research was conducted in the absence of any commercial or financial relationships that could be construed as a potential conflict of interest.

Publisher's note

References

1. Brown-Elliott BA, Brown JM, Conville PS, Wallace RJ Jr. Clinical and laboratory features of the Nocardia spp. based on current molecular taxonomy. *Clin Microbiol Rev*. (2006) 19:259–82. doi: 10.1128/CMR.19.2.259-282.2006

2. Ambrosioni J, Lew D, Garbino J. Nocardiosis: updated clinical review and experience at a tertiary center. *Infection*. (2010) 38:89–97. doi: 10.1007/s15010-009-9193-9

3. Martínez R, Reyes S, Menéndez R. Pulmonary nocardiosis: risk factors, clinical features, diagnosis and prognosis. *Curr Opin Pulm Med*. (2008) 14:219–27. doi: 10.1097/MCP.0b013e3282f85dd3

4. Muralidhar Reddy Y, Parida S, Jaiswal SK, Murthy JM. Nocardiosis-an uncommon infection in patients with myasthenia gravis: report of three cases and review of literature. *BMJ Case Rep*. (2020) 13:e237208. doi: 10.1136/bcr-2020-237208

5. Garcia RR, Bhanot N, Min Z. A mimic's imitator: a cavitary pneumonia in a myasthenic patient with history of tuberculosis. *BMJ Case Rep*. (2015) 2015:bcr2015210264. doi: 10.1136/bcr-2015-210264

6. Tang YL, Ruan Z, Su Y, Guo RJ, Gao T, Liu Y, et al. Clinical characteristics and prognosis of very late-onset myasthenia gravis in China. *Neuromuscul Disord*. (2023) 33:358–66. doi: 10.1016/j.nmd.2023.02.013

7. Traxler RM, Bell ME, Lasker B, Headd B, Shieh WJ, McQuiston JR. Updated review on Nocardia species: 2006-2021. *Clin Microbiol Rev*. (2022) 35:e0002721. doi: 10.1128/cmr.00027-21

8. Neumann B, Angstwurm K, Mergenthaler P, Kohler S, Schönenberger S, Bösel J, et al. Myasthenic crisis demanding mechanical ventilation: a multicenter analysis of 250 cases. *Neurology*. (2020) 94:e299–313. doi: 10.1212/WNL.0000000000008688

9. Liu Z, Lai Y, Yao S, Feng H, Zou J, Liu W, et al. Clinical outcomes of Thymectomy in myasthenia gravis patients with a history of crisis. *World J Surg*. (2016) 40:2681–7. doi: 10.1007/s00268-016-3599-6

10. Misra UK, Kalita J, Singh VK, Kumar S. A study of comorbidities in myasthenia gravis. *Acta Neurol Belg*. (2020) 120:59–64. doi: 10.1007/s13760-019-01102-w

11. Dumic I, Brown A, Magee K, Elwasila S, Kaljevic M, Antic M, et al. Primary lymphocutaneous *Nocardia brasiliensis* in an immunocompetent host: case report and literature review. *Medicina (Kaunas, Lithuania)*. (2022) 58:488. doi: 10.3390/medicina58040488

12. Dalakas MC. Immunotherapy in myasthenia gravis in the era of biologics. *Nat Rev Neurol*. (2019) 15:113–24. doi: 10.1038/s41582-018-0110-z

13. Aragonès JM, Altimiras J, Roura P, Alonso F, Bufill E, Munmany A, et al. Prevalence of myasthenia gravis in the Catalan county of Osona. *Neurologia*. (2017) 32:1–5. doi: 10.1016/j.nrl.2014.09.007

14. Melzer N, Ruck T, Fuhr P, Gold R, Hohlfeld R, Marx A, et al. Clinical features, pathogenesis, and treatment of myasthenia gravis: a supplement to the guidelines of the German neurological society. *J Neurol*. (2016) 263:1473–94. doi: 10.1007/s00415-016-8045-z

15. Park SY, Lee JY, Lim NG, Hong YH. Incidence and prevalence of myasthenia gravis in Korea: a population-based study using the National Health Insurance Claims Database. *J Clin Neurol*. (2016) 12:340–4. doi: 10.3988/jcn.2016.12.3.340

16. Xie R, Liu L, Wang R, Huang C. Traditional Chinese medicine for myasthenia gravis: study protocol for a network meta-analysis. *Medicine (Baltimore)*. (2020) 99:e21294. doi: 10.1097/MD.0000000000021294

17. Lafont E, Conan PL, Rodriguez-Nava V, Lebeaux D. Invasive Nocardiosis: disease presentation, diagnosis and treatment - old questions, new answers? *Infect Drug Resist*. (2020) 13:4601–13. doi: 10.2147/IDR.S249761

18. Restrepo A, Clark NM. Nocardia infections in solid organ transplantation: guidelines from the infectious diseases Community of Practice of the American Society of Transplantation. *Clin Transpl*. (2019) 33:e13509. doi: 10.1111/ctr.13509

19. Welsh O, Vera-Cabrera L, Salinas-Carmona MC. Current treatment for nocardia infections. *Expert Opin Pharmacother*. (2013) 14:2387–98. doi: 10.1517/14656566.2013.842553

20. Akcaglar S, Yilmaz E, Heper Y, Alver O, Akalin H, Ener B, et al. *Nocardia cyriacigeorgica*: pulmonary infection in a patient with Basedow-graves disease and a short review of reported cases. *Int J Infect Dis*. (2008) 12:335–8. doi: 10.1016/j.ijid.2007.06.014

21. Cargill JS, Boyd GJ, Weightman NC. *Nocardia cyriacigeorgica*: a case of endocarditis with disseminated soft-tissue infection. *J Med Microbiol*. (2010) 59:224–30. doi: 10.1099/jmm.0.011593-0

22. Chavez TT, Fraser SL, Kassop D, Bowden LP 3rd, Skidmore PJ. Disseminated *nocardia cyriacigeorgica* presenting as right lung abscess and skin nodule. *Mil Med*. (2011) 176:586–8. doi: 10.7205/MILMED-D-10-00346

23. Hadano Y, Ohmagari N, Suzuki J, Kawamura I, Okinaka K, Kurai H, et al. A case of pulmonary nocardiosis due to *Nocardia cyriacigeorgica* with prompt diagnosis by gram stain. *Nihon Kokyuki Gakkai zasshi*. (2011) 49:592–6.

24. Madden JL, Schober ME, Meyers RL, Bratton SL, Holland SM, Hill HR, et al. Successful use of extracorporeal membrane oxygenation for acute respiratory failure in a patient with chronic granulomatous disease. *J Pediatr Surg*. (2012) 47:E21–3. doi: 10.1016/j.jpedsurg.2011.12.029

25. Lavalard E, Guillard T, Baumard S, Grillon A, Brasme L, Rodríguez-Nava V, et al. Brain abscess due to *Nocardia cyriacigeorgica* simulating an ischemic stroke. *Ann Biol Clin*. (2013) 71:345–8. doi: 10.1684/abc.2013.0816

26. Severo CB, Oliveira Fde M, Hochhegger B, Severo LC. *Nocardia cyriacigeorgica* intracavitary lung colonization: first report of an actinomycetic rather than fungal ball in bronchiectasis. *BMJ Case Rep*. (2013) 2013:bcr2012007900. doi: 10.1136/bcr-2012-007900

27. Yagi K, Ishii M, Namkoong H, Asami T, Fujiwara H, Nishimura T, et al. Pulmonary nocardiosis caused by *Nocardia cyriacigeorgica* in patients with *Mycobacterium avium* complex lung disease: two case reports. *BMC Infect Dis*. (2014) 14:684. doi: 10.1186/s12879-014-0684-z

28. Eshraghi SS, Heidarzadeh S, Soodbakhsh A, Pourmand M, Ghasemi A, GramiShoar M, et al. Pulmonary nocardiosis associated with cerebral abscess successfully treated by co-trimoxazole: a case report. *Folia Microbiol*. (2014) 59:277–81. doi: 10.1007/s12223-013-0298-7

29. Berring DC, Nygaard U. Lung cavities caused by *Nocardia cyriacigeorgica* in an immunosuppressed boy. *Ugeskr Laeger*. (2014) 176:V01140077.

30. Castellana G, Grimaldi A, Castellana M, Farina C, Castellana G. Pulmonary nocardiosis in chronic obstructive pulmonary disease: a new clinical challenge. *Respir Med Case Rep*. (2016) 18:14–21. doi: 10.1016/j.rmcr.2016.03.004

31. Trastoy R, Manso T, García X, Barbeito G, Navarro D, Rascado P, et al. Pulmonary co-infection due to *Nocardia cyriacigeorgica* and *Aspergillus fumigatus*. *Rev espanola de quimioterapia*. (2017) 30:123–6.

32. Rivera K, Maldonado J, Dones A, Betancourt M, Fernández R, Colón M. *Nocardia cyriacigeorgica* threatening an immunocompetent host; a rare case of paramediastinal abscess. *Oxf Med Case Rep*. (2017):omx061. doi: 10.1093/omcr/omx061

33. Vignesh P, Rawat A, Kumar A, Suri D, Gupta A, Lau YL, et al. Chronic granulomatous disease due to neutrophil cytosolic factor (NCF2) gene mutations in three unrelated families. *J Clin Immunol*. (2017) 37:109–12. doi: 10.1007/s10875-016-0366-2

34. Wu J, Wu Y, Zhu Z. Pulmonary infection caused by *Nocardia cyriacigeorgica* in a patient with allergic bronchopulmonary aspergillosis: a case report. *Medicine*. (2018) 97:e13023. doi: 10.1097/MD.0000000000013023

35. Kobayashi K, Asakura T, Ishii M, Ueda S, Irie H, Ozawa H, et al. Pulmonary nocardiosis mimicking small cell lung cancer in ectopic ACTH syndrome associated with transformation of olfactory neuroblastoma: a case report. *BMC Pulm Med*. (2018) 18:142. doi: 10.1186/s12890-018-0710-9

36. Mahajan KR. Disseminated nocardiosis with cerebral and subcutaneous lesions on low-dose prednisone. *Pract Neurol*. (2019) 19:62–3. doi: 10.1136/practneurol-2018-002038

37. Karan M, Vučković N, Vuleković P, Rotim A, Lasica N, Rasulić L. Nocardial brain abscess mimicking lung cancer metastasis in immunocompetent patient with pulmonary nocardiasis: a case report. *Acta Clin Croat*. (2019) 58:540–5. doi: 10.20471/acc.2019.58.03.20

38. AlMogbel M, AlBolbol M, Elkhizzi N, AlAjlan H, Hays JP, Khan MA. Rapid identification of *Nocardia cyriacigeorgica* from a brain abscess patient using MALDI-TOF-MS. *Oxf Med Case Rep*. (2020):omaa088. doi: 10.1093/omcr/omaa088

39. Yu MH, Wu XX, Chen CL, Tang SJ, Jin JD, Zhong CL, et al. Disseminated Nocardia infection with a lesion occupying the intracranial space complicated with coma: a case report. *BMC Infect Dis*. (2020) 20:856. doi: 10.1186/s12879-020-05569-4

40. Saha BK, Chong WHH. Trimethoprim-induced hyponatremia mimicking SIADH in a patient with pulmonary nocardiosis: use of point-of-care ultrasound in apparent euvolemic hypotonic hyponatremia. *BMJ Case Rep*. (2020):13. doi: 10.1136/bcr-2020-235558

41. Lin J, Wu XM, Peng MF. *Nocardia cyriacigeorgica* infection in a patient with pulmonary sequestration: a case report. *World J Clin Cases*. (2021) 9:2367–72. doi: 10.12998/wjcc.v9.i10.2367

42. Browne WD, Lieberson RE, Kabbesh MJ. *Nocardia cyriacigeorgica* brain and lung abscesses in 77-year-old man with diabetes. *Cureus*. (2021) 13:e19373. doi: 10.7759/cureus.19373

43. Colaneri M, Lupi M, Sachs M, Ludovisi S, Di Matteo A, Pagnucco L, et al. A challenging case of SARS-CoV-2-AIDS and Nocardiosis coinfection from the SMatteo COvid19 REgistry (SMACORE). *New Microbiol*. (2021) 44:129–34.

44. Tsuchiya Y, Nakamura M, Oguri T, Taniyama D, Sasada S. A case of asymptomatic pulmonary *Nocardia cyriacigeorgica* infection with mild diabetes mellitus. *Cureus*. (2022) 14:e24023. doi: 10.7759/cureus.24023

45. Roy M, Lin RC, Farrell JJ. Case of coexisting Nocardia cyriacigeorgica and *Aspergillus fumigatus* lung infection with metastatic disease of the central nervous system. *BMJ Case Rep*. (2022):15. doi: 10.1136/bcr-2021-248381

46. Kobashi Y, Yoshioka D, Kato S, Oga T. Pneumococcal pneumonia co-infection with *Mycobacterium avium* and *Nocardia cyriacigeorgica* in an immunocompetent patient. *Int Med*. (2022) 61:1285–90. doi: 10.2169/internalmedicine.6895-20

47. Bejcek A, Owens J, Marella A, George A. Multiple rim-enhancing brain lesions and pulmonary cavitary nodules as the presentation of *Nocardia cyriacigeorgica* in a patient with non-small cell lung cancer. *Proc (Baylor Univ Med Cent)*. (2022) 35:555–6. doi: 10.1080/08998280.2022.2058831

48. Hong X, Ji YQ, Chen MY, Gou XY, Ge YM. *Nocardia cyriacigeorgica* infection in a patient with repeated fever and CD4(+) T cell deficiency: a case report. *World J Clin Cases*. (2023) 11:1175–81. doi: 10.12998/wjcc.v11.i5.1175

49. Ye J, Li Y, Hao J, Song M, Guo Y, Gao W, et al. Rare occurrence of pulmonary coinfection involving *Aspergillus fumigatus* and *Nocardia cyriacigeorgica* in immunocompetent patients based on NGS: a case report and literature review. *Medicine*. (2023) 102:e36692. doi: 10.1097/MD.0000000000036692

50. Gandham N, Kannuri S, Gupta A, Mukhida S, Das N, Mirza S. A post-transplant infection by *Nocardia cyriacigeorgica*. *Access Microbiol*. (2023):5. doi: 10.1099/acmi.0.000569.v3

51. Urbantat RM, Pioch CO, Ziegahn N, Stegemann MS, Stahl M, Mall MA, et al. Pleuropneumonia caused by *Nocardia cyriacigeorgica* in a 14-year-old girl with primary ciliary dyskinesia. *Pediatr Pulmonol*. (2023) 58:2656–8. doi: 10.1002/ppul.26536

52. Zhang LZ, Shan CT, Zhang SZ, Pei HY, Wang XW. Disseminated nocardiosis caused by *Nocardia otitidiscaviarum* in an immunocompetent host: a case report. *Zhonghua jie he he hu xi za zhi*. (2023) 46:1127–30. doi: 10.3760/cma.j.cn112147-20230516-00243

53. Bove A, Abdullah F, Saveeta F, Urena A, Martinez S. Unusual presentation of nocardiosis with pleural effusion in an immunocompetent host. *Cureus*. (2024) 16:e58686. doi: 10.7759/cureus.58686

frontiers | Frontiers in Medicine

TYPE Case Report
PUBLISHED 30 October 2024
DOI 10.3389/fmed.2024.1409323

OPEN ACCESS

EDITED BY
Karolina Henryka Czarnecka-Chrebelska,
Medical University of Lodz, Poland

REVIEWED BY
Ourania Papaioannou,
General University Hospital of Patras, Greece
Zainab Fatima,
University of South Florida, United States

*CORRESPONDENCE
Killen Harold Briones Claudett
killenbrio@hotmail.com

RECEIVED 29 March 2024
ACCEPTED 30 September 2024
PUBLISHED 30 October 2024

CITATION
Briones Claudett KH, Briones-Claudett MH, Murillo Vasconez R, Benitez Sólis JG, Briones Zamora KH, Freire AX, Barberan-Torres P and Grunauer M (2024) Bronchoscopy and molecular diagnostic techniques to identify superimposed infections in COVID-19-associated ARDS: a case series from Ecuador during the second wave. *Front. Med.* 11:1409323. doi: 10.3389/fmed.2024.1409323

Bronchoscopy and molecular diagnostic techniques to identify superimposed infections in COVID-19-associated ARDS: a case series from Ecuador during the second wave

Killen Harold Briones Claudett[1]*, Mónica H. Briones-Claudett[2], Roger Murillo Vasconez[3], Jaime G. Benitez Sólis[4], Killen H. Briones Zamora[5], Amado X. Freire[6], Pedro Barberan-Torres[7] and Michelle Grunauer[8]

[1]School of Medicine, Universidad Internacional del Ecuador (UIDE), Quito, Ecuador, [2]Intensive Care Unit, Ecuadorian Institute of Social Security (IESS), Babahoyo, Ecuador, [3]Intensive Care Unit, Ecuadorian Institute of Social Security (IESS), Ecuadorian Social Security Institute (IESS), Babahoyo, Ecuador, [4]Omni Hospital, Guayaquil, Ecuador, [5]Facultad de Ciencias Médicas, Universidad de Especialidades Espíritu Santo, Guayaquil, Ecuador, [6]Department of Medicine, University of Tennessee Health Science Center (UTHSC), Memphis, TN, United States, [7]Universidad Internacional del Ecuador (UIDE), Quito, Ecuador, [8]School of Medicine, Universidad San Francisco de Quito, Quito, Ecuador

Introduction: COVID-19-associated acute respiratory distress syndrome (CARDS) poses significant challenges in resource-limited settings. This case series explores the role of bronchoscopy and molecular techniques in identifying superimposed infections in CARDS patients during the second wave of the pandemic in Ecuador.

Methods: Nine critically ill CARDS patients underwent bronchoscopy and molecular testing to detect co-infections and superinfections. Clinical presentations, diagnostic findings, and outcomes were analyzed.

Results: Bronchoscopy and molecular techniques identified a range of secondary infections, including multidrug-resistant pathogens such as *Acinetobacter baumannii* and *Klebsiella pneumoniae*. The case series highlights the complexities of managing severe COVID-19 cases in resource-constrained environments.

Discussion: Early identification of microorganisms using PCR methods allows for rapid and accurate diagnosis, facilitating targeted management of critically ill CARDS patients. The study underscores the importance of advanced diagnostic tools and adaptable strategies in pandemic situations, particularly in low-resource settings.

KEYWORDS

COVID-19, ARDS, bronchoscopy, molecular techniques (RFLP), superimposed infections, resource-limited settings (RLS), second wave

Background

As of 2021, the global pandemic caused by severe acute respiratory syndrome coronavirus 2 (SARS-CoV-2), which first emerged in late 2019 in Wuhan, China, has resulted in at least 5 million deaths worldwide (1). The specific characteristics of severe COVID-19 led to the development of its nomenclature, CARDS, which refers to COVID-19-associated acute respiratory distress syndrome (2).

The clinical manifestations of SARS-CoV-2's biochemical behavior in CARDS are characterized by low blood oxygen levels and systemic hypoxemia, justifying the use of supplemental oxygen across a wide range (3). To diagnose CARDS, the Berlin 2012 ARDS diagnostic criteria must be met (4). The use of serum biomarkers, such as IL-6, C-reactive protein, ferritin, d-dimer, white blood cell count, and lymphocyte count, is crucial for staging the infection (5).

The management of COVID-19-associated acute respiratory distress syndrome (CARDS) has been the subject of extensive research, particularly regarding the use of immunomodulatory agents. A recent open-label, randomized controlled trial compared the efficacy of tocilizumab and baricitinib in hospitalized patients with severe COVID-19 (6). The study, which included 251 patients with a PaO2/fraction of inspired oxygen (FiO2) ratio of <200, found that baricitinib was non-inferior to tocilizumab for the primary composite outcome of mechanical ventilation or death at day 28. These findings highlight the ongoing efforts to optimize treatment strategies for severe COVID-19.

SARS-CoV-2 is primarily transmitted from person to person through respiratory droplets larger than 5 μm, especially when the patient presents with respiratory symptoms such as coughing and sneezing, and through contact with contaminated surfaces or fomites. Consequently, when managing patients under investigation, probable, or confirmed cases, it is crucial to implement standard precautions, contact precautions, and droplet transmission precautions. This is particularly crucial for healthcare workers performing bronchoscopy who are at high risk of exposure and require adequate personal protective equipment (7).

While airborne transmission by droplet nuclei or aerosols (capable of transmitting over distances >2 m) has not been definitively demonstrated for SARS-CoV-2, it is believed that this mode of transmission could occur during invasive respiratory tract procedures such as bronchoscopy (8).

In addition, the timing of presentation of other respiratory pathogen infections alongside SARS-CoV-2 poses a challenge, which can be categorized as follows: 1) coinfection, which refers to the presence of another pathogen at the time of diagnosis of SARS-CoV-2 infection, and 2) superinfection, which refers to the occurrence of another pathogen during the course of SARS-CoV-2 infection (9). Survival rate, length of hospital stay, and sequelae are critical factors, regardless of whether a patient exhibits coinfection or superinfection.

Furthermore, bronchoscopy and bronchoalveolar lavage (BAL) are powerful tools for sampling microbiological and molecular diagnostic testing, thereby identifying specific microorganisms growing in the bronchial environment and enabling targeted therapeutic interventions at the appropriate time (10).

During the second wave of COVID-19 in Ecuador, which lasted from November 2020 to May 2021, there was a significant increase in cases and hospitalizations. The peak occurred in mid-January 2021, with over 3,000 confirmed cases per week and nearly 1,600 hospitalizations (11). This context is crucial for understanding the cases presented in this study.

The role of bronchoscopy in the management of COVID-19 remains a subject of ongoing debate. For patients with severe COVID-19, particularly those admitted to the intensive care unit (ICU) (12), bronchoscopy may be essential to manage complications, such as atelectasis or hemoptysis, to address issues related to mechanical ventilation, and to identify superinfections. However, the use of bronchoscopy in COVID-19 patients is not without risk, notably the potential for viral transmission to healthcare staff. While various scientific societies have published guidelines to minimize heterogeneity in clinical practice (13), the evidence supporting these guidelines is limited and primarily consists of short series.

It is important to note that bronchoscopy can sometimes reveal unexpected findings in patients with suspected COVID-19 (14). In some cases, what initially appears to be an infection may be a different condition, such as vasculitis. A case report of granulomatosis with polyangiitis (GPA) presenting with a false positive COVID-19 antibody test highlights this potential for misdiagnosis (15). This underscores the importance of maintaining a broad differential diagnosis and the potential value of bronchoscopy in resolving complex cases, especially when the clinical presentation and initial test results are inconclusive.

Bronchoscopy should not be routinely used as a means to diagnose COVID-19 infection (16). This study aims to provide knowledge for the effective and safe use of bronchoscopy in patients with suspected or confirmed COVID-19 infection. The primary objective is to ensure maximum safety for our patients, the healthcare workers who care for them, and the broader community.

We present nine cases of critically ill patients with CARDS who underwent bronchoscopy and molecular diagnostic techniques to determine the presence of microorganisms associated with the presence of COVID-19. This case series provides valuable insight into the role of bronchoscopy in managing severe COVID-19 cases and identifying superimposed infections, contributing to the growing body of knowledge on optimal care strategies for these complex patients.

Case 1

A 51-year-old male patient with a history of obesity and high blood pressure was already admitted to the hospital with dyspnea, dry cough, fever, and headache for 11 days. The reverse transcription-polymerase chain reaction (RT-PCR) test for SARS-CoV-2 was positive. On day 2, the patient exhibited poor ventilatory mechanics and was transferred to the intensive care unit (ICU), where intubation and mechanical ventilation were initiated. A bronchoscopy with bronchoalveolar lavage (BAL) was performed on day 20. AL samples collected and processed by multiplex polymerase chain reaction (PCR) revealed multidrug-resistant *Acinetobacter baumannii* (1×107 copies), *Klebsiella*

Abbreviations: SARS-CoV-2, Severe acute respiratory syndrome coronavirus 2; ARDS, Acute respiratory distress syndrome; CARDS, COVID-19 associated acute respiratory distress syndrome.; ACE2, Angiotensin-converting enzyme; BAL, Bronchoalveolar lavage; RT-PCR, Multiplex polymerase chain reaction; ICU, Intensive care unit; IMV, Invasive mechanical ventilation; HFNC- High-flow nasal cannula; ECMO, Extracorporeal membrane oxygenation therapy; LVEF, Left ventricular eyection fracion; PASP, Pulmonary artery systolic pressure; CRAB, Carbapenem-resistant *Acinetobacter baumannii*; HIV, Infección por el virus de inmunodeficiencia humana; FiO_2, Fraction of inspired oxygen.

pneumoniae carbapenemase class A and D OXA (23 and 54 copies), *Candida albicans* (1×10^3 copies), and *Chryseobacterium indologenes*. Until day 23, the patient remained on invasive mechanical ventilation (IMV).

The patient's condition progressed unfavorably, with progressive deterioration of renal function leading to refractory septic shock and culminating in multiple organ failure. He died 47 days after his admission to the ICU.

Case 2

A 74-year-old female patient with a history of hypertension was presented to the hospital with dyspnea, cough, fever, diarrhea, and 80% saturation. An RT-PCR test for SARS-CoV-2 performed 7 days earlier returned a positive result. On day 1, supplemental oxygen was administered through a high-flow nasal cannula (HFNC) at a rate of 50 L/min and FiO2 **of** 60%, leading to an increase in oxygen saturation to 94%. On day 15, the patient became tachypneic and unable to **tolerate** the HFNC therapy; therefore, she was transferred to the ICU, requiring intubation and connection to mechanical ventilation under protective pulmonary ventilation parameters. A bronchoscopy with BAL was performed. Samples collected during the procedure were tested using PCR techniques, and *Klebsiella pneumoniae* **carbapenemase** class A and *Acinetobacter guillouiae* were isolated. On day 30, the patient presented with poor hemodynamic ventilation parameters, requiring greater vasopressor support and 100% FiO2, as well as very high airway pressures. The patient developed anuria and refractory metabolic acidosis, which led to multisystemic organ failure. The patient died within a few hours.

Case 3

A 68-year-old male patient without any significant medical history was admitted to the hospital with dyspnea, cough, fever, and oxygen saturation of 90% while using a mask and a reservoir at a flow rate of 15 liters per min. An RT-PCR test for SARS-CoV-2 performed 15 days earlier was obtained, showing a positive result. Supplemental oxygen was switched on and administered through an HFNC at a rate of 60 L/min, resulting in an oxygen saturation of 94%. On day 13, the patient developed symptoms of acute respiratory failure, which required oxygen at an FiO_2 of 80%. Therefore, he was transferred to the ICU where intubation was performed. On day 14, the patient exhibited persistent respiratory acidosis in gasometric controls despite previous measures, for which extracorporeal membrane oxygenation (ECMO) therapy was initiated. In the following days, the patient exhibited improved gasometric values but was unable to handle lower levels of sedation. On day 24, a tracheostomy was performed and a chest X-ray was conducted due to fever peaks, which showed an increase in bilateral bi-basal pulmonary condensation infiltrates.

On day 28, the bronchoscopy revealed evidence of clots along with areas of erythematous and hemorrhagic dots and minimal mucous secretion. Later, a BAL sample collected and tested through PCR testing revealed *Pseudomonas aeruginosa* and *Klebsiella pneumoniae* carbapenemase. The BAL culture isolated *Burkholderia cenocepacia,* which was resistant to ceftazidime but sensitive to meropenem and minocycline.

On day 53, during extracorporeal membrane oxygenation (ECMO) therapy, the patient presented with bleeding from the femoral cannula, which was controlled after hemostatic measures were applied. An echocardiogram was performed showing a decrease in left ventricular ejection fraction (LVEF) to 43%, which was previously 60%, and an increase in pulmonary artery systolic pressure (PASP) to 48 mmHg. The patient's clinical condition worsened and progressed to multiple organ failure, ultimately resulting in his death the following day.

Case 4

A 51-year-old female patient with no significant medical history was admitted to the hospital with dyspnea, asthenia, cough, expectoration, fever, and oxygen saturation of 90%. The result of an RT-PCR test for SARS-CoV-2 was positive. On day 3, the patient was transferred to the ICU due to failure to tolerate HFNC therapy, which prompted intubation and mechanical ventilation. On day 6, a BAL sample was collected. The sample was tested using PCR techniques and revealed *Klebsiella pneumoniae* carbapenemase class A. The galactomannan test was positive for *Aspergillus*. On day 10, diminished alveolar opacities were observed in both lungs, and the patient was extubated on day 16 and then connected to an HFNC. After receiving a fraction of inspired oxygen (FiO2) of 60%, the patient exhibited good ventilatory mechanics. After 3 days, high broad-spectrum antibiotics were suspended, and the patient was transferred to an intermediate care unit. On day 27, the patient, exhibiting a good prognosis, was switched from the HFNC to a simple nasal cannula, maintaining oxygen saturation of 94–96%. By day 32, the patient was discharged, and pulmonary rehabilitation was recommended, along with the use of supplemental oxygen through a nasal cannula at 2 L/min to maintain a SaPO2 level of 94–94% until total weaning.

Case 5

A 61-year-old female patient without a significant medical history was admitted to the hospital with fever, headache, arthromyalgia, anosmia, dry cough, diarrhea, and oxygen saturation of 94%. The result of an RT-PCR test for SARS-CoV-2 was positive. On day 2, the patient exhibited deterioration in lung function, with increased dyspnea and desaturation of up to 85%, prompting the initiation of HFNC therapy. The patient was transferred to the ICU, where intubation was performed, and placed on IMV. Soon after, a bronchoscopy with BAL was performed. SARS CoV-2 was isolated from the sample collected, and using PCR techniques, a viral load of 9,904 × 106 copies/μL was detected. On day 8, extubation was performed, and the patient was switched to HFNC with a FiO2 of 60% and a saturation of 96%. After a few days of improvement on the nasal cannula alone, the patient was finally discharged on day 18 with SaO2 >94% without any oxygen support and in good clinical condition.

Case 6

A 71-year-old male patient with a history of hypertension and type 2 diabetes mellitus was admitted to the ICU of the hospital with a 9-day history of respiratory symptoms that had been previously

treated at a private clinic where tocilizumab was administered 24 h before arrival. The result of an RT-PCR test for SARS-CoV-2 was positive.

On day 1, supplemental oxygen was administered through an HFNC without success, which prompted a switch to intubation and invasive mechanical ventilation. On day 3, a bronchoscopy with BAL was performed, and the sample was collected and sent to the molecular biology laboratory. Using multiplex PCR and mass spectrometry, *Trichosporon asahii*, *Klebsiella pneumoniae,* a KPC-producing strain, *Pseudomonas aeruginosa,* and *Aspergillus* were detected. These were identified by a galactomannan test, with a positive rate of 0.65. Antibiotic therapy was rotated; however, the patient developed multiple organ failure and eventually passed away.

Case 7

A 45-year-old male patient with a history of grade II obesity was admitted to the ICU due to respiratory symptoms that had developed over 10 days. He had been treated at home with penicillin and corticosteroids. He started experiencing respiratory difficulties 24 h before being admitted and tested positive for COVID-19 via PCR swab. Support was provided with high-flow nasal cannula oxygen therapy, which eventually failed, requiring invasive mechanical ventilation. On day 3 of the ICU admission, a fibrobronchoscopy with BAL was performed. The BAL sample was sent to the molecular biology laboratory, where *Staphylococcus aureus* was detected using multiplex PCR and mass spectrometry. mecA was resistant to vancomycin, and galactomannan was *Aspergillus* positive. Targeted antibiotic therapy with linezolid and voriconazole was started. He recovered favorably, with a decrease in acute phase reactants. He was weaned from mechanical ventilation and decannulated without complications. After 25 days of hospitalization in the ICU, he was discharged.

Case 8

A 55-year-old female patient with a history of depressive disorder tested positive for COVID-19 via PCR swab. She was admitted due to respiratory symptoms that had developed over 7 days, with the main concerns being persistent fever and worsening cough. She was transferred to the ICU, where she received support through a high-flow nasal cannula, which failed, prompting the initiation of IMV. On day 3 of the ICU admission, BAL was performed. No pathogens were detected using multiplex PCR and mass spectrometry. She died 72 h later due to refractory hypoxemia and multiple organ failure.

Case 9

A 66-year-old female patient with no pathological history of clinical importance was brought to the emergency service in a state of cardiorespiratory arrest, for which she received advanced cardiopulmonary resuscitation for 8 min and successfully regained spontaneous circulation. She was transferred to the ICU and placed on invasive mechanical ventilation. The results of the RT-PCR test for SARS-CoV-2 were positive.

On the 13th day in the ICU, a bronchoscopy with BAL was performed. Using multiplex polymerase chain reaction, multiresistant *Acinetobacter baumannii* was detected in the BAL, which was sensitive to colistin. Therefore, 100 mg of colistin was started every 12 h.

On the 17th day in the ICU, the patient's clinical condition worsened, and she died 48 h later.

During fiberoptic bronchoscopy, the ventilator settings were standardized as follows: FiO2 was increased to 100%, tidal volume (TV) set to 6–8 mL/kg of ideal body weight, respiratory rate (RR) set to 20 breaths per min, level of positive end-expiratory pressure (PEEP) set to 5 cm H2O, pressure limit set to 60 cm H2O, and the maximum inspiratory flow rate was set to 50 with a ramp wave and additional leak compensation. Furthermore, 15 min before the start of the procedure, the FiO2 was set to 100% and remained at that level throughout the procedure. During fiberoptic bronchoscopy, all ventilatory parameters remained constant (Figures 1, 2 and Table 1).

Discussion

In our case series of nine critically ill patients with COVID-19-associated ARDS (CARDS), we observed that SARS-CoV-2 infection can be associated with other microorganisms, highlighting the importance of early detection of secondary infectious etiologies. In this context, bronchoscopy is emerging as a valuable alternative for the early detection of secondary infectious etiologies and appropriate microbiological rescue (17).

Our findings corroborated that coinfections and superinfections in COVID-19 patients are associated with poor outcomes, including higher mortality rates and an increased need for invasive mechanical ventilation (IMV) (18). By focusing on identifying these infections through bronchoscopy and molecular diagnostic techniques, our case series addressed a critical aspect of COVID-19 management.

In our case series, the proper identification of coinfections and superinfections required pathogen isolation through microbiological culture from respiratory or blood samples, complemented by other molecular diagnostic techniques such as antigen detection or PCR for respiratory pathogens. We identified and reported on associated pathogens in our series of nine patients with coinfections and superinfections due to SARS-CoV-2 infection.

Although our case series focused on COVID-19, it is pertinent to consider insights from other viral infections. Previous studies have shown that after influenza virus infection, there is a reduced susceptibility to superinfections These findings may have implications for understanding the immune response to COVID-19 and its impact on secondary infections. However, further research is needed to confirm this finding in the context of SARS-CoV-2 infection.

Consistent with previous studies, we detected the presence of superinfections in the lower respiratory tract in patients with COVID-19, especially infections associated with *A. baumannii* and *S. aureus.* We employed early detection methods such as reverse transcription polymerase chain reaction (RT-PCR) (19). These pathogens were also identified through conventional culture, particularly *Staphylococcus aureus*, *Pseudomonas aeruginosa*, and *Klebsiella* spp. (20).

Notably, we observed carbapenem-resistant *Acinetobacter baumannii* (CRAB) in three of our patients. This finding aligns with several studies demonstrating how CRAB represents a common threat in the hospital setting, persisting on dry surfaces for extended periods

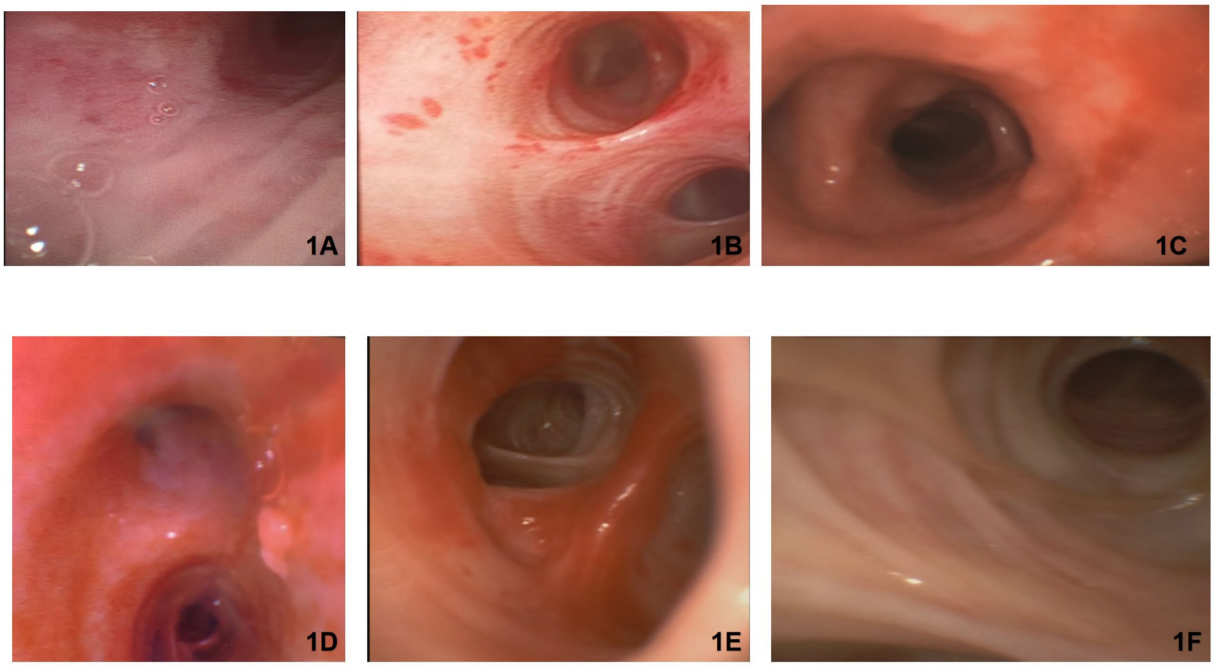

FIGURE 1
Bronchoscopic images provide valuable insights into the pathological changes that occurred in the airways of the patients with severe COVID-19. **(A)** Shows mucosal redness in the anterior wall of the subglottic region of the trachea, suggesting an infectious process. This finding is consistent with the known tropism of SARS-CoV-2 for the respiratory epithelium. **(B,D)** Show mucosal redness resulting from hemorrhagic bronchitis, characterized by small, confluent hemorrhagic areas that resemble "flea bites" on the tracheal mucosa. This finding may be a result of the increased vascular permeability and microvascular damage associated with COVID-19. **(C)** Shows edema and redness of the anterior wall of the right upper lobe bronchus, along with a dilated mucous gland orifice and mucopurulent secretions in the posterior segment. These changes suggest an ongoing inflammatory process and the presence of a secondary bacterial infection. **(E)** Shows irregularity of the mucosa in the left upper lobe, accompanied by vascular congestion and tortuosity. These findings are indicative of the extensive inflammatory response and microvascular alterations in the airways of patients with CARDS. **(F)** Shows blurred or indistinct cartilage in the left main bronchus and right lateral wall, which may be the result of pronounced mucosal edema and inflammation.

and resisting the majority of disinfectants. This translates to one of the leading causes of healthcare-associated infections, thus posing a risk for higher mortality rates in ICU patients.

A key strength of our case series is the use of molecular diagnostic techniques (21) for early specimen detection. This is vital because decisions regarding antibiotic treatments in severely ill patients often must be made without microbiological results.

All patients in our series received dexamethasone as an immunomodulatory therapy to reduce the inflammatory cascade. However, according to previous studies, inflammatory biomarkers such as C-reactive protein and procalcitonin may not be useful in identifying secondary infections in severely ill patients with SARS-CoV-2, similar to patients without infection. This presents a challenge at ICU admission since biomarker levels guide treatment initiation and continuation.

Our case series revealed co-infections in two of the patients, with *Pseudomonas and Aspergillus* being the most frequent. Regarding superinfections, we observed ESBL-and KPC-producing microorganisms, especially *Klebsiella pneumoniae* and *Pseudomonas aeruginosa* (22).

Although not observed in our case series, other microorganisms, particularly tuberculosis and HIV, have been reported in COVID-19 patients in other studies (23).

Despite the percentage of the presence of co-infections in our case series, the use of empirical antibiotics was very high (24), highlighting the potential overuse of antibiotics in COVID-19 (25). In some studies, leukocytosis increased absolute neutrophil count, and procalcitonin levels >0.5 ng/mL have been associated with a high probability of bacterial infection. However, these parameters lack sufficient sensitivity, specificity, and positive predictive value to accurately diagnose bacterial coinfections as independent tests, which is associated with a higher probability of treatment failure, especially in patients receiving immunomodulators, such as tocilizumab and corticosteroids (26).

It is worth noting that three of our cases (3, 6, and 8) received tocilizumab before their ICU admission. This biologic agent, which is known for increasing infection risk, was administered when these patients had high IL-6 levels, with the aim of managing the hyperinflammation associated with severe COVID-19. The use of tocilizumab before ICU admission highlights the delicate balance between early intervention in the inflammatory cascade and the risk of secondary infections. Our case series suggests careful monitoring for superinfections in patients treated with biologics, especially those requiring ICU care. The three patients in our cohort who received tocilizumab also had the highest levels of IL-6, a finding reflected in the literature. Recent research, including the study by Horby et al. (27), has shown that tocilizumab reduces mortality in hospitalized COVID-19 patients with hypoxia and systemic inflammation. However, the COVACTA trial (28) found no improvement in clinical outcomes or mortality with early

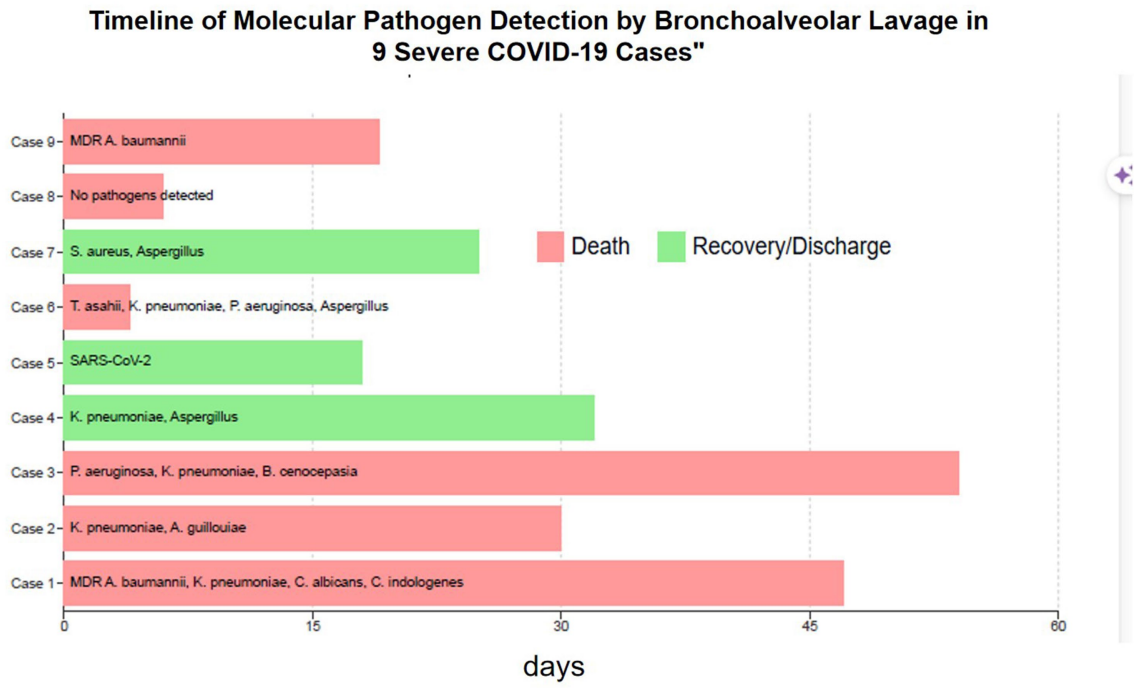

FIGURE 2
Timeline of the molecular pathogen detection by the bronchoalveolar lavage in the nine severe COVID-19 cases. This figure presents a detailed timeline of the key clinical events for the nine severe COVID-19 cases with superinfections. Each horizontal line represents an individual patient's hospitalization timeline, starting from the day of admission (A) and covering the entire duration of their hospital stay. Color Coding: Light Red Bar: Indicates the cases that resulted in patient death. Light Green Bar: Represents the cases that resulted in patient recovery and discharge. X-axis: Labeled "Days, "representing the duration of hospital stay. Y-axis: Displays case numbers, ranging from "Case 9" at the top to "Case 1" at the bottom. Bar Contents: The text within each bar indicates the pathogens detected via bronchoalveolar lavage (BAL) for each case. Pathogen Abbreviations: A comprehensive list below the graph explains the abbreviations used for the detected pathogens: DR: Multidrug-resistant; baumannii: *Acinetobacter baumannii*; pneumoniae: *Klebsiella pneumoniae*; albicans: *Candida albicans*; indologenes: *Chryseobacterium indologenes*; guillouiae: *Acinetobacter guillouiae*; aeruginosa: *Pseudomonas aeruginosa*; cenocepacia: *Burkholderia cenocepacia*; aureus: *Staphylococcus aureus*; asahii; *Trichosporon asahii*; and RS-CoV-2: Severe acute respiratory syndrome coronavirus 2.

tocilizumab use in severe COVID-19 pneumonia. Regarding superinfections, Kimmig et al. (29) reported no significant increase in secondary infections in tocilizumab-treated COVID-19 patients; however, vigilance is advised. Our small case series contributes to the discussion on tocilizumab use in severe COVID-19, emphasizing careful patient selection and monitoring for complications such as superinfections. Although causality cannot be established, these findings highlight challenges in managing severe COVID-19 and raise concerns about the use of biologics such as tocilizumab.

Our findings put into perspective the fact that the clinical course of ARDS in COVID-19 is usually marked by multiple superimposed infections, leading to high mortality rates. This observation emphasizes the importance of preventive measures, particularly vaccination, in containing the pandemic and reducing the incidence of COVID-19-induced ARDS. Seminal studies have shown that vaccination against COVID-19 is safe and effective in preventing severe disease (30). Moreover, population-based analyses have shown much better clinical outcomes in vaccinated patients compared to their unvaccinated counterparts. Such findings emphasize the critical role played by vaccination in the reduction of severe consequences of COVID-19, such as ARDS and associated superinfections. Our case series contributes significant insight as it was conducted at a time when vaccines were not widely available, suggesting that more widespread vaccination could potentially have averted such severe cases (31).

Our case series, conducted during the second wave of COVID-19 in Ecuador, acknowledges the unique conditions and challenges faced in resource-limited settings. The constraints of such environments necessitate innovative approaches and adaptation of standard practices to ensure effective patient management, particularly in severe COVID-19 cases where resources are limited (32).

The lessons learned from this case series are pivotal in the current pandemic context and have significant implications for future health crises. Understanding the dynamics and management strategies in resource-constrained settings, as observed in our patients from Ecuador, provides valuable insights into global health, emphasizing the need for adaptable and scalable solutions during pandemics (33).

Limitations and Future Research Directions: A notable limitation of this case series is the lack of a standard and consensus definition for the criteria determining the start and end of a COVID-19 epidemic wave (34). This has led to discrepancies in the established dates compared to other studies. In addition, accurately identifying the end of one wave and the beginning of the next is complex as virus transmission persists at baseline levels (35). This

TABLE 1 The baseline characteristics, laboratory tests, blood biomarkers, tomographic characteristics, and treatments associated with the isolated pathogens of each of the patients.

Clinical Characteristics	Patient 1	Patient 2	Patient 3	Patient 4	Patient 5	Patient 6	Patient 7	Patient 8	Patient 9
Age	51	74	68	51	61	71	45	55	66
Sex	Male	Female	Male	Female	Female	Male	Male	Female	Female
Past illness history	Hypertension*, Obesity	Hypertension	None	None	None	Hypertension, Diabetes type II	Obsesity type II	Depression	None
Disease history days prior hospital admission	11	7	16	5	7	9	10	7	12
Symptoms	Fever, dyspnea, dry cough, malaise, polyarthralgia.	Fever, dry cough, dyspnea, diarrhea.	Fever, dry cough, dyspnea, malaise.	Fever, asthenia, cough with expectoration	Fever, headache, arthromyalgia, anosmia, dry cough, and diarrheal stools	Fever, cough, dyspnea, malaise	Odynophagia, fever, dyspnea, malaise	Fever, odynophagia, dyspnea, malaise	Fever, malaise, dyspnea, cough, cardiorespiratory arrest during admission
RT-PCR Test for SARS-CoV-2	Positive	Positive	Positive	Positive	Positive	Positive	Positive	Positive	Positive
Oxygen saturation with HFNC device (%)	80	75	88	80	80	92	88	90	Not used*
Laboratory findings									
White cell count (per mm^3) (normal range 4,400 to 10,300)	23,790	20,000	20,340	15,320	11,260	25.20	15.11	26.27	19,950
Total neutrophils (normal range 1780 to 5,380)	22,410	18,550	19,270	14,160	10,730	24.30	13.90	22.89	16.95
Total lymphocytes (normal range 1,180 to 3,740)	430	870	530	740	210	520	770	261	243
CRP (mg/dl) (normal range 0 to 5)	44.31	8.45	43.98	4.25	27.82	53.20	–	16	34.54
Ferritin (ng/ml) (normal range 30 to 400)	1,736	2,221	1,435	1,133	1719	>2000	>2000	964	6,828

(Continued)

10.3389/fmed.2024.1409323

TABLE 1 (Continued)

Clinical Characteristics	Patient 1	Patient 2	Patient 3	Patient 4	Patient 5	Patient 6	Patient 7	Patient 8	Patient 9
**IL-6 (pg/ml) (normal range 0 to 6.5)	149.20	18.75	1,351	38.97	107.8	4,365	282	1,384	986.4
D-dimer (mg/l) (normal range 0 to 1.9)	0.79	2.95	4.14	2.59	0.60	6.8	1.18	9.2	4.27
Procalcitonine (ng/ml) (normal range < 0.046)	5.34	0.07	1.79	0.10	0.27	1.34	–	0.16	66.88
Radiological (CT-scan) findings:									
Ground-glass opacity	+++	+++	+++	++	+++	+++	+++	+++	+++
Condensation areas	Yes	No	Yes	Yes	Yes	Yes	Yes	No	Yes
Crazy paving pattern	No	+	No	+	+	+	No	No	+
Solitary nodule	No	No	No	No	No	No	No	No	No
Bronchoalveolar lavage findings									
Microorganisms	*Klebsiella pneumoniae* carbapenemase class A and class D OXA; Carbapenem-multiresistant *Acinetobacter baumannii* class D OXA 23 and class D OXA 51 *Candida albicans*, Cryseobacterium indologenes, Apergillus sp.	*Klebsiella pneumoniae* carbapenemase class A; *Acinetobacter guillouiae*.	Pseudomona aeruginosa; *Klebsiella pneumoniae* Carbapenemase; *Burkholderia cenocepacia*; *Candida albicans*; Aspergillus sp	GES-type carbapenemase-producing *P. aeruginosa*; Aspergillus	SARS CoV-2	Trichosporon asahii, Aspergillus; Klebsiella; pneumoniae carbapenemase; Pseudomonas; aeruginosa.	*Staphylococcus aureus* mecA; Aspergillus	SARS CoV-2	*Acinetobacter baumannii*

(Continued)

10.3389/fmed.2024.1409323

TABLE 1 (Continued)

Clinical Characteristics	Patient 1	Patient 2	Patient 3	Patient 4	Patient 5	Patient 6	Patient 7	Patient 8	Patient 9
Prescription	Supplemental oxygen (HFNC), meropenem, moxifloxacin, tigecycline, ceftazidime / avibactam, trimethoprim / sulfamethoxazole, unfractionated heparin, norepinephrine.	Supplemental oxygen (HFNC), meropenem, voriconazole, moxifloxacin, ivermectin, nebulized amikacin, enoxaparin, prednisone, atorvastatin, colchicine, antihypertensives	Supplemental oxygen (HFNC), received tocilizumab prior to their ICU admission. Colistin, tigecycline, meropenem, voriconazole, nebulized amikacin, enoxaparin, colchicine, ivermectin, atorvastatin, antihypertensives.	Supplemental oxygen (HFNC), colistin, minocycline, ceftazidime / avibactam, fosfomycin and voriconazole, rendisivir, dexamethasone, colchicine, atorvastatin, meropenem, and moxifloxacin	Supplemental oxygen (HFNC), dexamethasone, enoxaparin, atorvastatin, piperacillin / tazobactam, and moxifloxacin.	Received tocilizumab prior to their ICU admission. Mechanical ventilation, imipenem + cilastatin, levofloxacin, dexamethasone, enoxaparin, simvastatin	Mechanical ventilation, cefepime, levofloxacin, dexamethasone, enoxaparin, simvastatin.	Received tocilizumab prior to their ICU admission Mechanical ventilation, meropenem, vancomycin, voriconazole, dexamethasone, enoxaparin, simvastatin	Mechanical ventilation, meropenem, vancomycin, voriconazole, dexamethasone, enoxaparin, simvastatin
Mechanical ventilation needed	Yes	Yes	Yes	Yes	Yes	Yes	Yes	Yes	Yes
Survival	No	No	No	Yes	Yes	No	Yes	No	No

*Hypertension, high blood pressure; **C-RP, C reactive protein; ***IL-6, Interleukinae 6; ****HFNC, High flow nasal cannula.

study relied on confirmed case data, which can be influenced by external factors, such as variations in diagnostic capacity over time. Furthermore, the small number of cases in our series limits the generalizability of our findings. In addition, further research is needed to evaluate the long-term outcomes of patients with identified coinfections and superinfections.

In conclusion, this case series highlights the utility of bronchoscopy and molecular diagnostic techniques in detailing bronchial mucosal characteristics, underscoring their critical role in diagnosing and managing CARDS by identifying airway involvement and secondary infections. These techniques are particularly valuable when certain clinical and laboratory parameters are present in critically ill patients. Our findings suggest that BAL and the early use of molecular diagnostic techniques play an important role in the management of severe COVID-19 cases, particularly in resource-limited settings. Future studies should focus on optimizing these techniques and developing standardized protocols for their use in pandemic situations and should include larger patient populations to validate and expand upon our observations.

Data availability statement

The original contributions presented in the study are included in the article/Supplementary material, further inquiries can be directed to the corresponding author/s.

Ethics statement

The studies involving humans were approved by the Ecuadorian Ministry of Public Health's *ad hoc* ethics committee (code MSP-CGDES-2021-0065-O). As part of the REDCap study, the IESS Babahoyo Hospital complied with all ethical requirements for clinical research. The studies were conducted in accordance with the local legislation and institutional requirements. Written informed consent for participation in this study was provided by the participants' legal guardians/next of kin. Written informed consent was obtained from the individual (s) for the publication of any potentially identifiable images or data included in this article.

Author contributions

KB: Conceptualization, Data curation, Formal analysis, Funding acquisition, Investigation, Methodology, Project administration, Resources, Software, Supervision, Validation, Visualization, Writing – original draft, Writing – review & editing. MB-C: Conceptualization, Data curation, Formal analysis, Funding acquisition, Investigation, Methodology, Project administration, Resources, Software, Supervision, Validation, Visualization, Writing – original draft, Writing – review & editing. RM: Conceptualization, Data curation, Formal analysis, Investigation, Methodology, Project administration, Supervision, Validation, Writing – original draft, Writing – review & editing. JB: Conceptualization, Data curation, Formal analysis, Investigation, Methodology, Software, Supervision, Validation, Visualization, Writing – original draft, Writing – review & editing.

KB: Data curation, Formal analysis, Investigation, Methodology, Project administration, Resources, Supervision, Validation, Writing – original draft, Writing – review & editing. AF: Data curation, Formal analysis, Investigation, Methodology, Resources, Validation, Writing – original draft, Writing – review & editing, Conceptualization, Visualization. PB-T: Conceptualization, Data curation, Formal analysis, Investigation, Methodology, Resources, Visualization, Writing – original draft, Writing – review & editing, Funding acquisition, Project administration. MG: Conceptualization, Data curation, Formal analysis, Funding acquisition, Investigation, Methodology, Project administration, Resources, Visualization, Writing – original draft, Writing – review & editing, Software, Supervision, Validation.

Funding

The author(s) declare that no financial support was received for the research, authorship, and/or publication of this article.

Conflict of interest

The authors declare that the research was conducted in the absence of any commercial or financial relationships that could be construed as a potential conflict of interest.

Publisher's note

Supplementary material

The Supplementary material for this article can be found online at: https://www.frontiersin.org/articles/10.3389/fmed.2024.1409323/full#supplementary-material

References

1. Dong E, Du H, Gardner L (2020). An interactive web-based dashboard to track COVID-19 in real time. *Lancet Infect Dis* 20:533–4. doi: 10.1016/S1473-3099(20)30120-1

2. Maveddat A, Mallah H, Rao S, Ali K, Sherali S, Nugent K (2020). Severe acute respiratory distress syndrome secondary to coronavirus 2 (SARS-CoV-2). *Int J Occup Environ Med* 11:157–78. doi: 10.34172/ijoem.2020.2202

3. Xu Z, Shi L, Wang Y, Zhang J, Huang L, Zhang C, et al (2020). Pathological findings of COVID-19 associated with acute respiratory distress syndrome. *Lancet Respir Med* 8:420–2. doi: 10.1016/S2213-2600(20)30076-X

4. Ferguson ND, Fan E, Camporota L, Antonelli M, Anzueto A, Beale R, et al (2012). The Berlin definition of ARDS: an expanded rationale, justification, and supplementary material. *Intensive Care Med* 38:1573–82. doi: 10.1007/s00134-012-2682-1

5. Qeadan F, Tingey B, Gu LY, Packard AH, Erdei E, Saeed AI (2021). Prognostic values of serum ferritin and D-dimer trajectory in patients with COVID-19. *Viruses* 13:419. doi: 10.3390/v13030419

6. Karampitsakos T, Papaioannou O, Tsiri P, Katsaras M, Katsimpris A, Kalogeropoulos AP, et al (2023). Tocilizumab versus baricitinib in hospitalized patients with severe COVID-19: an open label, randomized controlled trial. *Clin Microbiol Infect* 3:372–8. doi: 10.1016/j.cmi.2022.10.015

7. Cordovilla R, Álvarez S, Llanos L, Nuñez Ares A, Cases Viedma E, Díaz-Pérez D, et al (2020). Recomendaciones de consenso SEPAR y AEER sobre el uso de la broncoscopia y la toma de muestras de la vía respiratoria en pacientes con sospecha o con infección confirmada por COVID-19 [SEPAR and AEER consensus recommendations on the use of bronchoscopy and airway sampling in patients with suspected or confirmed COVID-19 infection]. *Archivos Bronconeumol* 56:19–26. doi: 10.1016/j.arbres.2020.03.017

8. Pritchett MA, Oberg CL, Belanger A, De Cardenas J, Cheng G, Nacheli GC, et al (2020). Society for advanced bronchoscopy consensus statement and guidelines for bronchoscopy and airway management amid the COVID-19 pandemic. *J Thorac Dis* 12:1781–98. doi: 10.21037/jtd.2020.04.32

9. Musuuza JS, Watson L, Parmasad V, Putman-Buehler N, Christensen L, Safdar N (2021). Prevalence and outcomes of co-infection and superinfection with SARS-CoV-2 and other pathogens: a systematic review and meta-analysis. *PLoS One* 16:e0251170. doi: 10.1371/journal.pone.0251170

10. Bruyneel M, Gabrovska M, Rummens P, Roman A, Claus M, Stevens E, et al (2020). Bronchoscopy in COVID-19 intensive care unit patients. *Respirology* 25:1313–5. doi: 10.1111/resp.13932

11. National Emergency Operations Committee. Infografia-Nacional COVID19-Coe-Nacional-08h00-23072021 Second Wave [Pdf]. (2021) Available at: https://www.salud.gob.ec/wp-content/uploads/2021/07/INFOGRAFIA-NACIONALCOVID19-COE-NACIONAL-08h00-08072021.pdf

12. Barberi C, Castelnuovo E, Dipasquale A, Mrakic Sposta F, Vatteroni G, Canziani LM, et al (2021). Bronchoalveolar lavage in suspected COVID-19 cases with a negative nasopharyngeal swab: a retrospective cross-sectional study in a high-impact northern Italy area. *Intern Emerg Med* 16:1857–64. doi: 10.1007/s11739-021-02714-y

13. Saha BK, Saha S, Chong WH, Beegle S (2022). Indications, clinical utility, and safety of bronchoscopy in COVID-19. *Respir Care* 67:241–51. doi: 10.4187/respcare.09405

14. Patrucco F, Failla G, Ferrari G, Galasso T, Candoli P, Mondoni M, et al (2021). Bronchoscopy during COVID-19 pandemic, ventilatory strategies and procedure measures. *Panminerva Med* 63:529–38. doi: 10.23736/S0031-0808.21.04533-X

15. Tzouvelekis A, Karampitsakos T, Krompa A, Markozannes E, Bouros D (2020). False positive COVID-19 antibody test in a case of granulomatosis with Polyangiitis. *Front Med* 7:399. doi: 10.3389/fmed.2020.00399

16. Wahidi MM, Lamb C, Murgu S, Musani A, Shojaee S, Sachdeva A, et al (2020). American Association for Bronchology and Interventional Pulmonology (AABIP) statement on the use of bronchoscopy and respiratory specimen collection in patients with suspected or confirmed COVID-19 infection. *J Bronchology Interv Pulmonol* 27:e52–4. doi: 10.1097/LBR.0000000000000681

17. Rynda-Apple A, Robinson KM, Alcorn JF (2015). Influenza and bacterial superinfection: illuminating the immunologic mechanisms of disease. *Infect Immun* 83:3764–70. doi: 10.1128/IAI.00298-15

18. Paget C, Trottein F (2019). Mechanisms of bacterial superinfection post-influenza: a role for unconventional T cells. *Front Immunol* 10:336. doi: 10.3389/fimmu.2019.00336

19. Mobarak-Qamsari M, Jenaghi B, Sahebi L, Norouzi-Shadehi M, Salehi MR, Shakoori-Farahani A, et al (2023). Evaluation of *Acinetobacter baumannii*, *Klebsiella pneumoniae*, and *Staphylococcus aureus* respiratory tract superinfections among patients with COVID-19 at a tertiary-care hospital in Tehran. *Iran Eur J Med Res* 28:314. doi: 10.1186/s40001-023-01303-3

20. Bogdan I, Gadela T, Bratosin F, Dumitru C, Popescu A, Horhat FG, et al (2023). The assessment of multiplex PCR in identifying bacterial infections in patients hospitalized with SARS-CoV-2 infection: a systematic review. *Antibiotics* 12:465. doi: 10.3390/antibiotics12030465

21. Foschi C, Zignoli A, Gaibani P, Vocale C, Rossini G, Lafratta S, et al (2021). Respiratory bacterial co-infections in intensive care unit-hospitalized COVID-19 patients: conventional culture vs bio fire film Array pneumonia plus panel. *J Microbiol Methods* 186:106259. doi: 10.1016/j.mimet.2021.106259

22. Montrucchio G, Corcione S, Lupia T, Shbaklo N, Olivieri C, Poggioli M, et al (2022). The burden of Carbapenem-resistant *Acinetobacter baumannii* in ICU COVID-19 patients: a regional experience. *J Clin Med* 11:5208. doi: 10.3390/jcm11175208

23. Al-Kayali RS, Kashkash MF, Alhussein Alhajji AH, Khouri A (2023). Activation of tuberculosis in recovered COVID-19 patients: a case report. *Ann Med Surg* 85:280–3. doi: 10.1097/MS9.0000000000000188

24. Ali Mohammadi A, Chezani-Sharahi N, Hezaveh ZA, Abbasi E, Shariati A, Ghaznavi-Rad E (2023). The significant role of Carbapenems-resistant *Acinetobacter Baumannii* in mortality rate of patients with COVID-19. *Vacunas* 24:13–8. doi: 10.1016/j.vacun.2022.10.004

25. Granata G, Schiavone F, Pipitone G, Taglietti F, Petrosillo N (2022). Antibiotics use in COVID-19 patients: a systematic literature review. *J Clin Med* 11:7207. doi: 10.3390/jcm11237207

26. Sharifipour E, Shams S, Esmkhani M, Khodadadi J, Fotouhi-Ardakani R, Koohpaei A, et al (2020). Evaluation of bacterial co-infections of the respiratory tract in COVID-19 patients admitted to ICU. *BMC Infect Dis* 20:646. doi: 10.1186/s12879-020-05374-z

27. Horby P, Lim WS, Emberson JR, Mafham M, Bell JL, Linsell L, et al (2021). Dexamethasone in hospitalized patients with Covid-19. *N Engl J Med* 384:693–704. doi: 10.1056/NEJMoa2021436

28. Rosas IO, Bräu N, Waters M, Go RC, Hunter BD, Bhagani S, et al (2021). Tocilizumab in hospitalized patients with severe Covid-19 pneumonia. *N Engl J Med* 384:1503–16. doi: 10.1056/NEJMoa2028700

29. Kimmig LM, Wu D, Gold M, Pettit NN, Pitrak D, Mueller J, et al (2020). IL-6 inhibition in critically ill COVID-19 patients is associated with increased secondary infections. *Front Med* 7:583897. doi: 10.3389/fmed.2020.583897

30. Polack FP, Thomas SJ, Kitchin N, Absalon J, Gurtman A, Lockhart S, et al (2020). Safety and efficacy of the BNT162b2 mRNA Covid-19 vaccine. *N Engl J Med* 383:2603–15. doi: 10.1056/NEJMoa2034577

31. Papaioannou O, Karampitsakos T, Tsiri P, Sotiropoulou V, Koulousousa E, Tasiopoulos P, et al (2022). Clinical outcomes in vaccinated and unvaccinated patients with COVID-19: a population-based analysis. *Eur Rev Med Pharmacol Sci* 26:7705–12. doi: 10.26355/eurrev_202210_30047

32. Moreira-Soto A, Bruno A, de Mora D, Paez M, Garces J, Wulf B, et al (2023). Virological evidence of the impact of non-pharmaceutical interventions against COVID-19 in Ecuador, a resource-limited setting. *Emerg Microbes Infect* 12:2259001. doi: 10.1080/22221751.2023.2259001

33. Orellana-Manzano A, Cordeiro FB, Garcia-Angulo A, Centeno E, Vizcaíno-Tumbaco MJ, Poveda S, et al (2023). A report on SARS-CoV-2 first wave in Ecuador: drug consumption dynamics. *Front Pharmacol* 14:1197973. doi: 10.3389/fphar.2023.1197973

34. Alava JJ, Guevara A (2021). A critical narrative of Ecuador's preparedness and response to the COVID-19 pandemic. *Public Health Pract* 2:100127. doi: 10.1016/j.puhip.2021.100127

35. Zhang SX, Arroyo Marioli F, Gao R, Wang S (2021). A second wave? What do people mean by COVID waves?- a working definition of epidemic waves. *Risk Manag Healthc Policy* 14:3775–82. doi: 10.2147/RMHP.S326051

36. Harris PA, Taylor R, Minor BL, Elliott V, Fernandez M, O'Neal L, et al (2019). The REDCap consortium: building an international community of software platform partners. *J Biomed Inform* 95:103208. doi: 10.1016/j.jbi.2019.103208

37. Abood RN, McHugh KJ, Rich HE, Ortiz MA, Tobin JM, Ramanan K, et al (2019). IL-22-binding protein exacerbates influenza, bacterial super-infection. *Mucosal Immunol 12:1231–43. doi: 10.1038/s41385-019-0188-7*

frontiers | Frontiers in Immunology

TYPE Case Report
PUBLISHED 06 November 2024
DOI 10.3389/fimmu.2024.1452195

OPEN ACCESS

EDITED BY
Karolina Henryka Czarnecka-Chrebelska,
University of Lodz, Poland

REVIEWED BY
Xiangliang Liu,
The First Hospital of Jilin University, China
Qingquan Luo,
Shanghai Jiao Tong University, China

*CORRESPONDENCE
Lei Cao
BrawnyM80@163.com

†These authors have contributed equally to this work

RECEIVED 20 June 2024
ACCEPTED 21 October 2024
PUBLISHED 06 November 2024

CITATION
Fu C, Du H, Wang Q, Zhu W, Bian G, Zhong Z, Wang Y and Cao L (2024) Case report: A golden tail of immunotherapy: significant tail effect in a chemotherapy-resistant advanced pulmonary sarcomatoid carcinoma patient treated by Sintilimab combined with Anlotinib.
Front. Immunol. 15:1452195.
doi: 10.3389/fimmu.2024.1452195

Case report: A golden tail of immunotherapy: significant tail effect in a chemotherapy-resistant advanced pulmonary sarcomatoid carcinoma patient treated by Sintilimab combined with Anlotinib

Chenghao Fu[1,2†], Haonan Du[1†], Qiang Wang[3†], Weiyou Zhu[1], Guangli Bian[4], Zhujuan Zhong[5], Yuheng Wang[2] and Lei Cao[6*]

[1]Department of Oncology, The First Affiliated Hospital of Nanjing Medical University, Nanjing, Jiangsu, China, [2]Department of Thoracic Surgery, The First Affiliated Hospital of Nanjing Medical University, Nanjing, Jiangsu, China, [3]Department of Thoracic Surgery, Taizhou Fourth People's Hospital, Taizhou, Jiangsu, China, [4]Department of Radiology, The Affiliated Suqian First People's Hospital of Nanjing Medical University, Suqian, Jiangsu, China, [5]Department of Pathology, The Affiliated Suqian First People's Hospital of Nanjing Medical University, Suqian, Jiangsu, China, [6]Department of Oncology, The Affiliated Suqian First People's Hospital of Nanjing Medical University, Suqian, Jiangsu, China

Tail effect is a unique phenomenon in immunotherapy characterized by the prolonged maintenance of therapeutic efficacy. It can be observable even after treatment cessation. Immunotherapy has gradually become a vital regimen for the treatment of advanced lung cancer patients, among which immune-combined therapies based on immune checkpoint inhibitors (ICIs) have been applied clinically and demonstrates considerable clinical efficacy. In this case report, the patient was pathologically diagnosed with pulmonary sarcomatoid carcinoma (PSC), a rare and highly aggressive subtype of non-small cell lung cancer (NSCLC) known for its poor prognosis due to high invasiveness and metastatic potential. After developing resistance to chemotherapy, the patient was treated with a combined regimen of sintilimab and anlotinib, leading to initial clinical improvement. Following just three cycles of this regimen, treatment was discontinued, and the patient was discharged. Remarkably, over the subsequent months, the patient exhibited a significant tail effect, evidenced by sustained therapeutic stability, continuous tumor regression, stable low levels of serum carcinoembryonic antigen (CEA), and further improvement in clinical symptoms. Tail effect is a golden tail of immunotherapy. This case illustrates that the tail effect of immunotherapy can offer substantial survival benefits for patients with unresectable advanced lung cancer who have failed chemotherapy.

KEYWORDS

tail effect, immunotherapy, cancer therapy, PSC, ICI, Sintilimab

Introduction

Tail effect is a special phenomenon in clinical anti-tumor immunotherapy, referring to the long-term persistence of therapeutic efficacy, which continues to be observed even after treatment cessation. The underlying mechanism primarily involves the function of memory T cells (1–3), reflected at the molecular level by epigenetic regulation, long non-coding RNA (lncRNA), transcription factors, and cytokines (4). This phenomenon can provide considerable long-term clinical benefits to patients with advanced tumors, propelling immunotherapy to the forefront of advanced NSCLC treatment, and in some sense, altering the tumor progression pattern. In recent years, immunotherapy represented by ICIs has shown significant efficacy in the treatment of advanced NSCLC (5–7). Programmed death-1 (PD-1) inhibitory ICIs like sintilimab block the interaction between PD-1 and its ligand, programmed death-ligand 1 (PD-L1), thereby lifting the immune suppression imposed by tumor cells and activating T cell-mediated anti-tumor effects (8, 9). Combination regimens based on ICIs, including sintilimab combined with anlotinib, have been clinically applied (10–13). Anlotinib, a novel multi-target tyrosine kinase inhibitor, can inhibit angiogenesis and tumor cell proliferation, further enhancing the anti-tumor effects of ICIs (14, 15).

PSC is a rare and highly aggressive subtype of NSCLC, accounting for only 0.1%-0.4% of all lung malignancies (16, 17). Patients with PSC have a significantly higher risk of mortality compared to other types of NSCLC due to its high invasiveness and metastatic potential (16, 18). Chemotherapy is currently the primary treatment for advanced PSC, but its efficacy is often unsatisfactory due to the low sensitivity to chemotherapy and the rapid development of resistance (19–21). Other traditional treatment methods also have limited efficacy. Notably, PSC frequently exhibits high PD-L1 expression and high tumor mutation burden (TMB) (22), suggesting that it may benefit from ICIs. Several case reports have demonstrated significant efficacy of ICI-based combination therapies in advanced PSC patients (10, 23), potentially offering new treatment strategies for PSC.

This case report aims to illustrate the therapeutic process involving a combination of ICIs in the treatment of a patient with advanced, chemotherapy-resistant PSC, who exhibited a notable tail effect. This observation provides new perspectives on the comprehensive treatment strategies for patients with advanced NSCLC. While prior clinical trials have explored the combination of ICIs with anlotinib in PSC patients (23), this case is unique. It not only demonstrates the efficacy of combined ICIs therapy in an advanced chemotherapy-resistant PSC patient but also emphasizes the clinical benefit derived from the tail effect observed after the discontinuation of treatment. To date, this phenomenon has not been reported in PSC patients.

Case presentation

On May 19, 2022, a 59-year-old male patient presented with a one-month history of persistent dry cough and intermittent expectoration of white mucus. The patient had no family history of malignancy but had a history of smoking for over 30 years, with a smoking index of 600. He had recovered from pulmonary tuberculosis four years prior. The patient's ECOG performance status was 1, and the Numeric Rating Scale (NRS) score was 3. A chest computed tomography (CT) scan revealed a soft tissue density shadow approximately 58*38 mm in size with bronchial obstruction in the right middle lobe (RML) and a high-density mass lesion approximately 71*53 mm in the right lower lobe (RLL) with adjacent bronchial obstruction, lobulation, and patchy shadows. Enlarged mediastinal lymph nodes measuring approximately 30*19 mm were observed. Localized pleural thickening was noted around the lesion (Figures 1A–C). Bone scans and enhanced cranial MR showed no metastases. CEA level was abnormally elevated at 7.17 ng/ml (reference range: 0-4.7 ng/ml). White blood cell (WBC) level was 11.2*10^9/L (Figure 2).

To further clarify the pathological nature, the patient underwent a bronchoscopic biopsy on May 21, 2022. Pathological results indicated malignancy in both lesions in the right middle and lower lobes, pending further immunohistochemical (IHC) analysis. IHC results showed negative staining for TTF-1, Napsin-A, SYN, CD56, CgA, Cd56, Villin, P63, P40,CK20 and PSA (Figures 3G–P)as well as positive staining for CK-pan (+++), Ki67 (50%+), CK8/18 (+++), and CK7 (+++) (Figures 3C–F). Combined with hematoxylin-eosin (HE) staining (Figure 3B), the case was consistent with a poorly differentiated carcinoma, suggesting a sarcomatoid carcinoma phenotype. Next-generation sequencing (NGS) revealed mutations in the KRAS and TP53 genes, but no mutations were detected in the EGFR, ALK, or MET exon 14 genes. Unfortunately, according to the CSCO guidelines for driver gene definition, this patient is unlikely to benefit from targeted therapies aimed at these specific mutations (24). After multidisciplinary consultation by department of oncology and pathology in our hospital and department of thoracic surgery in the first affiliated hospital of Nanjing Medical University, the patient was diagnosed with stage IVa poorly differentiated PSC involving the RML/RLL with pleural involvement (cT4N2M1 IVa stage).

Considering the unresectable state of the tumor, the patient began a first-line chemotherapy regimen of cisplatin combined with albumin-bound paclitaxel on June 24, 2022, receiving two cycles from June 24 to August 19, 2022. However, the patient experienced decreased appetite, nausea, vomiting, significant weight loss, and grade II leukopenia (WBC level: 2.3*10^9/L) (Figure 2), indicating poor tolerance to the chemotherapy's toxic side effects. A follow-up chest CT on August 19, 2022, showed an increase in the size of the RML lesion to 61*37 mm, the RLL tumor to 73*56 mm, and mediastinal lymph nodes to 43 mm in diameter with partial fusion (Figures 1D–F). CEA levels further increased to 7.34 ng/ml (Figure 2) and the NRS score increased to 6. These signs indicated the appearance of chemotherapy resistance and progressive disease (PD).

In response to disease progression, we considered modifying the treatment regimen and evaluated the feasibility of immunotherapy. On August 20, 2022, with PD-L1 testing showing high expression (approximately 70%) (Figure 3A), we initially considered using sintilimab as ICIs medication and also took into account the favorable safety profile of anlotinib in combination therapy. Thus, the treatment regimen was finally adjusted to an immune-targeted combination of sintilimab and anlotinib. The patient received two

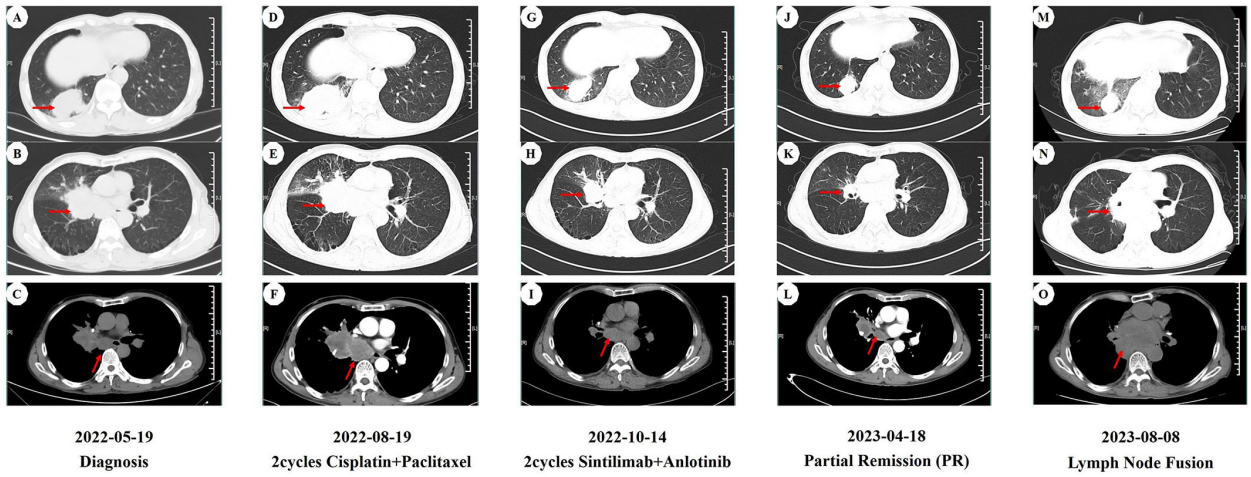

FIGURE 1
CT imaging assessment of lung lesions and mediastinal lymph nodes throughout the course of disease corresponding to their respective time points. **(A–C)** CT imaging of the lung window **(A, B)** and the mediastinal window **(C)** on May 19, 2022; **(D–F)** CT imaging of the lung window **(D, E)** and the mediastinal window **(F)** on August 19, 2022; **(G–I)** CT imaging of the lung window **(G,H)** and the mediastinal window **(I)** on October 14, 2022; **(J–L)** CT imaging of the lung window **(J, K)** and the mediastinal window **(L)** on April 18, 2023; **(M–O)** CT imaging of the lung window **(M, N)** and the mediastinal window **(O)** on August 8, 2023. **(A, D, G, J, M)** image manifests the lesion of the right lower lobe in the CT lung window. **(B, E, H, K, N)** image manifests the lesion of the right middle lobe in the CT lung window. **(C, F, I, L, O)** image manifests the mediastinal lymph nodes in the CT mediastinal window.

cycles of treatment from August 22 to October 14, 2022, during which the adverse reactions to chemotherapy disappeared, and the patient reported symptom improvement. A follow-up chest CT after the second cycle on October 14, 2022, showed a reduction in the size of the lesions in the RML and RLL by 34.4% and 19.8%, respectively. The mediastinal lymph nodes also showed reduction and clearer contours (Figures 1G–I). CEA levels were controlled at 4.42 ng/ml, and WBC levels decreased to 5.3*10^9/L (Figure 2). The NRS score decreased to 4. The efficacy evaluation showed stable disease (SD), confirming the preliminary effect of the combination therapy. But due to personal willingness and financial reasons, the patient decided to discontinue treatment after completing the third cycle on November 9, 2022, and was discharged after signing informed consent.

Given the patient's condition, we initially held a pessimistic outlook for follow-up results. However, surprisingly, during a follow-up visit on April 18, 2023, the patient exhibited a better mental state and further-improved clinical symptoms with a complete resolution of dry cough and chest pain, and an NRS score of 1. CT scans better confirmed the change: the RML lesion had shrunk to 27*21 mm, the RLL lesion to 51*31 mm, and the mediastinal lymph nodes to 21*19 mm (Figures 1J–L). The sizes were both better controlled than before: the RML lesion volume decreasing by 74% (compared with initial diagnosis) and 75% (compared with

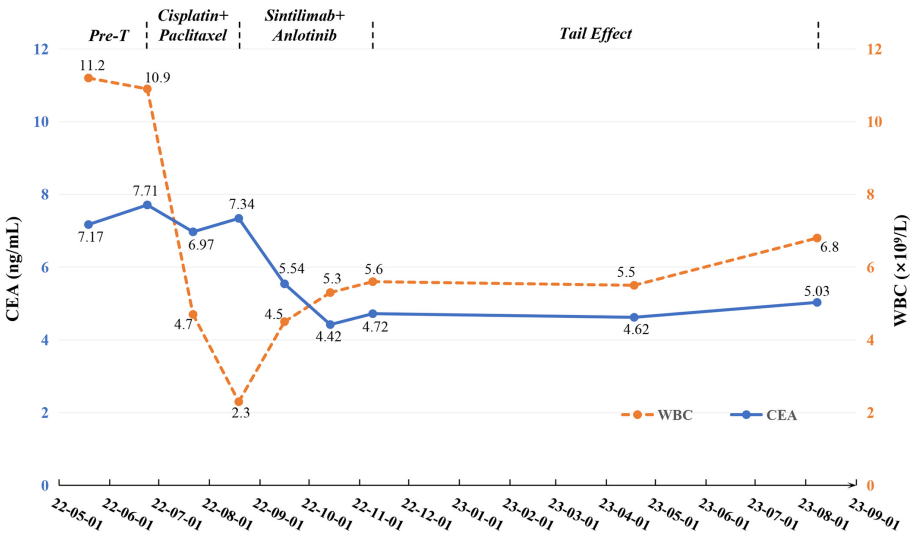

FIGURE 2
Changes of tumor markers and blood parameter during treatment. CEA, carcinoembryonic antigen; Pre-T, pre-treatment; WBC, white blood cell.

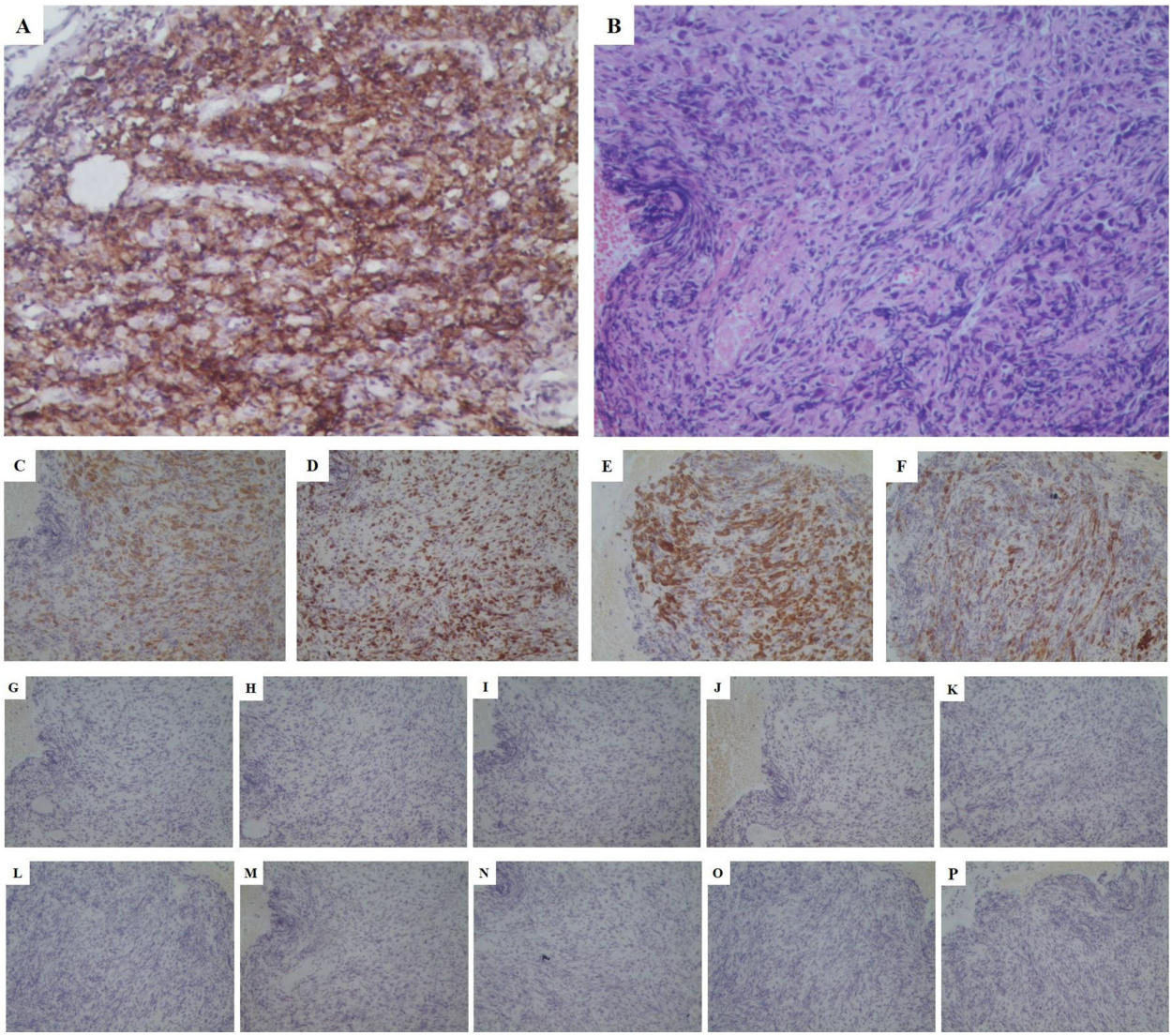

FIGURE 3
Pathological stained section (magnification:*200). **(A)** PD-L1 stained positive with a high expression (approximately 70%); **(B)** HE staining consistent with a poorly differentiated carcinoma, suggesting a sarcomatoid carcinoma phenotype; **(C)** CK-pan (+++); **(D)** Ki67 (50%+); **(E)** CK8/18 (+++); **(F)** CK7 (+++); **(G)** Napsin-A (-); **(H)** TTF-1 (-); **(I)** CgA (-); **(J)** SYN (-); **(K)** Cd56 (-); **(L)** Villin (-); **(M)** P63 (-); **(N)** P40 (-); **(O)** CK20 (-); **(P)** PSA (-). PD-L1, programmed death-ligand 1; HE, hematoxylin&eosin; CK, cytokeratin; TTF, thyroid transcription factor; SYN, synaptophysin; PSA, prostate specific antigen.

post-chemotherapy point), and the RLL lesion by 58% and 61%. CEA levels remained stable at 4.62 ng/ml, and WBC levels at 5.5*10^9/L (Figure 2). The efficacy evaluation showed partial response (PR). We considered this phenomenon the tail effect specific to immunotherapy. This is the first reported case of such a significant improvement: the patient's condition continued to improve substantially after short-cycle medication and long-term discontinuation, indicating the sustained anti-tumor efficacy of immunotherapy, providing the patient with direct and significant survival benefits.

Unfortunately, on August 8, 2023, a follow-up chest CT showed that the RML/RLL lesions remained well-controlled, and the NRS score remained at 1. CEA levels were 5.03 ng/ml (reference range: 0-4.7 ng/ml), and WBC levels were 6.8*10^9/L (Figure 2), maintaining good levels. However, the mediastinal lymph nodes showed abnormal enlargement and extensive irreversible fusion (Figures 1M–O). The patient, optimistic about his condition, refused further evaluation and passed away two weeks later at another hospital due to acute respiratory failure caused by a lung infection. The patient's treatment timeline is shown in Figure 4.

Discussion

Tail effect is a unique phenomenon associated with immunotherapy, referring to the prolonged maintenance of therapeutic efficacy which can be observable even after treatment cessation, providing long-term immune response and survival benefits for patients with advanced tumors. In this case, after the patient was diagnosed with PSC and exhibited chemotherapy

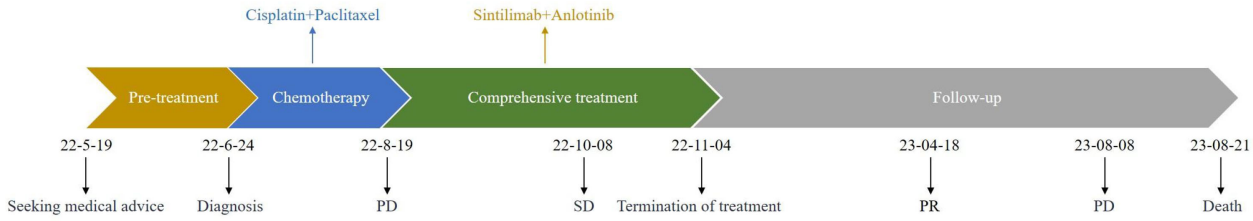

FIGURE 4
Patient treatment timeline.

resistance with disease progression; but initial clinical improvement was achieved following two cycles of immune-targeted combination therapy, with the efficacy evaluation being SD. Chemotherapy-induced adverse reactions disappeared, and pain was reduced. After completing three cycles of combination therapy, the patient discontinued treatment, but sustaining benefits continued to be observed for several months, with a significant tail effect: tumor size reduction, reversal of lymph node enlargement, substantial improvement in clinical symptoms, and a decrease in serum CEA levels. The efficacy evaluation was PR. This patient's significant clinical improvement after short-cycle medication and long-term discontinuation represents the first typical report of this kind.

Most current studies suggest that tail effect is primarily related to the function of memory T cells (1–3). Tissue-resident memory T cells (TRM) can persist in the tumor microenvironment for a long time and initiate specific immune responses upon encountering tumor-specific antigens, producing anti-tumor effects (1, 3). Stem memory T cells (TSCM) and central memory T cells (TCM) ensure their long-term survival and maintain anti-tumor immune responses through self-renewal and multi-directional differentiation (1, 2). Their downstream molecular mechanisms include histone modifications, chromatin remodeling, and the role of long non-coding RNA (lncRNAs) (4). H3K4me1 marks in enhancer regions help maintain an open chromatin state, promoting gene transcription while H3K4me3 marks in promoter regions facilitate efficient transcription initiation (25, 26). These mechanisms concurrently enable rapid activation of memory T cells and immune responses. Chromatin remodeling makes the chromatin structure of specific genes more relaxed, increasing transcription efficiency. Certain lncRNAs, such as UMLILO, guide histone modification enzymes WDR5 and MLL5 to specific genes, enhancing their H3K4me3 marks and increasing their sensitivity during immune responses (4, 27). Additionally, transcription factors like STAT1 rapidly activate via the JAK-STAT pathway and mediate chromatin opening in promoter or enhancer regions, participating in the efficient activation of memory T cells (26, 28–30). Meanwhile, the establishment of memory domains ensures the persistence of immune memory and the high reactivity of TRM. Memory domains refer to gene regions that remain open after immune activation, allowing rapid transcription initiation upon recognition and binding by specific transcription factors. These domains remain open after the immune response ends, ensuring rapid immune responses to specific antigens later (4, 31). The synergetical effects of these mechanisms ensure the long-lasting and effective immune responses mediated by memory T cells, clinically manifested as tail effect.

The presence of tail effect highlights the potential value of immunotherapy for treating advanced tumors. Traditional chemoradiotherapy focuses on tumor-related cellular changes, often resulting in rapid elimination upon exposure; in contrast, immunotherapy can maintain a certain level of anti-tumor activity through the sustained presence of therapeutic effects, providing considerable long-term clinical benefits to patients with advanced tumors and altering tumor progression models to some extent. Therefore, immunotherapy offers new prospects for treating chemotherapy-resistant unresectable tumors. It relies on detecting specific biomarkers to select suitable candidates, with PD-1 and its ligand PD-L1 receiving particular attention. Currently, PD-L1 expression level testing has been most widely used. Numerous domestic and international immunotherapy studies have explored the guidance provided by PD-L1 expression levels on treatment regimens, with a series of results confirming the close correlation between PD-L1 expression levels and the efficacy of immunotherapy (32–34). PD-1 is expressed on T cells, while PD-L1 is often expressed on tumor cells. The binding of PD-L1 to PD-1 activates signaling pathways that inhibit T cell proliferation and reduce cytokine secretion, mediating tumor cell evasion of T cell immune responses (8, 9). Studies have confirmed that PSC patients exhibit high PD-L1 expression, approximately 40% higher than conventional NSCLC (35, 36). Additionally, PD-L1 expression is associated with aggressive pathological features such as N2 involvement, local, and distant metastases (37). Thus, blocking the PD-1/PD-L1 pathway can relieve T cell inhibition and achieve anti-tumor effects.

PSC is a pathological subtype of NSCLC with extremely poor prognosis, characterized by biphasic nature, epithelial and sarcomatoid components, and epithelial-mesenchymal transition (EMT) during growth (38), leading to decreased cellular adhesion and increased migratory capacity (39). This feature causes cancer cells to invade surrounding stroma from the primary tumor (40), exhibiting high invasiveness and metastatic potential. There is currently no individualized treatment guideline for PSC, with treatment strategies typically referring to NSCLC. Advanced PSC is often treated with platinum-based chemotherapy.

the patient initially received two cycles of chemotherapy but experienced disease progression and adverse reactions such as

leukopenia, indicating chemotherapy resistance. Comparative studies indicate that chemotherapy has poor efficacy in PSC compared to conventional NSCLC and is prone to resistance (19–21). This suggests that the poor response to chemotherapy in PSC may be due to mechanisms such as continuous activation of EMT, leading to the spread of cancer cells to distant tissues and activation of tumor cells into cancer stem cells (CSCs) (41). CSCs, a rare subpopulation within tumors, contribute to intratumoral heterogeneity, a major cause of resistance (41). Wang's study confirmed the enrichment of CSCs in cisplatin-resistant NSCLC cells (42). Additionally, KRAS and TP53 mutations have been identified as poor prognostic factors in PSC, increasing genomic instability and reducing response to chemotherapy, leading to poor treatment outcomes (10, 43). The German Lung Cancer Genomic Medicine National Network (nNGM) study (44) found that patients with co-existing KRAS and TP53 mutations are more likely to develop chemotherapy resistance, consistent with the patient's case, suggesting the potential impact of genetic mutations on chemotherapy efficacy. Despite platinum-based doublet chemotherapy being the optimal first-line recommendation for advanced PSC patients, achieving satisfactory outcomes remains challenging. Therefore, the poor efficacy and adverse reactions to chemotherapy in advanced PSC patients highlight the urgent need for alternative treatment options.

Following poor response and adverse reactions to first-line chemotherapy, we rapidly conducted PD-L1 testing, obtaining high expression results, and selected the immune-targeted combination therapy of sintilimab and anlotinib after comprehensive evaluation of immunotherapy's specificity and safety (11, 12, 45, 46). Sintilimab, a highly selective human monoclonal antibody, is approved as a first-line treatment for advanced NSCLC. It binds to the PD-1 receptor on T cells, blocking the interaction with PD-L1 on tumor cells, thereby disrupting the immune suppression reaction, promoting T lymphocyte activation, increasing CD4+/CD8+ and Th1/Th2, reducing Treg levels, reconstructing the tumor immune surveillance mechanism, preventing tumor cells from evading the immune system, and ultimately exerting anti-tumor effects (47). Vascular invasion is another significant characteristic of PSC, and anti-angiogenic targeted drugs like anlotinib may offer potential benefits for PSC patients. Anlotinib, an effective small molecule tyrosine kinase inhibitor, inhibits angiogenesis and the activation of VEGFR2, PDGFRb, and FGFR1, as well as their shared downstream ERK signaling pathway. It normalizes blood vessels, enhances immune cell infiltration, and regulates the composition of immune cells within tumor tissues, alleviating the immune-suppressive state in the tumor microenvironment (14). Preclinical studies show that sintilimab combined with anlotinib can reduce the activity of myeloid-derived suppressor cells and regulatory T cells, remodeling the tumor microenvironment, converting the immune-suppressive state to an immune-permissive mode, normalizing tumor blood vessels, promoting T cell infiltration into the tumor, enhancing immune function, and blocking immune suppressive signals through multiple pathways, increasing anti-tumor activity (15). The combination of these two drugs targets multiple mechanisms, achieving tumor immune killing and surveillance, promoting immune responses, and improving objective response rates (ORR) and disease control rates (DCR) (10, 13). A retrospective study demonstrated positive outcomes in NSCLC patients unresponsive to chemotherapy receiving sintilimab and anlotinib combination therapy (11). Domestic and international cases have shown excellent results with this combination therapy: Zhimin Zeng's study confirmed that ICIs combined with anlotinib had better efficacy compared to chemotherapy or monotherapy (12). The phase 1b trial NCT03628521 reported an objective response rate of 72.7% and a median progression-free survival (PFS) of 15 months in 22 patients receiving sintilimab combined with anlotinib, with a significantly reduced incidence of treatment-related adverse events (TRAEs), indicating satisfactory and durable effects of the combination therapy (45). Peiliang Wang's research specifically targeted chemotherapy-resistant advanced PSC patients, demonstrating that this combination therapy not only had low toxicity but also maximized disease improvement (11), consistent with the patient's case: the patient showed significant improvement after receiving sintilimab and anlotinib, with disease control and substantial subjective symptom improvement.

Numerous clinical trials and case reports have indicated the existence of the tail effect in immunotherapy. A multicenter retrospective study found that patients achieving over six months of durable response from immunotherapy continued to benefit significantly after ICI discontinuation, showing long-term PFS (48). Phase III clinical trials KEYNOTE-024 and ASTRUM-005 compared PD-1 inhibitors with chemotherapy or placebo, showing similar survival curves: both PD-1 inhibitors produced significant differences from the control group around four cycles, with this difference increasing with extended treatment (49, 50), resulting in significantly better long-term survival outcomes for patients receiving immunotherapy. This indicates that immunotherapy's long-term efficacy remains at a high level, providing substantial long-term clinical benefits to patients, aided by the tail effect. The CheckMate 227 trial compared immunotherapy and chemotherapy in advanced NSCLC patients, showing that 27% of patients in the immunotherapy group maintained response five years later, compared to only 4% in the chemotherapy group (51), further suggesting the tail effect. Yue Hu's retrospective study analyzed treatment-free survival (TPS) in metastatic NSCLC (mNSCLC) patients after ICI discontinuation, finding that 35.5% of patients continued to benefit (52), with the tail effect during ICI-free periods providing nearly as much benefit as completing the treatment cycle, further confirming the widespread existence of tail effect and its high efficacy.

The significant tail effect observed in this case warrants exploration of the underlying mechanisms. The pronounced and persistent tail effect in this case may be related to PSC's characteristics. PSC has high TMB and leukocyte fraction (LF), resulting in high neoantigen burden and T-cell inflamed tumor microenvironment (TME) (22), continuously stimulating T cells to produce specific immune responses, making PSC highly responsive to immunotherapy. Additionally, the pharmacokinetics and

pharmacodynamics "disjunction phenomenon" of anti-PD-1 may contribute to the tail effect. A phase 1 study of anti-PD-1 (MDX-1106) found that although the drug's half-life in serum is only 12-20 days, more than 70% of PD-1 molecules on circulating T cells remained occupied two months after infusion, regardless of the infusion dose (53). This suggests that even at very low serum concentrations, the therapeutic effect of anti-PD-1 can persist, ensuring sustained efficacy. The patient's high PD-L1 expression also indirectly confirmed that blocking PD-1 with ICIs resulted in significant immune responses against tumor cells. Individual differences may also explain the patient's favorable outcomes: the patient achieved significant clinical improvement after only two cycles of immune-targeted combination therapy, with an efficacy evaluation of PR after five months of discontinuation, which is rare among similar patients. Nana Huang reported a PSC patient undergoing continuous 10-cycle immune-targeted therapy, maintaining SD, but with less pronounced efficacy compared to this case (23).

It is undeniable that while this regimen has produced a significant tail effect, it also presents some inevitable drawbacks: despite the patient's pulmonary lesion being evaluated as SD at the final follow-up, extensive fusion of the mediastinal lymph nodes was observed. This suggests that the combination of sintilimab and anlotinib may have limited efficacy in controlling lymph node lesions, potentially leading to lymph node recurrence or progression before the primary lesion. Additionally, the tail effect is difficult to quantify and monitor, and it may sometimes overlap with the effects of prior and subsequent treatments. The tail effect could also lead to patients and their families having an incomplete understanding of the disease status. Therefore, in clinical practice, we must balance risks and benefits, develop more detailed treatment plans, and enhance communication between doctors and patients about the treatment course of immune-targeted combination therapies.

The tail effect is often referred to as the "golden tail" of immunotherapy. As shown in this case, it has provided significant survival benefits for patients with chemotherapy-resistant or unresectable advanced lung cancer. In this case, the tail effect was maintained for several months following a short-term combination therapy regimen, and there are currently no reports of similar short-cycle treatment followed by long-term discontinuation. This further expands the available treatment options in clinical practice and holds important implications for future guidance. The diagnostic and therapeutic approach based on immune checkpoint inhibition may lead to breakthroughs in cancer treatment. However, based on this single case experience, more robust and comprehensive clinical trials or studies are needed to further validate the efficacy of these treatments.

Data availability statement

The original contributions presented in the study are included in the article/supplementary material, further inquiries can be directed to the corresponding authors.

Ethics statement

The studies involving humans were approved by Ethics Committee of the First People's Hospital of Suqian (2024-sl-0101). The studies were conducted in accordance with the local legislation and institutional requirements. The participants provided their written informed consent to participate in this study. Written informed consent was obtained from the individual(s) for the publication of any potentially identifiable images or data included in this article.

Author contributions

CF: Conceptualization, Data curation, Formal analysis, Funding acquisition, Investigation, Methodology, Project administration, Resources, Software, Supervision, Validation, Visualization, Writing – original draft, Writing – review & editing. HD: Conceptualization, Data curation, Formal analysis, Funding acquisition, Investigation, Methodology, Project administration, Resources, Software, Supervision, Validation, Visualization, Writing – review & editing. QW: Conceptualization, Data curation, Writing – review & editing. WZ: Data curation, Visualization, Writing – review & editing. GB: Methodology, Supervision, Visualization, Writing – review & editing. ZZ: Conceptualization, Project administration, Validation, Writing – review & editing. YW: Data curation, Software, Supervision, Writing – review & editing. LC: Conceptualization, Data curation, Formal analysis, Funding acquisition, Investigation, Methodology, Project administration, Resources, Software, Supervision, Validation, Visualization, Writing – original draft, Writing – review & editing.

Funding

The author(s) declare that no financial support was received for the research, authorship, and/or publication of this article.

Conflict of interest

The authors declare that the research was conducted in the absence of any commercial or financial relationships that could be construed as a potential conflict of interest.

Publisher's note

All claims expressed in this article are solely those of the authors and do not necessarily represent those of their affiliated organizations, or those of the publisher, the editors and the reviewers. Any product that may be evaluated in this article, or claim that may be made by its manufacturer, is not guaranteed or endorsed by the publisher.

References

1. Wang N. Research progress on differentiation and regulation of memory T cell subsets. *Chin J Immunol*. (2023) 39:1326–30. doi: 10.3969/j.issn.1000-484X.2023.06.044

2. Lin MX, Zang D, Chen J. Research progress on the relationship between central memory T cells and tumor immunotherapy. *Chin J Clin Oncol*. (2023) 50:1063–7. doi: 10.12354/j.issn.1000-8179.2023.20230627

3. Wu QL, Kang SP, Wu CY. The progress of tissue resident memory T-cells against tumors. *Sci Sin.-Vitae*. (2020) 50:1032–41. doi: 10.1360/SSV-2020-0024

4. Naik S, Fuchs E. Inflammatory memory and tissue adaptation in sickness and in health. *Nature*. (2022) 607:249–55. doi: 10.1038/s41586-022-04919-3

5. Xu L, Tao NN, Liang B, Li DW, Li HC, Su LL. Use of PD-1 inhibitor tislelizumab in the treatment of advanced pulmonary sarcomatoid carcinoma: A case report. *Thorac Cancer*. (2022) 13:502–5. doi: 10.1111/1759-7714.14290

6. Dai GY, He L, Yan Q, Li YM, Huang YD, Li B, et al. Case Report: Advanced pulmonary sarcomatoid carcinoma with adrenal gland metastasis after sintilimab combined with anlotinib treatment. *Front Oncol*. (2023) 13:1167516. doi: 10.3389/fonc.2023.1167516

7. Li YF, Zhao XF, Tian Y, Xiao XY, Yan CY, Shen H. Case Report: Pulmonary sarcomatoid carcinoma complicating TP53 mutation treated successfully with Tislelizumab combined with Anlotinib-a case report. *Front Genet*. (2022) 13:949989. doi: 10.3389/fgene.2022.949989

8. Pardoll DM. The blockade of immune checkpoints in cancer immunotherapy. *Nat Rev Cancer*. (2012) 12:252–64. doi: 10.1038/nrc3239

9. Tang Q, Chen Y, Li XJ, Long SQ, Shi Y, Yu YY, et al. The role of PD-1/PD-L1 and application of immune-checkpoint inhibitors in human cancers. *Front Immunol*. (2022) 13:964442. doi: 10.3389/fimmu.2022.964442

10. Chen FM, Gu QH, Hu CP, Cai XL, Lei SH. Poor prognosis of pulmonary sarcomatoid carcinoma with KRAS mutation and ALK fusion. *Onco Targets Ther*. (2019) 12:3321–5. doi: 10.2147/OTT.S196751

11. Wang PL, Fang XZ, Yin TW, Tian HR, Yu JM, Teng FF. Efficacy and safety of anti-PD-1 plus anlotinib in patients with advanced non-small-cell lung cancer after previous systemic treatment failure-A retrospective study. *Front Oncol*. (2021) 11:628124. doi: 10.3389/fonc.2021.628124

12. Qian XY, Wang Y, Liu FR, Yuan Y, Fang C, Zhang XW, et al. The efficacy and safety analysis of first-line immune checkpoint inhibitors in pulmonary sarcomatoid carcinoma. *Front Immunol*. (2022) 13:956982. doi: 10.3389/fimmu.2022.956982

13. Liu JR, Duan L, Wang WY, Sun XC, Yang G. Prospective, single arm, phase II Clinical study on the second-line treatment of advanced small cell lung cancer with sintilimab and anrotinib hydrochloride. *Pract J Cancer*. (2023) 38:839–42. doi: 10.3969/j.issn.1001-5930.2023.05.037

14. Lin BY, Song XM, Yang DW, Bai DS, Yao YY, Lu N. Anlotinib inhibits angiogenesis via suppressing the activation of VEGFR2, PDGFRβ and FGFR1. *Gene*. (2018) 654:77–86. doi: 10.1016/j.gene.2018.02.026

15. Su YD, Luo BY, Lu Y, Wang DW, Yan J, Zheng J, et al. Anlotinib induces a T cell-inflamed tumor microenvironment by facilitating vessel normalization and enhances the efficacy of PD-1 checkpoint blockade in neuroblastoma. *Clin Cancer Res*. (2022) 28:793–809. doi: 10.1158/1078-0432.CCR-21-2241

16. Yendamuri S, Caty L, Pine M, Adem S, Bogner P, Miller A, et al. Outcomes of sarcomatoid carcinoma of the lung: a Surveillance, Epidemiology, and End Results Database analysis. *Surgery*. (2012) 152:397–402. doi: 10.1016/j.surg.2012.05.007

17. Travis WD, Brambilla E, Burke AP, Marx A, Nicholson AG. Introduction to the 2015 world health organization classification of tumors of the lung, pleura, thymus, and heart. *J Thorac Oncol*. (2015) 10:1240–2. doi: 10.1097/JTO.0000000000000663

18. Steuer CE, Behera M, Liu Y, Fu C, Gillespie TW, Saba NF, et al. Pulmonary sarcomatoid carcinoma: an analysis of the national cancer data base. *Clin Lung Cancer*. (2017) 18:286–92. doi: 10.1016/j.cllc.2016.11.016

19. Ito K, Oizumi S, Fukumoto S, Harada M, Ishida T, Fujita Y, et al. Clinical characteristics of pleomorphic carcinoma of the lung. *Lung Cancer*. (2010) 68:204–10. doi: 10.1016/j.lungcan.2009.06.002

20. Lara PNJr, Redman MW, Kelly K, Edelman MJ, Williamson SK, Crowley JJ, et al. Disease control rate at 8 weeks predicts clinical benefit in advanced non-small-cell lung cancer: results from Southwest Oncology Group randomized trials. *J Clin Oncol*. (2008) 26:463–7. doi: 10.1200/JCO.2007.13.0344

21. Vieira T, Girard N, Ung M, Monnet I, Cazes A, Bonnette P, et al. Efficacy of first-line chemotherapy in patients with advanced lung sarcomatoid carcinoma. *J Thorac Oncol*. (2013) 8:1574–7. doi: 10.1097/01.JTO.0000437008.00554.90

22. Yang ZL, Xu JC, Li L, Li RD, Wang YL, Tian YH, et al. Integrated molecular characterization reveals potential therapeutic strategies for pulmonary sarcomatoid carcinoma. *Nat Commun*. (2020) 11:4878. doi: 10.1038/s41467-020-18702-3

23. Huang NN, Qu TH, Zhang CX, Li J. Case report: Successful treatment of advanced pulmonary sarcomatoid carcinoma with BUBIB-ALK rearrangement and KRAS G12C mutation by sintilimab combined with anlotinib. *Front Oncol*. (2024) 14:1269148. doi: 10.3389/fonc.2024.1269148

24. The Chinese Society of Clinical Oncogy. *Guidelines of Chinese Society of Clinical Oncology (CSCO)Non-Small Cell Lung Cancer*. Beijing: People's Medical Publishing House (2023).

25. Saeed S, Quintin J, Kerstens HH, Rao NA, Aghajanirefah A, Matarese F, et al. Epigenetic programming of monocyte-to-macrophage differentiation and trained innate immunity. *Science*. (2014) 345:1251086. doi: 10.1126/science.1251086

26. Lau CM, Adams NM, Geary CD, Weizman OE, Rapp M, Pritykin Y, et al. Epigenetic control of innate and adaptive immune memory. *Nat Immunol*. (2018) 19:963–72. doi: 10.1038/s41590-018-0176-1

27. Fanucchi S, Fok ET, Dalla E, Shibayama Y, Börner K, Chang EY, et al. Immune genes are primed for robust transcription by proximal long noncoding RNAs located in nuclear compartments. *Nat Genet*. (2019) 51:138–50. doi: 10.1038/s41588-018-0298-2

28. Naik S, Larsen SB, Gomez NC, Alaverdyan K, Sendoel A, Yuan S, et al. Inflammatory memory sensitizes skin epithelial stem cells to tissue damage. *Nature*. (2017) 550:475–80. doi: 10.1038/nature24271

29. Henikoff S, Shilatifard A. Histone modification: cause or cog? *Trends Genet*. (2011) 27:389–96. doi: 10.1016/j.tig.2011.06.006

30. Zaret KS. Pioneer transcription factors initiating gene network changes. *Annu Rev Genet*. (2020) 54:367–85. doi: 10.1146/annurev-genet-030220-015007

31. Larsen SB, Cowley CJ, Sajjath SM, Barrows D, Yang Y, Carroll TS, et al. Establishment, maintenance, and recall of inflammatory memory. *Cell Stem Cell*. (2021) 28:1758–1774.e8. doi: 10.1016/j.stem.2021.07.001

32. Brahmer JR, Rodríguez-Abreu D, Robinson AG, Hui R, Csőszi T, Fülöp A, et al. Health-related quality-of-life results for pembrolizumab versus chemotherapy in advanced, PD-L1-positive NSCLC (KEYNOTE-024): a multicentre, international, randomised, open-label phase 3 trial. *Lancet Oncol*. (2017) 18:1600–9. doi: 10.1016/S1470-2045(17)30690-3

33. Herbst RS, Baas P, Kim DW, Felip E, Pérez-Gracia JL, Han JY, et al. Pembrolizumab versus docetaxel for previously treated, PD-L1-positive, advanced non-small-cell lung cancer (KEYNOTE-010): a randomised controlled trial. *Lancet*. (2016) 387:1540–50. doi: 10.1016/S0140-6736(15)01281-7

34. Garon EB, Rizvi NA, Hui R, Leighl N, Balmanoukian AS, Eder JP, et al. Pembrolizumab for the treatment of non-small-cell lung cancer. *N Engl J Med*. (2015) 372:2018–28. doi: 10.1056/NEJMoa1501824

35. Stephan-Falkenau S, Streubel A, Mairinger T, Blum TG, Kollmeier J, Mairinger FD, et al. Integrated clinical, molecular and immunological characterization of pulmonary sarcomatoid carcinomas reveals an immune escape mechanism that may influence therapeutic strategies. *Int J Mol Sci*. (2023) 24:10558. doi: 10.3390/ijms241310558

36. Kim S, Kim MY, Koh J, Go H, Lee DS, Jeon YK, et al. Programmed death-1 ligand 1 and 2 are highly expressed in pleomorphic carcinomas of the lung: Comparison of sarcomatous and carcinomatous areas. *Eur J Cancer*. (2015) 51:2698–707. doi: 10.1016/j.ejca.2015.08.013

37. Yi XL, Xu WH, Tang GH, Zhang LY, Wang KS, Luo H, et al. Individual risk and prognostic value prediction by machine learning for distant metastasis in pulmonary sarcomatoid carcinoma: a large cohort study based on the SEER database and the Chinese population. *Front Oncol*. (2023) 13:1105224. doi: 10.3389/fonc.2023.1105224

38. Huang Y, Guo JH, Li SL, Liu JF, Xu JP, Ye W, et al. The correlation between histologic, immunophenotypic, and molecular characteristics of pulmonary sarcomatoid carcinoma reveals that sarcomatoid change is potentially derived from epithelial carcinoma cells undergoing epithelial-mesenchymal transition. *Appl Immunohistochem Mol Morphol*. (2023) 31:17–25. doi: 10.1097/PAI.0000000000001060

39. Hay ED. An overview of epithelio-mesenchymal transformation. *Acta Anat (Basel)*. (1995) 154:8–20. doi: 10.1159/000147748

40. Thiery JP, Sleeman JP. Complex networks orchestrate epithelial-mesenchymal transitions. *Nat Rev Mol Cell Biol*. (2006) 7:131–42. doi: 10.1038/nrm1835

41. Shibue T, Weinberg RA. EMT, CSCs, and drug resistance: the mechanistic link and clinical implications. *Nat Rev Clin Oncol*. (2017) 14:611–29. doi: 10.1038/nrclinonc.2017.44

42. Wang LH, Liu X, Ren Y, Zhang JY, Chen JL, Zhou WL, et al. Cisplatin-enriching cancer stem cells confer multidrug resistance in non-small cell lung cancer via enhancing TRIB1/HDAC activity. *Cell Death Dis*. (2017) 8:e2746. doi: 10.1038/cddis.2016.409

43. Liu XW, Wang F, Xu CW, Chen XR, Hou X, Li Q, et al. Genomic origin and intratumor heterogeneity revealed by sequencing on carcinomatous and sarcomatous components of pulmonary sarcomatoid carcinoma. *Oncogene*. (2021) 40:821–32. doi: 10.1038/s41388-020-01573-9

44. Bischoff P, Reck M, Overbeck T, Christopoulos P, Rittmeyer A, Lüders H, et al. Outcome of first-line treatment with pembrolizumab according to KRAS/TP53

mutational status for nonsquamous programmed death-ligand 1-high (≥50%) NSCLC in the german national network genomic medicine lung cancer. *J Thorac Oncol.* (2024) 19:803–17. doi: 10.1016/j.jtho.2023.12.015

45. Chu TQ, Zhong RB, Zhong H, Zhang B, Zhang W, Shi CL, et al. Phase 1b study of sintilimab plus anlotinib as first-line therapy in patients with advanced NSCLC. *J Thorac Oncol.* (2021) 16:643–52. doi: 10.1016/j.jtho.2020.11.026

46. Han BH, Li K, Wang QM, Zhang L, Shi JH, Wang ZH, et al. Effect of anlotinib as a third-line or further treatment on overall survival of patients with advanced non-small cell lung cancer: the ALTER 0303 phase 3 randomized clinical trial. *JAMA Oncol.* (2018) 4:1569–75. doi: 10.1001/jamaoncol.2018.3039

47. Zhu D, Li YY, Song YQ, Li YJ. The clinical research progress of PD-1 inhibitor: sintilimab. *Chin J Hosp Phamacy*. (2020) 40(1):120–3. doi: 10.13286/j.1001-5213.2020.01.20

48. Kim H, Kim DW, Kim M, Lee Y, Ahn HK, Cho JH, et al. Long-term outcomes in patients with advanced and/or metastatic non-small cell lung cancer who completed 2 years of immune checkpoint inhibitors or achieved a durable response after discontinuation without disease progression: Multicenter, real-world data (KCSG LU20-11). *Cancer.* (2022) 128:778–87. doi: 10.1002/cncr.33984

49. Reck M, Rodríguez-Abreu D, Robinson AG, Hui R, Csőszi T, Fülöp A, et al. Pembrolizumab versus chemotherapy for PD-L1-positive non-small-cell lung cancer. *N Engl J Med.* (2016) 375:1823–33. doi: 10.1056/NEJMoa1606774

50. Cheng Y, Han L, Wu L, Chen J, Sun HM, Wen GL, et al. Effect of first-line serplulimab vs placebo added to chemotherapy on survival in patients with extensive-stage small cell lung cancer: the ASTRUM-005 randomized clinical trial. *JAMA*. (2022) 328:1223–32. doi: 10.1001/jama.2022.16464

51. Hellmann MD, Paz-Ares L, Bernabe Caro R, Zurawski B, Kim SW, Carcereny Costa E, et al. Nivolumab plus ipilimumab in advanced non-small-cell lung cancer. *N Engl J Med.* (2019) 381:2020–31. doi: 10.1056/NEJMoa1910231

52. Hu Y, Liu S, Wang L, Liu YX, Zhang DH, Zhao YL. Treatment-free survival after discontinuation of immune checkpoint inhibitors in mNSCLC: a systematic review and meta-analysis. *Front Immunol.* (2023) 14:1202822. doi: 10.3389/fimmu.2023.1202822

53. Brahmer JR, Drake CG, Wollner I, Powderly JD, Picus J, Sharfman WH, et al. Phase I study of single-agent anti-programmed death-1 (MDX-1106) in refractory solid tumors: safety, clinical activity, pharmacodynamics, and immunologic correlates. *J Clin Oncol.* (2010) 28:3167–75. doi: 10.1200/JCO.2009.26.7609

frontiers | Frontiers in Medicine

TYPE Case Report
PUBLISHED 11 November 2024
DOI 10.3389/fmed.2024.1455978

OPEN ACCESS

EDITED BY
Giuseppe Fiorentino,
Colli Hospital, Italy

REVIEWED BY
Maria Paparoupa,
University Medical Center
Hamburg-Eppendorf, Germany
Elvira Gonzalez-Obeso,
Hospital Clínico Universitario de Valladolid,
Spain

*CORRESPONDENCE
Kaiyi Mao
✉ mky1159103@163.com

†These authors have contributed equally to this work and share first authorship

RECEIVED 27 June 2024
ACCEPTED 31 October 2024
PUBLISHED 11 November 2024

CITATION
Mao K, Wang L, Mao Y, Shang X, Zhou G, Zhao P, Wang C and Ma H (2024) Posterior mediastinal extralobar pulmonary sequestration in a neonate with pulmonary artery supply: a case report.
Front. Med. 11:1455978.
doi: 10.3389/fmed.2024.1455978

Posterior mediastinal extralobar pulmonary sequestration in a neonate with pulmonary artery supply: a case report

Kaiyi Mao[1,2*†], Leibo Wang[3†], Yuchen Mao[1,2], Xianhui Shang[1,2], Guangxu Zhou[1,2], Peng Zhao[1,2], Cao Wang[1,2] and Hong Ma[1,2]

[1]Department of Pediatric Surgery, Affiliated Hospital of Zunyi Medical University, Zunyi, China, [2]Department of Pediatric Surgery, Guizhou Children's Hospital, Zunyi, China, [3]Urology Surgery, Beijing Jishuitan Hospital Guizhou Hospital, Guiyang, China

This paper reports a rare case of extralobar pulmonary sequestration in the posterior mediastinum of a neonate with arterial supply from the pulmonary artery. A 3-day-old male neonate was diagnosed with type II congenital pulmonary airway malformation after prenatal color Doppler ultrasonography showed a lesion with blood supply from the pulmonary artery in the left lung. Post-birth chest computed tomography(CT) showed that the lesion was located in the posterior mediastinum with low density change, mild stripe enhancement after contrast, and no obvious blood supply vessels. A neurogenic tumor was considered for the preoperative diagnosis. The mass was removed by video-assisted thoracoscopic surgery. During the surgery, the mass was observed to be a dark red solid lump with a feeding vessel originating from the pulmonary artery. The postoperative histopathological diagnosis was extralobar pulmonary sequestration. Combined with the preoperative imaging results, it was considered that the nourishing vessels might have intermittent torsion. The patient recovered well after surgery, and no recurrence was observed after 6 months of follow-up. Therefore, the possibility of extralobar pulmonary sequestration cannot be ruled out for posterior mediastinal masses that are not supplied by the descending aorta or without identified feeding vessels.

KEYWORDS

extralobar pulmonary sequestration, neonate, posterior mediastinal mass, misdiagnosis, case report

Introduction

Pulmonary sequestration (PS) is a rare congenital abnormality involving lung tissue development, accounting for 0.15–6.4% of congenital lung malformations (1). Its main characteristic is the non-functional lung tissue that is separated from the trachea, bronchial tree, and pulmonary artery of normal lung tissue, forming cystic or solid mass structures. Pathologically, PS is classified into two types: intralobar pulmonary sequestration (ILS) and extralobar pulmonary sequestration (ELS), based on whether the abnormal lung tissue shares a pleural envelope with the surrounding lung tissue. ELS constitutes approximately 25% of PS cases and is typically found between the lower left lung and the diaphragm, with occasional occurrences in the mediastinum (2). The blood supply for ELS usually comes

from the thoracic aorta or the abdominal aorta, with origins from the pulmonary artery being very rare (3).

Here, we report a unique case of a child whose prenatal ultrasound suggested a mass in the left lung with a blood supply from the pulmonary artery. The lesion progressively enlarged over time. Postnatal enhanced chest CT showed the lesion located in the posterior mediastinum without obvious feeding arteries. During surgery, the lesion appeared dark red and was found to have a feeding artery originating from the pulmonary artery. After complete resection, the pathological results indicated ELS.

Case presentation

The male child was admitted to our department 3 days after birth due to prenatal findings of fetal lung abnormalities. During routine prenatal color ultrasound at 24 weeks of gestation, a slightly hyperechoic mass measuring approximately 24 mm × 15 mm × 16 mm was detected in the left thoracic cavity of the fetus, the mass had uniform internal echoes, clear boundaries, and blood supply from the pulmonary artery. Initially, this was suspected to be type II congenital pulmonary airway malformation (CPAM). Subsequent color ultrasound at 30 weeks showed the mass had grown to approximately 30 mm × 26 mm × 20 mm. But the post-birth chest plain CT scan shows the presence of an oval-shaped solid mass in the left posterior mediastinum, with no observed cystic structures, and having a CT value of 33 Hounsfield units (HU) (Figure 1A). After enhancement, no significant nourishing vessels were evident, with only mild strip enhancement observed within the lesion (Figure 1B). Based on these findings, the diagnosis of left type II CPAM was ruled out. The lesion, lacking obvious nourishing vessels and being low-density, located in the posterior mediastinum, initially suggested a neurogenic tumor before surgery. However, prenatal color ultrasound indicated the lesion received blood supply from the pulmonary artery. After consultation within the surgical team, thoracoscopic resection of the posterior mediastinal lesion was planned, focusing on identifying any blood supply artery during the operation.

During the operation, an oval-shaped solid mass, approximately 30 mm × 25 mm × 10 mm in size, was found in the left posterior mediastinum. The mass was encapsulated by its own visceral pleura and was separate from the normal lung tissue, with no connection to the normal bronchi (Figure 2A). Upon careful dissection of the lesion, a nourishing vessel with a diameter of approximately 3 mm was observed at its base, which was supplied by the pulmonary artery (Figure 2B), consistent with the blood supply source indicated by the prenatal ultrasound. Therefore, considered the lesion to be an ELS with atypical blood supply. Complete resection was achieved after clamping the nourishing vessels. Postoperative pathology revealed bronchioles, alveoli, and alveolar structures within the tissue. Bronchiectasis was covered with pseudostratified fibrous columnar epithelium, surrounded by fibromuscular tube walls. Cartilage plates were observed in some bronchial walls, consistent with ELS (Figures 2C,D). The patient recovered well post-surgery, with the thoracic drainage tube removed on the third day and discharge on the fifth day without complications such as pneumothorax, mediastinal emphysema, or atelectasis. Follow-up at 6 months showed the patient's general condition to be excellent, with no abnormalities detected on chest radiographs.

Discussion

Some studies indicate that approximately 80% of ELS cases receive arterial blood supply from the thoracic or abdominal aorta, while about 15% are supplied by other systemic arteries, with blood supply from the pulmonary artery being rare (3). In the case presented here, prenatal examination revealed an abnormal left-sided pulmonary lesion supplied by the pulmonary artery. Based on its imaging characteristics and nourishing vessels, prenatal diagnosis primarily considered type II congenital pulmonary airway malformation (CPAM). CPAM is caused by the failure of normal bronchoalveolar structures development, leading to adenomatoid or adenomatous hamartomatous proliferation in the terminal respiratory units without the formation of normal alveoli. Type II CPAM originates in terminal bronchioles, exhibiting smaller cysts and solid areas (4). The key difference between PS and CPAM in prenatal diagnosis lies in their vascular supply. PS derives blood from systemic arteries, often the thoracic aorta, whereas CPAM receives its blood supply from the pulmonary artery. In this case, the prenatal color ultrasound indicated a slightly hyperechoic mass supplied by the left pulmonary artery, making it difficult to distinguish from CPAM, resulting in a misdiagnosis before delivery. Neurogenic tumors are the most common tumors in the posterior mediastinum, whereas ELS is usually located between the left lower lobe of the lung and the diaphragm. Occasionally, it can also occur below the diaphragm, within the diaphragm, but ELS located in the posterior mediastinum is very rare (5). Postnatally, enhanced chest CT in this case indicated a lesion in the posterior mediastinum with low-density changes, slight strip enhancement, and no identifiable nourishing vessels, resembling neurogenic tumor imaging findings. Consequently, CPAM diagnosis was ruled out postnatally, leading to consideration of a neurogenic tumor.

CT examination is highly sensitive for diagnosing ELS, particularly enhanced CT, which can accurately identify the arterial blood supply from systemic circulation. However, studies have demonstrated that in cases where pulmonary sequestration experiences torsion, imaging features on enhanced scans may show non-enhancement or strip enhancement of the mass, without an identifiable abnormal supply artery from systemic circulation (6). In this particular case, enhanced CT after birth revealed minimal enhancement of the tumor with a few strip enhancements and no discernible supplying artery, contradicting prenatal color ultrasound findings. However, during thoracoscopic examination, the lesion appeared dark red with identifiable nourishing vessels. Based on these observations, we hypothesized that the mass may have undergone intermittent torsion, resulting in atypical postnatal imaging findings. Coleman et al. (7) first proposed the phenomenon of intermittent torsion of ELS nourishing arteries. Our case is similar to this phenomenon. In their case, fetal magnetic resonance imaging (MRI) detected the nourishing vessels of ELS. However, a subsequent ultrasound examination revealed no blood

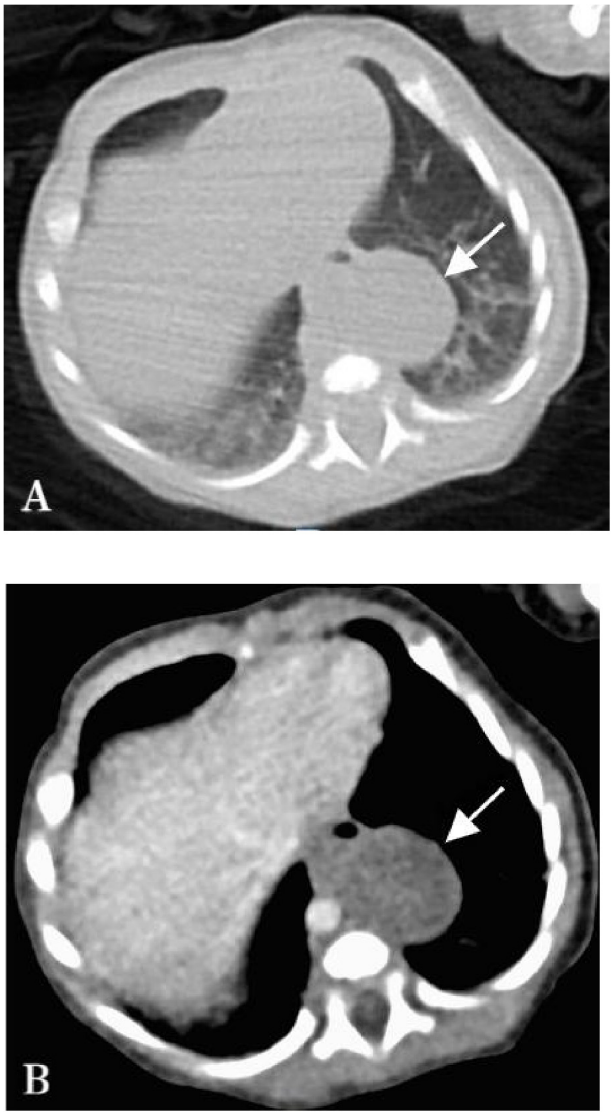

FIGURE 1
Chest CT image of the child on the 3rd day after birth. **(A)** The plain CT scan shows the presence of an oval-shaped solid mass in the left posterior mediastinum, with no observed cystic structures, measuring approximately 27 × 20 mm with a CT value of 33 HU (arrow). **(B)** Enhanced CT did not reveal significant nourishing vessels within the lesion, mild stripe enhancement was observed within the lesion, which had clear boundaries (arrow).

flow within the vascular pedicle. Interestingly, during surgery, the ultrasound once again detected the nourishing vessels, indicating possible intermittent torsion. Our case is, therefore, highlighting this phenomenon.

When ELS undergoes torsion necrosis, imaging typically fails to show the supplying arteries, and patients may present with severe abdominal pain, pleural effusion, and other symptoms (8). Some patients may also experience chest pain, dyspnea, and vomiting. Pathological reports often indicate diffuse hemorrhage of the pulmonary parenchyma (9). In our case, however, besides the imaging characteristics, other symptoms were absent. This may be because the nourishing blood vessels of the lesion in this case only underwent intermittent torsion with a relatively mild degree and short duration. Additionally, the child underwent surgery on the fourth day after birth, before the isolated lung tissue could develop ischemic necrosis. Reports suggest that MRI offers advantages in diagnosing ELS with torsion (10, 11). T1-weighted imaging (T1WI) of twisted lung tissue typically shows high signal intensity, indicating lesions combined with bleeding. Furthermore, MRI can visualize cystic or tubular shadows within the mass and accurately delineate the relationship between the lesion, pleura, and normal lung tissue. This capability makes MRI valuable in distinguishing between congenital lung developmental malformations and tumors.

In conclusion, this study presented a rare case of external posterior mediastinal pulmonary sequestration in a neonate with blood supply from the pulmonary artery. Prenatal color ultrasound indicated pulmonary artery supply to the lesion, while postnatal enhanced CT failed to detect nourishing vessels and showed the lesion in the posterior mediastinum, resembling imaging findings seen in neurogenic tumors. These factors collectively contributed to diagnostic challenges and misdiagnosis before surgery. For such

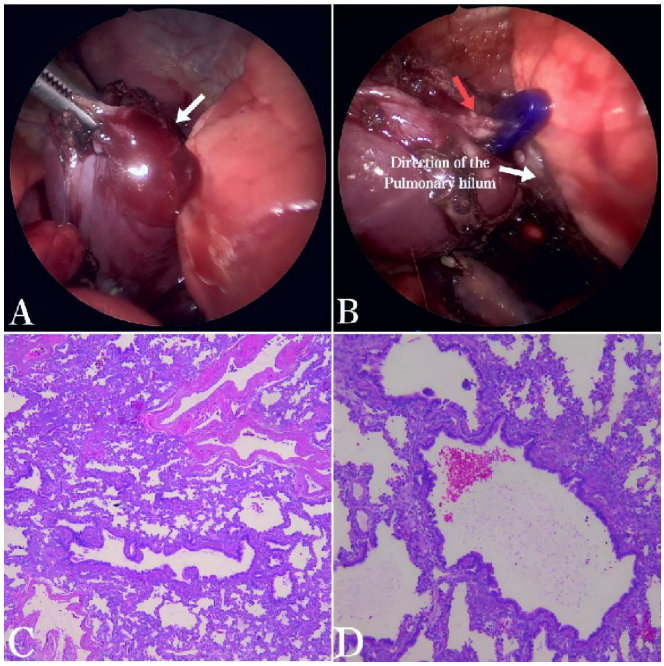

FIGURE 2
(A) During the thoracoscopic examination, a solid mass approximately 30 mm × 25 mm × 10 mm in size, dark red in color, was found in the left posterior mediastinum. The mass was encapsulated by its own visceral pleura, had a smooth surface, was independent of the normal lung tissue, and was not connected to the normal bronchi (arrow). **(B)** A nourishing vessel about 3 mm in diameter was identified at the base of the lesion (red arrow), which was supplied by the pulmonary artery. **(C,D)** Histopathological examination (HE × 50 and HE × 100) showed bronchioles, alveoli, and alveolar structures within the tissue. Bronchiectasis was covered with pseudostratified fibrous columnar epithelium, surrounded by fibromuscular tube walls. Cartilage plates were observed in some bronchial walls, consistent with extralobar pulmonary sequestration.

cases, relying solely on preoperative CT may not suffice for accurate diagnosis. Preoperative MRI could potentially provide better visualization of abnormal blood vessels and lesion characteristics. Furthermore, meticulous identification of abnormal blood vessels during surgery is crucial. Therefore, even for posterior mediastinal masses that lack blood supply from the descending aorta or have no identifiable nourishing blood vessels, the possibility of ELS should be considered to avoid misdiagnosis.

Data availability statement

The original contributions presented in this study are included in this article/supplementary material, further inquiries can be directed to the corresponding author.

Ethics statement

The studies involving humans were approved by the Ethics Committee of Zunyi Medical University Hospital. The studies were conducted in accordance with the local legislation and institutional requirements. Written informed consent for participation in this study was provided by the participants' legal guardians/next of kin. Written informed consent was obtained from the minor(s)' legal guardian/next of kin for the publication of any potentially identifiable images or data included in this article.

Author contributions

KM: Conceptualization, Data curation, Investigation, Writing – original draft, Writing – review and editing. LW: Conceptualization, Data curation, Investigation, Methodology, Writing – review and editing. YM: Writing – review and editing. XS: Writing – review and editing. GZ: Writing – review and editing. PZ: Writing – review and editing. CW: Writing – review and editing. HM: Writing – review and editing.

Funding

The author(s) declare that no financial support was received for the research, authorship, and/or publication of this article.

Acknowledgments

We thank all the reviewers for their assistance and support.

Conflict of interest

The authors declare that the research was conducted in the absence of any commercial or financial relationships that could be construed as a potential conflict of interest.

Publisher's note

References

1. Petty L, Joseph A, Sanchez J. Case report: pulmonary sequestration in an adult. *Radiol Case Rep.* (2018) 13:21–3. doi: 10.1016/j.radcr.2017.09.029

2. Zhang N, Zeng Q, Chen C, Yu J, Zhang X. Distribution, diagnosis, and treatment of pulmonary sequestration: report of 208 cases. *J Pediatr Surg.* (2019) 54:1286–92.

3. Corbett HJ, Humphrey GME. Pulmonary sequestration. *Paediatr Respir Rev.* (2004) 5:59–68. doi: 10.1016/j.prrv.2003.09.009

4. Aryal K, Regmi PR, Adhikari G, Bhhattarai U, Sedhain SP. Congenital pulmonary airway malformation (CPAM): a case report and review of the literature. *Radiol Case Rep.* (2023) 18:3483–6. doi: 10.1016/j.radcr.2023.07.018

5. Lupinski RW, Agasthian T, Lim CH, Chua YL. Extralobar pulmonary sequestration simulates posterior neurogenic tumor. *Ann Thorac Surg.* (2004) 77:2203–4. doi: 10.1016/S0003-4975(03)01290-6

6. Choe J, Goo HW. Extralobar pulmonary sequestration with hemorrhagic infarction in a child: preoperative imaging diagnosis and pathological correlation. *Korean J Radiol.* (2015) 16:662. doi: 10.3348/kjr.2015.16.3.662

7. Coleman AM, Merrow AC, Crombleholme TM, Jaekle R, Lim FY. Fetal MRI of torsed bronchopulmonary sequestration with tension hydrothorax and hydrops in a twin gestation. *Fetal Diagn Ther.* (2016) 40:156–60. doi: 10.1159/000371513

8. Son SA, Do YW, Kim YE, Lee SM, Lee DH. Infarction of torsed extralobar pulmonary sequestration in adolescence. *Gen Thorac Cardiovasc Surg.* (2020) 68:77–80. doi: 10.1007/s11748-019-01105-7

9. Li L, Yang Q, Wang YX, Yu DL, Chen JH, Wang WJ. [Clinical analysis of pulmonary sequestration with torsion in 4 cases and literature review]. *Zhonghua Jie He He Hu Xi Za Zhi Zhonghua Jiehe He Huxi Zazhi Chin J Tuberc Respir Dis.* (2021) 44:812–6. doi: 10.3760/cma.j.cn112147-20201117-01100

10. Walcutt J, Abdessalam S, Timmons Z, Winningham P, Beavers A. A rare case of torsion and infarction of an extralobar pulmonary sequestration with MR, CT, and surgical correlation. *Radiol Case Rep.* (2021) 16:3931–6. doi: 10.1016/j.radcr.2021.09.045

11. Yokota R, Sakamoto K, Urakawa H, Takeshita M, Yoshimitsu K. Torsion of right lung sequestration mimicking a posterior mediastinal mass presenting as acute abdomen: usefulness of MR imaging. *Radiol Case Rep.* (2019) 14:551–4. doi: 10.1016/j.radcr.2019.02.008

frontiers | Frontiers in Medicine

TYPE Case Report
PUBLISHED 18 November 2024
DOI 10.3389/fmed.2024.1476864

OPEN ACCESS

EDITED BY
Karolina Henryka Czarnecka-Chrebelska,
Medical University of Lodz, Poland

REVIEWED BY
Robson Leão,
Rio de Janeiro State University, Brazil
Po Lin Chen,
National Cheng Kung University, Taiwan

*CORRESPONDENCE
Yufeng Feng
jiqimaoke@163.com

RECEIVED 06 August 2024
ACCEPTED 04 November 2024
PUBLISHED 18 November 2024

CITATION
Sha J, Shao J, Lu S, Zhang M, Gu C, Deng Y, Zhang J and Feng Y (2024) A case report of severe pneumonia caused by *Aeromonas dhakensis* infection complicated with severe atrial septal defect. *Front. Med.* 11:1476864. doi: 10.3389/fmed.2024.1476864

A case report of severe pneumonia caused by *Aeromonas dhakensis* infection complicated with severe atrial septal defect

Jun Sha[1], Jie Shao[1], Sheng Lu[1], Mengmeng Zhang[1], Cheng Gu[1], Yimai Deng[2], Jianfeng Zhang[1] and Yufeng Feng[1]*

[1]Intensive Care Unit, Changshu No. 2 People's Hospital, Suzhou, China, [2]Changshu Medicine Examination Institute, Suzhou, China

Aeromonas dhakensis is an increasingly recognized human pathogen in recent years and was first isolated and reported in a sample of childhood diarrhea in Bangladesh. More and more cases of *Aeromonas dhakensis* infection have been reported in recent years. Here we report a case of severe pneumonia caused by *Aeromonas dhakensis* with severe atrial septal defect. The patient, a 56-year-old male, was admitted to the hospital with severe hypoxemia and severe septic shock. Detection of the patient's bronchoalveolar lavage fluid (BALF) and peripheral blood by the metagenomic next generation sequencing (mNGS) indicated *Aeromonas dhakensis* infection.

KEYWORDS

***Aeromonas dhakensis*, severe pneumonia, atrial septal defect, mNGS, ECMO**

Introduction

Aeromonas dhakensis is a highly pathogenic human pathogen discovered in recent years (1). *Aeromonas dhakensis* is a Gram-negative bacillus and widely distributed in water environments (1). *Aeromonas dhakensis* is extremely virulent and can cause severe sepsis and multiple organ failure in a short time (2), with a 14-day sepsis-related mortality rate of 25.5% (3). *Aeromonas dhakensis* has been reported to have multiple virulence factors and its strains have cytotoxic activity against human blood cell lines (4). *Aeromonas dhakensis*, for example, produces a cytotoxic enterotoxin (5) and also secretes a pathogenic exotoxin A (6). Clinically, it can lead to the most common intestinal infections in patients, but also can lead to extremely serious invasive parenteral infections, such as lung infections, biliary tract infections, and soft tissue infections. Patients with compromised immunity are more susceptible to infection of *Aeromonas dhakensis*, which can lead to severe sepsis and organ failure (7). Here, we report a case of a 56-year-old man diagnosed with *Aeromonas dhakensis* pneumonia with severe atrial septal defect.

Case report

A 56-year-old male presented to the hospital due to fever with chest tightness and asthma for 1 day. The patient was admitted to ICU after endotracheal intubation with mechanical ventilation due to severe hypoxemia. The patient had a history of atrial septal defect for more than 30 years. A blood routine examination showed that white blood cell count was 2.0×10^9/L, the percentage of neutrophils was 85.8%, and platelet

count was 43×10^9/L. C-reactive protein was 3.8 mg/L. Blood gas analysis showed that the oxygenation index was 39.5 mmHg. Procalcitonin was 91.8 ng/mL. The chest computer tomography (CT) scan displayed inflammation in both lungs, mainly in the upper lobe of the right lung (Figure 1). Cardiac ultrasound revealed that the atrial septal defect was 2.66 cm, and the pulmonary artery pressure is about 80 mmHg (Figure 2).

The patient was diagnosed with severe pneumonia, severe acute respiratory distress syndrome (ARDS), septic shock, sepsis, severe atrial septal defect, and severe pulmonary hypertension. The patient's empiric anti-infective therapy was omadacycline in combination with imipenem. The patient received the treatment of veno-arterio-venous extracorporeal membrane oxygenation (VAV-ECMO) immediately due to poor finger pulse oxygen and blood pressure. However, after ECMO treatment, the patient's finger pulse oxygen was still poor. Sildenafil, ambrisentan and inhaled NO were given to reduce pulmonary arterial pressure, considering the patient had severe atrial septal defect and pulmonary hypertension, and severe pulmonary shunt. At the same time, the metagenomic next generation sequencing (mNGS) tested by the company Nanjing KingMed for clinical laboratory through Illumina MiSeq sequencing platform was used to detect the pulmonary alveolar lavage fluid (BALF) and peripheral blood to identify the infectious pathogen. Direct microscopic examination of BALF and peripheral blood showed Gram-negative bacteria.

On the third day of hospitalization, the results of the mNGS showed that *Aeromonas dhakensis* was positive and the relative abundance of *Aeromonas dhakensis* was 95.68%. According to the results of drug sensitivity test, *Aeromonas dhakensis* was sensitive to omoxycycline and imipenem. Therefore, the anti-infection treatment plan would not be adjusted. After active treatment for 2 weeks, the inflammatory index of the patient decreased significantly, and the patient's consciousness became clear. However, due to pulmonary interstitial changes caused by infection and severe pulmonary hypertension, the patient still presented with moderate to severe respiratory failure and was unable to leave the ventilator (Figure 3). After 2 months of mechanical ventilation and rehabilitation exercise, the patient was successfully removed from the ventilator and transferred out of ICU (Figure 4). But the pulmonary interstitial changes caused by infection could not return to normal.

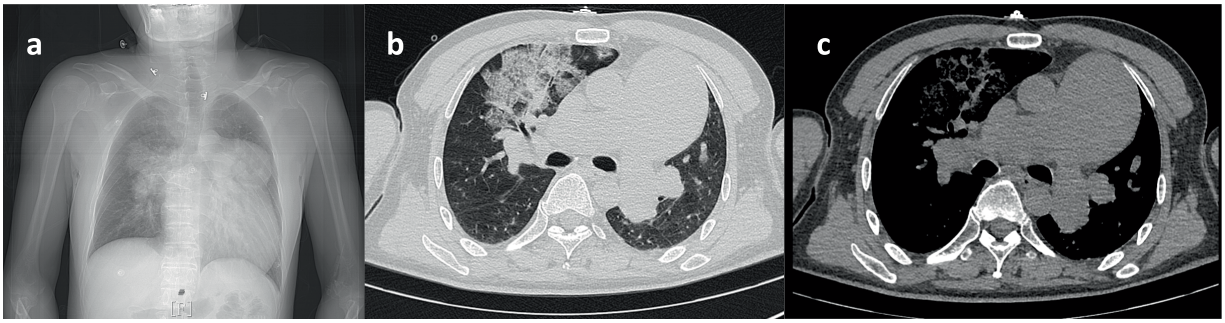

FIGURE 1
(a–c) The chest computer tomography (CT) scan displayed a double lung infection.

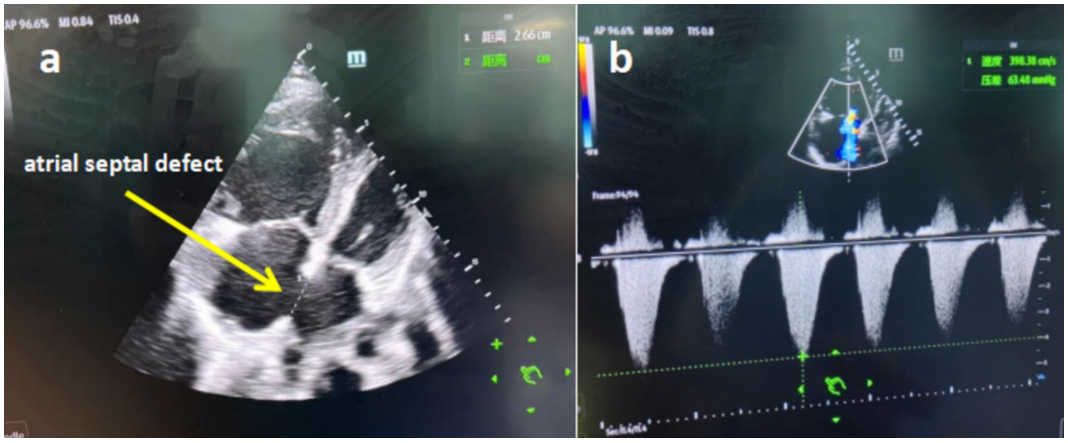

FIGURE 2
(a) Cardiac ultrasound showed the patient with severe atrial septal defect. (b) Cardiac ultrasound showed the patient with severe pulmonary hypertension.

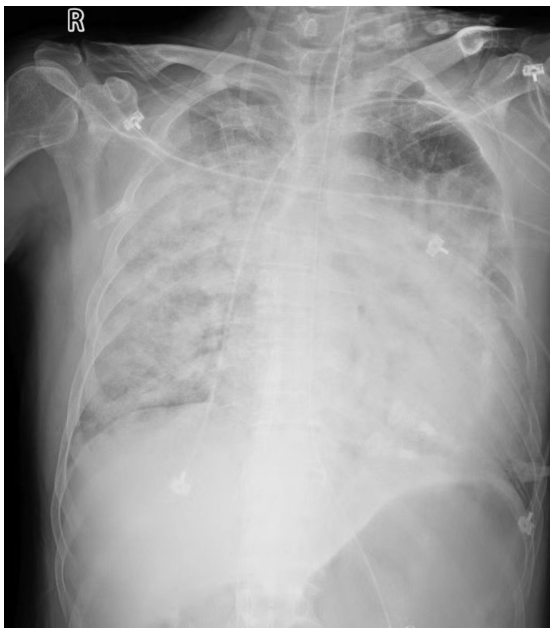

FIGURE 3
Chest X-ray of the patient after effective anti-infective treatment.

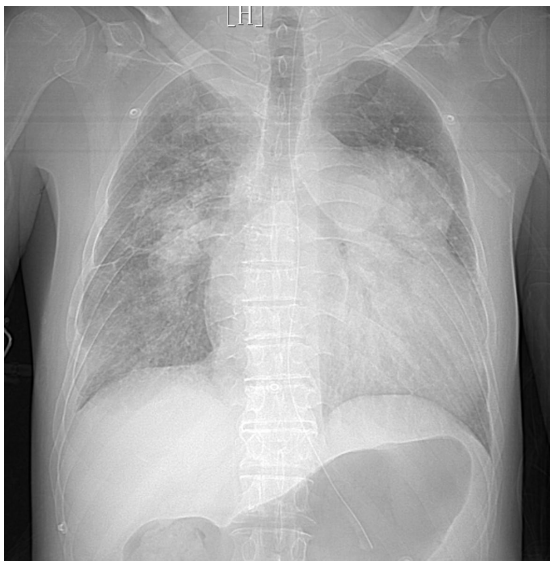

FIGURE 4
Chest X-ray of the patient after withdrawing ventilator successfully.

Discussion

Aeromonas is a Gram-negative bacterium. Human infections are usually caused by *Aeromonas hydrophila*, *Aeromonas veronii* biovar sobria, and *Aeromonas caviae* (8). *Aeromonas* is widely distributed in various kinds of freshwater waters, and the infection of *Aeromonas* in humans is usually through direct contact with water containing pathogenic bacteria (9). People with chronic underlying disease and low immunity are more susceptible to *Aeromonas*. *Aeromonas* can cause gastrointestinal tract, skin and soft tissue, respiratory infections, nervous system and biliary tract infections (10). The clinical manifestations of *Aeromonas* infection are usually rapid onset, severe symptoms and severe sepsis. It has been reported that the initial symptoms of *Aeromonas* infection may be diarrhea, cough, expectoration and hemoptysis (2).

Aeromonas dhakensis was previously considered a subspecies of *Aeromonas hydrophila* (11), which was first isolated from a sample of childhood diarrhea in Bangladesh (12). But according to the latest microbiology studies, whole genome sequence analyses unambiguously confirmed that *Aeromonas dhakensis* reached the level of species (13). *Aeromonas dhakensis* can also cause infections in the digestive, respiratory, urinary, hepatobiliary and skin and soft tissues (3). The mortality rate of *Aeromonas dhakensis* is much higher than other *Aeromonas* species (14), because *Aeromonas dhakensis* contains multiple pathogenic genes and can produce multiple exotoxins. *Aeromonas dhakensis* strains have toxic effects on human blood cell lines, which may result in a reduction in blood cell lines (15, 16). Up to now, the specific pathogenesis of *Aeromonas dhakensis* remains unclear (17).

Aeromonas dhakensis is sensitive to third or fourth generation cephalosporins, aminoglycosides, fluoroquinolones, and tetracyclines (18). *Aeromonas dhakensis* has been reported to produce a variety of β-lactamases resulting in resistance to a variety of penicillins, cephalosporins and even carbapenems (19). Clinicians should be cautious about the use of cephalosporins alone for anti-infective treatment if clinically suspected or confirmed *Aeromonas dhakensis* infection (20).

Conclusion

Clinically, we observed that the infection of *Aeromonas dhakensis* led to the rapid onset of severe septic shock and the possible complications of multiple organ failure Including heart failure, renal failure, respiratory failure, and decreased blood cell line. *Aeromonas dhakensis* is not a common pathogen in community-acquired pneumonia, but it can cause rapid onset, severe symptoms and multiple organ dysfunction in patients. At this time, clinicians should think of the possibility of a *Aeromonas dhakensis* infection. In this case, we used ECMO early to maintain the patient's vital signs, which bought time and opportunity for effective treatment.

Data availability statement

The original contributions presented in the study are included in the article/supplementary material, further inquiries can be directed to the corresponding author.

Ethics statement

The studies involving humans were approved by the Ethics Review Committee of Changshu No. 2 People's Hospital. The studies were conducted in accordance with the local legislation and institutional requirements. The participants provided their written informed consent to participate in this study. Written informed consent was obtained from the individual(s) for the publication of any potentially identifiable images or data included in this article.

Author contributions

JuS: Writing – original draft, Writing – review & editing. JiS: Project administration, Writing – review & editing. SL: Project administration, Writing – review & editing. MZ: Project administration, Writing – review & editing. CG: Project administration, Writing – review & editing. YD: Resources, Writing – review & editing. JZ: Project administration, Writing – review & editing. YF: Writing – review & editing.

Funding

The author(s) declare that no financial support was received for the research, authorship, and/or publication of this article.

Conflict of interest

The authors declare that the research was conducted in the absence of any commercial or financial relationships that could be construed as a potential conflict of interest.

Publisher's note

All claims expressed in this article are solely those of the authors and do not necessarily represent those of their affiliated organizations, or those of the publisher, the editors and the reviewers. Any product that may be evaluated in this article, or claim that may be made by its manufacturer, is not guaranteed or endorsed by the publisher.

References

1. Chen PL, Lamy B, Ko WC. *Aeromonas dhakensis*, an increasingly recognized human pathogen. *Front Microbiol*. (2016) 7:793. doi: 10.3389/fmicb.2016.00793

2. Luo D, Dai L. A 26-year-old man with multiple organ failure caused by *Aeromonas dhakensis* infection: a case report and literature review. *Front Med*. (2024) 11:1289338. doi: 10.3389/fmed.2024.1289338

3. Wu CJ, Chen PL, Hsueh PR, Chang MC, Tsai PJ, Shih HI, et al. Clinical implications of species identification in monomicrobial *Aeromonas* bacteremia. *PLoS One*. (2015) 10:e0117821. doi: 10.1371/journal.pone.0117821

4. Morinaga Y, Yanagihara K, Eugenin FL, Beaz-Hidalgo R, Kohno S, Figueras Salvat MJ. Identification error of *Aeromonas aquariorum*: a causative agent of septicemia. *Diagn Microbiol Infect Dis*. (2013) 76:106–9. doi: 10.1016/j.diagmicrobio.2013.01.019

5. Chopra AK, Houston CW. Enterotoxins in *Aeromonas*-associated gastroenteritis. *Microbes Infect*. (1999) 1:1129–37. doi: 10.1016/S1286-4579(99)00202-6

6. Ponnusamy D, Kozlova EV, Sha J, Erova TE, Azar SR, Fitts EC, et al. Cross-talk among flesh-eating *Aeromonas hydrophila* strains in mixed infection leading to necrotizing fasciitis. *Proc Natl Acad Sci USA*. (2016) 113:722–7. doi: 10.1073/pnas.1523817113

7. Patil SM, Hilker ED. *Aeromonas hydrophila* community-acquired bacterial pneumonia with septic shock in a chronic lymphocytic leukemia patient due to absolute neutropenia and lymphopenia. *Cureus*. (2022) 14:e23345. doi: 10.7759/cureus.23345

8. Janda JM, Abbott SL. The genus *Aeromonas*: taxonomy, pathogenicity, and infection. *Clin Microbiol Rev*. (2010) 23:35–73. doi: 10.1128/CMR.00039-09

9. Esteve C, Alcaide E, Blasco MD. *Aeromonas hydrophila* subsp. *dhakensis* isolated from feces, water and fish in Mediterranean Spain. *Microbes Environ*. (2012) 27:367–73. doi: 10.1264/jsme2.ME12009

10. Janda JM. Recent advances in the study of the taxonomy, pathogenicity, and infectious syndromes associated with the genus *Aeromonas*. *Clin Microbiol Rev*. (1991) 4:397–410. doi: 10.1128/CMR.4.4.397

11. Figueras MJ, Alperi A, Saavedra MJ, Ko WC, Gonzalo N, Navarro M, et al. Clinical relevance of the recently described species *Aeromonas aquariorum*. *J Clin Microbiol*. (2009) 47:3742–6. doi: 10.1128/JCM.02216-08

12. Huys G, Kämpfer P, Albert MJ, Kühn I, Denys R, Swings J. *Aeromonas hydrophila* subsp. *dhakensis* subsp. nov., isolated from children with diarrhoea in Bangladesh, and extended description of *Aeromonas hydrophila* subsp. *hydrophila* (Chester 1901) Stanier 1943 (approved lists 1980). *Int J Syst Evol Microbiol*. (2002) 52:705–12. doi: 10.1099/00207713-52-3-705

13. Beaz-Hidalgo R, Martínez-Murcia A, Figueras MJ. Reclassification of *Aeromonas hydrophila* subsp. *dhakensis* Huys et al. 2002 and *Aeromonas aquariorum* Martínez-Murcia et al. 2008 as *Aeromonas dhakensis* sp. nov. comb nov. and emendation of the species *Aeromonas hydrophila*. *Syst Appl Microbiol*. (2013) 36:171–6. doi: 10.1016/j.syapm.2012.12.007

14. Chen PL, Wu CJ, Tsai PJ, Tang HJ, Chuang YC, Lee NY, et al. Virulence diversity among bacteremic *Aeromonas* isolates: ex vivo, animal, and clinical evidences. *PLoS One*. (2014) 9:e111213. doi: 10.1371/journal.pone.0111213

15. Rasmussen-Ivey CR, Figueras MJ, McGarey D, Liles MR. Virulence factors of *Aeromonas hydrophila*: in the wake of reclassification. *Front Microbiol*. (2016) 7:1337. doi: 10.3389/fmicb.2016.01337

16. Tomás JM. The main *Aeromonas* pathogenic factors. *ISRN Microbiol*. (2012) 2012:256261–22. doi: 10.5402/2012/256261

17. Kitagawa H, Ohge H, Yu L, Kayama S, Hara T, Kashiyama S, et al. *Aeromonas dhakensis* is not a rare cause of *Aeromonas* bacteremia in Hiroshima, Japan. *J Infect Chemother*. (2020) 26:316–20. doi: 10.1016/j.jiac.2019.08.020

18. Chen PL, Wu CJ, Chen CS, Tsai PJ, Tang HJ, Ko WC. A comparative study of clinical *Aeromonas dhakensis* and *Aeromonas hydrophila* isolates in southern Taiwan: *A. dhakensis* is more predominant and virulent. *Clin Microbiol Infect*. (2014) 20:O428–34. doi: 10.1111/1469-0691.12456

19. Wu CJ, Chen PL, Wu JJ, Yan JJ, Lee CC, Lee HC, et al. Distribution and phenotypic and genotypic detection of a metallo-β-lactamase, CphA, among bacteraemic *Aeromonas* isolates. *J Med Microbiol*. (2012) 61:712–9. doi: 10.1099/jmm.0.038323-0

20. Wu CJ, Wang HC, Chen PL, Chang MC, Sunny Sun H, Chou PH, et al. AQU-1, a chromosomal class C β-lactamase, among clinical *Aeromonas dhakensis* isolates: distribution and clinical significance. *Int J Antimicrob Agents*. (2013) 42:456–61. doi: 10.1016/j.ijantimicag.2013.08.002

frontiers | Frontiers in Medicine

TYPE Case Report
PUBLISHED 19 November 2024
DOI 10.3389/fmed.2024.1464493

OPEN ACCESS

EDITED BY
Karolina Henryka Czarnecka-Chrebelska,
Medical University of Lodz, Poland

REVIEWED BY
Rafiye Ciftciler,
Hacettepe University, Türkiye
Roberto Giovanni Carbone,
University of Genoa, Italy

*CORRESPONDENCE
Yinhe Feng
✉ fengyinhe@sina.com

†These authors have contributed equally to this work

RECEIVED 14 July 2024
ACCEPTED 04 November 2024
PUBLISHED 19 November 2024

CITATION
Yue Y, Du R, Han D, Zhao T, Zeng C and Feng Y (2024) Three-year delay in diagnosis of pulmonary sarcoidosis due to presence of necrotizing granulomas: a cautionary case report. *Front. Med.* 11:1464493. doi: 10.3389/fmed.2024.1464493

Three-year delay in diagnosis of pulmonary sarcoidosis due to presence of necrotizing granulomas: a cautionary case report

Yubing Yue[1†], Rao Du[2†], Ding Han[1], Tianxia Zhao[1], Chunfang Zeng[1] and Yinhe Feng[1*]

[1]Department of Respiratory and Critical Care Medicine, Deyang People's Hospital, Affiliated Hospital of Chengdu College of Medicine, Deyang, China, [2]Department of Respiratory and Critical Care Medicine, West China Hospital, Sichuan University, Chengdu, China

Diagnosis of pulmonary sarcoidosis can be difficult and strongly dependent on clinical experience, especially when necrotizing granulomas are present. Here we report an individual who, 3 years after onset of symptoms, was definitively diagnosed with pulmonary sarcoidosis based on percutaneous lung biopsy under the guidance of computed tomography, after he failed to receive a specific diagnosis at other tertiary hospitals based on cervical lymph node biopsy and transbronchial needle aspiration under the guidance of endobronchial ultrasonography. After his definitive diagnosis at our medical center, he was given corticosteroids, which led to remission. Clinicians, especially in areas lacking suitably experienced pathologists, should be aware of how to diagnose sarcoidosis in the presence of abundant necrotizing granulomas in order to ensure timely diagnosis.

KEYWORDS

pulmonary sarcoidosis, puncture, biopsy, granuloma, case report

Introduction

Sarcoidosis is a systemic disease of unknown origin involving non-caseous, non-necrotizing epithelioid granulomas (1). The disease can vary substantially in its manifestations, affected tissues and response to treatment (2). Although it is self-limiting in most patients, approximately one quarter of patients may suffer a progressive, chronic course leading to irreversible injury, such as pulmonary fibrosis, cirrhosis, fatal arrhythmia, or blindness (3). Incidence around the world varies from ~2 to 11 cases annually per 100,000 people, and 90% of cases involve the lungs, with smaller proportions involving the skin or eyes (4). In recent years, bone marrow involvement have also been rarely reported in pediatric and adult sarcoidosis (5). More than 10% of cases of pulmonary sarcoidosis involve the pulmonary parenchyma as well as intrapulmonary and peripheral lymph nodes (6).

Pulmonary sarcoidosis is diagnosed by exclusion and based fundamentally on histopathology, typically of tissue from a superficial, easy-to-biopsy site as well as tissue from the affected area in the chest (7). Histopathology should indicate non-caseous, non-necrotizing epithelioid cell granulomas. However, the granulomatous-type inflammation that is also found in other pathological conditions often makes the diagnosis difficult and may confuse pathologists into misclassifying sarcoidosis as another disease.

Here we describe the case of an individual in China who, 3 years after onset of symptoms, was definitively diagnosed with pulmonary sarcoidosis involving the peripheral lymph nodes, liver and spleen after his diagnosis went undetected at other tertiary hospitals. We attribute the missed diagnosis to the presence of abundant necrotizing granulomas, which distracted pathologists from the true underlying condition. Clinicians and pathologists should be aware of the potential of sarcoidosis in the presence of necrotizing granulomas and which techniques may be more reliable for diagnosing the condition.

Case presentation

A 50-year-old Chinese man came to our tertiary hospital complaining of cough and progressive dyspnea lasting longer than 3 years, as well as dryness of the eyes and cervical lymph node enlargement lasting longer than 1 year. The patient reported no hemoptysis, chest pain, hot flashes, night sweats, or weight loss. During the previous 18 months, he had visited two other tertiary hospitals in western China. At the first hospital, histopathology of neck lymph node puncture indicated granulomatous inflammation with necrosis, and the patient was referred to the second hospital for further diagnostic work-up. At the second hospital, a chest computed tomography revealed regional lymphadenopathy, diffuse nodules in the lungs, and a mass in the right lower lobe. He then underwent transbronchial needle aspiration under the guidance of endobronchial ultrasonography (EBUS-TBNA), which indicated the same pathological results as the first hospital. Histology based on acid-fast, periodic acid Schiff, or hexamine silver stains were unremarkable, while a polymerase chain reaction test for the presence of *Mycobacterium tuberculosis* was negative. The patient was discharged from the hospital without diagnosis or treatment.

When he was admitted to our hospital, the patient reported no recent travel; no history of infectious or chronic diseases, trauma or clinical procedures other than the diagnostic procedures described above; and no history of alcohol or drug use. He reported having smoked at least 20 cigarettes per day for 30 years, then quitting more than 1 year before admission to our hospital. For 6 months prior to admission, he had been taking pregabalin (75 mg) twice daily to treat post-herpes neuralgia in his left chest.

At admission, the patient had normal body temperature (36.3°C), respiratory rate (19 breaths/min), heart rate (94 beats/min) and oxygen saturation in ambient air (97%), but his blood pressure was high (144/102 mmHg). Nothing remarkable was found on physical examination, routine blood tests, or assays of hypersensitive C-reaction protein, brain natriuretic peptide, liver function, coagulatory or connective tissue disease-associated antibodies, electrolytes or cardiac markers in serum, gases in arterial blood, or interferon-γ release. However, the patient showed elevated uric acid in serum (516.6 μmol/L).

Enhanced chest computed tomography displayed diffuse nodules and consolidation in the lungs. Additionally, enlarged axillary and paraspinal lymph nodes with calcification were found in the bilateral mediastinum. A mildly enhanced mass measuring 5.5 × 3.4 cm in the anterior basal segment of the right lower lobe and diffuse nodules in the liver and spleen were also detected (Figures 1A–D).

To rule out lung cancer, the mass underwent percutaneous lung biopsy under the guidance of computed tomography, which indicated granulomatous inflammation (Figure 2). Histology of the biopsy after periodic acid schiff or hexamine silver staining was unremarkable. Based on the above findings as well as the results of ophthalmological tests and abdominal computed tomography, the patient was definitively diagnosed with pulmonary sarcoidosis involving the liver, spleen, and peripheral lymph nodes.

The patient was prescribed oral prednisone at 30 mg daily. After 1 month on this therapy, the patient reported substantial improvement in coughing and dyspnea. After 2 months of treatment, a follow-up chest computed tomography showed significant improvement in the condition of nodules, consolidation, lymphadenopathy and the mass (Figures 1E–G). The patient was switched to oral prednisone at 20 mg daily, and follow-up 1 month later showed no evidence of sarcoidosis recurrence. The patient was switched to prednisone maintenance therapy at 10 mg daily.

Discussion

Clinical symptoms, computer imaging and physiological investigations of sarcoidosis are lack of specificity. Approximately one third of individuals with active sarcoidosis present non-specific manifestations such as fatigue, low fever, weight loss, night sweats, and joint pain (8). Hypercalcemia, even malignant hypercalcemia, is one of its manifestations (9). Dry cough, shortness of breath and chest pain are relatively common manifestations of pulmonary sarcoidosis (8), consistent with our patient's presentation of cough and progressive dyspnea, but respiratory symptoms may be neglected during diagnosis if the primary manifestations involve tissues other than the lungs. The causes and drivers of sarcoidosis remain unclear, and numerous factors have been implicated, including infection, dust, antigen-presenting cells, $CD4^+$ T cells, cytokines such as interleukin-2 and tumor necrosis factor-*A*, as well aspolymorphisms in genes encoding human leukocyte antigen and butyrophilin-like protein 2 (3).

Sarcoidosis is a systemic granulomatous disease that may affect all organs but preferably lungs and lymph nodes. Some of the organs involved are hidden and not easily detected. Although a recent meta-analysis study suggested that the sensitivity and specificity of positron emission-computed tomography (PET-CT) in the diagnosis of pulmonary sarcoidosis were 0.971 and 0.873, respectively, PET-CT also does not ensure identification all organ involvement of pulmonary sarcoidosis (10). Our patient showed bilateral hilar lymphadenopathy and pulmonary infiltrates consistent with Scadding stage II in pulmonary sarcoidosis (11). Pulmonary sarcoidosis more often involves the upper lobe of both lungs and shows diffuse nodules, but our patient had a mass in the right lower lobe, which led us to examine the possibility of lung cancer. Our patient showed macronodules, which presumably arose through coalescence of granulomata and indicate more extensive disease (12), consistent with the involvement of multiple organs in our patient. Similarly, Marc et al. reported a rare pulmonary sarcoidosis case presenting with a large, solitary lung mass with imaging features of lung cancer (13). In addition to rare lump-like image findings as our patient, non-specific interstitial pneumonia (NSIP) lookalike pattern have recently been reported as a distinct

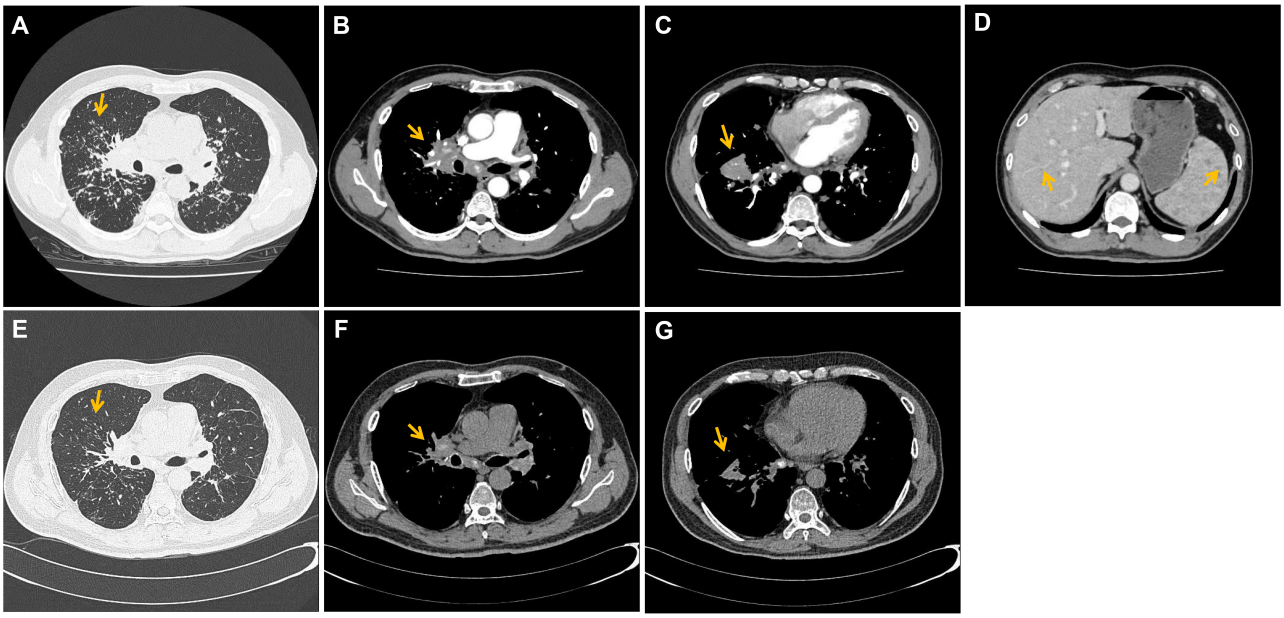

FIGURE 1
The initial and follow-up CT images of patient. **(A)** Computed tomography (CT) of the chest displayed diffuse nodules and consolidation in the lungs (yellow arrow). **(B)** Additionally, enlarged axillary and paraspinal lymph nodes with calcification and mild degree of enhancement were found in the bilateral mediastinum (yellow arrows); **(C)** as well as a mildly enhancement mass (about 5.5 × 3.4 cm) where a CT-guided percutaneous lung biopsy was performed (yellow arrows); **(D)** diffuse nodules in the liver and spleen were also detected (yellow arrows); **(E–G)** were after 2 months treatment. The condition of nodules, consolidation, lymphadenopathy and the mass showed significant improvement (yellow arrow).

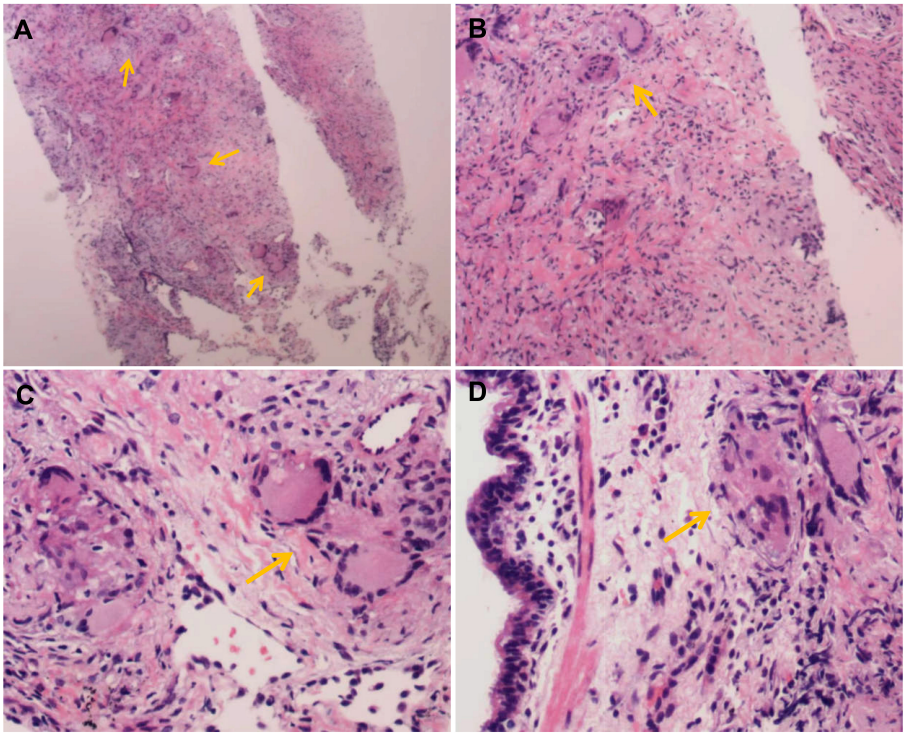

FIGURE 2
The histopathological staining of the lung sample. Tissue biopsy with multiple non-necrotizing granulomas (yellow arrow) at different magnification stained with hematoxylin-eosin (**A**: 40×), (**B**: 100×), (**C**: 200×), and (**D**: 200×).

pattern of pulmonary sarcoidosis on high-resolution computed tomography (HRCT) (14).

Our patient showed no signs of liver dysfunction but did show diffuse miliary-like nodules in the liver and spleen as well as enlargement of the spleen. The liver is involved in ~20% of cases of intrathoracic sarcoidosis (15), though autopsy-based studies suggest the real incidence may be as high as 80% (16). When the liver is affected, the spleen also tends to be affected. Hepatic sarcoidosis typically manifests as no symptoms or as mild, non-specific symptoms such as abdominal discomfort, exertion, vomiting, weight loss and fever, which is consistent with the presentation in our patient. Computed tomography of the liver and spleen typically reveals hepatosplenomegaly, diffuse nodules and rare solitary nodules, which are not specific for sarcoidosis. Up to 15% of patients with pulmonary sarcoidosis show spleen enlargement or splenic nodules on abdominal computed tomography (17). Diffuse splenic nodules associated with extensive tissue involvement outside the lungs and predicts worse prognosis (18), which may appear in our patient at longer follow-up.

Pulmonary sarcoidosis is a difficult condition to diagnose, and its diagnosis remains one of exclusion. Biopsy of peripheral lymph nodes and EBUS-TBNA failed to detect in our patient the non-necrotizing granulomas composed of epithelioid histiocytes and multinucleated giant cells, surrounded by palisading lymphocytes, plasma cells and fibroblasts, which are the hallmark of sarcoidosis (11). We attribute this failure to the abundance of necrotizing granulomas in the tissue sections, which distracted the pathologists and perhaps because of their lack of experience led them to focus more on the possibility of fungal or mycobacterial infection. Thus, our case highlights the need for clinicians and pathologists to consider the possibility of sarcoidosis even in the presence of abundant necrotizing granulomas. Indeed, one study has suggested that about 20% of cases of sarcoidosis involve some degree of necrotizing granulomas in biopsies (19). The riskier technique of percutaneous lung biopsy under the guidance of computed tomography did detect non-necrotizing granulomas in our patient and, after our careful exclusion of infection through appropriate histological stains, allowed us to diagnose him with pulmonary sarcoidosis. While sarcoidosis is the most frequent cause of granulomatous disease (whether necrotic or not), the second and third most frequent causes are tuberculosis and sarcoid reaction due to malignancy (20), which should therefore be considered during differential diagnosis. A rare finding, non-necrotizing granulomas formation in bone marrow biopsy have also been reported in Brucellosis (21). In some cases, other rare granulomatous diseases, such as drug-induced granulomatosis, Crohn's disease, granulomatosis with polyvasculitis, and eosinophilic granulomatosis need to be ruled out (22). Thus, the accuracy of the diagnosis involves a sensible differential for alternative diagnoses of infectious or non-infectious diseases.

The therapeutic management of pulmonary sarcoidosis is challenging due to the heterogenous of the clinical comorbid conditions, response to therapy and prognosis, thus should be individualized for each patient. Prednisone at an initial dose of 20–40 mg daily is the corticosteroid most frequently used to treat sarcoidosis. Daily doses above 40 mg appear not to provide additional benefit and instead increase risk of side effects (23). More recently, one study has used the proportions of circulating PD-1$^+$ CD4$^+$ memory T cells and PD-1$^+$ regulatory T cells to predict treatment response to prednisone in pulmonary sarcoidosis (24). In the absence of consensus guidelines on tapering off corticosteroid therapy, the dose is typically reduced gradually after 2–4 weeks of initial treatment, and maintenance therapy at a daily dose of 5–10 mg is usually continued for 6–24 months. Second-line treatments include immunosuppressive and cytotoxic drugs such as methotrexate, leflunomide, and azathioprine, while biological drugs can serve as third-line treatments (25). Recent evidence supports the potential therapeutic benefits of anti-fibrosis drugs such as nintedanib due to their ability to reduce lung inflammation (26). Steroid treatment of sarcoidosis can be a double-edged sword: while the disease rarely relapses if it resolves on own, it relapses in 37–74% of individuals within 3–6 months after they stop steroid therapy (25). Some effective evidence has been observed that inhaled corticosteroid maintenance after induced systemic corticosteroid therapy can reduce relapse, but mainly budesonide (27). The possible explanation could be that inhaled budesonide creates the systemic anti-inflammatory activity, which is induced by rapidly absorbed into systemic circulation. This is also an option to the maintenance therapy for our patient. Generally, patients should be followed up for at least 3 years after they stop steroid therapy, since recurrence beyond that point seems to be rare (25).

Our case highlights the complexity of diagnosing pulmonary sarcoidosis, especially when multiple tissues are involved and when necrotic granulomas are abundant. Infection and cancer should be carefully excluded through appropriate histological staining and other tests. Although riskier than other biopsy approaches, percutaneous lung biopsy under the guidance of computed tomography may be necessary to definitively diagnose difficult cases. Future research should devote more attention to the diagnosis and treatment of extrapulmonary sarcoidosis.

Data availability statement

The original contributions presented in the study are included in the article/supplementary material, further inquiries can be directed to the corresponding author.

Ethics statement

Written informed consent was obtained from the individual(s) for the publication of any potentially identifiable images or data included in this article.

Author contributions

YF: Writing – review & editing. YY: Writing – original draft. RD: Writing – original draft. DH: Writing – review & editing. TZ: Writing – review & editing. CZ: Writing – review & editing.

Funding

The author(s) declare financial support was received for the research, authorship, and/or publication of this article. This work was supported by the Deyang Science and Technology Project

(Grant No. 2023SZZ013) and Deyang People's Hospital incubation project (Grant No. FHS202302).

Conflict of interest

The authors declare that the research was conducted in the absence of any commercial or financial relationships that could be construed as a potential conflict of interest.

Publisher's note

References

1. Chong Y, Lee EJ, Kang CS, Kim TJ, Song JS, Shim H. Necrotizing sarcoid granulomatosis: possibly veiled disease in endemic area of mycobacterial infection. *J Pathol Transl Med.* (2015) 49:346–50. doi: 10.4132/jptm.2015.04.17

2. Schupp JC, Freitag-Wolf S, Bargagli E, Mihailović-Vučinić V, Rottoli P, Grubanovic A, et al. Phenotypes of organ involvement in sarcoidosis. *Eur Respir J.* (2018) 51:1700991. doi: 10.1183/13993003.00991-2017

3. Spagnolo P, Rossi G, Trisolini R, Sverzellati N, Baughman RP, Wells AU. Pulmonary sarcoidosis. *Lancet Respir Med.* (2018) 6:389–402. doi: 10.1016/S2213-2600(18)30064-X

4. Thillai M, Atkins CP, Crawshaw A, Hart SP, Ho LP, Kouranos V, et al. BTS Clinical Statement on pulmonary sarcoidosis. *Thorax.* (2021) 76:4–20. doi: 10.1136/thoraxjnl-2019-214348

5. Meshram RM, Gajimwar VS, Gholap S, Jhanwar M. Bone marrow involvement: atypical presentation of early-onset childhood sarcoidosis. *Eur J Rheumatol.* (2020) 7:190–4. doi: 10.5152/eurjrheum.2020.20076

6. Sève P, Pacheco Y, Durupt F, Jamilloux Y, Gerfaud-Valentin M, Isaac S, et al. Sarcoidosis: a clinical overview from symptoms to diagnosis. *Cells.* (2021) 10:766. doi: 10.3390/cells10040766

7. Hu MK, Mathur A, Dempsey OJ. Pulmonary sarcoidosis: a clinical update. *J R Coll Physicians Edinb.* (2020) 50:322–9. doi: 10.4997/jrcpe.2020.324

8. Carmona EM, Kalra S, Ryu JH. Pulmonary sarcoidosis: diagnosis and treatment. *Mayo Clin Proc.* (2016) 91:946–54. doi: 10.1016/j.mayocp.2016.03.004

9. Lakhal M, Kebbara S, Thouil A, Kouismi H. Malignant hypercalcemia revealing pulmonary sarcoidosis. *Cureus.* (2024) 16:e64454. doi: 10.7759/cureus.64454

10. Donnelly R, McDermott M, McManus G, Franciosi AN, Keane MP, McGrath EE, et al. Meta-analysis of [(18)F]FDG-PET/CT in pulmonary sarcoidosis. *Eur Radiol.* (2024). doi: 10.1007/s00330-024-10949-4

11. Belperio JA, Fishbein MC, Abtin F, Channick J, Balasubramanian SA, Lynch Iii JP. Pulmonary sarcoidosis: a comprehensive review: past to present. *J Autoimmun.* (2023) 19:103107. doi: 10.1016/j.jaut.2023.103107

12. Desai SR, Sivarasan N, Johannson KA, George PM, Culver DA, Devaraj A, et al. High-resolution CT phenotypes in pulmonary sarcoidosis: a multinational Delphi consensus study. *Lancet Respir Med.* (2024) 12:409–18. doi: 10.1016/S2213-2600(23)00267-9

13. Marc MS, Pescaru CC, Costin EO, Crisan AF, Maritescu A, Pescaru A, et al. Large lung consolidation: a rare presentation of pulmonary sarcoidosis. *Life.* (2023) 14:44. doi: 10.3390/life14010044

14. Xu R, Wang K, Li W, Liu D. Diagnosis of pulmonary sarcoidosis comorbid with non-specific interstitial pneumonia: a case report. *BMC Pulm Med.* (2024) 24:497. doi: 10.1186/s12890-024-03316-y

15. Abdelghaffar M, Hwang E, Damsky W. Cutaneous sarcoidosis. *Clin Chest Med.* (2024) 45:71–89. doi: 10.1016/j.ccm.2023.08.004

16. Kumar M, Herrera JL. Sarcoidosis and the liver. *Clin Liver Dis.* (2019) 23:331–43. doi: 10.1016/j.cld.2018.12.012

17. Bailey GL, Wells AU, Desai SR. Imaging of pulmonary sarcoidosis-a review. *J Clin Med.* (2024) 13:822. doi: 10.3390/jcm13030822

18. Tetikkurt C, Yanardag H, Pehlivan M, Bilir M. Clinical features and prognostic significance of splenic involvement in sarcoidosis. *Monaldi Arch Chest Dis.* (2017) 87:893. doi: 10.4081/monaldi.2017.893

19. Grutters JC. Establishing a diagnosis of pulmonary sarcoidosis. *J Clin Med.* (2023) 12:6898. doi: 10.3390/jcm12216898

20. Aydogan Eroglu S, Yildiz T, Sonkaya E, Kavas M, Ozbaki F, Sertçelik L, et al. Diagnosis distribution in cases with granulomatous inflammation in lung, pleura, and lymph node biopsies: an experience from a tertiary level single center chest diseases and thoracic surgery hospital. *Sarcoidosis Vasc Diffuse Lung Dis.* (2022) 38:e2021048. doi: 10.36141/svdld.v38i4.11914

21. Ciftciler R, Ozturk G. Non-necrotizing granulomas in bone marrow biopsy of a patient with bicytopenia: brucellosis case. *Med Sci Dis.* (2022) 9:260–2. doi: 10.36472/msd.v9i4.710

22. Valeyre D, Brauner M, Bernaudin JF, Carbonnelle E, Duchemann B, Rotenberg C, et al. Differential diagnosis of pulmonary sarcoidosis: a review. *Front Med.* (2023) 10:1150751. doi: 10.3389/fmed.2023.1150751

23. Broos CE, Poell L, Looman C, In 't Veen J, Grootenboers M, Heller R, et al. No evidence found for an association between prednisone dose and FVC change in newly-treated pulmonary sarcoidosis. *Respir Med.* (2018) 138S:S31–7. doi: 10.1016/j.rmed.2017.10.022

24. Miedema JR, de Jong LJ, Kahlmann V, Bergen IM, Broos CE, Wijsenbeek MS, et al. Increased proportions of circulating PD-1(+) CD4(+) memory T cells and PD-1(+) regulatory T cells associate with good response to prednisone in pulmonary sarcoidosis. *Respir Res.* (2024) 25:196. doi: 10.1186/s12931-024-02833-y

25. Gerke AK. Treatment of granulomatous inflammation in pulmonary sarcoidosis. *J Clin Med.* (2024) 13:378. doi: 10.3390/jcm13030738

26. Mata Salvador MC, Francesqui J, Sellarés J. The current state-of-the-art in pharmacotherapy for pulmonary sarcoidosis. *Expert Opin Pharmacother.* (2024) 25:1317–24. doi: 10.1080/14656566.2024.2377714

27. Selroos O, Brattsand R. Inhaled budesonide and pulmonary sarcoidosis revisited. *Sarcoidosis Vasc Diffuse Lung Dis.* (2024) 41:e2024037. doi: 10.36141/svdld.v41i3.15852

frontiers | Frontiers in Medicine

TYPE Case Report
PUBLISHED 27 November 2024
DOI 10.3389/fmed.2024.1491838

OPEN ACCESS

EDITED BY
Uday Kishore,
United Arab Emirates University,
United Arab Emirates

REVIEWED BY
Yutaka Yoshii,
The Jikei University School of Medicine,
Japan
Zheng Jin Tu,
Cleveland Clinic, United States

*CORRESPONDENCE
Dong Wang
✉ wangdongwuhan001@163.com

RECEIVED 05 September 2024
ACCEPTED 11 November 2024
PUBLISHED 27 November 2024

CITATION
Yan X, Fu H, Deng W, Zhang Z and Wang D (2024) Early and rapid diagnosis of *Chlamydia psittaci* pneumonia by tNGS in six patients: a case series.
Front. Med. 11:1491838.
doi: 10.3389/fmed.2024.1491838

Early and rapid diagnosis of *Chlamydia psittaci* pneumonia by tNGS in six patients: a case series

Xinsheng Yan[1], Huali Fu[2], Wenjun Deng[3], Zhenlu Zhang[1] and Dong Wang[1]*

[1]Department of Clinical Laboratory, Wuhan Asia General Hospital, Wuhan Asia General Hospital Affiliated to Wuhan University of Science and Technology, Wuhan, China, [2]Respiratory and Critical Care Medicine, Wuhan Asia General Hospital, Wuhan Asia General Hospital Affiliated to Wuhan University of Science and Technology, Wuhan, China, [3]Department of Radiology, Wuhan Asia General Hospital, Wuhan Asia General Hospital Affiliated to Wuhan University of Science and Technology, Wuhan, China

Background: Psittacosis is a zoonotic infectious disease caused by *Chlamydia psittaci* (*C. psittaci*) infection, which can be transmitted by birds, poultry and wild animals. The symptoms and imaging findings of *C. psittaci* pneumonia are atypical and primarily rely on etiological diagnosis. The incidence of *C. psittaci* infection has been significantly underestimated because of the low sensitivity and poor timeliness of traditional diagnostic methods. Therefore, early and accurate diagnosis of psittacosis remains a challenge.

Case presentation: A case series with six pneumonia patients who were admitted to our hospital in the period from January 2023 to June 2023 is presented. These patients exhibited acute onset and symptoms, including fever, cough, poor appetite, dry mouth, dizziness, chills, and chest tightness. Despite comprehensive laboratory and radiological examinations, the cause of the pneumonia remained unidentified. Therefore, a sample of bronchoalveolar lavage fluid (BALF) was tested via target next-generation sequencing (tNGS), which revealed a positive result for *C. psittaci*. Prompt adjustment of the treatment regimens upon identification of the pathogen led to favorable outcomes in all patients.

Conclusion: tNGS is a novel diagnostic technology that enables rapid, accurate and cost-effective detection of *C. psittaci* pneumonia. Early detection of *C. psittaci* can improve patient outcomes through timely adjustment of therapies.

KEYWORDS

psittacosis, *Chlamydia psittaci*, target next-generation sequencing, tNGS, pathogen detection

1 Introduction

According to the Global Burden of Disease Collaboration, it is estimated that nearly 600 million individuals were estimated to be affected by pneumonia and other lower respiratory tract infections globally in 2019, resulting in 2.5 million deaths (1). The epidemiologic distribution of pneumonia pathogens has shifted in recent years, with an increase in some rare pathogens. *C. psittaci*, an intracellular gram-negative pathogen, is commonly found in birds (especially parrots and pigeons) and mammals (2). Inhalation of aerosols from infected bird feathers or avian excreta can lead to *C. psittaci* pneumonia in humans. This pathogen is frequently misdiagnosed, leading to the potential misuse of

antimicrobials and the development of drug resistance (3, 4). Patients with *C. psittaci* pneumonia typically exhibit sepsis and a rapidly deteriorating condition. Early diagnosis and treatment are crucial for improving patient prognosis because of the rapid progression of the disease (5).

The diagnosis of *C. psittaci* pneumonia is challenging because of its nonspecific clinical presentation and often relies on laboratory testing for the pathogen. Currently, culture, serology and molecular testing are the main methods of detection. Cell cultures for *C. psittaci* are time-consuming and require a high level of laboratory biosafety, making them unsuitable for routine use, and serologic tests have limited early diagnostic value, as they are more appropriate for retrospective diagnosis (6). PCR reagents for *C. psittaci* are not readily available and are limited by clinician judgment, although PCR is considered the gold standard for detection (7). Metagenomic next-generation sequencing (mNGS) employs high-throughput sequencing technology to capture the comprehensive range of microbial nucleic acid sequences present in samples. These sequences are then compared and analyzed with existing microbial nucleic acid sequences stored in a database. This approach facilitates the efficient and accurate identification of suspected pathogenic microorganisms in samples. In recent years, many reported cases of *C. psittaci* pneumonia have been definitively diagnosed by mNGS (8, 9). More recently, target next-generation sequencing (tNGS), a new technology based on the combination of ultra-multiplex PCR amplification and high-throughput sequencing, has gradually entered clinic practice as a faster and less expensive molecular detection method than mNGS. However, reports on the application of tNGS for *C. psittaci* detection are scarce. Therefore, this study was conducted to analyze the clinical data of six patients with *C. psittaci* pneumonia at our hospital to evaluate the effectiveness of tNGS for early and rapid diagnosis and to better understand the clinical characteristics of these patients.

2 Case presentation

Between January 2023 and June 2023, a total of 297 inpatients underwent tNGS testing, and six of these patients were diagnosed with *C. psittaci* pneumonia. Data regarding the demographic characteristics of the six patients, including age, gender, occupational history, and avian exposure, were collected. Clinical manifestations, signs, as well as laboratory and imaging findings, were documented. The aetiological diagnosis was based on the sequence of the *C. psittaci* obtained from BALF samples via tNGS. Furthermore, the use of antibiotics prior to and following the diagnosis of *C. psittaci* pneumonia, along with the time intervals from symptom onset to admission and from admission to diagnosis, were recorded.

2.1 Baseline characteristics and clinical manifestations

Table 1 presents general information on the six patients, comprising three men and three women aged between 18 and 66 years, who were included in this study. Among them, two patients had a history of hypertension, three had a history of diabetes, one had a history of atrial fibrillation, one had a history of ulcers, and one had abnormal liver function. Additionally, three patients had a documented history of exposure to poultry, whereas two had a history of exposure to parrots. All patients experienced fever, with the highest body temperature recorded ranging from 38.0 to 40.0°C. Common accompanying symptoms included cough (3/6), headache (2/6), dizziness (2/6), cold symptoms (2/6), stiffness (3/6), chest tightness (2/6), pharyngeal pain (1/6), fatigue (4/6), muscle pain (2/6), and frequent urination urgency (2/6).

2.2 Clinical laboratory testing

Various parameters, including the white blood cell (WBC) count, neutrophil (NE) percentage, ultrasensitive c-reactive protein (hCRP) level, serum amyloid A (SAA) level, procalcitonin (PCT) level, erythrocyte sedimentation rate (ESR), alanine aminotransferase (ALT) level, aspartate aminotransferase (AST) level, glomerular filtration rate (eGFR) and interleukin 6 (IL-6) level, were assessed upon admission (Table 2). All six patients presented normal WBC counts, with three patients showing elevated NE percentages. Furthermore, all patients presented increased levels of hCRP, SAA, PCT, and IL-6. During the initial visit, the recorded levels ranged from 33.87–187.20 mg/L, 266.64–498.99 mg/L, 0.054–3.854 ng/mL and 26.90–61.90 pg./L, respectively. The ESR ranged from 13 to 88 mm/h, with increases noted in 4 of 6 patients. ALT levels ranged from 18 to 61 U/L, with elevated levels observed in 2 of the 6 patients. AST levels fell within the range of 16–50 U/L, and elevated levels were observed in 1 of the 6 patients. Additionally, the eGFRs ranged from 63 to 124 mL/min, with elevated levels noted in 5 of the 6 patients.

2.3 Imaging findings

Chest CT was conducted for all patients upon admission (Figure 1). Among the six patients, five had lesions affecting one lung, whereas one patient had bilateral lung involvement. The lesions were diffusely distributed ground-glass shadows with localized solid lesions, and two patients presented bronchial air signs.

2.4 Targeted next-generation sequencing

Six patients with suspected *C. psittaci* pneumonia underwent bronchoscopy to obtain BALF samples which were then sent to the KingMed Diagnostics Group Co., Ltd., Guangzhou, China for tNGS. *C. psittaci* was detected in all six cases, other pathogens were

Abbreviations: mNGS, metagenomics next-generation sequencing; tNGS, target next-generation sequencing; CT, computed tomography; hCRP, hypersensitive C-reactive protein; WBC, white blood cell; SAA, serum amyloid A; ALT, alanine aminotransferase; AST, aspartate aminotransferase; ESR, erythrocyte sedimentation rate; PCT, procalcitonin; IL-6, interleukin 6; eGFR, estimated glomerular filtration rate; C. psittaci, Chlamydia psittaci; BALF, bronchoalveolar lavage fluid; PCR, polymerase chain reaction; RPhK, reads per 100,000.

TABLE 1 Baseline characteristics and clinical manifestations of patients with *Chlamydia psittaci* pneumonia.

Case	Sex	Age (year)	Occupation	Past history	Contact history	Temperature peak (°C)	Initial symptoms	Concomitant symptoms
1	Male	63	Retired	Diabetes	No	38	Fever, headache, fear of the cold	Chest tightness and shortness of breath
2	Male	48	Company employee	Diabetes; Hypertension; Atrial fibrillation	No	40	Fever, giddy	Fatigue, poor appetite, cough
3	Female	66	Retired	Atherosclerosis of the aorta; Liver dysfunction	No	39	Fever, Fear of the cold	Fever, dry cough, fatigue, dysuria, cough
4	Female	37	Company employee	Diabetes; Hypertension	Parrot	38.5	Fever, chest distress	Cough, sore throat, headache, muscle aches
5	Female	58	Unemployed	Gastric ulcer; duodenal ulcer	Chicken	40	Fever	Muscle aches, dizziness, fatigue
6	Male	18	Student	No	Parrot	39.5	Fever	Weakness, poor stamina

TABLE 2 Laboratory results of the patients with *C. psittaci* pneumonia.

Case	WBC	NE	hCRP	SAA	PCT	ESR	ALT	AST	eGFR	IL-6
	(*10^9/L)	(%)	(mg/L)	(mg/L)	(ng/mL)	(mm/h)	(U/L)	(U/L)	(mL/min)	(pg/mL)
1	8.82	75.4	187.20	450.34	3.854	88	34	31	63	61.90
2	5.74	89.4	116.55	352.11	0.127	19	21	24	110	50.65
3	5.10	70.4	33.87	339.28	0.074	45	61	50	92	33.50
4	9.48	71.7	59.76	498.99	0.054	53	43	16	124	26.90
5	7.26	74.1	61.93	266.64	0.065	49	12	19	97	57.20
6	7.52	80.0	100.85	431.63	0.424	13	18	26	109	55.60
Ave	7.32	76.8	93.36	389.83	0.766	45	32	28	99	47.63
NR	3.5–9.5	40–75	0–3	0–10.8	0–0.046	0–26	7–40	16–50	66–143	0–7

Ave, average; NR, normal range.

identified in two of the cases (Table 3). The protocol for the tNGS assay is showed in Figure 2. After the samples were collected in the clinical laboratory, nucleic acids (DNA and RNA) were extracted, after which the tNGS target library was constructed and sequenced. The target 198 pathogens (Supplementary Table S1) of the tNGS assay include 80 bacteria, 79 viruses, 32 fungi and 7 atypical pathogens. Three amplicons (Supplementary Table S2) were designed for the detection of *C. psittaci*.

2.4.1 Material processing and nucleic acid extraction

BALF samples were collected according to the established standard procedures. For viscous BALF samples, an equal volume of 0.1 mol/L dithiothreitol (DTT) liquefaction agent was added to the collection tube; the mixture was then vortexed thoroughly and incubated at room temperature for 3–5 min to ensure complete liquefaction. Non-viscous BALF samples did not require a 0.1 mol/L DTT treatment step. A total of 13 μL of exogenous endogenous reference was added to 1.3 mL of the liquefied mix; the mixture was vortexed to ensure thorough mixing and then centrifuged at 12,000 rpm for 5 min. The supernatant was discarded, and the residual sample volume was adjusted to 500 μL by pipetting. This aliquot was transferred into the bead mill tube provided in the extraction kit, to which 50 μL of SDS was added, and the mixture was subjected to a wall-breaking apparatus for mechanical lysis. Following mechanical lysis, the samples were centrifuged at 12,000 rpm for 5 min, and 250 μL of the supernatant was used for nucleic acid extraction. The extraction was performed via the MagPure Pathogen RNA/DNA Extraction Kit (Magen Biotechnology, Guangzhou, China), following the manufacturer's protocol. The extracted nucleic acids were quantified via an Equalbit DNA HS Assay Kit (Vazyme Biotech, Nanjing, China) with an Invitrogen™ Qubit™ 4.0 (Thermo Fisher Scientific, Massachusetts, United States), and the input nucleic acids did not exceed 100 ng for library construction.

2.4.2 Library preparation and sequencing

Library preparation was performed via the RP100TM Respiratory Pathogen Microorganisms Multiplex Testing Kit (KingCreate Biotechnology, Guangzhou, China). cDNA was synthesized via reverse transcription of the extracted nucleic acids, followed by steps such as ultra-multiplex PCR amplification, PCR product purification, adapter ligation and library purification to complete library construction. The constructed libraries were pooled into homogeneous masses. The size of the library fragments was determined via the

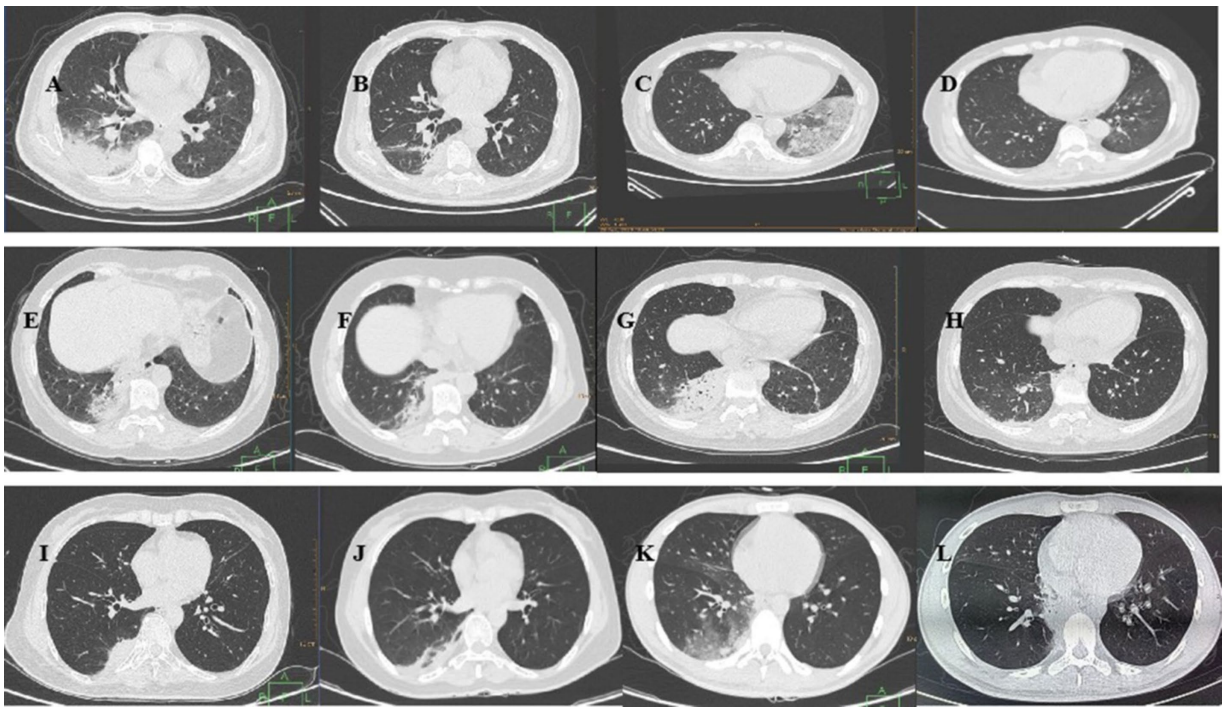

FIGURE 1
Chest CT of the six patients with *Chlamydia psittaci* pneumonia. Case 1: (A) On January 30, the lower lobe of the right lung had a large area of consolidation, and the ventilation bronchus was visible. (B) On February 10, shadow absorption in the lower lobe of the right lung was significantly reduced. Case 2: (C) On February 9, a chest CT revealed diffusely distributed ground–glass shadows with patchy solid shadows in the lower lobe of the left lung. (D) On February 28, a small number of pale shadows were observed in the lower lobe of the left lung, and the foci of intrapulmonary infection were mostly resorbed. Case 3: (E) On March 11, a solid lesion was detected in the posterior basal segment of the lower lobe of the right lung. (F) On March 18, there was a decreased lesional area and partial thinning of the posterior basal segment of the lower lobe of the right lung. Case 4: (G) On April 10, a chest CT revealed a large solid lesion in the lower lobe of the right lung and a striated shadow in the lower lobe of the left lung. (H) On April 17, chest CT revealed that the solid lesion in the original lung was largely absorbed, as was the striated shadow in the left lower lobe. Case 5: (I) On April 12, a chest CT revealed a solid shadow in the posterior basal segment of the lower lobe of the right lung. (J) On April 21, a chest CT revealed inflammatory thinning of the lower lobe of the right lung. Case 6: (K) On June 26, there were multiple ground glass shadows in the middle lobe and lower lobe of the right lung, and patchy consolidation was observed in the lower lobe of the right lung. (L) On July 8, a chest CT revealed that the inflammation in the lower lobe of the right lung had resolved.

TABLE 3 **Diagnosis and treatment of patients with *C. psittaci* pneumonia.**

Case	Anti-infective drugs used before diagnosis	Time from symptom onset to admission	Time from admission to diagnosis	Turnaround time of tNGS from sample receipt to final report	tNGS results (RPhK)	Anti-infective drugs used after diagnosis
1	Ceftazidime, Piperacillin/ Tazobactam, Moxifloxacin	7 d	4 d	12 h	*C. psittaci* 757	Moxifloxacin
2	Ceftazidime, Cefoperazone/ Sulbactam, Moxifloxacin	7 d	4 d	18 h	*C. psittaci* 2,718, *Staphylococcus aureus* 90	Moxifloxacin, Minocycline
3	Piperacillin/Tazobactam, Fosfomycin	5 d	4 d	21 h	*C. psittaci* 1735, *Cryptococcus neoformans* 97	Levofloxacin
4	Penicillin, Cefaclor	8 d	2 d	17 h	*C. psittaci* 22	Moxifloxacin
5	Cefminox, Biapenem, Minocycline	4 d	4 d	19 h	*C. psittaci* 8,048	Moxifloxacin, Minocycline
6	Cefpodoxime, Abidor, Etimicin, Amoxicillin/Clavulanic acid	4d	2d	16 h	*C. psittaci* 9,652	Moxifloxacin, Minocycline

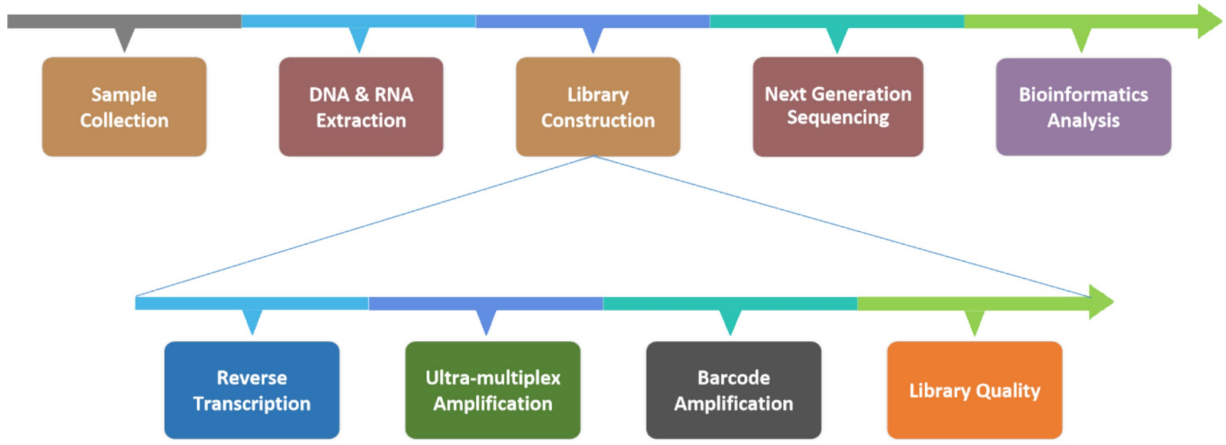

FIGURE 2
Protocol for the tNGS assay.

Qsep100 Bio-Fragment Analyzer (BiOptic, Taiwan, China). The size of the library fragments should be of from 250 to 350 bp. The qualified pooled library was diluted and denatured, 500 μL of which was subjected to the Illumina MiniSeq Platform (Illumina, California, United States) for sequencing.

2.4.3 Bioinformatics analysis

The raw sequencing read data were subjected to a quality control procedure. Fastp v0.20.1 was employed for adapter trimming and quality trimming using default parameters, followed by mapping to the reference via Bowtie2 v2.4.1 in 'very-sensitive' mode. The reference sequence used for read mapping was a database curated from various sources including the GenBank, RefSeq, and Nucleotide databases from NCBI.[1] To identify positive signals for specific pathogens, the number of mapped reads was counted and normalized to the number of reads per 100,000 (RPhK). Cases with specific RPhKs were considered positive for each sample.

2.4.4 Interpretation of tNGS results

For bacteria (excluding the *Mycobacterium tuberculosis* complex), fungi, viruses, and atypical pathogens, the criteria for positivity are as follows: (1) RPhK ≥10 when amplicon coverage is 100% and the number of amplicons is greater than 1; (2) RPhK ≥30 when 50% ≤ amplicon coverage <100% and the number of amplicons is equal to 1; (3) RPhK ≥50 when amplicon coverage is less than 50%. For *Mycobacterium tuberculosis* complex: a positive result is considered when RPhK ≥1, no other samples in the same batch detect *Mycobacterium tuberculosis*, and the retest result is ≥1. Additionally, the detected pathogens are classified according to their pathogenicity: (A) specifically pathogenic in respiratory specimens or clinically common pathogens; (B) opportunistic (conditional) pathogens in respiratory specimens that may cause infection in patients with systemic or local immunocompromise/compromise/deficiency, respiratory barrier disruption, or lower respiratory microecological imbalance; (C) the normal microecological flora of the respiratory tract, usually does not lead to infection. Finally, we need to perform a thorough assessment of the patient's clinical profile to determine the presence of a lung infection and the clinical relevance of the potential pathogen. This evaluation includes the patient's medical history, symptoms, imaging findings, tNGS results and other laboratory findings.

2.5 Treatment and outcome

The diagnosis and treatment histories of the six patients with *C. psittaci* pneumonia are shown in Table 3. All patients received empiric anti-infective therapy with two to four antibiotics sequentially prior to diagnosis, with one patient also receiving antiviral therapy using abidor. The six patients experienced a mean time of 5.8 days from symptom onset to hospital admission (range 4–8 days) and a mean time of 3.3 days from hospital admission to diagnosis (range 2–4 days). For all samples, the tNGS turnaround time from sample receipt to the final report was less than 24 h. Additional pathogens were found in the tNGS results of two patients, but were subsequently excluded by other laboratory findings and clinical manifestations. Six patients were eventually diagnosed with *C. psittaci* pneumonia. Following diagnosis, the treatment regimen was promptly adjusted to quinolone antibiotic therapy for anti-infection purposes. After 1 week of anti-infection treatment, all six patients were discharged once their body temperature normalized and their clinical symptoms significantly improved. Prior to discharge, all patients underwent chest CT examinations, which revealed the disappearance of inflammatory lesions.

3 Discussion

Studies have indicated that the global prevalence of *C. psittaci* infection in birds is as high as to 20%, with all birds posing a potential risk for *C. psittaci* infection in humans (10). In the present study, three patients had confirmed contact with birds in their prehistory. This case report suggests that since close contact with birds is one of

1 https://www.ncbi.nlm.nih.gov

the major risk factors for infection with the pathogen, it is important to elicit the patient's history in detail to provide direction for pathogen detection. All six patients in this case series experienced a fever between 38.0 and 40.0°C and symptoms such as cough, headache, sore throat, malaise and other flu-like symptoms. These signs and symptoms lack specificity and are similar to those of community-acquired pneumonia caused by various pathogens including viruses, fungi and bacteria. Owing to the diverse and atypical nature of the symptoms of psittacosis, its incidence has been significantly underestimated compared with that of other atypical pathogens (11). Our data further support previous reports on this matter.

Similarly, inflammatory biomarkers are nonspecific for *C. psittaci* pneumonia. The WBC count, PCT level, and ESR demonstrated limited diagnostic value for *C. psittaci* pneumonia in this study. hCRP, SAA, and IL-6 showed some diagnostic potential, but their elevation is not exclusive to this pathogen and lacks specificity. In summary, the laboratory findings in *C. psittaci* pneumonia are nonspecific, which aligns with the findings from previous studies (12). Chest CT scans of all patients revealed extensive lung lesions with varying degrees of pulmonary infiltrates. Unilateral lung involvement was common, but bilateral lesions were also observed, both of which were nonspecific. While *C. psittaci* infection is often linked to bird contact, it is not a prerequisite for diagnosis. Therefore, pathogen detection plays a crucial role in confirming the diagnosis of *C. psittaci* pneumonia (13).

Nonetheless, conventional methods for detecting pathogens such as culture or serological tests, are not suitable for early detection of the disease (14). Compared with traditional methods, mNGS, known for its high sensitivity and broad detection range, plays a crucial role in guiding the diagnosis and treatment of pneumonia (15). Previous studies have investigated the use of mNGS for the detection of *C. psittaci* infection, and this method has demonstrated high detection efficacy (8, 16–19). Moreover, mNGS has gained popularity for its ability to detect multiple pathogens simultaneously (20, 21). The rise in the diagnosis and reporting of psittacosis in recent years may be linked to the increased clinical utilization of mNGS (22). However, owing to its cost and long reporting time, mNGS may not be feasible in all cases and is typically used as a complementary option for challenging clinical scenarios. In China, the current price of mNGS in 2024 is US$ 500–700 per sample, whereas the price of tNGS is US$ 100–200. To control the cost of mNGS, batch processing of samples is often necessary, resulting in longer turnaround times. The tNGS test offers advantages such as fast detection speed, wide coverage and high accuracy, similar to those of the mNGS test, but incurs only a quarter of the cost (23). The time span from admission to diagnosis for the six patients in this study ranged from 2 to 4 days, which was notably shorter than the 5 to 11 days reported by Dai et al. for six patients diagnosed with *C. psittaci* pneumonia via mNGS (24). tNGS focuses on dozens to hundreds of clinically common and subrare pathogens, dramatically reducing the amount of sequencing data to 0.1 M through targeted enrichment technology, which in turn dramatically reduces the cost of testing (25). Furthermore, tNGS allows for dual-process DNA and RNA assays in a single experiment, is less impacted by prior antibiotic exposure, and excels in diagnosing rare, atypical pathogens while simultaneously identifying coinfecting pathogens. In this study, *C. psittaci* was consistently detected in all the BALF samples tested. Following prompt and targeted anti-infective treatment, the patients experienced a significant improvement in their symptoms, and imaging results revealed resolution of most of the infected foci. The use of tNGS technology in this study proved to be crucial in identifying the source of infection.

BALF is regarded as the most reliable specimen for the detection of pathogens in cases of lower respiratory tract infection (26, 27). However, BALF samples are challenging to obtain in some hospitals where bronchoscopy is unfeasible. Compared with BALF, sputum specimens are relatively easy to collect and have wider application and operability in practice. Zhenfeng Deng et al. (28) compared the detection of 209 sputum samples with tNGS and conventional microbiological testing methods, and found that the overall microbial detection rate of tNGS was significantly higher than that of conventional microbiological testing (96.7% vs. 36.8%). Their study suggests that tNGS may also be a valuable pathogenic diagnostic method for patients for whom alveolar lavage fluid collection is not appropriate.

In summary, the clinical manifestations of *C. psittaci* pneumonia can be complex, diverse and nonspecific. Clinicians should have a high index of suspicion for *C. psittaci* infection in patients with a history of live poultry exposure, who present with high fever and cough, along with significantly elevated levels of hCRP, SAA, and IL-6, slightly elevated PCT levels, normal WBC counts, and negative results of routine aetiological tests. Under the above circumstances, tNGS, as an emerging diagnostic technique for pathogenic microorganisms, is expected to be an economical, rapid and accurate method for diagnosing *C. psittaci* pneumonia.

Data availability statement

The original contributions presented in the study are included in the article/Supplementary material, further inquiries can be directed to the corresponding author.

Ethics statement

The studies involving humans were approved by the ethical review committee of the Wuhan Asia General Hospital. The studies were conducted in accordance with the local legislation and institutional requirements. The participants provided their written informed consent to participate in this study. Written informed consent was obtained from the individual(s) for the publication of any potentially identifiable images or data included in this article.

Author contributions

XY: Data curation, Writing – original draft. HF: Data curation, Writing – review & editing. WD: Data curation, Writing – review & editing. ZZ: Conceptualization, Writing – review & editing. DW: Data curation, Writing – review & editing.

Funding

The author(s) declare that financial support was received for the research, authorship, and/or publication of this article. This study was supported by the Fund of Wuhan Municipal Health Commission

(No. WX21Q29) and the Research and Innovation Fund of Wuhan Asia General Hospital (No. 2022KYCX1-B09).

Acknowledgments

We thank the Wuhan KingMed Diagnostics for their technical assistance. We also thank the colleagues in Wuhan Asia General Hospital for their contributions.

Conflict of interest

The authors declare that the research was conducted in the absence of any commercial or financial relationships that could be construed as a potential conflict of interest.

Publisher's note

Supplementary material

The Supplementary material for this article can be found online at: https://www.frontiersin.org/articles/10.3389/fmed.2024.1491838/full#supplementary-material

References

1. GBD. Global mortality associated with 33 bacterial pathogens in 2019: a systematic analysis for the global burden of disease study 2019. *Lancet (North American ed)*. (2022) 400:2221–48. doi: 10.1016/s0140-6736(22)02185-7

2. Stewardson AJ, Grayson ML. Psittacosis. *Infect Dis Clin N Am*. (2010) 24:7–25. doi: 10.1016/j.idc.2009.10.003

3. Han X, Liu X, Chen L, Wang Y, Li H, Zhou F, et al. Disease burden and prognostic factors for clinical failure in elderly community acquired pneumonia patients. *BMC Infect Dis*. (2020) 20:668. doi: 10.1186/s12879-020-05362-3

4. Torres A, Chalmers JD, Dela Cruz CS, Dominedò C, Kollef M, Martin-Loeches I, et al. Challenges in severe community-acquired pneumonia: a point-of-view review. *Intensive Care Med*. (2019) 45:159–71. doi: 10.1007/s00134-019-05519-y

5. Hogerwerf L, de Gier B, Baan B, van der Hoek W. *Chlamydia Psittaci* (psittacosis) as a cause of community-acquired pneumonia: a systematic review and Meta-analysis. *Epidemiol Infect*. (2017) 145:3096–105. doi: 10.1017/s0950268817002060

6. Missault S, de Meyst A, van Elslande J, van den Abeele AM, Steen E, van Acker J, et al. Three cases of atypical pneumonia with *Chlamydia Psittaci*: the role of laboratory vigilance in the diagnosis of psittacosis. *Pathogens*. (2023) 12:65. doi: 10.3390/pathogens12010065

7. Nieuwenhuizen AA, Dijkstra F, Notermans DW, van der Hoek W. Laboratory methods for case finding in human psittacosis outbreaks: a systematic review. *BMC Infect Dis*. (2018) 18:442. doi: 10.1186/s12879-018-3317-0

8. Tang J, Tan W, Luo L, Xu H, Li N, Li P. Application of metagenomic next-generation sequencing in the diagnosis of pneumonia caused by *Chlamydia Psittaci*. *Microbiol Spectr*. (2022) 10:e0238421. doi: 10.1128/spectrum.02384-21

9. Gu L, Liu W, Ru M, Lin J, Yu G, Ye J, et al. The application of metagenomic next-generation sequencing in diagnosing *Chlamydia Psittaci* pneumonia: a report of five cases. *BMC Pulm Med*. (2020) 20:65. doi: 10.1186/s12890-020-1098-x

10. Sukon P, Nam NH, Kittipreeya P, Sara-in A, Wawilai P, Inchuai R, et al. Global prevalence of chlamydial infections in birds: a systematic review and Meta-analysis. *Prev Vet Med*. (2021) 192:105370. doi: 10.1016/j.prevetmed.2021.105370

11. Rybarczyk J, Versteele C, Lernout T, Vanrompay D. Human psittacosis: a review with emphasis on surveillance in Belgium. *Acta Clin Belg*. (2020) 75:42–8. doi: 10.1080/17843286.2019.1590889

12. Shi Y, Chen J, Shi X, Hu J, Li H, Li X, et al. A case of *Chlamydia Psittaci* caused severe pneumonia and meningitis diagnosed by metagenome next-generation sequencing and clinical analysis: a case report and literature review. *BMC Infect Dis*. (2021) 21:621. doi: 10.1186/s12879-021-06205-5

13. Balsamo G, Maxted AM, Midla JW, Murphy JM, Wohrle R, Edling TM, et al. Compendium of measures to control *Chlamydia Psittaci* infection among humans (psittacosis) and pet birds (avian Chlamydiosis), 2017. *J Avian Med Surg*. (2017) 31:262–82. doi: 10.1647/217-265

14. Liu J, Gao Y. Tigecycline in the treatment of severe pneumonia caused by *Chlamydia Psittaci*: a case report and literature review. *Front Med (Lausanne)*. (2022) 9:1040441. doi: 10.3389/fmed.2022.1040441

15. Gu W, Miller S, Chiu CY. Clinical metagenomic next-generation sequencing for pathogen detection. *Annu Rev Pathol*. (2019) 14:319–38. doi: 10.1146/annurev-pathmechdis-012418-012751

16. Chen X, Cao K, Wei Y, Qian Y, Liang J, Dong D, et al. Metagenomic next-generation sequencing in the diagnosis of severe pneumonias caused by *Chlamydia Psittaci*. *Infection*. (2020) 48:535–42. doi: 10.1007/s15010-020-01429-0

17. Wu HH, Feng LF, Fang SY. Application of metagenomic next-generation sequencing in the diagnosis of severe pneumonia caused by *Chlamydia Psittaci*. *BMC Pulm Med*. (2021) 21:300. doi: 10.1186/s12890-021-01673-6

18. Liu K, Wu L, Chen G, Zeng D, Zhong Q, Luo L, et al. Clinical characteristics of *Chlamydia psittaci* infection diagnosed by metagenomic next-generation sequencing: a retrospective multi-center study in Fujian, China. *Infect Drug Resist*. (2024) 17:697–708. doi: 10.2147/idr.S443953

19. Teng XQ, Gong WC, Qi TT, Li GH, Qu Q, Lu Q, et al. Clinical analysis of metagenomic next-generation sequencing confirmed *Chlamydia Psittaci* pneumonia: a case series and literature review. *Infect Drug Resist*. (2021) 14:1481–92. doi: 10.2147/idr.S305790

20. Yin XW, Mao ZD, Zhang Q, Ou QX, Liu J, Shao Y, et al. Clinical metagenomic sequencing for rapid diagnosis of pneumonia and meningitis caused by *Chlamydia Psittaci*. *World J Clin Cases*. (2021) 9:7693–703. doi: 10.12998/wjcc.v9.i26.7693

21. Zhang Q, Li S, Zhou W, Zheng L, Ren Y, Dong L, et al. Application of metagenomic next-generation sequencing (Mngs) combined with rapid on-site cytological evaluation (Rosce) for the diagnosis of *Chlamydia Psittaci* pneumonia. *Int J Clin Exp Pathol*. (2021) 14:389–98. Available at: https://pubmed.ncbi.nlm.nih.gov/33936360

22. Xu W, Wang Q, Li L, Zhu B, Cai Q, Yi X, et al. Case report: metagenomic next-generation sequencing applied in diagnosing psittacosis caused by *Chlamydia Psittaci* infection. *FCIMB*. (2023) 13:1249225. doi: 10.3389/fcimb.2023.1249225

23. Li S, Tong J, Li H, Mao C, Shen W, Lei Y, et al. *L. pneumophila* infection diagnosed by tNGS in a lady with lymphadenopathy. *Infect Drug Resist*. (2023) 16:4435–42. doi: 10.2147/idr.S417495

24. Dai J, Lian X, Mo J, Li X, Mo W, Wang H, et al. Case report: a clinical case study of six patients with *Chlamydia Psittaci* pneumonia. *Front Cell Infect Microbiol*. (2023) 13:1084882. doi: 10.3389/fcimb.2023.1084882

25. Yin Y, Zhu P, Guo Y, Li Y, Chen H, Liu J, et al. Enhancing lower respiratory tract infection diagnosis: implementation and clinical assessment of multiplex Pcr-based and hybrid capture-based targeted next-generation sequencing. *EBioMedicine*. (2024) 107:105307. doi: 10.1016/j.ebiom.2024.105307

26. Liu J, Zhao F, Lu J, Xu H, Liu H, Tang X, et al. High *Mycoplasma Pneumoniae* loads and persistent long-term *Mycoplasma Pneumoniae* DNA in lower airway associated with severity of pediatric *Mycoplasma Pneumoniae* pneumonia. *BMC Infect Dis*. (2019) 19:1045. doi: 10.1186/s12879-019-4667-y

27. Li Z, Zhang Y, Zhang W, Zhang Y, Zhou S, Chen W, et al. Study on the detection and infection distribution of multidrug-resistant organisms in different specimens. *Infect Drug Resist*. (2022) 15:5945–52. doi: 10.2147/idr.S375682

28. Deng Z, Li C, Wang Y, Wu F, Liang C, Deng W, et al. Targeted next-generation sequencing for pulmonary infection diagnosis in patients unsuitable for Bronchoalveolar lavage. *Front Med (Lausanne)*. (2023) 10:1321515. doi: 10.3389/fmed.2023.1321515

frontiers | Frontiers in Medicine

TYPE Case Report
PUBLISHED 04 December 2024
DOI 10.3389/fmed.2024.1467541

OPEN ACCESS

EDITED BY
Talat Kilic,
İnönü University, Türkiye

REVIEWED BY
Gyaninder Pal Singh,
All India Institute of Medical Sciences, India
Kay Tetzlaff,
University Hospital of Tübingen, Germany

*CORRESPONDENCE
Jin Ma
✉ 103118900@qq.com

RECEIVED 20 July 2024
ACCEPTED 22 November 2024
PUBLISHED 04 December 2024

CITATION
Wu J, Yuan H, Guo Z, Feng Q and Ma J (2024) Negative pressure pulmonary edema: a case report and literature review.
Front. Med. 11:1467541.
doi: 10.3389/fmed.2024.1467541

Negative pressure pulmonary edema: a case report and literature review

Jian Wu, Hua Yuan, Zhiqiang Guo, Qiupeng Feng and Jin Ma*

Department of Emergency Medicine, Affiliated Kunshan Hospital of Jiangsu University, Kunshan, China

Negative pressure pulmonary edema (NPPE) is a form of non-cardiogenic pulmonary edema triggered by a swift increase in negative intrapleural pressure due to upper airway obstruction and represents a potential cause of acute respiratory failure. This study documents a case of NPPE post-endotracheal extubation subsequent to general anesthesia. The patient, a young female, underwent a "laparoscopy-assisted unilateral salpingectomy" under general anesthesia for an ectopic pregnancy. Immediately post-extubation, the patient exhibited a sudden decline in oxygen saturation and tachypnea. Pink frothy secretions were suctioned from the oral and nasal cavities. Swift interventions, including oxygen therapy, non-invasive ventilation, diuretics, and corticosteroids, were administered. The patient's condition was effectively managed, and after 6 days of treatment, she was discharged from the hospital following full recovery.

KEYWORDS

negative pressure pulmonary edema, non-cardiogenic pulmonary edema, post-anesthetic complication, patient prognosis, case report

Introduction

Negative pressure pulmonary edema (NPPE) represents non-cardiogenic pulmonary edema precipitated by a rapid escalation in intrathoracic negative pressure due to acute or chronic upper airway obstruction, potentially resulting in life-threatening hypoxemia (1). Since the initial documentation of NPPE (2), its incidence and mortality rates have demonstrated variability across various reports (1, 3). NPPE arises from multiple factors, with laryngospasm post-anesthetic extubation being the predominant cause. The fundamental pathophysiological mechanism entails the production of significant inspiratory pressure by patients to counteract upper airway obstruction, thereby causing a progressive rise in intrathoracic negative pressure and subsequent increase in pulmonary capillary pressure (1, 4). Clinically, NPPE manifests as severe respiratory distress, hypoxia, and expectoration of pink frothy sputum, with imaging typically indicating cardiogenic pulmonary edema (1, 5). Standard treatments encompass airway management, oxygen supplementation, positive pressure ventilation, and intensive care unit (ICU) care (3). Additionally, many patients achieve recovery through supportive care alone (1), although the use of pharmacological interventions remains a subject of debate (6). This report delineates a case of NPPE following general anesthesia and tracheal extubation, which was successfully managed in the Emergency Department of Kunshan Hospital Affiliated to Jiangsu University.

Case report

A 38-year-old married female with no previous history of cardiac disease, asthma, pneumonia, or allergies to food or medication presented with a ruptured ectopic pregnancy.

On March 9, 2022, at 19:45, she underwent an emergency laparoscopic-assisted salpingectomy under general anesthesia at a local hospital. All preoperative evaluations, including laboratory tests, imaging studies, and physical examinations, were within normal limits. The surgery concluded at 21:00 without complications, and the anesthesia was satisfactory. Intraoperative fluid replacement included 1,000 mL of normal saline. At 21:10, the endotracheal tube was removed, and the patient was alert with no complaints. At 21:15, cardiac monitoring indicated a decrease in peripheral oxygen saturation (SpO_2) to approximately 75%. The patient reported chest tightness and dyspnea, with pink frothy sputum. Physical examination revealed clear consciousness, tachypnea, and bilateral pulmonary rales. Immediate oxygen therapy via nasal cannula was started. Arterial blood gas analysis revealed: pH 7.31, partial pressure of arterial oxygen (PaO_2) 83 mmHg, partial pressure of arterial carbon dioxide ($PaCO_2$) 47 mmHg. A 12-lead electrocardiogram displayed sinus rhythm without signs of acute ischemia or infarction. After administration of 40 mg methylprednisolone and 20 mg furosemide intravenously, oxygen therapy was switched to a face mask, resulting in a SpO_2 of approximately 95%. Due to ongoing chest tightness and dyspnea, the patient was transferred to our emergency department. Upon admission, the patient reported chest tightness and mild dyspnea. Vital signs were: temperature 37.3°C, pulse 100/min, respiratory rate 26/min, blood pressure 108/72 mmHg, SpO_2 98% (with face mask oxygen). Physical examination revealed bilateral pulmonary rales, with normal cardiac and abdominal findings and no lower extremity edema. Non-invasive positive pressure ventilation was promptly initiated, along with 20 mg furosemide intravenously. Arterial blood gas analysis showed: pH 7.34, PaO_2 127 mmHg, $PaCO_2$ 47 mmHg, white blood cell count 16.47*109/l, neutrophil percentage 96.6%, hemoglobin 107 g/L, platelet count 202*109/l, D-Dimmer 1.98 mg/L fibrinogen equivalent units, N-terminal pro-B-type natriuretic peptide 86.5 pg/mL. Chest computed tomography (CT) revealed bilateral pulmonary exudative changes consistent with pulmonary edema (Figure 1). After 6 h, the patient's symptoms improved, with no dyspnea or chest pain and only a mild cough without sputum. Repeat arterial blood gas analysis showed: pH 7.46, PaO_2 285 mmHg, $PaCO_2$ 45.9 mmHg. A follow-up chest CT at 12 h demonstrated significant resolution of the bilateral pulmonary exudative changes (Figure 2). Contrast-enhanced CT showed no evidence of pulmonary embolism (Figure 3). The patient's respiratory status improved over the following days as the pulmonary edema resolved. She was discharged after 6 days without any complaints, and a final chest CT showed no significant abnormalities (Figure 4). A one-month follow-up revealed no residual symptoms.

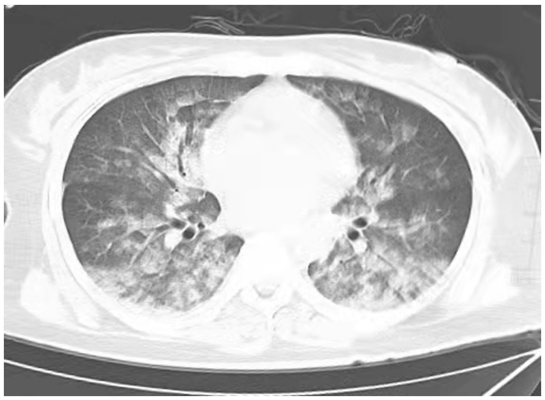

FIGURE 1
Chest CT scan depicting increase in diffuse density of the lungs, bilateral ground glass opacities, and dorsal consolidation of lungs because of pulmonary infiltrates, supporting acute pulmonary edema at 0.15 h after extubations. (Extensive, patchy ground-glass opacities and cloud-like shadows were observed in both lungs).

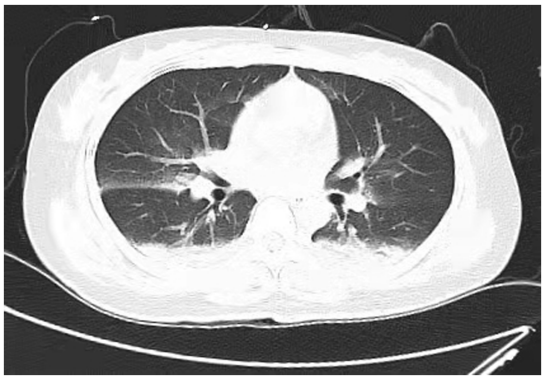

FIGURE 2
Chest CT scan depicting most of the lung infiltrates resolved at 6 h after extubations. (Scattered cloud-like opacities with blurred margins are observed in both lungs).

Discussion

First documented in 1973, NPPE has since been reported numerous times with varying incidence rates (2). The reported incidence of NPPE ranges from 0.1 to 12% (7–10), although the true incidence remains uncertain. Given the frequent occurrence of upper airway obstruction during the perioperative period, it is hypothesized that the actual incidence is likely much higher, with many cases potentially misdiagnosed or undiagnosed. Mortality rates also exhibit variability. Initially, the mortality rate for NPPE was reported to range from 11 to 40%. Subsequent literature reviews have indicated a mortality rate of 2% (11, 12). A recent systematic review of NPPE in adult otolaryngologic surgeries reported a mortality rate of 5%, identifying age and ICU admission as primary risk factors for mortality (3).

Airway obstruction from various factors is directly responsible for NPPE, with laryngospasm most frequently occurring during recovery from general anesthesia. In adults, 55% of NPPE cases are caused by perioperative laryngospasm, and studies indicate that the incidence of laryngospasm during extubation is 0.87% (1). Additionally, oropharyngeal surgery, obstructive respiratory distress, obesity, and laryngeal mask displacement significantly contribute to NPPE. Research involving 86,561 patients (13) revealed that active smokers and those undergoing endotracheal intubation for general anesthesia face a significantly higher risk of developing NPPE post-extubation in the operating room. NPPE has also been reported following extubation after general anesthesia for surgeries beyond the oropharyngeal region. This case involves a patient who underwent a laparoscopic-assisted unilateral salpingectomy under general

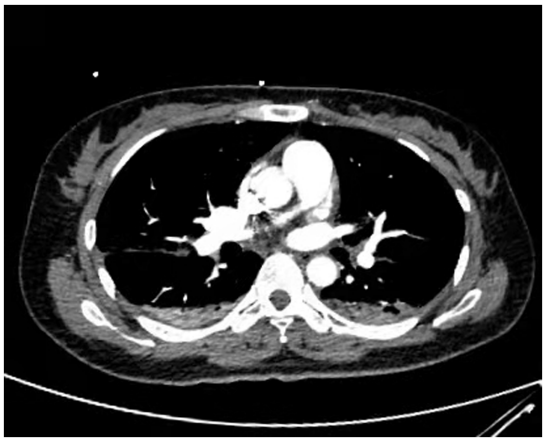

FIGURE 3
Contrast-enhanced CT showed no evidence of pulmonary embolism. (Pulmonary embolism angiography reveals two areas of pneumonia-related changes and extensive alveolar pulmonary edema).

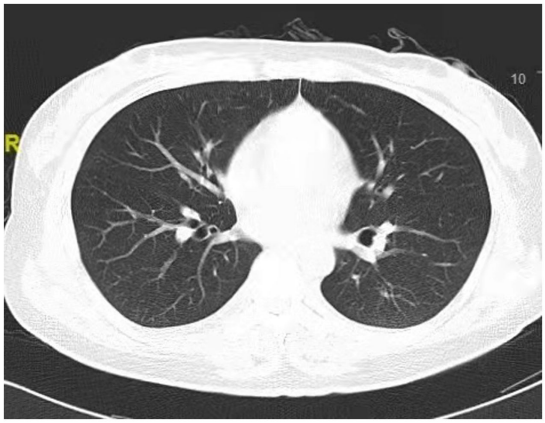

FIGURE 4
Chest CT scan depicting clear lung fields, indicating normal performance of the lungs at 6 days after extubations.

anesthesia. We believe that the cause of NPPE in this patient was likely laryngospasm following general anesthesia. Laryngospasm is the most common cause of NPPE, accounting for 55% of cases. In this instance, the patient was a young, previously healthy woman with no history of lung disease who experienced oxygen desaturation and dyspnea after extubation post-surgery, further supporting laryngospasm as the likely trigger.

The pathogenesis of NPPE is primarily attributed to the generation of substantial negative intrapleural pressure. In adults, inspiratory efforts against a closed upper airway can generate negative pressures up to approximately −140 mmHg (4). This degree of negative pressure is sufficient to significantly enhance venous return to the right heart and cause the interventricular septum to shift towards the left ventricle, thereby decreasing stroke volume. Concurrently, as venous return increases, more blood enters the pulmonary circulation, resulting in elevated hydrostatic pressure within the pulmonary circulation. The pulmonary microvascular system promotes fluid extravasation from the vascular bed into the interstitium (14). The formation and resolution of NPPE pulmonary edema are linked to the low protein concentration in the pulmonary edema fluid of most NPPE patients, suggesting that elevated hydrostatic pressure is responsible for NPPE development. Although negative intrathoracic pressure is the primary factor in NPPE pathogenesis, other factors are also significant. Ventilatory efforts against an obstructed airway ultimately lead to hypoxia and acidosis, which elevate pulmonary vascular resistance and adversely affect alveolar-capillary integrity. Moreover, significant inspiratory efforts trigger a high adrenergic response, further increasing pulmonary vascular resistance and directly promoting blood redistribution from the systemic to the pulmonary circulation (15).

Respiratory distress, hypoxia, cyanosis, pink frothy sputum, and hemoptysis are typical symptoms and signs of NPPE. Key diagnostic criteria include: (1) a history of the upper airway obstruction; (2) sudden onset of respiratory difficulty, hypoxia, and hypercapnia within minutes to hours after obstruction relief; (3) presence of pink frothy sputum; (4) radiological findings: X-ray showing diffusely increased density, widened vascular shadows, and bilateral, central alveolar and interstitial infiltrates. Given its similarity to aspiration pneumonia during anesthesia and other causes of pulmonary edema, clinicians must be vigilant in differential diagnosis. When the diagnosis is uncertain, it is crucial to exclude causes such as cardiogenic pulmonary edema, minor reflux aspiration, acute respiratory distress syndrome, allergic pulmonary edema, and neurogenic pulmonary edema. In this case, the patient presented with a clinical manifestation of coughing up frothy pink sputum, which can easily lead clinicians to misdiagnose NPPE as left heart failure, cardiogenic pulmonary edema, or aspiration pneumonia in an emergency, thereby delaying optimal treatment. In particular, imaging results are useful in differentiating NPPE from cardiogenic pulmonary edema (5). NPPE typically presents with prominent bilateral perihilar alveolar infiltrates, whereas cardiogenic pulmonary edema follows a more interstitial pattern and usually shows evident blood flow diversion to the lung apices (1). With the rapid advancement of bedside ultrasound technology, Zhang et al. (16) reported a case of rapid diagnosis and treatment of NPPE in a 35-year-old female patient using bedside ultrasound. This patient had a history of general anesthesia for a ruptured ectopic pregnancy. Considering symptoms such as rapid breathing and decreased oxygen saturation and differentiating from pulmonary embolism, enhanced CT showed no significant signs of pulmonary embolism. Given the patient's profile as a young female without underlying cardiac disease, the condition's changes occurring 5 min after extubation, and relevant auxiliary examination results, acute NPPE was diagnosed. Furthermore, acute NPPE can manifest as quickly as within seconds or as late as 4 h after the relief of airway obstruction.

The management of NPPE is primarily aimed at symptomatic relief, focusing on enhancing oxygenation and reducing pulmonary edema. The severity, progression, and outcome of NPPE are determined by the duration of obstruction. The decision to reintubate is crucially dependent on the ability to maintain effective oxygenation. Treatment involves vigilant monitoring, ensuring airway patency, oxygen therapy, and respiratory support through endotracheal intubation or non-invasive ventilation (1, 17, 18). In the presented case, the patient did not exhibit significant airway obstruction upon admission, and the condition had markedly improved with

non-invasive ventilation prior to hospitalization, thereby avoiding endotracheal intubation. The underlying pathology causing pulmonary edema must be considered when contemplating intubation. When mechanical ventilation is necessary, lung-protective ventilation strategies are advised, even for patients without acute respiratory distress syndrome (1). While diuretics are standard for cardiogenic pulmonary edema, they play a secondary role in NPPE management. Some studies suggest that the use of furosemide should be etiology-dependent (1, 4), whereas others argue that its use is controversial due to the risks of hypoperfusion and hypovolemia. However, in this instance, the patient's symptoms significantly improved following furosemide administration. Additionally, most NPPE cases can be effectively managed with ventilatory support, such as continuous positive airway pressure, bilevel positive airway pressure, or mechanical ventilation. In severe cases, venovenous extracorporeal membrane oxygenation has been successfully employed (19).

In conclusion, NPPE is recognized as a life-threatening post-anesthetic complication, necessitating prevention and early recognition as essential components of management. Early diagnosis and timely treatment result in improved outcomes. Perioperative patients should be vigilantly monitored for NPPE, particularly in the absence of a prior cardiac history or cardiovascular risk factors. In instances where acute pulmonary edema develops during recovery from general anesthesia, NPPE should be highly suspected. Additionally, immediate and assertive intervention is critical for enhancing patient prognosis.

Data availability statement

The raw data supporting the conclusions of this article will be made available by the authors, without undue reservation.

Ethics statement

The studies involving humans were approved by the Medical Ethics Committee of Affiliated Kunshang Hospital of Jiangsu University. The studies were conducted in accordance with the local legislation and institutional requirements. The participants provided their written informed consent to participate in this study. Written informed consent was obtained from the individual(s) for the publication of any potentially identifiable images or data included in this article.

Author contributions

JW: Conceptualization, Investigation, Resources, Writing – original draft, Writing – review & editing. HY: Conceptualization, Data curation, Formal analysis, Software, Supervision, Validation, Writing – original draft. ZG: Formal analysis, Methodology, Software, Supervision, Validation, Writing – original draft. QF: Data curation, Formal analysis, Investigation, Methodology, Software, Writing – review & editing. JM: Conceptualization, Funding acquisition, Investigation, Project administration, Writing – original draft, Writing – review & editing.

Funding

The author(s) declare that financial support was received for the research, authorship, and/or publication of this article. This work was supported by the Kunshan Social Development Science and Technology Project (KSZ2169).

Conflict of interest

The authors declare that the research was conducted in the absence of any commercial or financial relationships that could be construed as a potential conflict of interest.

Publisher's note

References

1. Bhattacharya M, Kallet RH, Ware LB, Matthay MA. Negative-pressure pulmonary edema. *Chest*. (2016) 150:927–33. doi: 10.1016/j.chest.2016.03.043

2. Capitanio MA, Kirkpatrick JA. Obstructions of the upper airway in children as reflected on the chest radiograph. *Radiology*. (1973) 107:159–61. doi: 10.1148/107.1.159

3. Din-Lovinescu C, Trivedi U, Zhang K, Barinsky GL, Grube JG, Eloy JA, et al. Systematic review of negative pressure pulmonary edema in otolaryngology procedures. *Ann Otol Rhinol Laryngol*. (2021) 130:245–53. doi: 10.1177/0003489420938817

4. Lemyze M, Mallat J. Understanding negative pressure pulmonary edema. *Intensive Care Med*. (2014) 40:1140–3. doi: 10.1007/s00134-014-3307-7

5. Holzgreve A, Fabritius MP, Conter P. CT findings in negative pressure pulmonary edema. *Diagnostics*. (2020) 10:749. doi: 10.3390/diagnostics10100749

6. Liu R, Wang J, Zhao G, Su Z. Negative pressure pulmonary edema after general anesthesia: a case report and literature review. *Medicine*. (2019) 98:e15389. doi: 10.1097/MD.0000000000015389

7. Tami TA, Chu F, Wildes TO, Kaplan M. Pulmonary edema and acute upper airway obstruction. *Laryngoscope*. (1986) 96:506–9. doi: 10.1288/00005537-198605000-00007

8. Park H, Nam S, Jang YJ, Ku S, Choi SS. Negative pressure pulmonary edema in a patient undergoing open rhinoplasty: a case report. *Medicine*. (2021) 100:e24240. doi: 10.1097/MD.0000000000024240

9. Tebay A, Bouti K, Tebay N. Negative pressure pulmonary edema following a cholecystectomy—a case report. *Rev Pneumol Clin*. (2017) 73:267–71. doi: 10.1016/j.pneumo.2017.08.006

10. Xiong J, Sun Y. Negative pressure pulmonary edema: a case report. *BMC Anesthesiol*. (2019) 19:63. doi: 10.1186/s12871-019-0730-x

11. Goldenberg JD, Portugal LG, Wenig BL, Weingarten RT. Negative-pressure pulmonary edema in the otolaryngology patient. *Otolaryngol Head Neck Surg*. (1997) 117:62–6. doi: 10.1016/s0194-5998(97)70208-0

12. Westreich R, Sampson I, Shaari CM, Lawson W. Negative-pressure pulmonary edema after routine septorhinoplasty: discussion of pathophysiology, treatment, and prevention. *Arch Facial Plast Surg*. (2006) 8:8–15. doi: 10.1001/archfaci.8.1.8

13. Tsai PH, Wang JH, Huang SC, Lin YK, Lam CF. Characterizing post-extubation negative pressure pulmonary edema in the operating room-a retrospective matched case-control study. *Perioper Med*. (2018) 7:28. doi: 10.1186/s13741-018-0107-6

14. Albergaria VF, Soares CM, Araújo Rde M, de Mendonça WL. Negative-pressure pulmonary edema after transsphenoidal hypophysectomy. Case report. *Rev Bras Anestesiol*. (2008) 58:391–6. doi: 10.1590/s0034-70942008000400009

15. Guru PK, Agarwal A, Pimentel M, McLaughlin DC, Bansal V. Postoperative pulmonary edema conundrum: a case of negative pressure pulmonary edema. *Case Rep Crit Care*. (2018) 2018:1584134–3. doi: 10.1155/2018/1584134

16. Zhang G, Huang X, Wan Q, Zhang L. Ultrasound guiding the rapid diagnosis and treatment of negative pressure pulmonary edema: a case report. *Asian J Surg*. (2020) 43:1047–8. doi: 10.1016/j.asjsur.2020.07.004

17. Lang SA, Duncan PG, Shephard DA, Ha HC. Pulmonary oedema associated with airway obstruction. *Can J Anaesth*. (1990) 37:210–8. doi: 10.1007/BF03005472

18. Ma J, Liu T, Wang Q, Xia X, Guo Z, Feng Q, et al. Negative pressure pulmonary edema (review). *Exp Ther Med*. (2023) 26:455. doi: 10.3892/etm.2023.12154

19. Koide M, Kitada T, Kogure M, Fukui K, Sogabe K, Kato Y, et al. Extraordinary delayed-onset negative pressure pulmonary hemorrhage resulting in cardiac arrest after general anesthesia for vocal cord polypectomy. *Case Rep Crit Care*. (2020) 2020:8830935–5. doi: 10.1155/2020/8830935

frontiers | Frontiers in Medicine

TYPE Case Report
PUBLISHED 17 December 2024
DOI 10.3389/fmed.2024.1420414

OPEN ACCESS

EDITED BY
Giuseppe Fiorentino,
Colli Hospital, Italy

REVIEWED BY
Eva Revilla-López,
Vall d'Hebron University Hospital, Spain
Miguel Angel Fernandez-Vaquero,
Clinica Universidad de Navarra, Spain

*CORRESPONDENCE
Rongjie Shi
✉ 13887215123@163.com

†These authors have contributed equally to this work

RECEIVED 09 July 2024
ACCEPTED 29 November 2024
PUBLISHED 17 December 2024

CITATION
Zi Y, Shi Y and Shi R (2024) Abdominal lymphangioleiomyomatosis in a man presenting with gastrointestinal hemorrhage as the first manifestation: a case report. *Front. Med.* 11:1420414. doi: 10.3389/fmed.2024.1420414

Abdominal lymphangioleiomyomatosis in a man presenting with gastrointestinal hemorrhage as the first manifestation: a case report

Ying Zi[1†], Yuchen Shi[2†] and Rongjie Shi[3*]

[1]The First Affiliated Hospital of Dali University, Dali, Yunnan, China, [2]The First Affiliated Hospital of Kunming Medical University, Kunming, Yunnan, China, [3]Department of Gastroenterology, The First Affiliated Hospital of Dali University, Dali, Yunnan, China

Lymphangioleiomyomatosis (LAM) is a rare, low-grade malignant condition that typically affects women of childbearing age and primarily involves the lungs. While cases involving males and affecting the gastrointestinal tract are exceedingly uncommon. This report discusses an unusual case of abdominal LAM in a male patient with gastrointestinal hemorrhage. The patient, a 70-year-old man, had been experiencing recurrent abdominal pain, occasional black stools, dizziness, and fatigue for over a month before being admitted to the hospital. Diagnostic electronic gastroscopy identified ulcers in the gastric and duodenal bulb with hemorrhage. An abdominal CT scan revealed multiple cystic foci in the retroperitoneum and mesentery, but no masses were found. Despite receiving medical treatment, the patient continued to have black stools and eventually underwent laparoscopic distal subtotal gastrectomy. The pathological results of the excised distal gastric specimens showed LAM-like lesions in the submucosal layer of the pylorus, mesentery of the side of the lesser curvature of the stomach, and small intestine, leading to a diagnosis of abdominal LAM. However, even after the surgery, the patient still experienced recurrent black stools and developed new symptoms of chest tightness and shortness of breath. A follow-up chest CT revealed bilateral pleural effusion and multiple lung cysts, indicating a worsening condition. The patient was then prescribed oral Sirolimus, which resulted in an improvement in symptoms, including black stool, chest tightness, and shortness of breath. This case report provides a detailed account of the progression of an unusual gastrointestinal LAM case and suggests that a combination of surgery and Sirolimus may be effective in managing the condition.

KEYWORDS

lymphangioleiomyomatosis, gastrointestinal hemorrhage, abdomen, male, case report

Introduction

Lymphangioleiomyomatosis (LAM) was first discovered and identified by Burrell in 1937 (1), and the first case reported in the Chinese mainland was in 1983 (2). LAM is a rare condition characterized by abnormal proliferation of smooth muscle cells around the lymphatic ducts, classified under the family of PEComas (3). The most common site of LAM is the lung, accounting for about 90% of all cases. Pulmonary LAM can cause progressive cystic changes in the lung, pneumothorax, chylothorax, and can lead to respiratory failure and ultimately death (4). LAM in the abdomen is generally rare, and gastrointestinal LAM is even rarer. In these cases, smooth muscle cell proliferation within the lymphatic system of the gastrointestinal tract forms tumor masses in the corresponding bowel wall areas (5). These lesions, typically multinodular in the gastrointestinal tract, often manifest as bleeding. Additionally, according to the published literature, gastrointestinal lymphangiomatosis mainly presents with non-specific chronic symptoms, such as abdominal pain, weakness, weight loss, abdominal distension, and, rarely, pitting edema due to hypoproteinemia, gastrointestinal bleeding, or obstruction (6). It is also noted that abdominal LAM can form large masses, but primary abdominal LAM typically shows non-specific imaging features apart from space-occupying lesions (7). This report highlights a rare instance of primary abdominal LAM in a male patient characterized by gastrointestinal bleeding to enhance the understanding of its clinical diagnosis and treatment.

Case presentation

Clinical history and the results of auxiliary examination in the first admission

A 70-year-old man was admitted to the hospital on 24 April 2023, with a month-long history of recurrent abdominal pain, intermittent black stools, dizziness, and fatigue. Upon admission, his physical examination showed a body temperature of 36.9°C, a heart rate of 80 beats per min, a respiratory rate of 20 breaths per min, and a blood pressure of 96/57 mm Hg. He exhibited noticeable pallor in his skin, mucous membranes, and eyelid conjunctiva, indicative of anemia. The patient appeared mentally weak. His lung examination revealed clear respiratory sounds bilaterally, and his heart rhythm was regular. His abdomen was soft and flat, with mild tenderness and active bowel sounds throughout, but there was no rebound pain, muscle tension, or shifting dullness. He had not experienced significant weight changes or body swelling since the onset of his symptoms. Prior to this illness, the patient has a 50-year smoking history and smoked about 20 cigarettes per day, besides this, he had been in good health with no history of diseases or medications and no known genetic disorders in his family history.

We performed several additional tests to evaluate the patient's overall health. His blood routine indicated moderate anemia with a red blood cell (RBC) count of 3.42×10^{12}/L while hemoglobin (HGB) was 65 g/L. The fecal occult blood test came back strongly positive, indicating possible hemorrhage. However, the digital rectal examination did not reveal any abnormalities, and tumor markers were negative. An abdominal CT scan showed multiple cystic hypodense shadows of varying sizes in the retroperitoneum and mesentery, with the largest measuring 4.2 cm × 3.4 cm and a density of 10.8 HU (Figure 1A), located in the right upper quadrant. This lesion did not show significant enhancement on the contrast scan, remaining at a density of 10.9 HU (Figure 1B). The chest CT revealed increased transparency in the lung fields, with scattered cystic translucent shadows in both lungs (Figure 1C). Electronic gastroscopy showed multiple ulcerative lesions in the gastric antrum, covered with white fur and surrounded by congested, bleeding mucosa, each measuring about 0.5 cm in diameter. The anterior and posterior walls of the duodenal bulb showed mucosal erosion, and a small, actively bleeding ulcer was found at the center of this erosion, with a congested bulge on the side of the stomach's lesser curvature (Figures 2A, B). Biopsy samples from the gastric antrum and duodenal bulb revealed mild chronic inflammation in the gastric antrum mucosa with abundant inflammatory exudates. The duodenal bulb's lamina propria showed congestion with infiltrations of lymphocytes, plasma cells, and medium neutrophils. Based on these histopathological findings, the patient was diagnosed with chronic gastritis (specifically, chronic superficial gastritis in the zero phase), as well as stomach and duodenal ulcers with bleeding (specifically, superficial ulcers in the active stage).

Based on his diagnosis, the patient received treatments aimed at managing his symptoms. These included suppressing gastric acid with Omeprazole (40 mg daily via intravenous drip), protecting the mucosa through oral administration of L-Glutamine and Sodium Gualenate Granules (0.67 g daily), stopping bleeding with Octreotide (0.6 mg daily, administered intravenously at 2.5 ml/h) and Carbazochrome Sodium Sulfonate Injection (80 mg daily via intravenous drip), and replenishing blood volume with red blood cell suspension through intravenous drip. Despite these interventions, the patient continued to experience black stools, indicating ongoing active bleeding in the digestive tract. A follow-up blood test on 15 May 2023, showed a RBC count of 4.34×10^{12}/L and a hemoglobin level of 94 g/L. A second gastroscopy revealed that the ulcerative lesions in the gastric antrum had enlarged, with the mucosa showing an orange and red coloration and signs of active bleeding. Additionally, the area from the duodenal bulb to the descending part was covered with mucosal bulges, and the surface was infused with blood (Figures 2C, D).

After careful consideration of the patient's ongoing active gastrointestinal bleeding and lack of response to conservative medical treatments, it was determined that surgery was necessary. Prior to the surgery, thorough evaluations were conducted to rule out any contraindications, including coagulation function tests, infectious disease screenings, and reviews of the previous surgical history and drug allergies. Consequently, a laparoscopic distal subtotal gastrectomy was performed on 16 May 2023. During the surgery, a bloody mass was observed in the gastric antrum, along with multiple small, unruptured bloody masses in the mesentery. The procedure involved clamping and cutting the duodenum 3 cm below the pylorus and carefully dissecting the associated arteries and veins. The lesser curvature of the stomach was mobilized upstream, and approximately one-third of the greater curvature was dissociated from left to right. The distal two-thirds of the stomach were then clamped and severed. To maintain digestive continuity, the jejunum was anastomosed laterally to the posterior wall of the stomach.

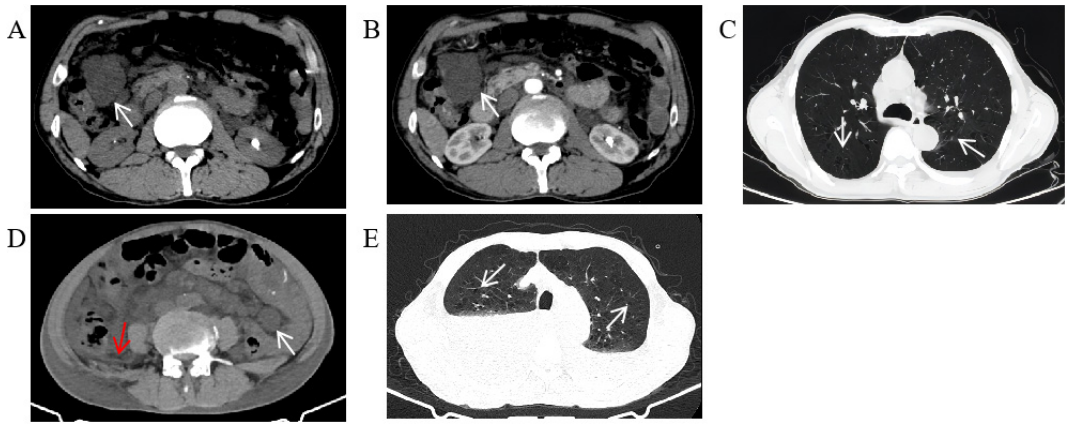

FIGURE 1
Abdominal and chest CT. **(A)** There were multiple round cystic hypodense shadows of different sizes in the retroperitoneum and mesentery. The white arrow points to the largest cystic hypodense shadows located in the right upper quadrant, about 4.2 cm × 3.4 cm in size and 10.8 Hu of density. **(B)** The largest cystic hypodense shadows saw no obvious enhancement on the contrast scan, 10.9 Hu of density. **(C)** The transparency of the two lung fields increased. The two lungs were scattered with cystic translucent shadows whose diameters were between 0.3 and 1.0 cm. **(D)** There were multiple round cystic hypodense shadows of different sizes in the retroperitoneum and mesentery. The white arrow points to the largest cystic hypodense shadows located in the left lower quadrant, about 2.5 cm × 2.1 cm in size and 10.3 Hu of density. A small amount of abdominopelvic effusion can be seen as the red arrow points. **(E)** The transparency of the two lung fields increased, and the two lungs were scattered with cystic translucent shadows as the arrow points. Bilateral pleural effusion can be seen with high-density liquid level.

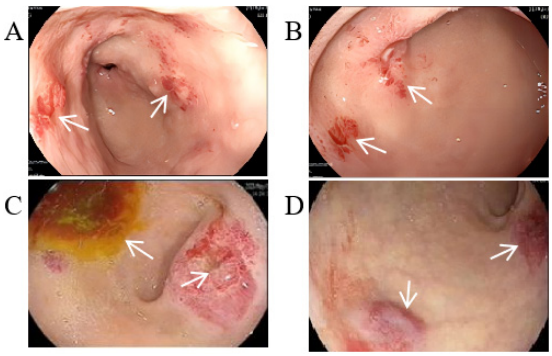

FIGURE 2
Gastroscopic image. **(A)** Multiple ulcerative lesions in the gastric antrum. **(B)** Mucosal erosion ulcer in the duodenal bulb. **(C)** Ulcerative lesions with enlarged surface and active bleeding. **(D)** Mucosal bulge in the duodenal bulb with surface congestion.

The excised distal gastric and small intestinal mucosa were sent for examination. Visible to the naked eye were nodular lesions of various sizes in the excised tissue, with the largest having a diameter of 1.6 cm. Pathological biopsy analysis revealed LAM-like lesions in the submucosal layer of the pylorus, the mesentery adjacent to the lesser curvature of the stomach, and the small intestine (Figure 3). These lesions were determined to be T1NxM0 in grade and phase II in stage. Immunohistochemical results of duodenal tissue showed Ki67 (+5%), D2-40 (+), CD34 (+), Desmin (+), SMA (+), S-100 (−), Melan-A (−), HMB-45 (−) (Figure 4). Based on a thorough evaluation of the abdominal CT findings and the pathology biopsy results, the patient was definitively diagnosed with abdominal LAM. He showed signs of improvement post-surgery and was discharged from the hospital on 30 May 2023.

Clinical history and the results of auxiliary examination in the second admission

On 3 October 2023, the patient was readmitted and reported experiencing chest tightness, and shortness of breath, besides the symptoms from his last hospitalization. The physical examination revealed persistent pallor in his skin, mucous membranes, and eyelid conjunctiva, indicating anemia. He still appeared mentally weak. Upon examination of the lungs, decreased respiratory sounds were noted, particularly in the right lung. His heart rhythm was regular, and scars from previous surgery were visible on his abdomen. He also reported mild tenderness in the epigastrium, especially below the xiphoid process. Active bowel sounds were present throughout the abdomen, and there were no signs of rebound pain or muscle tension, and shifting dullness was negative. He had gained 2 kg since his last discharge. Blood tests indicated severe anemia, with a RBC count of 2.48 × 10^{12}/L and HGB of 48 g/L. An abdominal CT scan showed multiple round, cystic, hypodense shadows of varying sizes in the retroperitoneum and mesentery, with the largest measuring 2.5 cm × 2.1 cm and a density of 10.3 HU, located in the left lower quadrant and a small amount of abdominopelvic effusion was also present (Figure 1D). A chest CT scan revealed increased lung field transparency, cystic translucent shadows scattered in both lungs, and bilateral pleural effusion (Figure 1E). To address the pleural effusion, closed drainage was performed on both sides of the patients' chest, draining mild bloody chylous fluid. Cytopathological analysis confirmed that the fluid did not contain any LAM cells or other malignant tumor cells. Due to the patients' shortness of breath, he was unable to cooperate with pulmonary function test. A peripheral blood whole-exome gene sequencing was performed, which did not reveal any pathogenic or potentially pathogenic gene variants related to the patient's clinical presentation. However, other potential pathogenic genes, including PEX7 and SLC26A4,

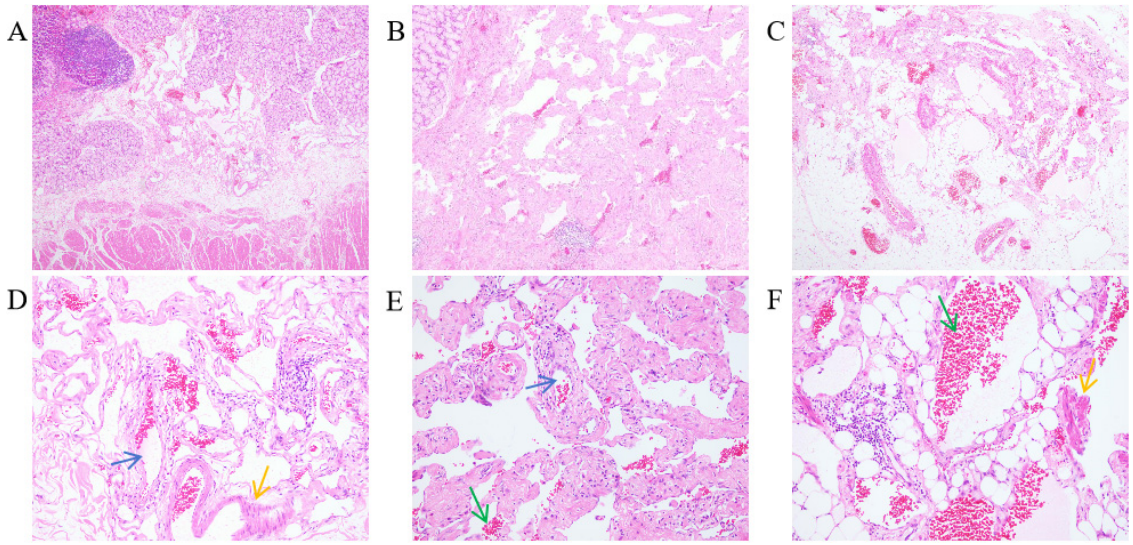

FIGURE 3
The mesentery of the duodenum and pylorus and the mesentery showed dilated lacuna-like structures (the blue arrow points) of varying sizes, covered with a single layer of flat epithelium. Pink lymphatic fluid was found in the lumen (the green arrow points). Proliferative smooth muscle cells (the yellow arrow points) around the focal lumen were observed. HE stains; **(A–C)** are 40× magnification; **(D–F)** are 200× magnification. **(A)** Submucosal layer of the pylorus. **(B)** Mesentery of the side of the lesser curvature of the stomach. **(C)** Mesentery of the small intestine. **(D)** Dilated lymphatic vessels and proliferative smooth muscle cells in the submucosal layer of the pylorus. **(E)** Dilated lymphatic vessels and lymphatic fluid in the mesentery of the side of the lesser curvature of the stomach. **(F)** Proliferative smooth muscle cells and lymphatic fluid in the mesentery of the small intestine.

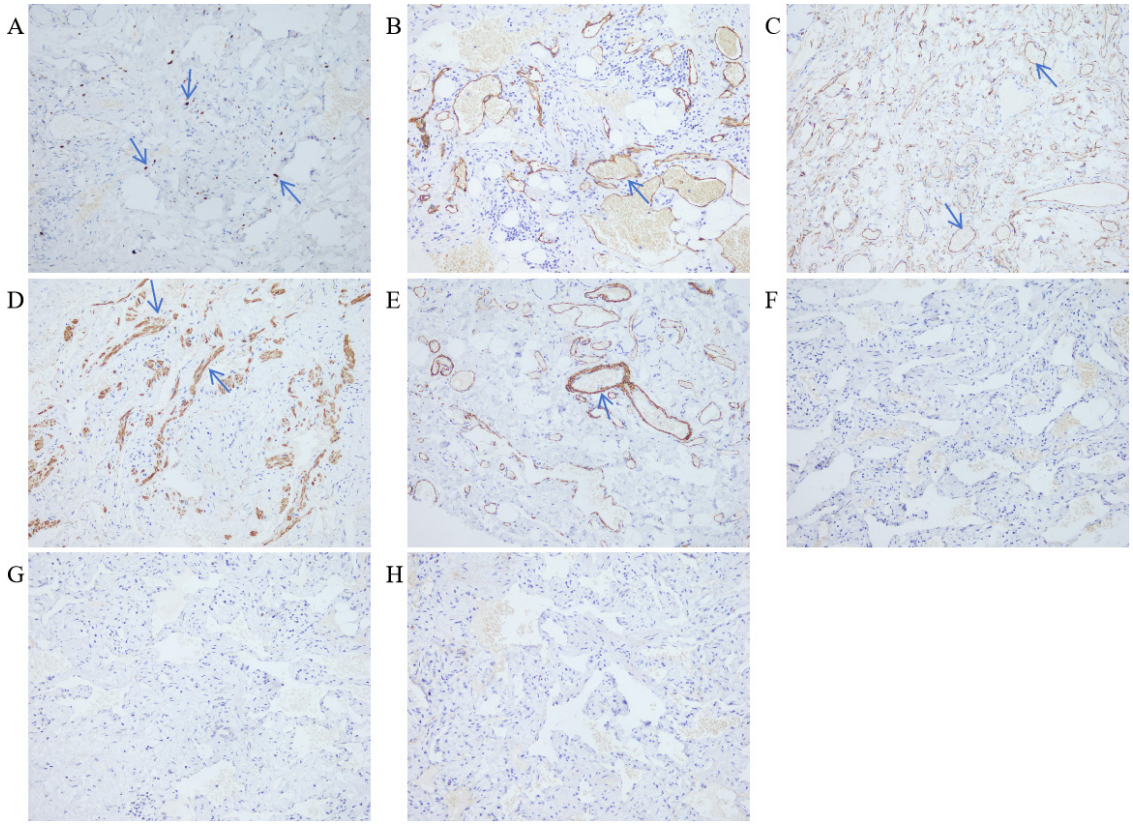

FIGURE 4
Immunohistochemistry of duodenal tissue. LDP staining; 200× magnification. **(A)** Ki67 (+5%). **(B)** Lymphatic vessel D2-40 (+). **(C)** Blood vessels CD34 (+). **(D)** Smooth muscle of the tube wall Desmin (+). **(E)** Smooth muscle of the tube wall SMA (+). **(F)** HMB-45 (–). **(G)** Melan-A (–). **(H)** S-100 (–).

10.3389/fmed.2024.1420414

TABLE 1 Results of whole exome gene detection.

Gene	Population frequency	Pathogenicity classification	Related diseases
PEX7	0.0007	Pathogenicity	1. Peroxisome biosynthesis disorder type 9B 2. Proximal limb punctiform chondrodysplasia type 1
SLC26A4	0.005	Pathogenicity	1. Often cryptogenetic deafness type 4 with enlarged vestibular aqueduct 2. Pendred syndrome
HMGCS2	0	Unclear meaning	3-hydroxy-3-methylglutaryl CoA synthetase type 2 deficiency
PRKCD	0	Unclear meaning	Autoimmune lymphocyte proliferation syndrome type III
MCMC4	0.002	Unclear meaning	Immune deficiency type 54

HMGCS2, PRKCD and MCMC4 of unknown significance were identified (Table 1). After a multi-disciplinary discussion and patient briefing, a new treatment plan was initiated on 18 October 2023, with the patient taking 1 mg of Sirolimus orally daily. During both hospital stays, the patient did not receive any adjuvant treatments, such as chemotherapy or radiotherapy, apart from the aforementioned methods. Following the initiation of Sirolimus treatment, the patient's symptoms, including black stool, chest tightness, and shortness of breath, improved, and he was discharged on 23 October 2023. Monthly hospital visits were scheduled for the first three months post-discharge to monitor treatment efficacy, followed by monthly follow-up calls. Throughout the Sirolimus treatment period, his condition remained stable, without recurrence or drug-related side effects, such as mucositis, canker sores, and diarrhea.

Discussion

Lymphangioleiomyomatosis (LAM) is a rare tumor caused by the proliferation of smooth muscle cells around lymph nodes and interstitial lymphatics (7). It is a slowly progressive, systemic disease associated with cystic lung destruction, abdominal tumors, and chylous fluid accumulations due to infiltration of neoplastic LAM cells. Women of childbearing age are more likely to be affected, and most cases manifest as pulmonary lesions (8). The prevalence of LAM is extremely low, with only 3.4–7.8 cases per 1 million females reported in the literature (9). While there have been documented instances of gastrointestinal LAM, cases involving male patients remain exceedingly rare. One case has been reported in the literature about a young man with diffuse abdominal LAM who experienced symptoms for six months, including vomiting, weight loss, intermittent abdominal pain, bloating, and constipation (6). Goh et al. (5) documented a case of a female with LAM affecting the ascending, transverse, and descending colon, primarily presenting with constipation. Song et al. (10) reported a case of a young man diagnosed with ascending colon LAM who manifested with intermittent right upper quadrant pain. Despite these similar cases, instances of LAM involving the alimentary canal and manifesting as gastrointestinal bleeding are seldom reported in the existing literature. This study provides a comprehensive account of the presentation and progression of this uncommon gastrointestinal LAM in males, which can help raise awareness among clinicians.

Most scholars believe that LAM is caused by gene mutation, specifically in the tuberous sclerosis complex (TSC) gene. There are two forms of LAM: Tuberous sclerosis LAM (TSC-LAM) and sporadic LAM (S-LAM) (11). Among the LAM patients, S-LAM accounts for about 85% of LAM cases, while TSC-LAM accounts for 15%. Both forms involve mutations in the TSC gene (12), including mutations of TSC1 and TSC2. The TSC gene is a tumor suppressor gene located on autosomes and is widely expressed in the body. When this gene is mutated in LAM patients, it loses its regulatory function of the TSC gene, leading to overactivation of the mammalian target of rapamycin (mTOR) (13), a key regulator of cell growth and proliferation (14). This results in the abnormal proliferation of smooth muscle cells, also known as LAM cells. In this case report, a whole exome gene test was performed, but no LAM-associated gene mutations were detected. Mutations in PEX7 and SLC26A4 were identified, but these are associated with different diseases. The significance of mutations in HMGCS2, PRKCD, and MCMC4 is still unclear. While the theory that TSC gene mutations cause LAM is primarily based on studies of female pulmonary LAM (PLAM), it does not rule out the potential role of other gene mutations in male LAM. In this patient, TSC gene mutation was not detected, allowing us to preliminarily exclude it as a cause. The mutated genes that were detected, their known clinical significance, and potential related diseases are listed in Table 1. Further research is needed to determine if these gene mutations are linked to the onset of this patient's condition.

Diagnosing LAM presents challenges. Typically, patients with LAM do not exhibit specific symptoms in the early stages, and many of their symptoms resemble those found in other lung conditions, such as asthma, chronic obstructive pulmonary disease (COPD), and bronchitis. The two most frequent clinical presentations of LAM are recurrent pneumothoraces and dyspnea (15). Respiratory symptoms are the first clinical presentation in most patients diagnosed with LAM (15–17). Less commonly, LAM may present with a chylous effusion, an abdominal or pelvic mass, coughing up blood, abdominal bleeding due to a renal angiomyolipoma, or as an incidental finding of lung cysts and abdominal tumors (4, 9, 18, 19). In our case, the patient experienced recurrent abdominal pain, intermittent black stool, dizziness, and fatigue for more than a month. Abdominal CT examination did not reveal any significant mass within the abdominal cavity. After completing a series of ancillary tests, the cause of persistent gastrointestinal bleeding remained unclear. Eventually, the pathological examination of the surgical excision specimen indicated that LAM-like lesions were observed in the submucosal layer of the pylorus, mesentery

of the side of the lesser curvature of the stomach and small intestine. The immunohistochemical results showed Ki67 (+5%), D2-40 (+), CD-34 (+), Desmin (+), SMA (+). It has been reported in the literature that Desmin (+), SMA (+), and D2-40 (+) are features of the immunohistochemistry of LAM. Desmin and SMA are myogenic markers for smooth muscle-like cells, while D2-40 is a marker of lymphatic endothelial cells (20–22). After correlating the abdominal CT findings, which revealed cystic lesions in the abdominal cavity, with the microscopic pathology and immunohistochemistry features, this case was ultimately diagnosed as abdominal LAM.

Lombard (23) proposed that LAM cells metastasize through the lymphatic tract. These LAM cells in the lymphatic fluid block the lymphatic duct outlet, resulting in increased lymphatic pressure (23). This can lead to the dilation of lymphatic vessels, as observed in the current patient. The patient's pathology sections revealed enlarged lymphatic vessels, and abdominal CT scans showed signs of cystic lesions. In the lungs, clusters or nests of LAM cells infiltrate the walls of vessels, disrupting these walls and ultimately causing bleeding into the alveoli (24). Based on these findings, it can be speculate that the proliferation of LAM cells infiltrating the walls of gastrointestinal vessels could cause bleeding at the corresponding sites, which may account for the patient's gastrointestinal bleeding symptoms. Moreover, the nodular lesions identified in the removed stomach and duodenal tissue are a manifestation of LAM cells proliferating in clusters.

Recent studies have shown that LAM cells, which are present in the blood and body fluids of S-LAM patients, have the ability to metastasize and spread to other areas of the body. This suggests that these cells are capable of moving away from their original location and implanting in new sites (25). The biological behavior of LAM is similar to that of low-grade neoplasms, and it has been found to metastasize (26). LAM cells within the abdominal cavity can travel through the lymphatic system and reach the lungs, where they can evenly distribute to both the left and right lobes. Once in the lungs, these cells invade and infiltrate the lung tissue, forming uniform lesions on both sides (23). In this case report, LAM cells metastasized from the abdominal cavity to the lungs, resulting in lung injury. This was expressed as a diffuse distribution of thin-walled cysts cavity and chylothorax in both lungs, leading to symptoms such as chest tightness and shortness of breath.

A portion of LAM located in the abdomen may initially not respond well due to the inability to identify the cause. However, a definitive diagnosis can often be made through a pathological biopsy following surgery (5, 7). When LAM occurs without a tumor mass, there are no established standardized treatment protocols. In cases where there is gastrointestinal bleeding or intestinal obstruction, surgical intervention may be necessary (6). In this study, surgical intervention was required when the patient's gastrointestinal symptoms did not improve with conservative medical treatment. However, after the surgery, the patient continued to experience intermittent black stools and symptoms of chest tightness and shortness of breath. This suggests that the surgery did not fully resolve the gastrointestinal bleeding, and the condition may have even worsened, as indicated by the emergence of pulmonary symptoms. As a result, new treatment options needed to be explored.

A study has reported that a female patient diagnosed with pulmonary and retroperitoneal LAM experienced significant improvement after taking 1 mg/day of Sirolimus orally. Her pulmonary symptoms notably improved after six months of treatment, and the retroperitoneal lymph node lesions were completely resolved following three years of regular therapy (27). Consequently, the same treatment regimen of orally administering 1 mg/day of Sirolimus was used to manage disease progression in the current case.

Currently, mTOR inhibitors, such as Sirolimus and Everolimus, are the primary clinical treatment for LAM (28). Sirolimus is a highly targeted small molecule that binds to an immunophilin called FK506 binding protein, forming a complex. This complex then interacts with mTOR, blocking the activation of kinases downstream of the mTOR pathway and reducing mTOR expression. This decrease in mTOR expression leads to a decrease in abnormal proliferation of LAM cells, thereby reducing the damage they cause to tissues and organs (29).

The American Thoracic Society/Japanese Respiratory Society (ATS/JRS) guidelines state that Sirolimus can improve lung function and quality of life in patients, as well as reduce the accumulation of angiomyolipoma, lymphangioleiomyoma, and chylous fluid. Sirolimus is recommended for LAM patients who have abnormal or decreased lung function. In cases where LAM patients experience symptomatic chylous fluid accumulation, such as chylous pleural fluid and ascites, it is advised to use Sirolimus before resorting to invasive treatments. These invasive treatments may include methods such as intermittent percutaneous drainage or the use of indwelling drainage devices (30). While the guidelines do not specify a precise duration for Sirolimus use, but in clinical practice, a low dose of 1–2 mg/day is often recommended. This dosage aims to maintain serum trough levels within the range of 5–15 ng/mL (31). However, studies have shown that using Sirolimus to treat LAM can lead to potential side effects, including mucositis, canker sores, diarrhea, nausea, hypercholesterolemia, acne-like rash, and lower limb swelling (32). To reduce the occurrence of drug-related adverse events, low-dose administration is recommended and may enhance the safety of long-term treatment with Sirolimus. It is important to note that discontinuing Sirolimus during treatment can result in further deterioration of lung function (30).

Currently, the clinical treatment effect of LAM is limited, and most treatment modalities can only delay the progression of the disease but cannot achieve a cure (28). During our follow-up period, we observed that the patient's black stool episodes were still intermittent, but the frequency had significantly decreased compared to his initial hospitalization. Additionally, the patient reported a significant improvement in his chest tightness and shortness of breath symptoms, and his lung condition did not worsen. The patient is currently undergoing ongoing follow-up, and his condition remains stable with no recurrence observed. The effectiveness of the treatment will continue to be monitored throughout the follow-up process.

Conclusion

This case report describes the progression and treatment of a male patient with LAM, which affects both the gastrointestinal tract and lungs. LAM is a rare disease characterized by progressive

involvement of multiple organs and is often irreversible once it occurs. Early diagnosis of LAM is challenging, and symptoms like gastrointestinal bleeding can be easily misdiagnosed as an ulcer. However, if a pulmonary or abdominal CT scan shows multiple cystic lesions, the diagnosis of LAM should be strongly considered as a potential diagnosis, regardless of whether the patient is experiencing symptoms such as hemoptysis or gastrointestinal bleeding. A pathological biopsy should be performed as soon as possible to confirm the diagnosis. In addition, once LAM is confirmed, the first-line medication, Sirolimus, should be initiated as early as possible after excluding any contraindications. A combined approach of surgery and Sirolimus may be a more effective strategy for slowing the progression of the disease. This case analysis provides valuable insights for clinicians in diagnosing and treating gastrointestinal LAM. Clinicians should be particularly attentive to LAM in male patients, as pulmonary symptoms may not always be the initial manifestation. However, further research is necessary to gain a better understanding of the mechanisms of gastrointestinal LAM and to develop more effective treatment options.

Data availability statement

The original contributions presented in this study are included in this article/supplementary material, further inquiries can be directed to the corresponding author.

Ethics statement

The studies involving humans were approved by The First Affiliated Hospital of Dali University. The studies were conducted in accordance with the local legislation and institutional requirements. The participants provided their written informed consent to participate in this study. Written informed consent was obtained from the individual(s) for the publication of any potentially identifiable images or data included in this article.

Author contributions

YZ: Conceptualization, Data curation, Formal analysis, Methodology, Project administration, Software, Writing – original draft. YS: Conceptualization, Data curation, Formal analysis, Methodology, Project administration, Software, Writing – original draft. RS: Conceptualization, Data curation, Methodology, Software, Supervision, Writing – review and editing.

Funding

The authors declare that no financial support was received for the research, authorship, and/or publication of this article.

Conflict of interest

The authors declare that the research was conducted in the absence of any commercial or financial relationships that could be construed as a potential conflict of interest.

Publisher's note

References

1. Ye L, Jin M, Bai C. Clinical analysis of patients with pulmonary lymphangioleiomyomatosis (PLAM) in mainland China. *Respir Med.* (2010) 104:1521–6.

2. Brunelli A, Catalini G, Fianchini A. Pregnancy exacerbating unsuspected mediastinal lymphangioleiomyomatosis and chylothorax. *Int J Gynaecol Obstet.* (1996) 52:289–90. doi: 10.1016/0020-7292(95)02619-3

3. Sbaraglia M, Bellan E, Dei Tos AP. The 2020 WHO classification of soft tissue tumours: News and perspectives. *Pathologica.* (2021) 113:70–84. doi: 10.32074/1591-951X-213

4. Ryu JH, Moss J, Beck GJ, Lee JC, Brown KK, Chapman JT, et al. The NHLBI lymphangioleiomyomatosis registry: Characteristics of 230 patients at enrollment. *Am J Respir Crit Care Med.* (2006) 173:105–11. doi: 10.1164/rccm.200409-1298OC

5. Goh SG, Ho JM, Chuah KL, Tan PH, Poh WT, Riddell RH. Leiomyomatosis-like lymphangioleiomyomatosis of the colon in a female with tuberous sclerosis. *Mod Pathol.* (2001) 14:1141–6. doi: 10.1038/modpathol.3880449

6. Belhasan D, Ghalim F. Diffuse abdominal lymphangiomatosis without tumoral masses: A case report. *Clin J Gastroenterol.* (2024) 17:430–3.

7. Erginoz E, Taskin HE, Cavus GH, Zengin AK. Leiomyomatosis-like lymphangioleiomyomatosis: A case report of the colonic manifestation of tuberous sclerosis. *Medicine (Baltimore).* (2021) 100:e27723.

8. McCarthy C, Gupta N, Johnson SR, Yu JJ, McCormack FX. Lymphangioleiomyomatosis: Pathogenesis, clinical features, diagnosis, and management. *Lancet Respir Med.* (2021) 9:1313–27.

9. Harknett EC, Chang WY, Byrnes S, Johnson J, Lazor R, Cohen MM, et al. Use of variability in national and regional data to estimate the prevalence of lymphangioleiomyomatosis. *QJM.* (2011) 104:971–9.

10. Song B, Yan JX, Zhao JC. Primary abdominal lymphangioleiomyomatosis with mucosa-associated lymphoid tissue lymphoma. *J Gastrointest Surg.* (2020) 24:2383–6. doi: 10.1007/s11605-020-04584-9

11. Zhang X, Travis WD. Pulmonary lymphangioleiomyomatosis. *Arch Pathol Lab Med.* (2010) 134:1823–8.

12. Baldi BG, Freitas CS, Araujo MS, Dias OM, Pereira DA, Pimenta SP, et al. Clinical course and characterisation of lymphangioleiomyomatosis in a Brazilian reference centre. *Sarcoidosis Vasc Diffuse Lung Dis.* (2014) 31:129–35.

13. Brakemeier S, Grohé C, Bachmann F, Budde K. [Sporadic Lymphangioleiomyomatosis (sLAM) and Tuberous Sclerosis Complex (TSC) - Pulmonary Manifestations]. *Pneumologie.* (2017) 71:86–95.

14. Gupta N, Vassallo R, Wikenheiser-Brokamp KA, McCormack FX. Diffuse cystic lung disease. Part II. *Am J Respir Crit Care Med.* (2015) 192:17–29.

15. Liu Y, Guo Z, Zhao C, Li X, Liu H, Chen J. Lymphangioleiomyomatosis: A case report and review of diagnosis and treatment. *Onco Targets Ther.* (2018) 11: 5339–47.

16. Barton EC, Johnson S, Collin N, Bhatt N, Maskell NA. A chylothorax in a young woman: The difficulties of medical management. *Respirol Case Rep.* (2024) 12:e01303. doi: 10.1002/rcr2.1303

17. Kirkeby MH, Bendstrup E, Rose HK. Case report: If it is not asthma-think of lymphangioleiomyomatosis in younger female patients. *Front Med (Lausanne).* (2024) 11:1328471. doi: 10.3389/fmed.2024.1328471

18. Cudzilo CJ, Szczesniak RD, Brody AS, Rattan MS, Krueger DA, Bissler JJ, et al. Lymphangioleiomyomatosis screening in women with tuberous sclerosis. *Chest.* (2013) 144:578–85.

19. McCormack FX. Lymphangioleiomyomatosis: A clinical update. *Chest.* (2008) 133:507–16.

20. Fu W, Li Y, Li H, Yang P, Xing X. Solitary extrapulmonary lymphangioleiomyomatosis of the liver: A case report and literature review. *Exp Ther Med.* (2016) 12:1499–502. doi: 10.3892/etm.2016.3502

21. Johnson SR, Taveira-DaSilva AM, Moss J. Lymphangioleiomyomatosis. *Clin Chest Med.* (2016) 37:389–403.

22. Suzuki K, Nagasaka K, Oda K, Abe H, Maeda D, Matsumoto Y, et al. A case of lymphangioleiomyomatosis associated with endometrial cancer and severe systemic lupus erythematosus. *BMC Cancer.* (2016) 16:390. doi: 10.1186/s12885-016-2413-z

23. Lombard CM. Pulmonary lymphangioleiomyomatosis: A proposed state of neoplastic senescence. *Med Hypotheses.* (2019) 132:109372. doi: 10.1016/j.mehy.2019.109372

24. Liu CP, Gu YY. Clinicopathological features of pulmonary lymphangioleiomyomatosis. *J Diagn Pathol.* (2022) 29:1037–40.

25. Prizant H, Hammes SR. Minireview: Lymphangioleiomyomatosis (LAM): The "Other" steroid-sensitive cancer. *Endocrinology.* (2016) 157:3374–83. doi: 10.1210/en.2016-1395

26. Wahid S, Chiang PC, Luo HL, Huang SC, Tsai EM, Chiang PH. Pelvic lymphangioleiomyomatosis treated successfully with everolimus: Two case reports with literature review. *Medicine (Baltimore).* (2017) 96:e4562. doi: 10.1097/MD.0000000000004562

27. Zong DD, Ouyang YR. Rapamycin successfully treated lung and retroperitoneal lymphangiomyomatosis in 1 case and literature review. *J Central South Univ (Medical Science).* (2012) 37:963–7.

28. Zhang HY, Song XY, Li SJ. Treatment status and research progress of lymphangioleiomyomatosis. *Bachu Med.* (2021) 4:115–8.

29. Sengupta S, Peterson TR, Sabatini DM. Regulation of the mTOR complex 1 pathway by nutrients, growth factors, and stress. *Mol Cell.* (2010) 40:310–22.

30. Gupta N, Finlay GA, Kotloff RM, Strange C, Wilson KC, Young LR, et al. Lymphangioleiomyomatosis diagnosis and management: High-resolution chest computed tomography, transbronchial lung biopsy, and pleural disease management. An Official American Thoracic Society/Japanese Respiratory Society Clinical Practice Guideline. *Am J Respir Crit Care Med.* (2017) 196:1337–48. doi: 10.1164/rccm.201709-1965ST

31. Bee J, Fuller S, Miller S, Johnson SR. Lung function response and side effects to rapamycin for lymphangioleiomyomatosis: A prospective national cohort study. *Thorax.* (2018) 73:369–75.

32. Interstitial Lung Disease Group, Chinese Thoracic Society, Chinese Medical Association; Expert Consensus Group of Lymphangioleiomyomatosis; Rare Diseases Research Center, Chinese Academy of Medical Sciences; Rare Diseases Society, Chinese Research Hospital Association. [Consensus Statement: sirolimus (rapamycin) as therapy for lymphangioleiomyomatosis (2018)]. *Zhonghua Jie He He Hu Xi Za Zhi.* (2019) 42:92–7. doi: 10.3760/cma.j.issn.1001-0939.2019.02.002

frontiers | Frontiers in Medicine

TYPE Case Report
PUBLISHED 08 January 2025
DOI 10.3389/fmed.2024.1519065

OPEN ACCESS

EDITED BY
Karolina Henryka Czarnecka-Chrebelska,
Medical University of Lodz, Poland

REVIEWED BY
Aleksandra Uzelac,
University of Belgrade, Serbia
Annibale Raglio,
SIMPIOS, Italy

*CORRESPONDENCE
Peisong Chen
✉ 13570474904@163.com

†These authors have contributed equally to this work

RECEIVED 29 October 2024
ACCEPTED 17 December 2024
PUBLISHED 08 January 2025

CITATION
Fang J, Fang H, Guo P, Peng Y and Chen P (2025) *Strongyloides stercoralis* combined with concurrent multiple pathogens infections in an immunosuppressed patient: a case report. *Front. Med.* 11:1519065. doi: 10.3389/fmed.2024.1519065

Strongyloides stercoralis combined with concurrent multiple pathogens infections in an immunosuppressed patient: a case report

Jingchun Fang[1,2†], Huimin Fang[1,2†], Penghao Guo[1], Yaqin Peng[1] and Peisong Chen*

[1]Department of Laboratory Medicine, The First Affiliated Hospital, Sun Yat-sen University, Guangzhou, China, [2]Department of Laboratory Medicine, Nansha Division, The First Affiliated Hospital, Sun Yat-sen University, Guangzhou, China

Background: *Strongyloides stercoralis* is an opportunistic pathogenic parasite. Most individuals with normal immune function may not exhibit significant symptoms, and the signs are atypical, which can easily lead to missed diagnoses and delayed treatment. People with underlying diseases and weakened immunity are prone to develop severe conditions after infection with *Strongyloides stercoralis*.

Case presentation: We report an immunocompromised patient in whom the pathogen was initially not detectable using traditional parasitic detection techniques. However, *Strongyloides stercoralis* was identified in both the alveolar lavage fluid and blood through metagenomic next-generation sequencing. Subsequently, *Strongyloides stercoralis* was detected in the alveolar lavage fluid after multiple rounds of testing using traditional microscopic examination techniques. Based on the mNGS results and other examination findings, the patient was diagnosed with *Strongyloides stercoralis* in combination with concurrent multiple pathogens infections. After the combined drug therapy of Meropenem, Vancomycin, and Albendazole, the patient's condition was gradually brought under control.

Conclusion: This case demonstrates the advantage of integrating traditional detection methods with metagenomics next-generation sequencing technology in the etiological diagnosis of immunocompromised individuals. It is conducive to clarifying the etiological diagnosis of patients and thereby facilitating the timely initiation of corresponding treatments.

KEYWORDS

***Strongyloides stercoralis*, pneumonia, metagenomic next-generation sequencing, co-infection, immunocompromisation**

Background

Strongyloides stercoralis (*S. stercoralis*) is a soil-transmitted nematode that is endemic to tropical and subtropical regions of the world (1). The lifecycle of *Strongyloides stercoralis* alternates between free-living and parasitic cycles. Under suitable environmental conditions, such as in warm and damp soil, the eggs of the *S. stercoralis* hatch into

rhabditiform larvae. After undergoing several molts, these larvae continue to develop into mature adult threadworms. When infective larvae (2) (filariform larvae) enter the human body, they make their way into the circulatory system. They then travel through the right ventricle of the heart to the lungs, where they penetrate the capillaries of the alveolar walls. Then, they move through the bronchial tubes and the pharynx to settle in the small intestine, where they mature and establish themselves. After *S. stercoralis* invades the human body, it can cause strongyloidiasis, and severe cases may even lead to death (3, 4). The diagnosis of *S. stercoralis* infection is difficult because the sensitivity of traditional methods is variable and there is the need to use more techniques such as Baermann concentration, Agar plate culture, Serology and RT-PCR. This paper employs a combination of metagenomic next-generation sequencing (mNGS) and traditional etiological examinations to rapidly and accurately detect a case of *S. stercoralis* co-infection with multiple other pathogens. This approach enables the patient to receive timely and effective treatment and enhances healthcare professionals' comprehension of co-infections associated with *S. stercoralis*.

Case presentation

A 75-year-old woman was admitted to the hospital (the First Affiliated Hospital of Sun Yat-sen University, Guangzhou, China) on account of a prolonged cough, expectoration, and recent manifestations of fever and shortness of breath. The patient, a farmer with a generally mediocre health condition, denied any history of exposure to epidemic areas or contaminated water. The patient had a history of COVID-19 infection, hypertension, and nephrotic syndrome. She had been administered irbesartan (150 mg QD), atorvastatin (20 mg QD), methylprednisolone (40 mg QD), and rivaroxaban (10 mg QD) for blood pressure control, lipid regulation, and anticoagulation therapy. Before this admission, she had been on long-term anti-infective therapy at the local hospital, but symptom control was poor. Then the patient presented to the emergency department due to worsening pneumonia, and her condition was complex, requiring airway intubation, mechanical ventilation, and urgent management. In this study, written consent for the publication of detailed information has been obtained from the legal guardians of the patients.

Upon admission, the physical examination revealed the following: body temperature 36.3°C, pulse rate 115 beats per minute, respiratory rate 25 breaths per minute, and blood pressure 95/58 mmHg. The patient was in a state of analgesic sedation, with pale skin and mucous membranes throughout the body, and scattered petechiae were present. The patient had mild edema in the lower extremities. Cardiac and pulmonary auscultation showed no abnormalities, however, coarse breath sounds both dry and wet crackles were heard in both lungs, indicating a lung infection. Abdominal examination showed no significant tenderness, rebound tenderness, or palpable masses, and bowel sounds were normal.

The Laboratory Examination revealed leukocytosis 4.77×10^9/L, and neutrophils percentage 85.8%, eosinophils percentage 1.2%, increased C-reactive protein (CRP) 51.83 mg/L (normal range 0–10 mg/L), and elevated procalcitonin 2.60 ng/mL (normal range 0–0.05 ng/mL), suggesting a possible infection or inflammation. Coagulation tests indicated prolonged prothrombin time, and gastric juice occult blood test showed a strongly positive result, consistent with gastrointestinal bleeding. Hemoglobin 55 g/L (normal range 115–150 g/L) and serum total protein 53.1 g/L (normal range 64–87 g/L), and serum albumin 31.9 g/L (normal range 35–50 g/L) were decreased. Cellular immunity chip testing showed a decreased CD4+ T cell count of 224 cell/μl (normal range, 500–1,440 cell/μl), CD8+ T cell count of 168 cell/μl (normal range, 238–1,250 cell/μl), and CD3+ T cell count of 420 cell/μl (normal range, 770–2,860 cell/μl), indicating severe cellular immunodeficiency. Chest CT revealed diffuse pulmonary inflammation with a small amount of pleural effusion (Figures 1A,B). Considering that the patient had been on long-term steroid therapy, and Cellular immunity chip testing showed decreased levels of CD3, CD4, and CD8, which indicate cellular immunodeficiency and an increased propensity for infectious diseases, the patient was considered the possibility of pneumonia. Then a combination of Meropenem (1 g iv Q8H), Compound Sulfamethoxazole (0.96 g p.o. Q6H), and Caspofungin (50 mg iv. drip QD) was administered for anti-infection therapy.

On the second day of admission, the patient experienced repeated fevers, with a maximum body temperature of 38.9°C, accompanied by a further increase in CRP (88.71 mg/L) and D-dimer (15.61 mg/L). Subsequently, the blood culture was sent for examination. Furthermore, the patient was tested for Aspergillus antigen, *Cryptococcus neoformans* antigen, rapid detection of *Mycobacterium tuberculosis* and rifampicin resistance gene, acid-fast bacillus smear,

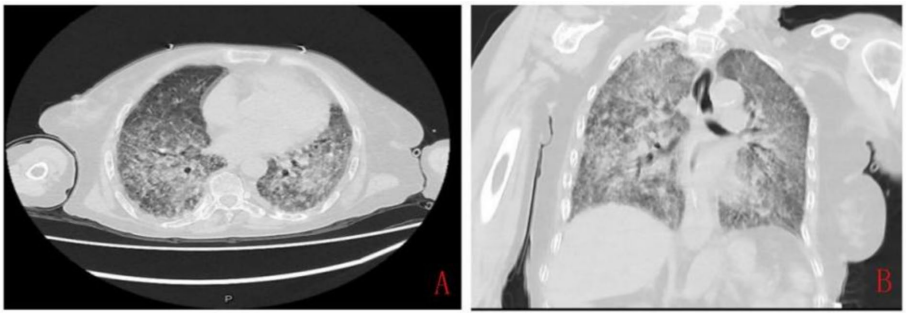

FIGURE 1
The chest computed tomography imaging at admission showed diffuse inflammation in both lungs. **(A)** Transverse image, showing markedly thickened, disorganized, and blurred pulmonary markings, with some areas presenting a reticular and honeycomb-like appearance. **(B)** Coronal image, showing diffuse patchy areas of increased density in both lungs with indistinct borders.

Streptococcus pneumoniae antigen, Influenza A virus, Influenza B virus, *Mycoplasma pneumoniae*, and *Legionella pneumophila*, all of which were negative. The examination cycles of blood and sputum culture were long, and the results had not been reported yet. Considering the patient was immunocompromised, and her condition was complex, but initial clinical tests failed to detect any pathogens, therefore, mNGS testing of blood and bronchoalveolar lavage fluid (BALF) was sent for the rapid identification of the pathogen. After sample processing and DNA extraction [QIAamp® UCP Pathogen DNA Kit (Qiagen)] for mNGS, libraries were constructed for the DNA samples using a Nextera XT DNA Library Prep Kit (Illumina, San Diego, America), sequencing was performed using Nextseq 550Dx sequencer (Illumina, San Diego, America). The mNGS of BALF identified *Enterococcus faecium* (307,810 reads), *Candida albicans* (296,337 reads), *Candida glabrata* (111,343 reads), *S. stercoralis* (347,139 reads), and *Human Parainfluenza Virus Type 3*, among others (Table 1). Moreover, the blood mNGS detected *S. stercoralis* (15 reads) (Table 2). After examination, the blood culture indicated the presence of *Enterococcus faecium*, and the *in vitro* drug susceptibility test demonstrated sensitivity to vancomycin and linezolid, while the sputum culture disclosed moderate growth of *Candida glabrata*. The other laboratory test results indicated that the patient's blood contains *Epstein–Barr virus* (EBV) DNA at a level of 1.26×10^3 copies/mL, *Cytomegalovirus* (CMV) DNA at a level of 8.19×10^3 copies/mL, and (1,3)-β-D-glucan at a level of 119.58 pg./mL.

Based on the mNGS results, a re-examination was conducted on the clinically submitted BALF, and a large quantity of Gram-positive cocci, fungal spores, and pseudohyphae (with observable phagocytosis of white blood cells) were identified. Through repeated smear microscopic examinations, *S. stercoralis* was detected (Figures 2A–D). Nevertheless, the result of the smear test for blood parasites was negative. Regrettably, the patient did not defecate during the hospitalization, so routine stool examination and stool parasite examination could not be performed.

With the mNGS results, the patient was ultimately diagnosed with *S. stercoralis* pneumonia complicated by multiple pathogen infections. BALF NGS and other examination findings suggested multiple bacterial, fungal, viral, and parasitic infections as well as bloodstream infections, prompting an adjustment in the treatment regimen. The patient was administered Meropenem (1 g iv Q8H), Vancomycin (0.5 g iv Q8H), Caspofungin (50 mg iv. drip QD), Oseltamivir (75 mg BID), Ganciclovir (250 mg p.o. Q12H), and Albendazole (0.4 g BID) to enhance antibacterial, antifungal, antiviral and antiparasitic effects.

With comprehensive treatment, the patient's vital signs stabilized, infection was controlled. The following figure (Figure 3) shows the changes throughout the entire course of the patient since admission and the process of anti-infection. One week after follow-up, the patient's infection markers (procalcitonin, 0.673 ng/mL) gradually declined, and the blood culture turned negative, and subsequently, the patient is gradually recovering.

Discussion

Strongyloidiasis, caused by the parasite *S. stercoralis*, is prevalent worldwide, but it is more common in resource-poor countries with hot and humid climates and poor sanitation conditions (5). This parasite has opportunistic pathogenic characteristics, with the most significant risk factors (5) including HIV infection, *Human T-lymphotropic virus type 1* infection (6), alcoholism, and prolonged soil contact. Generally, most individuals with normal immune function may not exhibit significant symptoms upon infection, while those with underlying health conditions and weakened immunity are more susceptible to developing severe cases (7). The symptoms of infected individuals typically include small localized hemorrhagic spots on the skin, migratory linear or serpiginous urticaria, fever, severe cough with expectoration, coughing, and difficulty breathing (8). Prolonged immunosuppression can escalate to more extensive, hemorrhagic, purpuric lesions, particularly around the umbilicus and limb roots (9). In severe cases of infection, complications such as multi-organ involvement and systemic toxicity may occur, potentially leading to death within a short period. Chest CT scans of those infected may reveal punctate, small patchy, or reticular localized or diffuse inflammatory opacities (10). The patient in this case was elderly and had multiple high-risk factors, including hypertension, nephrotic syndrome, and long-term steroid therapy. The patient had a cough and expectoration for over 50 days, and a chest CT revealed diffuse pulmonary inflammation in both lungs, indicating obvious symptoms of respiratory tract infection. Additionally, the patient presented with pallor of the skin and mucous membranes, scattered petechiae, and localized ecchymosis, suggesting the possibility of infection caused by *S. stercoralis*.

TABLE 1 The micro-organisms were detected by mNGS (bronchoalveolar lavage fluid).

Category	Pathogen	Reads	Coverage (%)	Relative abundance (%)
Bacteria	*Enterococcus faecium*	307,810	87.5	87.3
Fungi	*Candida albicans*	296,337	69.2	70.5
	Candida glabrata	111,343	43.8	29.4
Virus	Epstein–Barr virus	262	10.3	58.8
	Human Herpesvirus I	128	5.8	32.4
	Cytomegalovirus	54	1.5	8.8
	Human Parainfluenza Virus Type 3	304,108	100	100
Parasite	Strongyloides stercoralis	347,139	36.2	100
Human microbiota	Hemolytic Staphylococcus	33,869	53.8	9.2
	Neisseria flavescens	3,141	31.4	2.8

TABLE 2 The micro-organisms were detected by mNGS (Venous blood).

Category	Pathogen	Reads	Coverage (%)	Relative abundance (%)
Bacteria	–	–	–	–
Fungi	–	–	–	–
Virus	Epstein–Barr virus	3	0.1	3.4
	Cytomegalovirus	115	2.8	94.1
Parasite	Strongyloides stercoralis	15	36.2	100
Human microbiota	–	–	–	–

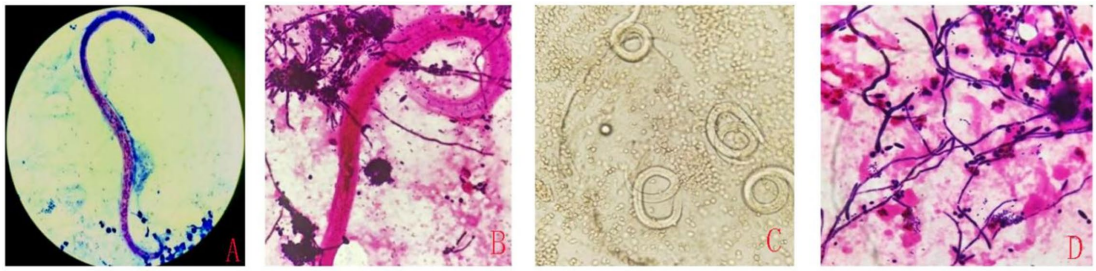

FIGURE 2
The detection of *S. stercoralis* in alveolar lavage fluid using different smear techniques. Acid-fast staining **(A)**, Gram staining **(B)**, Wet mount observation **(C)**, Gram staining **(D)**.

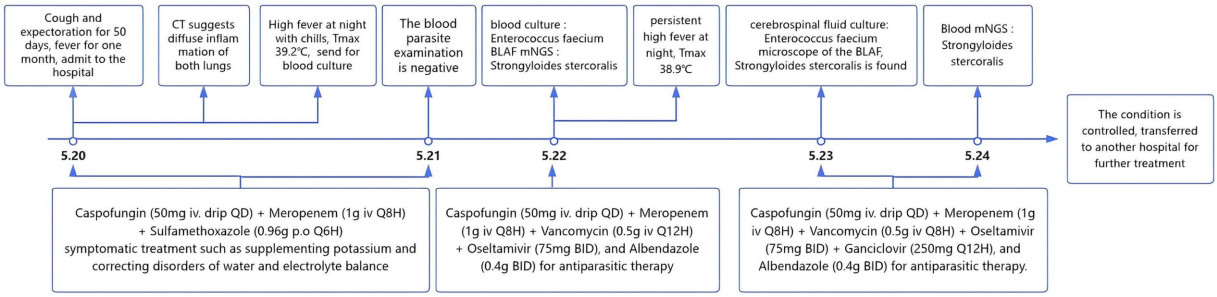

FIGURE 3
The changes in the whole course of the patient since admission and the process of anti-infection.

Currently, parasitological techniques are the gold standard for detecting *S. stercoralis* larvae in fecal samples under microscopes (11). However, the sensitivity may be inadequate (12), especially with reduced worm burden, and missed detections were prone to occur. Furthermore, microscopic examination is easily influenced by various factors, such as the specimen quality, the effect of specimen preparation and staining, and the experience of the inspectors. The serology test is also used to diagnose an infection of *S. stercoralis*. Immunodiagnostic tests for strongyloidiasis are indicated when infection is suspected and the organism is not detected by duodenal aspiration, string tests, or by repeated examinations of stool. Most antibody detection tests employ antigens derived from *S. stercoralis* (or from closely-related *S. ratti* or *S. venezuelensis*) filariform larvae, although recombinant antigens such as (e.g., NIE, SsIR) are increasingly being used. Although indirect fluorescent antibody (IFA), indirect hemagglutination (IHA) and antigen-linked fluorescent and magnetic bead tests are are available, enzyme immunoassay (EIA) is recommended because of its greater sensitivity. The filariform antigen-based EIA used at CDC has a sensitivity of 96% and a specificity of 98%. The commercial EIA kits that are currently available have comparable specificity but slightly lower sensitivity. Immunocompromised persons with disseminated strongyloidiasis usually have detectable IgG antibodies despite their immunosuppression, though false negative results can occur.[1] Hailu et al.'s study indicates that RT-PCR detected the highest number of *S. stercoralis* infections. A combination of RT-PCR with agar plate culture (APC) and/ or Baermann Concentration Test "BCT" better detected *S. stercoralis* from stool samples compared to other combinations or single diagnostic methods. Therefore, RT-PCR and combination of RT-PCR with APC and/or BCT diagnostic methods should be advocated for detection of S. stercoralis infection (13).

1 https://www.cdc.gov/dpdx/strongyloidiasis/index.html

Molecular techniques can play a confirmatory role in diagnosis, with their ability to circumvent both the low sensitivity of parasitological techniques and the low specificity of immunological techniques (14). The mNGS does not require pre-setting, cultivation, or selectivity. It directly extracts DNA/RNA from clinical samples and completes the detection of pathogens such as bacteria, fungi, viruses, and parasites in one go. This method has diagnostic advantages in populations prone to mixed infections, unexplained critical illnesses and patients with rapid disease progression, particularly those with impaired immune function. In this case, the patient was not initially considered to have a parasitic infection. Due to the deterioration of the condition and unidentified cause of infection, mNGS testing was sent for the rapid identification of the pathogen. Then the *S. stercoralis* was rapidly detected through mNGS. The mNGS provided a direction for the clinical diagnosis and treatment of this patient. Subsequently, based on the mNGS results indicating a significant presence of *Streptococcus constellatus* DNA, multiple and repeated microscopic examinations of the patient's BALF were conducted. It was through this rigorous and targeted re-examination that we were ultimately able to visualize the parasite under the microscope (Figure 2), confirming the infection caused by *S. stercoralis*. However, the blood parasitic examination remained negative, highlighting the limitations of traditional detection methods in the detection of mixed infections and rare pathogens. A challenge in this case was that the laboratory does not routinely perform smear examinations for BALF cultures, and due to the patient's condition, it was impossible to obtain feces for routine testing. Through this case, we have recognized the importance of simultaneous microscopic examination for routine cultures.

It is well documented that immunosuppressive agents (e.g., corticosteroids) increase the risk of opportunistic infections (15). On the other hand, several opportunistic infections were reported in COVID-19 patients, including *Candida* spp. (16), *Cytomegalovirus* (CMV) (17), *Herpes simplex virus* (HSV) (18) and *S. stercoralis* (19). In this case, in addition to detecting *S. stercoralis* in the patient's BALF mNGS results, *Enterococcus, Candida albicans, and Candida glabrata* were also detected. *Candida* spp. are commensal yeasts that are normally found on human skin, in mucosal and intestinal microbiota, and in the mycobiome. and up to 60% of people can be colonized with *Candida* spp. (20) *Candida* spp. can become pathogenic when the equilibrium between commensal organisms is disturbed, and risk factors for *Candida* spp. overgrowth and invasiveness are present. Such risk factors include immunosuppression, the presence of central lines, and exposure to antibiotics (21). As for *Enterococcus*, the most commonly reported infections are intra-abdominal infections, urinary tract infections, bacteremia and endocarditis, pneumonia is rarely described (22). Infections typically present in immunosuppressed patients who have received multiple courses of antibiotics in the past. It is generally believed that *Enterococcus and Candida* have a higher probability of colonization in the respiratory tract, and they generally do not require treatment. However, since the patient was immunocompromised, had previously been infected with COVID-19 and exposed to broad-spectrum antibiotics, the risk of opportunistic infections is relatively high. Based on the microscopic examination of the patient's sputum, which showed a large number of white blood cells, Gram-positive cocci being engulfed by white blood cells, and Candida hyphae were also visible. Combined with the elevated results of fungal serum (1,3)-β-D-glucan (119.58 pg./mL) and procalcitonin (2.6 ng/mL), empirical treatment targeting both *Enterococcus* and *Candida* is currently being considered.

Studies have indicated that strongyloidiasis complicated by CMV (23) infection often presents with non-specific gastrointestinal symptoms. CMV infection triggers a Th1 type cellular immune response and suppresses the Th2 type cellular immune response associated with *S. stercoralis* infection, which can increase the risk of disseminated strongyloidiasis (8, 24). *S. stercoralis* primarily causes intestinal disease and disrupts the intestinal immune microenvironment, increasing the body's susceptibility to intestinal bacteria. When both infections occur together, they may complicate the disease course (25). Clinical manifestations in patients with multiple pathogen co-infections are often non-specific, making clinical diagnosis and treatment more challenging (26). Therefore, for patients with compromised immune function (such as the immunosuppressed host with pneumonia in this case) who are prone to various types of opportunistic infections, it is necessary to pay attention to not only common pathogen infections but also to the infections caused by less common pathogens like fungi and parasites (27).

Eosinophils are one of the foremost components of the immune system, which play a prominent role in parasitic infections. Eosinophilia is a common, but not uniform, finding in *S. stercoralis* infection and is thought to be more marked in earlier infections, becoming less pronounced and more variable in chronic cases (28). However, previous reports suggest that patients who have an absence of eosinophilia in the setting of a Strongyloides infection tend to have a poorer prognosis (29). The reason for this observation is unclear, but it may be related to corticosteroid-induced neutrophilia and the fact that corticosteroids can promote the apoptosis of eosinophils (30). The patient's eosinophil count was normal upon admission, which might be associated with the patient's disease course, severity of the condition, and the use of glucocorticoids. Following the initiation of the anti-infective therapy, continuous monitoring of the complete blood count over several days disclosed eosinophil levels above the normal range, suggesting a favorable trend in the disease course and the efficacy of the treatment regimen. Through the timely administration of antibacterial, antifungal, antiviral, and antiparasitic treatments, the patient's condition was controlled.

We are aware that this report has limitations. Firstly, our clinical physicians had ordered routine stool tests, stool parasitic examinations, and stool culture tests early on. Regrettably, the patient did not defecate during the hospitalization, so routine stool examination and stool parasite examination could not be performed. Secondly, the specific cause of the patient's infection with *S. stercoralis* remains unclear. According to the medical history, we understand that the patient is a farmer, and we can only speculate that the patient might have been exposed to soil contaminated with *S. stercoralis*.

Conclusion

This case underlines the need to exclude *S. stercoralis* infection particularly in immunocompromised patient with risk factors and highlights the diagnostic power of NGS although it indicates the need not to lose knowledge of traditional methods.

Data availability statement

The datasets presented in this study can be found in online repositories. The names of the repository/repositories and

accession number(s) can be found in the article/supplementary material.

Ethics statement

The studies involving humans were approved by Clinical Research and Ethics Committee of the First Affiliated Hospital of Sun Yat-sen University. Written informed consent was obtained from the individual(s) for the publication of any potentially identifiable images or data included in this article. No animal studies are presented in this manuscript. And the study was conducted in accordance with the local legislation and institutional requirements.

Author contributions

JF: Data curation, Writing – original draft, Writing – review & editing. HF: Data curation, Writing – original draft, Writing – review & editing, Investigation. PG: Methodology, Writing – review & editing. YP: Methodology, Writing – review & editing. PC: Funding acquisition, Visualization, Writing – review & editing.

Funding

The author(s) declare that financial support was received for the research, authorship, and/or publication of this article. The research is supported by the Guangdong Natural Science Foundation-General Program (2023A1515011252) and the Development Plan "Biosafety Technology" Key Project (2022B1111020003).

Conflict of interest

The authors declare that the research was conducted in the absence of any commercial or financial relationships that could be construed as a potential conflict of interest.

Generative AI statement

The authors declare that no Gen AI was used in the creation of this manuscript.

Publisher's note

References

1. Nutman TB. Human infection with *Strongyloides stercoralis* and other related strongyloides species. *Parasitology*. (2017) 144:263–73. doi: 10.1017/S0031182016000834

2. Mora Carpio AL, Meseeha M. Strongyloidiasis In: StatPearls [internet]. Treasure Island, FL: StatPearls Publishing (2024)

3. Hu L, Teng J, Li GJ. A case report of fecal roundworm co-infection with Fungi. *Chinese J Infect Control*. (2023) 22:351–4. doi: 10.12138/j.issn.1671-9638.20233145

4. Wang Y, Tian J, Peng ZY, Hu F, Cai FY, Tang YB. Analysis and prevention of a severe infection case of fecal roundworm and pneumocystis Jirovecii. *Chinese J Hosp Infect*. (2019) 29:1772–1775+1785. doi: 10.11816/cn.ni.2019-190764

5. Czeresnia JM, Weiss LM. Strongyloides stercoralis. *Lung*. (2022) 200:141–8. doi: 10.1007/s00408-022-00528-z

6. Ye L, Taylor GP, Rosadas C. Human T-cell Lymphotropic virus type 1 and *Strongyloides stercoralis* co-infection: a systematic review and meta-analysis. *Front Med (Lausanne)*. (2022) 9:832430. doi: 10.3389/fmed.2022.832430

7. Liu HY, Zh AP, Dong LM, Wei H. A case of systemic lupus erythematosus complicated with fecal roundworm infection. *Trop Med Mag*. (2022) 22:1030–2. doi: 10.3969/j.issn.1672-3619.2022.07.032

8. Rahman F, Mishkin A, Jacobs SE, Caplivski D, Ward S, Taimur S. "*Strongyloides stercoralis*, human T-cell Lymphotropic virus Type-1 and cytomegalovirus coinfection in an allogeneic hematopoietic stem-cell transplant recipient." transplantation. *Direct*. (2020) 6:e573. doi: 10.1097/TXD.0000000000001021

9. Fernandez-Gonzalez P, Torres-Tienza S, Collantes-Rodríguez C, Sáez-García MÁ, Fonda-Pascual P. Cytology and dermatological findings: key diagnostic tools in *Strongyloides stercoralis* hyperinfestation. *Int J Dermatol*. (2024) 63:e443–5. doi: 10.1111/ijd.17280

10. Yashwanth Raj T, Vairakkani R, Harshavardhan TS, Srinivasaprasad ND, Dilli Rani V, Edwin FM. Post-renal transplant Miliary mottling: not always tuberculosis. *Ind J Nephrol*. (2020) 30:121–4. doi: 10.4103/ijn.IJN_141_19

11. Inês Ede J, Souza JN, Santos RC, Souza ES, Santos FL, Silva ML, et al. Efficacy of parasitological methods for the diagnosis of *Strongyloides stercoralis* and hookworm in faecal specimens. *Acta Trop*. (2011) 120:206–10. doi: 10.1016/j.actatropica.2011.08.010

12. Buonfrate D, Tamarozzi F, Paradies P, Watts MR, Bradbury RS, Bisoffi Z. The diagnosis of human and companion animal *Strongyloides stercoralis* infection: challenges and solutions. A scoping review. *Adv Parasitol*. (2022) 118:1–84. doi: 10.1016/bs.apar.2022.07.001

13. Hailu T, Amor A, Nibret E, Munshea A, Anegagrie M, Flores-Chavez MD, et al. Evaluation of five diagnostic methods for Strongyloides stercoralis infection in Amhara National Regional State, Northwest Ethiopia. *BMC Infect Dis*. (2022) 22:297. doi: 10.1186/s12879-022-07299-1

14. Chan AHE, Thaenkham U. From past to present: opportunities and trends in the molecular detection and diagnosis of *Strongyloides stercoralis*. *Parasit Vectors*. (2023) 16:123. doi: 10.1186/s13071-023-05763-8

15. Fishman JA. Opportunistic infections–coming to the limits of immunosuppression? *Cold Spring Harbor Perspect Med*. (2013) 3:a015669. doi: 10.1101/cshperspect.a015669

16. Abdoli A, Falahi S, Kenarkoohi A. COVID-19-associated opportunistic infections: a snapshot on the current reports. *Clin Exp Med*. (2022) 22:327–46. doi: 10.1007/s10238-021-00751-7

17. Le Balc'h P, Pinceaux K, Pronier C, Seguin P, Tadié J-M, Reizine F. Herpes simplex virus and cytomegalovirus reactivations among severe COVID-19 patients. *Crit Care*. (2020) 24:530. doi: 10.1186/s13054-020-03252-3

18. Whitley RJ, Roizman B. Herpes simplex virus infections. *Lancet*. (2001) 357:1513–8. doi: 10.1016/S0140-6736(00)04638-9

19. Berger R, Kraman S, Paciotti M. Pulmonary strongyloidiasis complicating therapy with corticosteroids. *Am J Trop Med Hyg*. (1980) 29:31–4. doi: 10.4269/ajtmh.1980.29.31

20. Kullberg BJ, Arendrup MC. Invasive Candidiasis. *N Engl J Med*. (2015) 373:1445–56. doi: 10.1056/NEJMra1315399

21. Lamoth F, Lockhart SR, Berkow EL, Calandra T. Changes in the epidemiological landscape of invasive candidiasis. *J Antimicrob Chemother*. (2018) 73:i4–i13. doi: 10.1093/jac/dkx444

22. O'Driscoll T, Crank CW. Vancomycin-resistant enterococcal infections: epidemiology, clinical manifestations, and optimal management. *Infect Drug Resist*. (2015) 8:217–30. doi: 10.2147/IDR.S54125

23. Rathor N, Khillan V, Sarin SK. *Strongyloides stercoralis* hyperinfection in patient with autoimmune hepatitis and purpura fulminans. *Ind J Crit Care Med*. (2016) 20:52–4. doi: 10.4103/0972-5229.173694

24. Puthiyakunnon S, Boddu S, Li Y, Zhou X, Wang C, Li J, et al. Strongyloidiasis—an insight into its global prevalence and management. *PLoS Negl Trop Dis*. (2014) 8:e3018. doi: 10.1371/journal.pntd.0003018

25. Barelli C, Donati C, Albanese D, Pafčo B, Modrý D, Rovero F, et al. Interactions between parasitic helminths and gut microbiota in wild tropical primates from intact and fragmented habitats. *Sci Rep*. (2021) 11:21569. doi: 10.1038/s41598-021-01145-1

26. Wen Q, Fu XY, Liu DY. Research Progress on co-infection of fecal roundworm with other pathogens. *Chinese J Schistosomiasis Control*. (2023) 35:206–12. doi: 10.16250/j.32.1374.2022156

27. Pei P, Liu TT, Lu YY, Lili T. A report of severe infection case of fecal roundworm. *Trop Med Mag*. (2020) 20:1503–4. doi: 10.3969/j.issn.1672-3619.2020.11.026

28. Klion AD, Nutman TB. The role of eosinophils in host defense against helminth parasites. *J Allergy Clin Immunol*. (2004) 113:30–7. doi: 10.1016/j.jaci.2003.10.050

29. Saradna A, Shenoy A, Ambesh P, Kamholz S. Strongyloides Hyperinfection and Miliary tuberculosis presenting with syndrome of inappropriate antidiuretic hormone secretion in a malnourished patient. *Cureus*. (2018) 10:e2349. Published 2018 Mar 20. doi: 10.7759/cureus.2349

30. Meagher LC, Cousin JM, Seckl JR, Haslett C. Opposing effects of glucocorticoids on the rate of apoptosis in neutrophilic and eosinophilic granulocytes. *J Immunol*. (1996) 156:4422–8. doi: 10.4049/jimmunol.156.11.4422

frontiers | Frontiers in Medicine

TYPE Case Report
PUBLISHED 24 January 2025
DOI 10.3389/fmed.2025.1457903

OPEN ACCESS

EDITED BY
Uday Kishore,
United Arab Emirates University,
United Arab Emirates

REVIEWED BY
Lilong Liu,
Huazhong University of Science and Technology, China
Dawei Yang,
Fudan University, China

*CORRESPONDENCE
Ming Chen
✉ tdyycm@163.com
Bo Yang
✉ jx321979219@163.com

†These authors have contributed equally to this work

RECEIVED 01 July 2024
ACCEPTED 08 January 2025
PUBLISHED 24 January 2025

CITATION
Wang J, Li X, Xu W, Jiang N, Yang B and Chen M (2025) Case report: The Montgomery T tube may be the preferred transition option for achieving a smooth extubation after tracheotomy when complicating airway pathology is present. *Front. Med.* 12:1457903. doi: 10.3389/fmed.2025.1457903

Case report: The Montgomery T tube may be the preferred transition option for achieving a smooth extubation after tracheotomy when complicating airway pathology is present

Jieqiong Wang[1†], Xun Li[2†], Weihua Xu[1], Nenghui Jiang[3], Bo Yang[4*] and Ming Chen[1*]

[1]Department of Pulmonary and Critical Care Medicine, Tongde Hospital of Zhejiang Province, Hangzhou, Zhejiang, China, [2]College of Medicine, Jiaxing University, Jiaxing, Zhejiang, China, [3]Department of Anesthesia Operating Room, The Second Affiliated Hospital of Jiaxing University, Jiaxing, Zhejiang, China, [4]Department of Pharmacy, Tongde Hospital of Zhejiang Province, Hangzhou, Zhejiang, China

Prolonged retention of tracheostomy tubes post-procedure often leads to complications, including granulation tissue overgrowth, airway narrowing, and laryngeal edema, necessitating delayed removal of the tracheostomy tube. Currently, a definitive therapeutic regimen capable of simultaneously resolving these complications and expediting tracheostomy decannulation remains elusive. Herein, we present an efficacious strategy addressing these airway morbidities and facilitating rapid tube removal. A 44-year-old male patient, who had undergone tracheostomy due to underlying disease, demonstrated substantial recovery following rehabilitation and was poised for tracheostomy tube extraction. However, bronchoscopic examination revealed severe granulation tissue at the stoma site and laryngeal edema, posing challenges to immediate decannulation. To tackle these issues concurrently while aiming for swift tube removal, we performed bronchoscopic intervention for granulation tissue excision, subsequently replacing the conventional tracheostomy tube with a Montgomery T tube as a transitional measure to restore normal ventilation. With additional rehabilitation fostering respiratory function enhancement, follow-up bronchoscopies confirmed no recurrence of granulations and significant reduction in laryngeal edema, thereby enabling the successful removal of the Montgomery T tube 2 months later, restoring the patient's unassisted respiratory capacity. This case underscores a clinically pertinent insight: following resolution of local airway abnormalities impeding tracheostomy decannulation, the strategic implementation of a Montgomery T tube as a transitional phase merits serious consideration among clinicians managing patients with long-term tracheostomies. Our findings contribute to the development of more streamlined approaches to overcoming complexities associated with tracheostomy tube removal in clinical practice.

KEYWORDS

tracheotomy, Montgomery T tube, tracheostomy cannula, suprastomal granulomas, case report

Introduction

For patients undergoing tracheotomy requiring an indwelling tracheostomy tube, the ultimate goal is early and safe extubation. In addition to conditions which limit extubation, complications associated with a long-term indwelling tracheostomy cannulae can occur such as infection, granulation tissue hyperplasia (1), subglottic stenosis, vocal cord paralysis, vocal cord edema, airway softening, and trachea-esophageal fistula can also lead to delayed extubation or extubation and reintubation (2, 3). Airway pathology complications, especially when Suprastomal granuloma is combined with severe vocal fold edema, further increases management difficulty. The need to address both the complications and to achieve the goal of early tracheostomy tube extubation undoubtedly complicates subsequent treatment strategy.

Here, we report the case of a patient with significant granulation tissue hyperplasia combined with severe glottic edema following tracheotomy with an indwelling tracheotomy tube. To facilitate early extubation, we performed a bronchoscopic excision of the granuloma followed by placement of a Montgomery T tube to replace the original tracheostomy tube as a transition before allowing the patient to resume normal respiration. After 2 months of rehabilitation, bronchoscopic examination showed no new edema and edema in the vocal cord area was significantly reduced. At that time the Montgomery T tube was removed and normal respiration was successfully restored. A search of the clinical literature reveals that similar cases involving this type of procedure have not been reported to date.

Case presentation

A 41-year-old male patient was admitted to the emergency ICU on April 10, 2022, with a diagnosis of "brainstem hemorrhage" resulting in "impaired consciousness for 1 day." He had a history of long term uncontrolled hypertension which resulting from failure to regularly take his medication. Due to his critical condition upon admission, tracheal intubation was performed and mannitol was given to reduce intracranial pressure along with several other treatments. Because long term ventilation was anticipated, a tracheotomy was performed on April 20, 2022 to maintain adequate respiratory support. After the initial treatment, the patient regained consciousness, blood oxygenation increased and the muscle strength in the left limb was determined to be grade 1 at that time. Ventilation was discontinued on April 26, 2022 and replaced with high-flow oxygen through the tracheotomy cannula. The patient was transferred to the Department of Respiratory and Critical Care Medicine on May 23, 2022. During this period, the patient experienced "hospital-related pneumonia," "urinary tract infection" and "catheter associated infection," however all of these conditions ameliorated following appropriate treatment. During this time, the patient became more lucid and was able to perform simple directed activities. At this point, the patient was recovery progress suggested that removal of the tracheostomy tube would permit normal respiration. However, in order to more accurately assess the condition of the airway, promptly manage possible airway complications, and reduce the risks associated with the removal of the tracheostomy tube, we performed the following procedure on July 1, 2022 under general anesthesia.

First, a ventilator was connected to the tracheostomy cannula used for respiratory support. A fiberoptic bronchoscope was introduced into the passage way of the tracheostomy tubing. This examination revealed no observable abnormalities at the lower end of the tube and in the distal extent of airway (Figure 1A).

Next, the bronchoscope was inserted through the nose to explore the pharyngeal airway region above the tracheostomy tube. It was found that severe edema and local tissue disfiguration in the pre-tracheal pharyngeal region (Figure 1B) did not permit, after several attempts, positive identification of the tracheal opening.

During the procedure, we requested that otolaryngologist use the laryngoscope observe the tissue of swollen glottic area (Figure 1C), expose the upper airway of the Tracheotomy incision. More granulomas were found in the upper airway which blocked almost the entire airway (Figure 1D).

Given the complications associated with the airway granulomatous lesions and glottic edema we hoped to remove the tracheostomy tube as soon as possible so that the patient could resume normal respiration. Therefore, an emergency multidisciplinary consultation was held with the anesthesiologist and otolaryngologist.

After consulting with them, we decided to use the laryngoscope to maintain a working channel within the airway. The granulomas were first removed using a fiberoptic bronchoscopic snare device (Figure 1E).

After removing the majority of the granuloma and establishing airway patency, the original PVC tracheostomy tube was removed and an 11-gauge Montgomery tracheal T tube was inserted (Figure 1F).

The horizontal branch of Montgomery T tube was left open postoperatively due to remaining edema in the vocal fold region. The horizontal branch of the Montgomery T tube was then plugged after edema in glottal area had subsided. The patient was evaluated to determine whether he could tolerate upper airway ventilation and was encouraged to talk and eat to simulate normal physiological activity. Around 2 weeks postoperatively, the patient was able to breathe when the Montgomery T tube horizontal branch was plugged. However, there were still excessive secretions in the patient's airway at that time, so the horizontal branch was opened regularly for fluid aspiration.

We performed a routine bronchoscopy on July 13, 2022. Microscopically we saw a partially diminished edematous condition of the glottis and surrounding tissues (Figure 2A), a well-positioned Montgomery T tube (Figure 2B), and no new granulomas in the airway (Figure 2C).

At this time, some edema remained in the glottic area (Figures 3A,B), but it did not appear to markedly affect the patient's breathing, so the Montgomery T tube was removed (Figures 3C,D). After this procedure, the patient recovered well and was able to breathe normally. At this point, the patient showed no dyspnea. The patient and their family expressed satisfaction with this.

Discussion

There is a lack of consensus regarding when a tracheostomy tube can be safely removed. Some studies suggest that extubation should be considered once the patient no longer requires mechanical ventilation, airway obstruction has been resolved, airway secretions are controlled, and swallowing function is largely restored (4, 5). Utilizing a standardized extubation protocol to guide the removal of

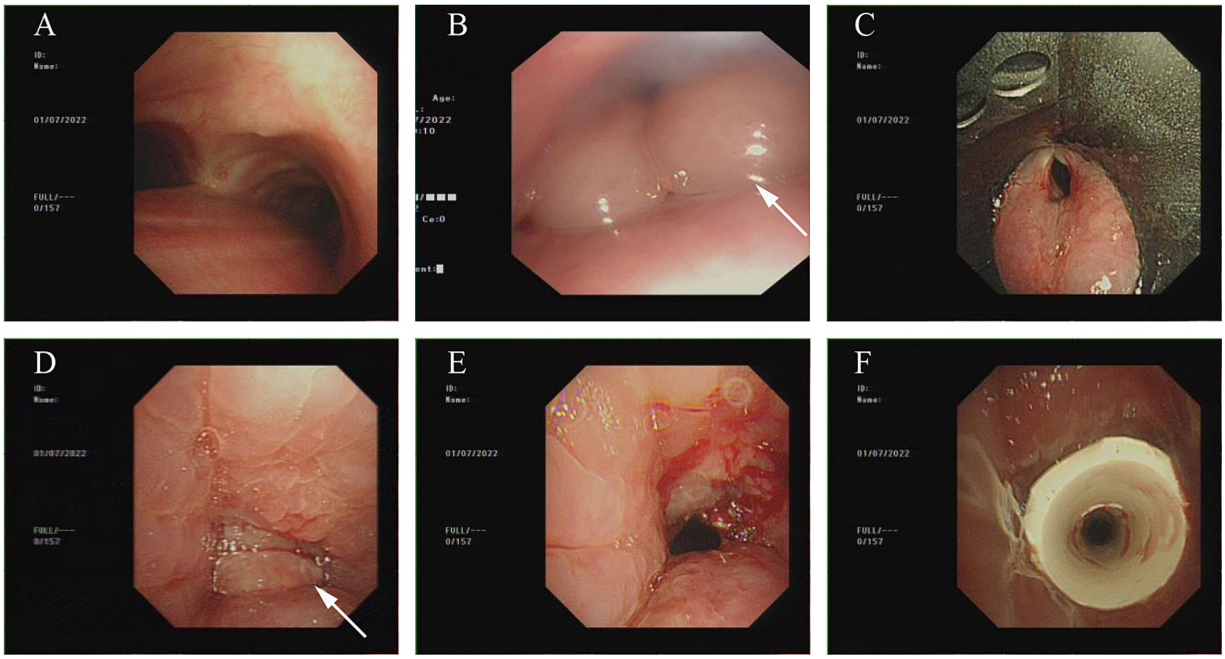

FIGURE 1
Bronchoscopy condition as of July 1, 2022. **(A)** No obvious abnormality were noted in the main airway below the tracheostomy sleeve. **(B)** Severe edema noted in throat and glottic region. **(C)** A view of severe glottal edema with support laryngoscope. **(D)** A Suprastomall granuloma obstructs the airway. **(E)** The majority of the granulomas were removed using the bronchoscope snare device allowing partial opening of the upper airway. **(F)** Montgomery T tube was inserted.

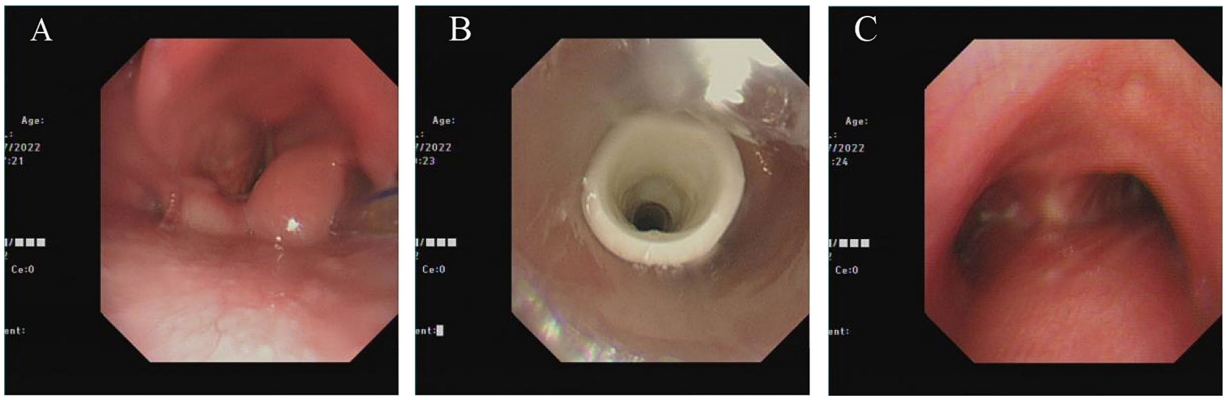

FIGURE 2
Bronchoscopy condition as of July 13, 2022. **(A)** Glottic edema was reduced, but was still obvious. **(B)** Montgomery T tube in optimal position. **(C)** No new granuloma appeared in the main part of the airway below Montgomery T tube.

tracheostomy tubes can reduce extubation time, decrease the failure rate, and minimize complications, thereby providing greater benefits to patients (6). Clearly, early and safe extubation is beneficial to the patient.

It has been shown that endoscopy to assess the presence of airway stenosis prior to the removal of the tracheostomy tube can help improve the success rate of extubation (7). Patients undergoing tracheotomy have a high probability of developing airway abnormalities. Common complications include granulation tissue hyperplasia and subglottic stenosis (8). Some researchers believe that most granulomas can be detected by bronchoscopy and that they do not significantly impact airway patency, thus not requiring special treatment. However, for patients with granulomas causing significant obstruction who require immediate extubation, aggressive management of these granulomas is necessary. In such cases, direct endoscopic resection is generally the method of choice (8, 9).

While the patient management protocol described above focuses on the attendant complications, the ultimate goal of our treatment was not only to relieve the airway obstruction caused by granulomas, but to take steps to remove the tracheostomy tube as soon as possible when sarcoidosis was anticipated to accompany the presence of an indwelling tracheotomy tube. Long-term placement of tracheostomy tubes has been shown to promote the formation of granulomas within the airway. This phenomenon is associated with the physical irritation

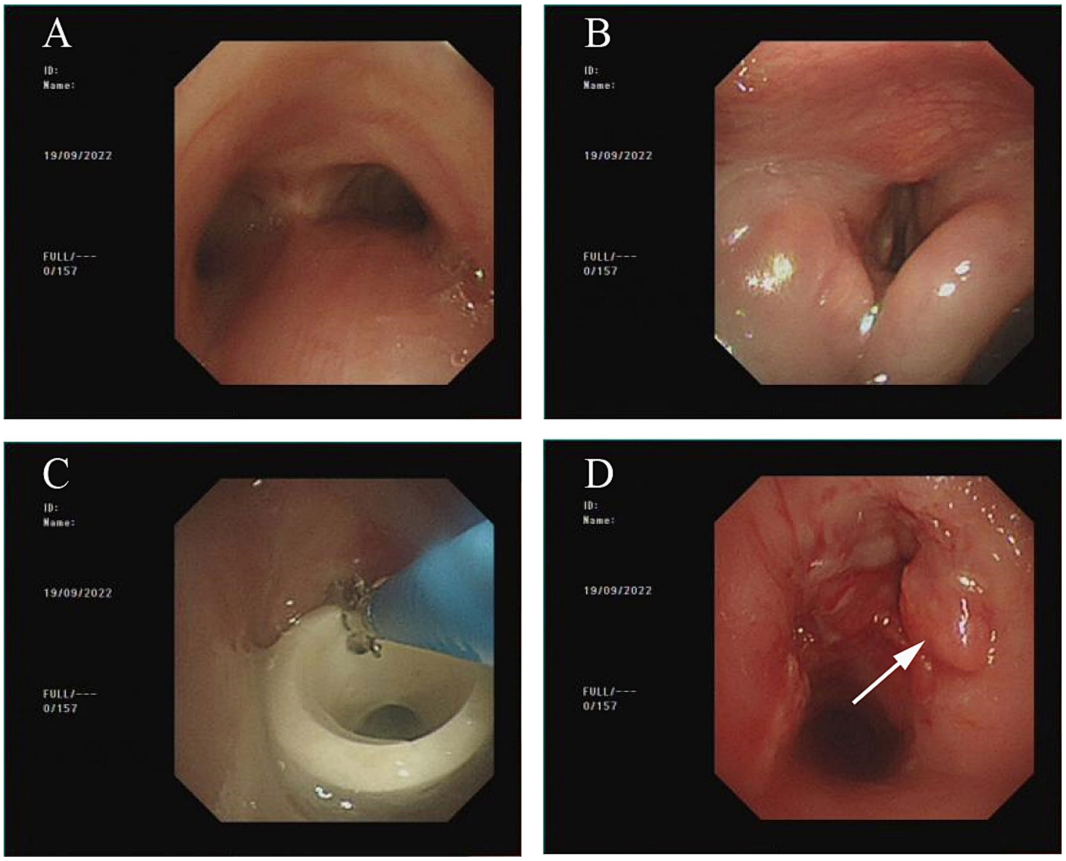

FIGURE 3
Bronchoscopy condition as of September 19, 2022. **(A)** No new granulomas noted in the airway below Montgomery T tube. **(B)** Glottic edema has notably subsided, but is not completely normal at this point. **(C)** Remove Montgomery T tube using biopsy forceps. **(D)** After removal of Montgomery T tube, the airway was essentially smooth.

caused by the presence of the tube and the excessive, non-physiological mechanical stress exerted on the airway walls (10).

When granulation tissue hyperplasia is combined with severe edema in the vocal area, subsequent treatment becomes further complicated. Even after the granulomas are eliminated, the tracheostomy tube should not be removed immediately. This is because severe asphyxiation can occur if the artificial lumen closes before the normal breathing passage reopens due to severe supraglottic edema (11).

When considering the risk of granuloma recurrence with a PVC tracheostomy cannula, a metal tracheostomy cannula can be used during the transition period. Metal tubes are usually made of silver or stainless steel and offer several advantages: durability, inhibition of bacterial growth, non-reactivity with surrounding tissue, resistance to biofilm formation, and ease of cleaning (12). A plug test can be performed to determine whether the metal tracheostomy cannula can be safely removed. However, some investigators disagree on whether the plugging test is a reliable indicator for removal of the tracheostomy cannula (13, 14).When edema is present in the vocal fold region, it is not possible to accurately determine whether effective respiration can be maintained after removing a metal tracheostomy tube. Additionally, the inability to speak affects the patient's quality of life. Rapid implementation of speech capabilities allows for more effective communication, improves swallowing function, and promotes recovery (14, 15).

Glucocorticoids have been shown to be an effective treatment during the acute phase of vocal fold edema (16, 17). However, there is no clear evidence that corticosteroids are beneficial for treating chronic vocal fold edema (18). This is because the edema only subsides after an extended period, and long-term hormonal therapy may increase the risk of complications such as secondary infections. Premature removal of the tracheostomy tube may necessitate re-intubation. Conversely, unnecessarily delaying extubation can lead to longer hospital stays and increased medical costs.

Therefore, the purpose of this report in describing the treatment of airway maintenance complications is not to focus on specific treatment measures but to present options for selecting appropriate treatment strategies. These strategies should not only effectively address urgent airway maintenance issues but also create optimal conditions for rapid extubation and the restoration of normal airway patency.

The insertion of the Montgomery T tube is primarily used to treat subglottic tracheal stenosis. It serves a dual role in supporting airway maintenance and stabilizing tracheal scarring (19). The Montgomery T tube is generally employed to address subglottic stenosis resulting from endotracheal intubation and tracheotomy. It is also utilized for

TABLE 1 Comparison of advantages and disadvantages of PVC tracheostomy tubes and Montgomery T tubes.

Characteristics/Parameters	PVC tracheostomy tube	Montgomery T tube
Replacement	Frequent, easy	Rarely needed, but complex if required
Airway complications	Common: mucosal injury, scarring, granulation, bleeding	Fewer complications; risk of stent fracture or displacement
Prevention of aspiration	Effective	Higher risk of aspiration pneumonia
Mechanical ventilation	Can connect to ventilator	Cannot connect to ventilator
Airway humidification	Requires enhanced humidification	Lower humidification needs
Microbial colonization	Higher risk	Lower risk
Speech and quality of life	Requires speaking valve, less esthetic	Easier speech, more esthetic

airway stenosis caused by rare conditions such as polychondritis (20) or glycogen storage disease (21). Additionally, the Montgomery T tube can be used both for short-term treatments and long-term management of chronic conditions like airway malacia (22).

At present, no studies have evaluated the efficacy of using a Montgomery T tube as a transitional device prior to the removal of a standard PVC tracheostomy tube or the specific circumstances that warrant its use before extubation. To provide a comprehensive comparison, we have outlined the advantages and disadvantages of PVC tracheostomy tubes versus Montgomery T tubes in Table 1.

We believe that for patients experiencing airway maintenance complications such as suprastomal granuloma combined with glottic edema, bronchoscopic granuloma resection followed by the placement of a Montgomery T tube can be beneficial prior to extubation. The Montgomery T tube's elasticity, toughness, and strong support help maintain structural integrity during long-term contact with the airway. Additionally, it exhibits good tissue compatibility and is non-toxic. Its optimal diameter, which is smaller than the airway diameter, effectively reduces irritation to the airway mucosa (23), thereby significantly decreasing the recurrence of granuloma formation at the tracheotomy incision and reducing glottic edema (24). It also allows for relatively flexible ventilation options. Approximately 2–3 days postoperatively, the horizontal branch can be closed to simulate normal respiration, depending on the resolution of inflammation, to assess whether severe edema in the vocal area impacts normal breathing. In this case, patients can attempt to breathe normally through the vertical branch about 1 week after the operation. Even with visible glottic edema, blood oxygen saturation can be maintained at over 90% at rest, suggesting that cannula removal may be possible even when some edema is still present. In our case, there was still some glottic edema when the Montgomery T tube was finally removed, but it did not affect normal respiration.

Additionally, the unique structure of the Montgomery T tube allows for the clearance of airway secretions through the lateral hole when the horizontal branch is open. When the horizontal branch is closed, patients can still speak through the vertical branch. This feature improves the patient's quality of life and facilitates smoother extubation.

In summary, this report describes the treatment of airway complications using specially selected indwelling tracheostomy cannulas. The treatment strategy outlined here can provide valuable guidance for physicians conducting respiratory interventions in similar cases.

Data availability statement

The raw data supporting the conclusions of this article will be made available by the authors, without undue reservation.

Ethics statement

The studies involving humans were approved by Medical Ethics Committee of Zhejiang Provincial Tongde Hospital. The studies were conducted in accordance with the local legislation and institutional requirements. The participants provided their written informed consent to participate in this study. Written informed consent was obtained from the individual(s) for the publication of any potentially identifiable images or data included in this article.

Author contributions

JW: Data curation, Resources, Writing – original draft. XL: Data curation, Validation, Visualization, Writing – original draft. WX: Conceptualization, Writing – review & editing. NJ: Conceptualization, Writing – review & editing. BY: Supervision, Writing – review & editing, Data curation. MC: Project administration, Resources, Validation, Visualization, Writing – review & editing.

Funding

The author(s) declare that financial support was received for the research, authorship, and/or publication of this article. This work was supported by the Zhejiang Traditional Chinese Medicine Science and Technology Plan Project (nos. 2020ZB050 and 2021AX003) and the Chai Xiujuan Famous Old TCM Expert Inheritance Studio Construction Project (no. GZS2021016).

Conflict of interest

The authors declare that the research was conducted in the absence of any commercial or financial relationships that could be construed as a potential conflict of interest.

Publisher's note

References

1. Mubashir T, Arif AA, Ernest P, Maroufy V, Chaudhry R, Balogh J, et al. Early versus late tracheostomy in patients with acute traumatic spinal cord injury: a systematic review and Meta-analysis. *Anesth Analg*. (2021) 132:384–94. doi: 10.1213/ANE.0000000000005212

2. Meenan K, Bhatnagar K, Guardiani E. Intubation-related laryngeal pathology precluding tracheostomy Decannulation: incidence and associated risk factors. *Ann Otol Rhinol Laryngol*. (2021) 130:1078–84. doi: 10.1177/0003489421995285

3. Fernandez-Bussy S, Mahajan B, Folch E, Caviedes I, Guerrero J, Majid A. Tracheostomy tube placement: early and late complications. *J Bronchol Interv Pulmonol*. (2015) 22:357–64. doi: 10.1097/LBR.0000000000000177

4. Cheung NH, Napolitano LM. Tracheostomy: epidemiology, indications, timing, technique, and outcomes. *Respir Care*. (2014) 59:895–915. doi: 10.4187/respcare.02971

5. Rosero EB, Corbett J, Mau T, Joshi GP. Intraoperative airway management considerations for adult patients presenting with tracheostomy: a narrative review. *Anesth Analg*. (2021) 132:1003–11. doi: 10.1213/ANE.0000000000005330

6. Komori M. Update on pediatric tracheostomy. *Auris Nasus Larynx*. (2024) 51:429–32. doi: 10.1016/j.anl.2024.01.003

7. Muhle P, Suntrup-Krueger S, Burkardt K, Lapa S, Ogawa M, Claus I, et al. Standardized endoscopic swallowing evaluation for tracheostomy Decannulation in critically ill neurologic patients - a prospective evaluation. *Neurol Res Pract*. (2021) 3:26. doi: 10.1186/s42466-021-00124-1

8. Al Bahri K, Liu CC. Surveillance endoscopy in pediatric tracheostomy: a systematic review. *Int J Pediatr Otorhinolaryngol*. (2021) 140:110533. doi: 10.1016/j.ijporl.2020.110533

9. Liu CC, Soares JJ, Elder L, Hill L, Abts M, Bonilla-Velez J, et al. Surveillance endoscopy after tracheostomy placement in children: findings and interventions. *Laryngoscope*. (2020) 130:1327–32. doi: 10.1002/lary.28247

10. Marchioni A, Tonelli R, Andreani A, Cappiello GF, Fermi M, Trentacosti F, et al. Molecular mechanisms and physiological changes behind benign tracheal and subglottic stenosis in adults. *Int J Mol Sci*. (2022) 23:2421. doi: 10.3390/ijms23052421

11. Cui W, Xiang J, Deng X, Qin Z. Difficult tracheostomy decannulation related to nasogastric tube syndrome: a case report. *Int J Surg Case Rep*. (2023) 110:108734. doi: 10.1016/j.ijscr.2023.108734

12. Hess DR, Altobelli NP. Tracheostomy tubes. *Respir Care*. (2014) 59:956. doi: 10.4187/respcare.02920

13. Flanagan F, Healy F. Tracheostomy decision making: from placement to decannulation. *Semin Fetal Neonatal Med*. (2019) 24:101037. doi: 10.1016/j.siny.2019.101037

14. Wirtz N, Tibesar RJ, Lander T, Sidman J. A pediatric Decannulation protocol: outcomes of a 10-year experience. *Otolaryngol Head Neck Surg*. (2016) 154:731–4. doi: 10.1177/0194599816628522

15. McGrath BA, Wallace S, Wilson M, Nicholson L, Felton T, Bowyer C, et al. Safety and feasibility of above cuff vocalisation for ventilator-dependant patients with tracheostomies. *J Intensive Care Soc*. (2019) 20:59–65. doi: 10.1177/1751143718767055

16. Ochi N, Yamane H, Honda Y, Takigawa N. Accidental aspiration of denture cleanser tablets caused severe mucosal edema in upper airway. *Clin Respir J*. (2018) 12:291–4. doi: 10.1111/crj.12468

17. Murphy Estes C, Chadwick K, Sadoughi B, Andreadis K, Sussman S, Sulica L. Performers' perceptions of vocal function during Oral steroid treatment of vocal fold edema. *Laryngoscope*. (2022) 132:2434–41. doi: 10.1002/lary.30072

18. Kovacs A, Haran S, Paddle P. Chronic non-granulomatous supraglottitis of a male adolescent and its successful management with azathioprine. *BMJ Case Rep*. (2019) 12:e227458. doi: 10.1136/bcr-2018-227458

19. Hu H, Zhang J, Wu F, Chen E. Application of the Montgomery T-tube in subglottic tracheal benign stenosis. *J Thorac Dis*. (2018) 10:3070–7. doi: 10.21037/jtd.2018.05.140

20. Jeong N, Jang HJ, Lee JH, Kim HK, Park JH, Lee YJ, et al. A case of tracheobronchomalacia due to relapsing polychondritis treated with Montgomery T-tube. *SAGE Open Med Case Rep*. (2019) 7:2050313X19832164. doi: 10.1177/2050313X19832164

21. Soni-Jaiswal A, Penney SE, Jones SA, Walker R, Rothera MP, Bruce IA. Montgomery T-tubes in the management of multilevel airway obstruction in mucopolysaccharidosis. *Int J Pediatr Otorhinolaryngol*. (2014) 78:1763–8. doi: 10.1016/j.ijporl.2014.06.015

22. Shi S, Chen D, Li X, Wen W, Shen X, Liu F, et al. Outcome and safety of the Montgomery T-tube for laryngotracheal stenosis: a single-center retrospective analysis of 546 cases. *J Otorhinolaryngol Relat Spec*. (2014) 76:314–20. doi: 10.1159/000362244

23. Wahidi MM, Ernst A. The Montgomery T-tube tracheal stent. *Clin Chest Med*. (2003) 24:437–43. doi: 10.1016/s0272-5231(03)00042-x

24. Rizzi MD, Thorne MC, Zur KB, Jacobs IN. Laryngotracheal reconstruction with posterior costal cartilage grafts: outcomes at a single institution. *Otolaryngol Head Neck Surg*. (2009) 140:348–53. doi: 10.1016/j.otohns.2008.11.035

frontiers | Frontiers in Medicine

TYPE Case Report
PUBLISHED 29 January 2025
DOI 10.3389/fmed.2025.1517389

OPEN ACCESS

EDITED BY
Giuseppe Fiorentino,
Colli Hospital, Italy

REVIEWED BY
Simona Alexandra Iacob,
Carol Davila University of Medicine and Pharmacy, Romania
Naheel Alamer,
Imam Abdulrahman Bin Faisal University, Saudi Arabia

*CORRESPONDENCE
Jian Zhu
zhujian0718@126.com
Xiang Yue
xibeixing@163.com
Wei Wen
wenwei@jsph.org.cn

†These authors have contributed equally to this work and share first authorship

RECEIVED 26 October 2024
ACCEPTED 03 January 2025
PUBLISHED 29 January 2025

CITATION
Zhang F, Wang J-L, Zhu J, Si S, Guo H, Yue X and Wen W (2025) When a sore throat turns into deadly multiple serous cavity effusions: the role of *Prevotella oris* in rapidly progressing infection—a case report. *Front. Med.* 12:1517389. doi: 10.3389/fmed.2025.1517389

When a sore throat turns into deadly multiple serous cavity effusions: the role of *Prevotella oris* in rapidly progressing infection—a case report

Fangqi Zhang[1†], Juan-Li Wang[2†], Jian Zhu[3*†], Shaokui Si[1], Hao Guo[4], Xiang Yue[4*] and Wei Wen[5*]

[1]Department of Pulmonary and Critical Care Medicine, The 987th Hospital of Joint Logistics Support Force of People's Liberation Army, Baoji, China, [2]Department of Child Healthcare, The Third Hospital of Wuhan, Wuhan, China, [3]Department of Thyroid and Breast Surgery, General Hospital of Central Theater Command of the People's Liberation Army, Wuhan, China, [4]Department of Thoracic Cardiovascular Surgery, The 987th Hospital of Joint Logistics Support Force of People's Liberation Army, Baoji, China, [5]Department of Thoracic Surgery, The First Affiliated Hospital with Nanjing Medical University, Nanjing, China

Severe infections that develop rapidly from ordinary symptoms not only increase patient misunderstandings but also lead to excessive detection of these symptoms by physicians. This case study describes a 19-year-old male individual who initially presented with a sore throat and subsequently developed multiple serous cavity effusions that lead to septic pulmonary embolism and septic shock. After multiple cultures of the patient's sputum yielded no identifiable pathogenic bacteria, the metagenomic next-generation sequencing (mNGS) revealed *Prevotella oris* as the predominant pathogen present in both the patient's peripheral blood and the pericardial drainage fluid. The subsequent antibiotic treatment, guided by the mNGS results, along with surgical drainage and mediastinal irrigation, effectively controlled and ultimately cured the patient's condition. This case is unique because it is the first to show that normally colonizing *Prevotella* can also cause fatal multiorgan infection as an opportunistic pathogen in a previously healthy young person with no immune-related diseases. The aim of this study is to expand clinical awareness of this common symptom and its potentially fatal outcome.

KEYWORDS

polyserous effusions, *Prevotella*, sore throat, necrotizing mediastinitis, case report

Introduction

Prevotella is often considered part of the Bacteroides complex, commonly associated with a healthy plant-based diet, and acts as a probiotic in the human body, throughout the entire digestive tract, from the mouth to the anus (1, 2). It can survive in atmospheric oxygen concentrations for up to 3 days (3).

Previous reports have shown that *Prevotella* species can lead to pleural infection (4, 5). However, there are no published reports discussing fatal multiple serous cavity effusions caused by *Prevotella oris* in a previously healthy young person with no immune-related diseases. This case study presents a 19-year-old male who initially presented with a sore throat and subsequently developed multiple serous cavity effusions, which led to septic pulmonary embolism and septic shock caused by *Prevotella oris*.

Case report

A 19-year-old male automobile manufacturing worker, previously healthy with no history of immune-related diseases, presented with a sore throat and fever lasting 1 day, with a maximum temperature of 38.9°C. He had neither a history of specific infectious diseases nor any exposure to pollen or pets. He denied a family history of hereditary diseases. He was diagnosed with tonsillitis at a community hospital and received cefixime treatment for 3 days. However, his condition did not improve, and he developed swelling on the right side of his neck. The computed tomography (CT) examination revealed no obvious abnormalities in the lungs or the chest cavity but showed suspicious swelling of the soft tissue on the right side of the neck (see Figure 1). The hemograms revealed a leukocyte count of 16.86×10^9/L (normal range: $3.5–9.5 \times 10^9$/L) and a neutrophil count of 93.6%. Based on these results, he was treated with intravenous moxifloxacin. Two days later, the above-mentioned symptoms continued to worsen, and he developed chest pain and shortness of breath. He was then admitted to the hospital. When asked about his recent lifestyle habits, he denied drinking probiotic drinks or consuming functional dairy products. He also denied eating raw or unclean food, including during the period of antibiotic treatment. The physical examination revealed an acute disease presentation, with pharyngeal congestion, bilateral tonsil enlargement (grade II), evident neck swelling, rapid breathing (45 breaths per min), audible wet rales in both upper lungs, diminished respiratory sounds in both lower lungs, a heart rate of 134 beats per min, a consistent rhythm, distant heart sounds, and abdominal tenderness. The dental examination revealed mild swelling of his gums, no decayed teeth, and good oral hygiene. He underwent a chest CT re-examination, which showed a large amount of fluid in the chest, pericardial, and abdominal cavities. The right lung was infected by a scattered pattern (see Figure 2). The microbiological testing of the pharyngeal swab did not detect the flu, coronavirus, or any bacterial microorganisms. The laboratory tests, including HIV tests and T-SPOT-TB tests, were negative. The hemograms revealed a leukocyte count of 25.74×10^9/L, with a neutrophil percentage (NEUT%) of 92.1%. Other results included a C-reactive protein level of 265.76 mg/L, procalcitonin of 4.2 ng/mL, albumin of 23.2 g/L, and the following arterial blood gas values (with 5 L/min oxygen mask): pH 7.39, PO2 80 mmHg, PCO2 36 mmHg, and lactate (Lac) 2.3 mmol/L. Therefore, he underwent emergency tracheal intubation and ventilator-assisted breathing, and his treatment regimen was changed to a combination of meropenem and linezolid as broad-spectrum antibiotics for severe sepsis.

Then, he underwent closed thoracic drainage for diagnosis and treatment, during which 1,000 mL of red and white, gradually stratified, turbid fluid was removed, emitting a foul odor. During this period, the patient was repeatedly cultured for bacteria, tuberculosis, and fungi in the pus, blood, and sputum collected from the breathing tube, and no positive findings were observed. The biochemical examination of the pleural effusion showed a WBC count of 172.11×10^9/L, a NEUT percentage of 91.0%, and a RBC count of (2+). Pericardial puncture fluid was also obtained, and the thoracic cavity, pericardial drainage fluid, and peripheral blood were examined for pathogenic bacteria using metagenomic next-generation sequencing (mNGS), which identified a large number of *Prevotella oris* (see Figure 3). A figure explicitly showcasing this timeline with clinical and diagnostic milestones is presented in Figure 4.

Subsequent antibiotic treatment, guided by the mNGS results, included intravenous piperacillin-tazobactam and metronidazole, along with aggressive surgical flushing and continuous drainage of the multilocular cavity. Within a few days, the patient made a rapid recovery, with a return to normal body temperature, resolution of respiratory symptoms, and quick healing of the drain site. Three months after discharge, the patient's CT re-examination showed that the lesion had mostly resolved (see Figure 5), and he expressed great satisfaction with the diagnosis and treatment he received during his hospital stay.

Discussion

The patient was a young adult with a healthy immune system. The main complaint was pharyngeal pain accompanied by fever, with the pain persisting throughout the course of the disease. The patient's condition rapidly progressed from neck symptoms (right-side neck swelling) to chest symptoms (pleural and pericardial effusions), eventually leading to fatal multiple serous cavity effusions. Factors that contributed to the progression to sepsis with *Prevotella oris* included the lack of positive results from the pathogen cultures and insufficient knowledge about infections caused by *Prevotella oris*. The key to obtaining an accurate diagnosis is recognizing that the patient has a typical persistent fever and the evidence of elevated white blood cells.

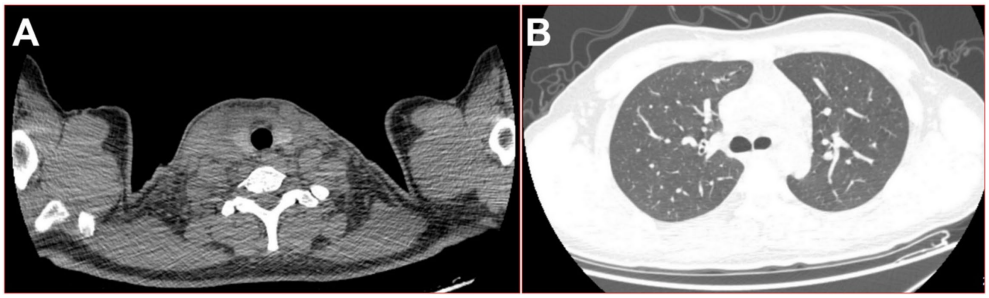

FIGURE 1
On the fourth day of the fever, 16-slice computed tomography (CT) images of the patient were obtained. **(A)** Swelling of the right side of the neck soft tissue; **(B)** lung window in the upper thoracic cavity.

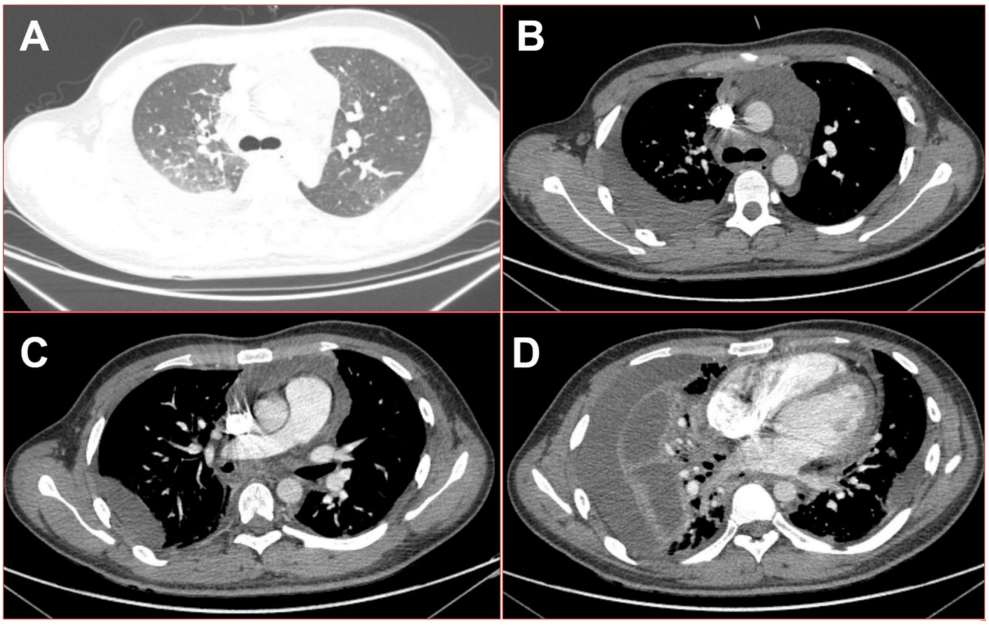

FIGURE 2
On the seventh day of the fever, 16-slice computed tomography images of the patient's chest revealed multiple serous cavity effusions. **(A)** Lung window in the upper thoracic cavity; **(B)** mediation window in the upper thoracic cavity; **(C)** mediation window in the middle part of the thoracic cavity; **(D)** mediation window in the lower thoracic cavity.

Moreover, rapid progression of the disease is not characteristic of tuberculous multiple serous cavity effusions. The patient was treated with a broad spectrum of antibiotics, and although the disease continued to progress, no positive findings were observed in the pus, blood, or sputum pathogen cultures. This indicates that the likelihood of detecting *Prevotella oris* in the blood or sputum pathogen cultures was low.

The presence of a red and white stratified turbid liquid suggested the possibility of chylous fluid. However, chylous fluid rarely causes symptoms of infection. Furthermore, there are three main causes of chylous leakage: (1) trauma, such as closed or open injuries to the neck and chest (6); (2) obstruction, such as lymphoma, metastatic cancer, or mediastinal granuloma (7); and (3) congenital thoracic duct hypoplasia or fistula formation (8). Other causes include tuberculosis, cirrhosis, sarcoidosis, and lymphatic malformations (9). The patient in this case had no history of neck trauma. Obstruction and congenital thoracic duct hypoplasia or fistula formation often occur in the abdomen, primarily affecting children. The symptoms and signs presented in this case were not consistent with the aforementioned etiologies or the disease characteristics of chylous fluid.

After escalating the empirical broad-spectrum antibiotic treatment, the patient continued to progress, and septic shock developed. Meanwhile, the patient's sputum drawn from the breathing tube was cultured repeatedly, but no obvious positive pathogenic bacteria were found. Fortunately, *Prevotella oris* was accurately detected as the pathogen using mNGS, which is theoretically able to detect any pathogen with a known genome sequence (10).

Prevotella is a genus of obligate anaerobic Bacteroides that colonize the human body extensively by binding to or attaching to other bacteria, rather than epithelial cells (1, 2, 11). *Prevotella* has a natural antibiotic resistance gene that prevents its elimination (12). When abundant, it is beneficial to human health and acts as a probiotic that can break down proteins and carbohydrates (1, 2, 13). It is even sold as an important ingredient in health drinks in some regions. However, this patient denied drinking probiotic drinks or consuming functional dairy products, and he also denied eating raw or unclean food. According to previous literature, the high abundance of this genus may be associated with diseases such as infections and hypertension (14, 15).

Prevotella oris, a species of the *Prevotella* genus, is commonly found in the mouth and causes periodontitis, but there have been few reports of it outside the oral cavity. *Prevotella* species, particularly *Prevotella intermedia* and *Prevotella denticola*, are notable for their role as opportunistic pathogens in various diseases, especially periodontitis. These Gram-negative anaerobic bacteria possess several virulence factors that enable them to adhere to host tissues, evade immune responses, and disrupt normal physiological processes. One of the primary virulence factors of *Prevotella* spp. is their ability to produce enzymes, such as cysteine proteases, which play a significant role in tissue degradation and immune evasion. These enzymes can degrade host proteins, thereby facilitating bacterial invasion and persistence in inflamed tissues. In addition, *Prevotella* species express adhesins that enhance their ability to bind to host cells, promoting colonization and biofilm formation. The interaction between *Prevotella* and other oral bacteria, such as *Streptococcus mutans*, can further enhance their virulence by creating a synergistic environment that supports the development of hypervirulent biofilms, which are more resistant to antimicrobial treatments (16, 17). The expression of virulence factors in *Prevotella* spp. is influenced by various environmental conditions, including the presence of host-derived signals and the local microenvironment within the oral cavity or inflamed tissues. For instance, the inflammatory milieu, characterized by elevated levels of cytokines

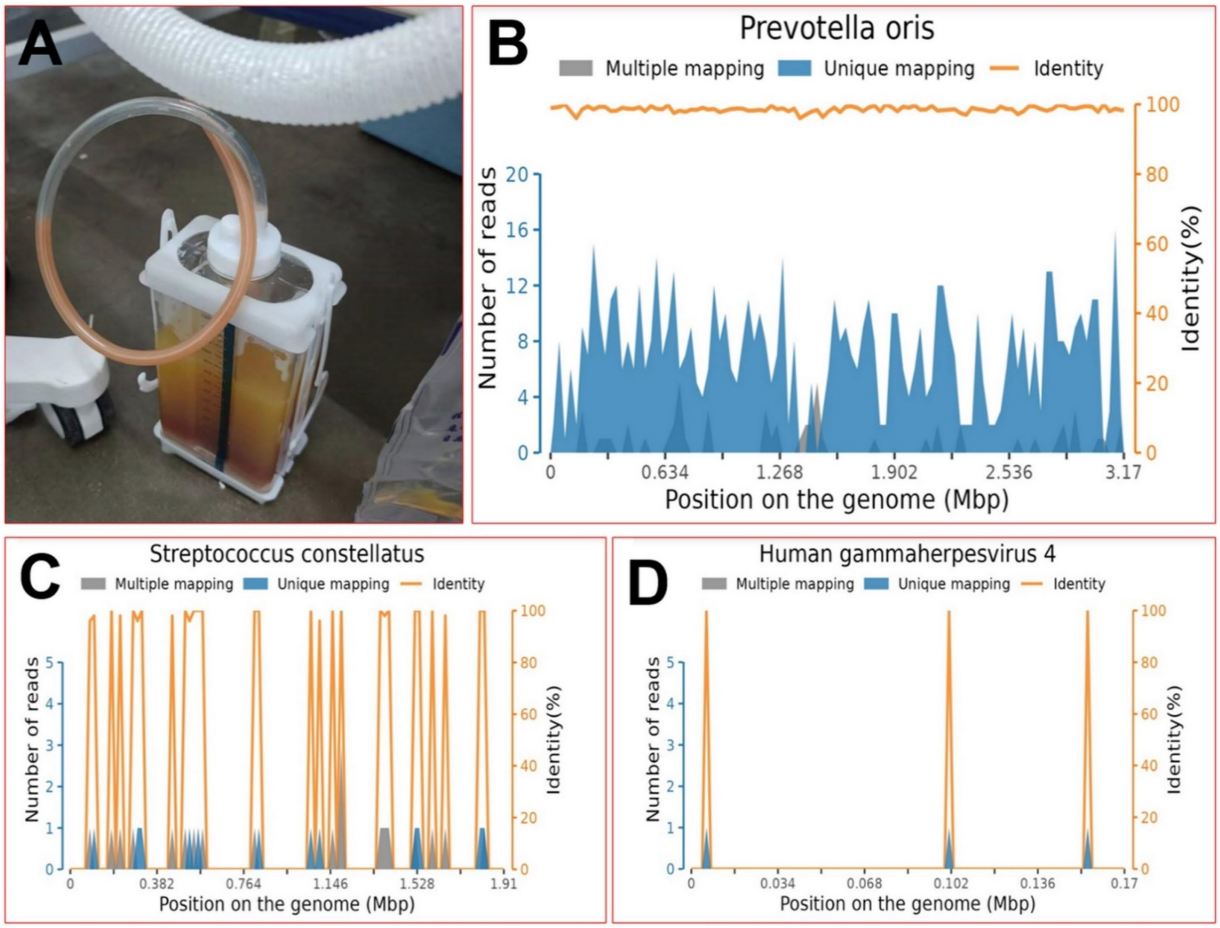

FIGURE 3
On the seventh day of the fever, the diagnosis was determined. **(A)** Appearance of pleural effusion; **(B)** position map of *P. oleracea* via metagenomic next-generation sequencing; **(C)** position map of *S. constellatus* via metagenomic next-generation sequencing; **(D)** position map of *HGM4* via metagenomic next-generation sequencing.

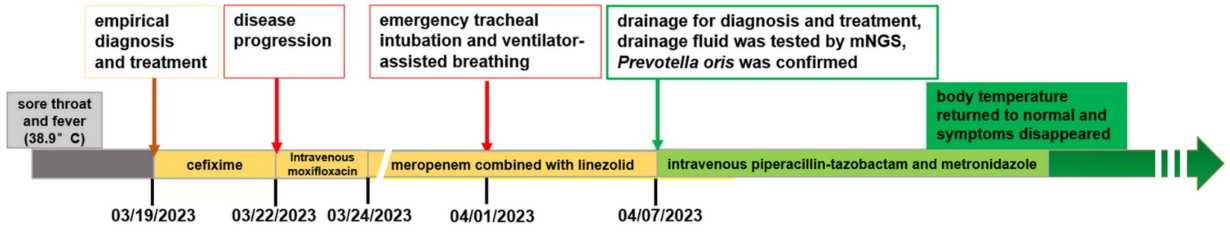

FIGURE 4
A figure explicitly showcasing the timeline with clinical and diagnostic milestones in this case.

and other immune mediators, can upregulate the expression of virulence genes in these bacteria. This response is critical during periods of dysbiosis, where the balance of microbial communities is disrupted, allowing *Prevotella* to thrive and contribute to disease progression (18). Furthermore, fatal multiple serous cavity effusions caused by *Prevotella oris* have not been reported.

On a microscopic level, *Prevotella oris* in the oropharynx can enter the lung microbiota through trace aspiration (19). Based on the theory of the gut–lung axis, *Prevoiella* in the gut may connect to and colonize the lung flora through the gut–lung axis and other pathways, resulting in similar trends of colonization by *Prevotella* in both the gut and lungs, as well as the crossover of dominant microbial communities (20). Research has indicated that the gut microbiota can produce various metabolites that enter the bloodstream and reach the lungs, where they can modulate immune responses. Short-chain fatty acids (SCFAs), for example, are produced by gut bacteria and have been shown to exert anti-inflammatory effects in the lungs. This underscores the potential therapeutic role of probiotics and prebiotics in managing respiratory diseases by restoring gut microbiota balance and enhancing gut–lung axis communication (20). Furthermore, the

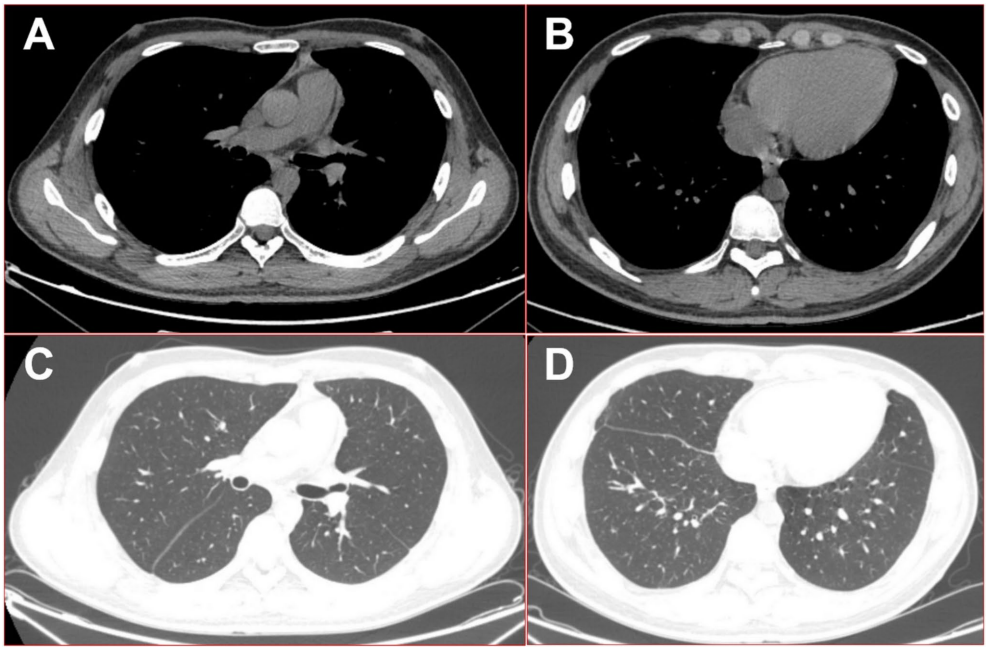

FIGURE 5
16-slice computed tomography images of the chest were obtained during the follow-up after the patient was cured. **(A)** Mediation window in the upper thoracic cavity; **(B)** mediation window in the lower thoracic cavity; **(C)** lung window in the upper thoracic cavity; **(D)** lung window in the lower thoracic cavity.

interplay between gut microbiota and lung health is not limited to inflammation; it also encompasses the modulation of immune cell activity and the regulation of systemic inflammation, both of which are crucial for preventing respiratory diseases.

In clinical practice, the accepted route of infection is through the oropharynx, which includes the submandibular space, parapharyngeal space, and retropharyngeal space, and is composed of the superficial, middle, and deep layers of the deep cervical fascia (21). Therefore, as in this case, *Prevotella* was likely the cause of the oropharyngeal infection that spread into these spaces and the mediastinum under centripetal force, causing pleural and pericardial effusions and subsequent hypoproteinaemia, which led to abdominal effusion and systemic polyscreening.

Early detection of pathogenic bacteria and multidisciplinary team discussions are essential for rapidly progressing multiple serous cavity effusions infections to obtain targeted treatment and avoid adverse prognoses (22). Detecting *Prevotella* species, particularly in clinical and environmental contexts, requires a nuanced understanding of their properties as anaerobic, Gram-negative bacteria. Their detection can be challenging due to their fastidious nature and the limitations of traditional culture methods. One effective approach for detecting *Prevotella* spp. involves the use of molecular techniques such as quantitative polymerase chain reaction (qPCR). This method has been utilized to develop species-specific primers that enhance the sensitivity and specificity of detection. For instance, a study designed specific primers based on the nucleotide sequence of a previously cloned DNA probe, which allowed for the accurate identification of *Prevotella nigrescens* in clinical samples (23). Furthermore, the application of metagenomic next-generation sequencing (mNGS) has proven beneficial in identifying rare pathogens such as *Prevotella intermedia*, which was detected in cerebrospinal fluid, showcasing the potential of advanced sequencing technologies in clinical diagnostics (24). In addition to molecular methods, the use of selective culture media can significantly improve the recovery of *Prevotella* species from clinical specimens. A systematic screening of various microbiological media has been shown to enrich for previously uncultivated target species associated with periodontal health or disease (25). This approach not only aids in isolating these bacteria but also provides insights into their ecological roles within the microbiome. Moreover, the dynamics of *Prevotella* spp. in the human gut microbiota have been extensively studied, revealing their complex interactions with other microbial communities and their implications for health. For example, a longitudinal study highlighted the transient nature of *Prevotella* abundance, suggesting that environmental factors and dietary habits can influence their detection and prevalence in the gut (26). This underscores the importance of considering both the biological and environmental contexts when developing detection strategies for *Prevotella* spp. Adequate clinical symptoms, signs, and medical imaging are also essential (4, 27, 28).

In summary, this case study exemplifies the complex journey of a physician's diagnosis and treatment of a previously healthy young man who experienced the progression of an infection, from an oral infection to multiple serous cavity effusions. Through this intricate process, the detrimental effects of *Prevotella oris* as a prevalent probiotic pathogen are highlighted, emphasizing its potential for disastrous consequences. This case study offers valuable insights into understanding a category of infectious diseases characterized by typical clinical symptoms but with severe outcomes, ultimately aiming to mitigate medical disputes and enhance the management of rare diseases.

Data availability statement

The original contributions presented in the study are included in the article/supplementary material, further inquiries can be directed to the corresponding authors.

Ethics statement

Written informed consent was obtained from the individual(s) for the publication of any potentially identifiable images or data included in this article.

Author contributions

FZ: Data curation, Formal analysis, Investigation, Writing – review & editing. J-LW: Funding acquisition, Writing – original draft. JZ: Funding acquisition, Investigation, Methodology, Project administration, Resources, Software, Supervision, Validation, Visualization, Writing – original draft, Writing – review & editing. SS: Data curation, Methodology, Resources, Writing – review & editing. HG: Data curation, Methodology, Writing – review & editing. XY: Data curation, Investigation, Methodology, Writing – review & editing. WW: Formal analysis, Funding acquisition, Investigation, Methodology, Writing – review & editing.

Funding

The author(s) declare that financial support was received for the research, authorship, and/or publication of this article. This work was supported by the "Three Heroes and One Team" Talent Project of the Central Theater Command General Hospital of the People's Liberation Army (no. 2023–1692) and the National Natural Scientific Foundation of People's Republic of China's General Program (no. 61971118).

Conflict of interest

The authors declare that the research was conducted in the absence of any commercial or financial relationships that could be construed as a potential conflict of interest.

Generative AI statement

The author(s) declare that no Gen AI was used in the creation of this manuscript.

Publisher's note

References

1. Tett A, Huang KD, Asnicar F, Fehlner-Peach H, Pasolli E, Karcher N, et al. The *Prevotella copri* complex comprises four distinct clades underrepresented in westernized populations. *Cell Host Microbe*. (2019) 26:666–679.e7. doi: 10.1016/j.chom.2019.08.018

2. Plummer EL, Sfameni AM, Vodstrcil LA, Danielewski JA, Murray GL, Fehler G, et al. Prevotella and Gardnerella are associated with treatment failure following first-line antibiotics for bacterial vaginosis. *J Infect Dis*. (2023) 228:646–56. doi: 10.1093/infdis/jiad261

3. Mangalam AK, Murray J. Microbial monotherapy with *Prevotella histicola* for patients with multiple sclerosis. *Expert Rev Neurother*. (2019) 19:45–53. doi: 10.1080/14737175.2019.1555473

4. Viswanath LS, Gunalan A, Jamir I. *Prevotella oris*: A lesser known etiological agent of pleural effusion. *Anaerobe*. (2022) 78:102644. doi: 10.1016/j.anaerobe.2022.102644

5. Cobo F, Lara-Oya A, Correa I, Rodríguez-Guerrero E, Pérez-Carrasco V, García-Salcedo JA, et al. Two rare cases of pleural infection due to Prevotella species. *Rev Esp Quimioter*. (2022) 35:503–5. doi: 10.37201/req/046.2022

6. Zheng X, Yang X, Lei S. Chylous leakage after esophagectomy for esophageal cancer: a systematic review. *J Cardiothorac Surg*. (2024) 19:240. doi: 10.1186/s13019-024-02764-1

7. Roumi Jamal B, Breim F, Souleman S, Maarawi G, Morjan M. Successful surgical treatment of congenital chylous ascites co-existed with congenital hypothyroidism: A rare case report. *Int J Surg Case Rep*. (2023) 111:108884. doi: 10.1016/j.ijscr.2023.108884

8. Gil González Y, Laseca-Modrego M, Arencibia-Sánchez O, González García-Cano D, Martin Martinez AI. Chylous ascites secondary to retroperitoneal Para-aortic lymphadenectomy: a case report. *Cureus*. (2022) 14:e22560. doi: 10.7759/cureus.22560

9. Duletzke NT, Kiraly LN, Martindale RG. Chylothorax and chylous ascites: overview, management, and nutrition. *Nutr Clin Pract*. (2023) 38:557–63. doi: 10.1002/ncp.10973

10. Li M, Wang B, Liu P, Wang H, Zhu J. Prostatitis as initial manifestation of *Chlamydia psittaci* pneumonia diagnosed by metagenome next-generation sequencing: a case report. *Open Life Sci*. (2023) 18:20220596. doi: 10.1515/biol-2022-0596

11. Gorvitovskaia A, Holmes SP, Huse SM. Interpreting Prevotella and Bacteroides as biomarkers of diet and lifestyle. *Microbiome*. (2016) 4:15. doi: 10.1186/s40168-016-0160-7

12. Ye S, Li S, Su C, Shi Z, Li H, Hong J, et al. Characterization of microbial community and antibiotic resistome in intra urban water. *Wenzhou China Front Microbiol*. (2023) 14:1169476. doi: 10.3389/fmicb.2023.1169476

13. Zhao Y, Feng Y, Ye Q, Hu J, Feng Y, Ouyang Z, et al. The oral microbiome in young women at different stages of periodontitis: Prevotella dominant in stage III periodontitis. *Front Cell Infect Microbiol*. (2022) 12:1047607. doi: 10.3389/fcimb.2022.1047607

14. Larsen JM. The immune response to Prevotella bacteria in chronic inflammatory disease. *Immunology*. (2017) 151:363–74. doi: 10.1111/imm.12760

15. Li J, Zhao F, Wang Y, Chen J, Tao J, Tian G, et al. Gut microbiota dysbiosis contributes to the development of hypertension. *Microbiome*. (2017) 5:14. doi: 10.1186/s40168-016-0222-x

16. Könönen E, Fteita D, Gursoy UK, Gursoy M. Prevotella species as oral residents and infectious agents with potential impact on systemic conditions. *J Oral Microbiol*. (2022) 14:2079814. doi: 10.1080/20002297.2022.2079814

17. Niu Y, Zhang C, Sun Y, Dong L, Si Y, Yang J, et al. Symbiotic relationship between Prevotella denticola and *Streptococcus mutans* enhances virulence of plaque biofilms. *Arch Oral Biol*. (2023) 151:105714. doi: 10.1016/j.archoralbio.2023.105714

18. Dahlen G, Basic A, Bylund J. Importance of virulence factors for the persistence of Oral Bacteria in the inflamed gingival crevice and in the pathogenesis of periodontal disease. *J Clin Med*. (2019) 8:1339. doi: 10.3390/jcm8091339

19. Ermolenko E, Kotyleva M, Kotrova A, Tichonov S, Lavrenova N, Voropaeva L, et al. Consortium of indigenous fecal Bacteria in the treatment of metabolic syndrome. *Microorganisms*. (2022) 10:1574. doi: 10.3390/microorganisms10081574

20. Narayana JK, Aliberti S, Mac Aogáin M, Jaggi TK, Ali NABM, Ivan FX, et al. Microbial dysregulation of the gut-lung Axis in bronchiectasis. *Am J Respir Crit Care Med*. (2023) 207:908–20. doi: 10.1164/rccm.202205-0893OC

21. Ogura I, Minami Y, Sugawara Y, Mizuhashi R, Mizuhashi F, Oohashi M, et al. Odontogenic infection pathway to the Parapharyngeal space: CT imaging assessment. *J Maxillofac Oral Surg*. (2022) 21:235–9. doi: 10.1007/s12663-020-01401-3

22. Walkty A, Embil J. Lemierre's Syndrome. *N Engl J Med*. (2019) 380:e16. doi: 10.1056/NEJMicm1808378

23. Kim MJ, Lee YS, Park JY, Kook JK. Development of *Prevotella nigrescens*-specific PCR primers based on the nucleotide sequence of a Pn23 DNA probe. *Anaerobe*. (2011) 17:32–5. doi: 10.1016/j.anaerobe.2010.12.005

24. Ye Z, He J, Ji H, Xu H, Zhang Y, Zhou K, et al. Case report: isolated *prevotella intermedia* causing intracranial infection detected using metagenomic next generation sequencing. *BMC Neurol*. (2023) 23:383. doi: 10.1186/s12883-023-03374-5

25. Davis IJ, Bull C, Horsfall A, Morley I, Harris S. The Unculturables: targeted isolation of bacterial species associated with canine periodontal health or disease from dental plaque. *BMC Microbiol*. (2014) 14:196. doi: 10.1186/1471-2180-14-196

26. Han N, Peng X, Zhang T, Qiang Y, Li X, Zhang W. Temporal dynamics and species-level complexity of Prevotella spp. in the human gut microbiota: implications for enterotypes and health. *Front Microbiol*. (2024) 15:1414000. doi: 10.3389/fmicb.2024.1414000

27. Wu XY, Ding F, Li K, Huang WC, Zhang Y, Zhu J. Analysis of the causes of solitary pulmonary nodule misdiagnosed as lung Cancer by using artificial intelligence: a retrospective study at a single center. *Diagnostics*. (2022) 12:2218. doi: 10.3390/diagnostics12092218

28. Civen R, Jousimies-Somer H, Marina M, Borenstein L, Shah H, Finegold SM. A retrospective review of cases of anaerobic empyema and update of bacteriology. *Clin Infect Dis*. (1995) 20:S224–9. doi: 10.1093/clinids/20.supplement_2.s224

frontiers | Frontiers in Medicine

TYPE Case Report
PUBLISHED 30 January 2025
DOI 10.3389/fmed.2025.1520644

OPEN ACCESS

EDITED BY
Talat Kilic,
İnönü University, Türkiye

REVIEWED BY
Sanjay Gautam,
International Vaccine Institute, Republic of Korea
Smriti Agrawal,
King George's Medical University, India

*CORRESPONDENCE
Aleksandra Cvetkovic
✉ alexxandra.cvetkovic@gmail.com

RECEIVED 31 October 2024
ACCEPTED 13 January 2025
PUBLISHED 30 January 2025

CITATION
Cvetkovic A, Blanka Protic A, Jovanovic J and Adzic Vukicevic T (2025) Should miliary tuberculosis be considered as a possible cause of infertility in the new era: a case report and literature review.
Front. Med. 12:1520644.
doi: 10.3389/fmed.2025.1520644

Should miliary tuberculosis be considered as a possible cause of infertility in the new era: a case report and literature review

Aleksandra Cvetkovic[1]*, Ana Blanka Protic[1], Jelena Jovanovic[1] and Tatjana Adzic Vukicevic[1,2]

[1]Clinic of Pulmonology, University Clinical Center of Serbia, Belgrade, Serbia, [2]Faculty of Medicine, University of Belgrade, Belgrade, Serbia

Introduction: Miliary tuberculosis (MTB) is a potentially lethal form of tuberculosis that can occur in pregnant women, especially those who have conceived by *in vitro* fertilization (IVF).

Case description: A 28-year-old, female patient, after IVF's fourth attempt, at the end of the first trimester, developed a dry cough, high fever, abdominal pain, and vaginal bleeding, which led to the pregnancy termination without resolution of systemic symptoms despite various antibiotics. Because of the appearance of headaches, brain nuclear magnetic resonance (NMR) was done, and diffuse nodular brain lesions were found, which were initially interpreted as metastatic cancer disease. Afterward, the miliary changes were discovered in various organ systems, and the presence of *Mycobacterium tuberculosis* was confirmed. The antituberculosis treatment was initiated with the standard antituberculosis regimen with excellent clinical response and resolution of miliary changes.

Conclusion: Miliary tuberculosis is more common in cases of pregnancies related to IVF. It should be taken into consideration as a possible risk for infertility in the presence of nonspecific symptoms. Screening methods for latent tuberculosis in IVF patients are needed even in a low-burden TB country.

KEYWORDS

miliary tuberculosis, pregnancy, *in vitro* fertilization, latent tuberculosis, low TB burden country

Introduction

Miliary tuberculosis (MTB) represents a form of tuberculosis that originates from the hematogenous spread of *Mycobacterium tuberculosis*. According to literature data (1), it is usually found in adults and is due to recent infection or reactivation of latent tuberculosis. The predominant symptoms are often nonspecific and dependent on the most affected organs. If it is not recognized and treated accordingly, miliary tuberculosis could be fatal. Considering that more than 200.000 active TB cases were registered among pregnant women worldwide, along with the increased use of *in vitro* fertilization (IVF) methods and the increased number of MTB cases, it becomes obvious that this is an important topic for further investigation (2).

Case description

A 28-year-old Caucasian woman, human immunodeficiency virus (HIV) seronegative, vaccinated at birth with the Bacillus Calmette-Guerin (BCG) vaccine, without any previous medical history, became pregnant after the fourth IVF attempt. According to the available clinical data, the patient did not have any multisystemic symptoms during the previous IVF attempts. During her childhood, when she was 7 years old, her father was treated for drug-sensitive tuberculosis (DST), and it is still unknown if she was evaluated at the time as a person from the household. The initial chest X-ray done at the time of the pregnancy initiation was without pathological changes (Figure 1). At the end of the third month of pregnancy, the patient started experiencing dry cough, intermittent high fever up to 39°C, abdominal pain, and vaginal bleeding. The pregnancy was terminated at the end of the first trimester by hysterotomy because of extensive vaginal bleeding, and two stillborn fetuses (male and female, weighing 60 and 80 g) were evacuated from the uterus. Methicillin-resistant *Staphylococcus aureus* (MRSA) was isolated from the uterine cavity. During the following post-partum period, the patient remained febrile despite the treatment with numerous antibiotics regimens containing carbapenems, vancomycin, and piperacillin-tazobactam. One month after delivery she underwent computerized tomography (CT) of pulmonary artery examination, which revealed scattered reticular and micronodular changes in the pulmonary parenchyma without evidence of pulmonary thromboembolic disease. Three months after delivery, the patient started experiencing nausea, vomiting, and weight loss, and in the next 6 months, she started having strong headaches. The nuclear magnetic resonance (NMR) of the brain was performed and showed multiple nodular lesions in the brain parenchyma which were characterized as possible metastatic changes (Figure 2). The patient was finally referred to the tertiary-level hospital institution for further diagnostic evaluation under the suspicion of having a disseminated malignant disease. At the time of hospital admission, the chest X-ray revealed diffuse miliary changes. The CT examination of the chest and upper abdomen revealed diffuse micronodular changes in both lungs (Figure 3). The patient underwent a bronchoscopy examination which showed signs of mild bronchial inflammation. Sputum and tracheobronchial samples were sent for GeneX-pert MTB/RIF assay analysis and came back positive. The antituberculosis treatment was initiated with the standard antituberculosis drug regimen consisting of isoniazid, rifampin, pyrazinamide, and ethambutol. To determine the extent of the disease, positron emission tomography (PET) was performed and revealed the enhanced metabolic activity in the brain, lungs, mediastinum, liver, ileocecal, and genitourinary area. The final microbiologic confirmation of tuberculosis infection we got later was in the form of positive Löwenstein-Jenssen cultures of the sputum, tracheobronchial lavage, blood, urine, and menstrual blood. *Mycobacterium tuberculosis* strain was sensitive to all standard antituberculosis drugs. After the initiation of antituberculosis treatment, the patient experienced a favorable clinical outcome, with the complete resolution of all previously described pathological findings, including the complete resolution of the brain lesions, as was shown on the follow-up NMR of the brain (Figure 4).

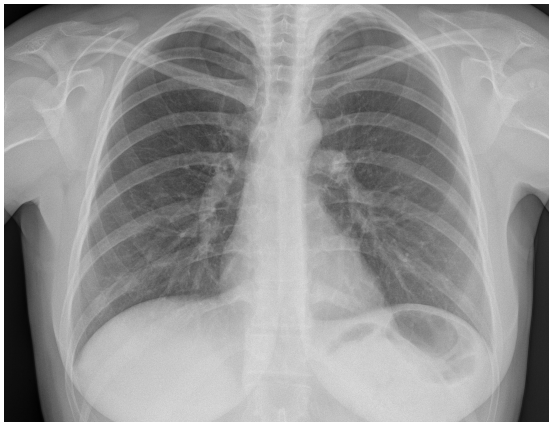

FIGURE 1
Chest X-ray done at the beginning of IVF treatment.

Discussion

It was already known that tuberculosis (TB) could have a tremendous impact on pregnancy outcomes and is an important cause of maternal and fetal morbidity and mortality. The disease progresses more rapidly in pregnant women and can lead to miscarriage (2). Furthermore, 15–30% of pregnant women with TB exhibit hematogenous dissemination and the development of miliary tuberculosis (3). It is also important to emphasize the significance of the possible existence of latent tuberculosis infection, since in the absence of appropriate treatment, there is an estimated lifetime risk of 8–10% for the reactivation of the disease, and that risk varies and can be much higher in case of immunosuppression (4).

As in the case of our patient, the clinical symptoms of infection are often nonspecific, most commonly including fever and cough, which often leads to misdiagnosis and delayed treatment. Also, diagnostic methods such as chest X-ray or chest CT are performed more conservatively during pregnancy because of the radiation exposure risk, so the diagnosis of miliary tuberculosis is often further delayed (5).

The use of IVF methods revolutionized modern infertility worldwide with generally good success rates. It is known that genital tuberculosis (GTB), as a form of extrapulmonary TB, can be a major cause of primary infertility among women in countries with high TB burden (6). The use of IVF and embryo transfer (ET) methods enables the bypassing of fallopian tubes damaged by TB, which consequently can lead to the coexistence of pregnancy and genital TB infection (7). There is an increasing number of reports of cases of miliary tuberculosis in patients who have undergone IVF treatment. The retrospective study of Wang et al. has shown that the incidence of miliary tuberculosis was significantly higher among IVF-ET patients than in the group of patients who have conceived naturally (8). Furthermore, Gai et al. also showed in their retrospective study that women with TB infection during IVF achieved pregnancy were more prone to the hematogenous dissemination of the disease (9). A possible explanation underlines the role of immune and endocrine disorders during pregnancy. It has been shown that during pregnancy cell-mediated immunity has

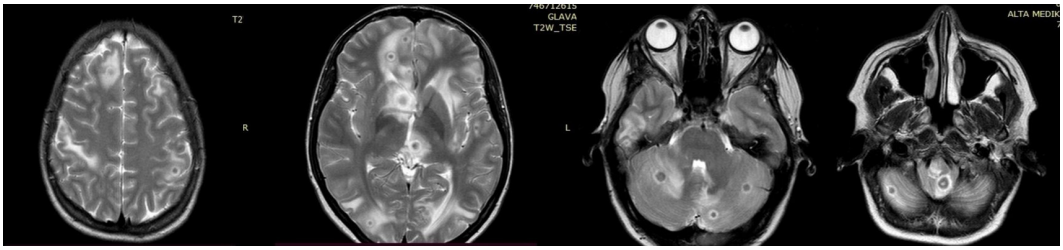

FIGURE 2
Diffuse nodular changes in the brain parenchyma seen on the nuclear magnetic resonance (NMR).

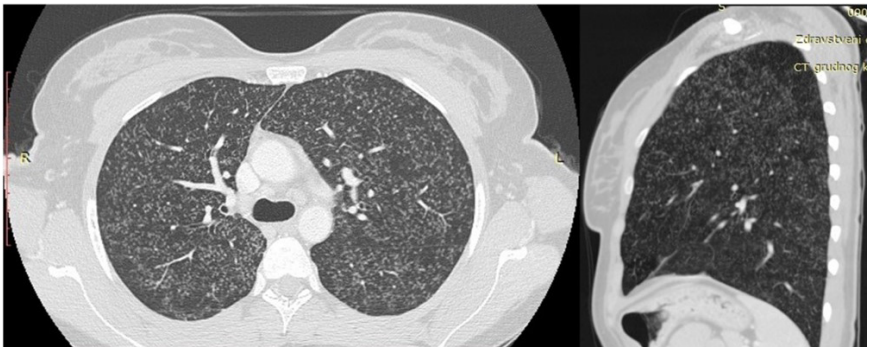

FIGURE 3
Computerized tomography (CT) of the chest with visible multiple micronodular changes in the lungs.

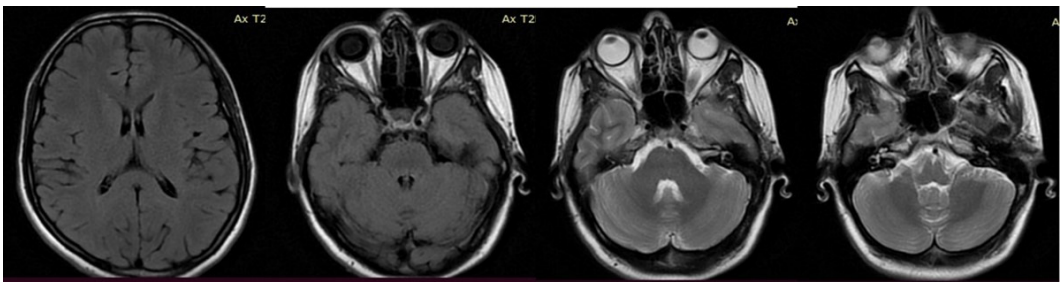

FIGURE 4
Follow-up brain NMR after 6 months of antituberculosis treatment.

been impaired because of a relative bias toward T-helper type 2 (Th2) immunity (10). This may explain increased susceptibility to certain infections or their reactivation during pregnancy, as in the case of tuberculosis infection. Furthermore, the equilibria between Th1 and Th2 cellular responses are crucial for the determination of the outcome of tuberculosis disease (11).

The role of endocrine mechanisms including effects of progesterone and estrogen could be responsible for immunity response. It is known that progestogens can have a role in a dose-dependent effect on the Th1/Th2 response leading to the reduction of T-cell proliferation and the suppression of host immunity, which is important because of the routine progestogen supplementation after IVF (12). In clinical practice, the progestogen supplementation is commonly given until the 8th to 10th gestational week, and as shown in previous retrospective studies a large proportion of patients develop symptoms a few weeks later, which was seen in our patient (13, 14). High estrogen levels can increase *Mycobacterium tuberculosis* proliferation, and it is also proposed that the existence of increased vascular permeability after pregnancy may also lead to the facilitated hematogenous dissemination of the disease (3). Lastly, the possible role of glucocorticoids, which are given to sensitize the ovaries to gonadotropin stimulation during IVF and their immunosuppressive effects, should not be overlooked in the development of the disease (15).

The differential diagnosis of miliary tuberculosis, especially based only on radiological findings, is broad and complex. Distinguishing miliary changes from widespread metastatic cancer can be a diagnostic challenge, as in our patient's case (16). Therefore, to make an appropriate and timely diagnosis, it is important to consider including radiological findings, the patient's signs and symptoms, immune status, and family history.

In the present case, the initial diagnosis of MRSA from the uterine cavity delayed the diagnosis of miliary tuberculosis. Concomitant infection due to MRSA and *Mycobacterium tuberculosis* is uncommon and demonstrates that the diagnosis of miliary tuberculosis can be hidden by the existence of other pathogens (17).

The Republic of Serbia is among low TB burden countries, with an average TB incidence of 7.14/100.000 (18). As was shown in the case of our patient, even in a low TB-burden country, with increased rates of immigration, clinicians should be aware of the increased possibility of the development of miliary tuberculosis in pregnant women, especially in cases of IVF. Furthermore, it is also important to consider the possibility of latent TB infection, and the need for appropriate testing and chemoprophylaxis implementation.

Based on the presented case and available literature data, miliary tuberculosis should be taken into consideration as a possible risk for infertility in the presence of nonspecific symptoms. Nevertheless, in order to be able to prove the presence of a definitive connection between infertility and TB, larger studies are needed to be done in the future. Furthermore, appropriate screening methods for latent tuberculosis infection within households are needed, even in a country with a low TB burden to prevent active disease.

Data availability statement

The original contributions presented in this study are included in this article/supplementary material, further inquiries can be directed to the corresponding author.

Ethics statement

Written informed consent was obtained from the individual(s) for the publication of any potentially identifiable images or data included in this article.

Author contributions

AC: Writing – original draft. AB: Resources, Writing – review and editing. JJ: Visualization, Writing – review and editing. TA: Writing – review and editing.

Funding

The author(s) declare that no financial support was received for the research, authorship, and/or publication of this article.

Conflict of interest

The authors declare that the research was conducted in the absence of any commercial or financial relationships that could be construed as a potential conflict of interest.

Generative AI statement

The authors declare that no Generative AI was used in the creation of this manuscript.

Publisher's note

References

1. Sugarman J, Colvin C, Moran A, Oxlade O. Tuberculosis in pregnancy: An estimate of the global burden of disease. *Lancet Glob Health.* (2014) 2:e710–6. doi: 10.1016/S2214-109X(14)70330-4

2. Bates M, Ahmed Y, Kapata N, Maeurer M, Mwaba P, Zumla A. Perspectives on tuberculosis in pregnancy. *Int J Infect Dis.* (2015) 32:124–7. doi: 10.1016/j.ijid.2014.12.014

3. Sobhy S, Babiker Z, Zamora J, Khan K, Kunst H. Maternal and perinatal mortality and morbidity associated with tuberculosis during pregnancy and the postpartum period: A systematic review and meta-analysis. *BJOG.* (2017) 124:727–33. doi: 10.1111/1471-0528.14408

4. Haley C. Treatment of latent Tuberculosis infection. *Microbiol Spectr.* (2017) 5:7–39. doi: 10.1128/microbiolspec.TNMI7-0039-2016

5. Gai X, Chi H, Cao W, Zeng L, Chen L, Zhang W, et al. Acute miliary tuberculosis in pregnancy after in vitro fertilization and embryo transfer: A report of seven cases. *BMC Infect Dis.* (2021) 21:913. doi: 10.1186/s12879-021-06564-z

6. Bhanothu V, Theophilus J, Reddy P, Rozati R. Occurrence of female genital tuberculosis among infertile women: A study from a tertiary maternal health care research centre in South India. *Eur J Clin Microbiol Infect Dis.* (2014) 33:1937–49. doi: 10.1007/s10096-014-2164-1

7. Gull I, Peyser M, Yaron Y, Jaffa A, Amit A, Lessing J. The effect of an in-vitro fertilization pregnancy on a woman with genital tuberculosis. *Hum Reprod.* (1995) 10:3052–4. doi: 10.1093/oxfordjournals.humrep.a135846

8. Wang K, Ren D, Qiu Z, Li W. Clinical analysis of pregnancy complicated with miliary tuberculosis. *Ann Med.* (2022) 54:71–9. doi: 10.1080/07853890.2021.2018485

9. Yip L, McCluskey J, Sinclair R. Immunological aspects of pregnancy. *Clin Dermatol.* (2006) 24:84–7. doi: 10.1016/j.clindermatol.2005.10.022

10. Lissauer D, Eldershaw S, Inman C, Coomarasamy A, Moss P, Kilby M. Progesterone promotes maternal-fetal tolerance by reducing human maternal T-cell polyfunctionality and inducing a specific cytokine profile. *Eur J Immunol.* (2015) 45:2858–72. doi: 10.1002/eji.201445404

11. Lienhardt C, Azzurri A, Amedei A, Fielding K, Sillah J, Sow O, et al. Active tuberculosis in Africa is associated with reduced Th1 and increased Th2 activity in vivo. *Eur J Immunol.* (2002) 32:1605–13. doi: 10.1002/1521-4141(200206)32:6<1605

12. Yu N, Yang J, Guo Y, Fang J, Yin T, Luo J, et al. Intrauterine administration of peripheral blood mononuclear cells (PBMCs) improves endometrial receptivity in mice with embryonic implantation dysfunction. *Am J Reprod Immunol.* (2014) 71:24–33. doi: 10.1111/aji.12150

13. Labarta E, Rodríguez C. Progesterone use in assisted reproductive technology. *Best Pract Res Clin Obstet Gynaecol.* (2020) 69:74–84. doi: 10.1016/j.bpobgyn.2020.05.005

14. Xia L, Mijiti P, Liu X, Hu Z, Fan X, Lu S. Association of in vitro fertilization with maternal and perinatal outcomes among pregnant women with active tuberculosis:

A retrospective hospital-based cohort study. *Front Public Health*. (2022) 10: 1021998.

15. Liu S, Shi L, Wang T, Shi J. Effect of low-dose dexamethasone on patients with elevated early follicular phase progesterone level and pregnancy outcomes in IVF-ET treatment: A randomized controlled clinical trial. *Clin Endocrinol (Oxf)*. (2018) 89:771–8. doi: 10.1111/cen.13824

16. Zhao W, Tian Y, Peng F, Long J, Liu L, Huang M, et al. Differential diagnosis of acute miliary pulmonary tuberculosis from widespread-metastatic cancer for postoperative lung cancer patients: Two cases. *J Thoracic Dis*. (2017) 9:E115–20. doi: 10.21037/jtd.2017.02.13

17. Moriyama Y, Sono Y, Nishioka H. Tuberculous arthritis of the hip with Staphylococcus aureus superinfection. *J Infect Chemother*. (2016) 22:752–4. doi: 10.1016/j.jiac.2016.04.006

18. Institut za javno zdravlje Srbije. Dr Milan Jovanović Batut. *National Public Health Institute of Serbia*. Available online at: https://www.batut.org.rs/index.php?content=2794 (accessed April 10, 2024).

frontiers | Frontiers in Medicine

TYPE Case Report
PUBLISHED 05 February 2025
DOI 10.3389/fmed.2025.1501192

OPEN ACCESS

EDITED BY
Giuseppe Fiorentino,
Colli Hospital, Italy

REVIEWED BY
Maurizio Sanguinetti,
Catholic University of the Sacred Heart, Italy
Stanimir S. Ivanov,
Louisiana State University Health Shreveport, United States

*CORRESPONDENCE
Jianqing Fang
✉ fangjianqing001@hotmail.com

†These authors have contributed equally to this work

RECEIVED 24 September 2024
ACCEPTED 13 January 2025
PUBLISHED 05 February 2025

CITATION
Fang J, Wang Z, Shen Y, Wu X, Fang H, Sun X, Yu T and Zhang Q (2025) Case report: The value of early application of mNGS technology in the diagnosis and treatment of severe Legionnaires' disease: reports of two cases with different outcomes. *Front. Med.* 12:1501192. doi: 10.3389/fmed.2025.1501192

Case report: The value of early application of mNGS technology in the diagnosis and treatment of severe Legionnaires' disease: reports of two cases with different outcomes

Jianqing Fang[1*†], Zhe Wang[1†], Yu Shen[2], Xuenong Wu[1], Hao Fang[3], Xiaokui Sun[1], Ting Yu[1] and Qingqing Zhang[1]

[1]Department of Respiratory and Critical Care Medicine, Hangzhou Linping Hospital of Traditional Chinese Medicine, Hangzhou, China, [2]Department of Ultrasound Medicine, Hangzhou Linping Hospital of Traditional Chinese Medicine, Hangzhou, China, [3]Department of Intensive Care Medicine, Hangzhou Linping Hospital of Traditional Chinese Medicine, Hangzhou, China

Background: Legionnaires' disease has a high clinical mortality rate, and early diagnosis and treatment are critical. Increasing evidence shows that metagenomic next-generation sequencing (mNGS) has excellent potential for the early identification of pathogens. To help clinicians better recognize Legionnaires' disease in its early stage and to illustrate the diagnostic value of mNGS technology, we reviewed and summarized two cases of severe Legionnaires' disease.

Methods and analysis: We selected two patients with severe Legionnaires' disease who were admitted to our department in recent years. We discuss experience with them and the shortcomings in their treatment by summarizing their medical history, disease evolution, tests, and diagnostic and therapeutic processes.

Results: In both patients, the diagnosis of Legionnaires' disease was confirmed through analysis of the bronchoalveolar lavage fluid (BALF). The middle-aged male patient was cured and discharged due to early detection and diagnosis. The elderly immunocompromised patient died due to a delay in diagnosis.

Conclusion: This study highlights the importance of the early recognition and diagnosis of severe Legionnaires' disease and the advantages of mNGS in identifying the pathogen.

KEYWORDS

legionellosis, Legionnaires' disease, case report, severe community-acquired pneumonia, severe hospital-acquired pneumonia

Introduction

Legionella spp. are intracellular-parasitic, aerobic, gram-negative bacilli, of which 58 species and more than 70 serotypes have been identified (1, 2). These pathogens were first recognized following an outbreak of Legionnaires' disease (LD) at the 1976 American Legion Convention in Philadelphia (3). As a conditionally pathogenic bacterium, *Legionella* is widespread in natural water systems, soil, air-conditioning systems, and water catchment systems (4, 5). *Legionella* is spread mainly by inhalation of bacterial aerosols arising from contaminated water or soil (1).

Legionella infection can present as mild, self-limiting, flu-like symptoms; this condition is known as Pontiac fever and usually does not require antimicrobial treatment (2, 6). Patients with high-risk factors for infection, including chronic lung disease, age > 50 years, glucocorticoid therapy, hematological malignancies or solid tumors, and organ transplantation (7), are prone to opportunistic infection leading to community-acquired or hospital-acquired LD (1). Smoking can also create an environment that is conducive to the proliferation of microbes within the bronchial tree (8). A previous study has demonstrated that smoking is the most significant risk factor in LD patients (9). LD can progress to severe pneumonia or even severe acute respiratory distress syndrome, requiring intensive care and extracorporeal membrane oxygenation (ECMO) treatment (10). In immunocompromised patients, *Legionella* can also cause extrapulmonary legionellosis through blood dissemination (11), such as pericarditis (12), endocarditis (13), meningitis (14), and liver infection (15). *Legionella pneumophila* (Lp), *Legionella micdadei*, *Legionella longbeachae*, *Legionella bozemanae*, and *Legionella dumoffii* are the species that are most commonly encountered clinically. Among all *Legionella* spp., *Legionella pneumophila* serogroup 1 (Lp1) is the most virulent and common causative agent of LD (16); approximately 90% of LD cases result from Lp1 infection (17, 18).

The clinical manifestations of LD vary and include chills, fever, cough, hemoptysis, general malaise, and relative bradypnea. Gastrointestinal and neurological symptoms such as diarrhea, nausea or vomiting, and headache may be more prominent than they are in other bacterial pneumonias (2). Laboratory tests of LD patients have revealed leukocytosis with relative lymphopenia and elevated C-reactive protein (CRP) and calcitoninogen levels. Hypernatremia, hypophosphatemia, elevated levels of liver enzymes, and creatine kinase are common in this disease (19). The imaging presentation lacks specificity; early lesions are located mainly in unilateral lobes of the lungs and present as patchy or interstitial exudative opacity with blurred borders; this appearance can rapidly progress to consolidation in the short term, and pleural effusions and necrotic cavities are sometimes observed (20). In immunosuppressed patients, extrapulmonary dissemination and recurrence are more likely, and pulmonary cavitation is also more common, resulting in a higher mortality rate (21).

Because *Legionella* parasitizes alveolar macrophages, antibiotics that do not penetrate the host cell membrane, such as common beta-lactams and aminoglycosides, are ineffective. The antibiotics available for treatment include fluoroquinolones, macrolides, and rifampicin. Fluoroquinolone or macrolide monotherapy for LD, typically involving the use of levofloxacin, moxifloxacin, azithromycin, or clarithromycin, is still the conventional regimen (22–25). In patients with severe pneumonia, especially those with severe comorbidities and immunocompromised patients who have failed to respond to monotherapy regimens, fluoroquinolones in combination with macrolides may be considered (26). *Legionella* remains susceptible to commonly used antibiotics, and reports of resistance are rare (27, 28). This article reports two typical cases of severe LD with different outcomes.

Case 1 presentation

An 80-year-old woman with a 5-day history of cough and shortness of breath was admitted to the respiratory department during the summer months. She had a medical history of chronic obstructive pulmonary disease (COPD), hypertension, and previous cerebral infarction and was regularly treated with a tiotropium powder inhaler, irbesartan dispersible tablets, and atorvastatin tablets. She had no history of smoking. Physical examination revealed a body temperature of 37.8°C, a blood pressure of 152/62 mmHg, a heart rate of 84 beats/minute, and a respiration rate of 20 breaths/minute. She was conscious, with a barrel chest. Bibasilar wheezing was detected on lung auscultation. Both lower limbs exhibited mild edema. The remaining examination results were unremarkable. Laboratory investigations revealed a white blood cell (WBC) count of 12.65×10^9/L, an absolute neutrophil count (ANC) of 10.12×10^9/L and a platelet (PLT) count of 153×10^9/L. The serum CRP level was 75 mg/L, and the serum PCT level was 0.53 ng/ml. Arterial blood gas (ABG) analysis revealed an FiO2 of 29.00%, pH of 7.39, pCO_2 of 62.1 mmHg, and pO_2 of 68.7 mmHg (oxygenation index of 237 mmHg). Serum IgM antibodies against atypical pathogens (including *Mycoplasma pneumoniae*, *Chlamydia pneumoniae* and LP), upper respiratory tract specimens PCR (including influenza virus, adenovirus and SARS-CoV-2), and blood and sputum cultures were all negative. Chest computed tomography (CT) on admission revealed emphysema and slight thickening of the bronchial wall (Figures 1A–D).

Diagnosis and treatment: The patient's initial diagnosis was acute exacerbation of chronic obstructive pulmonary disease (AECOPD). The treatment regimen included cefotaxime (2.0 g, ivgtt, q12h) as an anti-infective, methylprednisolone (20 mg, iv, qd) and nebulized inhalation (budesonide 2 mg plus terbutaline 5 mg, bid) to relieve airway spasms and the use of a non-invasive ventilator (Philips V60) to improve ventilation. On hospital day 6, the patient's temperature was normal, but she still experienced shortness of breath and had yellowish sputum. On physical examination, her oral mucosal leukoplakia was detected, and moist rales and phlegm sounds were heard on lung auscultation. Repeat laboratory tests revealed a WBC count of 11.37×10^9/L, an ANC of 9.34×10^9/L, and a PLT of 152×10^9/L. Her CRP level had increased to 80 mg/L, her PCT level was 0.71 ng/ml, and sputum culture revealed *Candida albicans* (+ +). The antibiotic coverage was broadened to include cefoperazone sulbactam (2.0 g, ivgtt, q8h) and fluconazole (0.2 g, ivgtt, qd) to cover *Pseudomonas aeruginosa* and *Candida albicans*, and methylprednisolone was discontinued. After 7 days of treatment, the patient's symptoms improved, her oral mucosal leukoplakia subsided, her CRP and PCT levels returned to normal, and a

10.3389/fmed.2025.1501192

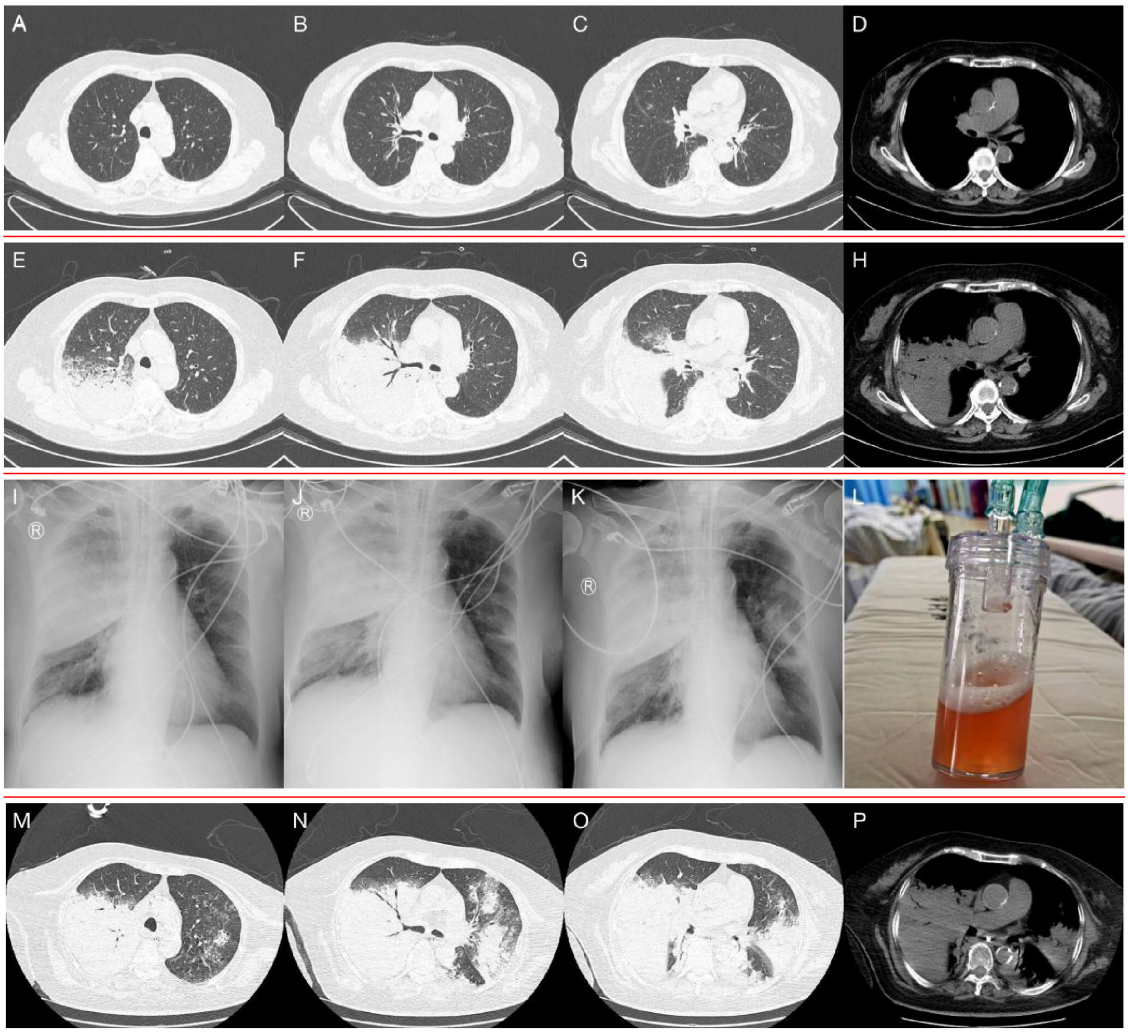

FIGURE 1
(A–D) Chest CT on admission, showed emphysema and slight thickening of the bronchial wall. **(E–H)** Chest CT on hospital day 16, showed a new sizeable consolidation in the upper right lung with blurred borders, a bronchial inflation sign, slightly patchy exudative opacity in the right middle lobe, and a small amount of pleural effusion on the right chest. **(I–K)** Bedside chest radiography on hospital day 18, 20, and 22, respectively, showed gradual enlargement of consolidation in the upper right lung and the development of new patchy exudative opacity in the upper left lung. **(L)** orange-colored BALF was collected at RB2 on hospital day 22. **(M–P)** Chest CT on hospital day 24, showed significant progression of the lesions and exudative consolidation in multiple lobes of both lungs.

repeat sputum culture was negative. Cefoperazone sulbactam was discontinued, fluconazole administration was switched to capsules (0.2 g, po, qd), non-invasive ventilator therapy was continued, and the patient was prepared for elective discharge. On hospital day 16, the patient developed chills and a high fever (39.2°C), with worsening dyspnoea. Examination revealed bilateral moist rales and marked upper right lung sounds. Laboratory investigations revealed that the WBC count had increased to 17.73 × 10^9/L, the CRP level was 94 mg/L, and the PCT level was 1.73 ng/ml. ABG analysis revealed an FiO2 of 33.00%, pH of 7.42, pCO2 of 40.3 mmHg, and pO2 of 55.1 mmHg (oxygenation index 167 mmHg). Repeat chest CT revealed a new sizeable consolidation with blurred borders in the upper right lung, a bronchial inflation sign, slightly patchy exudative opacity in the right middle lobe, and a small amount of pleural effusion in the right chest (Figures 1E–H). Imipenem cilastatin (0.5 g, ivgtt, q6h) was empirically used for G-bacilli therapy. The next morning, the patient's respiratory status worsened, with persistent dyspnea during sitting, slightly blurred consciousness, and coughing up of pale blood-colored sputum. Many bibasilar crackles were heard on lung auscultation. Considering severe nosocomial pneumonia with acute heart failure (PSI score: 160 points, class V; NYHA: cardiac function class IV), we transferred her to the intensive care unit (ICU) for invasive mechanical ventilation. The ICU physician performed endotracheal suction and bedside rapid microscopic detection of fungal fluorescence; fungal spores were positive. Antibiotic therapy was escalated to imipenem cilastatin (0.5 g, ivgtt, q6h) and voriconazole (0.2 g, ivgtt, q12h) to cover G-bacilli and fungi. As her condition became unstable, the patient underwent bedside chest radiography every 2 days; this revealed gradual enlargement of the consolidation in the upper right lung and the development of new patchy exudative opacity in the upper left lung (Figures 1I–K). Her CRP and PCT levels did not improve greatly. Both blood and sputum cultures and serum anti-Lp IgM antibodies were

negative. On hospital day 22, bronchoscopy was performed, and orange-colored bronchoalveolar lavage fluid (BALF) was collected at RB2 (Figure 1L). mNGS was performed using the PMseq platform, and the results were compared with those reported in the PMDB database. The mNGS results, which were obtained two days later, yielded 23,032 sequence reads for Lp (Table 1). The patient underwent chest CT, which revealed significant progression of the lesions and exudative consolidation in multiple lobes of both lungs (Figures 1M–P). On the basis of the patient's clinical presentation and mNGS results, she was diagnosed with severe, nosocomial LD. The physician adjusted the antibiotic regimen by discontinuing imipenem cilastatin with voriconazole and starting her on moxifloxacin (0.4 g, ivgtt, qd) in combination with azithromycin (0.5 g, ivgtt, qd) for anti-*Legionella* therapy. Despite a series of comprehensive treatments, the patient's condition continued to deteriorate, progressing to multiple organ failure (MOF), upper gastrointestinal bleeding, disseminated intravascular coagulation, and uncorrectable metabolic acidosis. The ICU physicians repeatedly recommended that the patient be transferred to a higher-level hospital for ECMO treatment, but the patient's family refused. On hospital day 29, the patient's family decided to abandon treatment. The patient died at home on the following day (Figure 2).

Case 2 presentation

A 50-year-old man who was a full-time taxi driver with no significant medical history was admitted to the respiratory department in early autumn, with a 3-day history of fever, cough and shortness of breath. His smoking index was 900. Physical examination revealed a body temperature of 40.4°C, a blood pressure of 108/63 mmHg, a heart rate of 126 beats/minute, and a respiration rate of 30 breaths/minute. He was conscious, with dyspnea and mild lip cyanosis. His lower left lung was turbid on percussion, and obvious moist rales were heard on auscultation. Laboratory investigations revealed a WBC of 17.88 $\times$ 10^9/L, an ANC of 16.52 $\times$ 10^9/L and a PLT of 137 $\times$ 10^9/L. CRP was 273 mg/L, and PCT was 18.35 ng/ml. Serum chemical tests revealed an alanine aminotransferase (ALT) level of 104.3 U/L, an aspartate aminotransferase (AST) level of 350.8 U/L, an LDH level of 1099.2 U/L, a creatine kinase (CK) level of 8602.9 IU/L, a blood urea nitrogen (BUN) level of 11.40 mmol/L, sodium level of 133.1 mmol/L and an inorganic phosphorus level of 1.42 mmol/L. ABG analysis revealed an FiO2 of 33.00%, pH of 7.45, pCO2 of 31.2 mmHg, and pO2 of 61.9 mmHg (oxygenation index 188 mmHg). Serum IgM antibodies against atypical pathogens (including *Mycoplasma pneumoniae*, *Chlamydia pneumoniae*, and *Legionella pneumophila*), upper respiratory tract specimen PCR (including probes for influenza virus, adenovirus and SARS-CoV-2), blood and sputum cultures, and sputum for antacid bacilli were all negative. Chest CT on admission revealed a large patchy exudative opacity with blurred borders and partial consolidation in the lower left lung, with thickening of the interlobular septum, a bronchial inflation sign and a small patch of exudative opacity in the lower lingual segment of the upper left lobe (Figures 3A–D).

The preliminary diagnosis was severe CAP (PSI score: 130, grade IV). As an empirical treatment regimen, moxifloxacin (0.4 g, ivgtt, qd) was given as an anti-infective agent against *Streptococcus pneumoniae* and atypical pathogens. After admission, the patient had pus-like, orange-yellow sputum (Figure 3M), but several sputum cultures were negative. Bronchoscopy under general anesthesia and endotracheal intubation were performed on hospital day 2, and orange-colored BALF was collected on LB10 (Figure 3N). The mNGS assay was performed using the PMseq platform; comparison of the results with the PMDB database, revealed 239 sequence readings for Lp 2 days later (Table 2). On the same day, repeat chest CT revealed rapid progression to consolidation in the entire lower left lung, accompanied by a small amount of bilateral pleural effusion (Figures 3E–H). The diagnosis of severe LD was confirmed on the basis of the patient's history, clinical presentation, laboratory results, chest radiographic findings, and mNGS results. Given the patient's severe condition at that time—he still had fever and dyspnea upon exertion, and a repeat ABG analysis revealed an oxygenation index of 176 mmHg—rifampicin (0.3 g, ivgtt, q12h) was added to his treatment. After 2 days of combination therapy, his fever subsided, and his clinical presentation improved markedly. However, on hospital day 11, the patient suddenly developed a generalized maculopapular rash (Figures 3O,P), without pain or itching, accompanied by a renewed high fever (40°C) without chills. The patient's respiratory symptoms, such as cough and dyspnea, did not deteriorate at this time. Furthermore, his CRP and PCT decreased to 26 mg/L and 0.72 ng/mL, respectively. Therefore, it appeared likely that the rash was associated with Lp infection or with a reaction to rifampicin rather than with worsening of the LD. Rifampicin was discontinued, and moxifloxacin was continued, with the addition of methylprednisolone (40 mg, iv, qd) and intravenous immunoglobulins (IVIGs) (10 g, ivgtt, qd) to combat antihypersensitivity reactions. Three days later, the patient's temperature returned to normal, and the rash gradually became lighter. Consequently, his methylprednisolone and IVIGs were discontinued, and his symptoms of fever and rash did not recur. On hospital day 20, the patient complained of only a slight dry cough with no other discomfort, and his CRP, PCT, liver function, renal function, electrolyte, and ABG results were all normal. Repeat chest CT revealed significant absorption of the consolidation in the left lung, resulting in partial thickening of the left pleura and contraction of the interlobar fissure (Figures 3I–L), and the patient was successfully discharged (Figure 4).

Discussion

The two typical cases reported in this article occurred in summer and autumn. Clinical studies have revealed an association between LD and climate; some 62% of cases occur in the summer and early autumn when precipitation increases (29), and 24% of cases are associated with travel (30). The first LD patient in this study presented with HAP, and she had high-risk factors for infection, such as a history of COPD and immunocompromising conditions (80 years old and steroid use). The second patient was a taxi driver who had worked in an air-conditioned environment for a long period, and had smoked for decades. These conditions are associated with a high risk of occupational exposure and infection with *Legionella* (31–33).

TABLE 1 mNGS results of the patient in case 1.

Genus name	Sequence number	Relative abundance%	Species name	Sequence number	Relative abundance%
Legionella	24392	99.95	*Legionella pneumophila* *Legionella anisa*	23032 23	94.38 /
Candida	3	/	*Candida tropicalis*	3	/
Cutibacterium	5	/	*Cutibacterium acnes*	3	/
Human Alphaherpesvirus 1	4	/			

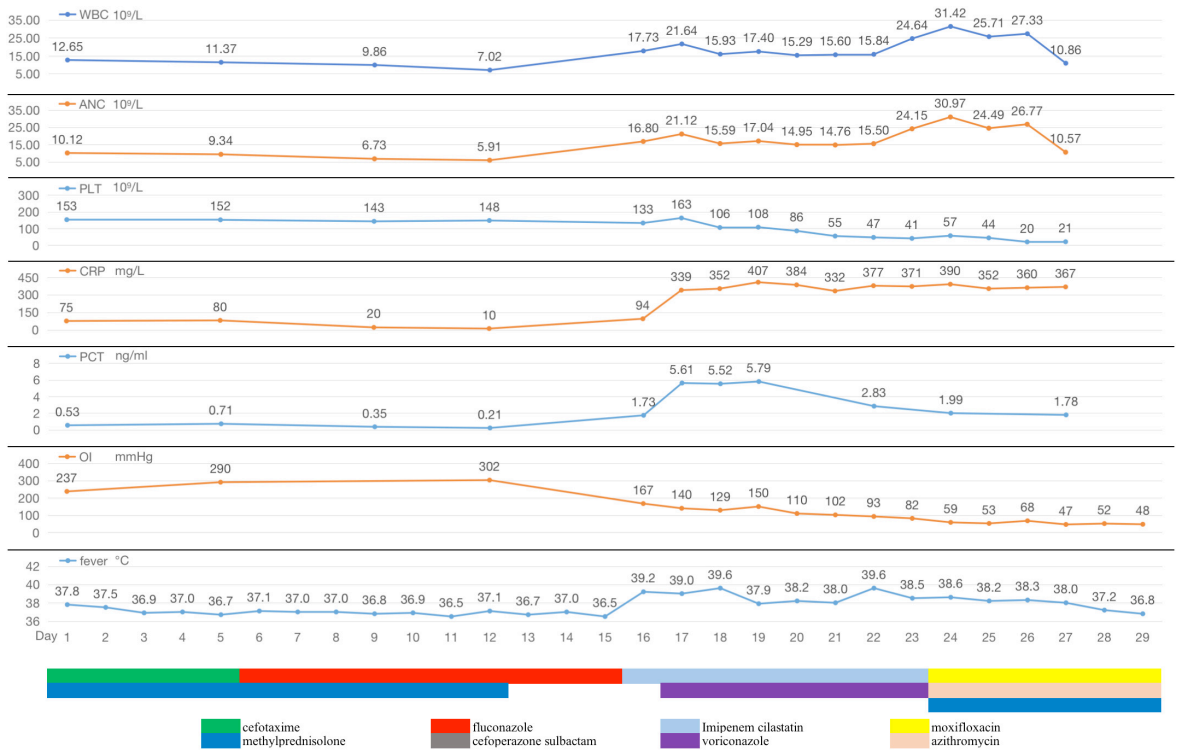

FIGURE 2
During hospitalization, the changes of body temperature, oxygenation index (OI), inflammatory indicators (WBC, ANC,PLT, CRP, and PCT), and antibiotic regimen adjustment process of Case 1.

Interestingly, in our patients, the lower respiratory secretions appeared orange in color; a similar finding has been reported both for patients with Lp pneumonia and for patients with *Legionella longbeachae* pneumonia and may be another clue that should prompt specific testing (34–36). The exact mechanism through which this color appears is unknown, and it is presumed to be due to the utilization of tyrosine in the alveolar epithelial cell lining fluid by *Legionella* (37). In the second patient, despite significant improvement in respiratory symptoms, a generalized maculopapular rash and a high fever suddenly developed on approximately hospital day 12. LD-associated rash is relatively rare (38), and its pathogenesis is poorly understood. Its occurrence may be related to the presence of *Legionella* toxins (39, 40), host immune responses (41), or drug reactions (42). Rifampicin-associated delayed drug eruptions have also been reported (43); in this patient's case, we also considered this as a possible cause of the rash, which subsided after appropriate treatment.

The etiological diagnosis of LD relies on microbiological laboratory tests. The culture of lower respiratory tract specimens, because it allows the isolation of strains for drug sensitivity testing and identification of all known strains of *Legionella* spp., is still the gold standard for diagnosis (44). However, it is rarely used in routine diagnosis because it requires stringent culture conditions, and the results can only be obtained after 3–5 days or even after 2 weeks (11).

Urine antigen tests (UATs) for *Legionella* are essential for the early diagnosis of LD (11) and have the advantages of convenience, timeliness and low cost. In Europe and the United States, diagnosis of LD is based on UATs in 70–80% of cases, and they have become the test of choice for diagnosing LD (45). However, most commercial UATs detect only Lp1 (46), which is isolated in approximately 80% of cases of Lp pneumonia (47, 48). In general, UATs are most sensitive to the Lp1 MAb 3/1 subtype, whereas their sensitivity in patients with Lp1 MAb 3/1-negative infection is approximately 40% (2). Although Lp1 is the major causative

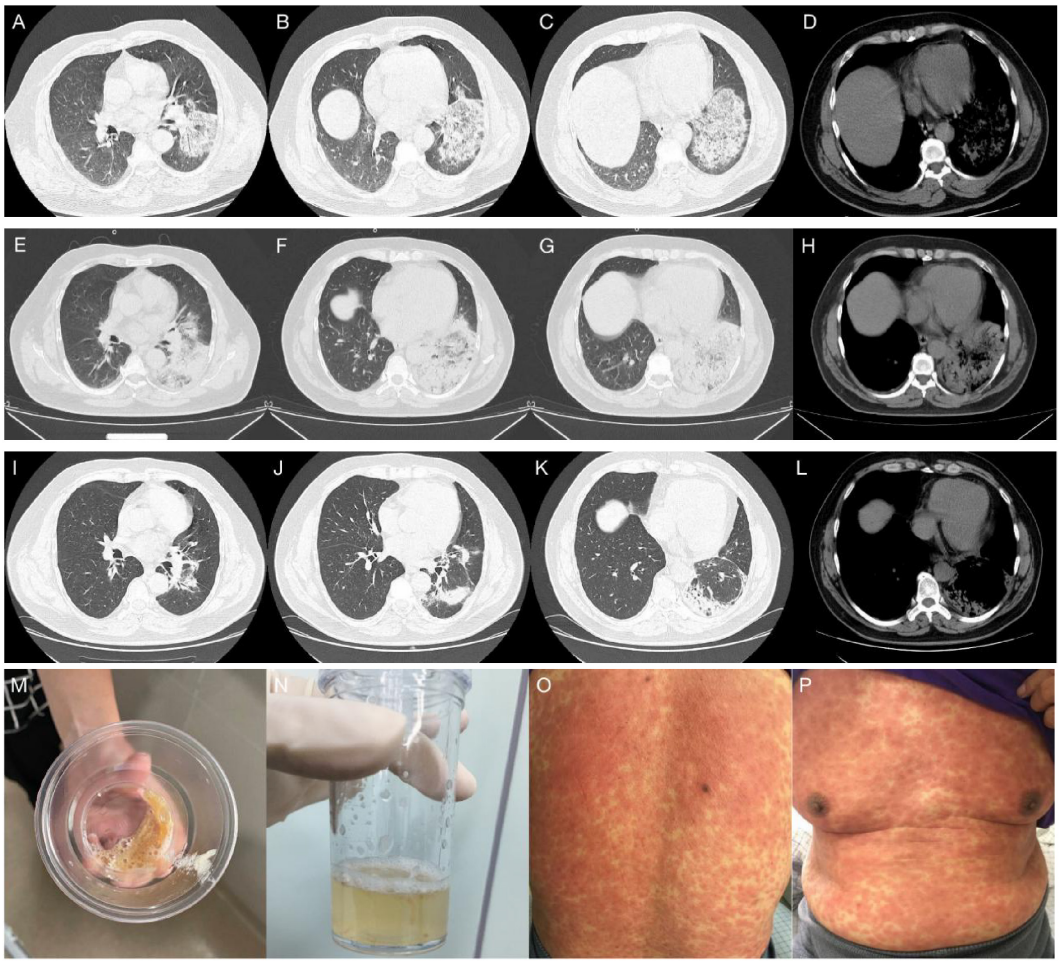

FIGURE 3
(A–D) Chest CT on admission, showed a large patchy exudative opacity with blurred borders and partial consolidation in the lower left lung, with thickening of the interlobular septum, a bronchial inflation sign and a small patch of exudative opacity in the lower lingual segment of the upper left lobe. **(E–H)** Chest CT on hospital day 4, showed rapid progression to consolidation in the whole lower left lung, accompanied by a small amount of bilateral pleural effusion. **(I–L)** Chest CT on hospital day 20, revealed significant absorption of consolidation in the left lung, leaving partial thickening of the left pleura and contraction of the interlobar fissure. **(M)** Pus-like, orange-yellow sputum. **(N)** orange-colored BALF was collected on LB10 on hospital day 2. **(O,P)** The patient suddenly developed a generalized maculopapular rash on hospital day 11.

TABLE 2 **mNGS results of the patient in case 2.**

Genus name	Sequence number	Relative abundance%	Species name	Sequence number	Relative abundance%
Legionella	255	81.73	*Legionella pneumophila*	239	76.60
Prevotella	34	/	*Prevotella bivia*	11	/
			Prevotella melaninogenica	9	/
Veillonella	11	/	*Veillonella dispar*	5	/
			Veillonella parvula	3	/
Granulicatella	9	/	*Granulicatella adiacens*	8	/
Rothia	3	/	*Rothia mucilaginosa*	3	/

pathogen of LD (47, 48), regional differences are significant. The Lp1 subtype is responsible for 87.1% of community-acquired LDs in Japan (49), and for 80–95% of cases in the United States and Europe but for only approximately 50% of cases in Australia and New Zealand (48, 50, 51).

UATs are typically positive within 48–72 h of symptom onset and remain positive for weeks or months (2); positive results have, in fact, been reported nearly one year after an infectious episode (52). UATs may yield false negative or false positive results in the acute phase of infection. In addition, the sensitivity of

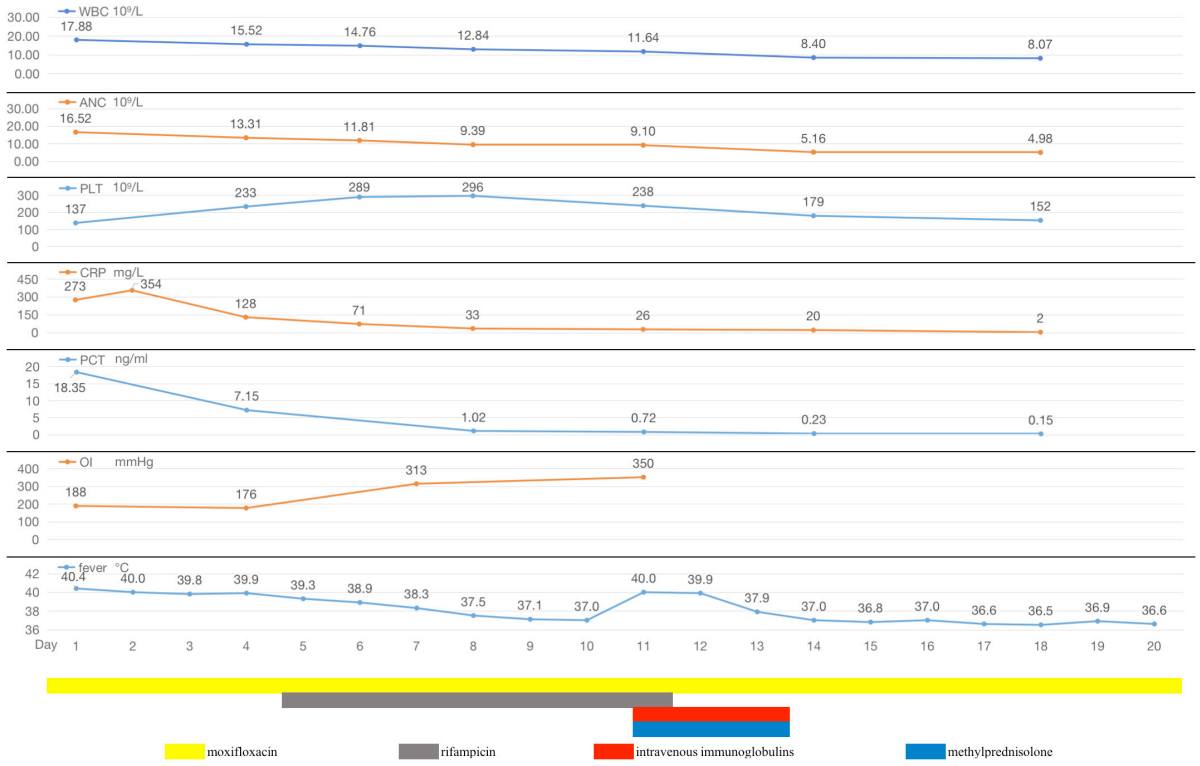

FIGURE 4
During hospitalization, the changes of body temperature, OI (oxygenation index), inflammatory indicators (WBC, ANC, PLT, CRP, and PCT), and antibiotic regimen adjustment process of Case 2.

UATs correlates with disease severity: they have 40–53% sensitivity for mild LD and 88–100% sensitivity for severe LD (53), likely due to differences in the antigen titers in urine samples. The use of highly concentrated urine samples can improve sensitivity, especially in cases involving mild disease, but samples are not routinely concentrated before testing (46, 54). A meta-analysis of 30 studies yielded a pooled sensitivity of 74.0% (95% CI, 68–81%) and a specificity of 99.1% (95% CI, 98.4–99.7%) for the UATs (55). As a result, in most cases in which the diagnosis is determined on the basis of UATs alone, epidemiological numbers may be underestimated compared with the actual incidence (44, 56).

PCR-based diagnosis of the presence of *Legionella* spp. is usually based on amplification of conserved regions of ribosomal RNA sequences. These regions are not specific and therefore can be used to detect any *Legionella* subspecies (57). In 35 studies that used respiratory samples, the summary sensitivity and specificity estimates of PCR for *Legionella* spp. were 97.4 and 98.6%, respectively (57). Compared with UATs, PCRs have better sensitivity and similar specificity. In the literature, patients with LDs that was acquired in the nosocomial setting or who are severely immunosuppressed are more likely to be infected by non-Lp1 strains (58, 59). For example, Head et al. reported that 36% of people living with HIV were coinfected with *Legionella* and that approximately one-third of LDs were caused by Lp, but none of these cases were caused by Lp1 (60). In such cases, the UATs might yield false negative results, and PCR might significantly improve the accuracy of diagnosis in these cases.

However, false negative results have been reported in some studies because of factors such as PCR inhibition, mismatch of primers and/or probes, the presence of *Legionella* targets in quantities below the limit of detection, and improper sample collection and handling (61). False positive results have also occurred due to cross-reaction of the *Legionella* species target (but not Lp) with *Stenotrophomonas maltophilia* (46). In addition, PCR kits are expensive, and the procedure requires specialized lab equipment and personnel. Although molecular tools such as specific PCR for *Legionella* spp. have been developed, they are rarely used in the clinic (62). In Europe, only 2% of 11,832 confirmed or suspected LD cases were identified by PCR (63).

mNGS enables the early detection of pathogenic microorganisms in specimens without hypothesis or bias, and it yields results that are not greatly influenced by previous administration of antibiotics (64). As a high-resolution and sensitive assay that covers the entire *Legionella* genus, including Lp and non-Lp, mNGS may circumvent the shortcomings of *Legionella* culture and UATs, and compensate for the inherent weaknesses of PCR in the diagnosis and surveillance of *Legionella* infection (65). In the literature coinfection with *Legionella* and other bacterial species, particularly *Streptococcus pneumoniae* and *Acinetobacter*, may occur (66). Tan et al. described six LD patients, all of whom had bacteremic coinfections (67). Other species that have been found to coinfect individuals infected with *Legionella* include *Pneumocystis jirovecii* (68), *Mycoplasma pneumoniae*, *Chlamydia pneumoniae*, *Chlamydia psittaci*, *Klebsiella pneumoniae*, and *Pneumocystis aeruginosa* (69). In cases such as

these, mNGS can more comprehensively identify the coinfecting pathogens in a timely manner, and the mNGS results can be used to select the antibiotic mixture needed for the successful treatment of pneumonia.

We are currently in an era of rapid development of novel techniques such as mNGS. These novel techniques should be considered new tools that provided rapid molecular methods for the detection of pathogens in pneumonia patients. mNGS also has the potential to identify pathogens present in the environment, including *Legionella*, for example in water samples, and thus to play a crucial role in outbreak control (66). Identifying *Legionella* as the causative agent of infection is essential for disease treatment and outbreak prevention (70, 71).

As a rapid and unbiased assay for the presence of specific microorganisms, mNGS has unique advantages in the detection of difficult-to-culture pathogens (72), especially in resource-limited healthcare settings. However, mNGS also has several shortcomings compared with other traditional microbiological tests; these shortcomings include its higher cost, its analytical sensitivity, the need for a complex laboratory workflow, and its susceptibility to contamination (73). Although the current cost of mNGS is relatively high (approximately 480$ per sample in China), early precise pathogenic diagnosis, treatment and optimal patient management may help reduce overall medical expenditures (65). On the other hand, patients' families often believe it is worthwhile to identify the pathogen early to improve patient prognosis. Nevertheless, the high cost of mNGS hinders its promotion and application in clinical practice. Therefore, targeted next-generation sequencing (tNGS) technology, which may be a good supplement for mNGS, is being developed and applied in China. Its sequencing volume is 1% that of mNGS, its cost is lower (approximately 164$ per sample in China), and it can detect hundreds of common DNA and RNA pathogens, thereby meeting the routine needs of clinical practice (74). However, if tNGS results are negative and the patient nevertheless has a highly suspicious infection, it is recommended that use of the mNGS test be considered to expand pathogen detection.

Given the vast amount of sequence information obtained through mNGS and the diversity of existing pathogen species, it can be extremely difficult to interpret mNGS reports correctly, and this increases the risk of false positive results (75). To date, there is a lack of internationally recognized standards for distinguishing whether pathogens identified by mNGS are truly pathogenic, colonized, or merely false positives. To address this issue, we combine the mNGS results with potentially useful information that may help identify the causative pathogen of lung infection; the other useful information includes the patient's medical history, immune status, serum inflammation values, microbial culture results, lung imaging and many other types of clinical information. In addition, at least two associate chief physicians jointly interpret the mNGS results to increase the authenticity and reliability of the conclusions and to reduce false positive rates as much as possible.

UATs and PCR for *Legionella* have not yet been performed at our hospital; the two cases of severe LD discussed here were ultimately confirmed by mNGS of BALF. We believe that with reductions in sequencing costs and continuous improvement in interpretation standards in China, mNGS-based pathogenic diagnosis can be increasingly used to greatly improve the choice of antimicrobial drug regimens and the timeliness of clinical pathogen treatment, especially in challenging cases of complicated infectious disease (76).

Conclusion

Overall mortality due to LD ranges from 4 to 18%, but it is close to 40% among immunocompromised patients and individuals requiring ICU admission (77–79). Therefore, early identification and diagnosis of LD is essential for effective treatment and accurate prognosis. Most clinical manifestations, laboratory findings, and radiographic features are non-specific. Orange-colored sputum and BALF appear to represent an important clues, but this needs to be explored in larger numbers of cases. The settings and incubation time required to culture *Legionella* are very strict, and not easy applied in clinical practice. UATs are convenient and fast, but mainly detect Lp1 and are not equally sensitive to all subtypes of *Legionella* (2), possibly resulting in underestimation of the actual incidence of the infection (44). PCR is more sensitive than UATs and can detect all *Legionella* subtypes, but it is technically demanding and is not widely used in the clinic (62). Therefore, mNGS could be considered for patients with severe pneumonia. In particular, causative pathogens cannot be identified by conventional detection methods (80) and patients may have coinfections. The use of mNGS can provide new diagnostic evidence that can be used to precisely guide precise antimicrobial therapy (81).

Data availability statement

The original contributions presented in the study are included in the article/supplementary material, further inquiries can be directed to the corresponding author.

Ethics statement

The studies involving humans were approved by the Hangzhou Linping Hospital of Traditional Chinese Medicine. The studies were conducted in accordance with the local legislation and institutional requirements. The participants provided their written informed consent to participate in this study. Written informed consent was obtained from the individual(s) for the publication of any potentially identifiable images or data included in this article.

Author contributions

JF: Supervision, Writing – original draft, Writing – review & editing. ZW: Data curation, Writing – original draft. YS: Data curation, Writing – original draft. XW: Data curation, Writing – original draft. HF: Data curation, Writing – original draft. XS: Methodology, Project administration, Supervision, Validation, Writing – original draft. TY: Methodology, Project administration, Supervision, Validation, Writing – original draft.

QZ: Methodology, Project administration, Supervision, Validation, Writing – original draft.

Funding

The author(s) declare that no financial support was received for the research, authorship, and/or publication of this article.

Acknowledgments

We wish to thank the patient for their consent to publish this case report.

Conflict of interest

The authors declare that the research was conducted in the absence of any commercial or financial relationships that could be construed as a potential conflict of interest.

Publisher's note

References

1. Burillo A, Pedro-Botet ML, Bouza E. Microbiology and epidemiology of Legionnaire's disease. *Infect Dis Clin N Am.* (2017) 31:7–27.

2. Cunha BA, Burillo A, Bouza E. Legionnaires' disease. *Lancet (London, England).* (2016) 387:376–85.

3. Fraser DW, Tsai TR, Orenstein W, Parkin WE, Beecham HJ, Sharrar RG, et al. Legionnaires' disease: Description of an epidemic of pneumonia. *N Engl J Med.* (1977) 297:1189–97.

4. Gonçalves IG, Simões LC, Simões M. Legionella pneumophila. *Trends Microbiol.* (2021) 29:860–1.

5. Brady MF, Awosika AO, Nguyen AD, Sundareshan V. "*Legionnaires disease*," in StatPearls [Internet]. StatPearls Publishing (2024).

6. Li S, Tong J, Li H, Mao C, Shen W, Lei Y, et al. L. pneumophila infection diagnosed by tNGS in a lady with lymphadenopathy. *Infect Drug Resist.* (2023) 16:4435–42. doi: 10.2147/IDR.S417495

7. Pouderoux C, Ginevra C, Descours G, Ranc AG, Beraud L, Boisset S, et al. Slowly or nonresolving Legionnaires' disease: Case series and literature review. *Clin Infect Dis.* (2020) 70:1933–40.

8. Almirall J, Blanquer J, Bello S. Community-acquired pneumonia among smokers. *Arch Bronconeumol.* (2014) 50:250–4.

9. Straus WL, Plouffe JF, File TM Jr., Lipman HB, Hackman BH, Salstrom SJ, et al. Risk factors for domestic acquisition of legionnaires disease. Ohio legionnaires Disease Group. *Arch Intern Med.* (1996) 156:1685–92.

10. Yue R, Wu X, Li T, Chang L, Huang X, Pan L. Early detection of *Legionella pneumophila* and Aspergillus by mNGS in a critically ill patient with legionella pneumonia after extracorporeal membrane oxygenation treatment: Case report and literature review. *Front Med.* (2021) 8:686512. doi: 10.3389/fmed.2021.686512

11. Rello J, Allam C, Ruiz-Spinelli A, Jarraud S. Severe Legionnaires' disease. *Ann Intens Care.* (2024) 14:51.

12. Teira A, Sánchez J, Santiago I, Zarauza J, Nan D, Teira R. Legionella endocarditis: A case report and review. *Enferm Infecc Microbiol Clin (English ed).* (2020). [Epub ahead of print].

13. Abdelghany M, Pruchnic W, Waseem S, Hussain KA. Legionella pericarditis, an unusual presentation. *Research* (2014). doi: 10.13070/rs.en.1.896

14. Grün D, Unger MM, Kauffmann J, Zimmer V, Fassbender K, Fousse M. Legionnaire's-disease-associated meningoencephalitis: A case report. *Pulmonology.* (2019) 25:128–30.

15. Lapidot R, Alawdah L, Köhler JR, Paulson V, Levy O. Hepatic *Legionella pneumophila* infection in an infant with severe combined immunodeficiency. *Pediatr Infect Dis J.* (2018) 37:356–8. doi: 10.1097/INF.0000000000001789

16. Stout JE, Yu VL. Legionellosis. *N Engl J Med.* (1997) 337:682–7.

17. Hlavsa MC, Cikesh BL, Roberts VA, Kahler AM, Vigar M, Hilborn ED, et al. Outbreaks associated with treated recreational water - United States, 2000-2014. *MMWR Morb Mortal Weekly Rep.* (2018) 67:547–51. doi: 10.15585/mmwr.mm6719a3

18. David S, Rusniok C, Mentasti M, Gomez-Valero L, Harris SR, Lechat P, et al. Multiple major disease-associated clones of *Legionella pneumophila* have emerged recently and independently. *Genome Res.* (2016) 26:1555–64. doi: 10.1101/gr.209536.116

19. Morimoto Y, Ishiguro T, Uozumi R, Takano K, Kobayashi Y, Kobayashi Y, et al. Significance of hypophosphatemia in patients with pneumonia. *Intern Med (Tokyo, Japan).* (2022) 61:979–88.

20. Viasus D, Di Yacovo S, Garcia-Vidal C, Verdaguer R, Manresa F, Dorca J, et al. Community-acquired *Legionella pneumophila* pneumonia: A single-center experience with 214 hospitalized sporadic cases over 15 years. *Medicine.* (2013) 92:51–60. doi: 10.1097/MD.0b013e31827f6104

21. Malani PN. Mandell, Douglas, and Bennett's principles and practice of infectious diseases. *JAMA.* (2010) 304:2067–8.

22. Cunha CB, Cunha BA. Antimicrobial therapy for Legionnaire's disease: Antibiotic stewardship implications. *Infect Dis Clin N Am.* (2017) 31:179–91. doi: 10.1016/j.idc.2016.10.013

23. Jasper AS, Musuuza JS, Tischendorf JS, Stevens VW, Gamage SD, Osman F, et al. Are fluoroquinolones or macrolides better for treating legionella pneumonia? A systematic review and meta-analysis. *Clin Infect Dis.* (2021) 72:1979–89.

24. Kato H, Hagihara M, Asai N, Shibata Y, Koizumi Y, Yamagishi Y, et al. Meta-analysis of fluoroquinolones versus macrolides for treatment of legionella pneumonia. *J Infect Chemother.* (2021) 27:424–33.

25. Allgaier J, Lagu T, Haessler S, Imrey PB, Deshpande A, Guo N, et al. Risk factors, management, and outcomes of legionella pneumonia in a large, nationally representative sample. *Chest* (2021) 159:1782–92. doi: 10.1016/j.chest.2020.12.013

26. Rello J, Gattarello S, Souto J, Sole-Violan J, Valles J, Peredo R, et al. Community-acquired Legionella Pneumonia in the intensive care unit: Impact on survival of combined antibiotic therapy. *Med Intens.* (2013) 37:320–6.

27. Bruin JP, Koshkolda T, Ep IJ, Lück C, Diederen BM, Den Boer JW, et al. Isolation of ciprofloxacin-resistant *Legionella pneumophila* in a patient with severe pneumonia. *J Antimicrob Chemother.* (2014) 69:2869–71. doi: 10.1093/jac/dku196

28. Ginevra C, Beraud L, Pionnier I, Sallabery K, Bentayeb H, Simon B, et al. Detection of highly macrolide-resistant *Legionella pneumophila* strains from a hotel water network using systematic whole-genome sequencing. *J Antimicrob Chemother.* (2022) 77:2167–70. doi: 10.1093/jac/dkac173

29. Cunha BA, Connolly J, Abruzzo E. Increase in pre-seasonal community-acquired Legionnaire's disease due to increased precipitation. *Clin Microbiol infect.* (2015) 21:e45–6. doi: 10.1016/j.cmi.2015.02.015

30. Garcia-Vidal C, Labori M, Viasus D, Simonetti A, Garcia-Somoza D, Dorca J, et al. Rainfall is a risk factor for sporadic cases of *Legionella pneumophila* pneumonia. *PLoS One.* (2013) 8:e61036. doi: 10.1371/journal.pone.0061036

31. Principe L, Tomao P, Visca P. Legionellosis in the occupational setting. *Environ Res.* (2017) 152:485–95.

32. Sakamoto R, Ohno A, Nakahara T, Satomura K, Iwanaga S, Kouyama Y, et al. Is driving a car a risk for Legionnaires' disease? *Epidemiol Infect.* (2009) 137:1615–22. doi: 10.1017/S0950268809002568

33. Polat Y, Ergin C, Kaleli I, Pinar A. [Investigation of *Legionella pneumophila* seropositivity in the professional long distance drivers as a risky occupation]. *Mikrobiyoloji Bulteni.* (2007) 41:211–7.

34. Sumi T, Suzuki K, Koshino Y, Ikeda T, Yamada Y, Chiba H. Sputum colour: An indicator of *Legionella pneumophila* pneumonia. *Respirol Case Rep.* (2024) 12:e01312. doi: 10.1002/rcr2.1312

35. Asami-Noyama M, Harada M, Murakawa K, Suizu J, Murakawa K, Chikumoto A, et al. Non-pneumophila Legionella species pneumonia with orange-coloured sputum. *Respirol Case Rep.* (2021) 9:e0814. doi: 10.1002/rcr2.814

36. Chen Y, Lu Y. Pay attention to clinical issues easy to be neglected in diagnosis and treatment of Legionella pneumonia. *J Intern Med Concepts Pract.* (2024) 19:6–12.

37. Fujita J, Touyama M, Chibana K, Koide M, Haranaga S, Higa F, et al. Mechanism of formation of the orange-colored sputum in pneumonia caused by *Legionella pneumophila*. *Intern Med (Tokyo, Japan).* (2007) 46:1931–4. doi: 10.2169/internalmedicine.46.0444

38. Carter CJ, Corley EM, Canepa H, Schmalzle SA. Legionnaires' disease presenting with exanthem; Case and review of previously published cases. *IDCases.* (2022) 27:e01376. doi: 10.1016/j.idcr.2022.e01376

39. Allen TP, Fried JS, Wiegmann TB, Hodges GR, Dixon AY, Lee SH, et al. Legionnaires' disease associated with rash and renal failure. *Arch Intern Med.* (1985) 145:729–30.

40. Calza L, Briganti E, Casolari S, Manfredi R, Chiodo F, Zauli T. Legionnaires' disease associated with macular rash: Two cases. *Acta Dermatovenereol.* (2005) 85:342–4.

41. Ziemer M, Ebert K, Schreiber G, Voigt R, Sayer HG, Marx G. Exanthema in Legionnaires' disease mimicking a severe cutaneous drug reaction. *Clin Exp Dermatol.* (2009) 34:e72–4. doi: 10.1111/j.1365-2230.2008.03176.x

42. Meyer RD, Edelstein PH, Kirby BD, Louie MH, Mulligan ME, Morgenstein AA, et al. Legionnaires' disease: Unusual clinical and laboratory features. *Ann Intern Med.* (1980) 93:240–3.

43. Dua R, Sindhwani G, Rawat J. Exfoliative dermatitis to all four first line oral anti-tubercular drugs. *Indian J Tubercul.* (2010) 57:53–6.

44. Pierre DM, Baron J, Yu VL, Stout JE. Diagnostic testing for Legionnaires' disease. *Ann Clin Microbiol Antimicrob.* (2017) 16:59.

45. European Centre for Disease Prevention and Control. *Legionnaires' Disease-Annual Epidemiological Report for 2021*. Stockholm: European Centre for Disease Prevention and Control (2023).

46. Peci A, Winter AL, Gubbay JB. Evaluation and comparison of multiple test methods, including real-time PCR, for legionella detection in clinical specimens. *Front Public Health.* (2016) 4:175. doi: 10.3389/fpubh.2016.00175

47. Miyashita N, Higa F, Aoki Y, Kikuchi T, Seki M, Tateda K, et al. Distribution of Legionella species and serogroups in patients with culture-confirmed Legionella pneumonia. *J Infect Chemother.* (2020) 26:411–7.

48. Yu VL, Plouffe JF, Pastoris MC, Stout JE, Schousboe M, Widmer A, et al. Distribution of Legionella species and serogroups isolated by culture in patients with sporadic community-acquired legionellosis: An international collaborative survey. *J Infect Dis.* (2002) 186:127–8. doi: 10.1086/341087

49. Amemura-Maekawa J, Kura F, Chida K, Ohya H, Kanatani JI, Isobe J, et al. *Legionella pneumophila* and other legionella species isolated from legionellosis patients in Japan between 2008 and 2016. *Appl Environ Microbiol.* (2018) 84:e721–718. doi: 10.1128/AEM.00721-18

50. Mandell LA, Wunderink RG, Anzueto A, Bartlett JG, Campbell GD, Dean NC, et al. Infectious diseases society of America/American Thoracic Society consensus guidelines on the management of community-acquired pneumonia in adults. *Clin Infect Dis.* (2007) 44 Suppl 2(Suppl. 2):S27–72. doi: 10.1086/511159

51. Mercante JW, Winchell JM. Current and emerging Legionella diagnostics for laboratory and outbreak investigations. *Clin Microbiol Rev.* (2015) 28:95–133.

52. Sopena N, Sabrià M, Pedro-Botet ML, Reynaga E, García-Núñez M, Domínguez J, et al. Factors related to persistence of Legionella urinary antigen excretion in patients with legionnaires' disease. *Eur J Clin Microbiol Infect Dis.* (2002) 21:845–8. doi: 10.1007/s10096-002-0839-5

53. Yzerman EP, den Boer JW, Lettinga KD, Schellekens J, Dankert J, Peeters M. Sensitivity of three urinary antigen tests associated with clinical severity in a large outbreak of Legionnaires' disease in The Netherlands. *J Clin Microbiol.* (2002) 40:3232–6. doi: 10.1128/JCM.40.9.3232-3236.2002

54. Garbino J, Bornand JE, Uçkay I, Fonseca S, Sax H. Impact of positive legionella urinary antigen test on patient management and improvement of antibiotic use. *J Clin Pathol.* (2004) 57:1302–5. doi: 10.1136/jcp.2004.018861

55. Shimada T, Noguchi Y, Jackson JL, Miyashita J, Hayashino Y, Kamiya T, et al. Systematic review and metaanalysis: Urinary antigen tests for Legionellosis. *Chest.* (2009) 136:1576–85.

56. Kinjo T, Ito A, Ishii M, Komiya K, Yamasue M, Yamaguchi T, et al. National survey of physicians in Japan regarding their use of diagnostic tests for legionellosis. *J Infect Chemother.* (2022) 28:129–34. doi: 10.1016/j.jiac.2021.12.008

57. Avni T, Bieber A, Green H, Steinmetz T, Leibovici L, Paul M. Diagnostic accuracy of PCR alone and compared to urinary antigen testing for detection of Legionella spp.: A systematic review. *J Clin Microbiol.* (2016) 54:401–11. doi: 10.1128/JCM.02675-15

58. Helbig JH, Uldum SA, Bernander S, Lück PC, Wewalka G, Abraham B, et al. Clinical utility of urinary antigen detection for diagnosis of community-acquired, travel-associated, and nosocomial legionnaires' disease. *J Clin Microbiol.* (2003) 41:838–40. doi: 10.1128/JCM.41.2.838-840.2003

59. Ranc AG, Carpentier M, Beraud L, Descours G, Ginevra C, Maisonneuve E, et al. *Legionella pneumophila* LPS to evaluate urinary antigen tests. *Diagn Microbiol infect Dis.* (2017) 89:89–91. doi: 10.1016/j.diagmicrobio.2017.06.013

60. Head BM, Trajtman A, Bernard K, Burdz T, Vélez L, Herrera M, et al. Legionella co-infection in HIV-associated pneumonia. *Diagn Microbiol Infect Dis.* (2019) 95:71–6.

61. Fields BS, Benson RF, Besser RE. Legionella and Legionnaires' disease: 25 years of investigation. *Clin Microbiol Rev.* (2002) 15:506–26.

62. Botelho-Nevers E, Grattard F, Viallon A, Allegra S, Jarraud S, Verhoeven P, et al. Prospective evaluation of RT-PCR on sputum versus culture, urinary antigens and serology for Legionnaire's disease diagnosis. *J Infect.* (2016) 73:123–8. doi: 10.1016/j.jinf.2016.04.039

63. Beauté J, Zucs P, de Jong B. Legionnaires disease in Europe, 2009-2010. *Euro Surveill.* (2013) 18:20417.

64. Zuo YH, Wu YX, Hu WP, Chen Y, Li YP, Song ZJ, et al. The Clinical Impact of Metagenomic Next-Generation Sequencing (mNGS) Test in hospitalized patients with suspected sepsis: A Multicenter Prospective Study. *Diagnostics (Basel, Switzerland.)* (2023) 13:323. doi: 10.3390/diagnostics13020323

65. Lei C, Zhou X, Ding S, Xu Y, Yang B, Guo W, et al. Case report: Community-acquired legionella gormanii pneumonia in an immunocompetent patient detected by metagenomic next-generation sequencing. *Front Med.* (2022) 9:819425. doi: 10.3389/fmed.2022.819425

66. Mizrahi H, Peretz A, Lesnik R, Aizenberg-Gershtein Y, Rodríguez-Martínez S, Sharaby Y, et al. Comparison of sputum microbiome of legionellosis-associated patients and other pneumonia patients: Indications for polybacterial infections. *Sci Rep.* (2017) 7:40114. doi: 10.1038/srep40114

67. Tan MJ, Tan JS, File TM Jr. Legionnaires disease with bacteremic coinfection. *Clin Infect Dis.* (2002) 35:533–9. doi: 10.1086/341771

68. Musallam N, Bamberger E, Srugo I, Dabbah H, Glikman D, Zonis Z, et al. *Legionella pneumophila* and Pneumocystis jirovecii coinfection in an infant treated with adrenocorticotropic hormone for infantile spasm: Case report and literature review. *J Child Neurol.* (2014) 29:240–2. doi: 10.1177/0883073813511148

69. Takayanagi N, Tokunaga D, Matsushima H, Ubukata M, Sato N, Kurashima K, et al. [Polymicrobial infections in patients with Legionella pneumonia]. *Nihon Kokyuki Gakkai zasshi.* (2004) 42:62–7.

70. Cho MC, Kim H, An D, Lee M, Noh SA, Kim MN, et al. Comparison of sputum and nasopharyngeal swab specimens for molecular diagnosis of Mycoplasma pneumoniae, Chlamydophila pneumoniae, and *Legionella pneumophila*. *Ann Lab Med.* (2012) 32:133–8. doi: 10.3343/alm.2012.32.2.133

71. White PS, Graham FF, Harte DJ, Baker MG, Ambrose CD, Humphrey AR. Epidemiological investigation of a Legionnaires' disease outbreak in Christchurch, New Zealand: The value of spatial methods for practical public health. *Epidemiol Infect.* (2013) 141:789–99. doi: 10.1017/S0950268812000994

72. Kolb M, Lazarevic V, Emonet S, Calmy A, Girard M, Gaïa N, et al. Next-generation sequencing for the diagnosis of challenging culture-negative endocarditis. *Front Med.* (2019) 6:203. doi: 10.3389/fmed.2019.00203

73. Greninger AL. The challenge of diagnostic metagenomics. *Exp Rev Mol Diagn.* (2018) 18:605–15.

74. Pei XM, Yeung MHY, Wong ANN, Tsang HF, Yu ACS, Yim AKY, et al. Targeted sequencing approach and its clinical applications for the molecular diagnosis of human diseases. *Cells.* (2023) 12:493.

75. Gaston DC, Miller HB, Fissel JA, Jacobs E, Gough E, Wu J, et al. Evaluation of metagenomic and targeted next-generation sequencing workflows for detection of respiratory pathogens from bronchoalveolar lavage fluid specimens. *J Clin Microbiol.* (2022) 60:e0052622.

76. He D, Quan M, Zhong H, Chen Z, Wang X, He F, et al. Emergomyces orientalis emergomycosis diagnosed by metagenomic next-generation sequencing. *Emerg Infect. Dis.* (2021) 27:2740–2.

77. Chidiac C, Che D, Pires-Cronenberger S, Jarraud S, Campèse C, Bissery A, et al. Factors associated with hospital mortality in community-acquired legionellosis in France. *Eur Respir J.* (2012) 39:963–70.

78. Pamparino S, Valente I, Tagliafico A, Dentone C, Bassetti M, Mennella S, et al. A very rare case of mycobacterium gordonae infection of the breast. *Breast J.* (2020) 26:2229–32.

79. Andrea L, Dicpinigaitis PV, Fazzari MJ, Kapoor S. Legionella pneumonia in the ICU: A tertiary care center experience over 10 years. *Crit Care Explor.* (2021) 3:e0508. doi: 10.1097/CCE.0000000000000508

80. Naccache SN, Federman S, Veeraraghavan N, Zaharia M, Lee D, Samayoa E, et al. A cloud-compatible bioinformatics pipeline for ultrarapid pathogen identification from next-generation sequencing of clinical samples. *Genome Res.* (2014) 24:1180–92. doi: 10.1101/gr.171934.113

81. Hilbi H, Jarraud S, Hartland E, Buchrieser C. Update on Legionnaires' disease: Pathogenesis, epidemiology, detection and control. *Mol Microbiol.* (2010) 76:1–11. doi: 10.1111/j.1365-2958.2010.07086.x

frontiers | Frontiers in Medicine

TYPE Case Report
PUBLISHED 11 February 2025
DOI 10.3389/fmed.2025.1518935

OPEN ACCESS

EDITED BY
Giuseppe Fiorentino,
Colli Hospital, Italy

REVIEWED BY
Eric Chun-Pu Chu,
EC Healthcare, Hong Kong SAR, China
Mohammed Alharthi,
Taif University, Saudi Arabia

*CORRESPONDENCE
Mei Hu
✉ humei306@126.com

†These authors have contributed equally to this work

RECEIVED 29 October 2024
ACCEPTED 24 January 2025
PUBLISHED 11 February 2025

CITATION
Zhai R, Su H, Wu Y, Tan R, Zhang X, Tian Y and Hu M (2025) Airway clearance technique therapy for atelectasis induced by scoliosis surgery: a case report.
Front. Med. 12:1518935.
doi: 10.3389/fmed.2025.1518935

Airway clearance technique therapy for atelectasis induced by scoliosis surgery: a case report

Rui Zhai[1†], Hairong Su[1†], Yaxu Wu[1], Rong Tan[2], Xiaoli Zhang[1], Ye Tian[1] and Mei Hu[1*]

[1]Department of Critical Care Medicine, Ninth Medical Center, General Hospital of the People's Liberation Army, Beijing, China, [2]Department of Spinal Surgery, Ninth Medical Center, General Hospital of the People's Liberation Army, Beijing, China

The patient, a 55-year-old female presenting with spinal deformity and exertional dyspnea, was referred to the hospital. Radiographic evaluation of her spine revealed an "S"-shaped scoliosis with a Cobb angle measuring 68°, indicative of severe scoliosis. Despite receiving medication for expectoration, postoperative symptoms including chest tightness, breathlessness, and ineffective coughing persisted and progressively worsened. Subsequent chest CT scans demonstrated extensive atelectasis, and pharmacological interventions proved to be ineffective. Considering the patient's clinical condition, we implemented airway clearance technique (ACT) along with prone ventilation to optimize cough effectiveness and mitigate atelectasis formation. The airway clearance techniques (ACT) employed include nebulization, continuous positive expiratory pressure (CPEP), and continuous high frequency oscillation (CHFO). Chest CT imaging confirmed that ACT substantially alleviated the patient's pulmonary atelectasis. Moreover, blood gas analysis indicated significant improvements in both the PaO_2/FiO_2 ratio and base excess of whole blood. Follow-up evaluation 1 year post-discharge revealed a favorable prognosis for the patient. We anticipate that our experience utilizing these novel therapeutic modalities will provide valuable insights for clinicians managing similar complications.

KEYWORDS

airway clearance technique, severe scoliosis, atelectasis, postoperative complications of scoliosis, case report

Introduction

The primary diagnostic criterion for scoliosis is a spinal curvature exceeding 10° on anterior and posterior X-rays. In the absence of other abnormal symptoms, such as hemivertebrae, it is referred to as idiopathic scoliosis (1). Despite the unknown pathogenesis of scoliosis, a review suggests four main pathogenetic mechanisms based on reported evidence: asymmetric bone growth dysregulation, susceptibility of bones to deformation, abnormal passive or disturbed active spinal system maintenance (2). Scoliosis restricts rib movement and impairs respiratory muscle function while displacing thoracic organs. Severe cases may lead to respiratory failure (3). Adult patients commonly experience pain and neurological symptoms compared to adolescent patients, with more complex procedures associated with higher rates of intraoperative and perioperative complications (4). A meta-analysis, which synthesized data from 17 clinical trials, demonstrated that the overall incidence of postoperative complications following scoliosis surgery was 23%, with pulmonary complications affecting 6.7% of cases (5). This emphasizes the significance of therapeutic management for postoperative complications. Herein we present a case

involving severe pulmonary atelectasis as a postoperative complication following scoliosis surgery. When conventional treatment regimens proved ineffective, our innovative approach utilizing noninvasive airway clearance technique combined with existing research led to significant improvements in patients suffering from atelectasis. We aim to provide clinicians with novel insights into managing such challenges.

Airway clearance techniques (ACT) are non-invasive interventions aimed at enhancing sputum clearance, thereby optimizing ventilation and mitigating the effects of coughing and dyspnea (6). ACT typically consists of four essential components. First, nebulization is utilized to loosen sputum or administer therapeutic medications. Second, continuous positive expiratory pressure (CPEP) is applied to maintain airway patency and dilation. Third, continuous high frequency oscillation (CHFO), a type of pneumatic chest physiotherapy, employs continuous high frequency oscillation within the airways to facilitate sputum mobilization. Finally, patients actively participate in expectoration. ACT is currently employed in the management of bronchiectasis, chronic suppurative lung disease, and cystic fibrosis (6–8). Pulmonary atelectasis is commonly managed through infection control, oxygen therapy, respiratory support, and surgical intervention when necessary. In this specific case, however, the patient exhibited inadequate response to conventional treatments including oxygen therapy, ambroxol hydrochloride, and budesonide. Given the patient's refusal of invasive procedures, the medical team faced the challenge of effectively managing the atelectasis while simultaneously alleviating the patient's discomfort. To address this issue, the physicians conducted an extensive literature review to learn the background and efficacy of airway clearance techniques (ACT). Based on clinical experience indicating ACT's potential in treating post-scoliosis surgery atelectasis, they discussed the treatment options with the patient and ultimately decided to proceed with ACT therapy. This innovative application of ACT not only successfully resolved the atelectasis but also minimized pain associated with invasive procedures and reduced overall treatment costs.

Case report

The patient, a 55-year-old female, had a surgical history of hydrocephalus correction at 6 weeks of age and underwent right-sided hip replacement 43 years ago. Additionally, she had a medical history of COPD. Following birth, the patient presented with spinal deformity characterized by deviation to one side. The patient eventually sought medical attention for curvature of the spine, chest tightness, and breath-holding with activity and continued aggravation.

On physical examination, the patient's height was 150 cm and weight was 42 kg. The body temperature was 36.1°C, pulse rate was 78 beats per minute, respiratory rate was 18 breaths per minute, and blood pressure was 110/70 mmHg. On thoracic auscultation, bilateral lung fields were clear; however, breath sounds were diminished. Following physical examination, it was determined that the patient exhibited a 4 cm elevation of the right shoulder compared to the left shoulder, a 3 cm elevation of the left side of the pelvis compared to the right side, unequal lower limb lengths, and distances from the anterior superior iliac crest to inner ankle measuring 77 cm on the left side and 74 cm on the right side. No abnormalities were observed in other areas of the patient's body. Ancillary X-rays (Figure 1A) and CT scans (Figure 2A) revealed an "S"-shaped scoliosis with a right convex kyphoscoliosis exhibiting a Cobb angle of 68° along with some vertebral dysplasia; the first 7, 9, and 10 thoracic vertebrae exhibited hemivertebrae with spinal cord cavities in cervical segments 4–6, longitudinal fissures of the spinal cord at the cervical-lumbar level, and formation of bony ridges in the spinal canal at the thoracic-lumbar level; bilateral lung striations with localised incomplete expansion of lung tissue. The results of blood gas analyses are summarized in Table 1. Detailed outcomes of

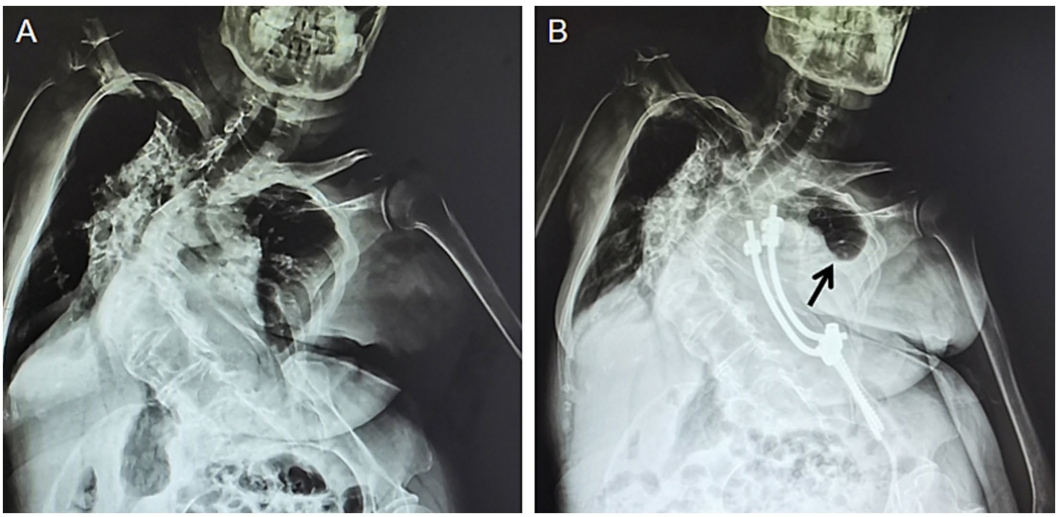

FIGURE 1
Radiological images of the patient's spine. **(A)** The preoperative state. **(B)** The postoperative state. The black arrow points to the location of pulmonary atelectasis in the patient's left lung.

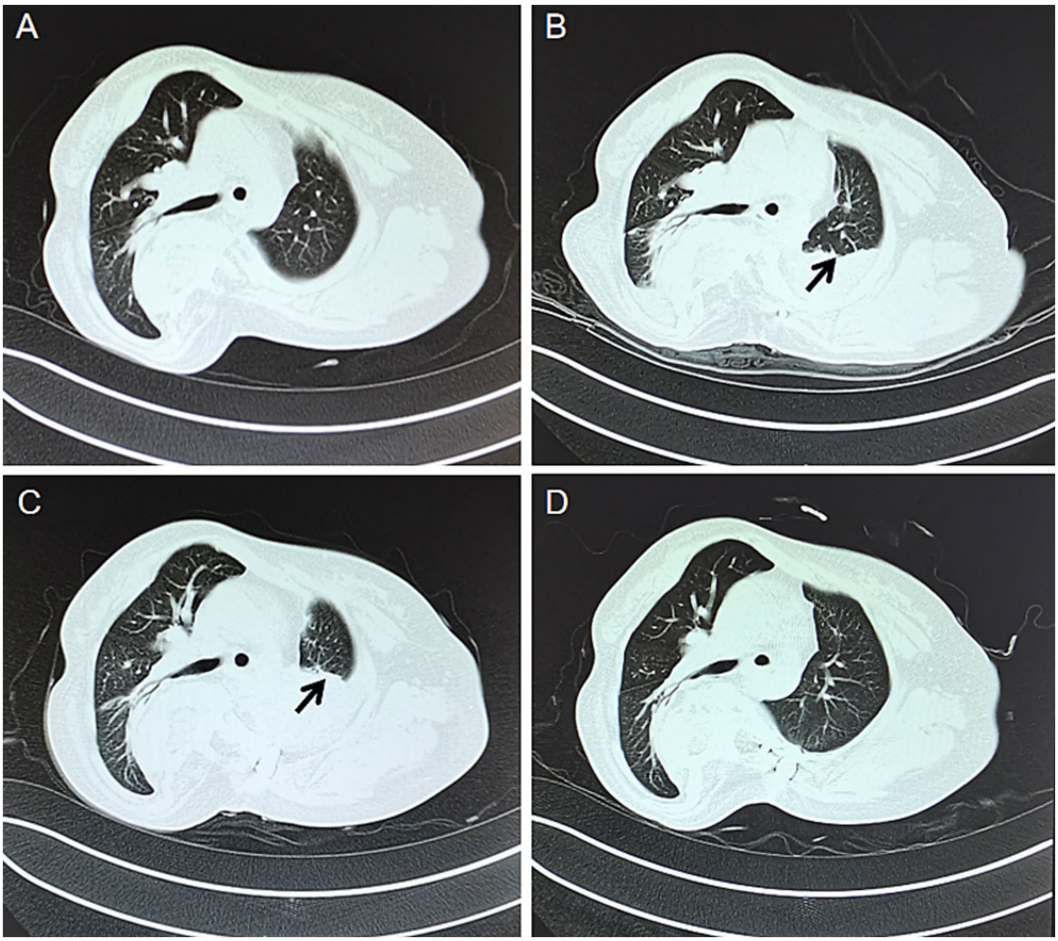

FIGURE 2
CT images of the patient's chest at different times. **(A)** Preoperative. **(B)** Post-surgery at 2 days. **(C)** Post-surgery at 13 days. **(D)** One week after airway clearance treatment. The black arrow points to the location of pulmonary atelectasis in the patient's left lung.

TABLE 1 Blood gas analysis results of patient.

Variable	Reference range, this hospital[a]	Admission	Day of surgery	1 day after surgery	13 days after surgery	Final test
Partial pressure of arterial oxygen (PaO_2), mmHg	83–108	71	103	130	85	68
Partial pressure of arterial carbon dioxide ($PaCO_2$), mmHg	35–45	57	67	62	62	45
PH	7.35–7.45	7.40	7.18	7.35	7.41	7.38
PaO_2/FiO_2 ratio, mmHg	>300	338	490	510	258	324
Base excess of whole blood (BEb), mmol/L	−3 to +3	8.8	−3.8	7.1	12.4	1
Actual bicarbonate (AB), mmol/L	22–26	35.3	25	34.2	39.3	26.6

[a]Reference values are influenced by many variables, including the patient population and the laboratory methods used. Therefore, our reference values may not apply to all patients.

pulmonary function tests are provided in Table 2; however, it should be noted that several tests were incompletely performed due to the patient's limited lung vital capacity. Given these findings, particularly the presence of hemivertebrae, the preliminary diagnosis was scoliosis with associated pulmonary dysfunction. Successful posterior orthopedic implant fusion and internal fixation for scoliosis were achieved under general anesthesia using a standardized anesthetic regimen, which included sufentanil 50 μg, cisatracurium besylate 10 mg, midazolam 10 mg, etomidate 20 mg, remifentanil 2 mg, and propofol 1 g. The operation lasted 145 min. To enhance the clarity of the treatment process, we have formulated a detailed timeline as illustrated in Figure 3. The patient reported a VAS pain score of 3 on the first postoperative day, which may have inadvertently

contributed to a reduced frequency of coughing. This reduction in coughing frequency could have subsequently led to symptoms of chest tightness, dyspnea, and difficulty expectorating that evening, persisting into the second postoperative day. The VAS pain rating scale is provided in Supplementary Figure S1. A chest CT examination conducted on the second day after surgery revealed bilateral lung striations, localized lung tissue distension insufficiency that was more progressive than preoperative findings, bilateral pleural effusions, and atelectasis (Figures 2A,B). The patient's VAS pain score decreased to 0 by the fourth post-operative day. Initial treatment with ambroxol hydrochloride injection (4 mL) and nebulized inhalation of budesonide suspension (1 mg) proved ineffective as symptoms worsened progressively. Subsequent chest CT at 13 days after operation indicated further exacerbation of atelectasis (Figure 2C), while radiological examination confirmed postoperative scoliosis (Figure 1B). Blood gas analysis revealed significant deterioration in several critical parameters, including the PaO_2/FiO_2 ratio, base excess in whole blood, and actual bicarbonate concentration (Table 1). The patient would not accept invasive treatment. Based on the original programme, an individualized airway clearance technique (ACT) protocol was developed considering the patient's specific condition. The ACT programme involved nebulisation with sterilised water for injection (10 mL) for 5 min, followed by continuous positive expiratory pressure (CPEP) for 2.5 min to promote lung expansion, and then switching to continuous high frequency oscillation (CHFO) for 2.5 min to facilitate sputum clearance, the above procedure is repeated a total of three times. ACT takes place once a day at 8/12/16 pm for 7 days. The treatment was administered in the prone position for a duration of 8 h per day along with respiratory muscle exercises, while the patient received instructions on effective coughing techniques. No adverse effects were observed during the course of treatment, which resulted in significant alleviation of the patient's symptoms that did not recur within 1 week after completion. Subsequent chest CT scans revealed significant improvement in pulmonary atelectasis (Figure 2D). Blood gas analysis also demonstrated substantial improvements in $PaCO_2$ levels, the PaO_2/FiO_2 ratio, whole blood base excess, and actual bicarbonate concentrations (Table 1). In light of the patient's suboptimal spirometry results, pulmonary function tests were not performed during the course of treatment. Prior to discharge, we reassessed the patient's pulmonary function and noted that although certain parameters, including FEV1/FVC, had demonstrated improvement, overall lung function remained less than optimal, providing only partial data (Table 2). The patient was discharged 9 days after the completion of ACT treatment. Discharge advice included avoiding strenuous exercise for 3 months, maintaining moderate low back muscle function exercise, adhering to respiratory function exercises, and scheduling regular follow-up appointments. The patient reported an excellent recovery and exhibited no abnormal symptoms during the 1-year follow-up after discharge. The patient expressed high satisfaction with the treatment outcomes.

TABLE 2 Patient pulmonary function test results.

Variable	Predicted values	Admission	Discharge
VC MAX, L	2.39	0.68	0.59
FVC, L	2.33	0.64	0.57
FEV1, L	1.95	0.4	0.4
FEV1/FVC, %	83.69	61.94	69.92
MVV, L/min	83.9	12.76	13.89
R5, $cmH_2O/(L/s)$	3.94	15.33	7.69
R20, $cmH_2O/(L/s)$	3.32	7.99	5.08
X5, $cmH_2O/(L/s)$	−0.71	−2.12	−4.06

VC, vital capacity; FVC, forced vital capacity; FEV1, forced expiratory volume in 1 second; MVV, maximum voluntary ventilation; R5, resistance at 5 Hz; R20, resistance at 20 Hz; X5, reactance at 5 Hz.

Discussion

Different surgical approaches for scoliosis treatment can impact pulmonary function and increase the risk of postoperative pulmonary complications (9). In adults with scoliosis, surgical interventions often present complex scenarios (10). Furthermore, a study demonstrated that approximately 2.3% of patients undergoing surgery for congenital scoliosis experienced postoperative complications related to atelectasis (11). In this particular case, the patient exhibited pre-existing pulmonary dysfunction and a history of COPD, which further complicated the procedure and escalated the risk of complications (12). Although the literature on postoperative complications of scoliosis has been documented, no relevant reports specifically address strategies for severe cases of atelectasis.

Atelectasis is a frequently encountered mechanical complication during the perioperative period, characterized by inadequate lung expansion into the chest wall (13, 14). Atelectasis not only impairs oxygenation and reduces lung compliance but also triggers inflammation, damages the alveolar-capillary barrier, and may lead to severe lung injury (14–16). Therefore, effective

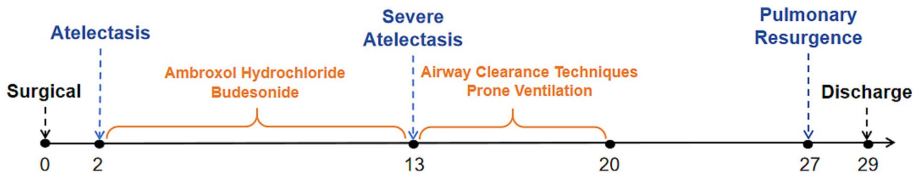

FIGURE 3
Roadmap of the time when the patient develops a post-operative complication—atelectasis and its treatment.

management of atelectasis is crucial for ensuring patient health and safety. Although continuous positive airway pressure ventilation has been reported as a preventive measure against partial lung collapse during anesthesia induction (17), it has not been considered as the treatment of choice for atelectasis (18). With the innovative application of ACT therapy tailored to individual patient's specific conditions, we achieved a more satisfactory therapeutic outcome in managing postoperative complications associated with atelectasis.

ACT is a non-invasive therapeutic modality that primarily utilizes continuous positive expiratory pressure (CPEP) ventilation to maintain airway patency, enhance alveolar ventilation, and promote sputum expulsion, thereby achieving its therapeutic objectives continuous high frequency oscillation. Additionally, it employs continuous high frequency oscillation to loosen secretions, while simultaneously accelerating ciliary movement to facilitate the migration of peripheral bronchial secretions towards the larger airways. In cases where pharmacological interventions are ineffective, clinicians actively explore alternative treatments to alleviate patient suffering. After conducting a comprehensive review of available literature to fully understand the benefits and limitations of ACT, and considering this information alongside their clinical experience, the clinician ultimately selected ACT as the treatment modality. The procedure and timing were also chosen in accordance with the European Respiratory Society's guidelines on airway clearance techniques for adults with bronchiectasis (19). To facilitate the patient's recovery, we implemented a prone position protocol based on clinical evidence from studies of COVID-19 patients, providing 8 h of daily prone positioning (20, 21). The patient's left lung was successfully re-expanded and blood gas indices were significantly improved through the implementation of ACT therapy (Figure 2; Table 1).

In this instance, ACT treatment played a crucial role in reversing atelectasis, a complication that can occur following lateral spinal surgery. This highlights the significant potential of ACT for managing postoperative pulmonary atelectasis associated with similar surgical procedures. The notable efficacy of ACT is consistent with the well-documented effectiveness of radiofrequency oscillation in addressing atelectasis in perioperative contexts (22). When considering the application of ACT, it is crucial for physicians to possess a thorough understanding of its mechanism of action and the specific advantages and limitations of each technique, as outlined in authoritative guidelines such as the European Respiratory Society statement, in order to mitigate potential unforeseen complications (19). However, individual cases exhibit unique characteristics, and it remains uncertain whether ACT is universally applicable to all patients who develop post-operative atelectasis. Future research should prioritize the design and implementation of rigorous randomized controlled clinical trials to ascertain the efficacy of ACT in addressing this particular postoperative complication.

Data availability statement

The original contributions presented in the study are included in the article/Supplementary material, further inquiries can be directed to the corresponding author.

Ethics statement

Written informed consent was obtained from the individual(s) for the publication of any potentially identifiable images or data included in this article.

Author contributions

RZ: Investigation, Methodology, Software, Writing – original draft, Writing – review & editing. HS: Investigation, Methodology, Software, Writing – original draft, Writing – review & editing. YW: Data curation, Writing – original draft. RT: Methodology, Writing – review & editing. XZ: Investigation, Writing – original draft. YT: Writing – original draft, Methodology. MH: Resources, Supervision, Writing – review & editing.

Funding

The author(s) declare that no financial support was received for the research, authorship, and/or publication of this article.

Conflict of interest

The authors declare that the research was conducted in the absence of any commercial or financial relationships that could be construed as a potential conflict of interest.

Generative AI statement

The authors declare that no Generative AI was used in the creation of this manuscript.

Publisher's note

Supplementary material

The Supplementary material for this article can be found online at: https://www.frontiersin.org/articles/10.3389/fmed.2025.1518935/full#supplementary-material

SUPPLEMENTARY FIGURE S1
VAS pain rating scale. The pain levels in the table are in ascending order from 0 to 10, where 0 is no pain and 10 is severe pain. The patient ticks the appropriate number for his/her situation.

References

1. Trobisch P, Suess O, Schwab F. Idiopathic scoliosis. *Dtsch Arztebl Int*. (2010) 107:875–84. doi: 10.3238/arztebl.2010.0875

2. De Sèze M, Cugy E. Pathogenesis of idiopathic scoliosis: a review. *Ann Phys Rehabil Med*. (2012) 55:128–38. doi: 10.1016/j.rehab.2012.01.003

3. Koumbourlis AC. Scoliosis and the respiratory system. *Paediatr Respir Rev*. (2006) 7:152–60. doi: 10.1016/j.prrv.2006.04.009

4. Heary RF. Evaluation and treatment of adult spinal deformity. Invited submission from the Joint Section Meeting on Disorders of the Spine and Peripheral Nerves, March 2004. *J Neurosurg Spine*. (2004) 1:9–18. doi: 10.3171/spi.2004.1.1.0009

5. Roser MJ, Askin GN, Labrom RD, Zahir SF, Izatt M, Little JP. Vertebral body tethering for idiopathic scoliosis: a systematic review and meta-analysis. *Spine Deform*. (2023) 11:1297–307. doi: 10.1007/s43390-023-00723-9

6. O'Neill K, O'Donnell AE, Bradley JM. Airway clearance, mucoactive therapies and pulmonary rehabilitation in bronchiectasis. *Respirology*. (2019) 24:227–37. doi: 10.1111/resp.13459

7. Schofield LM, Singh SJ, Yousaf Z, Wild JM, Hind D. Personalising airway clearance in chronic suppurative lung diseases: a scoping review. *ERJ Open Res*. (2023) 9:00010-2023. doi: 10.1183/23120541.00010-2023

8. Heinz KD, Walsh A, Southern KW, Johnstone Z, Regan KH. Exercise versus airway clearance techniques for people with cystic fibrosis. *Cochrane Database Syst Rev*. (2022) 6:CD013285. doi: 10.1002/14651858.CD013285

9. Bullmann V, Schulte TL, Schmidt C, Gosheger G, Osada N, Liljenqvist UR. Pulmonary function after anterior double thoracotomy approach versus posterior surgery with costectomies in idiopathic thoracic scoliosis. *Eur Spine J*. (2013) 22:164–71. doi: 10.1007/s00586-012-2316-x

10. Aebi M. The adult scoliosis. *Eur Spine J*. (2005) 14:925–48. doi: 10.1007/s00586-005-1053-9

11. Yin S, Tao H, Du H, Feng C, Yang Y, Yang W, et al. Postoperative pulmonary complications following posterior spinal instrumentation and fusion for congenital scoliosis. *PLoS One*. (2018) 13:e0207657. doi: 10.1371/journal.pone.0207657

12. Lagier D, Zeng C, Fernandez-Bustamante A, Vidal Melo MF. Perioperative pulmonary atelectasis: part II. Clinical implications. *Anesthesiology*. (2022) 136:206–36. doi: 10.1097/ALN.0000000000004009

13. Gillett D, Mitchell MA, Dhaliwal I. Avoid the trap: nonexpanding lung. *Chest*. (2021) 160:1131–6. doi: 10.1016/j.chest.2021.04.025

14. Zeng C, Lagier D, Lee JW, Vidal Melo MF. Perioperative pulmonary atelectasis: part I. biology and mechanisms. *Anesthesiology*. (2022) 136:181–205. doi: 10.1097/ALN.0000000000003943

15. Nguyen DM, Mulder DS, Shennib H. Altered cellular immune function in the atelectatic lung. *Ann Thorac Surg*. (1991) 51:76–80. doi: 10.1016/0003-4975(91)90454-x

16. Duggan M, McCaul CL, McNamara PJ, Engelberts D, Ackerley C, Kavanagh BP. Atelectasis causes vascular leak and lethal right ventricular failure in uninjured rat lungs. *Am J Respir Crit Care Med*. (2003) 167:1633–40. doi: 10.1164/rccm.200210-1215OC

17. Tusman G, Böhm SH. Prevention and reversal of lung collapse during the intra-operative period. *Best Pract Res Clin Anaesthesiol*. (2010) 24:183–97. doi: 10.1016/j.bpa.2010.02.006

18. Venus B. CPAP not the treatment of choice for atelectasis. *Chest*. (1983) 83:586–7. doi: 10.1378/chest.83.3.586b

19. Herrero-Cortina B, Lee AL, Oliveira A, O'Neill B, Jácome C, Dal Corso S, et al. European Respiratory Society statement on airway clearance techniques in adults with bronchiectasis. *Eur Respir J*. (2023) 62:2202053. doi: 10.1183/13993003.02053-2022

20. Bargoud CG, Jih T, Baskar D, Volk L, Siddiqui S, Suaray M, et al. Compliance of prone positioning in non-intubated COVID-19 patients. *Clin Med Res*. (2023) 21:171–6. doi: 10.3121/cmr.2023.1830

21. de Araújo MS, Santos MMPD, de Assis Silva CJ, de Menezes RMP, Feijão AR, de Medeiros SM. Prone positioning as an emerging tool in the care provided to patients infected with COVID-19: a scoping review. *Rev Lat Am Enfermagem*. (2021) 29:e3397. doi: 10.1590/1518-8345.4732.3397

22. Qin YJ, Zhang YQ, Chen Q, Wang Y, Li SY. Effect of high-frequency oscillation on reduction of atelectasis in perioperative patients: a prospective randomized controlled study. *Ann Med*. (2023) 55:2272720. doi: 10.1080/07853890.2023.2272720

frontiers | Frontiers in Medicine

TYPE Case Report
PUBLISHED 25 February 2025
DOI 10.3389/fmed.2025.1527556

OPEN ACCESS

EDITED BY
Giuseppe Fiorentino,
Colli Hospital, Italy

REVIEWED BY
Zonghui Zuo,
Tianjin Agricultural University, China
Zhenlu Zhang,
Wuhan Asia Heart Hospital, China

*CORRESPONDENCE
Jianping Liang
✉ ljpzhongshan@163.com
Xiuqiong Xia
✉ zhongshanxxq@126.com

†These authors have contributed equally to this work

RECEIVED 13 November 2024
ACCEPTED 06 February 2025
PUBLISHED 25 February 2025

CITATION
Zhang A, Huang T, Lao X, Ma J, Xia X and Liang J (2025) Severe *Chlamydia psittaci* pneumonia complicated by deep vein thrombosis: a case report.
Front. Med. 12:1527556.
doi: 10.3389/fmed.2025.1527556

Severe *Chlamydia psittaci* pneumonia complicated by deep vein thrombosis: a case report

Anbing Zhang[1†], Ting Huang[1,2†], Xiaoli Lao[1,3], Jun Ma[1,2], Xiuqiong Xia[1*] and Jianping Liang[1*]

[1]Department of Pulmonary and Critical Care Medicine, Zhongshan People's Hospital, Zhongshan, China, [2]Shenzhen University Medical School, Shenzhen University, Shenzhen, China, [3]Graduate School, Guangdong Medical University, Zhanjiang, China

Deep vein thrombosis (DVT) of the legs is a rare but clinically important complication of *Chlamydia psittaci* pneumonia. We report a case of a 51-year-old man who was admitted to the hospital with fever, cough, and dyspnea. Next-generation sequencing confirmed the diagnosis of *Chlamydia psittaci* pneumonia. His D-dimer level was elevated on admission, and ultrasound confirmed DVT in the legs. The patient was treated with intravenous doxycycline for the infection and rivaroxaban as an anticoagulant. His condition gradually improved and he was discharged after making a full recovery. In this paper, we explore the potential association between *Chlamydia psittaci* infection and venous thrombosis, as well as clinical management strategies.

KEYWORDS

psittacosis, next-generation sequencing, D-dimer, anticoagulant, deep vein thrombosis

Introduction

Chlamydia psittaci is a pathogen commonly found in birds that can also infect humans, causing psittacosis (1). In humans, psittacosis typically manifests as pneumonia, with clinical symptoms including fever, cough, and dyspnea. In severe cases, it can lead to life-threatening pneumonia (2). Although psittacosis is uncommon, the risk of transmission is increasing owing to globalization and the growing trade of poultry and pet birds (2).

Surgery, fractures, and cancer are common causes of venous thromboembolism (VTE), whereas infection-induced VTE is relatively rare (3). Deep vein thrombosis (DVT) of the lower legs and pulmonary thromboembolism are seldom reported in cases of *Chlamydia psittaci* infection. Fang and Xu (4) reported a case of pulmonary thrombosis induced by psittacosis pneumonia, suggesting a possible association between psittacosis and pulmonary thrombosis; however, this hypothesis requires further clinical evidence. He et al. (5) described a case of *Chlamydia psittaci* pneumonia complicated by atherosclerosis obliterans of the legs. Pulmonary thrombosis and venous thrombosis are pathophysiological processes linked to stasis, vascular endothelial injury, and hypercoagulability. The risk of these conditions is increased in individuals who are bedridden, recovering from surgery, and those with cancer (6). However, severe infections can lead to an excessive inflammatory response, causing endothelial injury and hypercoagulable states, thereby increasing the risk of pulmonary thrombosis and venous thrombosis (7).

We describe a rare case of *Chlamydia psittaci* pneumonia complicated by DVT of the legs. We performed a detailed case analysis to explore the potential association between

Chlamydia psittaci infection and venous thrombosis and provide a source of reference for clinical diagnosis and treatment.

Case description

The patient was a 51-year-old man who was admitted to hospital with a 5-day history of fever, cough, and dyspnea. He had no known underlying medical conditions. Five days previously, he had developed a persistent high fever (with a maximum temperature of 40°C), accompanied by cough and shortness of breath. On admission, physical examination revealed a temperature of 39°C, blood pressure of 138/98 mmHg, heart rate of 116 bpm, respiratory rate of 29 breaths/min, and oxygen saturation of 89% breathing room air. Auscultation of the lungs revealed coarse breath sounds and scattered moist rales. No peripheral edema was noted in his lower legs.

Laboratory tests on admission showed an elevated white blood cell, neutrophil, and platelet counts, and elevated D-dimer, C-reactive protein (CRP), procalcitonin, and interleukin-6 (IL-6) levels (Table 1). Arterial blood gas analysis showed pH 7.441, PO2 59.1 mmHg, PCO2 26.5 mmHg, and HCO3 20.6 mmol/L. Liver function tests revealed elevated alanine aminotransferase (ALT) and aspartate aminotransferase (AST) levels, Blood biochemistry revealed low total protein (57.1 g/L) and albumin (31.6 g/L) levels. His electrolyte levels were as follows: potassium 4.26 mmol/L, sodium 148 mmol/L, chloride 113 mmol/L, calcium 2.14 mmol/L, and phosphorus 0.8 mmol/L. Renal function tests showed a creatinine level of 68 μmol/L, uric acid level of 71 μmol/L, and urea level of 8.31 mmol/L. His creatine kinase (CK) level was 32 U/L, creatine kinase MB isoenzyme (CK-MB) level was 8 U/L, N-terminal-pro-brain natriuretic peptide (NT-proBNP) level was 60 pg/mL, and fibrinogen level was 3.2 g/L. Nucleic acid tests for influenza and SARS-CoV-2, a dengue antigen test, and a *Mycoplasma pneumoniae* antibody test all were negative. Chest computed tomography (CT) revealed extensive consolidation in both lungs and a small amount of pleural effusion on the right side (Figures 1A–C).

The patient was immediately intubated in the emergency room and mechanical ventilation was initiated. He was admitted to the intensive care unit and started on intravenous cefoperazone-sulbactam (1.5 g, 8-hourly) for infection control. Owing to the severity of his condition and the possibility of infection by a rare pathogen, bronchoscopy and bronchoalveolar lavage of the right lower lobe were performed on the day of admission. A sample of bronchoalveolar lavage fluid (BALF) was sent for next-generation sequencing (NGS). The next day, NGS identified *Chlamydia psittaci* (with 85,915 sequence reads) in the BALF. Further questioning revealed that the patient had a history of slaughtering poultry at home and had slaughtered a chicken 1 week prior to the onset of his symptoms. He was diagnosed with severe *Chlamydia psittaci* pneumonia and the antibiotic was switched to intravenous doxycycline (0.1 g, 12-hourly). Three days after starting doxycycline treatment, his fever resolved.

On admission, the patient's D-dimer level was considerably elevated (6.53 mg/L; reference < 0.5 mg/L), which made us consider the possibility of a clotting condition. Although he had no obvious swelling in his lower legs, a venous ultrasound was performed of both legs. This revealed thrombosis and complete occlusion in the intermuscular veins of both legs (Figures 2A, B). However, the patient's family refused pulmonary artery computed tomography angiography (CTA), so the presence of pulmonary thromboembolism could not be investigated. The patient was diagnosed with DVT of the legs and oral rivaroxaban (15 mg, twice daily) was initiated. The dose was reduced to 20 mg daily after 3 weeks.

Follow-up chest CT 1 week after starting doxycycline treatment revealed reduced lung consolidation and pleural effusion (Figures 1D–F). The patient was extubated and transferred to a general ward. Doxycycline therapy was continued and his symptoms improved after 1 week. He recovered and was discharged. Oral doxycycline (0.1 g/dose, orally, twice daily for 2 weeks) and rivaroxaban treatment were continued following discharge. Follow-up chest CT after 3 weeks of doxycycline therapy revealed marked improvement of the lung lesions (Figures 1G–I), and his D-dimer levels decreased to within the normal range. Follow-up venous ultrasound of the legs after 2 months of rivaroxaban therapy revealed complete resolution of the intermuscular vein thrombosis (Figures 2C, D).

Discussion

This report describes a rare case of *Chlamydia psittaci* pneumonia complicated by DVT of the legs. Psittacosis is a zoonosis and is primarily transmitted through contact with respiratory secretions, feces, and other excreta from poultry and other birds (8). However, our patient did not have an obvious history of bird contact, such as poultry rearing, and it was only on detailed questioning after receiving the NGS results showing *Chlamydia psittaci* in the BALF that the history of poultry exposure was discovered. This highlights the importance of detailed history-taking so as not to overlook atypical exposures. The clinical manifestations of *Chlamydia psittaci* infection are varied and can easily be confused with other types of pneumonia. Early and accurate identification of the infecting pathogen is critical for timely and effective treatment. In patients with community-acquired pneumonia that does not respond to empirical antibiotic treatment, NGS of BALF should be performed to identify the pathogen. The antibiotic treatment should be adjusted accordingly once the pathogen has been identified (9).

The main clinical manifestation of *Chlamydia psittaci* infection is pneumonia (2). Owing to the nonspecific clinical manifestations, it can easily be mistaken for pneumonia caused by other pathogens, which may lead to misdiagnosis or missed diagnosis. In this case, the patient initially presented with high fever, cough, and dyspnea, symptoms similar to common bacterial infections. However, he did not respond to standard broad-spectrum antibiotic treatment, leading us to suspect infection by an atypical pathogen. Ultimately, NGS confirmed *Chlamydia psittaci* infection. This highlights the importance of considering rare pathogens such as *Chlamydia psittaci* in cases of unexplained pneumonia.

In this case, the patient developed DVT of the legs during the course of *Chlamydia psittaci* infection. Although an association has been reported between infectious diseases and venous thrombosis (10–12), cases of psittacosis complicated by pulmonary thrombosis

TABLE 1 The patient's laboratory test results.

Test parameter	Normal range	On the day of admission	2 weeks after starting DOX
WBC count ($\times 10^9$/L)	4–10	8.8	7.76
Neutrophil count ($\times 10^9$/L)	2–7	7.3	5.47
Neutrophil (%)	40–75	83	74
Lymphocyte count ($\times 10^9$/L)	0.8–4	0.76	1.21
Lymphocyte (%)	20–40	8.6	15.6
Hemoglobin (g/L)	113–151	140	143
Platelets ($\times 10^9$/L)	101–320	407	240
CRP (mg/L)	0–8	97	5.14
PCT (ng/mL)	0–5	0.57	0.06
D-dimer (mg/L)	0–0.5	6.53	1.61
IL-6 (pg/mL)	0-7	197	9.73
ALT (U/L)	7–40	45	26
AST (U/L)	13–40	49	33
Creatinine (μmol/L)	45–84	68	50
CK (U/L)	26–174	32	28
K (mmol/L)	3.5–5.5	4.26	3.9
Na (mmol/L)	135–145	148	134
Cl (mmol/L)	95–105	113	98
Fibrinogen (g/L)	2–4	3.2	2.59
NGS *C. psittaci* reads (n)	/	85915	/

ALT, alanine aminotransferase; AST, aspartate aminotransferase; DOX, doxycycline; CK, creatine kinase; CRP, C-reactive protein; IL-6, interleukin-6; NGS, next-generation sequencing, PCT, procalcitonin; WBC, white blood cells.

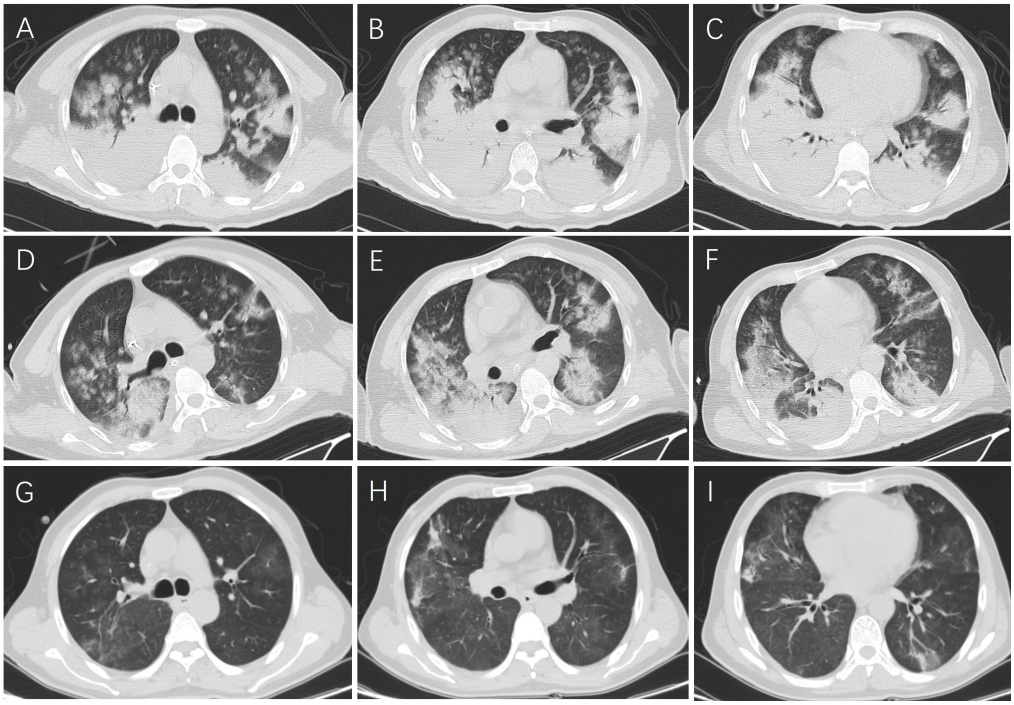

FIGURE 1
Chest computed tomography (CT) of the patient: The initial chest CT on admission showed bilateral pneumonia **(A–C)**. After 1 week of doxycycline treatment, the chest CT showed partial absorption of the pneumonia **(D–F)**. After 3 weeks of doxycycline treatment, the chest CT showed marked absorption of the pneumonia **(G–I)**.

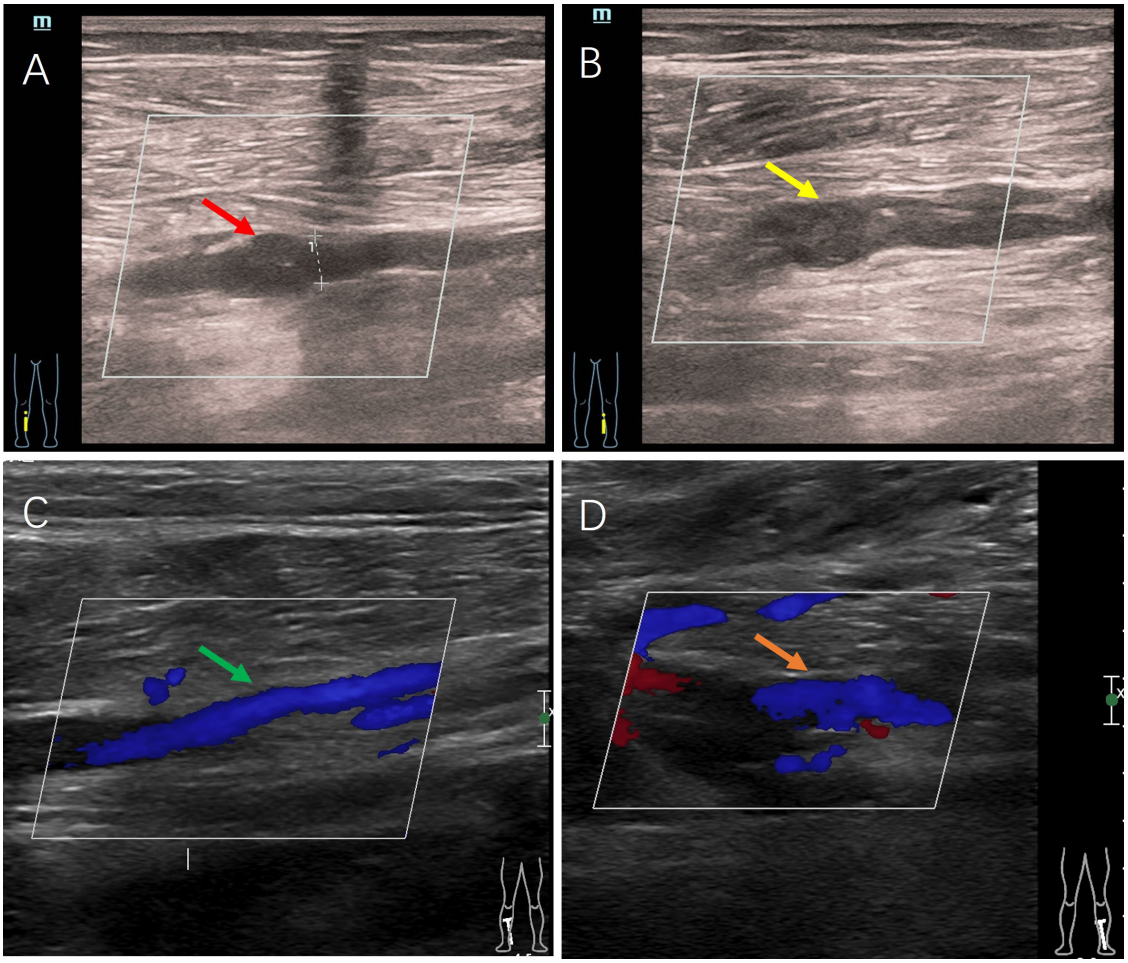

FIGURE 2
Venous ultrasound of the legs on admission showing intermuscular venous thrombosis in the right calf (**(A)**, red arrows); and left calf **(B)**, yellow arrows). Follow-up venous ultrasound of the legs after 2 months of rivaroxaban therapy revealed complete resolution of the intermuscular vein thrombosis (right calf, **(C)**, green arrows; and left calf, **(D)**, orange arrows).

or DVT are rare (4). The high incidence of thromboembolic events in patients hospitalized with COVID-19 has provided evidence of the effectiveness of anticoagulant therapy in infection-induced thrombosis (13, 14). COVID-19 is closely associated with venous thromboembolic diseases, including deep vein thrombosis and pulmonary embolism (15). Previous studies have shown that SARS-CoV-2 infection reduces the expression of ACE2 molecules on the cell surface, which may lead to activation of the renin-angiotensin system, promoting vascular constriction and endothelial injury. Endothelial injury, in turn, results in upregulated expression of tissue factors and an imbalance in the fibrinolytic system (16). *Chlamydia pneumoniae* infection may increase the risk of thrombosis by activating platelets (17), and may contribute to the development of atherosclerosis by inducing chronic inflammation (18). The exact mechanisms by which infection triggers thrombosis are not fully understood but may involve activation of inflammation, endothelial cell injury, autoimmune responses, and an imbalance between coagulation and anticoagulation (19, 20). In addition, infection can potentially cause VTE as a result of reduced mobility. Epaulard (21) reviewed previous research which showed that the risk of VTE during infection is mediated by the link between inflammation and activation of coagulation. IL-6 and CRP are nonspecific markers of inflammation and tissue injury (15). Studies have shown that elevated levels of IL-6 and CRP can promote pulmonary thrombosis (22). High CRP levels are also associated with an increased risk of VTE (23). CRP influences tissue factor synthesis, hemostasis activation, and fibrinolysis (24, 25), reflecting underlying inflammation or hypercoagulable states that may contribute to the occurrence of VTE (26). Although elevated IL-6 and CRP levels are seen in other conditions, their combination with an elevated D-dimer level led us to suspect VTE in this case. Fibrinogen can increase blood viscosity, thus increasing the risk of thrombosis (19).

Early recognition of VTE can be difficult when patients do not exhibit classic symptoms such as hemoptysis, chest pain, or swelling of the calves; therefore, monitoring of D-dimer levels is particularly important. Our patient had elevated D-dimer levels on admission, prompting immediate venous ultrasound examination of his legs, which confirmed the diagnosis of DVT. The patient's family declined pulmonary artery CTA, so it was not possible to determine whether the patient had an associated pulmonary

embolism. D-dimer testing is essential for patients clinically at high risk of VTE, as a negative D-dimer result can rule out acute pulmonary embolism (27).

In managing this case, the patient was immediately started on anticoagulant therapy after the DVT diagnosis, and doxycycline was used for infection control. This combined treatment strategy controlled the infection and prevented further expansion of the thrombosis and related complications. Anticoagulant therapy is crucial for patients with DVT; however, the benefit of anticoagulants must be carefully weighed against the risks. Novel anticoagulants such as rivaroxaban, dabigatran, argatroban, bivalirudin, apixaban, and edoxaban offer stronger anticoagulant effects with a lower risk of bleeding compared with traditional anticoagulants, and have recently become the preferred option for antithrombotic therapy (28). Compared with traditional anticoagulants such as warfarin, rivaroxaban is easier to administer, has more rapid onset of effect, and does not require monitoring (19). Rivaroxaban reduces the size of the thrombus and the risk of recurrence, without increasing the risk bleeding, making it a preferred option over standard anticoagulants (29).

Conclusion

Chlamydia psittaci pneumonia complicated by venous thromboembolism is extremely rare. In the absence of symptoms and signs such as chest pain, hemoptysis, and swelling of the lower legs, D-dimer monitoring can aid in the early identification of venous thromboembolism. Timely detection of thrombosis and initiation of anticoagulant therapy can improve the outcome.

Data availability statement

The datasets presented in this article are not readily available because of ethical/privacy restrictions. Requests to access the datasets should be directed to the corresponding authors.

Ethics statement

The studies involving humans were approved by the Ethics Committees of Zhongshan People's Hospital. The studies were conducted in accordance with the local legislation and institutional requirements. The participants provided their written informed consent to participate in this study. Written informed consent was obtained from the individual(s) for the publication of any potentially identifiable images or data included in this article.

Author contributions

JL: Conceptualization, Methodology, Project administration, Resources, Supervision, Writing – original draft, Writing – review and editing. AZ: Conceptualization, Data curation, Formal Analysis, Investigation, Methodology, Writing – original draft, Writing – review and editing. TH: Data curation, Formal Analysis, Investigation, Methodology, Software, Writing – review and editing. XL: Conceptualization, Data curation, Investigation, Methodology, Writing – review and editing. JM: Formal Analysis, Investigation, Methodology, Writing – review and editing. XX: Investigation, Methodology, Visualization, Writing – review and editing.

Funding

The author(s) declare that financial support was received for the research, authorship, and/or publication of this article. This study was supported by the Science and Technology Plan Project of Zhongshan (grant no. 2024B1041).

Acknowledgments

We thank the patient for his cooperation during the diagnostic process.

Conflict of interest

The authors declare that the research was conducted in the absence of any commercial or financial relationships that could be construed as a potential conflict of interest.

Generative AI statement

The authors declare that no Generative AI was used in the creation of this manuscript.

Publisher's note

References

1. Zhang A, Xia X, Yuan X, Liu Y, Niu H, Zhang Y, et al. Severe *Chlamydia psittaci* pneumonia complicated by rhabdomyolysis: A case series. *Infect Drug Resist.* (2022) 15:873–81. doi: 10.2147/IDR.S355024

2. Zhang A, Xia X, Yuan X, Lv Y, Liu Y, Niu H, et al. Clinical characteristics of 14 cases of severe *Chlamydia psittaci* pneumonia diagnosed by metagenomic next-generation sequencing: A case series. *Medicine (Baltimore).* (2022) 101:e29238. doi: 10.1097/MD.0000000000029238

3. Lutsey P, Zakai N. Epidemiology and prevention of venous thromboembolism. *Nat Rev Cardiol.* (2023) 20:248–62.

4. Fang C, Xu L. *Chlamydia psittaci* pneumonia-induced pulmonary thrombosis: A case report. *Infect Drug Resist.* (2023) 16:7063–9. doi: 10.2147/IDR.S435246

5. He Y, Wang S, Deng J, Pu Q, Chen H, Huang L. *Chlamydia psittaci* pneumonia complicated with lower extremity atherosclerotic occlusive disease. *Infect Drug Resist.* (2023) 16:2141–5. doi: 10.2147/IDR.S393256

6. Xiang L, Jin S, Yu Y, Wang D, Chen H. Risk of venous thromboembolism in patients undergoing gastric cancer surgery: A systematic review and meta-analysis. *BMC Cancer.* (2023) 23:933. doi: 10.1186/s12885-023-11424-x

7. Zerangian N, Erabi G, Poudineh M, Monajjem K, Diyanati M, Khanlari M, et al. Venous thromboembolism in viral diseases: A comprehensive literature review. *Health Sci Rep.* (2023) 6:e1085.

8. Hogerwerf L, Roof I, de Jong M, Dijkstra F, van der Hoek W. Animal sources for zoonotic transmission of psittacosis: A systematic review. *BMC Infect Dis.* (2020) 20:192. doi: 10.1186/s12879-020-4918-y

9. Huang W, Wang F, Cai Q, Xu H, Hong D, Wu H, et al. Epidemiological and clinical characteristics of psittacosis among cases with complicated or atypical pulmonary infection using metagenomic next-generation sequencing: A multi-center observational study in China. *Ann Clin Microbiol Antimicrob.* (2023) 22:80.

10. Cowan L, Lutsey P, Pankow J, Cushman M, Folsom A. Hospitalization with infection and incident venous thromboembolism: The ARIC study. *Thromb Res.* (2017) 151:74–8. doi: 10.1016/j.thromres.2017.01.008

11. Chen Y, Lin T, Huang W, Lin C, Dai M, Kao C. Association between pneumococcal pneumonia and venous thromboembolism in hospitalized patients: A nationwide population-based study. *Respirology.* (2015) 20:799–804. doi: 10.1111/resp.12501

12. Clayton T, Gaskin M, Meade T. Recent respiratory infection and risk of venous thromboembolism: Case-control study through a general practice database. *Int J Epidemiol.* (2011) 40:819–27. doi: 10.1093/ije/dyr012

13. Nopp S, Moik F, Jilma B, Pabinger I, Ay C. Risk of venous thromboembolism in patients with COVID-19: A systematic review and meta-analysis. *Res Pract Thromb Haemost.* (2020) 4:1178–91.

14. Vaughn V, Yost M, Abshire C, Flanders S, Paje D, Grant P, et al. Trends in venous thromboembolism anticoagulation in patients hospitalized with COVID-19. *JAMA Netw Open.* (2021) 4:e2111788.

15. Ren L, Wu M, Xiong J. [Preliminary progress in the study of the relationship between COVID-19 infection and partial arterial or venous diseases]. *Zhonghua Wai Ke Za Zhi.* (2023) 61:1119–23.

16. Tanzadehpanah H, Lotfian E, Avan A, Saki S, Nobari S, Mahmoodian R, et al. Role of SARS-CoV-2 and ACE2 in the pathophysiology of peripheral vascular diseases. *Biomed Pharmacother.* (2023) 166:115321. doi: 10.1016/j.biopha.2023.115321

17. Lichota A, Gwozdzinski K, Szewczyk E. Microbial modulation of coagulation disorders in venous thromboembolism. *J Inflamm Res.* (2020) 13:387–400. doi: 10.2147/JIR.S258839

18. Piñon-Esteban P, Núñez L, Moure R, Marrón-Liñares G, Flores-Rios X, Aldama-Lopez G, et al. Presence of bacterial DNA in thrombotic material of patients with myocardial infarction. *Sci Rep.* (2020) 10:16299. doi: 10.1038/s41598-020-73011-5

19. Song S, Xu YA. retrospective study of the clinical characteristics of 9 children with pulmonary embolism associated with *Mycoplasma pneumoniae* pneumonia. *BMC Pediatr.* (2023) 23:370. doi: 10.1186/s12887-023-04188-7

20. Iba T, Helms J, Levi M, Levy J. Thromboinflammation in acute injury: Infections, heatstroke, and trauma. *J Thromb Haemost.* (2024) 22:7–22.

21. Epaulard O, Foote A, Bosson J. Chronic infection and venous thromboembolic disease. *Semin Thromb Hemost.* (2015) 41:644–9.

22. Zhang Y, Zhang Z, Wei R, Miao X, Sun S, Liang G, et al. IL (interleukin)-6 contributes to deep vein thrombosis and is negatively regulated by miR-338-5p. *Arterioscler Thromb Vasc Biol.* (2020) 40:323–34. doi: 10.1161/ATVBAHA.119.313137

23. Olson N, Cushman M, Lutsey P, McClure L, Judd S, Tracy R, et al. Inflammation markers and incident venous thromboembolism: The REasons for Geographic And Racial Differences in Stroke (REGARDS) cohort. *J Thromb Haemost.* (2014) 12:1993–2001. doi: 10.1111/jth.12742

24. Cermak J, Key N, Bach R, Balla J, Jacob H, Vercellotti GM. C-reactive protein induces human peripheral blood monocytes to synthesize tissue factor. *Blood.* (1993) 82:513–20.

25. Bisoendial R, Kastelein J, Levels J, Zwaginga J, van den Bogaard B, Reitsma P, et al. Activation of inflammation and coagulation after infusion of C-reactive protein in humans. *Circ Res.* (2005) 96:714–6. doi: 10.1161/01.RES.0000163015.67711.AB

26. Vormittag R, Funk M, Mannhalter C, Schönauer V, Vukovich T, Minar E, et al. C-reactive protein 3' UTR +1444C>T polymorphism in patients with spontaneous venous thromboembolism. *Atherosclerosis.* (2006) 188:406–11. doi: 10.1016/j.atherosclerosis.2005.11.006

27. Kearon C, de Wit K, Parpia S, Schulman S, Afilalo M, Hirsch A, et al. Diagnosis of pulmonary embolism with D-dimer adjusted to clinical probability. *N Engl J Med.* (2019) 381:2125–34.

28. Bartholomew J. Update on the management of venous thromboembolism. *Cleve Clin J Med.* (2017) 84:S39–46.

29. Male C, Lensing A, Palumbo J, Kumar R, Nurmeev I, Hege K, et al. Rivaroxaban compared with standard anticoagulants for the treatment of acute venous thromboembolism in children: A randomised, controlled, phase 3 trial. *Lancet Haematol.* (2020) 7:e18–27. doi: 10.1016/S2352-3026(19)30219-4

frontiers | Frontiers in Medicine

TYPE Case Report
PUBLISHED 27 February 2025
DOI 10.3389/fmed.2025.1501242

OPEN ACCESS

EDITED BY
Talat Kilic,
İnönü University, Türkiye

REVIEWED BY
Florian Missey,
Aix Marseille Université, France
Haralampos Gouveris,
Johannes Gutenberg University Mainz, Germany

*CORRESPONDENCE
Ruchir P. Patel
✉ rpatel@sleeplessinarizona.com

RECEIVED 24 September 2024
ACCEPTED 10 February 2025
PUBLISHED 27 February 2025

CITATION
Patel RP and Rohrscheib CE (2025) The activation, clinical course, and clinical outcome of using an unconventional electrode configuration in a patient newly implanted with Inspire® therapy: a case report.
Front. Med. 12:1501242.
doi: 10.3389/fmed.2025.1501242

The activation, clinical course, and clinical outcome of using an unconventional electrode configuration in a patient newly implanted with Inspire® therapy: a case report

Ruchir P. Patel[1]* and Chelsie E. Rohrscheib[2]

[1]The Insomnia and Sleep Institute of Arizona, Scottsdale, AZ, United States, [2]Wesper, Inc., New York, NY, United States

Hypoglossal nerve stimulation therapy via the Inspire® implant is a common alternative to positive airway pressure (PAP) treatment for obstructive sleep apnea (OSA). While hypoglossal nerve stimulation (HGNS) therapy offers a high rate of successful treatment outcomes, the post-activation care pathway, which involves gradual titration of the amplitude to achieve both subjective and objective improvements, can be lengthy, ranging from 3 to 12 months post-activation. Here, we report a case of a 55-year-old man with severe obstructive sleep apnea and a history of hypertension who underwent successful activation and titration of the Inspire® implant to achieve subjective and objective relief within 8 weeks post-implantation and 5 weeks post-activation, using an unconventional starting electrode configuration. This case highlights the need for further exploration of alternative Inspire® activation and management protocols that may lead to improved patient outcomes and higher success rates.

KEYWORDS

obstructive sleep apnea, sleep disorders, hypoglossal nerve stimulation, Inspire®, hypoxic burden, CPAP intolerance, care pathways

Introduction

The Inspire® hypoglossal nerve stimulation (HGNS) device by Inspire Medical Systems Inc. is a common treatment for patients with moderate to severe obstructive sleep apnea (OSA). This device improves OSA by stimulating the hypoglossal nerve (HN), which controls the muscles of the tongue, preventing it from blocking the airway (1). The use of Inspire® as an alternative to positive airway pressure (PAP) therapy has seen substantial growth in recent years, with over 70,000 patients treated as of 2023 (2). While research supports the potential for excellent outcomes with Inspire®, the post-activation care pathway involving gradual titration of the amplitude can be lengthy, ranging from 3 to 12 months (3). This time-consuming process often leads to patient frustration and dissatisfaction. Furthermore, frustration among physicians can result in a lack of consideration of Inspire® as a viable treatment option for their patients.

The Inspire® device consists of several key components, including an implantable pulse generator, a stimulation lead, a respiratory sensing lead, and an external remote control. The single-cuff stimulation lead can be configured to operate in five different electrode

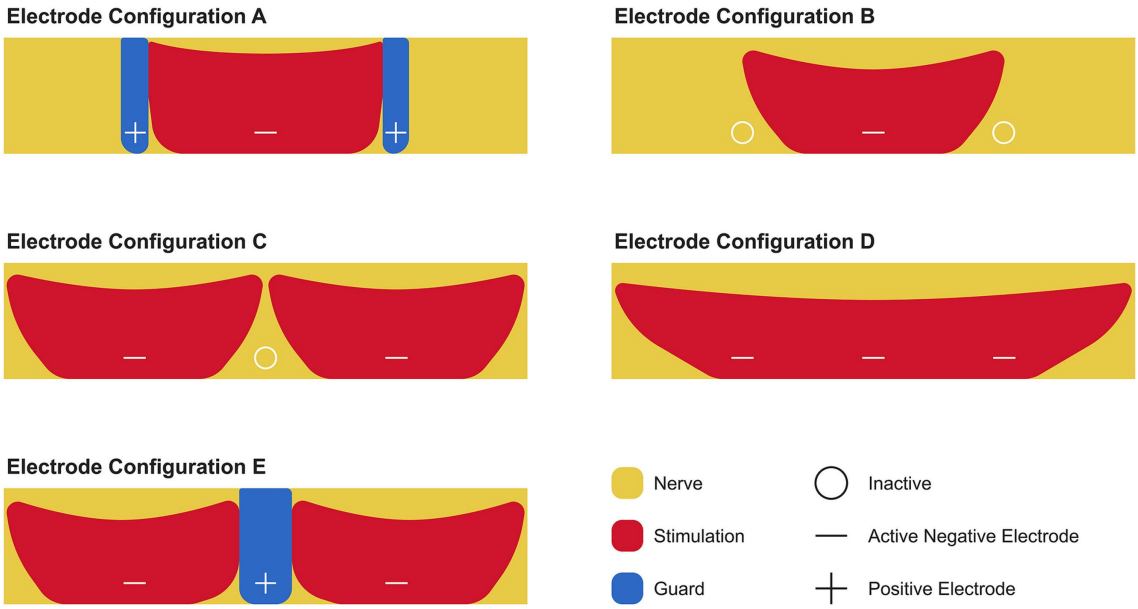

FIGURE 1
Electrode configurations for stimulating the hypoglossal nerve using the Inspire® device. The distal branch of the hypoglossal nerve (yellow) is stimulated via the cuff, which contains a system of three electrodes. These electrodes can be programmed to function as a positive (+) or negative (–) electrode or switched off (o). The positive electrode acts as a guard (blue) that limits the area of stimulation (red). The recommended electrode configuration by Inspire Medical Systems Inc. is Electrode A.

configurations (Figure 1). Inspire Medical Systems Inc. refers to these configurations as Electrode A (+ – +), a bipolar configuration with a guarded cathode; Electrode B (o – o), an unipolar configuration with a single centered cathode; Electrode C (– o –), an unipolar configuration with dual outer cathodes; Electrode D (– – –), a grouped cathode (broad unipolar); and Electrode E (– + –), a bipolar configuration with dual outer cathodes and a center guard (3). Each can be strategically positioned along the length of the distal branch of the HN to stimulate the nerve in synchronization with the patient's breathing, resulting in tongue protrusion, which prevents airway obstruction (4, 5).

Based on the STAR trial published in 2014, Inspire Medical Systems Inc. chose the electrode configuration known as Electrode A, or plus-minus-plus (+ – +), as the standard default electrode configuration to activate all patients (6). Electrode A applies stimulation to the distal branch of the HN through the middle electrode, which serves as the anode, while the two outer electrodes serve as the cathodes. To date, Inspire Medical Systems Inc. has not explored or recommended using alternative electrode configurations as a means to improve outcomes in patients who do not respond to (+ – +) or to reduce the length of titration time.

This case study outlines a novel Inspire® activation approach using the unipolar electrode configuration of Electrode B, or off-minus-off (o – o), in which the middle electrode is utilized to deliver stimulation over a broader area across the distal branch of the HN. The use of this electrode configuration allows for a wider energy field to be applied across the distal branch of the HN, thereby resulting in a different effect on nerve fiber recruitment, muscle activation, and consequently, tongue movement.

Case description

A 55-year-old man with a medical history significant for hypertension and severe OSA [the Apnea–Hypopnea Index (AHI) ≥30] was presented for Inspire® therapy due to difficulty tolerating PAP therapy. His OSA was re-evaluated over two nights using Wesper's home sleep apnea test (HSAT) in August 2023 (7). During the first night, his AHI was 28.6 with an HSAT-O2 nadir value of 76%. On the second night, his AHI was 30.9 with an O2 nadir value of 75%.

Inspire® was implanted on 22 December 2023 and activated 3 weeks later (Figure 2). The patient agreed to participate in a novel activation approach using Electrode B (o – o) (Table 1). In this configuration, the electrode labeled "o" is inactive, meaning no electrical stimulation is delivered, whereas the "–" negative electrode is active, serving as a cathode and generating electrical current to stimulate the HN. Initially, before activating, programming, and titrating Electrode B (o – o), the patient underwent the standard activation protocol with Electrode A (+ – +) for the documentation of these settings. Electrode B was selected due to its more powerful unipolar configuration, which allows for effective midline protrusion of the tongue at lower amplitudes. The primary advantage of Electrode B lies in the way the energy field is applied to the nerve, leading to a distinct muscle recruitment pattern of the genioglossus and geniohyoid muscles. This often results in a more centralized activation, generating symmetric forward traction on the tongue base and achieving greater airway opening. In addition, the lower amplitude required with this configuration enhances patient comfort while achieving superior airway patency, compared to Electrode A. As per Inspire Medical Systems Inc., there are no known contraindications for Electrode B.

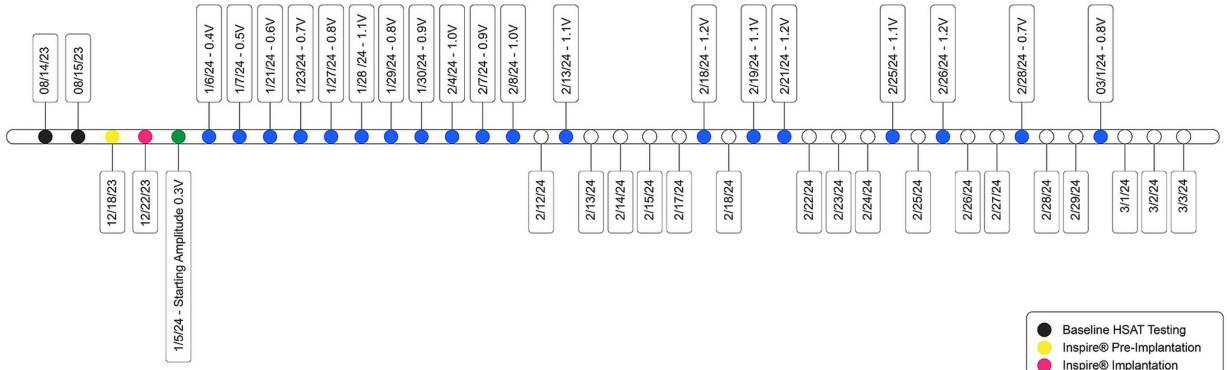

FIGURE 2
Timeline of patient care, from Inspire® implantation through activation and amplitude titration.

TABLE 1 Inspire® activation parameters.

Initial activation parameters		
	Electrode A (+ – +)	Electrode B (o – o)
Sensational threshold	0.6 V	0.2 V
Functional threshold	0.9 V	0.3 V
Tongue movement	Symmetric midline protrusion	

Initial programming		
Electrode configuration	(o – o)	
Amplitude configuration	0.2 V – 1.2 V	
Starting amplitude	0.3 V	
Rate	40 Hz	
Pulse width	60 µs	
Start delay	30 min	
Pause delay	15 min	
Total therapy duration	8 h	

Novel initial Inspire® activation protocol for Electrode A (+ – +) and Electrode B (o – o), along with initial programming for the novel Electrode B configuration setting. The patient initially underwent the standard activation protocol with Electrode A (+ – +) to document these settings before activating, programming, and titrating Electrode B (o – o).

The patient was advised to increase the amplitude at a frequency of every fifth to seventh night, depending on tolerance. If an amplitude level was uncomfortable, he was instructed to decrease it by one level until his next clinic visit. At the 2-week follow-up visit, the patient was titrated to an amplitude of 0.8 V and reported feeling comfortable with the stimulation. He noted that he was sleeping 90–120 min longer per night compared to before starting Inspire® therapy, as well as a reduction in daytime sleepiness.

The patient was seen 2 weeks after titrating to an amplitude of 1.0 V and was doing well, but he felt the stimulation was too strong. Therefore, the rate was reduced to 30 Hz, and the amplitude was increased to 1.1 V. At the subsequent 2-week follow-up, the patient reported that an amplitude of 1.2 V began disrupting his sleep, so he remained at 1.1 V. The pulse width was then increased to 120 µs, and the rate was increased to 33 Hz, while the amplitude was reduced to 0.7 V. In these settings, the stimulation felt comfortable, and the patient continued to maintain good tongue protrusion.

During the titration process, the patient's OSA was re-evaluated using Wesper's HSAT ($n = 17$) after each amplitude voltage adjustment. These results were compared to the patient's pre-implantation ($n = 2$) results (Figures 3A–E). Significance was determined using a t-test. The patient's AHI, oxygen desaturation index (ODI), O2 nadir, and hypoxic burden (HB) were assessed to evaluate improvements in OSA. The patient's average post-activation AHI [Baseline AHI: 29.7, SD = 1.62; Post-activation AHI: 7.5, SD = 2.64; $t(17) = 11.44$; $p < 0.0001$; Figure 3A], ODI [Baseline ODI: 32.0; SD = 2.54; Post-activation ODI: 8.29; SD = 2.74; $t(17) = 11.60$; $p < 0.0001$; Figure 3B], O2 nadir [Baseline nadir: 75.5%; SD = 0.70; Post-activation nadir: 86.8%; SD = 2.27; $t(17) = 6.85$; $p < 0.0001$; Figure 3C] and HB [Baseline HB: 546.58%min/h; SD = 38.0; Post-activation HB: 67.65%min/h; SD = 25.66; $t(17) = 24.13$; $p < 0.0001$; Figure 3D] showed significant improvements with the (o – o) electrode configuration.

The testing process determined that his AHI improvement at the final amplitude of 0.8 V was not significantly different compared to higher amplitudes of ≥1.0 V (Figure 3A), further confirming that 0.8 V was the ideal amplitude setting for both objective and subjective improvements. His most recent HSAT result on 3rd March 2024 revealed a residual AHI value of 3.16, ODI value of 4.43, O2 nadir value of 90%, and HB value of 34.6%min/h. The titration process was completed 8 weeks after the implantation and 5 weeks after the activation compared to the average recommended completion time of 12–17 weeks.

The patient presented for his final follow-up visit 1 week later, reporting that he was sleeping very well at an amplitude of 0.8 V and no longer noticing the stimulation after the adjustments made to the stimulation parameters the previous week. His most recent HSAT result revealed a residual AHI value of 3.2 and an O2 nadir value of 90%. In

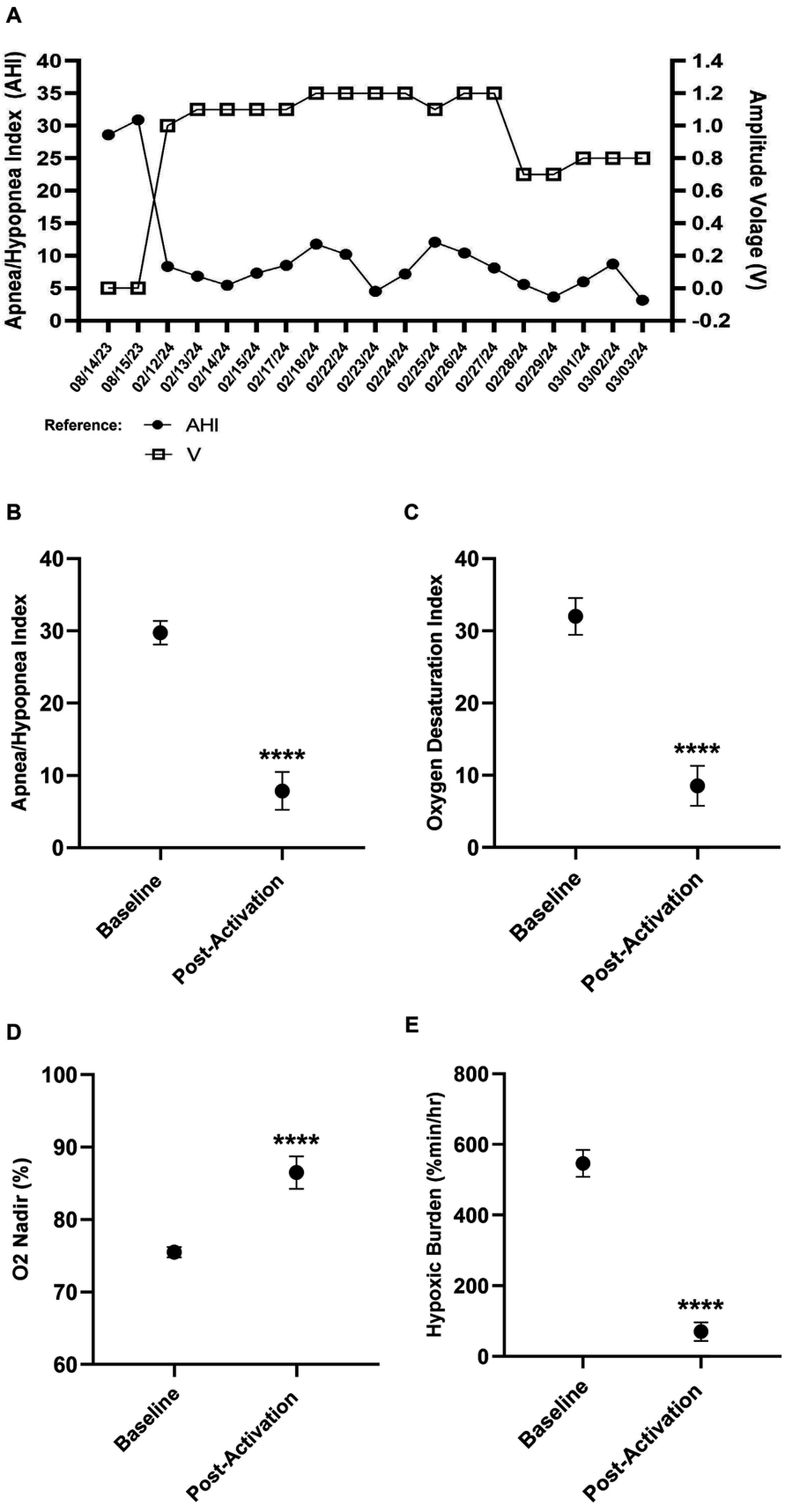

FIGURE 3
Improvements in key obstructive sleep apnea indices after Inspire® activation. Baseline data represent pre-activation. **(A)** Pre-activation and postactivation Apnea-Hypopnea Index (AHI) versus amplitude. **(B)** Pre-activation and post-activation AHI. **(C)** Pre-activation and post-activation oxygen desaturation index. **(D)** Pre-activation and post-activation minimum SpO2. **(E)** Pre-activation and post-activation hypoxic burden.

addition, his score on the Epworth Sleepiness Scale decreased from 10 at baseline to 6 post-treatment, and his Insomnia Severity Index score decreased from 10 to 6. The titration process was completed 8 weeks after the implantation and 5 weeks after the activation, compared to the average recommended completion time of 12–17 weeks.

Discussion

The Inspire® implant was approved by the FDA in 2014 and has since become a powerful alternative therapeutic option for patients with moderate to severe OSA. While patient selection is of great importance to ensure treatment appropriateness and optimize outcomes, it is also understood that even the most optimal patient may not achieve both subjective and objective improvements with the recommended default electrode configuration within the estimated 90-day titration timeframe. This case successfully demonstrates that alternative Inspire® electrode configurations can be used to achieve both subjective and objective improvements in obstructive sleep apnea (OSA), as well as reduce titration time. A limitation of this study is that electrode configurations A, C, D, and E were not tested, which may limit the generalizability of the findings and highlights the need for further research involving a broader range of configurations.

There are multiple individual factors that may result in an individual not having a successful subjective and/or objective outcome with Inspire® therapy. Common reasons include comorbid conditions such as generalized anxiety disorder, chronic insomnia, restless legs syndrome, a low arousal threshold, or chronic pain syndrome. The patient's beliefs and behaviors may also affect the outcomes. These include unrealistic expectations, difficulty operating the remote control correctly, a lack of understanding of the self-titration protocol, or even fatigue during the lengthy titration period.

Many patients are unable to be successfully titrated to an effective amplitude within the initial 90-day post-activation period to achieve subjective and/or objective improvement. This can lead to patient dissatisfaction, distrust of the therapy, and a loss of confidence due to the lack of a successful treatment outcome after such a lengthy titration process. The process of initiating Inspire® therapy is often described as a journey rather than a sprint, but even a journey has its limit. As a result, protocols must be evaluated and re-evaluated to determine if there is a more effective and efficient method that can achieve the same or even better outcomes, ultimately improving patient satisfaction and even increasing physician acceptance of this therapeutic alternative.

To improve patient satisfaction, physician satisfaction, clinical workflows, and patient outcomes, more streamlined protocols need to be established utilizing alternative electrode configurations. It is well established that the different electrode configurations currently available for the Inspire® implant produce unique patterns of neurostimulation. These patterns may influence the patient's tolerance of the therapy and the movement of the tongue. Thus, alternative configurations have unique effects on nerve fiber recruitment and the activation of the genioglossus and geniohyoid muscles, resulting in varying patterns of airway dilatation (4, 8).

Furthermore, the availability of longitudinal efficacy data during the titration phase of hypoglossal nerve stimulation therapy enables clinicians to make faster and more informed management decisions. The current model of care does not allow for the regular collection of efficacy data as minor or major programming adjustments are being made. Access to this type of data could potentially shorten the titration period and also provide the option of alternative electrode configurations for initiating the therapy, rather than recommending only a single electrode configuration.

In conclusion, this case report demonstrates the potential of alternative Inspire® electrode configurations to improve both subjective and objective outcomes in patients with obstructive sleep apnea (OSA). The use of the unipolar Electrode B configuration resulted in significant improvements in the AHI, oxygen saturation, and overall sleep quality, while also shortening the titration period compared to standard practices. However, a limitation of this study is that not all electrode configurations were tested, which may limit the generalizability of the findings. Further research is needed to explore a broader range of electrode configurations and develop more efficient activation protocols to improve patient outcomes, reduce titration time, and enhance both patient and physician satisfaction with Inspire® therapy.

Data availability statement

The datasets presented in this study can be found in online repositories. The names of the repository/repositories and accession number(s) can be found below: https://doi.org/10.6084/m9.figshare.26870662.v1.

Ethics statement

Ethical approval was not required for the study involving humans in accordance with the local legislation and institutional requirements. Written informed consent to participate in this study was not required from the participants or the participants' legal guardians/next of kin in accordance with the national legislation and the institutional requirements. Written informed consent was obtained from the individual(s) for the publication of any potentially identifiable images or data included in this article.

Author contributions

RP: Conceptualization, Data curation, Formal Analysis, Investigation, Methodology, Resources, Writing – original draft, Writing – review & editing. CR: Data curation, Formal Analysis, Visualization, Writing – original draft, Writing – review & editing.

Funding

The author(s) declare no financial support was received for the research, authorship, and/or publication of this article.

Acknowledgments

The authors would like to thank the staff at The Insomnia and Sleep Institute of Arizona for their assistance in caring for the patient

in this case study. We would also like to acknowledge Antonio Moura for his consultation on the statistical analysis, as well as Maria Belen Cabello and Brett Figliozzi for their assistance in creating the artwork for the figures presented in this case study.

Conflict of interest

CR reports that they are an employee of Wesper Inc., the home sleep apnea test that was used to collect sleep data for the patient featured in this case report.

The remaining author declares that the research was conducted in the absence of any commercial or financial relationships that could be construed as a potential conflict of interest.

Publisher's note

All claims expressed in this article are solely those of the authors and do not necessarily represent those of their affiliated organizations, or those of the publisher, the editors and the reviewers. Any product that may be evaluated in this article, or claim that may be made by its manufacturer, is not guaranteed or endorsed by the publisher.

References

1. Costantino A, Rinaldi V, Moffa A, Luccarelli V, Bressi F, Cassano M, et al. Hypoglossal nerve stimulation long-term clinical outcomes: a systematic review and meta-analysis. *Sleep Breath*. (2020) 24:399–411. doi: 10.1007/s11325-019-01923-2

2. Verbraecken J, Dieltjens M, Op de Beeck S, Vroegop A, Braem M, Vanderveken O, et al. Non-CPAP therapy for obstructive sleep apnoea. *Breathe (Sheff)*. (2022) 18:220164. doi: 10.1183/20734735.0164-2022

3. Steffen A, Jeschke S, Soose RJ, Hasselbacher K, König IR. Impulse configuration in hypoglossal nerve stimulation in obstructive sleep apnea: the effect of modifying pulse width and frequency. *Neuromodulation*. (2022) 25:1312–6. doi: 10.1111/ner.13490

4. Journal of Clinical Sleep Medicine. (2023). Available at: https://jcsm.aasm.org/pb-assets/documents/Decision%20Care%20Pathway%20and%20Management%20of%20UAS-1683912826853.pdf (Accessed March 4, 2024).

5. Vanderveken OM, Beyers J, Op de Beeck S, Dieltjens M, Willemen M, Verbraecken JA, et al. Development of a clinical pathway and technical aspects of upper airway stimulation therapy for obstructive sleep apnea. *Front Neurosci*. (2017) 11:523. doi: 10.3389/fnins.2017.00523

6. Strollo PJ Jr, Soose RJ, Maurer JT, de Vries N, Cornelius J, Froymovich O, et al. Upper-airway stimulation for obstructive sleep apnea. *N Engl J Med*. (2014) 370:139–49. doi: 10.1056/NEJMoa1308659

7. Raphelson JR, Ahmed IM, Ancoli-Israel S, Ojile J, Pearson S, Bennett N, et al. Evaluation of a novel device to assess obstructive sleep apnea and body position. *J Clin Sleep Med*. (2023) 19:1643–9. doi: 10.5664/jcsm.10644

8. Fleury Curado T, Oliven A, Sennes LU, Polotsky VY, Eisele D, Schwartz AR. Neurostimulation treatment of OSA. *Chest*. (2018) 154:1435–47. doi: 10.1016/j.chest.2018.08.1070

frontiers | Frontiers in Oncology

TYPE Case Report
PUBLISHED 28 March 2025
DOI 10.3389/fonc.2025.1496752

OPEN ACCESS

EDITED BY
Karolina Henryka Czarnecka-Chrebelska,
Medical University of Lodz, Poland

REVIEWED BY
Swarna Kanchan,
Marshall University, United States
Hamadi Madhi,
University of Michigan, United States

*CORRESPONDENCE
Hongying Zhang
hy_zhang@scu.edu.cn

†These authors have contributed equally to this work

RECEIVED 15 September 2024
ACCEPTED 04 March 2025
PUBLISHED 28 March 2025

CITATION
Shi C, Qiu Y, He K, Li Y, Wan Q, Yao J and Zhang H (2025) Case Report: Intestinal metastasis from *ALK*-rearranged pulmonary pleomorphic carcinomas mimicking inflammatory myofibroblastic tumors. *Front. Oncol.* 15:1496752. doi: 10.3389/fonc.2025.1496752

Case Report: Intestinal metastasis from *ALK*-rearranged pulmonary pleomorphic carcinomas mimicking inflammatory myofibroblastic tumors

Changle Shi[1†], Yan Qiu[1†], Kang He[2], Yuli Li[1], Qingsong Wan[3], Jin Yao[4] and Hongying Zhang[1*]

[1]Department of Pathology, West China Hospital, Sichuan University, Chengdu, Sichuan, China, [2]Department of Pathology, Panzhihua steel general hospital, Panzhihua, Sichuan, China, [3]Department of Radiology, Panzhihua steel general hospital, Panzhihua, Sichuan, China, [4]Department of Radiology, West China Hospital, Sichuan University, Chengdu, Sichuan, China

Lung carcinomas usually spread to the liver, lungs, pleura, pericardium, adrenal glands, brain, and bones. Anaplastic lymphoma kinase gene (*ALK*) fusion occurs in approximately 5% of non-small cell lung cancer (NSCLC) cases and most frequently in adenocarcinoma. Here, we report a rare case of intestinal metastasis originating from pulmonary pleomorphic carcinoma in a 49-year-old male heavy smoker. At the local hospital, the patient was initially considered to have an ALK-positive intestinal tumor, leading to a differential diagnosis of inflammatory myofibroblastic tumor (IMT). Due to the tumor's peculiar morphology (including epithelioid and spindle cell components), pathologists of the local hospital sent slides of the case to our hospital for further consultation. Immunohistochemical analysis revealed that the epithelioid and spindle neoplastic cells were positive for CK7, TTF1, and ALK-V. Fluorescence *in situ* hybridization (FISH) confirmed the presence of the echinoderm microtubule-associated protein-like 4 (*EML4*):: *ALK* fusion. Based on these findings, we established the final diagnosis as intestinal metastasis of ALK-positive pulmonary pleomorphic carcinoma. A subsequent enhanced CT scan of the chest revealed a 3.0 cm solid mass in the right upper lung, further supporting the diagnosis of intestinal metastasis originating from pulmonary pleomorphic carcinoma. In conclusion, this case exhibited highly unusual clinicopathological features that could easily lead to misdiagnosis as primary intestinal tumors with *ALK* rearrangement. Pathologists must know this possibility to ensure accurate diagnosis and appropriate management.

KEYWORDS

ALK, inflammatory myofibroblastic tumor, epithelioid inflammatory myofibroblastic sarcoma, lung carcinoma, intestinal metastasis

Introduction

Lung cancer is mainly divided into small-cell lung carcinoma (SCLC) and non-small cell carcinoma (NSCLC). The NSCLC primarily includes squamous cell carcinoma (SqCC), adenocarcinoma (ADC), large cell carcinoma, adenosquamous carcinoma, and other types of NSCLC (1). Pulmonary pleomorphic carcinoma (PLC) is a pretty rare type of NSCLC, which is composed of a mesenchymal component of spindle cells, giant cells, or both, with a sarcomatoid tumor component of more than 10% according to the 2021 World Health Organization's (WHO) histological classification of lung tumors. Moreover, reports indicate that it accounts for no more than 0.5% of lung carcinomas (1).

There are many genetic abnormalities that have been described, the most common genes including tumor protein p53 (*TP53*), KRAS proto-oncogene (*KRAS*), and epidermal growth factor receptor (*EGFR*) (1). Notably, anaplastic lymphoma kinase gene (ALK) rearrangement occurs in approximately 5% of pulmonary PLCs (2), which is similar to that in cases with non-small cell lung cancer (NSCLC) and is most often seen in ADC (3).

The most frequent metastatic sites of pulmonary PLC are the liver, adrenal glands, brain, and bones. Metastases to the intestine from lung cancer are uncommon and only account for about 8% of all lung cancer cases in autopsy (4) and even less in clinical incidence (5, 6), let alone the first clinical indication.

Researchers have only reported a small number of lung cancers with intestinal metastasis, including few ones with *ALK* rearrangement, but most of them are ADC subtypes instead of PLCs (7–9). Here, we described an extremely rare case of *EML4*::*ALK* positive pulmonary PLC with intestinal metastasis, which histologically mimics inflammatory myofibroblastic tumor (IMT).

Case presentation

A 49-year-old heavy-smoker (37 pack per year) male patient was admitted to the local hospital with acute abdomen pain. The patient has no history of chronic diseases. Neither the patient nor their family members have a history of cancer. An enhanced computed tomography (CT) scan revealed a 4.0 cm soft tissue mass within the lumen of the small intestine and mid-lower intestine intussusception (Figure 1).

The patient was admitted to the general surgery ward, and an intussusception surgery was performed on April 8, 2019. An irregular, hard, solid white mass involving the intestine was identified during surgery. The patient underwent complete resection of the mass with a partial small intestine resection. The resected specimen comprised a multinodular mass with a tan-white cut surface and firm consistency, whereas a thin envelope was observed in the periphery of the mass. ALK-positive IMT was diagnosed and was highly suspicious for epithelioid inflammatory myofibroblastic sarcoma (EIMS) for showing ALK(5A4) positive in neoplastic cells immunochemically. Our department received the consultation slides from the local hospital.

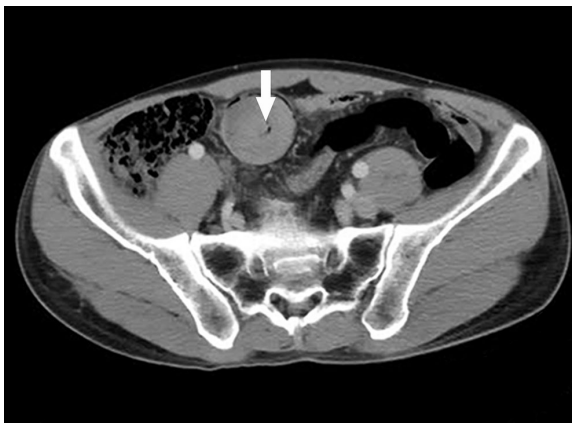

FIGURE 1
Enhanced computed tomography (CT) scan showing a well-defined soft tissue mass (arrow) in the lumen of the ileum.

Histologically, in low-power fields, the tumor was located within the submucosa and lamina propria of the intestinal wall with mucosal erosion (Figure 2A), and the neoplastic cells were embedded within the inflammatory background. In high power fields, it showed that neoplastic components of fat spindle-shaped cells and large epithelioid cells with ovoid nuclei interwoven with each other distributed in the background of many neutrophil cells (Figure 2B, C). Mitotic activity was frequent (up to 10 per 10 high-power fields), and atypical forms were observed. The neoplastic cells showed moderate cytoplasmic positivity for ALK (OTI1H7) and were negative for CD30, CD45, desmin, smooth muscle actin, DOG1, CD117, CD34, and S-100 protein. After reviewing those consultation slides, additional immunostainings were performed and results showed that the neoplastic cells were positive for ALK-V (D5F3) (cytoplasmic pattern) (Figure 2D), ALK (5A4), thyroid transcription factor 1 (TTF-1, 8G7G3) (Figure 2E), TTF-1(SPT2), epithelial membrane antigen (EMA), cytokeratin AE1/AE3, and cytokeratin seven (CK7) (Figure 2F). The tumor cells were negative for p63, cytokeratin 5/6, and Napsin-A. Fluorescence *in situ* hybridization analysis revealed *ALK* gene rearrangement in spindle, oval, and epithelial-like neoplastic cells (Figure 3A). Subsequently, next-generation sequencing involving 68 lung cancer-related genes identified an *EML4* (exon 6):: *ALK* (exon 20) gene fusion(V3) (Figure 3B). No genetic abnormality of *EGFR*, *KRAS*, *TPM3*, or other genes was detected.

Given that the neoplastic cells were positive for CK7 and TTF1, this strongly suggests that the tumor likely originated from the pulmonary epithelium rather than the soft tissue of the intestine. Additionally, this case revealed the presence of an *EML4* (exon 6):: *ALK* (exon 20) (V3) fusion, which was one of the most common genetic alterations observed in lung cancer. In contrast, EIMS typically harbored *RANBP2*::*ALK* or *RRBP1*::*ALK* fusions (10). Based on these findings, we considered this case to represent intestinal metastasis of an ALK-rearranged pulmonary adenocarcinoma. Therefore, we recommend further clinical investigations to confirm the diagnosis.

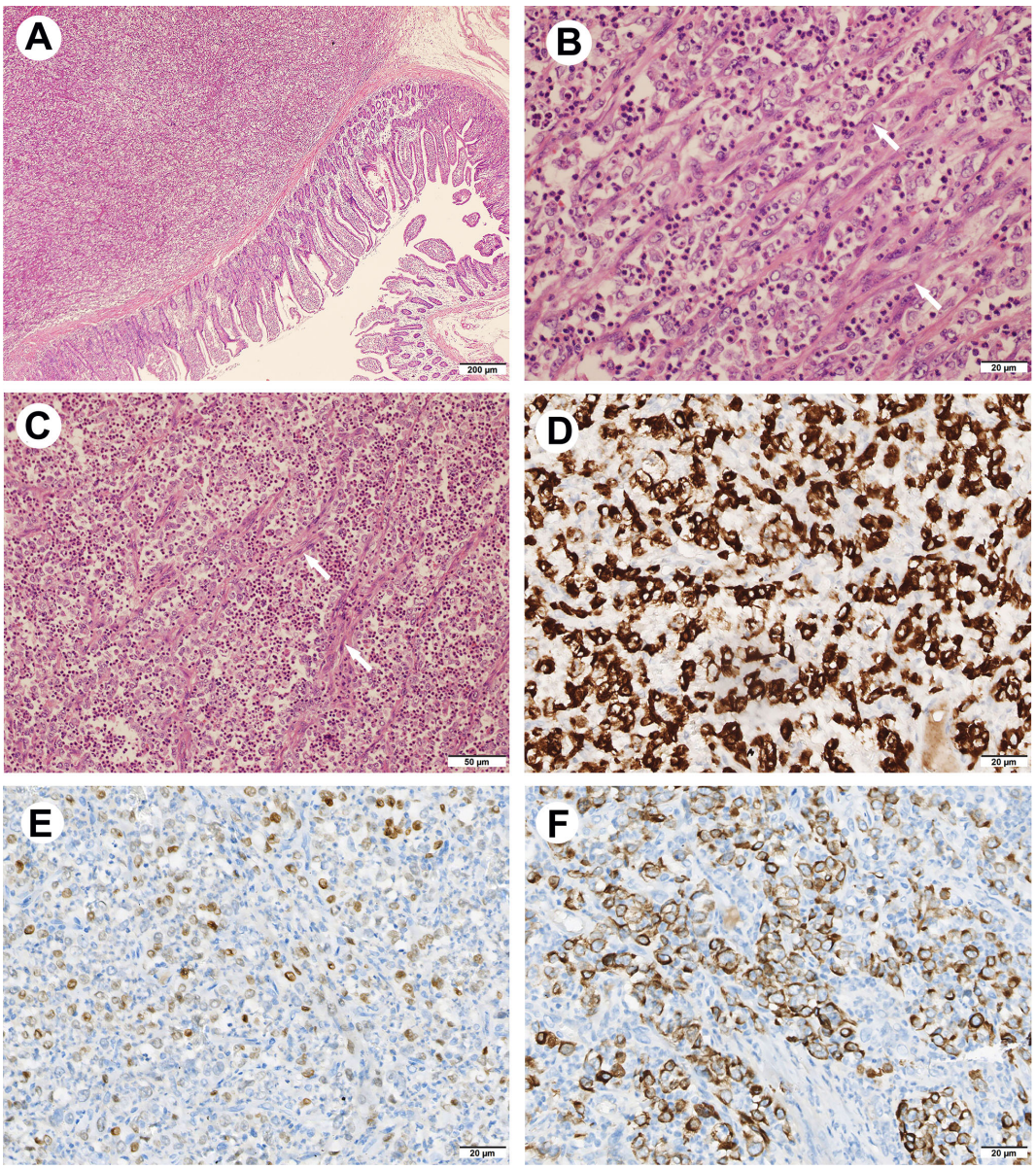

FIGURE 2
Hematoxylin & eosin and immunohistochemical findings of the tumor. **(A)** Low-power view showing the tumor located within the intestinal wall (HE, 40×). **(B, C)** The neoplastic components of fat spindle-shaped cells (arrow) and large epithelioid cells with ovoid nuclei interwoven with each other distributed in the background of large number of neutrophil cells ((HE, 200x&400×). **(D)** The neoplastic cells show cytoplasmic positivity for ALK (D5F3) (IHC, 400×). **(E)** The nuclear of neoplastic cells are positivity for TTF-1(8G7G3) (IHC, 400×). **(F)** The neoplastic cells show cytoplasmic reactivity for CK7 (IHC, 400×).

A subsequent enhanced CT scan of the chest revealed a 3.0 cm solid mass in the right upper lung, further confirming the diagnosis. Therefore, the oncologists recommended the ALK-tyrosine kinase inhibitors (TKI) therapy to the patient. Unfortunately, the patient refused to apply therapeutic approaches despite the doctor firmly suggesting them. Enhanced CT was performed seven months later; it identified a mass of 9.3cm×8.5cm invading the abdominal ln the lower abdomen, which is considered a metastasis or recurrence. The patient showed rapid disease progression and died in December 2019, 6 months after surgery.

Discussion

Metastases to the intestine from lung cancer are rare. Historically, clinical incidence rates of intestinal metastasis of lung cancer have been reported to be no more than 1% (4). However, a review study showed that small bowel obstruction caused by lung carcinoma was up to 11.1% in all secondary tumors (5), implying that some cases may be overlooked in clinical diagnoses.

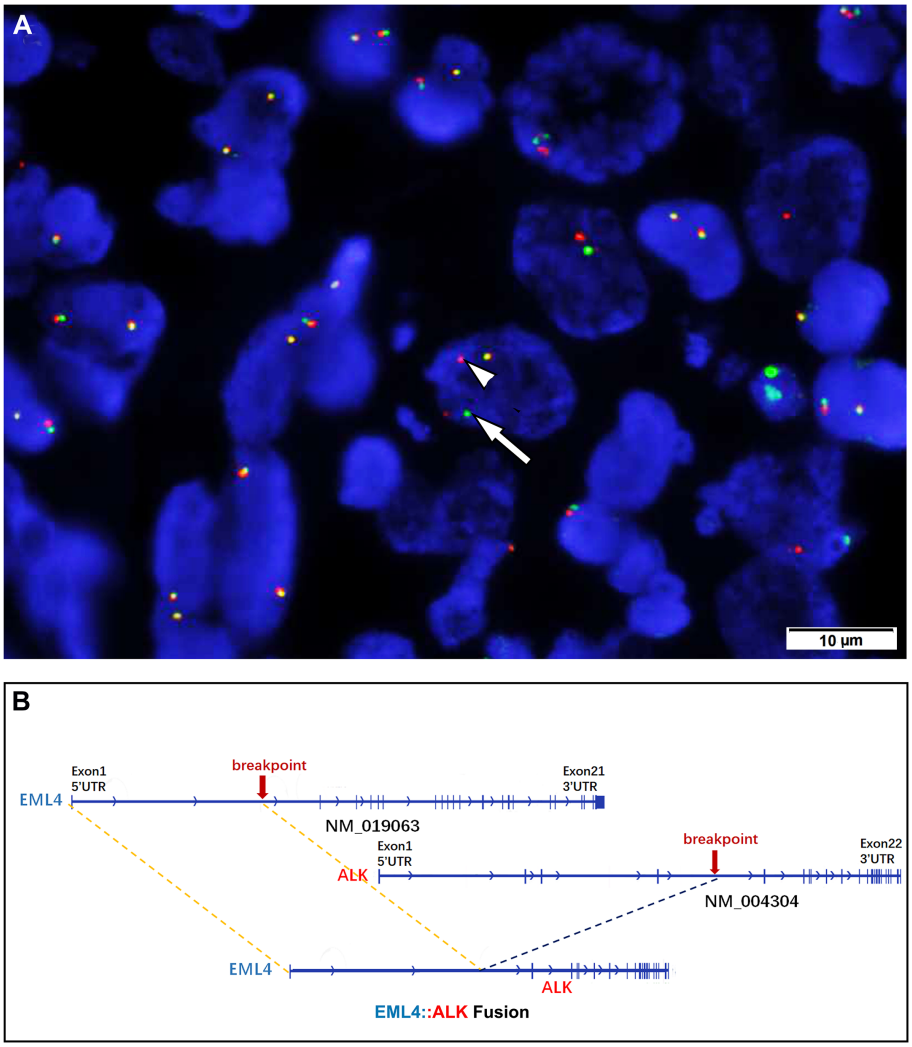

FIGURE 3
(A) Fluorescence *in situ* hybridization demonstrating a rearrangement of the ALK locus in the neoplastic cells (separation of the red [arrow] and green [arrowhead] signals). **(B)** Next-generation sequencing involving 68 lung cancer-related genes identified an *EML4* (exion 6)::*ALK* (exon 20)(V3) gene fusion.

A SNOMED search of the West China Hospital surgical pathology files from January 2009 to May 2023 identified 73132 lung carcinomas, whereas only 24 cases (0.03%) of lung carcinomas metastasized to the intestine have been identified. Among the 24 lung carcinomas (including the present one), ADC (11/24, 45.8%) was the most common subtype, followed by SqCC (5/24,20.8%), PLC (4/24, 8.7%), small cell lung carcinoma (3/24, 12.5%) and large cell carcinoma (1/24, 4.2%). Four patients have performed ALK protein detection (one ADC, one SCC, and one PLC), and the present case is the only positive for ALK. In our hospital, the current case is the only *ALK*-positive PLC confirmed by FISH. Additionally, the data we summarized demonstrated that most cases of intestinal metastasis involved the small intestine (17/24, 70.8%), and only a minimal number of cases involved the large intestine (3/24, 12.5%), the ileocecal junction (2/24, 8.3%) and appendix (2/24, 8.3%). As far as we know, carcinoma originating from the small bowel is sporadic, which would remind clinicians to preferentially explore the primary sites for carcinomas in the small intestine.

A search of the English literature indicated that only 21 cases of *ALK*-rearranged pulmonary pleomorphic carcinomas had been reported so far (including the present one) (Supplementary Table) (2, 11–23). All patients with available age data (13 cases) are adults aged from 38 to 87 years old (median, 58 years old). Among those 14 cases with gender information, males comprised far more than females, with a ratio of 9 to 5. Of those patients (13 cases) with smoking information, 3 have a smoking history, while 10 denied it. The tumor size was 2.4 cm to 7 cm (median, 3cm). For the morphology, most cases (9/11, 81.8%) were composed of sarcomatoid spindle cell components and ADC in varying proportions, while a majority of cases (2/11, 18.2%) comprised giant cells and other components (spindle cells, SqCC or ADC). All those patients with *ALK* rearrangement with ALK immunostaining results (17 cases) showed positive for ALK (17/17,100%). *EML4* is the only fusion partner of the *ALK* gene in those patients with identified fusion partners (8/8, 100%). Among those five patients with follow-up information, local or distant metastases occurred in four patients,

10.3389/fonc.2025.1496752

and the present case is the only one that metastasized to the small intestine. There were two patients who died in 3 and 23 months after surgery, despite they adopt aggressive treatment. Two patients have survived for 11 months after admission. The present case died 6 months ago after refusing any treatments after diagnosis, considering his poor physical condition.

Small intestine metastasis in *ALK*-rearrangement lung cancer is infrequent. Four cases (including the present one) have been reported in the literature (7–9), and details was shown in Table 1. They shared some clinical and pathological features but also showed differences. In two of these cases, abdominal pain was the initial symptom, and they were admitted to the hospital with intestinal lesions as the primary concern. Intestinal metastasis presents with more pronounced symptoms than lung symptoms, which might be one of the reasons for misdiagnosis. Notably, all three cases with detailed genetic findings involved the *EML4::ALK* (V3) fusion type, which has been reported to be associated with poor prognosis of *ALK*-rearranged non-small cell lung cancer (24). All these four patients were already showed distant metastasis at the initial consultation and two of the passed away in 14 months after diagnosis; however, whether this is related to the V3 fusion type requires further investigation. Among the four pathological cases, three contained only ADC components. In contrast, the present case comprised epithelioid and spindle cell components, and it was the only case of pleomorphic carcinoma among these four cases. Currently, there is no definitive experimental evidence regarding the mechanisms of lung cancer metastasis. Still, previous studies suggest it might be related to the intestine's abundant blood supply and lymphatic tissue (8, 9).

Compared with other reported *ALK*-rearranged PLC cases, the present case exhibited peculiar clinicopathological and molecular features. Epidemiologically, the initial clinical indications of intestinal metastasis of lung cancer and PLC are sporadic. Histologically, this tumor is rich in inflammatory cells and diffusely scattered in epithelioid and spindle cell areas. Molecularly, this tumor harbors *ALK* gene rearrangement. All of the above-mentioned characteristics make the diagnosis of the present case more challenging. For the present case, inflammatory spindle cell lesions of the cavum abdominals should be dominantly considered as differential diagnosis, where IMT and anaplastic large cell lymphoma (ALCL) would be much more likely to be identified as ALK-positive tumors, especially IMT (including its subtypes). IMTs are the much more common types of ALK-positive gastrointestinal neoplasm, far outnumbering metastatic NSCLCs. Besides, some classic IMTs can express focal positivity for cytokeratin, and a minority of tumors can harbor *EML4::ALK* fusion, making the diagnosis more confusing (6). In the present case, the morphology is more prone to be a high-grade tumor, and epithelioid inflammatory fibroblastic sarcoma (IMS), an aggressive subtype of IMTs, should be excluded. IMS has a marked predilection for the abdominal cavity and comprises large epithelioid cells. However, we should emphasize that most EIMSs show a nuclear membrane or a perinuclear accentuated cytoplasmic pattern of ALK staining and usually have *RANBP2*:: *ALK* or *RRBP1*:: *ALK* fusions (10). The current case showed a cytoplasmic pattern and harbored *EML4*::

TABLE 1 Clinicopathologic and molecular features of ALK-rearrangement lung carcinomas with small intestinal metastases.

No.	References	Age/ Sex	Smoking history	Family history of cancer	Psychosocial history	Morphology	Diagnosis	Clinical stage	Initial symptoms	Size (cm)	Treatment	Metastasis sites	Clinical outcome	Molecular findings of ALK		
														ALK (IHC)	ALK (FISH)	ALK (NGS)
1	Cha et al. (2016) (7)	72/ M	Yes	NA	NA	ADC	ADC	IV	Hoarseness and dyspnea	3.4	Chemotherapy +Crizotinib	Liver, jejunum, abdominal wall peri-gastric LN	Survival with disease, 9m	+(D5F3)	Rearrangement	ND
2	Zhu et al. (2024) (8)	45/ M	No	NA	NA	ADC	ADC	IV	Cough and chest discomfort	NA	Ensartinib +Radiotherapy+Chemotherapy	Mediastinal, right hilar, and supraclavicular region, jejunum	Died,14m	ND	ND	EML4::ALK (V3)
3	Liu et al. (2025) (9)	66/ M	No	NA	NA	ADC	ADC	IV	Abdominal pain and diarrhea	NA	Right hemicolectomy and mesenteric tumor resection + Lung partial resection + Alectinib	Small intestine	Survival with disease, NA	ND	ND	EML4::ALK (V3)
4	Present case (2024).	49/ M	No	No	NA	ADC+SpC	PLC	IV	Acute abdomen pain	3	None	Small intestine	Died, 6m	+(D5F3)	Rearrangement	EML4::ALK (V3)

NA, not available; ND, not done; F, female; M, male; GC, giant cells; SpC, spindle cells; PLC, pleomorphic carcinoma.

ALK fusion. ALCL is a common type of tumor that harbors ALK gene fusion; furthermore, about 10% of ALCLs present large round neoplastic cells admixed with a large number of reactive histiocytes (25), which is similar to the morphology of the present case. Although the gastrointestinal tract is not the common site for ALCL, it does occur in the gastrointestinal tract (26). However, the hallmark cells of anaplastic large cell lymphoma (ALCL) are absent in the present case. As reported, these cells usually have a variable proportion, with eccentric, horseshoe- or kidney-shaped nuclei and often an adjacent eosinophilic region (25). In addition, ALCL is generally positive for CD30. All the above-mentioned characteristics assist us in ruling out the possibility of ALCL. Notably, positive TTF1 staining combined with detailed clinical findings can be valuable in confirming the diagnosis.

The present case exhibited extremely peculiar clinicopathological features and can easily be misdiagnosed as primary intestinal tumors with ALK rearrangement. A comprehensive analysis from clinical, histological, immunohistochemical, and molecular aspects offers a full view of these case. It reminded that pathologists should be aware of the possibility of other ALK-positive neoplasms, including metastatic lesions, in the diagnosis-making process. However, being a single case study, its findings lacked generalizability and there was no experimental evidence on metastasis mechanisms, and more cases are needed to clarify it.

Data availability statement

The original contributions presented in the study are included in the article/Supplementary Material. Further inquiries can be directed to the corresponding author/s.

Ethics statement

The studies involving humans were approved by West China Hospital Institutional Review Board. The studies were conducted in accordance with the local legislation and institutional requirements. The participants provided their written informed consent to participate in this study. Written informed consent was obtained from the participant/patient(s) for the publication of this case report.

Author contributions

CS: Formal Analysis, Resources, Writing – original draft. YQ: Writing – review & editing, Writing – original draft. KH: Resources, Writing – review & editing. YL: Data curation, Writing – review & editing. QW: Resources, Writing – review & editing. JY: Resources, Writing – review & editing. HZ: Writing – review & editing.

Funding

The author(s) declare that financial support was received for the research and/or publication of this article. This work was supported by the National Natural Science Foundation of China (No. 81972520, 82203180); Natural Science Foundation Project of Science & Technology Department of Sichuan Province (No.2024NSFSC0763, 2024NSFSC7843) and the Cadre Health Research Project of Sichuan Province (No.2024-113).

Conflict of interest

The authors declare that the research was conducted in the absence of any commercial or financial relationships that could be construed as a potential conflict of interest.

Publisher's note

Supplementary material

The Supplementary Material for this article can be found online at: https://www.frontiersin.org/articles/10.3389/fonc.2025.1496752/full#supplementary-material

References

1. WHO Classification of tumors Editorial Board Thoracic Tumors. *WHO Classification of Tumor*. Lyon: International Agency for Research on Cancer (2021).

2. Huang Y, Guo J, Li S, Liu J, Xu J, Ye W, et al. The correlation between histologic, immunophenotypic, and molecular characteristics of pulmonary sarcomatoid carcinoma reveals that sarcomatoid change is potentially derived from epithelial carcinoma cells undergoing epithelial-mesenchymal transition. *Appl Immunohistochem Mol Morphol*. (2023) 31:17–25. doi: 10.1097/PAI.0000000000001060

3. Soda M, Choi YL, Enomoto M, Takada S, Yamashita Y, Ishikawa S, et al. Identification of the transforming EML4-ALK fusion gene in non-small-cell lung cancer. *Nature*. (2007) 448:561–6. doi: 10.1038/nature05945

4. Rossi G, Marchioni A, Romagnani E, Bertolini F, Longo L, Cavazza A, et al. Primary lung cancer presenting with gastrointestinal tract involvement: clinicopathologic and immunohistochemical features in a series of 18 consecutive cases. *J Thorac Oncol*. (2007) 2:115–20. doi: 10.1016/S1556-0864(15)30037-X

5. Idelevich E, Kashtan H, Mavor E, Brenner B. Small bowel obstruction caused by secondary tumors. *Surg Oncol*. (2006) 15:29–32. doi: 10.1016/j.suronc.2006.05.004

6. Coffin CM, Hornick JL, Fletcher CD. Inflammatory myofibroblastic tumor: comparison of clinicopathologic, histologic, and immunohistochemical features including ALK expression in atypical and aggressive cases. *Am J Surg Pathol*. (2007) 31:509–20. doi: 10.1097/01.pas.0000213393.57322.c7

7. Cha YJ, Cho BC, Kim HR, Lee HJ, Shim HS. A case of ALK-rearranged adenocarcinoma with small cell carcinoma-like transformation and resistance to crizotinib. *J Thorac Oncol*. (2016) 11:e55–8. doi: 10.1016/j.jtho.2015.12.097

8. Zhu L, Zhao Y, Zhang Y, Liu Z, Ma W, Guo Y, et al. Small intestinal metastasis in a lung adenocarcinoma patient with concurrent EML4-ALK V3 and TP53 mutations after distinct responses to tyrosine kinase inhibitors: A case report. *Heliyon*. (2024) 10: e38839. doi: 10.1016/j.heliyon.2024.e38839

9. Liu TH, Chen YZ, Xu ZQ, Dong M. Oncogenic ALK fusion in rare subtype of small intestine metastasis from occult lung cancer. *Lung Cancer Manag*. (2025) 14:2364582. doi: 10.1080/17581966.2024.2364582

10. Lee JC, Li CF, Huang HY, Zhu MJ, Mariño-Enríquez A, Lee CT, et al. ALK oncoproteins in atypical inflammatory myofibroblastic tumours: novel RRBP1-ALK fusions in epithelioid inflammatory myofibroblastic sarcoma. *J Patho*. (2017) 241:316–23. doi: 10.1002/path.4836

11. Yoshida A, Tsuta K, Nakamura H, Kohno T, Takahashi F, Asamura H, et al. Comprehensive histologic analysis of ALK-rearranged lung carcinomas. *Am J Surg Pathol*. (2011) 35:1226–34. doi: 10.1097/PAS.0b013e3182233e06

12. Lee HY, Ahn HK, Jeong JY, Kwon MJ, Han JH, Sun JM, et al. Favorable clinical outcomes of pemetrexed treatment in anaplastic lymphoma kinase positive non-small-cell lung cancer. *Lung Cancer*. (2013) 79:40–5. doi: 10.1016/j.lungcan.2012.10.002

13. Kodama T, Motoi N, Ninomiya H, Sakamoto H, Kitada K, Tsukaguchi T, et al. A novel mechanism of EML4-ALK rearrangement mediated by chromothripsis in a patient-derived cell line. *J Thorac Oncol*. (2014) 9:1638–46. doi: 10.1097/JTO.0000000000000311

14. Shiroyama T, Tanaka A, Tamiya M, Hamaguchi M, Osa A, Takeoka S, et al. A rare case of pleomorphic carcinoma of the lung harboring an anaplastic lymphoma kinase (ALK) rearrangement. *Intern Med*. (2015) 54:2741–3. doi: 10.2169/internalmedicine.54.4474

15. Murakami Y, Saka H, Oki M. Response to crizotinib and clinical outcome in ALK-rearranged pulmonary pleomorphic carcinoma. *J Thorac Oncol*. (2015) 10:e28–9. doi: 10.1097/JTO.0000000000000450

16. Maruyama R, Matsumura F, Shibata Y, Takahashi H, Okabayashi H, Kosai S, et al. Detection of ALK rearrangement in an octogenarian patient with pleomorphic carcinoma of the lung. *Gen Thorac Cardiovasc Surg*. (2016) 64:167–9. doi: 10.1007/s11748-014-0428-4

17. Jang JS, Bi L, Kipp BR, Jen J, Yi ES, Boland JM. Molecular characterization of pulmonary sarcomatoid carcinoma: analysis of 33 cases. *Mod Pathol*. (2016) 29:824–31. doi: 10.1038/modpathol.2016.89

18. Li X, Wang D, Zhao Q, Ren D, Ren F, Chen G, et al. Clinical significance and next-generation sequencing of Chinese pulmonary sarcomatoid carcinoma. *Sci Rep*. (2017) 7:3947. doi: 10.1038/s41598-017-04296-2

19. Chen X, Zhang Y, Lu J, Xu C, Liang J, Wang F, et al. Pulmonary sarcomatoid carcinoma with ALK rearrangement: frequency, clinical-pathologic characteristics, and response to ALK inhibitor. *Transl Oncol*. (2017) 10:115–20. doi: 10.1016/j.tranon.2016.11.009

20. Lin L, Huang F, Chen F, He Y, Hu J, Cao X. Anaplastic lymphoma kinase (ALK)-rearranged pulmonary pleomorphic carcinoma successfully treated with crizotinib. *J Int Med Res*. (2018) 46:3491–7. doi: 10.1177/0300060517748262

21. Alì G, Bruno R, Poma AM, Affinito O, Monticelli A, Piaggi P, et al. Whole transcriptome targeted gene quantification provides new insights on pulmonary sarcomatoid carcinomas. *Sci Rep*. (2019) 9:3536. doi: 10.1038/s41598-019-40016-8

22. Manabe S, Kasajima R, Murakami S, Miyagi Y, Yokose T, Kondo T, et al. Analysis of targeted somatic mutations in pleomorphic carcinoma of the lung using next-generation sequencing technique. *Thorac Cancer*. (2020) 11:2262–9. doi: 10.1111/1759-7714.13536

23. Hashimoto H, Komori K, Kameda K, Taguchi S, Ozeki Y. Successful salvage surgery followed by second ALK-TKI after alectinib failure in a patient with ALK-positive NSCLC. *Surg Case Rep*. (2022) 8:59. doi: 10.1186/s40792-022-01408-7

24. Noh KW, Lee MS, Lee SE, Song JY, Shin HT, Kim YJ, et al. Molecular breakdown: a comprehensive view of anaplastic lymphoma kinase (ALK)-rearranged non-small cell lung cancer. *J Pathol*. (2017) 243:307–19. doi: 10.1002/path.4950

25. Tsuyama N, Sakamoto K, Sakata S, Dobashi A, Takeuchi K. Anaplastic large cell lymphoma: pathology, genetics, and clinical aspects. *J Clin Exp Hematop*. (2017) 57:120–42. doi: 10.3960/jslrt.17023

26. Lee YY, Takata K, Wang RC, Yang SF, Chuang SS. Primary gastrointestinal anaplastic large cell lymphoma. *Pathology*. (2017) 49:479–85. doi: 10.1016/j.pathol.2017.05.007

frontiers | Frontiers in Medicine

TYPE Case Report
PUBLISHED 03 April 2025
DOI 10.3389/fmed.2025.1524248

OPEN ACCESS

EDITED BY
Giuseppe Fiorentino,
Colli Hospital, Italy

REVIEWED BY
Lamine Mahi,
Axelys Santé, France
Valentina Chiavieri,
University of Milan, Italy
Stefano Tigano,
IRCCS University Hospital of Bologna Sant Orsola Polyclinic, Italy

*CORRESPONDENCE
Xiao-Qi Li
✉ lxq20190125@foxmail.com

RECEIVED 07 November 2024
ACCEPTED 17 March 2025
PUBLISHED 03 April 2025

CITATION
Yang X-J, Wu Y-J, Wang J-Z, Zheng Y-L and Li X-Q (2025) Pulmonary artery pseudoaneurysm-induced massive hemoptysis after chemotherapy combined with tislelizumab for lung squamous cell carcinoma: a case report.
Front. Med. 12:1524248.
doi: 10.3389/fmed.2025.1524248

Pulmonary artery pseudoaneurysm-induced massive hemoptysis after chemotherapy combined with tislelizumab for lung squamous cell carcinoma: a case report

Xue-Jiao Yang[1], Yong-Juan Wu[2], Jing-Zhong Wang[2], Yu-Lan Zheng[1] and Xiao-Qi Li[2]*

[1]Department of Respiratory and Critical Care Medicine, Xiangyang Central Hospital, Affiliated Hospital of Hubei University of Arts and Science, Xiangyang, China, [2]Department of Interventional Radiology, Xiangyang Central Hospital, Affiliated Hospital of Hubei University of Arts and Science, Xiangyang, China

Lung squamous cell carcinoma (SCC) is a subtype of non-small cell lung cancer with high incidence and mortality rates. While chemotherapy and immune checkpoint inhibitors (ICIs) have become crucial treatment options for SCC, these may be associated with unforeseen complications. Here, we present a 65-year-old male of hemoptysis caused by a pulmonary artery pseudoaneurysm (PAP) after chemotherapy combined with tislelizumab for lung SCC. After confirmation with angiography, successful embolization was performed to occlude the pseudoaneurysm and proximal artery. To our knowledge, this is the first reported case of PAP formation after chemotherapy combined with tislelizumab for lung SCC.

KEYWORDS

lung squamous cell carcinoma, massive hemoptysis, pulmonary artery pseudoaneurysm, tislelizumab, tumor necrosis

Highlights

- After undergoing anti-tumor treatment for pulmonary squamous cell carcinoma, the occurrence of hemoptysis warrants vigilance for pulmonary artery pseudoaneurysm (PAP).
- Tumor necrosis leading to cavitation may be a contributing factor in the formation of a PAP.
- CT angiography can confirm the diagnosis of PAP.
- Endovascular embolization is an effective treatment method.

1 Introduction

With advancements in medical technology, chemotherapy and immune checkpoint inhibitors (ICIs) have become crucial treatment options for lung squamous cell carcinoma (SCC) (1). Tislelizumab is a modified antibody targeting programmed death protein-1 (PD-1) that was approved for treating non-small cell lung cancer (NSCLC) in combination with chemotherapy (2). Tislelizumab can specifically bind to the PD-1 on T cell surface, effectively blocking its interaction with programmed death-ligand 1 (PD-L1) expressed on tumor cells (2). By preventing this binding, tislelizumab reverses PD-1-mediated immunosuppression, restores T cell activation, and enhances anti-tumor immune responses. However, combination therapy may be potentially associated with unforeseen complications that severely affect patient prognosis. This report describes a case of massive hemoptysis caused by a pulmonary artery pseudoaneurysm (PAP) after chemotherapy combined with tislelizumab for lung SCC, providing a reference for clinical practitioners.

2 Case report

A 65-year-old male was admitted to our hospital with sudden massive hemoptysis. The patient denied experiencing chest pain, dyspnea, or fever. He had a 20-year history of chronic obstructive pulmonary disease, but no other significant comorbidities such as vascular diseases, and was not receiving any other chronic therapies at the time of presentation. Two months prior, an enhanced CT scan suggested a tumor in the right upper lung (Figure 1), and a biopsy confirmed right upper lung SCC (TNM stage T2bNXM1c1). The patient received two cycles of albumin-bound paclitaxel, nedaplatin, and tislelizumab. A follow-up CT scan performed showed partial remission of the tumor with cavitation (Figure 2).

Upon physical examination, the patient's hemodynamics were stable, and he exhibited no dyspnea but had hemoptysis with an oxygen saturation of 93%, a blood pressure of 132/67 mmHg, and a heart rate of 88 bpm. Approximately 200 mL of blood loss was estimated based on clinical observation. Auscultation revealed a few wet rales in the upper right lung. Laboratory tests showed hemoglobin at 78 g/L (normal range 130–175 g/L), white blood cell count at 13.46 x 10^9/L (normal range 3.50–9.50 x 10^9/L), neutrophil percentage at 87.9% (normal range 40–75.0%), and C-reactive protein at 143.0 mg/L (normal range 0–10 mg/L). Coagulation tests indicated a slightly prolonged prothrombin time (PT) of 13.5 s (normal range 9.0–13.0 s), a normal thrombin time (TT) of 15.7 s (normal range 14.0–21.0 s), an international normalized ratio (INR) of 1.17 (normal range 0.76–1.24), a PT activity of 67.6% (normal range 70.0–150.0%), and an activated partial thromboplastin time (APTT) of 29.4 s (normal range 21.5–37.0 s). Plasma fibrinogen was elevated at 6.15 g/L (normal range 2.00–4.00 g/L), and D-dimer was at the upper normal limit of 0.55 mg/L (normal range 0.00–0.55 mg/L).

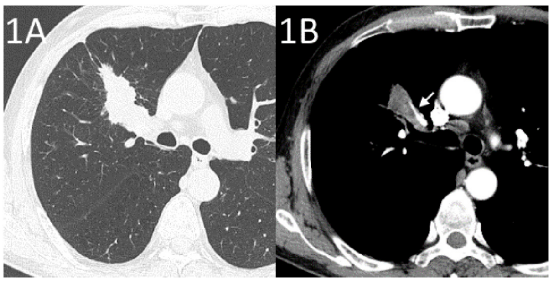

FIGURE 1
Enhanced CT at the diagnosis of lung cancer. **(A)** Lung window showing a tumor in the right upper lung. **(B)** Mediastinal window showing the margin of the tumor in the right upper lung in relation to the pulmonary artery (arrow).

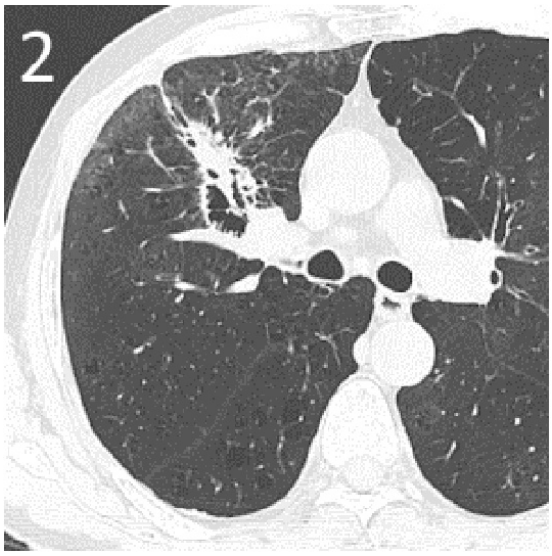

FIGURE 2
Re-examination plain CT after one cycle of chemotherapy combined with tislelizumab treatment. Lung window showing extensive necrosis of the tumor in the right upper lung with cavity formation.

Emergency CTA revealed pseudoaneurysm formation in the right upper pulmonary artery located at the SCC cavity wall with an intraluminal hematoma (Figure 3). The bronchial and non-bronchial systemic arteries showed no significant dilation. Emergency endovascular intervention was performed: after angiography confirmed the presence of a pseudoaneurysm, a 5F sheath (Outlook, Terumo, Tokyo, Japan) was inserted via the right femoral vein. Using a guidewire exchange, a 5F single-curve catheter (Cordis Corp., Miami Lakes, FL, USA) was advanced to the opening of the right upper pulmonary artery. A 2.1F microcatheter (Soft; Asahi Intecc Co., Ltd., Seto, Japan) was then super selectively inserted into the PAP. After confirmation via angiography, embolization was performed using microcoils (one with 4-mm diameter and 14-cm length, two with 3-mm diameter and 3-cm length; Cook, Bloomington, Ind) to occlude the PAP and proximal artery (Figure 4A). Post-procedure angiography confirmed the disappearance of the PAP (Figure 4B).

The patient experienced no active bleeding postoperatively, and follow-up over 6 months showed no recurrence of hemoptysis. Computed tomography (CT) scan 3 months post-embolization showed absorption of the tumor cavity with significant tumor

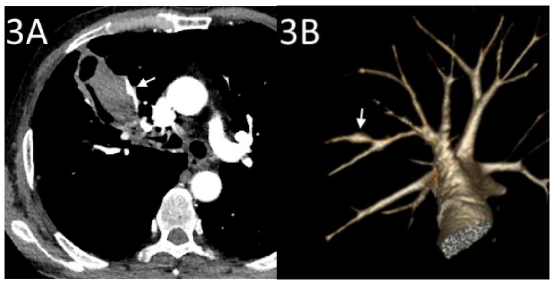

FIGURE 3
CT angiography (CTA) conducted after hemoptysis. **(A)** CTA showing a pseudoaneurysm of the pulmonary artery (arrow) at the edge of the cavity in the right upper lung tumor with hematoma inside the cavity. **(B)** Volume rendering reconstruction showing a pseudoaneurysm in a small branch of the left upper pulmonary artery (arrow).

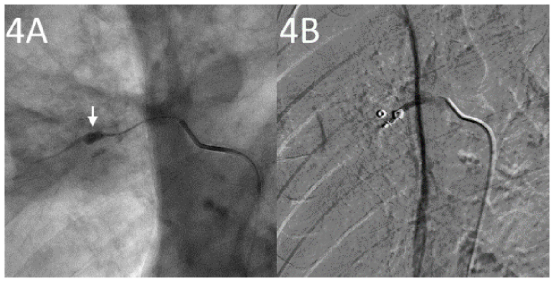

FIGURE 4
Angiography studies. **(A)** Super selective insertion of a microcatheter into the involved pulmonary artery showing a pulmonary artery pseudoaneurysm (arrow). **(B)** Post-embolization with coils showing pulmonary artery pseudoaneurysm success embolization.

reduction (Figure 5). Informed consent has been obtained for this report.

3 Discussion

Pulmonary artery pseudoaneurysm is a rare but extremely dangerous complication encountered in clinical practice (3, 4). Its formation mechanisms may include trauma, infection, tumor invasion, and iatrogenic factors (5). Primary lung cancer or pulmonary metastases can lead to PAP, a rare phenomenon involving direct tumor invasion and vascular wall erosion (4). SCC is the most common tumor because of its biological propensity for necrosis, and cavity formation is an independent risk factor for severe hemoptysis (4, 6). Additionally, studies have indicated that radiotherapy and chemotherapy can promote PAP formation by damaging the tumor and vascular walls (4, 6). ICIs enhance the immune response and significantly impact tumor cell death, leading to severe complications such as diffuse alveolar hemorrhage (7). While no reports have previously linked ICIs to PAP formation, a recent case report described fatal hemoptysis following treatment with tislelizumab and anlotinib in a patient with pulmonary sarcomatoid carcinoma, suggesting a potential association between ICI-based combination therapy and

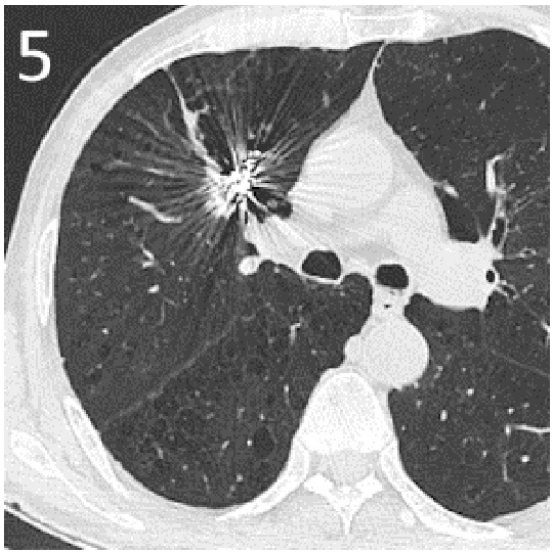

FIGURE 5
A CT scan 3 months post-embolization showed absorption of the tumor cavity with significant tumor reduction.

an increased risk of bleeding (8). Meanwhile, acquired PAP has been identified as a rare complication of systemic chemotherapy, as reported in another case report (9); unfortunately, no causal relationship was confirmed. In our case, the patient had no recent trauma, pulmonary infection, or history of receiving other invasive procedures. Additionally, he was not undergoing any other chronic treatments that could have compromised vascular integrity and did not show coagulation disorders according to laboratory tests. Therefore, the formation of PAP may result from dual damage to the pulmonary artery wall by SCC invasion and combined chemotherapy with tislelizumab, with exposed pulmonary arterial regions in the tumor necrotic cavity lacking tissue coverage, leading to pseudoaneurysm formation and rupture. Targeted treatment was immediately initiated upon diagnosis. Endovascular embolization was performed using interventional radiology to treat the pseudoaneurysms successfully (5, 10).

Reflecting on the clinical management of this case, early identification of high-risk factors, such as rapid tumor necrosis and cavitation, and close monitoring with periodic computed tomography angiography (CTA) might have facilitated earlier detection and potentially prevented severe hemoptysis (11). Despite successful embolization, closer monitoring during the initial cycles of combined therapy could have helped identify the early signs of vascular complications. Given the favorable outcome achieved by prompt embolization, we advocate immediate interdisciplinary consultation with interventional radiology or vascular surgery when PAP is suspected. In particular, patients presenting moderate-to-massive hemoptysis require continuous monitoring of vital signs and prompt initiation of emergency endovascular embolization, and potentially escalated care. Patients experiencing respiratory failure, hemorrhagic shock, or other severe complications should be immediately transferred to an intensive care unit for advanced supportive management. However, it remains uncertain whether routine advanced imaging would significantly improve outcomes, highlighting the need for further studies.

There are a few limitations to this case report. Firstly, while we hypothesize that the combination of tislelizumab and chemotherapy contributed to PAP formation through tumor necrosis and immune-mediated vascular injury, there is no direct evidence establishing a causal relationship. PD-L1 testing was also not performed prior to initiating chemotherapy and tislelizumab therapy for this patient because PD-L1 expression analysis was not available at our hospital at the time of treatment. Due to the lack of relevant reports and mechanistic studies, it remains unclear whether tislelizumab played a critical role in this case. Secondly, this is a single-case report, limiting the generalizability of our findings. Larger case series and retrospective studies are required to evaluate the potential risk associated with tislelizumab, or ICI-based combination therapy. Despite these limitations, this case highlights the need for vigilance regarding rare but severe complications, such as PAP, in the treatment of lung SCC with chemotherapy and tislelizumab. Cavitation within tumors may be an important factor in the formation of PAPs. Endovascular embolization is a safe and effective treatment method.

Data availability statement

The original contributions presented in this study are included in this article/supplementary material, further inquiries can be directed to the corresponding author.

Ethics statement

The studies involving humans were approved by Ethics Committee of Xiangyang Central Hospital. The studies were conducted in accordance with the local legislation and institutional requirements. The participants provided their written informed consent to participate in this study. Written informed consent was obtained from the individual(s) for the publication of any potentially identifiable images or data included in this article.

Author contributions

X-JY: Investigation, Writing – original draft. Y-JW: Investigation, Methodology, Supervision, Validation, Writing – review and editing. J-ZW: Investigation, Supervision, Validation, Writing – review and editing. Y-LZ: Conceptualization, Supervision, Validation, Writing – review and editing. X-QL: Writing – original draft, Writing – review and editing.

Funding

The author(s) declare that no financial support was received for the research and/or publication of this article.

Conflict of interest

The authors declare that the research was conducted in the absence of any commercial or financial relationships that could be construed as a potential conflict of interest.

Generative AI statement

The authors declare that no Generative AI was used in the creation of this manuscript.

Publisher's note

References

1. Wang J, Lu S, Yu X, Hu Y, Sun Y, Wang Z, et al. Tislelizumab plus chemotherapy vs chemotherapy alone as first-line treatment for advanced squamous non-small-cell lung cancer: A phase 3 randomized clinical trial. *JAMA Oncol.* (2021) 7:709–17. doi: 10.1001/jamaoncol.2021.0366

2. Zhang L, Geng Z, Hao B, Geng Q. Tislelizumab: A modified anti-tumor programmed death receptor 1 antibody. *Cancer Control.* (2022) 29:10732748221111296. doi: 10.1177/10732748221111296

3. Plessinger V, Jolly P. Rasmussen's aneurysms and fatal hemorrhage in pulmonary tuberculosis. *Am Rev Tuberc.* (1949) 60:589–603. doi: 10.1164/art.1949.60.5.589

4. Fukuda Y, Homma T, Uno T, Murata Y, Suzuki S, Shiozawa E, et al. Fatal rupture of pulmonary artery pseudoaneurysm after thoracic radiation therapy against lung squamous cell carcinoma: A case report and literature review. *Clin Case Rep.* (2021) 9:737–41. doi: 10.1002/ccr3.3647

5. Zugazaga A, Stachno M, García A, Tovar G, Benito V, Guasch I, et al. Pulmonary artery pseudoaneurysms: Endovascular management after adequate imaging diagnosis. *Eur Radiol.* (2021) 31:6480–8. doi: 10.1007/s00330-021-07819-8

6. Ito M, Niho S, Nihei K, Yoh K, Ohmatsu H, Ohe Y. Risk factors associated with fatal pulmonary hemorrhage in locally advanced non-small cell lung cancer treated with chemoradiotherapy. *BMC Cancer.* (2012) 12:27. doi: 10.1186/1471-2407-12-27

7. Singer, Faiz S, Qdaisat A, Abdeldaem K, Dagher J, Chaftari P, et al. Hemoptysis in cancer patients. *Cancers (Basel).* (2023) 15:4765. doi: 10.3390/cancers15194765

8. Pu C, Ma Y, Peng J, Wang Z. Case report: fatal hemoptysis after effective treatment with tislelizumab and anlotinib in pulmonary sarcomatoid carcinoma. *Front Oncol.* (2024) 14:1445358. doi: 10.3389/fonc.2024.1445358

9. Garg S, King G, Varadi G. Pseudoaneurysm of pulmonary artery: Rare complication of systemic chemotherapy. *Clin Case Rep.* (2015) 3:845–8. doi: 10.1002/ccr3.363

10. Zhang J, Jiang S. Massive haemoptysis from a central pulmonary arterial pseudoaneurysm secondary to advanced lung cancer: Successful treatment by Guglielmi detachable coil embolization. *Clin Respir J.* (2017) 11:258–62. doi: 10.1111/crj.12333

11. Noë G, Jaffé S, Molan MP. CT and CT angiography in massive haemoptysis with emphasis on pre-embolization assessment. *Clin Radiol.* (2011) 66:869–75. doi: 10.1016/j.crad.2011.03.001

frontiers | Frontiers in Medicine

TYPE Case Report
PUBLISHED 28 April 2025
DOI 10.3389/fmed.2025.1544843

OPEN ACCESS

EDITED BY
Talat Kilic,
İnönü University, Türkiye

REVIEWED BY
Hassan Soleimanpour,
Tabriz University of Medical Sciences, Iran
Berna Botan Yıldırım,
Baskent University, Türkiye

*CORRESPONDENCE
Ji-xiang Ni
✉ jxnee77@163.com

†These authors have contributed equally to this work

RECEIVED 13 December 2024
ACCEPTED 03 March 2025
PUBLISHED 28 April 2025

CITATION
Kong L-x, Li Z-h and Ni J-x (2025) Case Report: A case of reversible tracheal diameter Mounier-Kuhn syndrome and literature review.
Front. Med. 12:1544843.
doi: 10.3389/fmed.2025.1544843

Case Report: A case of reversible tracheal diameter Mounier-Kuhn syndrome and literature review

Lu-xia Kong†, Zhen-hua Li† and Ji-xiang Ni*

The Central Hospital of Wuhan, Tongji Medical College, Huazhong University of Science and Technology, Wuhan, China

Mounier-Kuhn syndrome (MKS), also known as tracheobronchomegaly (TBM) or tracheomegaly, is an extremely rare and chronic airway disease characterized by significant dilation of the trachea and central bronchi. Currently, there is a paucity of epidemiological studies on MKS, with the majority of data derived from case reports, resulting in limited understanding of this disease among clinicians. We encountered an 81-year-old male MKS patient whose diagnosis was delayed, and subsequently experienced a significant decrease in tracheal diameter post-diagnosis, marking the first documented case of reversible tracheal diameter in MKS patients. Concurrently, we conducted a review of 76 cases published within the past decade to procure comprehensive insights into the clinical characteristics of MKS patients. Based on our findings, we draw two key conclusions. First, at present, clinicians and radiologists have insufficient understanding of this disease, which often leads to missed diagnosis, misdiagnosis or delayed diagnosis. Second, the tracheal diameter of MKS has the potential to be reversible with appropriate treatment. This is the first case where the tracheal diameter has been found to be reversible.

KEYWORDS

tracheobronchomegaly, Mounier-Kuhn syndrome, reversible, tracheal diameter, tracheomegaly

Introduction

Mounier-Kuhn syndrome (MKS), also known as tracheobronchomegaly (TBM) or tracheomegaly, is an extremely rare and chronic airway disease characterized by significant dilation of the trachea and central bronchi. The condition may be hereditary or acquired, and is associated with the atrophy of the airway elastic fibers, thinning of smooth muscle, and diverticulum formation between the cartilage rings.

MKS, a highly misdiagnosed condition, was first identified by Czyhlarz in an autopsy in 1897, but it was not until 1932 that Mounier-Kuhn proposed a link between airway dilation and recurrent respiratory infections (1). To date, approximately 400 cases have been described (1), with a prevalence between 0.4 and 1.6% (2).

MKS is a rare clinical-radiological entity that can be diagnosed radiographically through chest radiographs, computed tomography (CT) scans, endoscopically, or through bronchoscopy or tracheoscopy. Furthermore, during this bronchoscopy, punch biopsies can be taken and may show a loss of elastic fibers, atrophy of longitudinal muscles, and muscularis mucosae thinning (3).

For patients with MKS, discharge of secretions is affected due to defective clearance and ineffective cough mechanisms. As a result, recurrent lung infections and bronchiectasis often occur (4).

We report on a patient with MKS who presented to our hospital in 2023 with reversible airway changes. Given the rarity of the disease, it was not possible to collect enough cases in the clinic, so we decided to retrospectively analyze previously published cases to further explore the characteristics of the disease. We performed a literature search using the keywords 'Mounier-Kuhn Syndrome,' 'Tracheobronchomegaly,' 'tracheomegaly' or 'Bronchomegaly' to identify relevant case reports in the database (primarily PubMed) in the past decade by 16 October 2024. Only cases involving patients aged 18 years or older were included. Non-English articles and those lacking clear measurements of tracheal or main bronchial diameter were excluded. A total of 76 MKS cases were collected and analyzed.

Case description

On January 3, 2023, an 81-year-old male was admitted with dyspnea and decreased appetite for 1 week. The patient, a Chinese national, had pulmonary tuberculosis, treated surgically in 1964. Since 2018, the patient has been hospitalized in our hospital for several times due to acute exacerbation of chronic obstructive pulmonary disease, bronchiectasis with infection, and recurrent lung infections. The patient was conscious when he was admitted, and his oxygen saturation was 92% without oxygen. He had a thick breathing sound in both lungs, and wet crackles could be heard in the lower right lung. Blood routine examination showed white blood cells 11.76*10^9/L (3.5 ~ 9.5*10^9/L), neutrophil count 82.10% (40 ~ 75%), C-reactive protein 7.07 mg/dL (0 ~ 6 mg/L), interleukin 6 22.52 pg/mL (<7 pg/mL), procalcitonin 1.30 ng/mL (0 ~ 0.1 ng/mL). And novel coronavirus nucleic acid was positive. As shown in Figure 1, the patient's chest CT showed double lung infection, bronchiectasis, and significant tracheobroncho enlargement. He was given symptomatic treatment such as high-flow oxygen inhalation, anti-virus, anti-infection, asthmatic relief, phlegm reduction and nutritional support. Two weeks later, the symptoms improved and the patient was discharged from the hospital. The chest CT examination 1 year later showed that the trachea and the right main bronchus were less enlarged than before.

Discussion

MKS is a rare condition that is frequently overlooked due to its atypical symptoms and limited awareness among clinicians. In the case we present, the patient exhibited an enlarged trachea in 2018 but was not diagnosed until 2023. To enhance clinicians' understanding of the condition, we conducted a review of cases over the past decade. In our study, 76 cases were included, and seriously, the average time from symptom onset to diagnosis was 14.24 ± 11.17 years, as detailed in Table 1 (see the Supplementary Table for the list of cases included).

Consistent with previous findings, MKS predominantly affected males (5), with males accounting for 83.12% (64/77) of cases. In fact, in 1984, conventional chest X-ray showed that the size of the trachea was only related to gender, not weight or height (6). MKS is typically diagnosed in the 5th and 6th decades of life (4). The older the age group, the higher the incidence, patients >60 years old accounted for 49.35% (38/77). The oldest age was 94 years old. Smoking and exposure to air pollutants are significant risk factors (7). A history of smoking was reported in 16 cases (20.78%).

MKS can be diagnosed when chest CT shows (female/male) trachea transverse diameter > 21/25 mm, sagittal diameter > 23/27 mm, and when the trachea transverse diameter of the right and left main bronchi are >19.8/21.1 mm and > 17.4/18.4 mm, respectively (8). Krustins et al. reported an average tracheal diameter of 36 mm (range, 25–65 mm) in MKS patients (9). Our findings are consistent with this, as the average tracheal diameter in our cohort of 77 MKS cases was 36.31 ± 7.95 mm, with a maximum diameter of 62.6 mm. The average diameters of the right and left main bronchi were

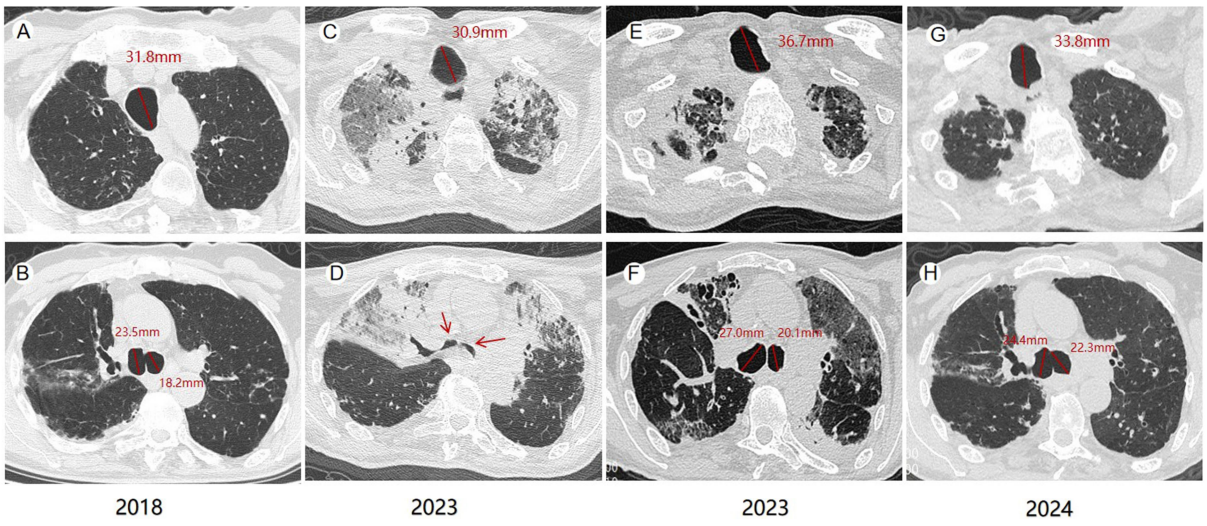

FIGURE 1
Computed tomography (CT) changes of the patient. In 2018, the maximum diameter of the patient's trachea, right and left main bronchi were 31.8 mm, 23.5 mm and 18.2 mm **(A,B)**, respectively. Collapse of the tracheal walls during exhalation was seen on CT at admission in 2023 **(C,D)**. The maximum diameters of the trachea, right and left, main bronchi in 2023 were 36.7 mm, 27.0 mm and 20.1 mm, respectively **(E,F)**. Chest CT in 2024 showed that the maximum diameters of trachea, right and left main bronchi were 33.8 mm, 24.4 mm and 22.3 mm, respectively **(G,H)**.

TABLE 1 Characteristics of the eligible cases for analysis.

Variable	Statistics
Age (years), Mean ± SD	57.22 ± 17.43
Oldest	94
Youngest	21
Age distribution, n/total n (%)	
20–39 years	13/77 (17.88)
40–59 years	26/77 (33.77)
>60 years	38/77 (49.35)
Sex, n/total n (%)	
Male	64/77 (83.12)
Female	13/77 (16.88)
Smokers, n/total n (%)	16/77 (20.78)
Average tracheal diameter (mm), Mean ± SD	36.31 ± 7.95
Largest	62.6
Average bronchial diameter (mm), Mean ± SD	
Right bronchus	23.71 ± 5.41
Left bronchus	22.27 ± 5.13
Tracheal diverticulosis, n/total n (%)	39/77 (50.65)
Bronchiectasis, n/total n (%)	49/77 (63.64)
Tracheobronchial dyskinesia, n/total n (%)	16/77 (20.78)
Recurrent respiratory infections, n/total n (%)	50/77 (64.94)
Comorbidities, n/total n (%)	
PTB	3/77 (3.90)
COPD	12/77 (15.58)
IPF	3/77 (3.90)
Tumor	1/77 (1.30)
Pulmonary embolism	1/77 (1.30)
Three types of MKS, n/total n (%)	
Type 1	37/77 (48.05)
Type 2	18/77 (23.38)
Type 3	22/77 (28.57)
Lung function test, n/total n (%)	
Normal	9/40 (22.50)
Obstructive	21/40 (52.50)
Restrictive	8/40 (20.00)
Mixed	2/40 (5.00)
Symptoms, n/total n (%)	
Fever	16/77 (20.78)
Dry cough	16/77 (20.78)
Productive cough	44/77 (57.14)
Hemoptysis	15/77 (19.48)
Dyspnea	47/77 (61.04)
Chest pain	11/77 (14.29)
Weight loss	4/77 (5.19)
Anorexia	1/77 (1.30)
Pharyngeal discomfort	3/77 (3.90)
Respiratory failure	12/77 (15.58)
Dysphagia	1/77 (1.30)
Club-finger	6/77 (7.79)
Asymptomatic	2/77 (2.60)
Changes upon auscultation (wheezes, rhonchi, crepitation)	29/77 (37.66)
Unilateral	3/77 (3.90)
Bilateral	26/77 (33.77)

n, number of patients; SD, standard deviation; PTB, pulmonary tuberculosis; COPD, chronic obstructive pulmonary disease; IPF, idiopathic pulmonary fibrosis; n/total n denotes the available number/total number because of some missing data.

23.71 ± 5.41 mm and 22.27 ± 5.13 mm, respectively. To date, few MKS cases with long-term follow-up have been reported, and in these cases, the tracheal diameter tends to increase progressively. In a single patient diagnosed with MKS, the tracheal diameter increased from 35 mm to 42 mm, the left bronchial diameter increased from 20 mm to 25 mm, and the right bronchial diameter increased from 18 mm to 23 mm over a seven-year follow-up period (10). Our patient represents the first documented case of reversible tracheal enlargement in MKS. From 2023 to 2024, the diameter of his trachea decreased from 36.7 mm to 33.8 mm, and the diameter of his right main bronchus decreased from 27.0 mm to 24.4 mm.

In addition, MKS is also diagnosed by the cross-sectional area of the trachea, which exceeds 371 mm^2 in men and 299 mm^2 in women (8). Interestingly, from a physiological perspective, airflow is inversely proportional to the fourth power of the radius. If the tracheal radius is increased by 2 times, the flow rate should be reduced by 16 times. The decrease in airflow rate leads to increased difficulty in clearing the airway, which leads to obstructions in removing secretions (11).

Bronchoscopy remains a strong diagnostic tool that can detect the dilation in the trachea and main bronchi during inspiration; their constriction, and even collapse, during expiration and coughing. This tracheobronchial dyskinesia may also manifest on CT in our patients, with 20.78% (16/77) exhibiting this finding. Biopsy of the trachea can show atrophy of elastic fibers and smooth muscle tissue or complete absence of cartilaginous elements (12).

Although pulmonary function testing is not considered diagnostic, some authors propose that it can assist in determining supportive care (3). Enlarged airways affect spirometry results due to weakness in tracheobronchial walls and hypotonia of myoelastic elements. These pathological changes lead to dynamic airway compression (manifested as expiratory collapse during forced exhalation) and dynamic restriction. Among the 40 patients who underwent pulmonary function testing, obstructive patterns were observed in 21 cases (52.5%), restrictive patterns in 8 (20%), mixed patterns in 2 (5%), with normal results in 9 patients (22.5%).

In addition to increased tracheal diameter, another common radiographic manifestation of MKS is airway diverticula. Diverticula were more frequently observed in the posterolateral wall, at the junction of the extrathoracic and intrathoracic parts of the trachea, which may be attributed to anatomical defects at this level or increased intracavitary pressure secondary to chronic cough (4, 8). Diverticula were present in 39 (50.65%) of 77 patients, and MKS could be classified into three types according to the presence or absence of diverticula and the anatomical distribution of diverticula. Type 1 is characterized by mild diffuse dilation of the trachea and main bronchi, while Type

2 exhibits abnormal and varying widenings accompanied by diverticula in the major airways. In Type 3, diverticula and sacculations accompany widening in the main airways extending to the distal bronchi (13). Among the 77 patients, type 1, type 2 and type 3 patients accounted for 48.05% (37/77), 23.38% (18/77) and 28.57% (22/77), respectively. Additionally, the tracheal diverticulum may serve as a reservoir for secretions, exacerbating the illness in MKS patients and increasing their susceptibility to recurrent respiratory infections (64.94%) and bronchiectasis (63.64%) (14).

The clinical presentations of MKS patients were diverse, including asymptomatic cases (2.60%). Typical symptoms resembling lung infection included: fever (20.78%), dry cough (20.78%), sputum production (57.14%), throat discomfort (3.90%), hemoptysis (19.48%), chest pain (14.29%), dyspnea (61.04%), and respiratory failure (15.58%) (15). Atypical symptoms such as anorexia (1.30%) and dysphagia (1.30%) were also observed in some cases (1, 16). Physical examination may reveal rales and/or rhonchi upon pulmonary auscultation, as well as digital clubbing (7.79%), tachycardia, tachypnea, and respiratory failure.

At present, whether MKS is congenital or acquired is still under debate (17). Two siblings with MKS were reported in the literature, as well as possible MKS cases in Cousins, leading to the initial belief that MKS was an autosomal recessive disorder (5). It was later found that MKS was also seen in patients with Tetany, Ehlers-Danlos syndrome, Marfan syndrome, and cutis laxa (8).

In 2014, Mitterbauer et al. performed a chromosomal analysis and an array-CGH to search for genetic abnormalities. The MKS patient's genome was completely unremarkable, the karyogram as well as the genome hybridization showed no significant gain or loss in known coding regions. Histological and immunohistochemical findings indicate that MKS is a chronic inflammatory condition characterized by the matrix metalloproteinase-mediated degradation of submucosal elastic fibers (18).

More and more people are recognizing that MKS is a secondary condition, associated with numerous chronic muscular, respiratory, or autoimmune diseases. These include pulmonary fibrosis, cystic fibrosis, bronchiectasis, emphysema, chronic bronchitis, amyotrophic lateral sclerosis (ALS) (19), sarcoidosis, chronic progressive histoplasmosis, giant cell arteritis (20), ankylosing spondylitis, rheumatoid arthritis, primary tracheobronchial amyloidosis (21), Sjogren's syndrome (22), and Homocystinuria (23).

In addition, MKS has also been observed in a number of conditions found in critically ill patients requiring prolonged hyperinflation of their endotracheal or tracheostomy tube cuffs; including those with acute respiratory distress syndrome (ARDS) and respiratory failure (8). Tracheal enlargement is a recognized complication of prolonged tracheal intubation, especially when cuff pressure exceeds 30 cmH_2O (24). In recent years, cases of MKS have also been reported in patients with COVID-19 (3, 25, 26).

Furthermore, Parris and Johnson described a case of MKS secondary to radiotherapy for the treatment of oropharyngeal carcinoma (26). Mohammed et al. described a case of fluoroquinolone-induced MKS, in which the diameter of the right main bronchus increased from 16.2 mm to 22.5 mm and the left main bronchus increased from 17.4 mm to 19.7 mm after 2 years of treatment (27).

Unfortunately, due to the limited understanding of the condition, there is scant evidence regarding effective remedies. And there are few interventions specifically targeting anatomical airway abnormalities, with treatment primarily focused on supportive symptomatic care. In our series of 77 cases, the treatment approaches were predominantly supportive care (67 cases), followed by tracheal stent placement (3 cases), tracheostomy tube placement (5 cases), lung transplantation (3 cases), and one case in which the specific treatment method was not mentioned.

In fact, for patients with both acute and chronic MKS, bronchodilators, mucolytic therapy, and intermittent steroid therapy have been shown to be beneficial. Appropriate antibiotic treatment is necessary for cases with bacterial infections. Additional supportive care options may include mobilization assistance and chest physical therapy to facilitate the clearance of secretions in these patients.

The management of chronic MKS in patients primarily focuses on symptom control and prevention of future infections. Firstly, smoking cessation is highly advantageous. Secondly, it is recommended to administer influenza and pneumococcal vaccinations to all adult MKS patients, irrespective of age or symptomatic status (5). Noninvasive mechanical ventilation (NIMV) has the potential to enhance expiratory flow and manage symptoms by reducing lung resistance and respiratory work load. In outpatient settings, some chronic patients have experienced symptom improvement with noninvasive continuous positive airway pressure (CPAP). However, it is important to note that NIMV may only provide temporary relief of clinical symptoms and may not achieve the intended treatment outcomes.

In patients with critical illness, if supportive care and medication fail to achieve desired outcomes, it may be necessary to consider surgical interventions. These interventions could encompass placement of a tracheostomy tube, tracheal stent placement, tracheobronchoplasty, laser therapy, or lung transplantation (15).

Due to the enlarged diameter of the airway, Ushakumari et al. recommend the use of endotracheal tubes with the largest diameter, through the glottic opening, an inflatable cuff to prevent air leakage, and wet gauze if necessary to reduce further leakage (7). Cheon et al. also chose a thicker tracheal tube than usual (inner diameter 8.0 mm, outer diameter 11.0 mm, maximum cuff size 28 mm) (28). Kim et al. observed that the standard tracheostomy tube is insufficient in length for proper placement within the dilated trachea of patients with MKS, resulting in significant peritubular sleeve leakage and subsequent hypercapnia. During tracheotomy and insertion, an undiagnosed case presented with tracheal enlargement secondary to massive cuff leakage resulting in ventilation failure (24). Hence, a customized tracheal catheter was shortened and carefully placed into the tracheostomy (3).

For patients with MKS, a primary anesthesia consideration is air leakage around the tracheal cannula, resulting in anesthetic gas leakage and inhalation hazards, catheter detachment, and passive airway collapse. These risks can complicate the process of obtaining adequate humidification during mechanical ventilation (28). Therefore, for MKS patients undergoing anesthesia, epidural anesthesia or lumbar anesthesia may be considered as alternative approaches (29).

Stent placement poses a significant challenge due to the need for using a large stent to stabilize an already enlarged airway, leading to common complications such as stent migration and mucus plug impaction. To mitigate the risk of stent migration, Y-type stents have been utilized with improved outcomes. Additionally, tracheobronchoplasty offers an alternative approach by restoring

normal airway anatomy while preserving mucociliary function (12). However, stent implantation also has complications such as secretion retention, infection and restenosis due to granulation.

Laser bronchoplasty represents a novel and minimally invasive technique, capable of mitigating local nodule contraction and scar formation, thereby ameliorating airway collapse. Both domestic and international studies have reported favorable clinical outcomes, with patients experiencing significant improvement in symptoms within 1 week post-surgery. Consequently, laser bronchoplasty stands as a safe and effective approach for addressing cartilaginous nodules to achieve recanalization. Nonetheless, further research is warranted to comprehensively evaluate the efficacy of this technique (30).

Surgical intervention and lung transplantation are reserved for patients with advanced disease or those who have exhausted options such as CPAP, airway stenting, tracheoplasty, and laser therapy (23, 31). However, technical challenges arise due to the need to connect the graft to the original dilated bronchus. Surgical treatment carries significant risks and complications, with certain limitations impacting patient outcomes.

Conclusion

Overall, there is a bias present in this study. The majority of cases are sourced from previously published journals, resulting in a focus on imaging descriptions and treatment modalities, and lack descriptions of patients' symptoms and signs. In addition, two key conclusions can be drawn from our patients' data: First, clinicians and radiologists have insufficient understanding of this disease, leading to frequent missed diagnosis, misdiagnosis, or delayed diagnosis. Although this syndrome is extremely rare, it significantly impacts patients' quality of life. Diagnosis and management require a comprehensive assessment, including computed tomography and a multidisciplinary approach involving pulmonologists and radiologists. Understanding its clinical features, association with other respiratory diseases, and treatment options is critical to managing this rare respiratory disease. Second, the tracheal diameter of MKS has the potential to be reversible with appropriate treatment. This study reports the first documented case of reversible tracheal diameter in MKS patients.

Data availability statement

The original contributions presented in the study are included in the article/Supplementary material, further inquiries can be directed to the corresponding author.

Ethics statement

Written informed consent was obtained from the participant/patient(s) for the publication of this case report.

Author contributions

L-xK: Conceptualization, Data curation, Formal analysis, Investigation, Methodology, Software, Visualization, Writing – original draft. Z-hL: Conceptualization, Formal analysis, Supervision, Writing – review & editing. J-xN: Conceptualization, Supervision, Validation, Writing – review & editing.

Funding

The author(s) declare that no financial support was received for the research and/or publication of this article.

Conflict of interest

The authors declare that the research was conducted in the absence of any commercial or financial relationships that could be construed as a potential conflict of interest.

Generative AI statement

The authors declare that no Gen AI was used in the creation of this manuscript.

Publisher's note

Supplementary material

The Supplementary material for this article can be found online at: https://www.frontiersin.org/articles/10.3389/fmed.2025.1544843/full#supplementary-material

References

1. Rossi S, Volpi F, Castellana R, Pancani R, Dente F, Gaeta R, et al. A case report of unusual recurrent bronchopneumonia infections in Mounier-Kuhn syndrome. *Radiol Case Rep*. (2024) 19:2525–30. doi: 10.1016/j.radcr.2024.03.028

2. Estrada DE, Uribe-Buritica FL, Vargas CA, García C, Martínez W. Recurrent pneumonias in a previously healthy and immunocompetent young adult: a case report Mounier-Kuhn syndrome. *Am J Case Rep*. (2020) 21:e918535. doi: 10.12659/ajcr.918535

3. Collins NE. Acquired Tracheomegaly in critically ill patients with COVID-19: a literature review. *J Nurse Pract*. (2022) 18:857–61. doi: 10.1016/j.nurpra.2022.05.014

4. Akgedik R, Karamanli H, Kizilirmak D, Kurt AB, Öztürk H, Yildirim BB, et al. Mounier-Kuhn syndrome (tracheobronchomegaly): an analysis of eleven cases. *Clin Respiratory J*. (2018) 12:885–9. doi: 10.1111/crj.12600

5. Krustins E, Kravale Z, Buls A. Mounier-Kuhn syndrome or congenital tracheobronchomegaly: a literature review. *Respiratory Med*. (2013) 107:1822–8. doi: 10.1016/j.rmed.2013.08.042

6. Breatnach E, Abbott GC, Fraser RG. Dimensions of the normal human trachea. *Am Roentgen Ray Soc*. (1984) 142:903–6. doi: 10.2214/ajr.142.5.903

7. Shahin S, Hoffman T, van Es W, Grutters J, Mateyo K. Congenital tracheobronchomegaly (Mounier-Kuhn syndrome) in a 28-year-old Zambian male: a case report. *Pan Afr Med J*. (2021) 40:153. doi: 10.11604/pamj.2021.40.153.31703

8. Imzil A, Bounoua F, Amrani HN, Moubachir H, Serhane H. Tracheobronchomegaly (Mounier-Kuhn syndrome) with CT and bronchoscopic correlation: a case report. *Radiol Case Rep*. (2022) 17:3611–5. doi: 10.1016/j.radcr.2022.06.077

9. Krustins E. Mounier-Kuhn syndrome: a systematic analysis of 128 cases published within last 25 years. *Clin Respiratory J*. (2014) 10:3–10. doi: 10.1111/crj.12192

10. Gouder C, Bilocca D, Fsadni P, Montefort S. A delayed diagnosis of Mounier-Kuhn syndrome. *BMJ Case Rep*. (2014) 2014:bcr2014203674. doi: 10.1136/bcr-2014-203674

11. Satia I, Dua B, Singh N, Killian K, O'Byrne PM. Tracheobronchomegaly, cough and recurrent chest infection: Mounier-Kuhn syndrome. *ERJ Open Res*. (2020) 6:00138. doi: 10.1183/23120541.00138-2020

12. O'Bryan CJ, Espinosa R, Chittivelu S, Wrenn V. Recurrent lower respiratory tract infections due to Mounier-Kuhn syndrome. *Cureus*. (2021) 13:e15437. doi: 10.7759/cureus.15437

13. Shin MS, Jackson RM, Ho KJ. (1988) Tracheobronchomegaly (Mounier-kuhn syndrome): CT diagnosis. AJR Am J Roentgenol *150*(777–779), doi: 10.2214/ajr.150.4.777

14. Liang C, Zhang L, Yu J, Miao C. Complicated airway management because of multiple tracheal diverticula in a patient with Mounier–Kuhn syndrome. *Anesthesiology*. (2024) 140:291–2. doi: 10.1097/aln.0000000000004813

15. Chandran A, Sagar P, Bhalla AS, Kumar R. Mounier-Kuhn syndrome. *BMJ Case Rep*. (2020) 14:e239876. doi: 10.1136/bcr-2020-239876

16. Sullivan S. An unusual cause of dysphagia. *Dysphagia*. (2016) 31:717–8. doi: 10.1007/s00455-016-9706-x

17. Babiker S, Hajalamin M. An atypical encounter: Mounir-Kuhn syndrome and aspergilloma coexistence: a case report. *Radiol Case Rep*. (2024) 19:3962–5. doi: 10.1016/j.radcr.2024.06.001

18. Mitterbauer A, Hoetzenecker K, Birner P, Mildner M, Prosch H, Streubel B, et al. Clinical-radiological, histological and genetic analyses in a lung transplant recipient with Mounier–Kuhn syndrome and end-stage chronic obstructive pulmonary disease. *Clin Respir J*. (2014) 9:375–9. doi: 10.1111/crj.12139

19. Lee DH, Yoon TM, Lee JK, Lim SC. Tracheomegaly secondary to tracheotomy tube cuff in amyotrophic lateral sclerosis. *Medicine*. (2015) 94:e1763. doi: 10.1097/md.0000000000001763

20. Damian LO, Manole S, Pamfil CAM, Rogojan L, Rednic S, Maniu AA, et al. Tracheal enlargement or Mounier-Kuhn syndrome in giant cell arteritis: a possible causal association with therapeutic implications. *Romanian J Morphol Embryol*. (2018) 59:595–9.

21. Uddin AK, Mansfield DR, Farmer MW, Lau KK. Primary tracheobronchial amyloidosis associated with tracheobronchomegaly evaluated by novel four-dimensional functional CT. *Respirol Case Rep*. (2015) 3:151–4. doi: 10.1002/rcr2.134

22. Geng Y, Zhou J, Liu Z. Tracheobronchomegaly in intubated ventilation of ARDS. *Arch Bronconeumol*. (2018) 54:99. doi: 10.1016/j.arbres.2017.05.019

23. Suliman AM, Alamin MA, Hamza MM. Tracheobronchomegaly (Mounier-Kuhn syndrome) and bronchiectasis as rare manifestations of Homocystinuria. *Respir Med Case Rep*. (2023) 42:101808. doi: 10.1016/j.rmcr.2023.101808

24. Harper S, Robinson M, Manning G, Jones A, Hobson J, Shelton CL. Management of tracheostomy-related tracheomegaly in a patient with COVID-19 pneumonitis. *Anaesthesia Rep*. (2020) 8:159–62. doi: 10.1002/anr3.12076

25. Jafari R, Cegolon L, Dehghanpoor F, Javanbakht M, Izadi M, Saadat SH, et al. Early manifestation of ARDS in COVID-19 infection in a 51- year-old man affected by Mounier-Kuhn syndrome. *Heart Lung*. (2020) 49:855–7. doi: 10.1016/j.hrtlng.2020.05.005

26. Choudhury S, Chohan A, Taweesedt PT, Dadhwal R, Vakil A. Coronavirus disease 2019-induced Tracheomegaly: a case report. *Cureus*. (2022) 14:e23810. doi: 10.7759/cureus.23810

27. Awad MT, Iftikhar S, Spetz SL, Kattan A, Banifadel M, Arndt K, et al. Tracheobronchial dilation (Mounier–Kuhn-like syndrome) secondary to fluoroquinolones. *Am J Ther*. (2020) 29:e248–50. doi: 10.1097/MJT.0000000000001215

28. Cheon B, Lee JH, Kim JH, Hwang SM. Airway management of a patient with Mounier-Kuhn syndrome during general anesthesia, a case report. *Anesthesia Pain Med*. (2024) 19:156–60. doi: 10.17085/apm.23172

29. Chuang C-C, Lee C-C, Lin B-S, Chen J-Y. Anesthesia for a patient with unexpected giant tracheobronchomegaly. *Tzu Chi Med J*. (2017) 29:59–61. doi: 10.4103/tcmj.tcmj_1_17

30. Li ZH, Kong L-X, Zhu S, Hu Y, Gao S. Tracheobronchomegaly associated with tracheobronchopathia osteochondroplastica: a case report. *Front Med*. (2024) 11:1540232. doi: 10.3389/fmed.2024.1444995

31. Rjimati M, Serraj M, Elbiaze M, Benjelloun MC, Amara B. Mounier-Kuhn syndrome (Tracheobronchomegaly): radiological diagnosis. *Radiol Case Rep*. (2021) 16:2546–50. doi: 10.1016/j.radcr.2021.06.021

frontiers | Frontiers in Medicine

TYPE Case Report
PUBLISHED 29 April 2025
DOI 10.3389/fmed.2025.1483405

OPEN ACCESS

EDITED BY
Giuseppe Fiorentino,
Colli Hospital, Italy

REVIEWED BY
Gionata Fragomeni,
Magna Græcia University, Italy
Konda Mani Saravanan,
Bharath Institute of Higher Education and Research, India

*CORRESPONDENCE
Darja Smirnova
darja.smirnova@rsu.lv

RECEIVED 19 August 2024
ACCEPTED 14 April 2025
PUBLISHED 29 April 2025

CITATION
Smirnova D, Steina E, Klibus M, Prozorovskis E, Strike E and Sabelnikovs O (2025) Case Report: VV-ECMO as a bridge to recovery from ACE inhibitor induced post-obstructive negative pressure pulmonary edema.
Front. Med. 12:1483405.
doi: 10.3389/fmed.2025.1483405

Case Report: VV-ECMO as a bridge to recovery from ACE inhibitor induced post-obstructive negative pressure pulmonary edema

Darja Smirnova[1,2]*, Eva Steina[1], Mara Klibus[1,2], Edgars Prozorovskis[3,4], Eva Strike[4] and Olegs Sabelnikovs[1,2]

[1]Department of Anesthesiology and Intensive Care, Pauls Stradiņš Clinical University Hospital, Riga, Latvia, [2]Department of Anesthesiology, Intensive Care and Clinical Simulations, Riga Stradiņš University, Riga, Latvia, [3]Extracorporeal Organ Support Center, Pauls Stradiņš Clinical University Hospital, Riga, Latvia, [4]Department of Cardiac Surgery Anesthesia and Intensive Care, Pauls Stradiņš Clinical University Hospital, Riga, Latvia

The indications for extracorporeal membrane oxygenation (ECMO) are becoming increasingly widespread nowadays. This case report describes the unique presentation of an adult patient with a combination of two rare complications: life-threatening angioedema caused by angiotensin-converting enzyme inhibitors (ACEi) and subsequent post-obstructive negative pressure pulmonary edema (NPPE). In this case, worsening angioedema that was unresponsive to medication led to severe airway obstruction and near-fatal acute respiratory syndrome due to NPPE. The worsening clinical course required a multidisciplinary approach and immediate initiation of extracorporeal membrane oxygenation (VV-ECMO). The literature reports that most NPPE cases resolve with oxygenation. However, in our case, the NPPE was refractory to mechanical ventilatory support, and we had to initiate VV-ECMO to prevent the patient from going into cardiac arrest due to severe hypoxia. This case underscores the critical role of VV-ECMO as a bridge to recovery from severe NPPE. It also highlights the need to raise clinicians' awareness of the potential life-threatening side effects of the commonly used antihypertensive drug perindopril.

KEYWORDS

case report, angiotensin-converting enzyme inhibitors, angioedema, negative pressure pulmonary edema, venovenous extracorporeal membrane oxygenation

Introduction

ACE inhibitors (ACEi) are the first-line treatment for hypertension in adults according to World Health Organization (WHO) recommendations (1) and are among the most commonly prescribed antihypertensive drugs in general practice (2). Although rare (between 0.1 and 0.7% of patients taking the drug) (3), the occurrence of angioedema is a severe side effect caused by a reduction in bradykinin degradation following ACEi administration (4, 5). Mild cases can be successfully treated with the oxygen supply, severe cases usually require short term invasive mechanical ventilation (6, 7).

Negative pressure pulmonary edema or post-obstructive non-cardiac pulmonary edema is a rare complication with an estimated incidence rate of between 0.1 and 12% (8). It usually occurs after a sudden, severe obstruction of the upper airway, e.g., asphyxia, laryngospasm after extubation or endotracheal tube obstruction (8–10). Although ACEi-induced angioedema could potentially trigger NPPE, no documented cases have been

reported in the literature to date. In most cases, NPPE resolves with positive pressure ventilation and adequate diuresis. In severe cases, acute respiratory distress syndrome (ARDS) may occur, necessitating invasive mechanical ventilation (8). To date, however, only a few cases requiring extracorporeal membrane oxygenation (ECMO) have been reported (11–13). In the case reports discussed, laryngospasm was the primary trigger for NPPE — occurring post-extubation in two cases [Augustin et al. (11) and Matsumura et al. (12)] and following direct laryngoscopy in a patient with laryngeal papillomatosis [Grant et al. (13)]. According to the ELSO International Registry Report 2022 (14), the use of extracorporeal membrane oxygenation has steadily increased, with indications expanding over time. Considering that NPPE can lead to prolonged and severe ARDS, the application of ECMO in severe, near-fatal NPPE cases is both reasonable and expected.

In this case report, we aimed to present a unique case of severe NPPE following ACE inhibitor use, which was successfully treated with veno-venous ECMO. This case highlights the need for early recognition, prompt airway management and the use of advanced supportive therapies in managing such critical complications.

Case description

A 72-year-old obese male (173 cm; 110 kg; body mass index, BMI 36.8) presented to the emergency department of Pauls Stradiņš Clinical University Hospital in early Saturday morning. He had a two-hour history of sore throat, bilateral swollen tongue, dysphonia and difficulty swallowing after waking up from sleep due to these complaints. Notably, he had no associated skin rashes or pruritus. Inspiratory stridor, wheezing and rhonchi were absent too. He denied any invasive procedure in the last few months that could be a trigger for angioedema, and there are no known similar cases in his family history.

The patient had a 10-year history of hypertension and diabetes mellitus, managed with daily antihypertensive medication (perindopril for 2 years without recent changes) and metformin. Over the past 18 months, he had experienced three similar episodes of tongue and lip swelling. Two resolved with an antihistamine (*Chloropyramini hydrocloridum*) taken perorally at home, while one required oxygen supply and short-term admission to the secondary health care hospital's emergency department. All previous episodes were attributed to food allergies and the patient was discharged with the recommendation to consult an allergist and eliminate the allergic product from his daily diet.

He received oxygen therapy via a face mask at 4 L/min, along with glucocorticoids (dexamethasone 12 mg) and intramuscular epinephrine as initial treatment prior to hospitalization. However, these interventions did not lead to clinical improvement and the patient was transferred to hospital. On admission to the emergency department, his vital signs were stable, and all laboratory parameters revealed unremarkable findings. His laboratory analyzes showed normal values for C4, C1 inhibitor protein (C1-INH protein) and C1-INH functions. Given the history of recurrent episodes of angioedema, the absence of laboratory findings suggestive of hereditary angioedema, and the temporal association with ACE inhibitor use, the clinical diagnosis of perindopril-induced angioedema was made.

Over the next 6 h in the emergency department, the patient's respiratory status deteriorated and oxygen therapy was increased to a high-flow mask at 10 L/min. Additional treatment with high-dose glucocorticoids (Solumedrol 500 mg), antihistamines (*Chloropyramini hydrochloridum* 20 mg), intravenous epinephrine, tranexamic acid (1 g), and two units of fresh frozen plasma was administered as part of the management strategy for severe ACEi-induced angioedema. However, these interventions did not lead to any improvement. Secondary physical examination revealed marked swelling of the tongue and increasing shortness of breath. As the angioedema continued to worsen despite medical treatment, the decision was made to proceed with invasive mechanical ventilation. However, due to difficult intubation, an acute tracheostomy was performed. The patient was then transferred to the intensive care unit (ICU) for further management and mechanical ventilation. Despite these interventions, he remained dependent on a high oxygen concentration to maintain adequate oxygenation, requiring an FiO2 of 0.7.

On the second day, despite maximum ventilatory support, the patient developed progressive hypoxia. On physical examination, his face and neck were cyanotic, and oxygen saturation was 80–82% with a 100% fraction of inspired oxygen (FiO2). The patient was agitated, and to optimize patient-ventilator synchronization, continuous infusions of fentanyl, midazolam, propofol, and cisatracurium were initiated. Optimal diuresis (>1.1 mL/kg/h) achieved with 80 mg furosemide and lung protective ventilation was initiated without any improvement in respiratory status. Despite maximal medical optimization, hypoxia continues to worsen with P/F ratio values ranging between 39 and 43 and SpO2 from 63 to 72% at 100% FiO2 over the next 6 h.

The portable chest X-ray showed bilateral lung field opacification (Figure 1A). The level of B-type natriuretic peptide (BNP) was 112 pg./mL. Transthoracic echocardiography was unremarkable, showing only a slightly enlarged left atrium with a preserved ejection fraction of 55%, making cardiogenic pulmonary edema an unlikely cause of respiratory deterioration. A computed tomography scan of the chest performed on admission to the intensive care unit revealed no evidence of aspiration, secondary pulmonary infection or associated complications. The patient showed no signs of inflammation, as inflammatory markers were not elevated (C-reactive protein 23.59 mg/L, interleukin-6 0 pg./mL, procalcitonin 0.13 ng/mL) and microbiologic cultures were sterile. In addition, bronchoscopy revealed the presence of pink foamy fluid. These findings, in the context of difficult airway management, strongly suggested NPPE as the primary contributor to the development of ARDS.

Despite the treatment applied, including optimal diuresis, synchronization with mechanical ventilation and maximal oxygen support, the patient remained in severe hypoxia (P/F ratio as low as 39 at FiO2 100%), leading to hemodynamic instability and bradycardic episodes. For this reason, the ECMO team specialists were consulted. The decision to initiate veno-venous ECMO for respiratory support was made based on the patient's Respiratory Survival Prediction Score (RESP) of zero, risk class III and a predicted in-hospital survival rate of 57%. Due to the patient's constitution, the right femoral vein was cannulated with a 29 Fr cannula for venous access and the right internal jugular vein was cannulated with a 21 Fr cannula for venous return, followed by a heparin bolus of 10,000 units. ECMO was initiated via MAQUET Cardiohelp System. As the patient was hypoxic and normocapnic, the initial ECMO pump flow was 3 L/min at 2200

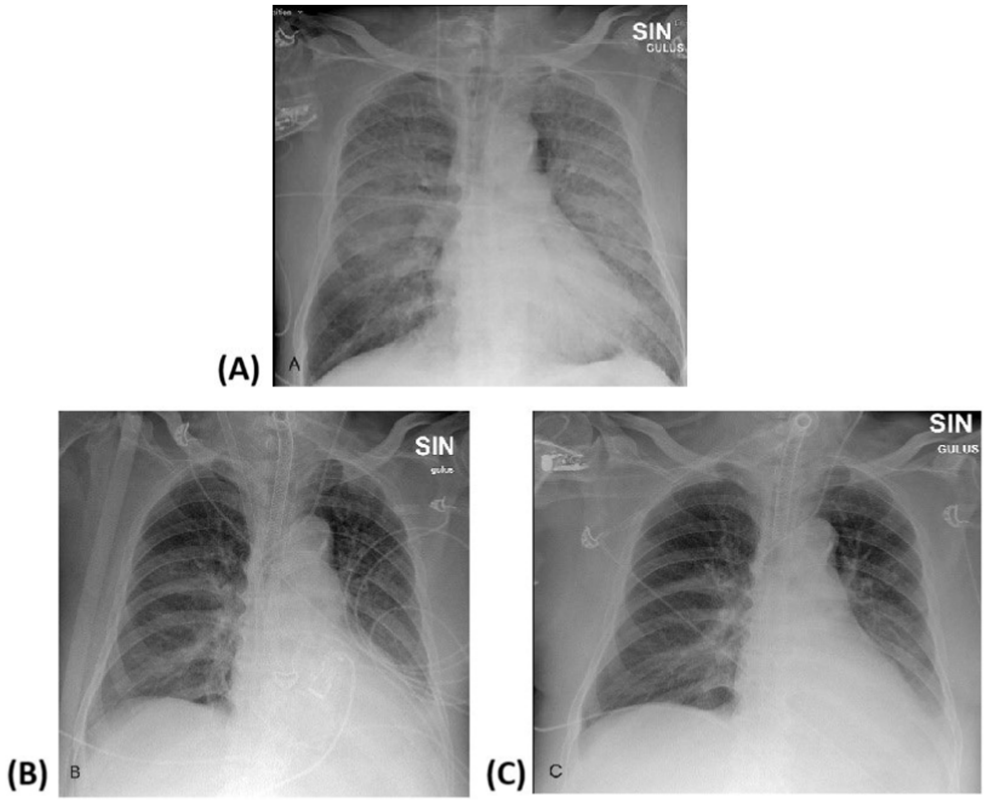

FIGURE 1
Portable chest X-rays. **(A)** X-ray taken on ICU day 2 (prior VV-ECMO cannulation). This radiograph demonstrates acute lung failure, with almost complete opacification of both lung fields. The bronchovascular pattern is accentuated, with uneven alveolar infiltrative changes bilaterally, more pronounced on the left side, suggesting pulmonary edema. The lung roots are homogenized, and the diaphragmatic domes are visible. There is no significant volume of contents in the pleural spaces. The heart and aorta shadows appear of normal size and configuration. **(B)** Day 8, before decannulation of VV-ECMO: The ECMO cannula is visible in the right internal jugular vein, with its tip reaching the distal third of the superior vena cava. Slight bronchovascular infiltrative changes are seen in the perihilar regions. Bilateral pulmonary ventilation has further improved, and the volume and intensity of atypical infiltrative changes have further decreased. **(C)** Day 9, after VV-ECMO decannulation: Compared to the previous examination, there is a significant improvement in bilateral lung ventilation, with a decrease in both the volume and intensity of atypical infiltrative changes.

RPMS and the «sweep gas» was 3 L/min with a FiO2 of 100%. The ventilator settings were adjusted to lung-protective ventilation (FiO2 40%, PEEP 10 cm H2O, RR 10, tidal volume (Tv) 450 mL) throughout the ECMO period. Immediately after ECMO support was initiated, serial arterial blood gas (ABG) analyzes showed a rapid improvement in the patient's oxygenation (Table 1, Figure 2) and vital signs. To maintain ECMO support, heparin anticoagulation was administered, targeting an aPTT goal of 40–60 s. The circuit was set to a flow of 3.5–4.0 L/min with a FiO2 of 100%, RPMs of 2,200–2,400, and a sweep gas flow of 3–4 L/min, adjusted according to the ABG analysis.

Over the next 6 days, the chest x-ray and hypoxia (Figures 1B,C) gradually improved and VV-ECMO was discontinued on day eight after admission to the hospital. He was further weaned from mechanical ventilation over the next 10 days and transferred to the ward on day 18 without the need for oxygen therapy. He was discharged home on day 23 after rehabilitation (Table 2) with a recommendation to consult a geneticist to screen for known mutations underlying a possible HAE-nC1-INH. Three months after discharge from our hospital, the patient stated in a telephone interview that he had resumed his daily life without sequelae. However, the patient had not yet undergone genetic counseling by the time of the follow-up examination, which was justified by a lack of necessity. After discharge, treatment with the angiotensin II receptor blocker telmisartan was initiated, with the dose being gradually increased to 80 mg once daily. No allergic reactions were observed in the following 3 months and hypertension remained well controlled.

On the first day, there was a small amount of bleeding from the cannulation site of the venous ECMO access, but this was resolved by suturing and did not require transfusion of blood components. No further complications related to ECMO occurred during the treatment period.

Discussion

The clinical course of the presented case is highly unusual and includes two rare but severe complications: angioedema induced by an ACE inhibitor perindopril and subsequent post-obstructive negative pressure pulmonary edema, successfully managed with VV-ECMO.

Angiotensin-converting enzyme inhibitors, such as perindopril, are widely prescribed for managing hypertension and other cardiovascular diseases, yet they can cause severe side effects (4, 5). Although angioedema is a rare side effect of ACE inhibitors and affects

TABLE 1 Dynamics of arterial blood gas analysis during major clinical events.

	pH	pO2 (mmHg)	pCO2 (mmHg)	Fi02	P/F ratio (mmHg)	Sp02 (%)
On admission to emergency department (Day 1)	7.32	117	36	0.4	292	100
Prior to mechanical ventilation (Day 1)	7.18	62	56	0.65	95	84
In the intensive care unit (Day 1)	7.33	81	36	0.7	115	97
Prior to VV-ECMO cannulation (Day 2)	7.39	39	36	1.00	39	48
Immediately post VV-ECMO cannulation (Day 2)	7.35	74	39	0.4	185	95
Prior de-cannulation (Day 8)	7.46	87	36	0.6	145	97
Post de-cannulation (Day 8)	7.42	148	39	0.6	246	99

The FiO_2 values shown in the table are taken from the settings of the invasive mechanical ventilators. The values presented in Table 1 highlight key clinical turning points, including marked deterioration prior to mechanical ventilation, severe hypoxemia before VV-ECMO cannulation, and a subsequent rapid improvement in respiratory parameters during and after VV-ECMO therapy—supporting its role as an effective bridge to recovery.

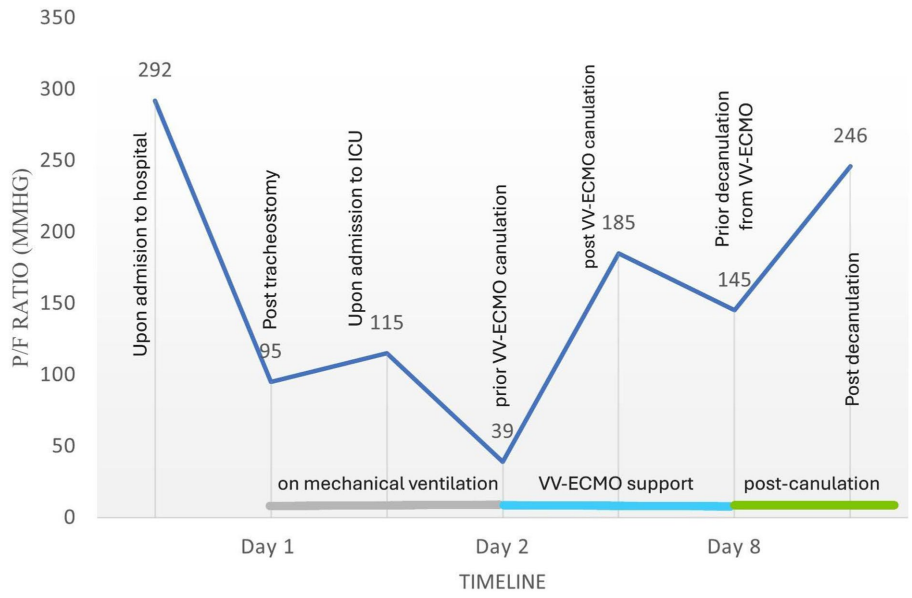

FIGURE 2
Flow chart illustrating the course of the PaO_2/FiO_2 (P/F) ratio in relation to key clinical events.

only a small percentage of patients (3), its clinical significance remains high due to the widespread use of ACEi as a commonly prescribed medication.

The pathophysiology of the development of all forms of angioedema is complex and can be defined as either hereditary (bradykinin-mediated) or acquired (histamine-or bradykinin-mediated angioedema). ACEi-induced angioedema is an acquired bradykinin-mediated angioedema and is associated with an accumulation of bradykinin (4, 5). As a vasoactive peptide, bradykinin increases vasodilation and alters vascular permeability, which can lead to life-threatening airway obstruction, as seen in our patient. Typical laboratory findings of ACEi-induced angioedema include normal levels of C1-INH function, C1-INH protein and C4, as in our case. This laboratory finding helps to differentiate acquired bradykinin-mediated angioedema from hereditary angioedema (HEA) type I or type II, which is caused by a mutation in the SERPING1 gene encoding C1-INH and therefore will presented with low levels of C1-INH and C4 (15, 16). However, it does not help to exclude the very rare disease as HEA type III or HEA with normal values of C1-INH (HAE-nC1-INH) (16–18).

TABLE 2 Timeline of relevant clinical events.

Day	Events
1	• Admission to the emergency department (early morning) • Treatment: Methylprednisolone, Epinephrine, antihistamines, fresh frozen plasma transfusion, tranexamic acid. • Oxygen supply with low concentration face mask
	• Worsening angioedema unresponsive to medication • Acute tracheostomy, transfer to the intensive care unit (early afternoon). • Lung protective mechanical ventilation (tidal volume of 6 mL/kg, a respiratory rate of 10 to 16 breaths per minute, a positive end-expiratory pressure (PEEP) of 8 cmH2O and a plateau pressure of 26 cmH2O)
2	• X-ray with opacification of the bilateral lung fields • Sedation, loop diuretics for optimal diuresis • VV ECMO cannulation (late afternoon, 42 h after admission to hospital)
3–8	• Improvement of the respiratory status • Decannulation of VV-ECMO on day 8
18	• Oxygen therapy no longer required • Transfer to the pulmonary department
23	• Discharge to home

An overview of the main clinical events is provided, with the table also listing the main interventions during the course of admission to the intensive care unit and throughout hospitalization.

Therefore, the WAO/EAACI international guideline for the management of hereditary angioedema recommends that patients suspected of having HAE who have normal C1-INH levels and function should be screened for known mutations underlying HAE-nC1-INH (15).

Distinguishing between different forms of angioedema is always challenging but crucial as the underlying pathophysiology influences clinical presentation and treatment recommendations. Bradykinin-mediated angioedema tends to be more severe, longer lasting and often results in upper airway swelling without urticaria, compared to histamine-mediated or allergic angioedema (7, 19, 20). According to the literature, the most important part of the treatment protocol for ACEi angioedema involves immediate cessation of the trigger (in our case perindopril) (4–6, 21). However, antihistamines, corticosteroids, and epinephrine are also prescribed to counteract vasodilation and increased vascular permeability (19). Although these medications do not directly affect bradykinin levels, they are commonly administered for ACEi-induced angioedema. This practice can be attributed to the challenges in establishing a definitive diagnosis and the urgency of initiating treatment. From a clinical practice perspective, the absence of a specific laboratory marker for the rapid diagnosis of angioedema necessitates a reliance on clinical factors. A lack of response to antihistamines, a history of ACE inhibitor use and the rapid onset of upper airway swelling may be helpful in identifying ACEi-induced angioedema (21).

In recent years, several new drugs have been developed for the treatment of hereditary angioedema. Some have also been investigated for ACEi-induced angioedema, based on the suspected common pathophysiological mechanism — excessive accumulation of bradykinin. Although specific therapy with Icatibant, a bradykinin B2 receptor antagonist currently approved for the treatment of HAE (15), has shown inconsistent results in the treatment of ACEi-induced angioedema, as evidenced by a recent meta-analysis of randomized controlled trials (20, 22). In some cases, an additional treatment strategy - tranexamic acid, fresh-frozen plasma transfusions and C1-esterase inhibitor concentrate - has shown beneficial results, also well-designed trials are lacking (18, 23–25).

The administration of Icatibant or C1-esterase inhibitor concentrate was not feasible in the clinical case we reported. The event occurred in the early morning hours of a weekend when the medication was not available in the emergency department. Current evidence suggests that Icatibant is most effective when administered immediately, as delayed administration reduces its efficacy (26–28). In addition, there is no high-quality randomized trial confirming the efficacy of Icatibant, and due to its high cost, this therapy is not included in the local treatment protocol for ACEi-induced angioedema. These factors further limited the options for specific treatment as the condition progressed.

In the reported case, the angioedema was refractory to treatment and led to severe airway obstruction requiring emergency tracheostomy. The patient's condition continued to deteriorate, leading to the development of severe ARDS with a near-fatal P/F ratio of 39, indicating critical hypoxemia and extreme respiratory failure.

We identified negative pressure pulmonary edema (NPPE) as the main cause of ARDS. Negative pressure pulmonary edema is a complication resulting from acute or chronic upper airway obstruction and often presents challenges to clinicians in recognition and diagnosis. NPPE occurs when significant upper airway obstruction generates highly negative intrathoracic pressure leading to pulmonary edema. The clinical manifestations of negative pressure pulmonary edema include dyspnea, tachypnea, cyanosis, and the production of a profuse pink foamy sputum in combination with hypoxia and hypercapnia as a result of underlying respiratory dysfunction and impaired gas exchange. All these clinical features were evident in our case.

However, consideration of possible differential diagnoses is crucial for appropriate management. One of the differential diagnoses is cardiogenic pulmonary edema, which can present with similar symptoms (29). In our case, however, the echocardiographic examination revealed no evidence of systolic or diastolic dysfunction of the left ventricle, no significant valvular abnormalities and normal left atrial pressure. In addition, the level of BNP was slightly increased. Based on these findings, a cardiogenic etiology was effectively ruled out. The second differential diagnosis is infectious pneumonia, including aspiration pneumonia, which is a relevant consideration given the patient's difficult airway. Although aspiration was a potential concern, the absence of characteristic CT findings, normal inflammatory markers, and sterile respiratory cultures made an infectious process unlikely (30). Another potential differential diagnosis in our case is aspiration pneumonitis, especially considering the difficult intubation. In contrast to aspiration pneumonia, aspiration pneumonitis is caused by sterile gastric contents causing chemical lung injury. Clinically, it presents with acute hypoxemia, tachycardia, fever and bilateral infiltrates, often following an aspiration event, typically in unconscious patients (30, 31). In our case, no massive aspiration was detected during bronchoscopy after intubation. However, since even minimal gastric content can cause lung injury and the clinical and radiologic features overlap with NPPE, we cannot

entirely exclude aspiration pneumonitis as a contributory cause for the development of severe ARDS. Nevertheless, given the clinical course and supportive diagnostic findings, NPPE remained the most plausible etiology of ARDS in our clinical case.

Although most NPPE cases respond well to conservative treatments like oxygen therapy and mechanical ventilation (9), our patient's NPPE was refractory to mechanical ventilation, leading to severe hypoxemia and the imminent risk of cardiac arrest associated with near fatal bradycardia. This rare and severe presentation necessitated the initiation of veno-venous ECMO. Only some cases of severe NPPE were managed with ECMO, according to the previous literature (11–13). However, none of them were caused by ACEi angioedema. In this case, VV-ECMO provided the essential respiratory support needed to maintain adequate oxygenation and allowed the lungs to rest and recover, demonstrating its critical role in managing severe respiratory failure unresponsive to conventional treatments.

The management of this case required a multidisciplinary approach with the involvement of intensivists and ECMO specialists. Both the timely recognition of the severity of the clinical course and the decision to initiate VV-ECMO were crucial for the stabilization of the patient. This case demonstrates the importance of a well-coordinated ECMO team within the hospital that is able to rapidly deploy this life-saving technology. The expertise and preparedness of such a team can significantly improve outcomes for patients with severe, refractory respiratory failure.

Effective data transmission and availability among all healthcare providers involved in a patient's care is critical to the management of severe clinical conditions. In this case, the patient had previously experienced similar symptoms three times, which recurred 6 months after initiating perindopril. However, due to inadequate communication, this information did not reach the patient's primary care physician and ACEi was not discontinued. Strategies aimed at improving physician and patient education regarding ACE inhibitor cessation after primary angioedema, along with proper documentation of adverse drug reactions in medical records are essential. These measures can help prevent severe complications and reduce the need for critical interventions such as VV-ECMO.

The management of hypertension in patients with a history of ACEi induced angioedema requires careful consideration. The main step is to discontinue the ACEi and switch to an alternative agent. Angiotensin II receptor blockers (ARBs) are often recommended due to their significantly lower risk of angioedema compared to ACEi. However, ARBs should be started at a low dose and titrated gradually under close monitoring, as cross-reactivity between ACEi and ARBs is possible. If ARBs are not appropriate or there is a high risk of recurrence, other antihypertensive options such as calcium channel blockers or thiazide diuretics should be considered (3, 32).

In summary, this case highlights the importance of early recognition and aggressive management of ACEi-induced angioedema and underscores the potential of ACE inhibitors to cause life-threatening complications. Increased awareness of the severe side effects of commonly prescribed medications such as perindopril can lead to better patient outcomes through prompt and appropriate intervention. In addition, awareness of NPPE as a potential consequence of severe airway obstruction is critical. While NPPE typically responds to conservative measures, this case demonstrates that refractory cases may require advanced interventions such as VV-ECMO.

Conclusion

We present the case of an obese middle-aged man with a unique clinical course of negative pressure pulmonary edema due to severe upper airway obstruction caused by perindopril angioedema. This case highlights the need for data sharing between healthcare providers involved in the patient's treatment to improve early detection of potential complications and qualitative management. Raising awareness of the potential side effects of commonly prescribed medications such as perindopril and the potential complications of angioedema can improve patient outcomes through early recognition and appropriate intervention. This case also emphasizes the benefits of timely initiation of veno-venous ECMO for respiratory support in severe refractory NPPE cases such as this one. This broadens the indications for extracorporeal membrane oxygenation and emphasizes the need for a well-coordinated ECMO team within the hospital.

Data availability statement

The original contributions presented in the study are included in the article/supplementary material, further inquiries can be directed to the corresponding author.

Ethics statement

Written informed consent was obtained from the individual(s) and/or the individual's next of kin/legal guardians for the publication of any potentially identifiable images or data included in this article.

Author contributions

DS: Conceptualization, Data curation, Writing – original draft, Writing – review & editing. ESte: Data curation, Writing – review & editing. MK: Data curation, Writing – review & editing. EP: Writing – review & editing. EStr: Supervision, Writing – review & editing. OS: Supervision, Writing – review & editing.

Funding

The author(s) declare that financial support was received for the research and/or publication of this article. This work was supported by Riga Stradins University, Department of Anesthesiology, Intensive Care and Clinical simulations.

Conflict of interest

The authors declare that the research was conducted in the absence of any commercial or financial relationships that could be construed as a potential conflict of interest.

Publisher's note

References

1. World Health Organization. Guidelines for the pharmacological treatment of hypertension in adults. Geneva: World Health Organization (2021).

2. Mancia G, Kreutz R, Brunström M, Burnier M, Grassi G, Januszewicz A, et al. 2023 ESH guidelines for the management of arterial hypertension: the task force for the management of arterial hypertension of the European Society of Hypertension: endorsed by the International Society of Hypertension (ISH) and the European renal association (ERA). *J Hypertens*. (2023) 41:1874–2071. doi: 10.1097/HJH.0000000000003480

3. Rubin S, Tomaszewski M. Prediction and prevention of ACE-inhibitor-induced angioedema—an unmet clinical need in management of hypertension. *Hypertens Res*. (2024) 47:257–60. doi: 10.1038/s41440-023-01491-9

4. Montinaro V, Cicardi M. ACE inhibitor-mediated angioedema. *Int Immunopharmacol*. (2020) 78:106081. doi: 10.1016/j.intimp.2019.106081

5. Wilkerson RG, Patel BM, Nappe TM, Holguin D. Angiotensin-converting enzyme inhibitor–induced angioedema. *Emerg. Med. Clin. N. Am*. (2022) 40:79–98. doi: 10.1016/j.emc.2021.09.004

6. Al-Khudari S, Loochtan MJ, Peterson E, Yaremchuk KL. Management of angiotensin-converting enzyme inhibitor–induced angioedema. *Laryngoscope*. (2011) 121:2327–34. doi: 10.1002/lary.22349

7. Banerji A, Clark S, Blanda M, LoVecchio F, Camargo CA Jr. Multicenter study of patients with angiotensin-converting enzyme inhibitor-induced angioedema who present to the emergency department. *Ann Allergy Asthma Immunol*. (2008) 100:327–32. doi: 10.1016/S1081-1206(10)60594-7

8. Ma J, Liu T, Wang Q, Xia X, Guo Z, Feng Q, et al. Negative pressure pulmonary edema (review). *Exp Ther Med*. (2023) 26:455. doi: 10.3892/etm.2023.12154

9. Lang SA, Duncan PG, Shephard DA, Ha HC. Pulmonary oedema associated with airway obstruction. *Can J Anaesth*. (1990) 37:210–8. doi: 10.1007/BF03005472

10. Bhattacharya M, Kallet RH, Ware LB, Matthay MA. Negative-pressure pulmonary edema. *Chest*. (2016) 150:927–33. doi: 10.1016/j.chest.2016.03.043

11. Augustin KJ, Creel-Bulos CM, Budhrani GF, Miller CF, Fiza B. Extracorporeal membrane oxygenation as acute rescue therapy for negative pressure pulmonary edema in the post anesthesia care unit (case report). *Clin Case Rep*. (2023) 11:e7606. doi: 10.1002/ccr3.7606

12. Matsumura K, Toyoda Y, Matsumoto S, Funabiki T. Near-fatal negative pressure pulmonary oedema successfully treated with venovenous extracorporeal membrane oxygenation performed in the hybrid emergency room (case report). *BMJ Case Rep*. (2020) 13:e234651. doi: 10.1136/bcr-2020-234651

13. Grant BM, Ferguson DH, Aziz JE, Aziz S. Successful use of VV ECMO in managing negative pressure pulmonary edema. *J Card Surg*. (2020) 35:930–3. doi: 10.1111/jocs.14472

14. Tonna JE, Boonstra PS, MacLaren G, Paden M, Brodie D, Anders M, et al. Extracorporeal life support organization registry international report 2022: 100,000 survivors. *ASAIO J*. (2024) 70:131–43. doi: 10.1097/MAT.0000000000002128

15. Maurer M, Magerl M, Betschel S, Aberer W, Ansotegui IJ, Aygören-Pürsün E, et al. The international WAO/EAACI guideline for the management of hereditary angioedema—the 2021 revision and update. *Allergy*. (2022) 77:1961–90. doi: 10.1111/all.15214

16. Kaplan AP, Greaves MW. Angioedema. *J Am Acad Dermatol*. (2005) 53:373–88. doi: 10.1016/j.jaad.2004.09.032

17. Santacroce R, D'Andrea G, Maffione AB, Margaglione M, d'Apolito M. The genetics of hereditary angioedema: a review. *J Clin Med*. (2021) 10:2023. doi: 10.3390/jcm10092023

18. Terreehorst I, Reitsma S, Cohn DM. Current treatment of angioedema induced by ACE inhibitors. *Curr Treat Options Allergy*. (2019) 6:18–26. doi: 10.1007/s40521-019-0203-y

19. Weisman DS, Arnouk N, Asghar MB, Qureshi MR, Kumar A, Desale S, et al. ACE inhibitor angioedema: characterization and treatment versus non-ACE angioedema in acute hospitalized patients. *J Community Hosp Intern Med Perspect*. (2020) 10:16–8. doi: 10.1080/20009666.2020.1711641

20. Kostis WJ, Shetty M, Chowdhury YS, Kostis JB. ACE inhibitor-induced angioedema: a review. *Curr Hypertens Rep*. (2018) 20:55. doi: 10.1007/s11906-018-0859-x

21. Rosenbaum S, Wilkerson RG, Winters ME, Vilke GM, Wu MYC. Clinical practice statement: what is the emergency department management of patients with angioedema secondary to an ACE-inhibitor? *J Emerg Med*. (2021) 61:105–12. doi: 10.1016/j.jemermed.2021.02.038

22. Jeon J, Lee YJ, Lee SY. Effect of icatibant on angiotensin-converting enzyme inhibitor-induced angioedema: a meta-analysis of randomized controlled trials. *J Clin Pharm Ther*. (2019) 44:685–92. doi: 10.1111/jcpt.12997

23. Erickson DL, Coop CA. Angiotensin-converting enzyme inhibitor-associated angioedema treated with C1-esterase inhibitor: a case report and review of the literature. *Allergy Rhinol*. (2016) 7:168–71. doi: 10.2500/ar.2016.7.0166

24. Hasara S, Wilson K, Amatea J, Anderson J. Tranexamic acid for the emergency treatment of angiotensin-converting enzyme inhibitor-induced angioedema. *Cureus*. (2021) 13:e18116. doi: 10.7759/cureus.18116

25. Perza M, Koczirka S, Nomura JT. C1 esterase inhibitor for ACE-inhibitor angioedema: a case series and literature review. *J Emerg Med*. (2020) 58:e121–7. doi: 10.1016/j.jemermed.2019.10.031

26. Bas M, Greve J, Stelter K, Havel M, Strassen U, Rotter N, et al. A randomized trial of icatibant in ACE-inhibitor-induced angioedema. *N Engl J Med*. (2015) 372:418–25. doi: 10.1056/NEJMoa1312524

27. Sinert R, Levy P, Bernstein JA, Body R, Sivilotti MLA, Moellman J, et al. Randomized trial of icatibant for angiotensin-converting enzyme inhibitor-induced upper airway angioedema. *J Allergy Clin Immunol Pract*. (2017) 5:1402–1409.e3. doi: 10.1016/j.jaip.2017.03.003

28. Straka BT, Ramirez CE, Byrd JB, Stone E, Woodard-Grice A, Nian H, et al. Effect of bradykinin receptor antagonism on ACE inhibitor-associated angioedema. *J Allergy Clin Immunol*. (2017) 140:242–248.e2. doi: 10.1016/j.jaci.2016.09.051

29. McDonagh TA, Metra M, Adamo M, Gardner RS, Baumbach A, Böhm M, et al. 2021 ESC guidelines for the diagnosis and treatment of acute and chronic heart failure: developed by the task force for the diagnosis and treatment of acute and chronic heart failure of the European Society of Cardiology (ESC) with the special contribution of the heart failure association (HFA) of the ESC. *Eur Heart J*. (2021) 42:3599–726. doi: 10.1093/eurheartj/ehab368

30. DiBardino DM, Wunderink RG. Aspiration pneumonia: a review of modern trends. *J Crit Care*. (2015) 30:40–8. doi: 10.1016/j.jcrc.2014.07.011

31. Hu X, Lee JS, Pianosi PT, Ryu JH, Limper AH. Aspiration-related pulmonary syndromes. *Chest*. (2015) 147:815–23. doi: 10.1378/chest.14-1049

32. Brown T, Gonzalez J, Monteleone C. Angiotensin-converting enzyme inhibitor–induced angioedema: a review of the literature. *J Clin Hypertens*. (2017) 19:1377–82. doi: 10.1111/jch.13097

frontiers | Frontiers in Medicine

TYPE Case Report
PUBLISHED 07 May 2025
DOI 10.3389/fmed.2025.1467001

OPEN ACCESS

EDITED BY
Uday Kishore,
United Arab Emirates University,
United Arab Emirates

REVIEWED BY
Lautaro De Vedia,
University of Buenos Aires, Argentina
Juan Nahuel Quiroz,
CONICET Centre for Research in Clinical Biochemistry and Immunology (CIBICI), Argentina
Robbie Christian,
Louis Stokes Cleveland VA Medical Center, United States

*CORRESPONDENCE
Guansong Wang
✉ wanggs@tmmu.edu.cn;
✉ wanggs2003@163.com
Daohui Gong
✉ aprilyz@126.com

RECEIVED 26 July 2024
ACCEPTED 14 April 2025
PUBLISHED 07 May 2025

CITATION
Gao Z, Jiang Y, Zhang M, Luo C, Wei Z, Gong D and Wang G (2025) Case Report: Drug-induced pneumonia caused by moxifloxacin and a literature review. *Front. Med.* 12:1467001. doi: 10.3389/fmed.2025.1467001

Case Report: Drug-induced pneumonia caused by moxifloxacin and a literature review

Zhan Gao, Yunqiu Jiang, Mingzhou Zhang, Chenjing Luo, Zhenghua Wei, Daohui Gong* and Guansong Wang*

Department of Pulmonary and Critical Care Medicine, Xinqiao Hospital, Third Military Medical University (Army Medical University), Chongqing, China

Drug-induced pneumonia is a rare and potentially life-threatening adverse drug reaction. Moxifloxacin is a fluoroquinolone antibiotic with broad-spectrum antimicrobial activity. Despite reports of moxifloxacin-related side effects such as interstitial nephritis, recurrent tendinitis, and pseudoallergic reactions, moxifloxacin-induced pneumonia is exceedingly rare. We report the case of a 45-year-old male who developed fever and cough, and progressed to hypersensitivity syndrome related to drug-induced pneumonia following moxifloxacin therapy. Discontinuation of moxifloxacin led to resolution of fever with significant resolution of pulmonary lesions. Comprehensive laboratory investigations ruled out other causes, confirming drug-induced pneumonia due to moxifloxacin. This case report provides typical clinical manifestations and pulmonary imaging changes, as well as an analysis of differential diagnosis of pulmonary lesions and key management strategies. The case and related literature review contribute to enhancing our understanding of moxifloxacin-related pneumonia, with important clinical significance in promptly correcting adverse reactions and improving patient outcomes.

KEYWORDS

moxifloxacin, drug-induced pneumonia, allergic reaction, hypersensitivity syndrome, adverse reactions

Introduction

Drug-induced pneumonia is an iatrogenic condition caused by drugs and their metabolites, leading to pulmonary inflammation through direct cytotoxicity and allergic reactions (1). It primarily affects the interstitial lung tissue and is termed drug-associated interstitial lung disease (DI-ILD). DI-ILD represents a distinct subtype of interstitial pneumonia. Epidemiological studies report an annual incidence of DI-ILD ranging from 4.1 to 12.4 cases per million population, accounting for 3–5% of all interstitial lung disease (ILD) cases (2). Clinical assessment of drug-induced pneumonia is challenging, as it is typically diagnosed through exclusion. Both the incidence of drug-induced pneumonia and the spectrum of causative drugs have evolved temporally. Before 1980, the main causative drugs were anticancer drugs and gold salts. In recent years, there has been an increase in pneumonia cases caused by antibiotics, chemotherapeutic drugs and anti-inflammatory drugs (3). Notably, 6–26% of DI-ILD cases in contemporary studies are associated with antibiotic use (4–9).

Moxifloxacin is a fluoroquinolone antibiotic widely used for respiratory tract infections (10). It exerts antimicrobial effects by inhibiting DNA gyrase in Gram-negative bacteria and topoisomerase IV in Gram-positive bacteria, resulting in DNA cleavage and rapid bactericidal activity (11). Although fluoroquinolones are generally regarded as having a favorable safety

profile, they are associated with a non-negligible incidence of adverse effects. Common adverse reactions to moxifloxacin include QT interval prolongation (12), hepatic and renal dysfunction, mental behavioral abnormalities, gastrointestinal, central nervous system, and skin reactions (13). Rare side effects such as recurrent tendonitis (14), interstitial nephritis (15), and allergic-like reactions, bilateral acute iridocyclitis (16), and cardiotoxicity have also been reported. Despite these known risks, moxifloxacin-induced pneumonia remains scarcely reported. To our knowledge, there are literature reports of pulmonary involvement in DRESS syndrome caused by moxifloxacin, which is considered to be related to allergic reactions.

Herein, we present a rare case of moxifloxacin-triggered pneumonia in a 45-year-old male, alongside a discussion of diagnostic strategies and a review of severe adverse reactions attributed to this agent. Written informed consent was obtained from the patient for publication.

Case presentation

A 45-year-old male patient was admitted with a persistent cough of over 10 days. He had no history of hypertension, diabetes, smoking, or alcohol consumption. The patient experienced paroxysmal coughing for over 10 days after catching a cold, with exacerbated symptoms at night, producing a small amount of sticky white sputum that was difficult to expectorate. He did not present with chills, high fever, purulent sputum, night sweats, chest pain, hemoptysis, or respiratory distress. Hospitalization at the local hospital revealed mild lung infection on chest CT (Figures 1A,B) and no significant abnormalities in the complete blood count and renal and liver function tests. He was then treated with moxifloxacin 400 mg IV daily, however, five days later, he developed fever, with a maximum body temperature of 39.6°C, without apparent chills or shivering. Moxifloxacin was discontinued, and the antibiotic was changed to piperacillin-tazobactam sodium 4.5 g IV q8h. Post-antibiotic treatment, a follow-up chest CT revealed infective lesions in the right upper lobe and bilateral lower lobes that were significantly more extensive than before (Figures 1C,D). The patient came to our hospital for further treatment, upon admission, laboratory investigations showed a C-reactive protein (CRP) of 82.9 mg/L and WBC count of 4.5×10^9/L, with a neutrophilic count of 2.4×10^9/L. He was once again administered moxifloxacin 400 mg IV daily for the infection and underwent a bronchoscopy examination 3 days later, yielding no significant findings. Bronchopulmonary biopsy was performed on the posterior segment of the upper right lobe, and pathology revealed chronic inflammation with fibrous tissue hyperplasia (Figure 2). Both the Periodic Acid-Schiff staining and Cytomegalovirus (CMV) tests were negative. During this period, his cough and sputum improved, and his CRP reduced to 6.8 mg/L. However, on the 6th day of admission, the patient developed a fever with a body temperature of 38°C, without chills, shivering, runny nose, sneezing or other symptoms. The lavage Metagenomic next-generation sequencing did not reveal significant bacteria, viruses, or mycobacterium tuberculosis. Symptomatic treatment was administered, and a repeat CRP measurement recorded 114.2 mg/L. The blood routine test showed a WBC count of 4.57×10^9/L, with a neutrophil count of 3.48×10^9/L and a normal eosinophil count (0.3×10^9/L), with no observed rash. The patient was given piperacillin-tazobactam sodium 4.5 g IV q8h for the infection; however, the fever persisted, and his cough and sputum worsened, with shortness of breath during fever. Acyclovir (0.25 g IV daily) antiviral treatment was added for 3 days, and a follow-up chest CT on the 9th day of hospitalization revealed scattered nodular lesions, ground-glass opacity, and interlobular septal

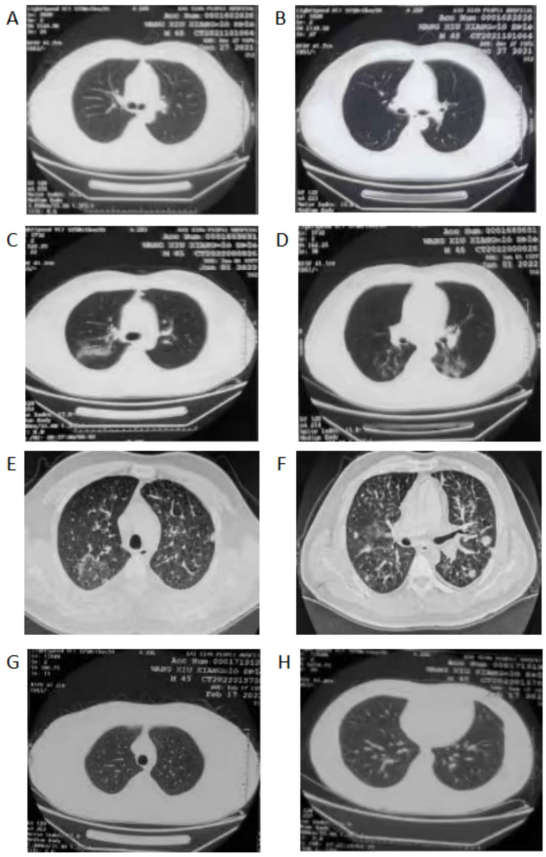

FIGURE 1
CT images of patients at different times [**(A,B)** show the lung CT of D-10, **(C,D)** show the lung CT of D-5, **(E,F)** show the lung CT of D 9, **(G,H)** show the lung CT of D 47].

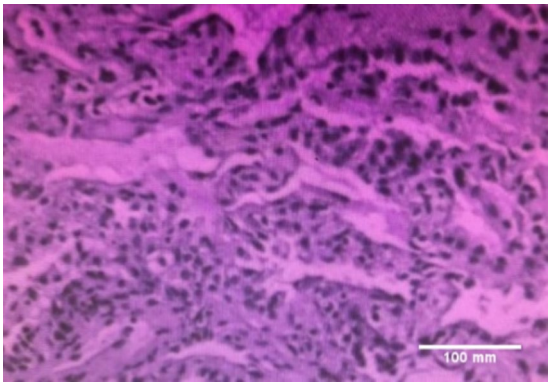

FIGURE 2
Pathology of the posterior segment of the right upper lobe lung. Bronchopulmonary biopsy was performed on the posterior segment of the upper right lobe, and pathology revealed chronic inflammation with fibrous tissue hyperplasia. Scar bar = 100 mm.

thickening in both lungs (Figures 1E,F). The results of the antinuclear antibody spectrum and anti-neutrophil antibody testing were negative. Moxifloxacin was discontinued on the 10th day of hospitalization, after which the patient remained afebrile and his cough improved. Two days later (January 17, 2022), methylprednisolone 40 mg daily was added for anti-inflammatory treatment, and a follow-up chest CT on the 17th day of hospitalization showed significant resolution and improvement of the lung lesions. Upon discharge, the patient continued to take oral Prednisone 30 mg daily, with a weekly reduction of 5 mg. A follow-up chest CT 1 month later showed complete resolution of the lesions (Figures 1G,H), with no significant coughing or sputum symptoms. During the hospitalization period, the patient took compound licorice oral liquid for cough relief (the patient had used it previously without adverse reactions), with no other special medications.

In summary, the patient exhibited symptoms of fever and pneumonia following two courses of moxifloxacin therapy. The temporal association and resolution after discontinuation supported the diagnosis of moxifloxacin-induced fever and pulmonary changes. Throughout the treatment process, the patient actively communicated his symptoms and concerns, enabling timely adjustments to the care plan and ultimately achieving favorable outcomes. The diagnostic and therapeutic timeline is summarized in Figure 3.

A literature review of adverse reactions caused by moxifloxacin

Moxifloxacin, a broad-spectrum antibiotic with favorable tissue penetration and a prolonged half-life, is widely used in the clinical management of infectious diseases. Notably, moxifloxacin may modulate pulmonary vascular permeability (17). A study reported that moxifloxacin administration and CMV replication within the first year post-transplantation were associated with an elevated risk of skin squamous cell carcinoma (SCC) (18). Specifically, moxifloxacin exposure increased the risk for SCC development during follow-up [hazard ratio (HR) = 2.9, 95% CI: 1.5–5.7; $p = 0.001$].

Drug-induced hypersensitivity syndrome (DIHS), also known as drug reaction with eosinophilia and systemic symptoms (DRESS), is a severe adverse reaction syndrome caused by moxifloxacin, characterized by systemic involvement includes pulmonary manifestations. Zhang et al. (19) reported a case of a 47-year-old woman who developed cough, fever, rash, hematologic abnormalities, shortness of breath, and interstitial lung changes after oral moxifloxacin therapy. Another report documented a patient with an upper respiratory infection who developed moxifloxacin-induced hypersensitivity pneumonitis. High-resolution chest CT scan revealed diffuse interlobular septal thickening and ground-glass opacities in both lower lung lobes. Skin prick testing and enzyme-linked immunosorbent assay for detecting specific IgE antibodies to moxifloxacin yielded negative results (20).

The hypersensitivity response caused by moxifloxacin also involves other organs, Chatzikyrkou et al. (15) reported a case of moxifloxacin-induced acute interstitial nephritis, renal biopsy revealed dense eosinophilic infiltrates and severe interstitial edema. Other severe adverse reactions, such as acute generalized exothermic hypersensitivity (21), Stevens Johnson syndrome (22), toxic episode neolysis and acute life failure (23), all of which are linked to the hypersensitivity reaction of moxifloxacin (Table 1). Fortunately, prompt recognition and accurate diagnosis can significantly improve clinical outcomes.

Discussion

Antibiotics remain the cornerstone of treating respiratory infectious diseases. In clinical practice, attention must be paid not only

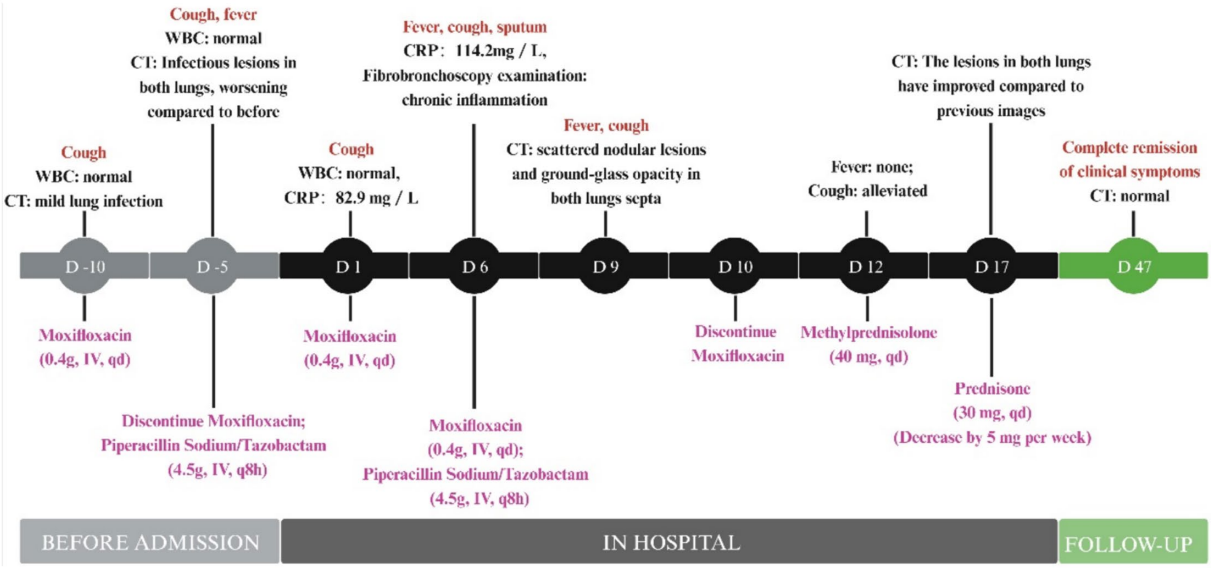

FIGURE 3
Flow chart of patient diagnosis and treatment.

TABLE 1 Summary of adverse reactions caused by moxifloxacin.

	Adverse reactions					
Features	DRESS	AKI	ALF	SJS	TEN	AGEP
Latentperiod	2–6 weeks	2–3 weeks	1–4 weeks	36 h	1 weeks	3–6 weeks
Fever	Yes	Yes	No	Yes	No	No
Skin damage	Yes	No	No	Server	Server	Yes
Viscus damage	Yes	Yes	Yes	Yes	Yes	Yes
Pathology	Mild keratinization of the epidermis, swelling around small blood vessels in the dermis, and proliferation of collagen fibers	Interstitial edema with eosinophilic infiltration	None	None	None	None
Treatment	None	Drug withdrawal + hormone therapy	Drug withdrawal + *combined therapy*	Drug withdrawal	Drug withdrawal	drug withdrawal

DRESS, drug reaction with eosinophilia and systemic symptoms; AKI, acute kidney injury; ALF, acute liver failure; SJS, stevens-johnson syndrome; TEN, toxic epidermal necrolysis; AGEP, acute generalized exanthematous pustulosis,

to antibiotic allergies and resistance, but also to potential adverse drug reactions (24). Although moxifloxacin-associated adverse effects are widely reported, cases of moxifloxacin-induced pneumonia remain scarce. Diagnosing moxifloxacin-induced pneumonia is particularly challenging, as non-infectious lung injury caused by moxifloxacin often mimics bacterial or viral pneumonia and requires exclusion of infectious etiologies to avoid life-threatening delays in management.

In the currently reported cases, hypersensitivity symptoms (fever, pulmonary inflammation) typically emerged 5 days after initiating moxifloxacin. Discontinuation led to prompt defervescence and radiographic improvement on chest CT. Notably, moxifloxacin-induced pneumonia lacks pathognomonic features. CT findings consistently demonstrate pulmonary infiltrates (20), and diagnosis relies on temporal associations between drug exposure/symptom resolution. The Naranjo Adverse Drug Reaction Probability Scale aids causality assessment, particularly when reactions are reversible or reproducible upon rechallenge. In this case, re-exposure to moxifloxacin triggered fever and radiographic progression, which resolved after withdrawal (Naranjo score = 6, "probable" causality) (25), fulfilling diagnostic criteria for drug-induced pneumonia (26).

Mechanistically, drug-induced pneumonia primarily manifests as interstitial lung disease through dual pathways: 1. Direct cytotoxicity: Moxifloxacin metabolites may damage alveolar epithelial and capillary endothelial cells, disrupting lung architecture and inciting inflammation (27). 2. Immune-mediated injury: Moxifloxacin metabolites act as haptens, forming antigenic complexes that trigger T-cell-dominated immune responses. This involves cytokine release, T-cell activation (3, 27), and delayed-type hypersensitivity (evidenced by normal IgE levels and symptom latency) (28). Cross-reactivity among quinolones is common due to MHC-dependent T-cell recognition (21, 29, 30). Notably, rapid symptom resolution post-drug withdrawal aligns with acute hypersensitivity-driven injury, akin to nitrofurantoin-induced pneumonitis (31). However, whether moxifloxacin's immunomodulatory properties directly contribute to lung injury remains unclear, warranting further mechanistic exploration.

This study has several limitations. First, the classification of moxifloxacin-associated pneumonia as interstitial pneumonia in this case was not definitively confirmed through histopathological examination. Second, the precise pathophysiological mechanisms underlying moxifloxacin-induced lung injury remain poorly characterized, necessitating further mechanistic investigations. Additionally, we were unable to obtain patient perspective due to privacy constraints.

In conclusion, this case underscores moxifloxacin as a potential culprit in drug-induced pneumonia and highlights the imperative to consider pharmacologic etiologies in patients with unexplained fever and pulmonary infiltrates.

Data availability statement

The original contributions presented in the study are included in the article/supplementary material, further inquiries can be directed to the corresponding authors.

Ethics statement

The studies involving humans were approved by Ethics Board of Army Medical University. The studies were conducted in accordance with the local legislation and institutional requirements. The participants provided their written informed consent to participate in this study. Written informed consent was obtained from the individual(s) for the publication of any potentially identifiable images or data included in this article.

Author contributions

ZG: Investigation, Project administration, Writing – original draft. YJ: Writing – original draft, Investigation, Project

administration. MZ: Writing – original draft, Project administration. CL: Writing – original draft, Investigation. ZW: Writing – original draft, Investigation. DG: Writing – review & editing. GW: Resources, Supervision, Writing – review & editing.

Funding

The author(s) declare that financial support was received for the research and/or publication of this article. This work was supported by The Major Project from Chongqing Municipal Science and Health Joint Medical Research Program (2024GGXM001).

Conflict of interest

The authors declare that the research was conducted in the absence of any commercial or financial relationships that could be construed as a potential conflict of interest.

Publisher's note

References

1. Gyotoku H, Yamaguchi H, Ishimoto H, Sato S, Taniguchi H, Senju H, et al. Prediction of anti-Cancer drug-induced pneumonia in lung Cancer patients: novel high-resolution computed tomography fibrosis scoring. *J Clin Med*. (2020) 9:1045. doi: 10.3390/jcm9041045

2. Skeoch S, Weatherley N, Swift AJ, Oldroyd A, Johns C, Hayton C, et al. Drug-induced interstitial lung disease: a systematic review. *J Clin Med*. (2018) 7:356. doi: 10.3390/jcm7100356

3. Depta JP, Pichler WJ. Cross-reactivity with drugs at the T cell level. *Curr Opin Allergy Clin Immunol*. (2003) 3:261–7. doi: 10.1097/00130832-200308000-00005

4. Kakugawa T, Yokota S, Ishimatsu Y, Hayashi T, Nakashima S, Hara S, et al. Serum heat shock protein 47 levels in patients with drug-induced lung disease. *Respir Res*. (2013) 14:133. doi: 10.1186/1465-9921-14-133

5. Tamura M, Saraya T, Fujiwara M, Hiraoka S, Yokoyama T, Yano K, et al. High-resolution computed tomography findings for patients with drug-induced pulmonary toxicity, with special reference to hypersensitivity pneumonitis-like patterns in gemcitabine-induced cases. *Oncologist*. (2013) 18:454–9. doi: 10.1634/theoncologist.2012-0248

6. Ohnishi H, Yokoyama A, Yasuhara Y, Watanabe A, Naka T, Hamada H, et al. Circulating KL-6 levels in patients with drug induced pneumonitis. *Thorax*. (2003) 58:872–5. doi: 10.1136/thorax.58.10.872

7. Piciucchi S, Romagnoli M, Chilosi M, Bigliazzi C, Dubini A, Beomonte ZB, et al. Prospective evaluation of drug-induced lung toxicity with high-resolution CT and transbronchial biopsy. *Radiol Med*. (2011) 116:246–63. doi: 10.1007/s11547-010-0608-y

8. Romagnoli M, Bigliazzi C, Casoni G, Chilosi M, Carloni A, Dubini A, et al. The role of transbronchial lung biopsy for the diagnosis of diffuse drug-induced lung disease: a case series of 44 patients. *Sarcoidosis Vasc Diffuse Lung Dis*. (2008) 25:36–45.

9. Akira M, Ishikawa H, Yamamoto S. Drug-induced pneumonitis: thin-section CT findings in 60 patients. *Radiology*. (2002) 224:852–60. doi: 10.1148/radiol.2243011236

10. Alexander E, Goldberg L, Das AF, Moran GJ, Sandrock C, Gasink LB, et al. Oral Lefamulin vs moxifloxacin for early clinical response among adults with community-acquired bacterial pneumonia: the LEAP 2 randomized clinical trial. *JAMA*. (2019) 322:1661–71. doi: 10.1001/jama.2019.15468

11. Hooper DC. Mechanisms of action of antimicrobials: focus on fluoroquinolones. *Clin Infect Dis*. (2001) 32:S9–S15. doi: 10.1086/319370

12. Radtke KK, Hesseling AC, Winckler JL, Draper HR, Solans BP, Thee S, et al. Moxifloxacin pharmacokinetics, cardiac safety, and dosing for the treatment of rifampicin-resistant tuberculosis in children. *Clin Infect Dis*. (2022) 74:1372–81. doi: 10.1093/cid/ciab641

13. De Sarro A, De Sarro G. Adverse reactions to fluoroquinolones. An overview on mechanistic aspects. *Curr Med Chem*. (2001) 8:371–84. doi: 10.2174/0929867013373435

14. Burkhardt O, Kohnlein T, Pap T, Welte T. Recurrent tendinitis after treatment with two different fluoroquinolones. *Scand J Infect Dis*. (2004) 36:315–6. doi: 10.1080/00365540410019390

15. Chatzikyrkou C, Hamwi I, Clajus C, Becker J, Hafer C, Kielstein JT. Biopsy proven acute interstitial nephritis after treatment with moxifloxacin. *BMC Nephrol*. (2010) 11:19. doi: 10.1186/1471-2369-11-19

16. Mendez BI, Ramirez ME, Ayala RS, Ruiz-Justiz AJ, Rodriguez-Garcia EJ, Gonzalez M, et al. Bilateral acute Iris Transillumination syndrome following Oral moxifloxacin overdose. *Cureus*. (2023) 15:e47426. doi: 10.7759/cureus.47426

17. Saito K, Tanaka N, Ikari J, Suzuki M, Anazawa R, Abe M, et al. Comprehensive lipid profiling of bleomycin-induced lung injury. *J Appl Toxicol*. (2019) 39:658–71. doi: 10.1002/jat.3758

18. Aranda A, Mayorga C, Ariza A, Dona I, Rosado A, Blanca-Lopez N, et al. In vitro evaluation of IgE-mediated hypersensitivity reactions to quinolones. *Allergy*. (2011) 66:247–54. doi: 10.1111/j.1398-9995.2010.02460.x

19. Zhang Y, Wang X, Cheng Y, Wang X, Zhang Y. A typical presentation of moxifloxacin-induced DRESS syndrome with pulmonary involvement: a case report and review of the literature. *BMC Pulm Med*. (2022) 22:279. doi: 10.1186/s12890-022-02064-1

20. Son CH, Kim HI, Kim KN, Lee KN, Lee CU, Roh MS, et al. Moxifloxacin-associated drug hypersensitivity syndrome with drug-induced hypersensitivity pneumonitis. *J Investig Allergol Clin Immunol*. (2008) 18:72–3.

21. Schmid DA, Depta JP, Pichler WJ. T cell-mediated hypersensitivity to quinolones: mechanisms and cross-reactivity. *Clin Exp Allergy*. (2006) 36:59–69. doi: 10.1111/j.1365-2222.2006.02402.x

22. Dhavaleshwar A, Nayak V, Hande M, Pai R. Topical moxifloxacin-induced toxic epidermal necrolysis and Stevens-Johnson syndrome. *J Postgrad Med*. (2019) 65:125–6. doi: 10.4103/jpgm.JPGM_535_18

23. Nori S, Nebesio C, Brashear R, Travers JB. Moxifloxacin-associated drug hypersensitivity syndrome with toxic epidermal necrolysis and fulminant hepatic failure. *Arch Dermatol*. (2004) 140:1537–8. doi: 10.1001/archderm.140.12.1537

24. Irfan O, Gilani JA, Irshad A, Irfan B, Khan JA. Pharmacological threat to lungs: a case series and literature review. *Cureus*. (2017) 9:e1232. doi: 10.7759/cureus.1232

25. Naranjo CA, Busto U, Sellers EM, Sandor P, Ruiz I, Roberts EA, et al. A method for estimating the probability of adverse drug reactions. *Clin Pharmacol Ther*. (1981) 30:239–45. doi: 10.1038/clpt.1981.154

26. Kubo K, Azuma A, Kanazawa M, Kameda H, Kusumoto M, Genma A, et al. Consensus statement for the diagnosis and treatment of drug-induced lung injuries. *Respir Investig*. (2013) 51:260–77. doi: 10.1016/j.resinv.2013.09.001

27. Baba K, Matsubara Y, Hirata Y, Ota Y, Takahashi S, Boku N. Case report: irinotecan-induced interstitial lung disease in an advanced colorectal cancer patient resurfacing decades after allogeneic bone marrow transplantation for aplastic anemia; a case report and narrative review of literature. *Front Oncol*. (2023) 13:1215789. doi: 10.3389/fonc.2023.1215789

28. Dona I, Moreno E, Perez-Sanchez N, Andreu I, Hernandez FDRD, Torres MJ. Update on quinolone allergy. *Curr Allergy Asthma Rep*. (2017) 17:56. doi: 10.1007/s11882-017-0725-y

29. Blanca-Lopez N, Ariza A, Dona I, Mayorga C, Montanez MI, Garcia-Campos J, et al. Hypersensitivity reactions to fluoroquinolones: analysis of the factors involved. *Clin Exp Allergy*. (2013) 43:560–7. doi: 10.1111/cea.12099

30. Azimi SF, Mainella V, Jeffres MN. Immediate hypersensitivity to fluoroquinolones: a cohort assessing cross-reactivity. *Open Forum Infect Dis*. (2022) 9:ofac106. doi: 10.1093/ofid/ofac106

31. Sovijarvi AR, Lemola M, Stenius B, Idanpaan-Heikkila J. Nitrofurantoin-induced acute, subacute and chronic pulmonary reactions. *Scand J Respir Dis*. (1977) 58:41–50.

frontiers | Frontiers in Medicine

TYPE Case Report
PUBLISHED 09 July 2025
DOI 10.3389/fmed.2025.1461269

OPEN ACCESS

EDITED BY
Uday Kishore,
United Arab Emirates University,
United Arab Emirates

REVIEWED BY
Ourania Papaioannou,
General University Hospital of Patras, Greece
Moustafa Ali Saad,
Cairo University, Egypt
Sahar Rostamian,
Harvard Medical School, United States

*CORRESPONDENCE
Taehun Kim
✉ taehunlung@gmail.com

RECEIVED 08 July 2024
ACCEPTED 16 June 2025
PUBLISHED 09 July 2025

CITATION
Kim T, Song BW and Shin HC (2025) Case Report: Rescue "awake" extracorporeal membrane oxygenation for acute respiratory failure in severe granulomatosis with polyangiitis with multisystem involvement. *Front. Med.* 12:1461269. doi: 10.3389/fmed.2025.1461269

Case Report: Rescue "awake" extracorporeal membrane oxygenation for acute respiratory failure in severe granulomatosis with polyangiitis with multisystem involvement

Taehun Kim[1]*, Byung Wook Song[2] and Hyeong Chan Shin[3]

[1]Division of Pulmonary Medicine, Department of Internal Medicine, Keimyung University School of Medicine, Dongsan Hospital, Daegu, Republic of Korea, [2]Division of Rheumatology, Department of Internal Medicine, Keimyung University School of Medicine, Dongsan Hospital, Daegu, Republic of Korea, [3]Department of Pathology, Keimyung University School of Medicine, Dongsan Hospital, Daegu, Republic of Korea

We present the case of a 40-year-old man who developed severe acute respiratory failure along with hemoptysis and was subsequently diagnosed with granulomatosis with polyangiitis (GPA). He was initially treated with high-dose corticosteroids, cyclophosphamide, plasmapheresis, and mechanical ventilation (MV). The patient's condition deteriorated after being weaned from MV, leading to his transfer to our medical center without reintubation. Upon admission, a high-flow nasal cannula delivering FiO2 of 1.0 was immediately initiated. Despite the severity of hypoxemia, the patient exhibited neither tachypnea nor subjective dyspnea, and was subsequently initiated on "awake" venovenous extracorporeal membrane oxygenation (VV-ECMO) without MV. Anticoagulation therapy was initiated, and continuous renal replacement therapy was commenced to manage anuria associated with acute renal failure. Due to treatment failure after initial immunosuppressive therapy with cyclophosphamide, rituximab was administered as an induction agent. Following four cycles of rituximab, the patient's respiratory function showed marked improvement. Subsequently, a splenic artery hemorrhage occurred but was effectively managed through prompt embolization, resulting in immediate hemodynamic stabilization. The patient was successfully weaned off VV-ECMO support on day 22 after starting ECMO. After the transfer from the intensive care unit, the patient began active rehabilitation, during which he reported episodes of dizziness. Magnetic resonance imaging of the brain revealed multiple acute infarctions, which are presumed to be caused by vasculitis, leading to the initiation of adjunctive antiplatelet therapy. This represents the first reported case of refractory severe GPA affecting the kidneys, splenic artery, and central nervous system and resulting in respiratory failure, which was managed using "awake" VV-ECMO. The patient remains on maintenance hemodialysis and continues treatment with corticosteroids and rituximab. No disease relapse has occurred until now (June 2025), and the patient is undergoing rehabilitation for intensive care unit-acquired weakness.

KEYWORDS

granulomatosis with polyangiitis, extracorporeal membrane oxygenation, rituximab, acute respiratory distress syndrome, splenic artery vasculopathy

Introduction

Antineutrophil cytoplasmic antibody (ANCA)-associated vasculitis, comprising granulomatosis with polyangiitis (GPA), microscopic polyangiitis, and eosinophilic granulomatosis with polyangiitis, is a systemic disorder that affects small- and medium-sized vessels. Severe cases are characterized by life-threatening multiorgan failure, involving alveolar hemorrhage, glomerulonephritis, central nervous system vasculitis, and cardiac manifestations. Refractory disease is defined as persistent disease activity despite an adequate course of immunosuppressive therapy (1). In GPA, some patients develop acute respiratory distress syndrome (ARDS) secondary to diffuse alveolar hemorrhage. ARDS commonly leads to severe impairment of oxygenation, and its severity is classified based on the ratio of partial pressure of oxygen (pO2) to the fraction of inspired oxygen (FiO2), according to the Berlin Criteria (2). A recent review indicated that although diffuse alveolar hemorrhage is relatively uncommon, it predominantly affects men and critically ill patients, often involves renal impairment, and frequently necessitates MV (3). Current guidelines for severe ARDS recommend the use of rescue extracorporeal membrane oxygenation (ECMO) to decrease mortality rates and reduce ventilator-associated lung injury (4). While venovenous (VV) ECMO is typically employed as a rescue therapy following mechanical ventilation, an alternative approach called "awake" ECMO has been introduced for use in non-intubated patients (5). ECMO has demonstrated success as a rescue therapy in cases of ANCA-associated vasculitis (6), GPA presenting with respiratory failure in adults (7–10), and in pediatric patients (11). This report describes a case of refractory severe GPA that affected the kidneys, splenic arteries, and central nervous system and was complicated by diffuse alveolar hemorrhage, respiratory failure, and cytomegalovirus pneumonitis. The patient was successfully treated using "awake" venovenous ECMO (VV-ECMO) without intubation, alongside induction therapy with rituximab.

Case description

A 40-year-old man was admitted to a local medical center's intensive care unit (ICU) due to respiratory failure and hemoptysis, and MV was initiated immediately (Figure 1A). The patient had no prior medical history and no known family history of autoimmune disease. The patient had a body mass index of 31.9, which is classified as obesity (height: 177 cm; body weight: 100 kg), and his anti-proteinase-3 (PR3) antibody level was greater than 100 U/mL. Progressive renal dysfunction was noted (blood urea nitrogen: 65 mg/dL, serum creatinine: 6.76 mg/dL), and continuous renal replacement therapy was initiated. Induction therapy was initiated with pulse steroids, specifically methylprednisolone, administered at 500 mg every 12 h from 31 August 2023 to 4 September 2023, and cyclophosphamide, administered at 500 mg/m^2 on 1 September 2023, in response to the anti-PR3 antibody level exceeding 100 U/mL. A diagnosis of diffuse alveolar hemorrhage associated with vasculitis and severe GPA was established. Plasmapheresis was performed on 1 August 2023. After 5 days of pulse steroid therapy, the patient showed clinical improvement and was successfully weaned off MV. The corticosteroid dose was reduced to 125 mg every 12 h from 5 August 2023 to 12 August 2023. However, 7 days later, the patient experienced deterioration in oxygenation, accompanied by recurrent hemoptysis. Consequently, the patient was transferred to our tertiary medical center for advanced respiratory support and rescue therapy.

Upon arrival at the emergency department, the patient was not intubated; therefore, high-flow nasal cannula (HFNC) therapy with FiO_2 of 1.0 was initiated. On presentation, the vital signs upon presentation were as follows: blood pressure 170/68 mmHg, heart rate 114 bpm, respiratory rate 14 breaths per min, and body temperature 36.7°C. Arterial blood gas analysis revealed a pCO_2 of 32.2 mmHg, pH of 7.551, and pO_2 of 67.4 mmHg. Although the pO2/FiO2 ratio was measured without MV and positive end-expiratory pressure, the values met the criteria for severe ARDS. The patient was admitted to the ICU for further respiratory support, and the initiation of rescue therapy was considered. The patient exhibited no signs of respiratory distress. Point-of-care cardiac echo ultrasonography revealed preserved systolic function without significant abnormalities. VV-ECMO was initiated via right internal jugular and left femoral vein cannulation without prior MV. Following ECMO application, the patient's respiratory pattern remained stable, with subsequent improvement in oxygenation (Table 1). Formal echocardiography

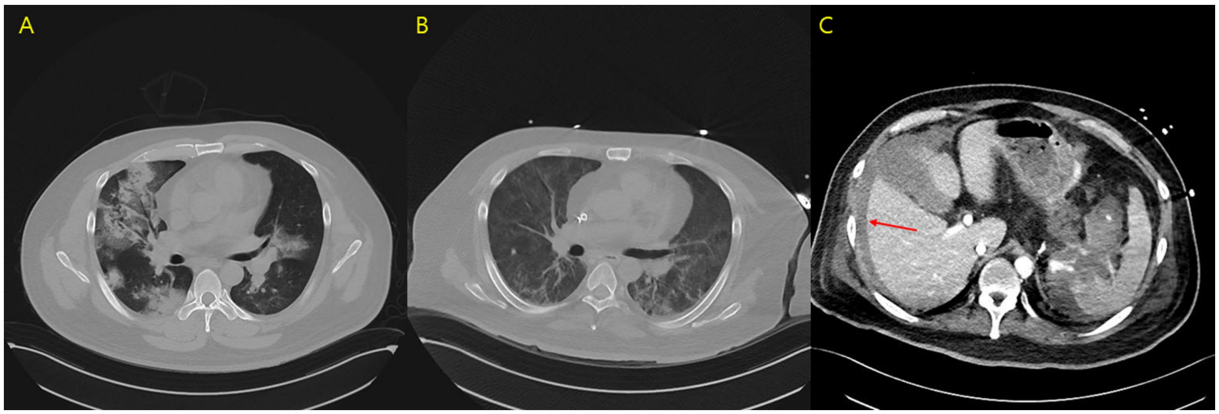

FIGURE 1
(A) Initial chest computed tomography scan. **(B)** Chest computed tomography scan on day 13 of hospitalization. **(C)** Abdominal computed tomography scan on day 13, revealing free fluid collection, hemoperitoneum (arrow), and contrast extravasation from the splenic artery.

conducted after ECMO initiation revealed an ejection fraction of 45%, without evidence of valvular heart disease or pulmonary hypertension. The patient did not report chest pain, and cardiac enzyme levels were within the normal range [troponin I < 0.16 ng/mL (0.0–0.3), CK-MB 1.74 ng/mL (0.0–4.87)]. The patient remained anuric, with renal failure evidenced by a blood urea nitrogen level of 65 mg/dL and a creatinine level of 6.76 mg/dL; therefore, continuous renal replacement therapy was continued via the ECMO circuit. Argatroban was administered for anticoagulation during the ECMO procedure. At the time of ECMO initiation, the patient exhibited thrombocytopenia without the clinical features of disseminated intravascular coagulation. Laboratory findings included a white blood cell count of 6.65×10^3/μL (4.00–10.00), a hemoglobin count of 6.70 g/dL (13.0–17.0), a platelet count of 89×10^3/μL (130–400), a prothrombin time of 13.0 s (10.0–14.0), an activated partial thromboplastin time of 28.8 s (20.0–33.5), and a C-reactive protein level of 6.1 mg/dL (0.0–0.5). Heparin-induced thrombocytopenia could not be ruled out.

Connective tissue disease-related serological tests were repeated upon admission to our medical center. The results showed no detectable anti-nuclear or anti-double-stranded DNA antibodies. Additionally, antibodies including anti-centromere (0.7 U/mL), anti-glomerular basement membrane (1.4 U/mL), anti-Jo-1 (0.8 U/mL), anti-myeloperoxidase (1.0 U/mL), anti-ribonucleoprotein (1.7 U/mL), anti-Scl-70 (2.1 U/mL), anti-Smith (0.2 U/mL), anti-Ro (0.3 U/mL), and anti-La (2.0 U/mL) were all within the negative range. In contrast, the anti-PR3 antibody remained positive at >100.0 U/mL (Table 2). The patient was diagnosed with refractory severe GPA based on a total score of 8, according to the 2022 American College of Rheumatology/European League Against Rheumatism classification criteria at the time of ICU admission. High-dose corticosteroids combined with rituximab were selected for induction therapy (12). As the patient experienced treatment failure with cyclophosphamide and plasmapheresis, we decided to use rituximab along with pulse steroid therapy. Immunosuppressive therapy for vasculitis was administered concurrently with the initiation of VV-ECMO. High-dose methylprednisolone (500 mg every 12 h) was administered from 15 to 18 August 2023, followed by a tapering regimen: 500 mg/day from 19 to 22 August, 250 mg/day from 23 to 25 August, 125 mg/day from 26 to 28 August, 60 mg/day from 29 August to 2 October, and 30 mg/day beginning 3 October 2023. Rituximab was administered at a dosage of 375 mg/m^2 weekly, with doses given on 15, 22, and 29 August, followed by a final dose on 6 October 2023. On the day of ICU admission (15 August 2023), cytomegalovirus (CMV) polymerase chain reaction (PCR) testing revealed a viral load of 5,700 copies/mL. However, the results of the CMV PCR became available 1 week later due to processing time. Despite clinical improvement following rituximab induction, qualitative CMV testing of the bronchoalveolar lavage fluid was positive, indicating a possible concurrent CMV infection. Therefore, ganciclovir (250 mg/day; 2.5 mg/kg/day) was administered for 3 weeks. Given the severity of the clinical condition

TABLE 1 Extracorporeal membrane oxygenation flow sheet.

Day	Pump RPM	Blood flow (L/min)	Air flow (L/min)	FiO_2 (%)	pH	pCO_2	pO_2
D1 (initial)					7.55	32.2	67.4
D1 ECMO	3,510	3.3	2.5	1	7.52	32.6	490
D2	3,510	4.8	2.5	1	7.37	39.9	535
D3	3,510	4.8	2.5	1	7.379	39	512
D4	2,385	4.8	2.5	1	7.39	36.6	391
D5	2,385	3	2	0.95	7.38	33.9	446
D6	2,385	2.9	2.5	0.95	7.44	32.5	390
D7	2,385	2.8	2.5	0.9	7.41	35.5	518
D8	2,385	2.8	2.5	0.9	7.38	34.8	501
D9	2,385	2.8	2.5	0.9	7.4	35	480
D10	2,385	2.8	2.5	0.9	7.42	33.4	445
D11	2,385	2.8	2.5	0.9	7.41	36.7	501
D12	2,385	2.8	2.5	0.85	7.4	35.5	459
D13	2,385	2.9	2.5	0.8	7.42	34.5	461
D14	2,900	2.9	2.5	0.8	7.4	35.2	440
D15	2,700	2.7	2.5	0.75	7.44	33.4	384
D16	2,700	2.7	2.5	0.75	7.4	36.1	390
D17	2,500	2.5	2.3	0.7	7.39	33.4	398
D18	2,500	2.7	2.3	0.7	7.4	33.6	400
D19	2,700	2.5	2.3	0.65	7.28	28.6	400
D20	1,500	1.5	1.7	0.6	7.41	38.4	299
D21	1,650	1.65	1.7	0.5	7.43	34	239
D22	1,600	1.6	0	0	7.37	39.2	102

ECMO, extracorporeal membrane oxygenation; RPM, rotations per minute; FiO_2, fraction of inspired oxygen; pCO_2 partial pressure of carbon dioxide; pO_2, partial pressure of oxygen.

TABLE 2 Autoimmune and laboratory tests flow sheet.

	September 15, 2023	September 22, 2023	September 29, 2023	October 06, 2023	October 31, 2023
Anti-GBM Ab (U/mL)	Negative (1.4)	Negative (0.3)	Negative (0.5)	Negative (0.9)	Negative (0.1)
Anti-MPO Ab (U/mL)	Negative (1.0)	Negative (0.8)	Negative (0.8)	Negative (0.8)	Negative (0.7)
Anti-PR3 Ab (U/mL)	Positive (>100)	Positive (27.1)	Positive (13.3)	Positive (5.4)	Positive (6.6)
CMV DNA Real-time PCR (copies/mL)	5,700	14,356	24,746	74,569	15,365
KL-6 (U/mL)	562.1	693.6	972.8	631.8	
Interleukin 6 (pg/mL)	30.4				

Anti-GBM Ab (negative <20 U/mL), anti-glomerular basement membrane antibody; anti-MPO Ab (negative <5 U/mL), anti-myeloperoxidase antibody; anti-PR3 Ab (negative <5 U/mL), anti-proteinase-3 antibody; CMV DNA, cytomegalovirus deoxyribonucleic acid; KL-6, Krebs von den Lungen-6; PCR, polymerase chain reaction.

and the patient's prior hospitalization, additional antimicrobial agents were administered, including carbapenem, teicoplanin, and prophylactic trimethoprim-sulfamethoxazole.

Anticoagulation therapy with argatroban was administered during the treatment period, and no further episodes of hemoptysis were observed. Following medical management, including volume reduction via continuous renal replacement therapy, chest radiography showed improvement in bilateral parenchymal consolidations. The anti-PR3 antibody level decreased from >100 U/mL on day 1 to 27.1 U/mL on day 8 (Table 2), and oxygenation parameters showed progressive improvement (Table 1; Figure 1B). On day 13 following ECMO initiation, although hemoptysis did not recur, a sudden drop in hemoglobin levels was detected along with hypotension. The patient reported dull abdominal pain, and point-of-care ultrasonography revealed the presence of fluid in the right subphrenic area. Consequently, chest and abdominal computed tomography scans were performed, revealing hemoperitoneum caused by splenic artery bleeding with contrast dye extravasation, which was presumed to be secondary to underlying vasculopathy (Figure 1C). A blood transfusion was conducted, consisting of four units of packed red blood cells (400 mL) and two units of fresh frozen plasma (400 mL), and anticoagulation therapy was discontinued. Emergent angioembolization of the splenic artery was promptly performed (Supplementary Figures S1A,B). No further decline in hemoglobin levels was observed after the embolization, and the patient's hemodynamic status stabilized rapidly, with normalized blood pressure and heart rate, leading to the discontinuation of nootropics. By day 21, the FiO2 of HFNC was reduced to 0.6. As the patient remained clinically stable, ECMO weaning was initiated. The patient was successfully weaned from VV-ECMO support on day 22 after starting ECMO. The patient exhibited favorable clinical recovery, enabling a gradual reduction and eventual discontinuation of supplemental oxygen. A renal biopsy was performed to confirm the diagnosis, which demonstrated crescentic glomerulonephritis (Figures 2A,B) and acute tubular necrosis (Figure 2C). As the anuric state persisted and renal biopsy findings suggested irreversible damage, long-term hemodialysis was initiated via a permanent catheter. During active rehabilitation, the patient experienced episodes of dizziness. Magnetic resonance imaging of the brain revealed multiple acute infarctions in the superior right frontal cortex and left parietal cortex (Supplementary Figures S2A–C). The cerebral infarctions were attributed to vasculitis; therefore, an additional antiplatelet agent, aspirin 100 mg/day, was prescribed. After receiving intensive care, the patient was discharged with ongoing maintenance therapy including hemodialysis, corticosteroids, and rituximab. No relapse has been observed until now (June 2025), and the patient continues rehabilitation for ICU-acquired weakness.

Discussion

A case of severe GPA was presented, in which induction therapy with cyclophosphamide was unsuccessful; however, successful disease control was achieved following rituximab-based induction (Supplementary Figure S3). As clinical improvement was consistently observed following rituximab induction, the deterioration before hospitalization was attributed to cyclophosphamide induction failure rather than CMV pneumonia. Given the patient's critical condition and the requirement for ongoing immunosuppressive therapy, ganciclovir was concurrently administered. In the critical care setting, this case represented successful management of severe ARDS using ECMO without MV as a rescue therapy. The patient initially presented with multiorgan dysfunction involving both the pulmonary and renal systems. Additionally, the involvement of both the splenic artery and the cerebrovascular system was identified. Splenic artery involvement is uncommon and has been documented in a limited number of cases (13–16). Cerebrovascular events are also infrequent; although central nervous system involvement was reported in 32.3–33.6% of patients, cerebrovascular manifestations occurred in only 4.0% of 146 patients (17, 18).

For the rescue management of ARDS, both VV-ECMO and prone positioning are considered viable options. Prone positioning is strongly recommended in conjunction with MV (19). However, recent evidence indicates that prone positioning does not significantly reduce the duration of successful weaning or mortality when compared to the supine position in patients undergoing VV-ECMO (20). In this case, the clinical team had to decide between initiating invasive mechanical ventilation with prone positioning or proceeding with VV-ECMO as the initial rescue therapy. Initial concerns were raised regarding the use of prone positioning; however, due to the absence of labored breathing, VV-ECMO with induction therapy was initiated without mechanical ventilation, and prone positioning was consequently not implemented.

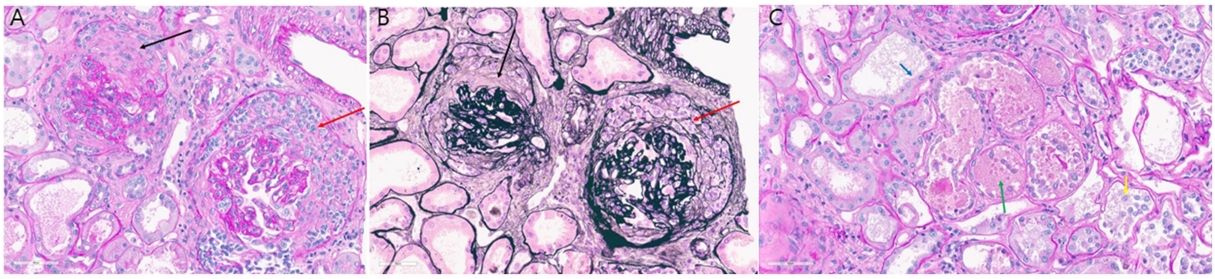

FIGURE 2
(A,B) Glomerular crescents: **(A)** circumferential fibrocellular crescent (black arrow) and cellular crescent (red arrow) accompanied by glomerular basement membrane wrinkling (periodic acid–Schiff stain; original magnification, ×40); **(B)** corresponding findings stained with periodic acid–methenamine silver (original magnification, ×40). **(C)** Acute tubular necrosis: loss of brush border (blue arrow), denuded tubular epithelial cells (yellow arrow), and tubular cast containing fibrin debris (green arrow) as seen on periodic acid–Schiff staining (original magnification, x40).

Anticoagulation was maintained during VV-ECMO, which may have contributed to the splenic artery hemorrhage in the context of underlying vasculopathy. Therefore, the use of anticoagulants during ECMO should be cautiously considered in severe GPA cases with multiorgan involvement. ARDS is a frequent complication of severe GPA and often necessitates ECMO support (9). In selected cases, "awake" ECMO without endotracheal intubation is feasible; however, meticulous monitoring of bleeding complications caused by vasculopathy is essential.

During the SARS-CoV-2 pandemic, it is essential to carefully assess the etiology of disorientation in patients with respiratory failure, particularly in immunocompromised individuals receiving immunomodulatory therapies. GPA associated with ARDS may clinically resemble infectious diseases that necessitate distinct treatment approaches (21, 22). PCR testing at our center was negative for SARS-CoV-2; however, CMV infection was confirmed. In patients with autoimmune diseases, both infection and the level of immunosuppression must be carefully managed to maintain effective disease control. Although this can be challenging, treatment decisions should be guided by the patient's clinical trajectory.

Although diagnostic biopsy plays a crucial role, its timing may be deferred based on the patient's clinical severity and overall condition, as seen in this case. However, when ANCA positivity indicates a severe disease course, such as in GPA, timely initiation of appropriate therapy is essential. Timely induction with an appropriate agent significantly improves survival outcomes. A randomized, double-blind, non-inferiority trial demonstrated that a rituximab-based regimen is not inferior to a cyclophosphamide-based regimen (23–25). For induction therapy in GPA, current options include rituximab or cyclophosphamide, both administered in combination with glucocorticoids (26). However, the 2021 American College of Rheumatology/Vasculitis Foundation guidelines recommend rituximab over cyclophosphamide for induction therapy in severe GPA (1). Successful induction can still be achieved in patients with prior treatment failure or early relapses following immunosuppressive therapy, as demonstrated in this case.

In conclusion, this report describes a case of severe GPA with multiorgan involvement, including pulmonary, renal, splenic arterial, and central nervous system manifestations. The condition was successfully managed using "awake" VV-ECMO in combination with rituximab-based induction therapy. This case underscores the importance of guideline-directed therapy when selecting induction regimens. For carefully selected patients, "awake" VV-ECMO without MV may offer a viable alternative to the routine application of invasive ventilation.

Data availability statement

The datasets presented in this article are not readily available because the data that support the findings of this study are not openly available due to the fact that consent to share data was not obtained from participants. However, the datasets used and analyzed in the current study are available from the corresponding author on reasonable request. Requests to access the datasets should be directed to TK, taehunlung@gmail.com.

Ethics statement

The study protocol was approved by the Institutional Review Board (IRB) of Keimyung University Dongsan Hospital (IRB N 2023-07-087-002). The study was conducted in compliance with the principles of the Declaration of Helsinki. The studies were conducted in accordance with the local legislation and institutional requirements. The ethics committee/institutional review board waived the requirement of written informed consent for participation from the participants or the participants' legal guardians/next of kin because the nature of this study was a retrospective case report.

Author contributions

TK: Conceptualization, Data curation, Formal analysis, Investigation, Methodology, Visualization, Writing – original draft, Writing – review & editing. BS: Conceptualization, Formal analysis, Methodology, Writing – review & editing. HS: Conceptualization, Investigation, Visualization, Writing – review & editing.

Funding

The author(s) declare that no financial support was received for the research and/or publication of this article.

Conflict of interest

The authors declare that the research was conducted in the absence of any commercial or financial relationships that could be construed as a potential conflict of interest.

Publisher's note

All claims expressed in this article are solely those of the authors and do not necessarily represent those of their affiliated organizations, or those of the publisher, the editors and the reviewers. Any product that may be evaluated in this article, or claim that may be made by its manufacturer, is not guaranteed or endorsed by the publisher.

Supplementary material

The Supplementary material for this article can be found online at: https://www.frontiersin.org/articles/10.3389/fmed.2025.1461269/full#supplementary-material

SUPPLEMENTARY FIGURE S1
Angiographic images obtained before **(A)** and after **(B)** splenic artery embolization. Contrast extravasation.

SUPPLEMENTARY FIGURE S2
Brain magnetic resonance images of superior frontal cortex infarction **(A)** and left parietal cortex infarction **(B,C)**.

SUPPLEMENTARY FIGURE S3
Flow chart.

References

1. Chung SA, Langford CA, Maz M, Abril A, Gorelik M, Guyatt G, et al. 2021 American College of Rheumatology/Vasculitis Foundation guideline for the management of antineutrophil cytoplasmic antibody–associated vasculitis. *Arthritis Rheumatol.* (2021) 73:1366–83. doi: 10.1002/art.41773

2. Ranieri VM, Rubenfeld GD, Taylor Thompson B, Ferguson ND, Caldwell E, Fan E, et al. Acute respiratory distress syndrome: the Berlin definition. *JAMA*. (2012) 307:2526–33. doi: 10.1001/jama.2012.5669

3. Da Silva RC, Adhikari P. Granulomatosis with polyangiitis presenting with diffuse alveolar hemorrhage: a systematic review. *Cureus*. (2022):14. doi: 10.7759/cureus.29909

4. Tasaka S, Ohshimo S, Takeuchi M, Yasuda H, Ichikado K, Tsushima K, et al. ARDS clinical practice guideline 2021. *J Intensive Care*. (2022) 10:32. doi: 10.1186/s40560-022-00615-6

5. Langer T, Santini A, Bottino N, Crotti S, Batchinsky AI, Pesenti A, et al. "Awake" extracorporeal membrane oxygenation (ECMO): pathophysiology, technical considerations, and clinical pioneering. *Crit Care*. (2016) 20:1–10. doi: 10.1186/s13054-016-1329-y

6. Wang L, Wang J, Xu Y, Jiao J, Xie L, Mo G. A novel therapeutic strategy using extracorporeal membrane oxygenation in patients with anti-neutrophil cytoplasmic antibodies-associated vasculitis: a case report and literature review. *Ann Transl Med*. (2021) 9:1267. doi: 10.21037/atm-21-3133

7. Wan R, Yang W, Ma X, Yang W, Pan P, Hu C, et al. Ecmo rescues patients with acute respiratory failure related to GpA. *Front Med*. (2021) 8:671396. doi: 10.3389/fmed.2021.671396

8. Yin K, March RJ, Hoopes CW, Balk RA, Raman J, Lateef OB, et al. Extracorporeal membrane oxygenation in the management of granulomatosis with polyangiitis. *J Card Surg*. (2021) 36:743–7. doi: 10.1111/jocs.15252

9. Delvino P, Monti S, Balduzzi S, Belliato M, Montecucco C, Caporali R. The role of extra-corporeal membrane oxygenation (ECMO) in the treatment of diffuse alveolar haemorrhage secondary to ANCA-associated vasculitis: report of two cases and review of the literature. *Rheumatol Int*. (2019) 39:367–75. doi: 10.1007/s00296-018-4116-z

10. Rawal G, Kumar R, Yadav S. ECMO rescue therapy in diffuse alveolar haemorrhage: a case report with review of literature. *J Clin Diagn Res*. (2016) 10:OD10-1. doi: 10.7860/JCDR/2016/20649.7969

11. Finkel R, Honig J, Chao CP, Rescoe E, Solomon S. The use of ECMO in pediatric granulomatosis with polyangiitis. *Pediatr Rheumatol*. (2022) 20:35. doi: 10.1186/s12969-022-00693-8

12. Robson JC, Grayson PC, Ponte C, Suppiah R, Craven A, Judge A, et al. 2022 American College of Rheumatology/European Alliance of associations for rheumatology classification criteria for granulomatosis with polyangiitis. *Arthritis Rheumatol*. (2022) 74:393–9. doi: 10.1002/art.41986

13. Fishman D, Isenberg DA. Splenic involvement in rheumatic diseases. *Semin Arthritis Rheum*. (1997) 27:141–55. doi: 10.1016/s0049-0172(97)80013-3

14. Katikineni VS, Kant S, Gapud EJ, Antiochos B, Manno RL, Phillips M, et al. Uncommon presentations in ANCA vasculitis: clinical characteristics and outcomes. *Clin Rheumatol*. (2019) 38:2195–9. doi: 10.1007/s10067-019-04568-4

15. Stone JH. Limited versus severe Wegener's granulomatosis: baseline data on patients in the Wegener's granulomatosis etanercept trial. *Arthritis Rheum*. (2003) 48:2299–309. doi: 10.1002/art.11075

16. Ahmad Y, Morawietz G, Ksouri H, Schefold JC, Zuercher P. Granulomatosis with polyangiitis (Wegener's) complicated by splenic rupture and severe acute respiratory distress syndrome: a case report. *Clin Case Reports*. (2021) 9:e04369. doi: 10.1002/ccr3.4369

17. Zhang W, Zhou G, Shi Q, Zhang X, Zeng XF, Zhang FC. Clinical analysis of nervous system involvement in ANCA-associated systemic vasculitides. *Clin Exp Rheumatol*. (2009) 27 (1 Suppl 52):S65-9.

18. Nishino H, Rubino FA, DeRemee RA, Swanson JW, Parisi JE. Neurological involvement in Wegener's granulomatosis: an analysis of 324 consecutive patients at the Mayo Clinic. *Ann Neurol*. (1993) 33:4–9. doi: 10.1002/ana.410330103

19. Grasselli G, Calfee CS, Camporota L, Poole D, Amato MBP, Antonelli M, et al. ESICM guidelines on acute respiratory distress syndrome: definition, phenotyping and respiratory support strategies. *Intensive Care Med*. (2023) 49:727–59. doi: 10.1007/s00134-023-07050-7

20. Schmidt M, Hajage D, Lebreton G, Dres M, Guervilly C, Richard JC, et al. Prone positioning during extracorporeal membrane oxygenation in patients with severe ARDS: the PRONECMO randomized clinical trial. *JAMA*. (2023) 330:2343–53. doi: 10.1001/jama.2023.24491

21. Tzouvelekis A, Karampitsakos T, Krompa A, Markozannes E, Bouros D. False positive COVID-19 antibody test in a case of granulomatosis with polyangiitis. *Front Med*. (2020) 7:399. doi: 10.3389/fmed.2020.00399

22. Karampitsakos T, Papaioannou O, Tsiri P, Katsaras M, Katsimpris A, Kalogeropoulos AP, et al. Tocilizumab versus baricitinib in hospitalized patients with severe COVID-19: an open label, randomized controlled trial. *Clin Microbiol Infect*. (2023) 29:372–8. doi: 10.1016/j.cmi.2022.10.015

23. Specks U, Merkel PA, Seo P, Spiera R, Langford CA, Hoffman GS, et al. Efficacy of remission-induction regimens for ANCA-associated vasculitis. *N Engl J Med*. (2013) 369:417–27. doi: 10.1056/NEJMoa1213277

24. Stone JH, Merkel PA, Spiera R, Seo P, Langford CA, Hoffman GS, et al. Rituximab versus cyclophosphamide for ANCA-associated vasculitis. *N Engl J Med*. (2010) 363:221–32. doi: 10.1056/NEJMoa0909905

25. Geetha D, Specks U, Stone JH, Merkel PA, Seo P, Spiera R, et al. Rituximab versus cyclophosphamide for ANCA-associated vasculitis with renal involvement. *J Am Soc Nephrol*. (2015) 26:976–85. doi: 10.1681/ASN.2014010046

26. Hellmich B, Sanchez-Alamo B, Schirmer JH, Berti A, Blockmans D, Cid MC, et al. EULAR recommendations for the management of ANCA-associated vasculitis: 2022 update. *Ann Rheum Dis*. (2024) 83:30–47. doi: 10.1136/ard-2022-223764

Frontiers in Medicine

Translating medical research and innovation into improved patient care

A multidisciplinary journal which advances our medical knowledge. It supports the translation of scientific advances into new therapies and diagnostic tools that will improve patient care.

Discover the latest Research Topics

See more →

Frontiers

Avenue du Tribunal-Fédéral 34
1005 Lausanne, Switzerland
frontiersin.org

Contact us

+41 (0)21 510 17 00
frontiersin.org/about/contact